LMS/BLU/S11381

Site Status Report: Groundwater Flow and Contaminant Transport in the Vicinity of the Bluewater, New Mexico, Disposal Site

November 2014

U.S. DEPARTMENT OF ENERGY | Legacy Management

This page intentionally left blank

Contents

Abbreviations vii
Executive Summary ix
1.0 Introduction and Objectives 1
1.1 Introduction 1
1.2 Groundwater Issues 2
1.3 Objectives 3
2.0 Study Area 7
2.1 Study Area Description 7
2.2 Bluewater Site History 8
2.2.1 Milling 8
2.2.2 Site Decommissioning 11
2.2.3 Historical Site Groundwater Issues 13
2.2.4 Historical Groundwater Monitoring 14
2.3 Site Groundwater Monitoring System 15
2.4 Homestake Mill Site 15
2.5 Regional Groundwater Monitoring 21
3.0 Geology 23
3.1 Geologic Mapping 23
3.2 Structure 24
3.2.1 Regional Structure 24
3.2.2 Site Structure 27
3.3 Stratigraphy 37
3.3.1 Precambrian Rocks 37
3.3.2 Permian Rocks 37
3.3.2.1 Abo Formation 37
3.3.2.2 Yeso Formation 38
3.3.2.3 Glorieta Sandstone 38
3.3.2.4 San Andres Limestone 38
3.3.3 Triassic Rocks 40
3.3.3.1 Moenkopi Formation 40
3.3.3.2 Chinle Formation 41
3.3.4 Neogene Volcanic Rocks 42
3.3.4.1 El Calderon Flow 42
3.3.4.2 Bluewater Basalt 42
3.3.4.3 Zuni Canyon Flow 43
3.3.5 Quaternary Deposits 43
3.3.5.1 Ancestral Rio San Jose Alluvium 43
3.3.5.2 Surficial Alluvium 44
4.0 Regional Hydrology 45
4.1 Surface Water 45
4.2 Hydrogeologic Units 46
4.2.1 Quaternary Alluvium 46
4.2.2 Basalts 48
4.2.3 Chinle Formation 48
4.2.4 San Andres Aquifer 49
4.2.5 Yeso Formation 52

4.2.6 Abo Formation 52
4.2.7 Precambrian Rocks 53
4.3 Regional Groundwater Flow System 53
4.3.1 Recharge and Discharge 53
4.3.1.1 Alluvial Aquifer 53
4.3.1.2 San Andres Aquifer 54
4.3.2 Information Sources Relevant to Groundwater Flow 55
4.3.3 Potentiometric Surfaces 56
4.3.3.1 Flow Patterns in the San Andres Aquifer 66
4.3.3.2 Average Linear Velocities 66
4.3.4 Influence of Faults 78
4.3.5 Regional Hydrographs 79
5.0 Regional Water Chemistry 85
5.1 Surface Water 85
5.2 Hydrogeologic Units 95
5.2.1 Quaternary Alluvium 95
5.2.2 Basalts 97
5.2.3 Chinle Formation 98
5.2.4 San Andres Aquifer 98
5.3 Background Uranium Concentration 99
6.0 Disposal Cell Performance 101
6.1 Tailings Disposal History 101
6.2 Main Tailings Impoundment Seepage 102
6.3 Disposal Cell Performance 107
6.3.1 Cell Cover Design and Construction 107
6.3.2 Existing Conditions of the Cell Cover 108
6.3.3 Cell Cover Evolution 111
6.3.4 Cell Cover Hydraulic Performance 111
6.4 Disposal Cell Seepage 112
6.4.1 Conditions for Seepage 112
6.4.2 Seepage Rate 113
6.4.3 Estimated Seepage Quantity 114
6.4.3.1 Water-Balance Equation 114
6.4.3.2 Inflow 114
6.4.3.3 Change in Storage 115
6.4.3.4 Outflow 115
6.4.4 Estimated Seepage Contaminant Mass 116
6.5 Disposal Cell Performance Summary 117
7.0 Site Hydrogeology and Water Chemistry 119
7.1 Local Groundwater Flow System 119
7.1.1 Aquifer Characterization 119
7.1.1.1 Aquifer Hydraulic Properties 119
7.1.1.2 Effects of Pumping Anaconda Production Wells 124
7.1.1.3 Aquifer Flow Conditions 127
7.2 Groundwater Chemistry in the Vicinity of the Bluewater Site 128
7.2.1 General Water Chemistry 128
7.2.1.1 Alluvial Aquifer 130
7.2.1.2 San Andres Aquifer 132

7.2.2 Uranium Mobility in Site Groundwater 133
7.2.2.1 Uranium Adsorption 134
7.2.2.2 Mineral Saturation 136
7.2.2.3 Oxidation-Reduction Analysis 137
7.2.3 Uranium Isotopes 138
8.0 Groundwater Contamination and Uranium Transport 149
8.1 Contaminant Source History 149
8.1.1 Main Tailings Impoundment 149
8.1.2 Anaconda Injection Well 149
8.2 Uranium Contamination in the Alluvial Aquifer 150
8.2.1 Uranium Plume Maps 150
8.2.2 Uranium Concentration Histories 154
8.3 Uranium Contamination in the San Andres Aquifer 158
8.3.1 Uranium Plume Maps 158
8.3.2 Uranium Concentration Histories 163
8.3.3 Uranium Concentrations at Municipal Wells 167
8.4 Uranium Transport Processes 169
8.4.1 Advection 169
8.4.2 Dispersion 169
8.4.3 Plume Stability 171
8.4.4 Merged Plumes 173
8.4.5 Geochemical Reactions 174
8.4.6 Uranium Adsorption 174
8.4.7 Dual-Domain Effects 174
8.5 Projected Fate of Uranium Contamination 175
8.6 Potential Effects of Increasing Regional Groundwater Levels 175
8.7 Potential for Source Removal 175
9.0 Groundwater Conceptual Model 177
9.1 Sources of Groundwater Contamination 177
9.2 Geological Features that Affect Groundwater Flow 177
9.3 Groundwater Sources and Flow 178
9.3.1 Alluvial Aquifer 178
9.3.2 San Andres Aquifer 179
9.4 Ambient Chemistry of Water Resources 181
9.4.1 Surface Water 181
9.4.2 Alluvial Aquifer 181
9.4.3 San Andres Aquifer 182
9.5 Performance of the Bluewater Disposal Cell 182
9.6 Mechanisms for Mobilization of Uranium and Other Constituents 184
9.7 Migration and Distribution of Uranium Contamination 184
9.7.1 Alluvial Aquifer 184
9.7.2 San Andres Aquifer 185
9.8 Physicochemical Phenomena that Influence Contaminant Transport 186
9.9 Fate of Uranium 188
9.10 Potential Risk to Downgradient Groundwater Users 188
9.11 Summary of Groundwater Conceptual Model 189
10.0 Uncertainties 191
11.0 References 197

Figures

Figure 1. Regional Location Map ... 1
Figure 2. Location Map for the Bluewater Disposal Site ... 4
Figure 3. Conceptual Model Study Area ... 9
Figure 4. Bluewater Site and Surrounding Area ... 12
Figure 5. Private Offsite Wells Monitored by DOE ... 19
Figure 6. Grants Reclamation Project at the Homestake Site ... 20
Figure 7. Geologic Features of the Study Area ... 25
Figure 8. Geologic Features of the Bluewater Site ... 26
Figure 9. Study Area Geologic Cross Sections A-A′ and B-B′ ... 29
Figure 10. Site Geologic Cross Sections A-A′, B-B′, and C-C′ ... 30
Figure 11. Site Geologic Cross Sections D-D′, E-E′, and F-F′ ... 31
Figure 12. Block Diagram of Site Geologic Cross Section A-A′ ... 32
Figure 13. Block Diagram of Site Geologic Cross Section B-B′ ... 33
Figure 14. Block Diagram of Site Geologic Cross Section F-F′ ... 34
Figure 15. Perspective Block Diagram of Geologic Cross Sections C-C′ and E-E′ ... 35
Figure 16. Monitoring Wells in the Study Area, Map 1 of 4 ... 57
Figure 17. Monitoring Wells in the Study Area, Map 2 of 4 ... 58
Figure 18. Monitoring Wells in the Study Area, Map 3 of 4 ... 59
Figure 19. Monitoring Wells in the Study Area, Map 4 of 4 ... 60
Figure 20. Hydraulic Heads in the Alluvial Aquifer in 1980 ... 61
Figure 21. Hydraulic Heads in the Alluvial Aquifer in 2012 ... 62
Figure 22. Hydraulic Heads and Flow Directions in the Alluvial Aquifer in 2012 ... 63
Figure 23. Potentiometric Surface in the San Andres Aquifer in 1980 ... 67
Figure 24. Potentiometric Surface in the San Andres Aquifer in 2012 ... 68
Figure 25. Ambient Flow Directions in the San Andres Aquifer ... 69
Figure 26. USGS Monitoring Wells in the Study Area ... 80
Figure 27. Hydrographs for USGS Wells Screened in the San Andres Aquifer in the Bluewater Area ... 81
Figure 28. Hydrographs for USGS Wells Screened in the San Andres Aquifer in the Mid-Valley Area ... 81
Figure 29. Hydrographs for USGS Wells Screened in the San Andres Aquifer in the South Valley Area ... 82
Figure 30. Hydrographs for USGS Wells Screened in the San Andres Aquifer near the Homestake Site ... 82
Figure 31. Hydrographs for USGS Wells Screened in the Alluvial Aquifer and the Bluewater Basalt ... 83
Figure 32. Background Sample Locations ... 87
Figure 33. Piper Diagrams for (a) Surface Water and (b) Basalt Background Samples ... 94
Figure 34. Piper Diagrams for (a) Quaternary Alluvium and (b) San Andres Aquifer Background Samples ... 96
Figure 35. Saturation Indexes for Calcite and Gypsum in Background Samples ... 97
Figure 36. Site Marker near the Southwest Corner of the Main Tailings Disposal Cell ... 101
Figure 37. Approximate Distribution of Materials Within the Main Tailings Impoundment ... 103
Figure 38. Schematic of the Tailings Impoundment Water Cycle ... 105
Figure 39. Estimated Cumulative Seepage from the Main Tailings Impoundment Through 1995 ... 106

Figure 40. Ponds in Depressions on the Main Tailings Disposal Cell in August 2012, Following a Summer Storm Event 109
Figure 41. Radon Measurement Location RF-05 in the Area of Cell Cover Depressions 110
Figure 42. Potentiometric Surface in the San Andres Aquifer in August 1978 125
Figure 43. Locations of Bluewater Site Wells Sampled in May 2013 129
Figure 44. Piper Diagrams for Onsite Groundwater Samples: (a) Alluvial Aquifer and (b) San Andres Aquifer 131
Figure 45. Saturation Indexes for Calcite and Gypsum in Onsite Alluvial Aquifer and San Andres Aquifer Samples 132
Figure 46. Variation in Uranium Concentrations (µg/L) in Equilibrium with 1 g/L of Hydrous Ferric Oxide and Variable pH and Varying Dissolved Inorganic Carbon Concentrations. Black and White dots Represent Background and Onsite Bluewater Groundwater Compositions, Respectively 135
Figure 47. pH-pE Diagram of the U-CO_2 System 139
Figure 48. pH-pE Diagram of the Iron System 140
Figure 49. Uranium Isotope Activity Ratios (ARs) for Alluvial Aquifer Wells at the Bluewater Site and in Surrounding Areas 145
Figure 50. Uranium Isotope Activity Ratios (ARs) for San Andres Aquifer Wells at the Bluewater Site and in Surrounding Areas 146
Figure 51. Regional Uranium Concentrations in the Alluvial Aquifer in 1980–1981 151
Figure 52. Regional Uranium Concentrations in the Alluvial Aquifer in 1996–1997 155
Figure 53. Regional Uranium Concentrations in the Alluvial Aquifer in 2012–2013 156
Figure 54. Temporal Plot of Uranium Concentrations in Alluvial Aquifer Wells at the Bluewater Site 157
Figure 55. Regional Uranium Concentrations in the San Andres Aquifer in 1980–1981 159
Figure 56. Regional Uranium Concentrations in the San Andres Aquifer in 1996–1997 160
Figure 57. Regional Uranium Concentrations in the San Andres Aquifer in 2008 161
Figure 58. Regional Uranium Concentrations in the San Andres Aquifer for the Period 2008–2013 162
Figure 59. Temporal Plot of Uranium Concentrations in San Andres Aquifer Wells at the Bluewater Site 165
Figure 60. Temporal Plot of Uranium Concentrations in San Andres Aquifer Wells near the Homestake Site 166
Figure 61. Uranium Concentration Data for Municipal Wells in the Grants-Bluewater Valley 168
Figure 62. Graphical Depiction of Contaminant Plume Evolution—Concentration Profiles Along the Plume Centerline at Successive Times t_1 Through t_6 173
Figure 63. Current Estimated Uranium Plume in the San Andres Aquifer 187
Figure 64. Stylized Cross Section of San Andres Aquifer Uranium Contamination and Risk 190

Tables

Table 1. Monitoring Wells at the Bluewater Site in 1997 15
Table 2. Construction Information for Wells Monitored at the Bluewater Site 17
Table 3. Estimated Ranges for Average Linear Velocity in Regional Aquifers Based on Previous Studies 70
Table 4. Average Linear Velocity Calculations for the Alluvial Aquifer 73
Table 5. Average Linear Velocity Calculations for the San Andres Aquifer 74
Table 6. Field Parameters 88
Table 7. Major Ion Concentrations (mg/L) 91
Table 8. Estimated Saturated Hydraulic Conductivities for the Bluewater Disposal Cell 113
Table 9. Footprint of Tailings Materials 115
Table 10. Potential Annual Outflow if the Tailings Become Saturated 116
Table 11. Estimated Seeped Contaminant Mass Prior to Disposal Cell Completion 117
Table 12. Hydraulic Properties for the Alluvial and San Andres Aquifers Derived from Aquifer Tests 120
Table 13. Uranium Mineral Saturation Indexes for Groundwater Samples from Six Bluewater Site Wells That Had the Highest Uranium Concentrations in May 2013 137
Table 14. Data from DOE Environmental Database for Samples with Reported Concentrations of Dissolved Iron and Redox Parameters 141
Table 15. $^{234}U/^{238}U$ Activity Ratios (ARs) in Groundwater Samples Collected from Alluvial Aquifer Wells at the Bluewater Site and Surrounding Areas 142
Table 16. $^{234}U/^{238}U$ Activity Ratios (ARs) in Groundwater Samples Collected from San Andres Aquifer Wells at the Bluewater Site and Surrounding Areas 143
Table 17. Uncertainties and Their Effects on Study Conclusions 192

Appendixes

Appendix A Water-Balance Assessment for the Bluewater Main Tailings Impoundment and Disposal Cell, Bluewater, New Mexico
Appendix B Well Information
Appendix C Water Level and Water Chemistry Data
Appendix D Information Sources
Appendix E Glossary
Appendix F Processes Affecting Contaminant Plumes

Plates

Plate 1 Conceptual Model Study Area
Plate 2 Geologic Map of the Study Area
Plate 3 Geologic Map of the Bluewater Site
Plate 4 Study Area Geologic Cross Sections A-A′ and B-B′
Plate 5 Site Geologic Cross Sections A-A′, B-B′, and C-C′
Plate 6 Site Geologic Cross Sections D-D′, E-E′, and F-F′
Plate 7 Well Locations

Abbreviations

ACLs	alternate concentration limits
amsl	above mean sea level
Anaconda	Anaconda Copper Company
AR	uranium activity ratio
ARCO	Atlantic Richfield Company
bgs	below ground surface
cfs	cubic feet per second
cm/s	centimeters per second
DO	dissolved oxygen
DOE	U.S. Department of Energy
EPA	U.S. Environmental Protection Agency
ft	foot or feet
ft^2	square feet
ft^3	cubic feet
ft/day	feet per day
ft^2/day	square feet per day
ft/yr	feet per year
gpm	gallons per minute
GRP	Grants Reclamation Project
HMC	Homestake Mining Company
Ks	saturated hydraulic conductivity
LiDAR	light detection and ranging
LTSP	Long-Term Surveillance Plan
MCL	maximum concentration limit
µg/L	micrograms per liter
µS/cm	microsiemens per centimeter
mi	mile or miles
mg/L	milligrams per liter
NMED	New Mexico Environment Department
NRC	U.S. Nuclear Regulatory Commission
pCi/L	picocuries per liter
pCi/m^2s	picocuries per square meter per second

redox	oxidation-reduction
SRNL	Savanah River National Laboratory
TDS	total dissolved solids
U-234	uranium-234
U-238	uranium-238
UMTRCA	Uranium Mill Tailings Radiation Control Act
USGS	U.S. Geological Survey

Executive Summary

This site status report presents an assessment of the groundwater systems impacted by the Bluewater, New Mexico, Disposal Site (Bluewater site; the site), a former uranium milling facility in Cibola County, New Mexico. The Anaconda Copper Company (Anaconda) and Atlantic Richfield Company (ARCO) processed uranium ore at the site from 1953 to 1982. Onsite areas impacted by the mill were reclaimed in following years, and the site was transferred to the U.S. Department of Energy (DOE) in 1997 for long-term surveillance and maintenance.

The DOE Office of Legacy Management manages the facility and is responsible for monitoring groundwater quality at the site. Monitoring results indicate that the upper two aquifers at the site are contaminated with mill-related constituents and that groundwater containing elevated concentrations of uranium is migrating beyond the site boundary. This is a serious concern because water is withdrawn from these aquifers downgradient of the site for drinking water, irrigation of agricultural land, and various industrial uses.

The primary objective of this study was to develop a groundwater conceptual model that describes the aquifers associated with the Bluewater site and the potential exposure of downgradient groundwater users to mill-related contamination. A study area encompassing approximately 195 square miles incorporates the contaminant source areas, the hydrologic and hydrogeologic features that most directly influence groundwater flow and contaminant transport in the Grants-Bluewater Valley, and the points of use, particularly the downgradient communities of Milan and Grants.

This study has found that numerous hydrogeologic processes affect contaminant transport in the region. The complex nature of these processes and the limited data to fully characterize them makes it challenging to accurately delineate the extent of subsurface milling-related contamination at the Bluewater site. This report includes a summary of uncertainties that impact the understanding of contaminant migration and fate in the region, and their significance regarding the conclusions drawn for the conceptual model. Despite the uncertainties, certain conclusions, including those summarized below, can be drawn from the evaluation of existing data. These conclusions are organized into the following three topics: sources of contamination, groundwater flow and transport, and potential risks to groundwater users.

Sources of Contamination

- The Anaconda/ARCO Bluewater uranium milling operations contaminated the aquifer in the ancestral Rio San Jose alluvial system and also contaminated the deeper bedrock San Andres aquifer in the San Andres Limestone and Glorieta Sandstone formations. Seepage of tailings fluid from the mill's tailings impoundments not only entered the two aquifers but apparently created a mineralized zone in the geologic strata (basalt, alluvium, limestone, and sandstone) and fault zones under the impoundments.
- Several billion gallons of tailings fluid (leachate) seeped through the bottom of the Bluewater main tailings impoundment and into the underlying aquifers prior to construction of the disposal cell cover in 1995. Estimated hydraulic properties of the cell cover and the tailings materials suggest that tailings fluids may continue to seep from the disposal cell indefinitely. However, the volume of fluid and mass of contaminants seeping from the cell

since it was constructed are very small compared to the volume and mass that seeped through the bottom of the tailings impoundment during milling operations.

- Uranium is mobilized in the alluvial and San Andres aquifers primarily by release of solid-phase uranium in the mineralized zone beneath the Bluewater site's main tailings disposal cell to groundwater flowing beneath the cell.
- The uranium release mechanisms in the subsurface at the site constitute a continuous contaminant source that produces uranium concentrations in onsite monitoring wells that are effectively constant or decreasing very slowly. It is assumed that this contaminant source will remain indefinitely.
- Operations at the Homestake uranium mill, located several miles southeast of the Bluewater site, contaminated the San Mateo Creek alluvial aquifer underlying the Homestake tailings piles. This is the primary source of contaminated alluvial groundwater in the vicinity of Milan.

Groundwater Flow and Transport

- Groundwater in the Rio San Jose alluvium flows southeast from the Bluewater site and merges with San Mateo Creek alluvial groundwater. The combined flow, which contains contaminants from both the Bluewater and Homestake sites, continues southeast toward Milan.
- Flow paths for the groundwater migrating from the Bluewater site in the San Andres aquifer are in the east-southeast direction from the site and, consequently, do not intersect municipal wells for the communities of Bluewater and Milan. Groundwater flow paths from the site appear to head toward areas north of Grants.
- The geology of the San Andres Limestone and Glorieta Sandstone provides an environment for a highly productive aquifer. Wells completed in karst features in the upper portion of the San Andres Limestone have high production rates with minimal drawdown. Fault, fracture, and solution channel and cavity features within both formations enhance the productivity of the aquifer and serve as conduits for high groundwater flow rates. Groundwater flows at much lower rates through the unfractured sandstone units within the aquifer.
- Groundwater flowing beneath and downgradient of the site in both the alluvial and San Andres aquifers is in an oxidized state. Consequently, dissolved uranium migrates with the groundwater flow instead of precipitating out of solution. Groundwater flow paths and uranium transport are correlated.
- Uranium concentrations in both aquifers decrease in transport distance from the Bluewater site, indicating that natural contaminant attenuation processes are active in the aquifers.
- The volume of flow and contaminant mass contributed by San Mateo Creek alluvial groundwater to the Milan area appear to be much greater than those contributed by Rio San Jose alluvial groundwater. The actual proportion of Bluewater-derived uranium in the alluvial aquifer downgradient from where flows from the respective sources merge is unknown.
- Evaluation of historical and current uranium concentrations in groundwater suggests that the uranium plume in the alluvial aquifer is shrinking, primarily due to remediation at the Homestake site. The uranium plume in the San Andres aquifer has been stable since the

early 1980s, such that uranium concentrations above the regional background concentration are essentially constant.

Potential Risk to Groundwater Users

- DOE sampled several private wells near the Bluewater site, completed in the alluvial and San Andres aquifers, in 2012 and 2013. The closest alluvial well to the site, although not used for drinking water, has uranium concentrations well below the drinking water standard. A groundwater sample from the closest San Andres aquifer well, which is not permitted or used for drinking water, had a uranium concentration higher than the drinking water standard. None of the private drinking water supply wells that DOE sampled in the vicinity of the Bluewater site have uranium concentrations exceeding the drinking water standard.
- Available groundwater data suggest that Bluewater-derived contamination does not adversely affect any private wells used for drinking water. However, not all of the well owners near the site allowed DOE to sample their wells. Although the unsampled wells do not appear to be within the groundwater flow paths emanating from the Bluewater site, it cannot be stated with certainty that groundwater in all private drinking water wells in the vicinity of the Bluewater site have uranium concentrations below the drinking water standard.
- The municipal water supply wells for Bluewater, Milan, and Grants pump water from the San Andres aquifer. Reported concentrations of dissolved uranium for those wells have all been less than the New Mexico drinking water standard and do not show an upward trend in uranium concentrations.
- Collectively, the direction of groundwater flow in the San Andres aquifer, the apparent stability of the uranium plume in the aquifer, and the locations of municipal supply wells indicate that Bluewater site–derived uranium contamination does not pose a current or future risk for community water systems in the Grants-Bluewater Valley.

Conclusions drawn from this conceptual model can only be confirmed through continued groundwater monitoring and evaluation of groundwater data. Existing and future activities involving Bluewater site–related contamination must continue to focus on protection of public health and the environment. This conceptual model is considered to be an important tool for use by DOE and other public entities to accomplish this goal.

This page intentionally left blank

1.0 Introduction and Objectives

1.1 Introduction

The Bluewater, New Mexico, Disposal Site (the Bluewater site; the site) is a former uranium milling facility in Cibola County in the northwest region of New Mexico (Figure 1). The Anaconda Copper Company (Anaconda) and Atlantic Richfield Company (ARCO) processed uranium ore at the site from 1953 to 1982. Milling operations contaminated the upper two aquifers at the Bluewater site. The U.S. Department of Energy (DOE) Office of Legacy Management (LM) currently manages the site and its responsibilities include monitoring the contaminated aquifers.

Figure 1. Regional Location Map

Groundwater in the region is used for several purposes. Alluvial groundwater is used primarily as drinking and livestock water by residences that are not connected to municipal water supply systems. The primary water supply source in the region is a bedrock aquifer, which is used by the communities of Bluewater, Milan, and Grants and is used for local industrial and agricultural purposes.

Because of the importance of groundwater in the region, DOE is evaluating impacts to human health and the environment from groundwater contamination associated with the mill operations. To help meet this objective, this report includes a conceptual model of contaminant transport processes in the aquifers impacted by the Bluewater site.

1.2 Groundwater Issues

Processing of uranium ore at the Bluewater mill produced radioactive tailings, which were stored onsite at two locations referred to as the carbonate tailings pile and the main tailings impoundment. As early as the late 1950s, the tailings had been identified as sources of contamination for two aquifers beneath the mill property. Some of the contamination impacted an alluvial aquifer that occurs in river sediments of the ancestral Rio San Jose that were covered by a succession of basalt lava flows. Significant contamination was detected in two bedrock formations at the site—the San Andres Limestone and the Glorieta Sandstone. These formations together act as a single, prolific regional source of groundwater referred to in this report as the San Andres aquifer. As discussed in Chapter 6, Anaconda and ARCO took multiple steps to reduce the capacity of the main tailings impoundment to be a source of contamination in the alluvial and San Andres aquifers.

During early milling operations, nitrate was identified as a site-related contaminant that impacted the alluvial and San Andres aquifers. In following years, the metals molybdenum, selenium, and uranium became the main constituents of concern stemming from the leaching of tailings. Additionally, studies of the Bluewater site in the late 1970s and early 1980s suggested that locally elevated concentrations of dissolved chloride and sulfate indicated mill-related contamination.

Accordingly, water chemistry parameters reflective of total salinity, such as total dissolved solids (TDS) concentration, have been used to help delineate the spatial extent of conservative (i.e., nonretarded) constituents in groundwater. Measured concentrations of chloride, sulfate, and TDS in the regional groundwater are generally not high enough to be significant threats to human health and the environment. In contrast, uranium is a contaminant that potentially poses a risk to drinking water users, and it is mobile and widespread in regional groundwater. For this reason, much of this study focuses on the assessment of uranium concentrations in the alluvial and San Andres aquifers and on physicochemical processes that affect subsurface uranium transport.

Dissolved uranium in the alluvial and San Andres aquifers is of particular interest in this assessment because of another significant source of uranium contamination in the Grants-Bluewater Valley. The Homestake site, a former uranium mill, is about 3.5 miles (mi) east-southeast of the Bluewater site. Homestake Mining Company (HMC) owns the facility, which processed ore from 1958 to 1990. Today the Homestake property and surrounding areas are also referred to as the Grants Reclamation Project (GRP), as the company's focus is on site reclamation and remediation of the underlying alluvial aquifer. The alluvial aquifer at the

Homestake site has been contaminated by HMC mill operations and by former uranium mining and milling operations in upgradient parts of the San Mateo Creek drainage basin. Groundwater in this alluvial aquifer not only flows southwest from the Homestake site toward Milan, but also to the west, where it merges with Rio San Jose alluvial groundwater coming from the Bluewater site.

In addition to uranium, much of the contamination in the San Mateo Creek alluvium at the Homestake site consists of dissolved selenium. According to HMC, none of the contamination generated by the milling has migrated as deep as the San Andres aquifer beneath the facility, primarily because a thick section of the low-permeability Chinle Formation acts locally as an effective aquitard between the alluvial and San Andres aquifers. Extensive subsurface remediation operations at the Homestake site complicate flow and transport processes in a groundwater system that is complex even under natural flow conditions.

Milan and Grants are hydraulically downgradient of the Bluewater and Homestake sites (Figure 2). The two municipalities withdraw groundwater from the San Andres aquifer for drinking water using multiple pumping wells located from about 2.5 to 7 mi from the Bluewater site. Given their respective locations relative to the former mill sites, both Milan and Grants monitor dissolved uranium in their municipal wells to verify that levels remain below the State of New Mexico maximum concentration limit (MCL) for the constituent, which is 0.03 milligram per liter (mg/L). Publicly available water chemistry data for all of the Milan and Grants municipal wells indicate that uranium concentrations are below the MCL. This observation also holds true for a single community well tapping the San Andres aquifer that is used to supply drinking water to the Village of Bluewater, about 1.5 mi west-southwest of the Bluewater site.

1.3 Objectives

The primary objective of this study is to develop a groundwater conceptual model that describes the extent of contamination associated with the Bluewater site and the potential risk to downgradient groundwater users. Developing the model of the groundwater system requires an understanding of milling history, site and regional geology, site and regional hydrogeology and groundwater chemistry, disposal cell performance, and groundwater contamination and uranium transport.

The scope of work necessary to develop the conceptual model includes addressing the following specific objectives.

- Identify the sources of groundwater contamination at the site and within the study area, addressing the contributions of contaminants from the Bluewater and Homestake mill sites.
- Describe the geology of the study area, identifying geologic features that affect the groundwater systems.
- Evaluate site and regional hydrology and hydrogeology to determine the sources of groundwater and how groundwater flows through the study area.
- Describe the ambient chemistry of water resources in the study area, including the water quality of surface water resources and chemistry of groundwater in the alluvial and San Andres aquifers and the interlying Chinle Formation.

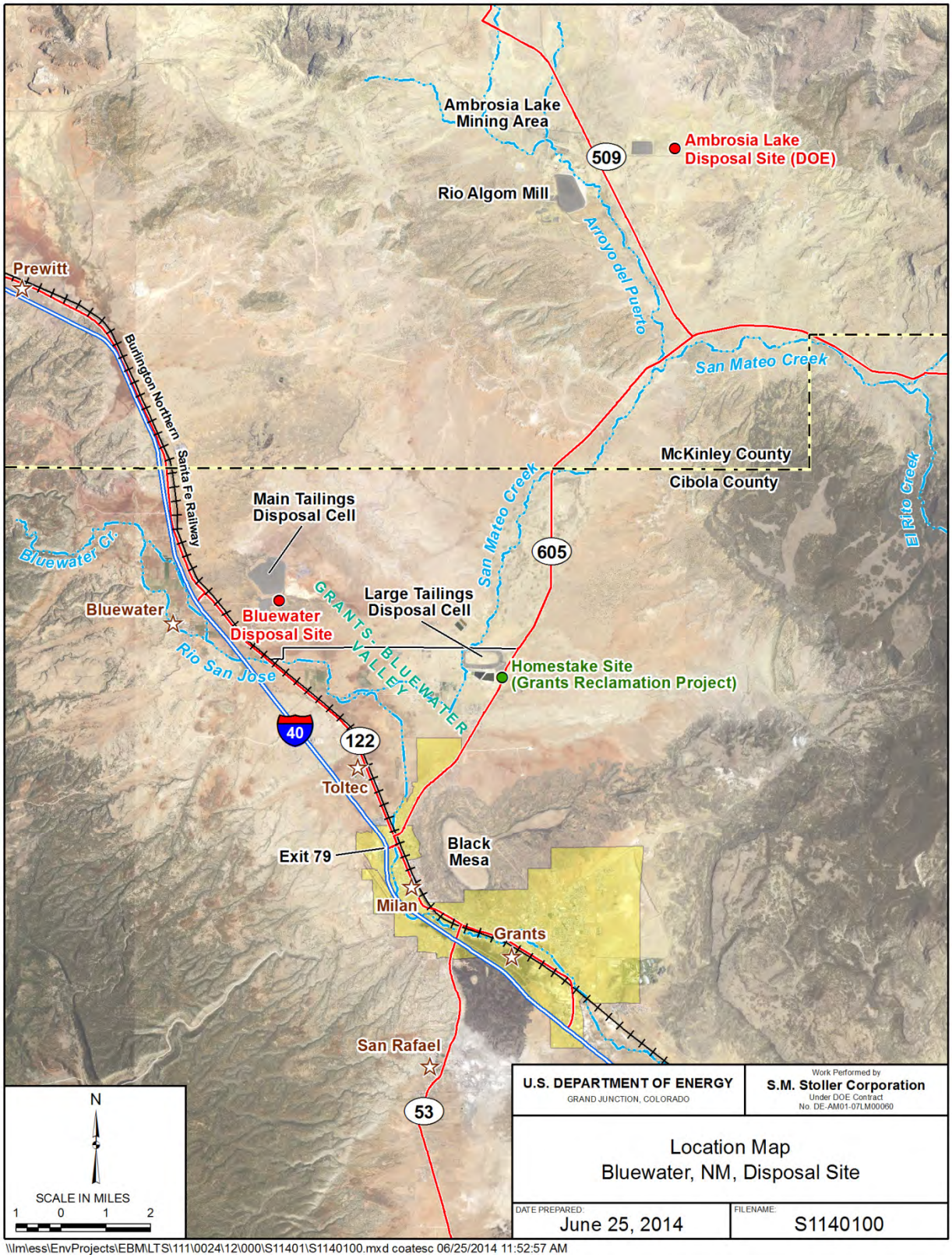

Figure 2. Location Map for the Bluewater Disposal Site

- Evaluate the performance of the main tailings disposal cell to determine if it is a continuing source of contamination to the local aquifers.
- Describe the most likely mechanisms for mobilizing uranium and other dissolved constituents in the aquifers.
- Describe the history of uranium contamination originating at the Bluewater site and its spatial distribution within the site and the region.
- Develop a comprehensive assessment of physicochemical phenomena that likely influence contaminant transport in the regional and site groundwater systems.
- Assess the potential fate of uranium and other contaminants in the study area.
- Evaluate the potential risk of site-related contamination impacting regional groundwater users, particularly the municipal water supplies for Bluewater, Milan, and Grants.
- Describe uncertainties associated with components of the conceptual model and how they affect the model's conclusions.

Geologic reports, groundwater investigations conducted at both site and regional scales, and data collected by DOE were used to develop the conceptual model. Appendix D presents summaries of reports from previous studies pertinent to development of the conceptual model.

This page intentionally left blank

2.0 Study Area

The Bluewater site is in Cibola County, about 9 mi northwest of Grants, the county seat. The Grants-Bluewater Valley, which contains the site and the communities of Bluewater, Milan, and Grants, lies within the Acoma-Zuni section of the southeast part of the Colorado Plateau physiographic province. The climate of this part of New Mexico is semiarid to arid, with a mean annual precipitation at Grants of about 10 inches. Precipitation generally increases with altitude in the region.

A transportation corridor comprising Interstate 40, State Highway 122, and the Burlington Northern Santa Fe Railway traverses the region in a southeast-northwest direction (Figure 2). State Highway 605, starting at Milan, is in the San Mateo Creek valley and passes by the Homestake site. From its intersection with Interstate 40 on the northwest end of Grants, State Highway 53 heads south toward San Rafael (Figure 2).

2.1 Study Area Description

Given the relatively high mobility of contaminants like uranium, the regional presence of community water systems dependent on groundwater in the San Andres aquifer, and the presence of another contaminant source due to milling, DOE has developed a conceptual model that accounts for hydrogeologic processes over a much larger geographic area than the Bluewater site itself. In addition to incorporating parts of the regional groundwater flow system hydraulically downgradient of the former Bluewater mill, the model also includes areas upgradient of the site that contribute recharge to, and therefore constitute sources of, groundwater flowing beneath the Bluewater site. The regional approach to assessing flow and transport processes is considered crucial to fully address potential risks to offsite users of groundwater in the alluvial and San Andres aquifers.

The geographic region of the conceptual model is a rectangular area about 13 mi east to west and 15 mi north to south (Figure 3). The north boundary of the study area roughly coincides with the Cibola County border with McKinley County, and the south boundary is about 4 mi south of Grants. The area's west boundary is about 5 mi west of the Bluewater site, and the east boundary captures the Homestake site and the east portion of Grants. With a total area of about 195 square mi, the study area completely covers four townships and a portion of each of five additional townships. Previous geologic mapping and hydrogeologic investigations encompass this study area and were used extensively in the preparation of this report.

Figure 3 and Plate 1 show a topographic map of the study area assembled from U.S. Geological Survey (USGS) quadrangles. Significant topographic features in the study area include Black Mesa, northwest of Grants, and the Zuni Mountains on the southwest side of the Grants-Bluewater Valley. The highest point in the study area (approximately 9,000 feet [ft] above mean sea level [amsl]) is in the Zuni Mountains. The basalt-covered Black Mesa has an elevation of about 7,200 ft amsl. A basalt-covered area (Bluewater Basalt) is also found to the west, south, and southeast of the Bluewater site, within a broad fluvial valley cut by the ancestral Rio San Jose. Major basalt flows (Zuni Canyon Basalt and El Calderon Basalt) are also seen at ground surface in areas south of Grants (Figure 3). The Homestake site is distinguished by the footprint of the large tailings disposal cell.

Principal land uses in the study area include agriculture in the form of irrigated farming and cattle ranches, small business along the Interstate 40 corridor, and industrial land use in Milan and Grants. Residential land use occurs in Milan, Grants, Bluewater, San Rafael, at five subdivisions south of the Homestake site, and at scattered single residences. The economy of the area is based on ranching, alfalfa and hay production, and tourism. Land ownership in the region is varied. In addition to privately owned property, the federal, state, county, and municipal governments own land, and portions of the Grants-Bluewater Valley and the Zuni Mountains contain Native American land.

Bluewater Creek, which emerges from Bluewater Canyon at the foot of the Zuni Mountains and joins with Mitchell Draw in the northwest corner of the study area (Figure 3) to form the present Rio San Jose, is significant because it is the only stream in the area that maintains flow in most years. Under historical natural conditions, the creek was perennial to the mouth of Bluewater Canyon. Since 1927, however, flow in the creek has been regulated where it empties out of Bluewater Lake, which is about 5 mi west of the study area's west boundary. Bluewater Lake and Bluewater Creek are major sources of recharge to groundwater that flows beneath the Bluewater site. A major surface water diversion structure on Bluewater Creek, about 0.5 mi south of the mouth of Bluewater Canyon (Figure 3), routes water to canals delivering irrigation water to land in the Grants-Bluewater Valley.

2.2 Bluewater Site History

Anaconda constructed the uranium mill at the Bluewater site in 1953 and began processing ore the same year. The U.S. Atomic Energy Commission was the first regulator of operations at the Bluewater mill. The State of New Mexico later assumed regulatory authority for the site in accordance with provisions in the Atomic Energy Act of 1954. The U.S. Nuclear Regulatory Commission (NRC) became the site regulator in 1986 after the State relinquished its regulatory responsibilities.

No uranium mining occurred on the Bluewater site or within the study area. The effects that uranium mining and milling activities in the San Mateo Creek basin have had on groundwater hydrology in the study area are addressed in subsequent chapters of this report.

2.2.1 Milling

ARCO purchased Anaconda in 1977, and the Anaconda Bluewater mill became known as the ARCO Bluewater mill in the early 1980s. The site was licensed under provisions of the Uranium Mill Tailings Radiation Control Act of 1978 (UMTRCA). The Bluewater mill was considered an UMTRCA Title II site, which applies to uranium mill sites that were active at the time the act was passed. Title II of the legislation required that, upon completion of remediation at a site, either the federal government or the state in which a mill was located would assume long-term custodial responsibilities.

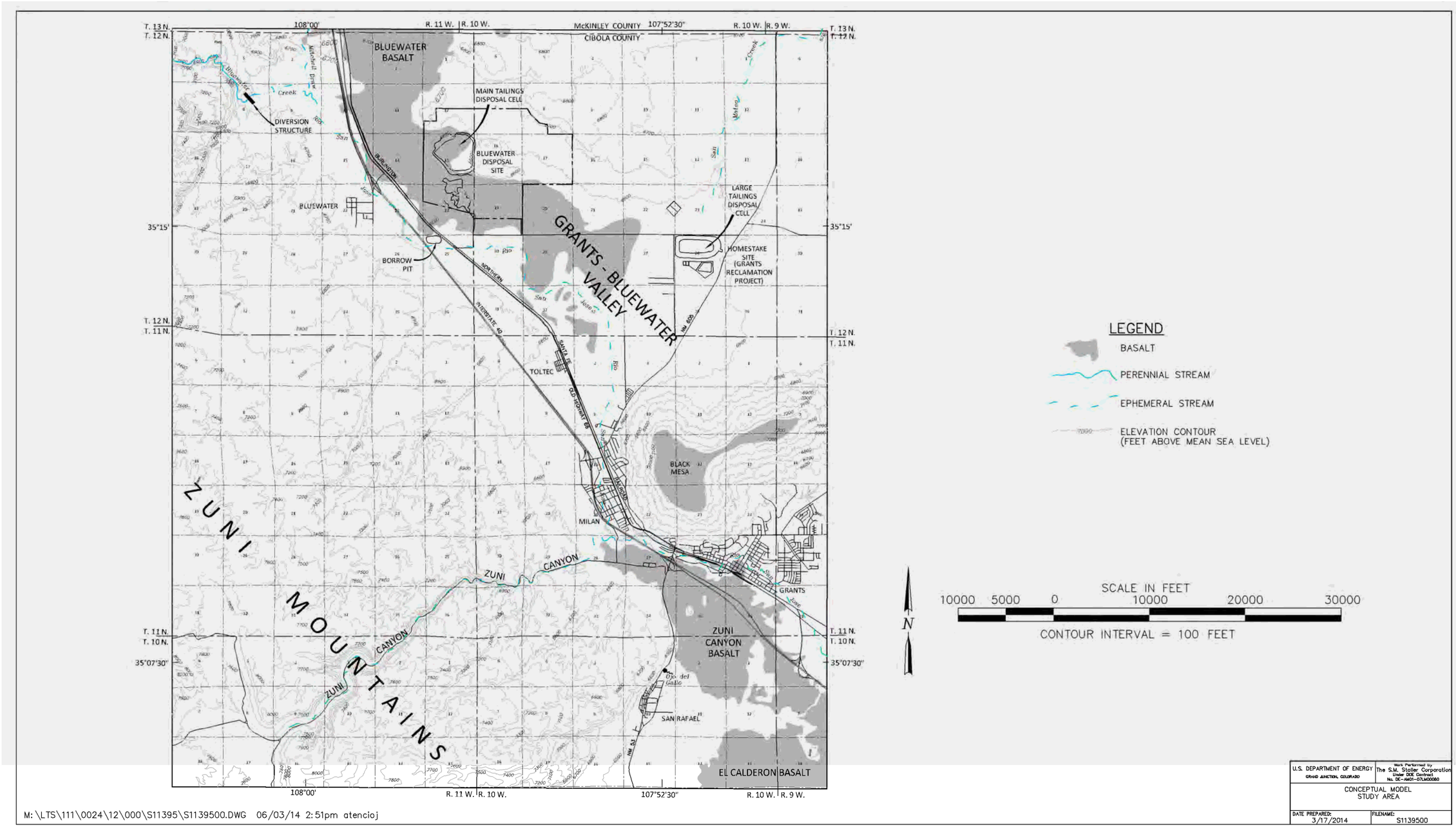

Figure 3. Conceptual Model Study Area

This page intentionally left blank

The Bluewater mill initially used a carbonate-leach process to extract uranium from ore mined from nearby mines in the Todilto Limestone, processing 300 tons of ore per day. Tailings produced from the carbonate process were disposed of in natural depressions in the Bluewater Basalt adjacent to the mill; these tailings were eventually encapsulated within the carbonate tailings cell (Figure 4). An acid-leach process replaced the carbonate-leach process in 1955 after discovery of sandstone uranium ores and development of mines on the Laguna Reservation east of Grants. The ore-processing rate eventually reached 6,000 tons per day.

Tailings from the acid-leach process were placed in a natural basin north of the carbonate tailings that became the main tailings impoundment. Heavier, coarse sand material settled near the south end of the impoundment, and finer materials settled in the north end. Chapter 6 discusses the spatial distribution of tailings materials in the main tailings impoundment. The last year of uranium ore milling at the site was 1982; mill operations to recover uranium from leachate fluids continued for several more years. Upon completion of site reclamation in 1995, the encapsulated tailings piles became known as the carbonate and main tailings disposal cells.

To reduce the amount of tailings fluids seeping from the main tailings impoundment into the underlying aquifers, Anaconda began disposing of fluids in a deep injection well located about a mile northeast of the impoundment (shown as the Anaconda injection well in Figure 4). This well was used between 1960 and 1977. Beginning in 1977, the tailings fluids were pumped to lined evaporation ponds north and northeast of the impoundment (Figure 4). These disposal processes are described further in Chapter 6 and Appendix A.

2.2.2 Site Decommissioning

ARCO submitted a decommissioning plan for the Bluewater mill to NRC in 1987. Upon NRC's approval of the plan in 1989, ARCO began demolition of buildings on the facility as well as residences in an Anaconda housing area south of the mill. The decommissioning process and site reclamation, including stabilizing the two tailings piles in place as engineered disposal cells and remediating the evaporation ponds, was completed in 1995.

During site reclamation activities, the tailings and other contaminated materials were encapsulated in six onsite disposal areas: the main tailings disposal cell (354 acres), the carbonate tailings disposal cell (54 acres), Disposal Area No. 1 (11 acres) containing mill debris, a small cell containing radiologically contaminated polychlorinated biphenyl materials within Disposal Area No. 1, another small cell containing radiologically contaminated asbestos materials, and two small landfills (totaling 2 acres) containing miscellaneous waste and milling byproduct material (ARCO 1996). All of these disposal areas contain potential groundwater contamination sources. Additionally, about 210 acres of undisturbed basalt surfaces containing contaminated windblown materials were not remediated because of the rough surfaces (ARCO 1996, DOE 1997); the affected areas are also potential contamination sources.

Site reclamation included an unsuccessful attempt to remediate the aquifers. ARCO abandoned and plugged the deep injection well in late 1995 in accordance with requirements of the New Mexico Office of the State Engineer and the New Mexico Water Quality Control Commission.

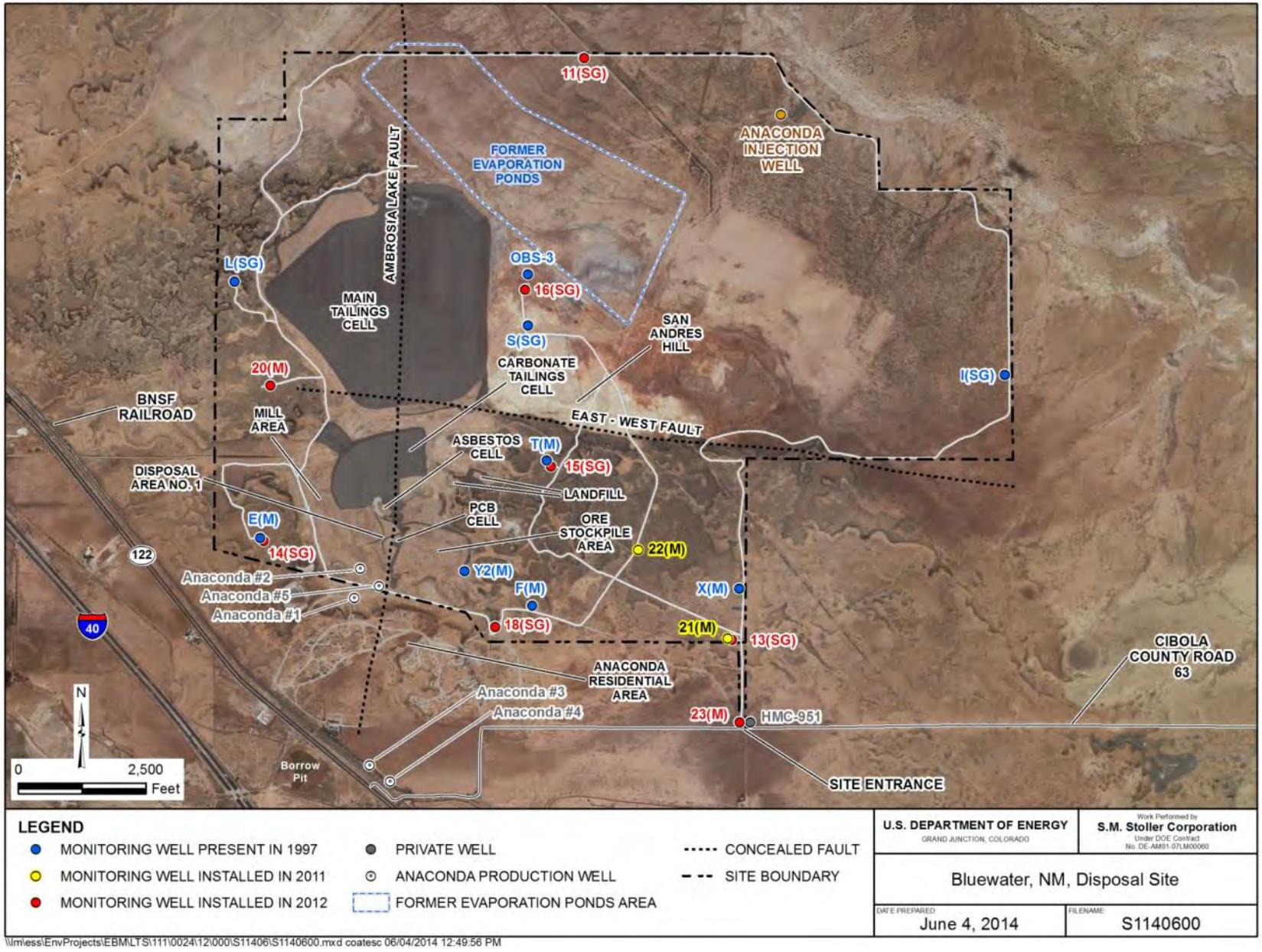

Figure 4. Bluewater Site and Surrounding Area

DOE assumed responsibility for the Bluewater mill site in 1997 after the State of New Mexico declined to take over long-term management duties. DOE manages the site in accordance with an NRC-approved Long-Term Surveillance Plan (LTSP) to ensure protection of human health and the environment. Requirements of the LTSP (DOE 1997) include ensuring that reclaimed features at the facility (disposal cells and landfills) function as designed and that onsite groundwater chemistry meets approved water quality standards.

2.2.3 Historical Site Groundwater Issues

Anaconda became aware as early as the late 1950s that contaminated mill process water from the main tailings impoundment was impacting the alluvial and San Andres aquifers (West 1972). This observation was supported further in consulting reports produced in the late 1970s by Hydro-Search (1977, 1981a), and again in the early- to mid-1980s in reports by Dames & Moore (1986a, 1986b).

Downward seepage of liquids from sandy and clay-rich tailings in the main tailings impoundment to underlying geologic units was considered to be the source of the contamination in the aquifers beneath and near the impoundment. ARCO estimated that approximately 5.7 billion gallons of tailings fluids seeped from the main tailings impoundment prior to encapsulation in 1995, with about 2.7 billion gallons occurring prior to 1960 when deep-well injection began. These seepage estimates are described in greater detail in Chapter 6 and Appendix A.

Contaminated groundwater in the alluvial aquifer resulted from downward seepage from both tailings piles through underlying porous basalt and into the buried sand and gravel deposits of the ancestral Rio San Jose. The contaminated alluvial groundwater was then transported southeastward, mostly within the Rio San Jose paleodeposits.

Downward-seeping contaminants from the main tailings impoundment also entered the San Andres aquifer, particularly where the base of the southeast portion of the impoundment directly contacts the San Andres Limestone. Additionally, some of the contamination in the San Andres aquifer was caused by tailings liquids that first migrated through a thin layer of basalt in direct contact with the tailings, and then to limestone and sandstone in the bedrock. It is also possible that some tailings leachate feeding ancestral Rio San Jose alluvium south of the impoundment subsequently migrated northeastward into the San Andres aquifer east of the main tailings impoundment.

The role that faults in the vicinity of the tailings played in affecting groundwater flow and contaminant transport during and shortly after milling years was not fully understood at the time. A north-striking fault (Ambrosia Lake Fault), which bisects the bedrock formations under the main tailings impoundment, is known to intersect an east-striking fault (East-West Fault) under the south side of the main tailings impoundment. Though both features may represent partial barriers to San Andres aquifer groundwater flow, each also likely acts as a conduit, helping to convey groundwater vertically from alluvium to the San Andres aquifer as well as horizontally along the fault zone.

During the milling period, some contamination was detected in the San Andres aquifer as far as 0.75 mi directly south of the main tailings impoundment (i.e., south of the East-West Fault). In particular, uranium and nitrate concentrations above background levels were detected in Anaconda #2 water-supply well used by Anaconda for milling. Anaconda pumped this well and

other San Andres aquifer production wells south of the mill (Anaconda #1, #3, #4, and #5 shown in Figure 4), creating a cone of depression that had the potential to induce southward flow of groundwater in the San Andres aquifer. It appears likely that the Ambrosia Lake Fault provided a conduit for the southward transport of contaminants from seepage from the main tailings impoundment. However, ARCO did not consider contamination in the San Andres aquifer south of the East-West Fault to be of concern because a downgradient private well (Sabre-Piñon well, currently known as HMC-951) had background uranium concentrations. ARCO assumed that incoming fresh groundwater was diluting the contaminants to acceptable concentrations.

In 1989, ARCO began pumping groundwater from the alluvial and San Andres aquifers using wells located around the perimeter of the main tailings impoundment as part of an effort to reduce local contaminant concentrations to background levels. This attempt at remediation proved unsuccessful, as no reductions in constituent concentrations were observed. As a consequence, ARCO recommended establishing alternate concentration limits (ACLs) for the two aquifers (Applied Hydrology Associates Inc. 1990, 1995). Subsequently, NRC approved ACLs for uranium of 0.44 mg/L and 2.15 mg/L for point-of-compliance wells in the alluvial aquifer and San Andres aquifer, respectively. These approved levels were significantly below the New Mexico drinking water standard for uranium at the time, which was 5 mg/L. In 2004, New Mexico adopted the U.S. Environmental Protection Agency (EPA) drinking water MCL for uranium of 0.03 mg/L for groundwater. Consequently, the current MCL for uranium is significantly below the former MCL, which ARCO was required to meet, and substantially below the approved ACLs.

Assessments made by ARCO in the 1990s indicated that the highest uranium concentrations at the site would be observed in the San Andres aquifer north of the East-West Fault, and that uranium concentrations would continue to meet health-based requirements (<5 mg/L) beyond the site's east boundary. Sample data from recent years at wells along the east boundary indicate that ARCO's expectations are being met but that groundwater leaving the site exceeds the current uranium MCL.

2.2.4 Historical Groundwater Monitoring

Anaconda and ARCO monitored an extensive network of onsite and private offsite wells. ARCO decommissioned many of the onsite wells prior to transferring the site to DOE. Consequently, DOE inherited only nine of the ARCO onsite monitoring wells (Table 1), which were considered to be sufficient by ARCO and NRC to ensure regulatory compliance in the alluvial and San Andres aquifers. The LTSP (DOE 1997) lists these nine wells and associated monitoring requirements. Since 1997, groundwater quality issues have led DOE to install an additional 10 wells at the site. DOE continues to monitor all of the wells for the purpose of protecting human health and the environment. Although the water quality monitoring accounts for multiple contaminants, uranium is the sole constituent that exceeds regulatory standards at onsite wells. Uranium concentrations exceed the ACL in one alluvial well and exceed the MCL in both aquifers in several wells located in the east and south portions of the site.

Table 1. Monitoring Wells at the Bluewater Site in 1997

Well	Aquifer	Purpose of Well
E(M)	Alluvial	Background
F(M)	Alluvial	Point of Compliance
T(M)	Alluvial	Point of Compliance
X(M)	Alluvial	Point of Exposure
Y2(M)	Alluvial	Point of Compliance for PCB Monitoring
L(SG)	San Andres	Background
OBS-3	San Andres	Point of Compliance
S(SG)	San Andres	Point of Compliance
I(SG)	San Andres	Point of Exposure

2.3 Site Groundwater Monitoring System

DOE currently conducts groundwater monitoring at the Bluewater site twice a year. A total of 20 wells are sampled during each event. Figure 4 shows the monitoring locations, and Table 2 lists the wells and relevant construction information. In addition to the nine ARCO wells that DOE inherited in 1997 and the 10 wells that DOE installed in 2011 and 2012, DOE began to include offsite private well HMC-951 in 2013. HMC owns this well, which draws water from the San Andres aquifer and is located a short distance east of the Bluewater site entrance.

To assess the spatial extent of constituents of concern in areas surrounding the Bluewater site, DOE has sampled other offsite wells shown in Figure 5. The Simpson well was sampled in 2012, and the other private wells were sampled in 2013. No formal procedures determine which offsite wells are sampled or the frequency of offsite sampling. Depending on the purpose of the offsite sampling, DOE may attempt to occasionally resample these wells or sample alternative wells.

2.4 Homestake Mill Site

The Homestake site is about 5 mi north-northeast of Milan and about 3 mi east-southeast of the Bluewater site. In addition to a decommissioned mill, the site contains a large and a small tailings disposal cell. Both cells have a radon barrier with an overlying interim soil cover. The site also contains collection ponds, evaporation ponds, and a reverse osmosis water treatment system for groundwater remediation (Figure 6).

Tailings produced by the milling, which began in 1958, were deposited in the small and large tailings piles, which were unlined. The tailings were deposited on San Mateo Creek alluvium, which is about 100 ft thick at the site. Fluids seeping from the piles entered the alluvial aquifer and subsequently entered aquifers in sandstone units of the underlying Chinle Formation where those units are in contact with the alluvium.

HMC's long-term goal is to restore the alluvial aquifer and the Chinle Formation aquifers by reducing the concentrations of contaminants to background concentrations. Background concentrations for the aquifers were based on water quality of the aquifers in areas unaffected by site-generated contamination.

HMC has installed several hundred wells for groundwater extraction, water injection, and monitoring on and in the vicinity of the large tailings disposal cell. Water for the disposal cell injection wells, which is intended to push contaminated tailings leachate through the bottom of the disposal cell, is supplied by HMC-owned wells tapping the alluvial aquifer and relatively permeable layers in the Chinle Formation. A series of toe drains have been installed around the large tailings disposal cell to capture tailings fluids from both natural cell drainage and fluids pushed through the bottom of the cell.

A network of extraction wells in the alluvial aquifer south (downgradient) of the tailings disposal cells is operated to capture remnant groundwater contamination from milling and tailings leachate that has escaped the toe drains. These wells also capture San Mateo Creek alluvial aquifer groundwater flowing beneath the large tailings disposal cell from areas north of the Homestake site. A portion of the water collected by this system of wells is delivered to the reverse osmosis plant for treatment, and remaining pumped water is routed to the collection ponds. The treated effluent is re-injected into the alluvial aquifer and parts of the underlying Chinle Formation. The remaining pumped water is routed to the evaporation ponds. A series of injection wells and infiltration trenches placed along the perimeter of the groundwater extraction area are operated to prevent migration of contaminated groundwater farther to the south, in the direction of Milan.

HMC operates a second groundwater restoration system to remediate those portions of the groundwater contaminant plumes that have migrated off the mill site and beyond the influence of the primary groundwater collection and injection system. This system includes extraction of affected groundwater and land application treatment using an irrigation delivery network. The irrigation network consists of two center-pivot spray irrigation systems and two flood irrigation locations (Figure 6) and provides land application treatment of the collected contaminated groundwater. Irrigation is now permitted for only one center-pivot irrigation area.

Alluvial groundwater entering the Homestake site from the north has elevated levels of uranium and other constituents. Contaminant sources are erosion of uranium-bearing formations and historical contaminant releases from former uranium mines and mills in the San Mateo Creek drainage basin north of the Homestake site. This incoming contaminated groundwater complicates efforts to distinguish Homestake-related contamination from offsite sources.

Determination of contaminant provenance is also a concern in parts of the alluvial aquifer lying about midway between the Bluewater site and the Homestake site. As described in Chapter 4, a significant volume of contaminated San Mateo Creek alluvial groundwater flows directly west from the Homestake site; specifically, from the area under the large tailings disposal cell. In parts of the aquifer where these flows merge with southeastward flow in the Rio San Jose alluvium from the Bluewater site, it becomes difficult to identify respective sources of contamination. The combined flow of the two aquifer systems is to the southeast toward Milan (see Figure 22).

Table 2. Construction Information for Wells Monitored at the Bluewater Site

Well	Date Installed	Northing	Easting	Surface Elevation	Borehole Bottom Elevation	Borehole Diameter	Casing Top Elevation	Casing Bottom Elevation	Casing Diameter	Screen Top Elevation	Screen Bottom Elevation	Casing Depth	Borehole Depth	Depth to Screen	Screen Length
		(ft)	(ft)	(ft amsl)	(ft amsl)	(inches)	(ft amsl)	(ft amsl)	(inches)	(ft amsl)	(ft amsl)	(ft bgs)	(ft bgs)	(ft)	(ft)
San Andres Aquifer Wells															
11(SG)	7/14/2012	1558335.2	469874.8	6636.50	6330.80	8.5	6639.19	6339.00	4	6371.50	6341.50	300.19	305.7	265	30
13(SG)	6/27/2012	1546949.5	472765.8	6591.03	6276.63	8.5	6593.57	6288.53	4	6321.03	6291.03	305.04	314.4	270	30
14(SG)	7/11/2012	1548886.2	463599.0	6614.75	6279.55	8.5	6617.2	6297.35	4	6329.75	6299.75	319.85	335.2	285	30
15(SG)	6/18/2012	1550341.0	469224.4	6610.12	6222.12	8.5	6612.53	6236.77	4	6269.12	6239.12	375.76	388	341	30
16(SG)	6/14/2012	1553798.9	468714.9	6615.55	6380.55	8.5	6618.25	6388.05	4	6420.55	6390.55	230.2	235	195	30
18(SG)	6/7/2012	1547203.3	468136.1	6598.72	6293.72	8.5	6601.32	6306.32	4	6338.72	6308.72	295	305	260	30
I(SG)	7/23/1979	1552131.2	478106.1	6624.84	6294.84	7.875	6625.93	6389.84	5.56	6389.84[a]	6295.93[a]	236.09	330	236.09[a]	93.91[a]
L(SG)	1/18/1981	1553955.4	463034.6	6604.81	5994.81	9.88	6606.09	6192.81	5.56	6192.81[a]	5996.09[a]	413.28	610	413.28[a]	196.72[a]
S(SG)	2/13/1981	1553097.9	468775.2	6623.82	6287.82	7.875	6625.25	6343.82	8.62	6464.82	6343.82	281.43	336	159	121
OBS-3	2/6/1981	1554101.3	468776.2	6613.39	6250.39	6.5	6617.22	6260.39	5.56	6460.99	6263.39	356.83	363	152.4	197.6
HMC-951	2/1/1957	1545336.0	473124.1	6576.95	6301.95	12	6576.79	6334.79	10	6334.79[a]	6304.79[a]	242	272	242[a]	30[a]
Alluvial Aquifer Wells															
20(M)	7/19/2012	1551924.4	463734.8	6610.54	6481.04	10	6613.38	6483.04	4	6500.54	6485.54	130.34	129.5	110	15
21(M)	7/11/2011	1546974.1	472680.7	6590.85	6433.85	8.25	6593.8	6438.85	4	6451.25	6441.25	154.95	157	139.6	10
22(M)	7/14/2011	1548706.3	470929.9	6603.61	6450.61	8.25	6606.48	6454.36	4	6466.78	6456.78	152.12	153	136.8	10
23(M)	6/30/2012	1545333.7	472920.0	6576.6	6455.6	10	6579.22	6465.1	4	6487.6	6467.6	114.12	121	89	20
E(M)	5/31/1978	1548937.6	463534.8	6614.79	6514.79	7.875	6616.32	6581.79	4.5	6546.19	6524.99	34.53	100	68.6	21.2
F(M)	6/6/1978	1547617.6	468854.4	6602.22	6466.19	7.875	6603.59	6466.19	4.5	6508.02	6487.35	137.4	136.03	94.2	20.67
T(M)	11/16/1980	1550460.9	469141.1	6612.1	6470.1	6.5	6612.65	6477.1	4.5	6484.1	6479.1	135.55	142	128	5
X(M)	12/18/1980	1547948.8	472906.9	6597.04	6462.54	7.875	6598.91	6462.54	4.5	6474.04	6465.04	136.37	134.5	123	9
Y2(M)	9/11/1986	1548289.2	467531.8	6611.96	6481.96	8.75	6614.13	6485.96	4	6513.96	6488.96	128.17	130	98	25

amsl = above mean sea level; bgs = below ground surface; ft = feet

[a] Well screen was not installed; the borehole was left open below the bottom of the casing

This page intentionally left blank

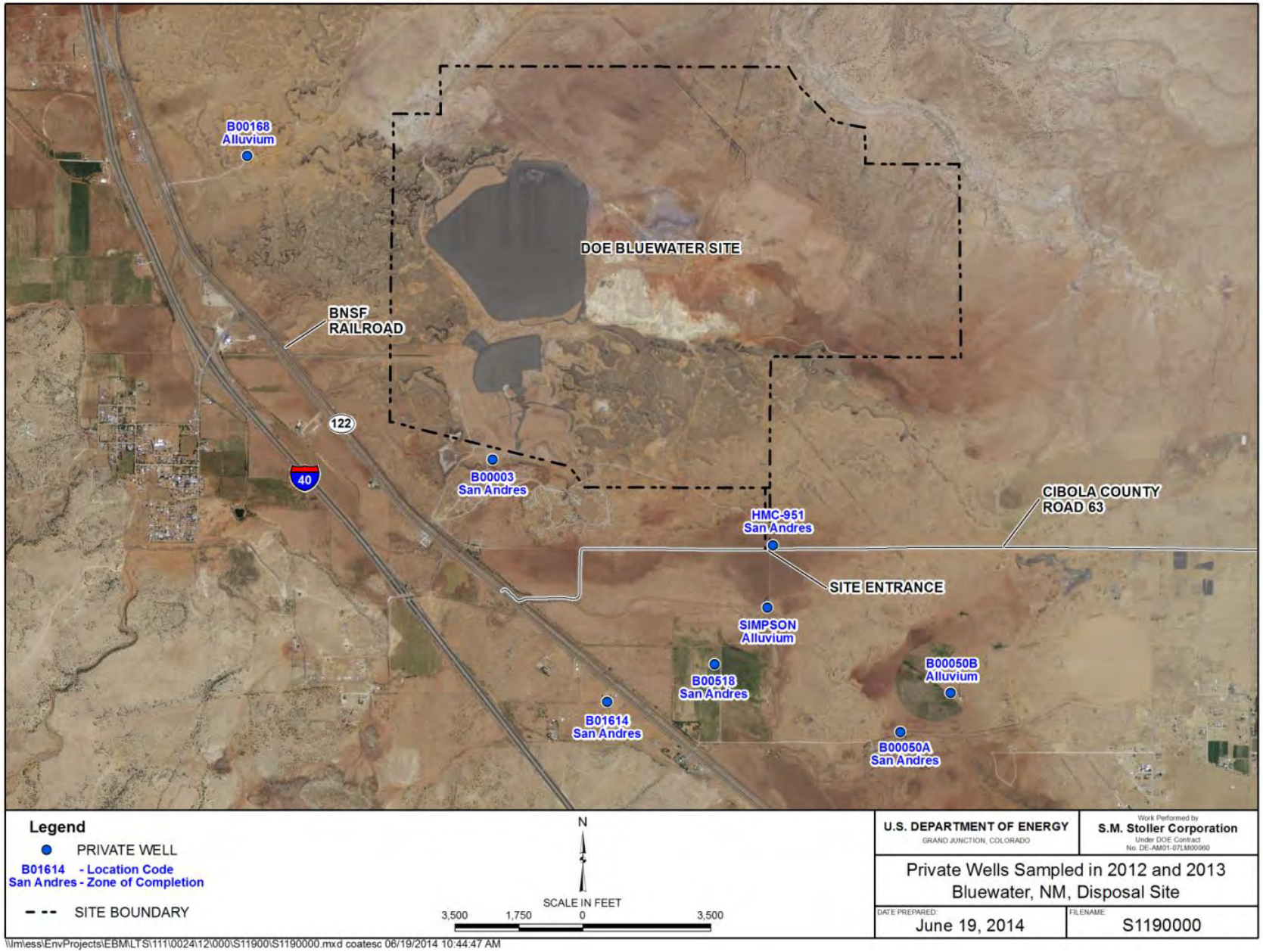

Figure 5. Private Offsite Wells Monitored by DOE

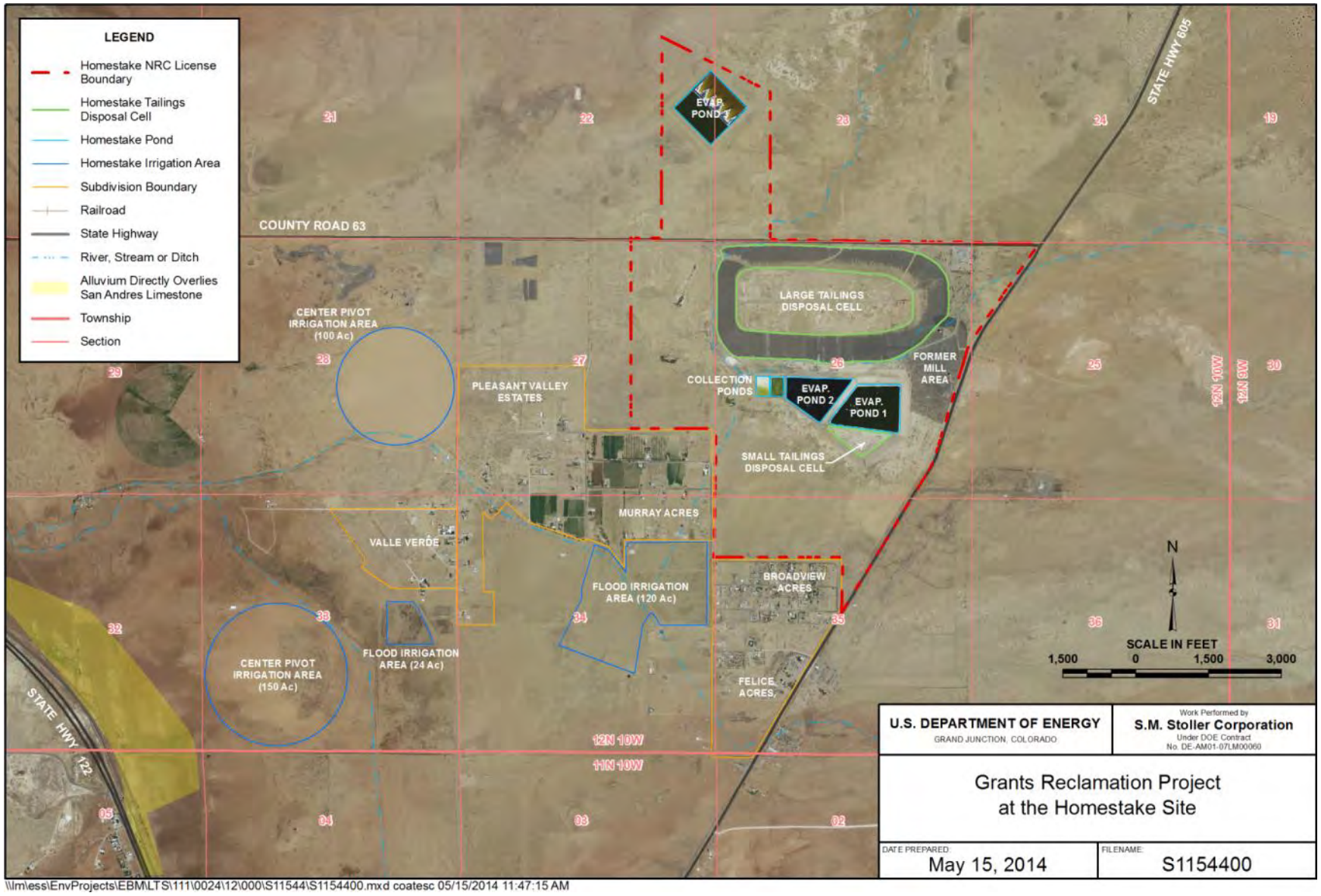

Figure 6. Grants Reclamation Project at the Homestake Site

2.5 Regional Groundwater Monitoring

Aquifers within the study area were affected by uranium-milling operations at the Bluewater and Homestake sites and by mining and milling activities in the San Mateo Creek drainage basin. In addition to groundwater monitoring by DOE and HMC, the USGS and the New Mexico Environment Department (NMED) have historically monitored and continue to monitor wells in the Grants-Bluewater Valley. The communities of Bluewater, Milan, and Grants also monitor their groundwater supply well networks. Water level and constituent concentration data from these sources are included in the groundwater evaluations in this report.

This page intentionally left blank

3.0 Geology

3.1 Geologic Mapping

Figure 7 and Figure 8 show regional and site geologic features, respectively. The regional geologic map, also shown at a scale of 1:48,000 in Plate 2, covers the study area and includes part of the Zuni Uplift, which is a recharge area for the San Andres aquifer. Also included in the regional map are downgradient and discharge areas for this aquifer in the Milan, Grants, and San Rafael areas. The site geologic map on a 2 ft topographic base, shown at a scale of 1:12,000 in Plate 3, covers about 8 square miles and includes the Bluewater site and bordering area. DOE geologists have verified many of the regional geologic features.

The regional geologic map was derived, with a few modifications, from the geohydrologic map by West (1972), which was mainly a compilation by Gordon (1961) of geologic mapping in the Grants-Bluewater area. Earlier, Gordon et al. (1960) with the USGS had completed the areal mapping and collection of detailed information on the water-supply wells; the later report by Gordon (1961) was a summary of the earlier work. Gordon et al. (1960) also mapped much of the area south of the Bluewater site (covering mainly the Milan and San Rafael 7.5-minute quadrangles) in the mid to late 1950s.

Other sources of geologic mapping that Gordon et al. (1960) included in their compiled map were work on other 7.5-minute quadrangles in the mid to late 1950s by the USGS in preliminary form by Thaden and Ostling (1967) for Bluewater, Thaden et al. (1967a) for Dos Lomas, and Thaden et al. (1967b) for Grants. Smaller-scale geologic maps that include and cover areas larger than the regional geologic map are available for the Grants 1:100,000-scale quadrangle (Dillinger 1990), the Albuquerque 1:250,000-scale quadrangle (Wyant and Olson 1978), and the Gallup 1:250,000-scale quadrangle (Hackman and Olson 1977); the southernmost part of the regional map is included in the 1:62,500-scale geologic map of the El Malpais lava field by Maxwell (1986).

Revised geologic mapping has recently been published for most of the regional geologic map area (7.5-minute quadrangles east of 108 degrees longitude). These new maps are a product of the STATEMAP program of the National Cooperative Geologic Mapping Act and were published by the New Mexico Bureau of Geology and Mineral Resources. The new maps are Bluewater (Rawling 2013), which includes most of the Bluewater site; Dos Lomas (Cather 2011); Grants (Zeiglar et al. 2012), which includes the Homestake site; and Milan (Rawling 2012). The San Rafael and Grants SE quadrangles along the south edge of the regional map have also been recently revised. Few changes are noted from the new geologic mapping on and near the Bluewater site (Bluewater, Dos Lomas, and Grants quadrangles). The most significant changes are in the Milan quadrangle, where geologic contacts and faults are more accurately shown. These changes are discussed in Sections 3.2 and 3.3.

3.2 Structure

3.2.1 Regional Structure

The site region is on the gently dipping northeastern flank of the Zuni Uplift (locally known as the Zuni Mountains), a northwest-striking structure with a complex tectonic history that developed during the latter part of the Laramide orogeny (Eocene time) along the south edge of the San Juan basin (Chapin and Cather 1981). The region is in the southeastern part of the larger Colorado Plateau physiographic province. Precambrian metamorphic and igneous rocks are exposed in the core (highest part) of the Zuni Uplift, and directly overlying Upper Paleozoic (Permian) sedimentary rocks gently dip northeast off the flank of the uplift. Sedimentary rocks of Permian and Triassic age, Neogene extrusive volcanic rocks, and Quaternary unconsolidated alluvial deposits in the regional and site areas are shown in the respective geologic maps (Figure 7 and Figure 8). Each sedimentary formation, volcanic rock unit, and Quaternary unit is discussed in detail in Section 3.3.

North- to northeast-striking faults are the most significant structural feature in the northern slope of the Zuni Uplift where the Bluewater site is located. Chamberlin and Anderson (1989) suggest that these faults are a result of Laramide indentation-extrusion tectonics. They describe this tectonic process as follows: as the Zuni block was being pushed north and northeast into the San Juan basin, large slivers of strata were shoved laterally to the east and west along strike-slip faults. These strike-slip normal and reverse faults bound large blocks. Several of these north- to northeast-striking faults are shown in the regional geologic map (Figure 7); from west to east, these faults are Big Draw, Ambrosia Lake, San Mateo (West and East branches), and San Rafael. The fault blocks are evident by the abrupt uplift and exposures of the Permian San Andres Limestone along the faulted boundaries of the blocks.

The Limekiln Canyon block, about 2 mi south of the Bluewater site, is a prominent northeasterly extrusion that has been uplifted and extruded north from the Zuni Uplift. Faults that bound the Limekiln Canyon block are the West branch of the San Mateo Fault to the southeast and what is probably a south extension (along Limekiln Canyon) of the Ambrosia Lake Fault to the northwest. These faults and two other north- to northeast-striking faults, Big Draw and the East branch of San Mateo, have vertically displaced sedimentary rocks as much as 100 to 300 ft along their lengths. Displacement along the San Rafael Fault is greater, ranging from about 200 ft in the Ojo del Gallo spring area to about 1,000 ft to the north in the Grants area (Frenzel 1992). Sedimentary rocks along the edges of the faulted blocks are drag folded and show monoclinal fold characteristics in places with dips as much as 30 degrees in the involved rocks.

Two other significant normal faults in the region that strike west and northwest displace sedimentary rocks by as much as 400 ft. The first fault, shown in Figure 7, extends from near the Mitchell Draw–Bluewater Creek confluence (which marks the start of the Rio San Jose) and extends southeast along the Rio San Jose valley to the West branch of the San Mateo Fault, and probably farther. This fault has about 250 ft of displacement at its northwest end about 1 to 2 mi northwest of Bluewater Village. This displacement is similar to the southeast along the fault, and the fault appears to abruptly displace the San Andres Limestone at the north ends of several of the extruded fault blocks (particularly the Limekiln Canyon block). Displacement along the downthrown side of this fault appears to have provided favorable topography for the course of the Rio San Jose.

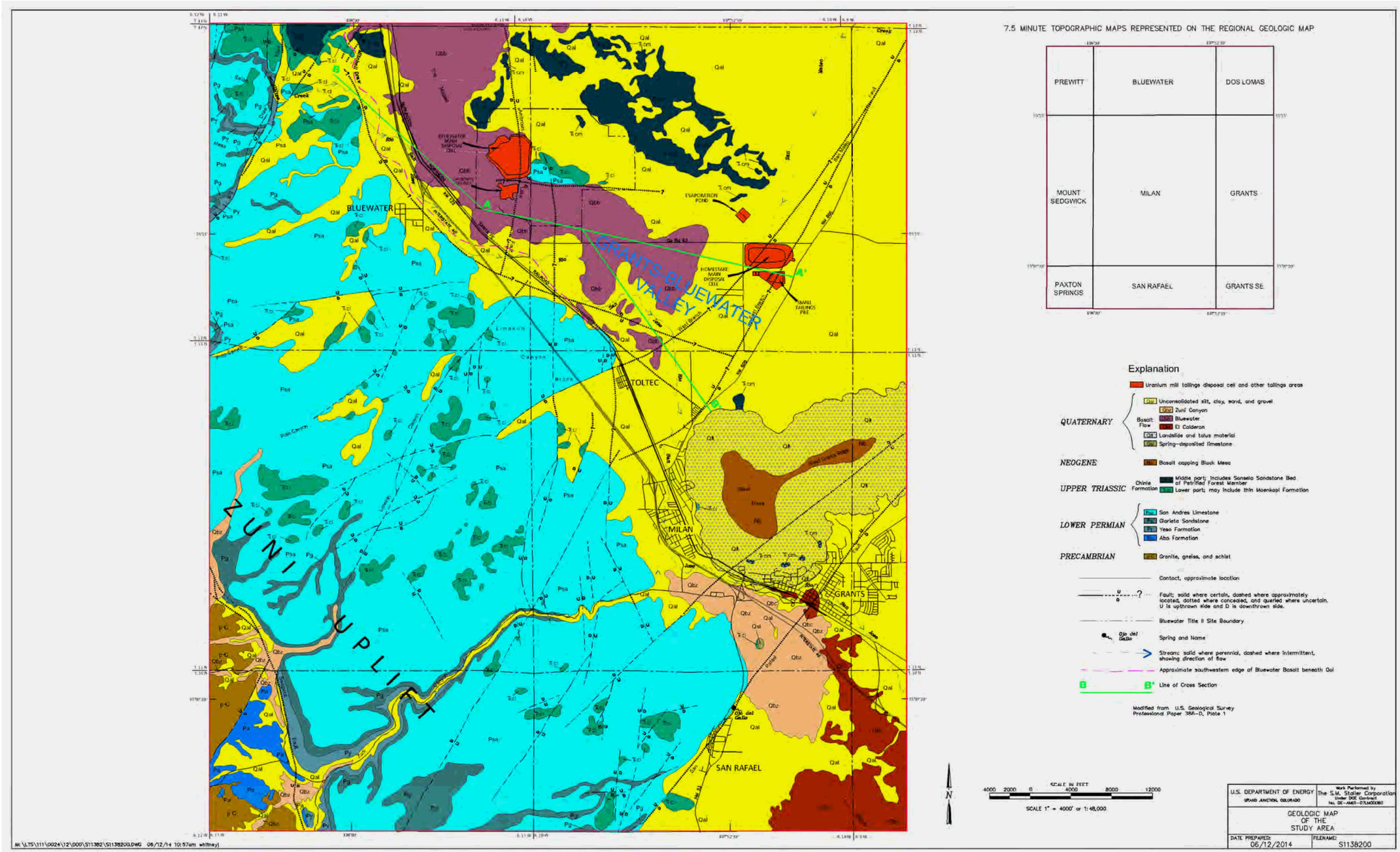

Figure 7. Geologic Features of the Study Area

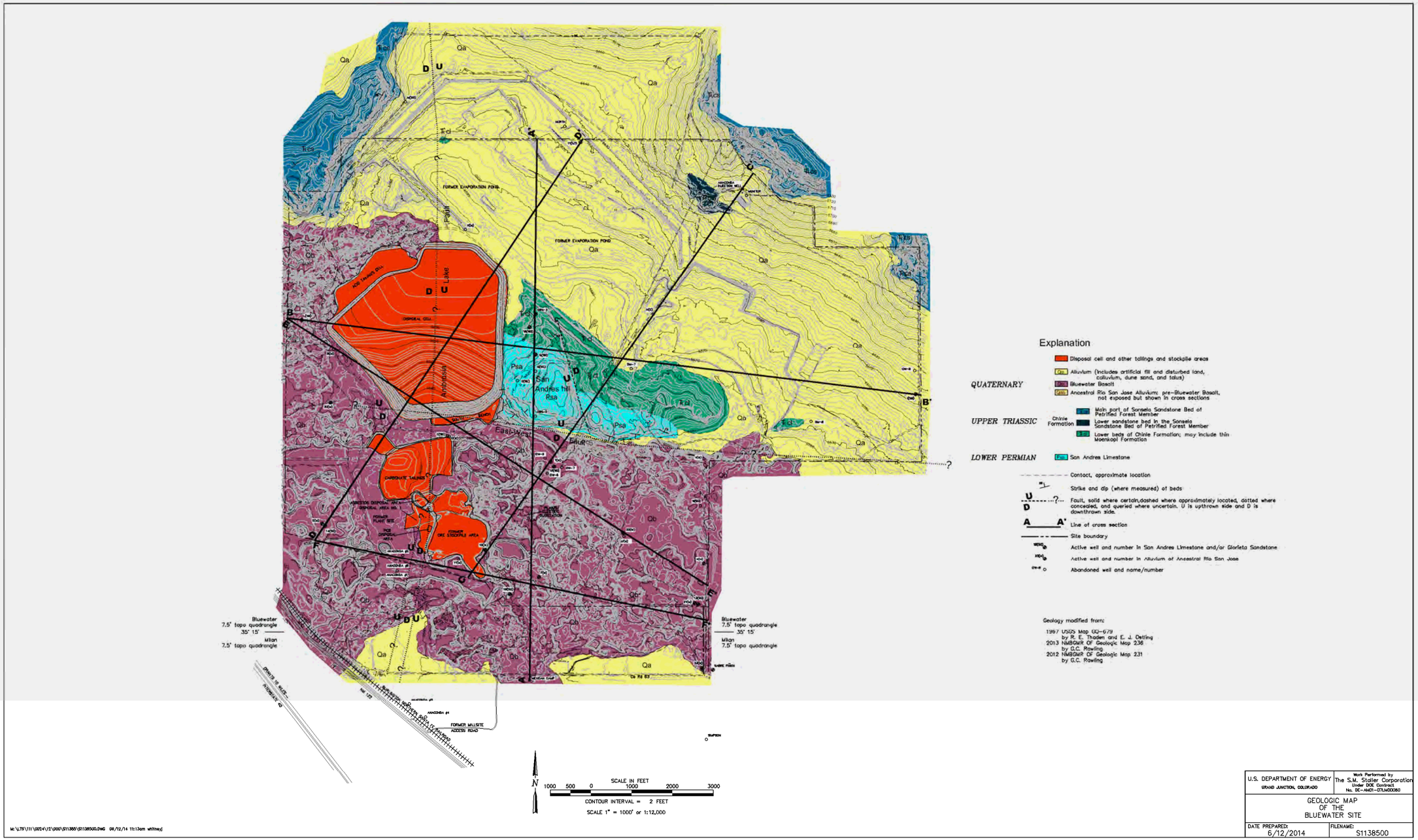

Figure 8. Geologic Features of the Bluewater Site

The second fault, shown in Figure 7 and in more detail in the site geologic map (Figure 8), is called the East-West Fault and extends for about 3 mi through the Bluewater site. On the north (upthrown) side of this high-angle normal fault, a block of resistant San Andres Limestone forms a prominent hill (San Andres hill) that rises up about 80 ft adjacent to the southeast corner of the main tailings impoundment. The west side of the resistant block is bounded by the Ambrosia Lake Fault, which intersects the East-West Fault.

Displacement on the East-West Fault is the largest (about 370 ft) in its western part near the southeast end of the Bluewater site main tailings disposal cell. Displacement decreases to the east; about 1 mi east, the displacement is about 270 ft, and about 2 mi to the east, displacement is uncertain and the fault may not extend much farther east. The East-West Fault may exist for about 0.5 mi or more west of the intersection of the Ambrosia Lake Fault, but its displacement is uncertain. Fault-created drag of the limestone and sandstone beds in the San Andres Limestone just north of the fault on San Andres hill has produced dips toward the south and southwest; dip of strata in this area away from the fault is typically about 3 degrees to the northeast.

The regional geologic map (Figure 7 and Plate 2) shows the locations of two geologic cross sections. The two cross sections are constructed along a northwest to southeast direction: one (A-A′) from the Bluewater site area southeast toward Milan and Grants, and the other (B-B′) from the mouth of Bluewater Creek to the Bluewater site area and eastward to the Homestake site. Figure 9 shows these two cross sections, and Plate 4 shows them in larger scale. Subsurface data for the sections were from borehole lithologic logs for holes drilled from the 1950s to wells installed by Homestake and DOE as recently as 2012. Surface data for the sections were from geologic mapping by Rawling (2012, 2013) and Zeiglar et al. (2012).

3.2.2 Site Structure

The Bluewater site geologic map (Figure 8 and Plate 3) shows the locations of six geologic cross sections. These cross sections show the complex structural variation within the site. Figure 10 shows three of the cross sections (A-A′, B-B′, and C-C′), and Figure 11 shows the other three (D-D′, E-E′, and F-F′). Plates 5 and 6 show larger-scale versions of the respective sections. Subsurface data for the sections were from borehole lithologic logs for holes drilled from the 1940s to DOE-installed wells in 2012. Surface data for the sections were from the site geologic map (Figure 8), which was compiled from recent geologic mapping by DOE geologists and geologic mapping by Thaden and Ostling (1967) and Rawling (2012, 2013). Cross sections A-A′ and C-C′ (Figure 10) show the displacement along the East-West Fault. Figure 12 shows a three-dimensional perspective (block diagram) of cross section A-A′.

Cross section B-B′ (Figure 10) and block diagram B-B′ (Figure 13) show the displacement along the north part of the Ambrosia Lake Fault. South of the East-West Fault, displacement along the Ambrosia Lake Fault is smaller; the fault may branch about 1 mile to the south, where different depths for the upper contact of the San Andres Limestone in Anaconda #2 and #5 wells suggest that the fault may split into two segments with a graben between them. Cross section F-F′ (Figure 11) and block diagram F-F′ (Figure 14) show the displacement across the southern part of the fault and the possible graben structure.

The Ambrosia Lake Fault may extend several miles farther south and join the fault in Limekiln Canyon, which bounds the northwest side of the Limekiln Canyon extruded block. North of the main tailings disposal cell, the Ambrosia Lake Fault is concealed, but its presence and relative displacement are implied by the location and attitude of sandstone beds at the northwest corner

of the Bluewater site boundary. These sandstone beds in the Triassic Chinle Formation dip to the northwest as much as 25 degrees and represent drag on the downthrown side of the fault.

Four miles north of the disposal cell, the Ambrosia Lake Fault was the conduit for the Quaternary Bluewater Basalt flows, which emerged from the area of El Tintero cinder cone. This strike-slip fault, which Chamberlin and Anderson (1989) describe as a right-lateral shear zone, continues northward to the Ambrosia Lake area. Subsurface structural relations are highly uncertain in the area of the Bluewater site where the Ambrosia Lake and East-West Faults intersect. The only well control in this area are abandoned wells C(SG) and C(M), which were south of the East-West Fault and east of the Ambrosia Lake Fault. Interpretations of the complexity of this area are shown by the two cross sections D-D′ and E-E′ (Figure 11), and the perspective block diagram based on cross sections C-C′ and E-E′ (Figure 15).

A high-angle, north-northwest striking normal fault with about 20 to 25 ft of displacement (downthrown on the east) borders the east side of the San Andres hill north of the East-West Fault. Although the displacement on this fault is small, its surface trace is obvious and marked by the red siltstone beds of the lowermost Chinle Formation placed against the gray San Andres Limestone. Cross sections B-B′ and C-C′ (Figure 10) show the displacement across this fault. Thaden and Ostling (1967) and Gordon (1961) mapped this fault.

Only the three faults mentioned above (East-West, Ambrosia Lake, and the small normal fault on the east side of the San Andres hill) have been verified at the Bluewater site. The exact position and extent of the East-West and Ambrosia Lake Faults are uncertain: in many places, the Bluewater Basalt or alluvial material, or both, have covered geomorphic and geologic indications of faulting. Subsurface lithologic data from water wells and monitoring wells installed during the past 50 years have helped determine the approximate position and displacement of faults on the site. Additional drilling would be necessary to more precisely determine the position and displacement along the two major faults that cut through the site. Highest uncertainty on the site involving the faults is the area where the East-West and Ambrosia Lake Faults intersect beneath the south end of the main tailings disposal cell (Figure 8 and Plate 3).

Two evaluations of faulting at the site are more recent than the early fault mapping by Thaden and Ostling (1967) and Gordon (1961). The first, on the hydrogeology of the Bluewater site mill tailings impoundment area (Hydro-Search 1977), indicated on their Plate I of the site only the three faults verified by DOE. The second, by Dames & Moore (1981a), was in conjunction with an evaluation of seepage from a proposed subgrade tailings disposal area 1 to 2 mi east of the main tailings disposal cell. That evaluation investigated the validity of the numerous faults mapped in the site area earlier by Thaden and Ostling (1967) and Gordon (1961).

The Dames & Moore evaluation found no evidence for several of the earlier mapped faults, but the presence and approximate position of the Ambrosia Lake and East-West Faults was confirmed. Their revised fault location map is shown on their Plate C-2, which shows four faults south of the East-West Fault. The evidence for these four faults, which generally are the same as the ones mapped by Gordon (1961), was not given. The Bluewater Basalt covers these four faults, and no subsurface evidence from more recent boreholes can suggest their presence. Because of lack of evidence, it is doubtful that these four faults exist.

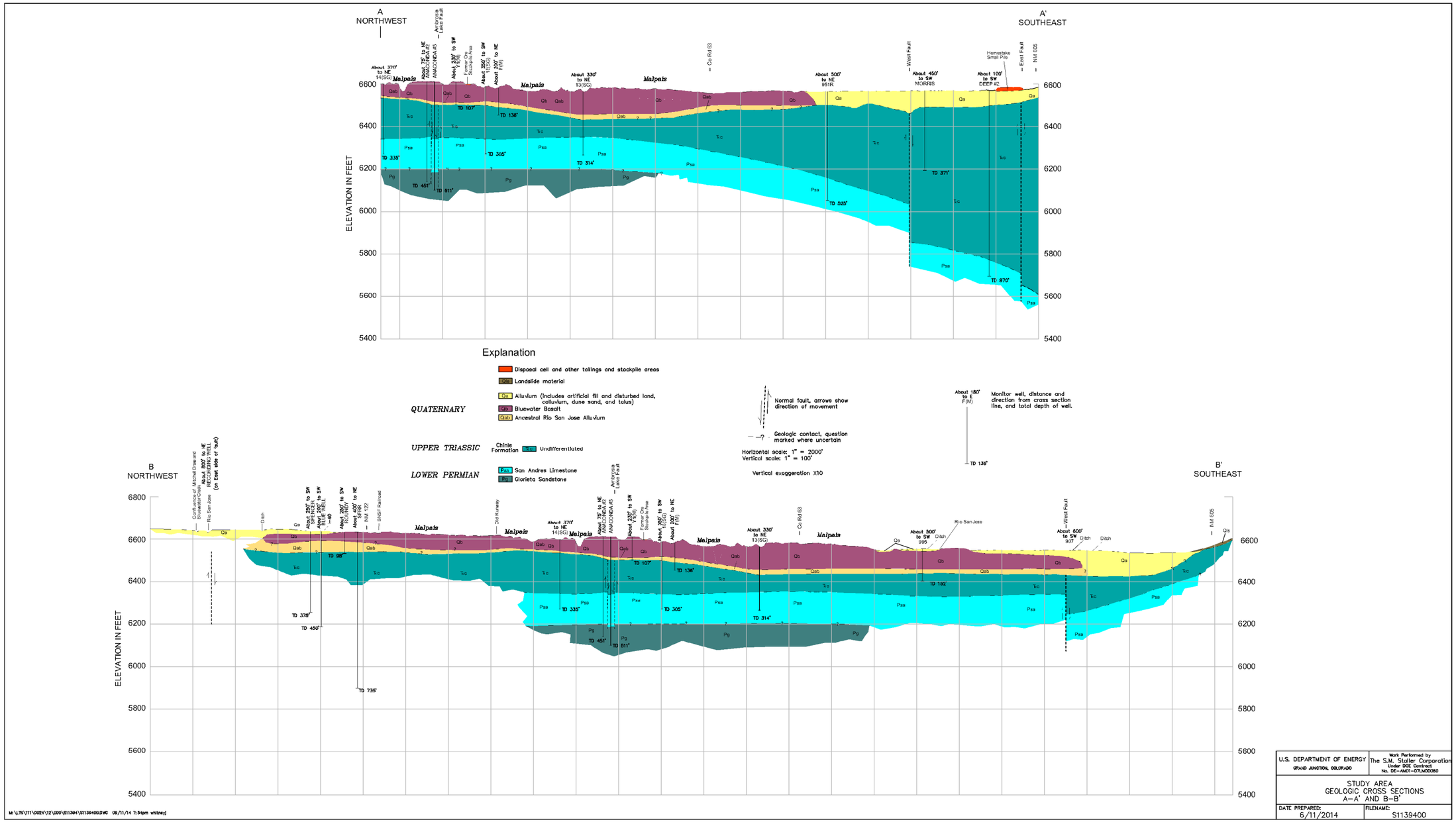

Figure 9. Study Area Geologic Cross Sections A-A' and B-B'

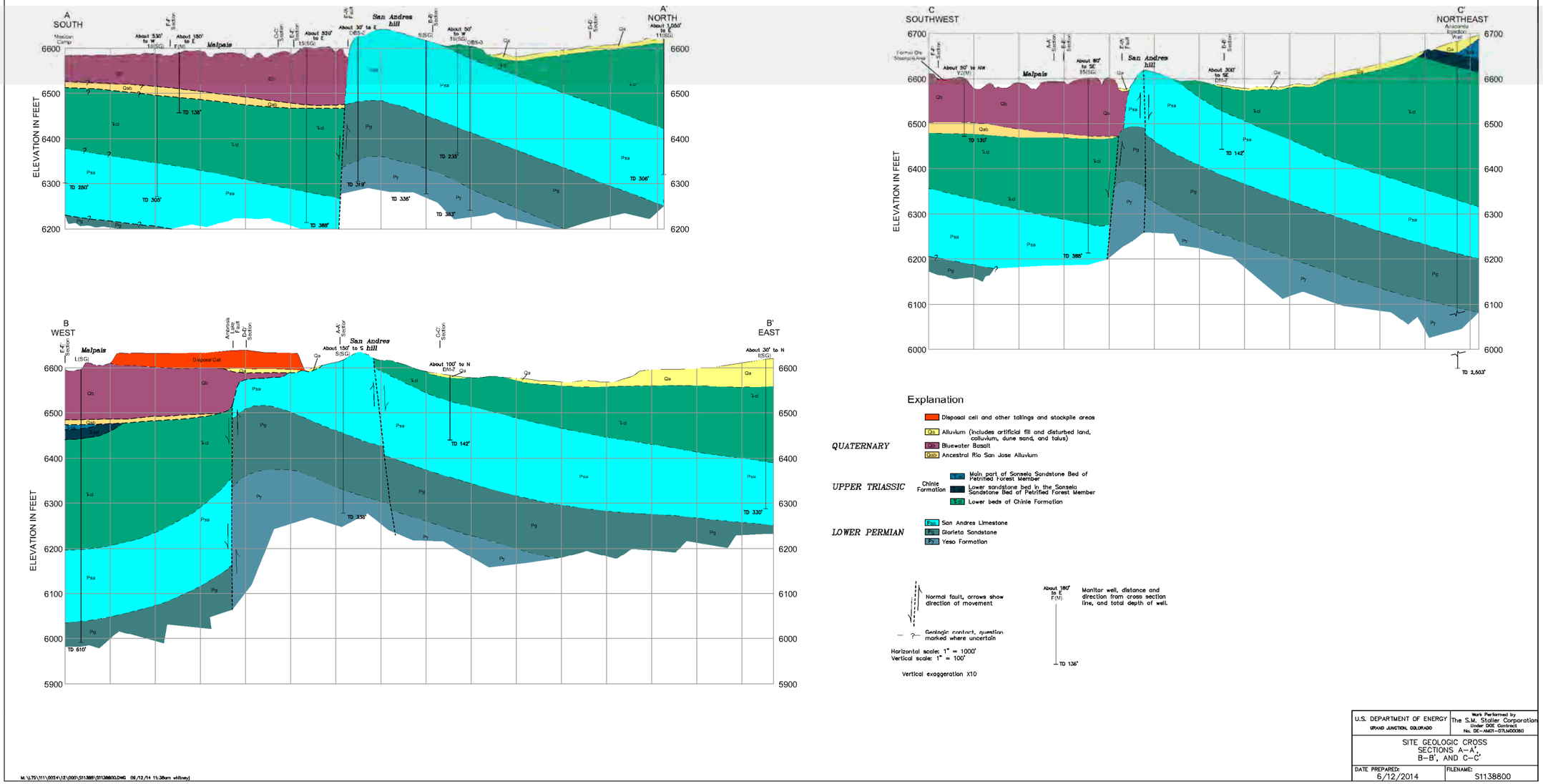

Figure 10. Site Geologic Cross Sections A-A', B-B', and C-C'

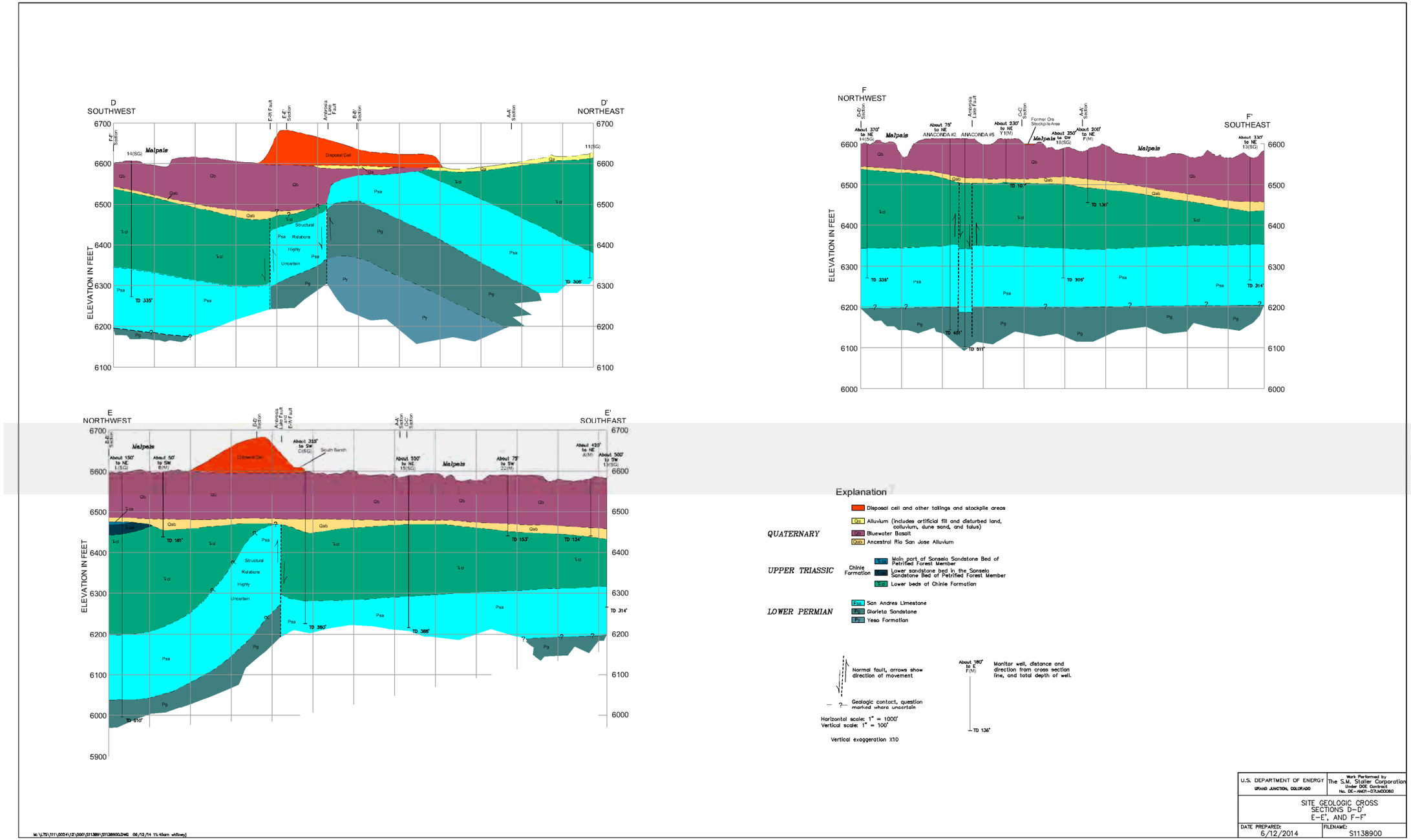

Figure 11. Site Geologic Cross Sections D-D', E-E', and F-F'

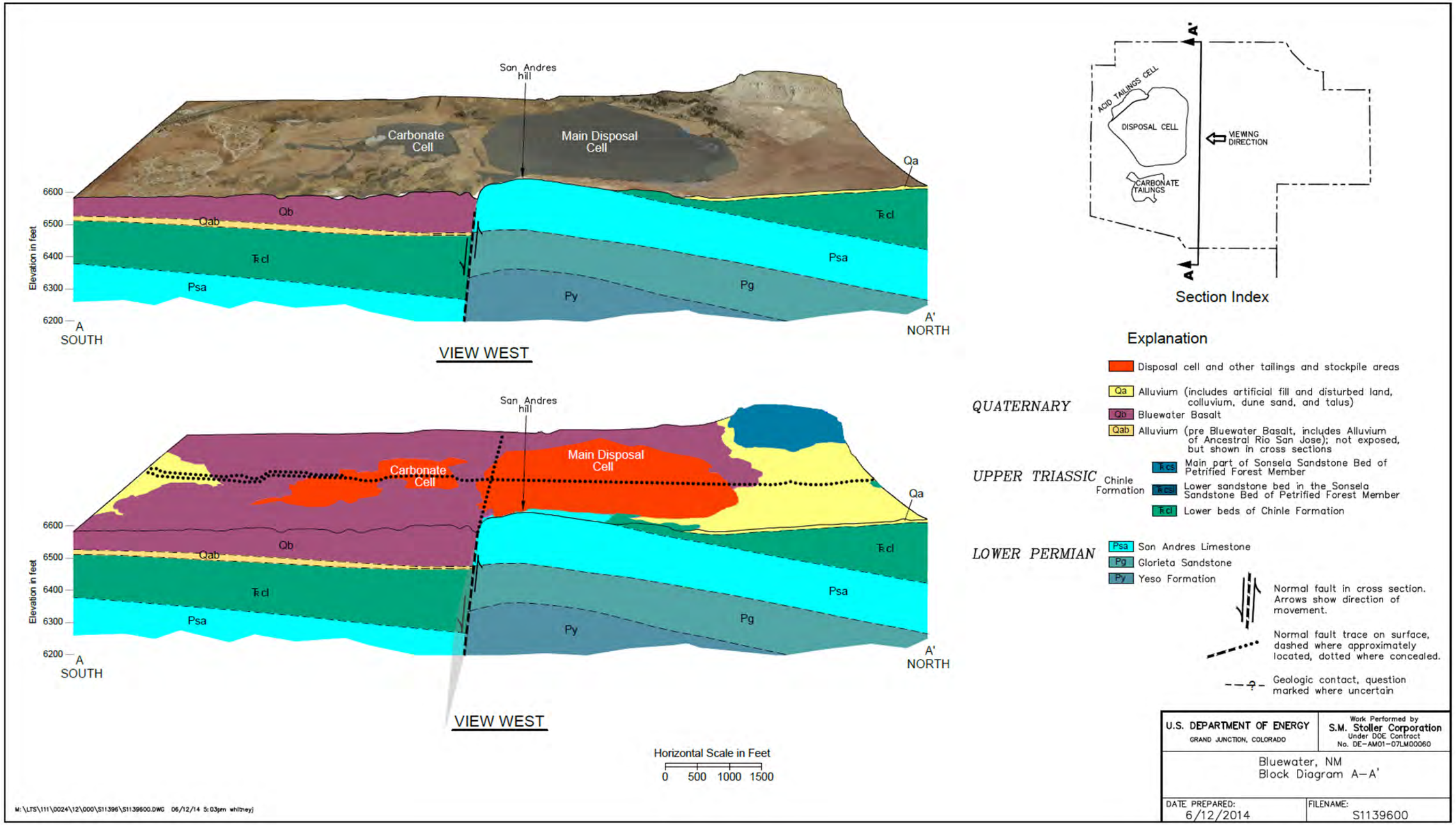

Figure 12. Block Diagram of Site Geologic Cross Section A-A'

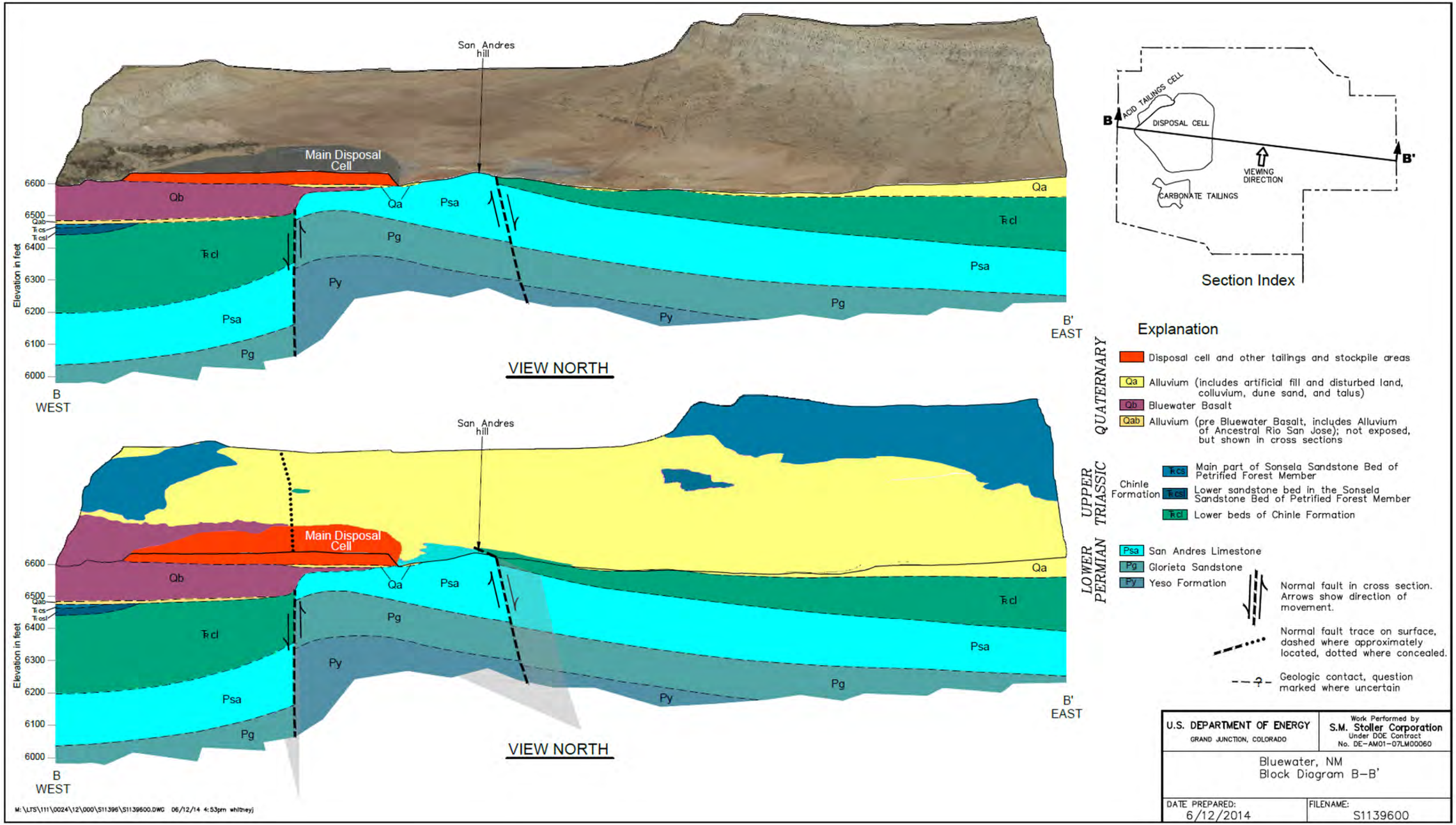

Figure 13. Block Diagram of Site Geologic Cross Section B-B'

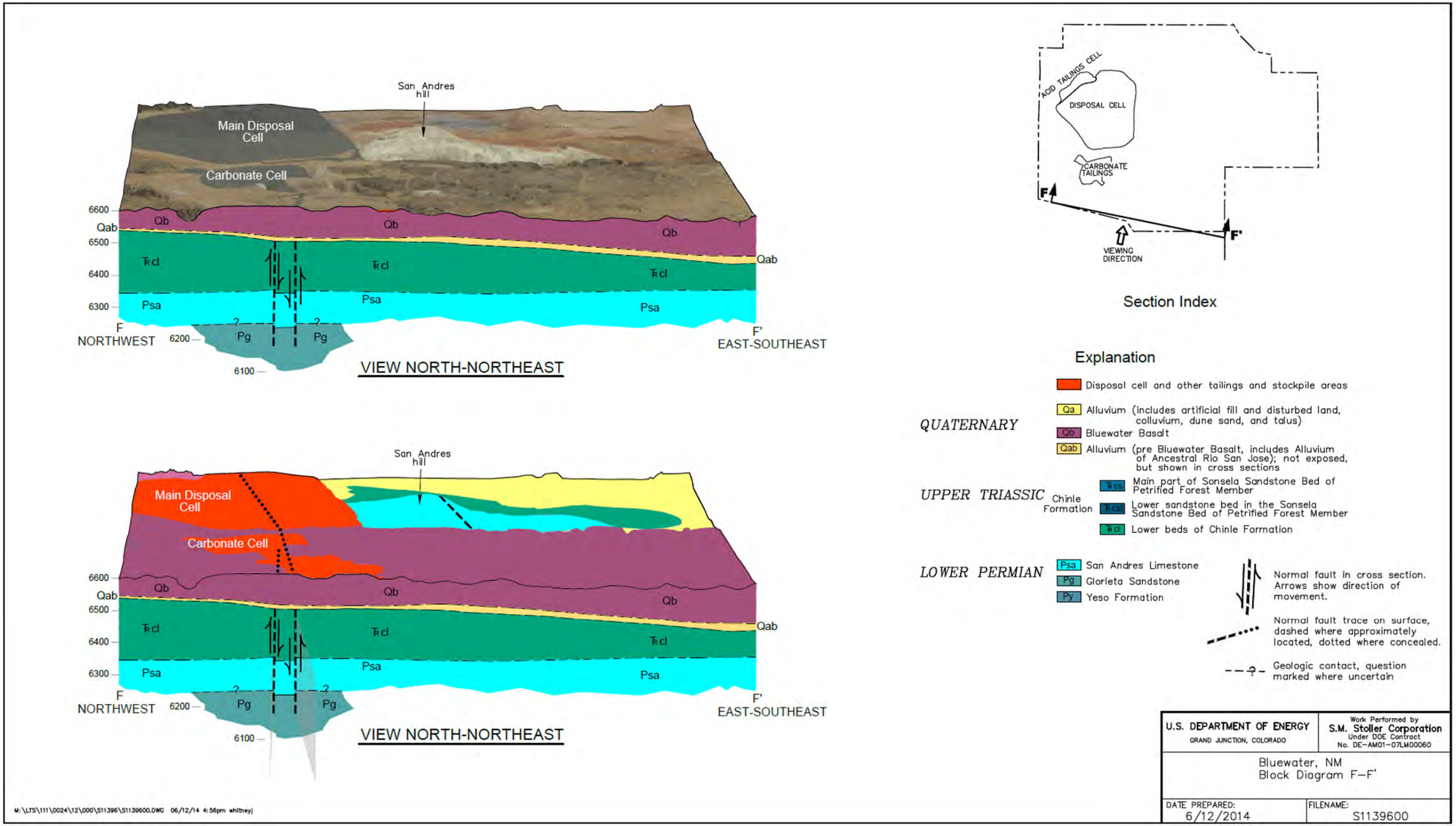

Figure 14. Block Diagram of Site Geologic Cross Section F-F'

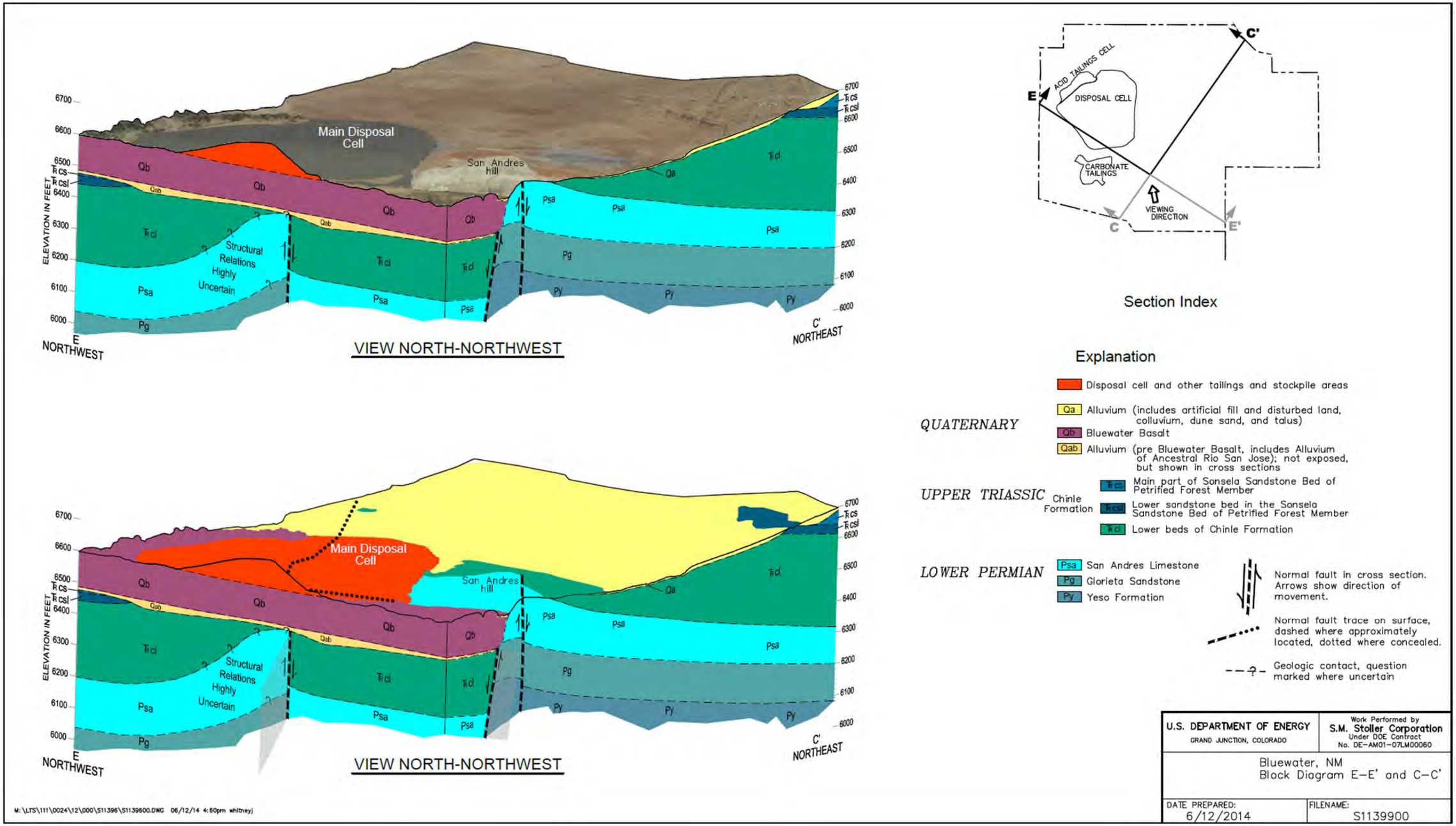

Figure 15. Perspective Block Diagram of Geologic Cross Sections C-C' and E-E'

This page intentionally left blank

Dames & Moore (1981a) included joints in their field investigations. They measured orientations of 600 joints in the site area. About 200 joints were from the San Andres Limestone just north of the East-West Fault, and the remainder were from the Chinle Formation east of the site and in the northeast part of the site. They concluded that the joints were vertical or very nearly so, had an average spacing of about 3 ft, generally closed with depth, and were very tight to nonexistent in the subsurface.

Major and intermediate joint orientations in the San Andres Limestone are N. 66° E. (east-northeast) and N. 16° W. (north-northwest), respectively. DOE geologic investigations on the site in 2009 noted a general north-northwest strike of joints in the San Andres Limestone east of the San Andres hill. This direction is similar to the strike trend of the small normal fault on the east side of the San Andres hill. One major and two intermediate joint orientations in the Chinle Formation in the northeastern part of the site area are N. 46° E. (northeast), and N.86° W. (west) and N. 8° W. (north), respectively.

3.3 Stratigraphy

Geologic formations and units from Precambrian to Quaternary age exposed in the study area are described in this section. These formations are shown in the order of their geologic age in the Explanations for Figure 7 and Plate 2. An additional geologic unit that is buried and not exposed, but is described in this section, is the ancestral Rio San Jose alluvium of Quaternary age.

3.3.1 Precambrian Rocks

Basement metamorphic rocks of Paleoproterozoic age are exposed in the Zuni Mountains about 7.5 mi southwest of the Bluewater site in the core of the Zuni Uplift, as shown west of the Sedgwick Fault on the regional geologic map (Figure 7 and Plate 2). Much of the rocks are foliated calc-alkaline granitoids (mostly quartz monzonite) that are about 1,655 million years old (Timmons and Cikoski 2012). Also exposed are smaller areas of hornblende gneiss and felsic volcanic schist. Estimated depth to the Precambrian in the Bluewater site area is 1,500 to 2,500 ft; the depth to Precambrian at the Anaconda injection well was 2,432 ft (West 1972).

3.3.2 Permian Rocks

3.3.2.1 Abo Formation

The Lower Permian Abo Formation, which unconformably overlies Precambrian metamorphic basement rock, is a thick section of mixed siliciclastics ranging from mudstone to conglomerates. These sediments were deposited mainly in a floodplain environment and are exposed in the core of the Zuni Uplift where the formation is 500 to 800 ft thick. At the Anaconda injection well, shown in Figure 8 and Plate 3 and in cross section C-C′ in Figure 10 and Plate 5, the depth to the Abo Formation is 1,466 ft, and the formation is 770 ft thick (West 1972). Between the Abo Formation and Precambrian basement at the Anaconda injection well is 196 ft of the Pennsylvanian Madera Limestone (it is not present in the core of the Zuni Uplift and, therefore, is not described here).

3.3.2.2 Yeso Formation

Conformably overlying the Abo Formation, the Lower Permian Yeso Formation in the region consists of two members: the Meseta Blanco Sandstone Member and the overlying San Ysidro Member. The formation is exposed around the core of the Zuni Uplift, in some of the deeper canyons incised into the northeast flank of the uplift (such as in Zuni Canyon), and along the west (upthrown) side of the Big Draw Fault about 4 mi west of the Bluewater site. Deposited in a marginal marine to lagoonal environment, the Yeso Formation consists of cross-bedded, fine-grained, reddish-brown quartzose sandstone in its lower part, and cross-bedded, fine-grained clayey sandstone and siltstone with several thin limestone beds in its upper part. The formation grades upward into the Glorieta Sandstone. Not exposed at the Bluewater site, the Yeso Formation at the Anaconda injection well is 877 ft thick (West 1972).

3.3.2.3 Glorieta Sandstone

The Lower Permian Glorieta Sandstone is exposed in bold, yellow to light-brown cliffs in Bluewater and Zuni Canyons and in several other canyons along the northeast flank of the Zuni Uplift. Deposited in a marginal marine environment, the formation generally consists of light gray, fine- to medium-grained sandstone composed of well-sorted, rounded to subrounded quartz grains. Beds are thick and massive, with some tabular cross beds in the upper part of the formation. Calcareous-cemented beds are soft and friable in the lower part of the formation; some beds in the upper part of the formation may be hard owing to cementation by silica. A few greenish-gray clay interbeds separate the thick sandstone beds. The upper Glorieta intertongues with the overlying San Andres Limestone, and the top of the Glorieta is described as the base of the first limestone bed in the San Andres.

The Glorieta Sandstone does not crop out at the Bluewater site; however, it was penetrated by the Anaconda injection well as shown in cross section C-C′ (Figure 10 and Plate 5), where its thickness is 120 ft (West 1972). Three other wells (S(SG), OBS-2, and OBS-3) on the site penetrated the entire thickness of the Glorieta Sandstone. These wells are in the area of the uplifted San Andres hill and are shown in cross section A-A′ (Figure 10 and Plate 5); well S(SG) is also shown in cross section B-B′ (Figure 10 and Plate 5). At all three wells, the thickness of the Glorieta Sandstone is approximately 130 ft. The thickness of the Glorieta Sandstone increases to 150 to 200 ft to the west and south of the site in Bluewater and Zuni Canyons.

3.3.2.4 San Andres Limestone

The Lower Permian San Andres Limestone forms the extensive gray, dissected slope that dips gently off the northeast flank of the Zuni Uplift. Deposited in marine conditions on a shallow shelf environment, the San Andres Limestone consists of limestone, dolomite, sandstone, and chert. After deposition, a long period of erosion (approximately 25 to 40 million years) from Middle Permian to Middle Triassic time exposed the formation to extensive solution action resulting in development of karst topography in some of the limestone beds. Following this erosional event, which created a major regional unconformity, the thick red beds of the Upper Triassic Chinle Formation were deposited.

Formation thickness and amount of limestone in the San Andres Limestone vary across the region. The thickness varies from about 110 to 190 ft in the region, and the variation is due to the

amount of pre-Triassic erosion and where the base and top of the formation are described. At the Anaconda injection well in the northeast part of the Bluewater site, the San Andres Limestone thickness is only 116 ft (West 1972), whereas the formation is typically 150 to 160 ft thick in wells in the central and western parts of the site. South of the Bluewater site on the flanks of the Zuni Uplift, the thickness increases to as much as 190 ft (Rawling 2012). The amount of limestone in the formation decreases with increasing distance north and northeast of the Zuni Uplift. At the injection well, the formation contains only about 10 percent limestone; in the central and south parts of the Bluewater site, limestone is about 30 to 40 percent of the formation; and to the south in the Milan quadrangle, limestone may be as much as 70 percent of the formation.

Gordon (1961) divided the San Andres Limestone into three informal members in the Grants-Bluewater area.

- **Lower member**—20 to 40 ft thick, composed of massive bluish-gray, dolomitic limestone, with interbedded sandstone and sandy limestone in the lower part.
- **Middle member**—15 to 30 ft thick, composed of light-gray to yellowish-buff sandstone that is well-sorted, friable, and locally cross-bedded.
- **Upper member**—60 to 100 ft thick, composed of massive gray, fossiliferous limestone, with the upper part being classified as sandy limestone in places and the occurrence of cherty material in some places.

These members are apparent in the lithologic log of core from the Anaconda #2 well (Gordon 1961). In that log, karstic cavities were reported from limestone in the lower and upper members. A thickness of 102 ft for the San Andres Limestone was shown in the Anaconda #2 well core log. Using the definition for the top of the underlying Glorieta Sandstone as the base of the first limestone bed, the base of the San Andres Limestone in the Anaconda #2 well core log was extended downward 51 ft to include interbeds of sandy limestone. This correction makes the thickness of the San Andres Limestone at the Anaconda #2 well at 153 ft. This thickness, along with a similar San Andres Limestone thickness of 150 ft penetrated by the Anaconda #5 well, is shown in cross section F-F′ (Figure 11 and Plate 6).

Nine wells in the Bluewater site area extended below the base of the San Andres Limestone. These wells are L(SG), S(SG), G(SG), D(SG), Anaconda #2, Anaconda #5, Anaconda injection well, OBS-2, and OBS-3. Of these, five (S(SG), G(SG), D(SG), OBS-2, and OBS-3) are in the area of the San Andres hill east of the main tailings disposal cell. Thicknesses of San Andres Limestone were used from these wells in construction of the six cross sections across the site. Other wells, which did not penetrate the entire thickness of the San Andres, provided data for the top of the formation that were useful for cross sections.

Several lithologic characteristics at the surface and in the subsurface identify the top of the San Andres Limestone at the regional Permian-Triassic unconformity. Surface characteristics include karst features and siliceous masses. Subsurface characteristics include abundant pyrite and color change.

- **Karst features:** Karstic solution processes and other erosion reportedly produced as much as 100 ft of relief in places on the surface at the top of the San Andres in and on the flanks of the Zuni Uplift. Little or no karst relief on the erosion surface was seen in the Bluewater site area or the immediate surrounding region to the south. The most evident karstic solution

features seen in the area are small-scale etching and fluting on outcrops of limestone and limey sandstone. These features were seen on outcrops at various levels through the San Andres Limestone thickness. In most places at the Bluewater site area, sandstone is exposed at the top of the San Andres Limestone, and karstic features had not developed.

- **Siliceous masses:** Silicification in the form of large, resistant masses of white to brown, iron-stained chert in thicknesses up to 5 ft are at scattered locations on the top of the San Andres Limestone. Two notable locations of the chert are at the Bluewater site on the uplifted San Andres hill and at the northeast end of the Limekiln Canyon block just southwest of State Highway 122. At both locations, the chert masses appear to be associated with an iron-stained sandstone bed that occurs at the top of the San Andres Limestone. It is possible that the chert masses filled channels cut into the top of the sandstone bed, but field exposures have not confirmed it. Only traces of chert have been found in drill cuttings from a few monitoring wells at the Bluewater site.
- **Abundant pyrite:** In most boreholes from monitoring well installations at the Bluewater site, drill cuttings from just below the top of the San Andres Limestone show an abrupt increase in fine-grained pyrite crystals. The abundant pyrite appears to be associated with fine-grained sandstone found at the top of the San Andres.
- **Color change:** Drill cuttings abruptly change color from brown-red, grayish-red, and greenish-gray of the lower Chinle Formation rocks to pale yellowish-brown and grayish-orange of uppermost sandstones in the San Andres Limestone. The yellow and orange color represents the oxidized conditions (increase in pyrite being oxidized, and limonite) in rocks of the San Andres Limestone below the unconformity.

3.3.3 Triassic Rocks

Triassic stratigraphy involving the Moenkopi and Chinle Formations is complicated in west-central New Mexico. During the past 50 years, improved understanding of regional stratigraphy has resulted in refinements in nomenclature. Heckert and Lucas (2003) present the current Triassic stratigraphic framework for the site region and the subdivision of the Chinle Formation (now Group status) into various formations. The older stratigraphic terminology of Gordon (1961) is used in this report because it is simple, and the important hydrologic units fit into its framework.

3.3.3.1 Moenkopi Formation

A small thickness of Middle Triassic Moenkopi Formation unconformably overlies the San Andres Limestone at the Bluewater site and southward on the flank of the Zuni Uplift. Thaden and Ostling (1967) mapped a 26 ft thickness of the formation, a reddish-brown arkosic and micaceous siltstone and sandstone, on the northeast flank of the San Andres hill on the Bluewater site. As much as 60 ft of Moenkopi Formation is shown in scattered remnants on the San Andres Limestone dip slope in recent mapping south of the Bluewater site in the Milan and San Rafael quadrangles (Rawling 2012, and Timmons and Cikowski 2012, respectively). Gordon (1961) did not think that the Moenkopi Formation extended this far east, and he mapped the red siltstone and sandstone directly overlying the San Andres Limestone as lower beds of the Chinle Formation. Because the thin Moenkopi Formation is not physically or chemically distinguishable from the overlying Chinle Formation, the Moenkopi is included in the lower beds of the Chinle Formation in the regional and site geologic maps and cross sections.

3.3.3.2 Chinle Formation

The Upper Triassic Chinle Formation is exposed or is present in subcrops along a wide northwest-striking valley (Grants-Bluewater Valley) from Grants to the Homestake and Bluewater sites. Most of the formation consists of grayish-red and reddish-brown mudstone, siltstone, and sandstone; lesser amounts of white to yellow and brown sandstone and conglomeratic sandstone are mainly in the middle and upper parts of the formation. The formation disconformably overlies the Moenkopi Formation, was deposited in a continental environment, and has an estimated thickness of 1,400 to 1,600 ft.

Only the lower and middle parts of the Chinle Formation, as mapped by Gordon (1961), are shown in the regional and site geologic maps. Upper parts of the Chinle Formation are not exposed in the study area; they occur along with other younger rocks northeast and downdip from the study area. Included in the lower part of the Chinle Formation is the thin Moenkopi Formation overlain by approximately 250 ft of predominantly red-brown claystone and siltstone. The middle part of the Chinle Formation, as described by Gordon (1961), consists of as much as 200 ft of thick beds of poorly sorted, cross-bedded sandstone and conglomeratic sandstone with interbeds of siltstone and mudstone. This sequence correlates with the Petrified Forest Member of the Chinle Formation, which Lucas and Hayden (1989) describe as the thick (about 1,000 ft) member in the middle of the Chinle. Specifically, within the Petrified Forest Member, the Sonsela Sandstone Bed (Sonsela), as much as 200 ft thick, is also described as consisting of light-gray to yellowish-brown, fine-grained to conglomeratic, cross-bedded sandstone with thin layers of grayish-purple mudstone (Lucas and Hayden 1989). Fossil (silicified) wood occurs in places in sandstone beds of the Sonsela, which crops out in the northwest portion of the Bluewater site. In the northeast part of the Bluewater site, a thick-bedded sandstone about 20 to 30 ft thick forms a conspicuous outcrop about 0.25 mi southwest of (and below) the main Sonsela outcrops. This white to pale-tan, cross-bedded sandstone is mapped as a lower sandstone bed within the Sonsela.

Much of the Chinle Formation in the region is covered by Quaternary unconsolidated alluvial, eolian (wind-deposited), and landslide material, or by one of four Neogene basalt flows. The lower part of the Chinle Formation is shown in the six cross sections for the site area and in the two cross sections for the region. The thickness of the lower part shown in the cross sections varies, depending on the degree of post-Triassic erosion. The entire thickness of the lower part of the Chinle Formation was penetrated in two wells (L(SG) and Anaconda injection well) at the Bluewater site. At well L(SG), the lower part of the Chinle Formation is nearly 250 ft thick, and about 25 ft of the overlying lower sandstone bed of the Sonsela also was penetrated (cross section B-B′ in Figure 10 and Plate 5, and cross section E-E′ in Figure 11 and Plate 6). At the Anaconda injection well, the lower part of the Chinle Formation is nearly 300 ft thick, and nearly 30 ft of the overlying lower sandstone of the Sonsela was penetrated (cross section C-C′ in Figure 10 and Plate 5).

Eastward from about 1 to 2 mi east of the Bluewater site entrance, the thickness of the Chinle Formation becomes much greater, owing in part to crossing to the downthrown sides of the West and East branches of the San Mateo Fault, as shown in regional cross section A-A′ (Figure 9 and Plate 4). In this area, lithologic borehole logs for the wells are not sufficiently detailed to allow the sandstones in the middle part of the Chinle Formation to be identified, and the larger

thicknesses of the Chinle Formation are designated as undifferentiated. At the east end of regional cross section A-A′, just east of HMC's small tailings disposal cell, the thickness of the Chinle Formation is approximately 900 ft. HMC has identified three aquifers in the Chinle Formation in the subsurface vicinity of their site. These aquifers are in parts of the Chinle Formation that contain sandstone beds that dip to the northeast.

3.3.4 Neogene Volcanic Rocks

Three basalt flows within the Quaternary Zuni-Bandera volcanic field are represented in the region around the Bluewater site. These flows are, from oldest to youngest, El Calderon, Bluewater, and Zuni Canyon. An older basalt flow about 50 ft thick of Late Pliocene age, dated at approximately 2.5 million years old (Laughlin et al. 1993), is preserved as the cap on Black Mesa that rises 700 to 800 ft above Grants and Milan. The three Quaternary basalt flows that cover alluvial deposits in the Rio San Jose valley are discussed below.

3.3.4.1 El Calderon Flow

Referred by Gordon (1961) as the Laguna basalt flow, El Calderon flow is exposed in the Grants area and in the large area south of San Rafael known as El Malpais. It consists of a series of flows that originated at El Calderon center on the south side of the Zuni Mountains and extended for about 25 mi around the east side of the Zuni Uplift to the Grants area. The flows have been dated at 110,000 to 128,000 years old (Laughlin et al. 1993). Much of this basalt is covered by eolian sand and silt south of San Rafael.

3.3.4.2 Bluewater Basalt

El Tintero ("the inkwell"), a small scoria cinder cone on top of a small shield volcano about 4 mi north of the Bluewater main tailings disposal cell, was the source of the Bluewater basalt flows. Several flows—Thaden and Ostling (1967) indicated at least five, and Hydro-Search (1977) mapped two separate flows—erupted from El Tintero and coursed south and southeast, filling the ancestral valley of the Rio San Jose. The tholeiitic composition of the dense to vesicular basalt contains small olivine and plagioclase phenocrysts in a groundmass of plagioclase and clinopyroxene. The flows extended to their last surface exposure just northeast of Toltec; they may extend a small distance farther south in the subsurface, but probably did not reach Milan or the area covered by the younger Zuni Canyon flow. Figure 7 and Plate 2 show the approximate southwest edge of the basalt beneath the Quaternary alluvial material (from Hydro-Search 1977). Thickness of the basalt is variable; in the Bluewater site and nearby area, it is generally 70 to 130 ft, as shown in the cross sections in Figure 10 and Plate 5, and Figure 11 and Plate 6. Sims et al. (2007) determined that eruption of the Bluewater Basalt began approximately 68,000 years ago.

The exposed rough surface of the flow is referred to as El Malpais ("the badlands"), and many of the primary flow structures are still preserved. The upper surface of the flows commonly show collapse features and pressure ridges, and the flow edges in many places show a steep carapace of pahoehoe crust and hexagonal cooling joints. The upper parts of the flows typically contain more vesicles, the flows are fractured in places, and lava tubes and other void spaces are present. A lava tube was encountered during drilling of the initial borehole for well 20(M) in the west part of the Bluewater site in 2012.

3.3.4.3 Zuni Canyon Flow

The Zuni Canyon flow consists of alkali-olivine basalt that originated from the Paxton Springs volcano, a small scoria cone within the Precambrian crystalline rocks in the core of the Zuni Mountains. It occurs as scattered remnants in Zuni Canyon where it flowed northeast down the canyon and spread out on the valley floor of the Rio San Jose south and southeast of Milan. The flow is as much as 50 ft thick south of Milan where it displays characteristics typical of an aa flow, and it covers part of the older El Calderon flow southwest of Grants. The flow has been determined to be about 20,700 years old (Dunbar and Phillips 2004).

3.3.5 Quaternary Deposits

Two types of unconsolidated alluvial deposits are represented in the region around the Bluewater site: ancestral Rio San Jose alluvium and surficial alluvium. The ancestral Rio San Jose alluvium is not exposed because it was buried by the Bluewater Basalt flows. The surficial alluvium includes thin material that has covered parts of the basalt flows and thicker material that has accumulated in areas outside the basalt flows, including the San Mateo Creek alluvium. Other Quaternary deposits include landslide (and slump), talus, and colluvial deposits around the flanks of Black Mesa and a small area of spring-deposited limestone (travertine) between Grants and San Rafael. The two alluvial deposit types are described below.

3.3.5.1 Ancestral Rio San Jose Alluvium

During the Middle and Late Pleistocene, stream courses in the region (Rio San Jose and San Mateo Creek) eroded to depths of 150 to 200 ft below the elevation of the present land surface. The ancestral Rio San Jose channel, which was cut into beds of the lower part of the Chinle Formation, follows a sinuous path southeastward that was controlled in places by the position of faults and uplifted blocks of resistant San Andres Limestone. Geologic cross sections A-A′ and C-C′ in Figure 10 and Plate 5 show the relationship of the ancestral Rio San Jose channel to the uplifted block of San Andres Limestone on the Bluewater site.

Alluvium accumulated in and along the Rio San Jose channel and attained a thickness of as much as 30 ft prior to being covered by flows of Bluewater Basalt beginning about 68,000 years ago. The thickness of the alluvium varies across the ancestral Rio San Jose valley; thicknesses found during drilling to install monitoring wells at the Bluewater site range from just a few feet to approximately 25 ft.

Ancestral Rio San Jose alluvium, indicated on the geologic cross sections as Qab, consists mainly of sand and gravel. The coarsest material (bed load) is in the base of channels, which contain coarse sand and gravel (poorly rounded clasts as large as 1-inch diameter). Finer-grained material (medium- and fine-grained sand and silt) is in shallower parts of channels and laterally away from channels. Composition of the sediment represents the nearby parent materials. Coarser gravels are composed of limestone, chert, and sandstone fragments, and a few Precambrian metamorphic clasts derived mostly from the Zuni Uplift to the southwest. Finer-grained sands are arkosic and are derived mostly from the Chinle Formation. Some distinct beds of laterally continuous sands and gravels occur.

Along the east, south, and southwest margins of the Bluewater Basalt flows, the underlying ancestral Rio San Jose alluvium merges laterally with a thicker sequence of surficial alluvium. This subsurface relationship at the east and southeast ends of the basalt flows is shown in the regional geologic cross sections A-A′ and B-B′, respectively, in Figure 9 and Plate 4.

3.3.5.2 Surficial Alluvium

Shown as Qal on the regional geologic map (Figure 7 and Plate 2) and Qa on the Bluewater site geologic map (Figure 8 and Plate 3), surficial alluvium consists of sand, gravel, and clay-silt deposited in fluvial (river), eolian, and lacustrine (lake) environments from the Middle Pleistocene to the present. Thickness is variable, depending on the presence or absence of basalt flows. Where basalt flows are not present, the alluvium may be 100 to 150 ft thick, as in the Homestake site area (represented by the San Mateo Creek alluvium), the area between Toltec and Milan, and the area northwest of the Bluewater site along the course of the present Rio San Jose north of Bluewater Village. In these areas, the age of the lowest part of the alluvium extends back to at least Middle Pleistocene time.

Fluvial deposits are generally sand to gravel sized and are represented along the present courses of the Rio San Jose, San Mateo Creek, the stream in Zuni Canyon, Bluewater Creek, and Mitchell Draw. Material from eolian deposition is Holocene age, is generally silt, covers parts of basalt flows, and covers the surface of open expanses such as the San Mateo Creek valley and the area north and northeast of the Bluewater main tailings disposal cell. Lacustrine deposition, of clay-silt size, is not exposed but is represented in the subsurface around and north of the Homestake site where the terminus of the Bluewater Basalt flows periodically blocked or dammed the flow of San Mateo Creek, creating intermittent lakes or playas. The Zuni Canyon basalt flow may have created a similar lacustrine depositional environment when it reached the valley of the Rio San Jose and likely blocked its flow.

4.0 Regional Hydrology

4.1 Surface Water

Streams in the study area include Bluewater Creek, Mitchell Draw, Rio San Jose, and San Mateo Creek. With the exception of Bluewater Creek, most reaches of the watercourses are dry throughout each year, largely because of the semiarid to arid climate of west-central New Mexico. Surface water flow in stream channels tends to occur only during large precipitation events in the region. The Rio San Jose, the dominant watercourse in the study area, has the potential under natural (undeveloped) conditions to maintain surface water flow along several miles of its main channel. However, flows in the river are rarely seen, primarily because it is heavily used for agriculture. Irrigation diversions of water from Bluewater Creek, the main source of flow to the Rio San Jose, cause most of the river between about 2 mi upstream of Bluewater Village and a few miles downstream of Grants to remain dry most of the time. As a result, the Rio San Jose is generally considered to be an ephemeral stream within the study area.

As previously mentioned, Bluewater Creek (Figure 3) is the only stream in the study area that tends to maintain perennial flows. The creek flows into Bluewater Canyon from Bluewater Lake, a reservoir about 5.5 mi upstream from where the creek empties into the Grants-Bluewater Valley. Flows in Bluewater Creek are diverted into an irrigation canal system about 0.5 mi south of the mouth of Bluewater Canyon at the base of the Zuni Mountains. About 1.3 mi downstream of the diversion structure (Figure 3), the Bluewater Creek channel joins Mitchell Draw, a typically ephemeral watercourse, to form the Rio San Jose. The combination of limited flows in both Mitchell Draw and Bluewater Creek downstream of the irrigation diversions explains the mostly ephemeral nature of the Rio San Jose in the Grants-Bluewater Valley.

In the northeast corner of the study area, the 4.5-mile reach of San Mateo Creek between the Cibola-McKinley county line and the large tailings disposal cell at GRP is considered an ephemeral stream. Six to 11 mi upstream of this reach, near and downstream of the community of San Mateo, the creek is fed by several springs, making year-round streamflow possible. El Rito Creek, also fed by springs, is a significant tributary to San Mateo Creek in this area (Figure 2). However, downstream of the confluence of the two creeks, seepage losses and water diversions for various purposes tend to limit flows in the main channel of San Mateo Creek. Farther downstream and about 3.5 mi north of the Cibola-McKinley county line, Arroyo del Puerto, an ephemeral watercourse that drains from the Ambrosia Lake mining area, is a significant tributary to San Mateo Creek. Because San Mateo Creek is ephemeral in the study area as well as just north of the Cibola-McKinley county line, surface water flows within the creek's drainage reach as far south as the Homestake site only during major flood events.

Despite the limited amount of surface water flow in the study area, surface watercourses have an impact on the hydrology of the Grants-Bluewater Valley. Seepage losses from Bluewater Lake and Bluewater Creek contribute recharge to both the alluvial aquifer and the San Andres aquifer. In addition, seepage losses from the irrigation canals fed by Bluewater Creek constitute recharge sources from about 3.5 mi north of Bluewater Village to variable distances downstream of the village. Unlike the reach of Bluewater Creek between the outlet of Bluewater Lake and the Grants-Bluewater Valley, the remaining watercourses draining the northeast flank of the Zuni Mountains are ephemeral. However, seepage losses from these drainages contribute significantly to groundwater recharge, especially in the San Andres aquifer near the base of the mountains.

Though San Mateo Creek is typically dry for several miles north of the Homestake site, the creek does play a role in the hydrology of the Grants-Bluewater Valley. Occasional floodwaters in the creek's drainage seep into underlying alluvium, contributing recharge to alluvial aquifer groundwater flowing south-southwestward to the Homestake site.

Historically, a spring called Ojo del Gallo, just north of San Rafael (Figure 3), was a significant source of surface water flow in the study area. In the 1930s, discharge from the spring of about 7 cubic feet per second (cfs) was common. Flow from Ojo del Gallo began declining in the mid-1940s due to increasing groundwater pumping for irrigation. During the period 1946 to 1953, flow from the spring decreased from about 4.5 cfs to a rate that was insufficient for irrigation of gardens (Baldwin and Anderholm 1992). Discharge from the spring was absent from 1954 to 1982, but some flow did return to the spring's outlet in the mid-1980s. Virtually no flow has been observed at Ojo del Gallo during the past two decades.

Discharges at Ojo del Gallo (Figure 3) are caused by blockage of southward-migrating groundwater in the San Andres aquifer due to vertical offset of geologic units at the San Rafael Fault (Frenzel 1992). The flows from the spring have changed with time because of variable hydrologic stresses on the San Andres aquifer. Above-average precipitation in the study area can result in more recharge to the aquifer, which increases the spring's discharge, whereas years of low precipitation and recharge to the aquifer cause decreases in spring flow. Similarly, decreases in hydraulic head due to extensive groundwater pumping in the region, which began in the mid-1940s and increased in the 1950s, reduces discharge at Ojo del Gallo.

4.2 Hydrogeologic Units

Given the limited flows in streams within the study area, groundwater is the most dependable and most heavily accessed source of water in Cibola County. Sections 4.2.1 through 4.2.7 describe the roles that geologic formations in the study area play in forming the regional groundwater system.

4.2.1 Quaternary Alluvium

The alluvial aquifer in the Grants-Bluewater Valley consists primarily of Quaternary-age alluvium. The expression "alluvial aquifer" is also sometimes used to describe saturated subsurface flow within both the alluvium and overlying basalt.

Other than the extraction of alluvial groundwater for remediation purposes at the GRP, most of the water withdrawn from the alluvial aquifer is for agricultural needs. In much of the study area, saturated alluvium rests on the Chinle Formation, which is generally considered to be an aquitard. Accordingly, the alluvial aquifer is not in direct hydraulic connection with the San Andres aquifer in parts of the Grants-Bluewater Valley where the Chinle Formation is present. In areas where the Chinle Formation is absent, the alluvium lies directly on the San Andres Limestone, facilitating direct hydraulic connection between the two aquifers. Near the base of the Zuni Mountains, the Chinle Formation is mostly absent. The occurrence of alluvium directly overlying the San Andres Limestone depends on the location of and vertical displacement of strata along faults.

The alluvial aquifer occurs in three general areas. Much of the aquifer consists of sands, gravels, silts, and clays deposited along a northwest-southeast alignment beneath and adjacent to the current channel of the Rio San Jose, near the base of the Zuni Mountains. These sediments are referred to in this report as recent Rio San Jose alluvium, or recent river alluvium. The area containing recent river alluvium is several miles long, extending from near the confluence of Bluewater Creek and Mitchell Draw to the east end of Grants. The thickness of the recent river alluvium varies from about 100 to 150 ft. A geologic map prepared by Hydro-Search (1981a) for the Grants-Bluewater Valley suggested that recent river alluvium in areas at the base of the mountains west of the Bluewater site directly overlie the San Andres Limestone. Such areas of direct contact between the alluvium and the San Andres Limestone are found at the mouth of Bluewater Canyon and near Bluewater Village. A much larger area in which alluvium appears to directly overlie the San Andres Limestone at the base of the mountains occurs from about 1 mi north of Toltec to about 1 mi south of Milan (Plate 7).

Another major portion of the alluvial aquifer occurs within sediments that were deposited by the ancestral Rio San Jose and are now covered by Bluewater Basalt. Lying northeast of the recent Rio San Jose alluvium, these deposits are called ancestral Rio San Jose alluvium, or ancestral river alluvium. The ancestral Rio San Jose alluvium extends southeastward from the north boundary of the study area to areas underneath the Bluewater site, and terminates about 4 mi east-southeast of the main tailings impoundment, near the West Branch of the San Mateo Fault. The thickness of the ancestral river alluvium at wells in the vicinity of the Bluewater site ranges from about 5 to 35 ft.

The third area containing alluvial sediments considered part of the regional alluvial aquifer is associated with San Mateo Creek, in the east half of the Grants-Bluewater Valley. This alluvium was deposited by San Mateo Creek over thousands of years and is commonly referred to as San Mateo Creek alluvium. Much of the alluvium associated with the creek consists of materials eroded from the Chinle Formation and younger formations in the drainage basin, including uranium-ore-bearing formations. The San Mateo Creek alluvium extends from the northeast corner of the study area to the GRP, and then on to the Rio San Jose just north of Milan. Saturated alluvium upgradient of the GRP is about 1.5 to 2 mi wide, and it expands to about 3 to 4 mi wide in the vicinity of the large tailings disposal cell at the Homestake site. Near its intersection with ancestral and recent Rio San Jose alluvium, the San Mateo Creek alluvium is as much as 5 mi wide. However, a significant portion of the subsurface in this widened portion of the alluvium is unsaturated due to the presence of a buried ridge of the Chinle Formation, which is the bedrock underlying the alluvium in the GRP. The thickness of San Mateo Creek alluvium in the vicinity of the Homestake site varies from about 50 to 150 ft, and saturated thickness in the alluvium at and near the Homestake site ranges from 0 to about 100 ft.

The transmissivity of the alluvial aquifer varies widely depending primarily on the grain size and the saturated thickness of the alluvial sediments. Aquifer-test data collected from pumping and monitoring wells in the Grants-Bluewater Valley indicate that the aquifer's transmissivity ranges from about 50 to 350,000 square feet per day (ft^2/day). Dividing these values by corresponding aquifer thicknesses at sites where aquifer tests have been performed results in aquifer hydraulic conductivities that range from 0.2 ft/day to 700 ft/day. Estimated hydraulic conductivities for alluvium in the vicinity of the Bluewater site range from 75 to 150 ft/day. Reported values for hydraulic conductivity of San Mateo Creek alluvium tend to be lower than those ascribed to alluvium deposited by the ancestral and recent Rio San Jose and typically range from

10 to 70 ft/day. However, hydraulic conductivities as large as 300 ft/day have been measured in a paleochannel containing San Mateo Creek alluvium directly west of the large tailings disposal cell at the Homestake site (HMC 2012).

The higher values of hydraulic conductivity in recent and ancestral Rio San Jose alluvium are associated with high-energy sand and gravel deposits along paleochannels of the river, whereas the lower values of hydraulic conductivity are attributed to finer-grained deposits in non-channel, overbank environments. The paleochannel containing San Mateo Creek alluvium just west of the large tailings disposal cell at the Homestake site also contains sands and gravels deposited in a high-energy fluvial environment.

The alluvial aquifer has been described as unconfined in some locations and confined in others. Confined conditions appear to occur where groundwater levels in ancestral Rio San Jose alluvium exceed the base elevation of overlying Bluewater Basalt. Relatively large depths to saturated alluvium (100 ft or more) at the Homestake site, including areas miles to the north of the large tailings disposal cell, suggest that groundwater in San Mateo Creek alluvium might be at least partially confined by shallower, less permeable strata (e.g., lacustrine deposits). In contrast, unconfined conditions would be expected where depth to groundwater is small (e.g., less than 30 ft), or where the water level in ancestral Rio San Jose alluvium falls below the base elevation of overlying Bluewater Basalt.

Where unconfined, the alluvial aquifer's specific yield is between 0.1 and 0.25 (dimensionless). Where confined, the storativity of the alluvial aquifer is reported to be about 1×10^{-3} (dimensionless). Numerous livestock and domestic (drinking water or household use) wells are completed in Quaternary alluvium (Baldwin and Anderholm 1992).

4.2.2 Basalts

In areas where hydraulic heads in ancestral river alluvium are higher than the base of overlying Bluewater Basalt, groundwater has the potential to flow horizontally within both the alluvium and the basalt. Such combined flow becomes apparent where the basalt is relatively permeable due to presence of fractures. Saturated volcanic rock in such areas is capable of yielding large quantities of water to wells. In some reports that discuss the hydrology of the Grants-Bluewater Valley, the coupled alluvium and basalt are referred to as the basalt-alluvium aquifer, whereas in others, they are simply called the alluvial aquifer. The latter convention is used in this report. In areas where the permeability of the basalt is very low, the basalt tends to act more as a confining layer for the underlying alluvium rather than an extended part of the alluvial aquifer.

Historically, saturated basalt in the region has been an important water resource. Springs reportedly issue from basalts along the margins of mesas near Grants (Baldwin and Rankin 1995), providing water for stock and domestic use.

4.2.3 Chinle Formation

The Chinle Formation generally acts as a confining unit, or aquitard, between the alluvial aquifer and the San Andres aquifer. The capacity of the Chinle to locally confine groundwater in the San Andres aquifer depends on its thickness and lithology. In areas where the San Andres aquifer is confined, the clay content within the Chinle causes the rocks to deform and squeeze in, thus

preventing upward or downward flow of groundwater across the formation (Baldwin and Anderholm 1992). The tendency of clay zones in the Chinle to squeeze in on fractures has been observed during the drilling of test holes that penetrate as deep as the San Andres Limestone.

In much of the study area, the Chinle Formation is unsaturated because of its low permeability. Where it is saturated, the Chinle is typically too fine-grained to transmit sufficient water to be considered an aquifer. However, water yields from some of the more sandy units of the Chinle are sometimes adequate for supplying domestic or stock water (Baldwin and Anderholm 1992).

Hydraulic properties of the Chinle Formation are based on reported values in hydrologic literature. Reported values for hydraulic conductivity in a formation of this kind are highly variable, ranging from 10^{-8} to 0.1 ft/day (Baldwin and Rankin 1995). Recharge to Chinle rocks in areas where it is possible occurs mostly by downward seepage of alluvial aquifer water into upper parts of the formation. Some seepage of water through the Chinle Formation (inter-aquifer leakage) is reported to occur near the base of the Zuni Mountains, in areas where the Chinle is relatively thin. Studies of the San Andres aquifer by the USGS (e.g., Baldwin and Anderholm 1992) suggest that pumping groundwater from the aquifer in areas where it underlies Chinle Formation rock has the potential to induce downward seepage of Chinle Formation water into the pumped horizons.

4.2.4 San Andres Aquifer

The San Andres aquifer is the most productive aquifer in the study area and the primary water source for municipal, commercial, irrigation, domestic, and livestock uses. The San Andres Limestone and the Glorieta Sandstone are generally treated as one aquifer, partly because the contact between them is gradational and difficult to identify. In addition, good hydraulic connection between the two units suggests that they can be collectively thought of as a single aquifer.

Though the San Andres Limestone is called a limestone, it consists mostly of sandstone in the vicinity of the Bluewater site. A map of limestone thicknesses in White and Kelly (1989) indicates that the cumulative thickness of limestone facies in the formation near Bluewater Village is less than 50 ft, with the remaining thickness of the San Andres Limestone consisting of sandstone facies. Given that the thickness of the San Andres Limestone in the vicinity of the Bluewater site varies between about 120 and 160 ft, sandstone in the formation at and near the site generally constitutes more than half the full formation thickness Though sandstone is more prevalent than limestone in the San Andres aquifer in the study area, regional and local hydrogeologic studies indicate that the largest amounts of water in the San Andres Limestone, and the San Andres aquifer as a whole, are transmitted in solution channels, cavernous zones, and fractures, which are characteristic of a karst environment. The channels, zones, and fractures appear to be well connected in the Grants-Bluewater Valley and are most developed near the Zuni Mountains. Karst features are abundant near the base of the mountains because limestone there was subjected to weathering, dissolution, and fracturing during periods of uplift and exposure (White and Kelly 1989). Areas of the San Andres Limestone farther from and north of the mountains have been less affected by these processes.

Karst horizons in the San Andres Limestone are attributed to geologic events of significant erosion (White and Kelly 1989). One such event occurred at the conclusion of the Permian

Period, which eventually helped lead to the filling of solution channels and cavities by Chinle Formation sediments. In some parts of the study area, prolonged erosion removed most or all of the San Andres Limestone and exposed the Glorieta Sandstone prior to deposition of Chinle materials in Triassic time. Erosion removed much of the upper part of the San Andres Limestone where it is exposed east of the main tailings impoundment and just north of the East-West Fault.

The combined thickness of the San Andres Limestone and the Glorieta Sandstone at the Bluewater site generally varies between about 250 and 350 ft (see Section 5.3). For calculation purposes, the mean thickness for the combined formations is assumed in this chapter to be 300 ft. Though porous medium flow of groundwater through the sandstones of the Glorieta is not as large as flow through solution channels in limestones of the San Andres, the sandstones are nevertheless much more permeable than regional formations dominated by shales, siltstones, and evaporite facies and are thus capable of transmitting relatively large quantities of subsurface water. In addition, fractures in the Glorieta Sandstone add secondary permeability, increasing the amount of flow through the sandstone.

Aquifer testing performed at wells screened in the San Andres aquifer typically attribute measured transmissivities to the combined thickness of the San Andres Limestone and Glorieta Sandstone, despite the fact that many wells in the aquifer tap only the uppermost 40 to 50 ft of the San Andres Limestone. Estimated transmissivity values from the testing are highly variable, ranging from 10 to 450,000 ft^2/day (Frenzel 1992, Baldwin and Rankin 1995). Using aquifer-test results, information on lithology of and saturated thicknesses in San Andres aquifer sediments, and potentiometric surface maps for the aquifer, Baldwin and Anderholm (1992) divided their region of study into seven transmissivity zones. Of those, two zones apply to almost the entire study area. A third transmissivity zone relevant to this conceptual model study is located in the southeast corner of the study area, on the southeast side of the San Rafael Fault.

One of the transmissivity zones identified by Baldwin and Anderholm (1992) occupies a north-south trending area on the west side of the Ambrosia Lake Fault that is about 5 mi wide (from Ambrosia Lake Fault to within a mile of the study area's west boundary). Though hydraulic testing of a well in this zone yielded a transmissivity of 24,000 ft^2/day, the zone was assigned a representative transmissivity of 10,000 ft^2/day. Baldwin and Anderholm (1992) surmised that wells drilled in this area west of the Bluewater site would not encounter a significant amount of limestone, and that the transmissivity values used to represent it were generally reflective of the Glorieta Sandstone, including fractured sandstone.

The San Andres aquifer transmissivity zone located east of the Ambrosia Lake Fault has some of the highest transmissivity values identified by Baldwin and Anderholm (1992), with the largest value being 450,000 ft^2/day. Extending east-southeastward to the San Rafael Fault, this zone was considered one of the most permeable due to the presence of cavernous zones, solution channels, and fractures in the aquifer. Reported well yields in this part of the study area can be as large as 2,800 gallons per minute (gpm), which is equivalent to 6.25 cfs. Though such pumping rates tend to be observed in wells that are associated with some of the largest transmissivity values measured in the aquifer, hydraulic testing at other wells in this zone resulted in estimated transmissivities as small as 100 ft^2/day. This demonstrated that San Andres aquifer transmissivities in the area lying between the Bluewater site and Grants can be quite variable. A map of posted aquifer-test results in Baldwin and Anderholm (1992) suggested that the largest transmissivity values are encountered near the base of the Zuni Mountains, and values become

less with distance north of the mountains. A transmissivity of 50,000 ft^2/day was considered by Baldwin and Anderholm (1992) to be representative of the transmissivity zone between the Ambrosia Lake Fault and Grants.

Baldwin and Anderholm (1992) reported that calculated transmissivity values for the zone in the southeast corner of the study area ranged from 70 to 200,000 ft^2/day. The larger transmissivity values were again attributed to cavernous or highly fractured zones in limestone. In addition to the large transmissivities identified through aquifer hydraulic testing, physical evidence for cavernous limestone rock was seen in some wells drilled in areas east of the San Rafael Fault. However, the wells with such physical evidence were outside the study area, either to the east or south of the study area's border. Baldwin and Anderholm (1992) selected a transmissivity of 50,000 ft^2/day as being representative of this zone.

Estimated hydraulic conductivities for the San Andres aquifer in the Grants-Bluewater Valley vary from about 0.25 to 1,800 ft/day (Baldwin and Rankin 1995). In comparison, Freeze and Cherry (1979) reported that a range of 1 to 10,000 ft/day is representative of hydraulic conductivity of cavernous limestone. Compilations of hydraulic properties for numerous karst aquifers presented in Huntoon (1995) and Worthington and Ford (2009) suggest that hydraulic conductivities in most cases range from 1 to about 3,000 ft/day.

In most parts of the study area, groundwater flow in the San Andres aquifer occurs under confined conditions. The aquifer storage parameter of interest in a confined aquifer is storativity, whereas the relevant storage parameter in an unconfined aquifer is specific yield. Storativity is calculated as the product of the aquifer's thickness and its specific storage, the latter of which is defined as the volume of water released from storage from a unit volume of aquifer under a unit decline in hydraulic head. USGS studies of the San Andres aquifer (Baldwin and Anderholm 1992, Frenzel 1992) reported that measured storativity values from aquifer hydraulic tests at wells screened in the San Andres aquifer were frequently on the order of 1×10^{-4} to 5×10^{-4}, and that the full range of measured storativities was from about 5×10^{-5} to 0.01. The high end of this range is relatively large for storativity and is probably more representative of a specific yield at a well that tends to respond to aquifer stresses, such as pumping, as if it were unconfined. In contrast, the low storativity value in the cited range is reflective of water being released from a confined aquifer because its matrix and the groundwater in it are slightly compressible. Dividing the low storativity value in the cited range by 300 ft, the estimated thickness of the San Andres aquifer at the Bluewater site, results in a specific storage of 1.7×10^{-7} ft^{-1}. This value is typical of specific storage in unfractured sandstones (Freeze and Cherry 1979).

The effective porosity of an aquifer affects the rate at which groundwater moves through it. Hydrologic assessments of the San Andres aquifer in the past have used variable estimates of its effective porosity, ranging from 0.02 to 0.25. The low end of this range was chosen to represent secondary permeability and porosity features of limestone that contains fractures and solution channels (Dames & Moore 1984a, 1986a). In comparison, the maximum value for the effective porosity is usually meant to be representative of water migrating in the pores between individual sand grains in unfractured sandstone layers. For a given hydraulic conductivity and horizontal hydraulic gradient, calculation of the average linear velocity of groundwater using the maximum value of effective porosity results in a value that is much lower than the water velocity in solution channels and fractures within limestone.

It is important in this conceptual model study to account for the highest velocities of groundwater in the San Andres aquifer, since these high velocities dictate when contaminants are first observed at specific locations downgradient of the Bluewater site, which lie east and southeast of the site. With this understanding, calculated velocities in limestone containing fractures and solution channels are best estimated using effective porosities that are relatively small, such as less than or equal to 0.05. Calculated velocities in fractured sandstone are also best estimated using relatively low effective porosities because most of the cross-sectional area of flow in fractured sandstone is typically taken up by matrix as opposed to fractures. In contrast, use of the high effective porosity of 0.25 mentioned above is probably more appropriate for estimating groundwater velocity in unfractured sandstone within the San Andres aquifer. However, it is also likely that the effective porosity of unfractured sandstone in portions of the San Andres aquifer is lower than 0.25 due to the presence of calcareous and silica cements between individual sand grains (e.g., see Section 3.3.2.3).

Rather than assuming that a single value of hydraulic conductivity and a single effective porosity apply to the entire vertical thickness of the San Andres aquifer at any given location, it is assumed in this conceptual model study that these parameters vary, both increasing and decreasing, with depth in the aquifer. With this conceptualization, horizontal water velocities and contaminant concentrations will also vary with depth in the aquifer. As a result, the contaminant concentration measured at a well screened over the full aquifer thickness at a location downgradient of a contaminant source will represent a mixture of different concentrations that are fed into the well at different rates. An assessment of estimated average linear velocities in the San Andres aquifer in Section 4.3.3.2 further examines how variable hydraulic properties of the aquifer media affect rates of transport to specific locations east and south of the Bluewater site.

4.2.5 Yeso Formation

The Yeso Formation is not a major source of groundwater in Cibola County. Reported transmissivities for the formation tend to be less than 1,000 ft^2/day (Baldwin and Anderholm 1992), indicating that hydraulic conductivity values for the formation are typically low. Water-level and well-yield data are generally not available for the Yeso Formation.

4.2.6 Abo Formation

The Abo Formation is not a significant source of water in the study area, largely because of low permeabilities and high mineral contents in anhydrite and gypsum strata composing much of this bedrock unit. The Abo Formation occurs at depths greater than 3,000 ft in much of the study area (Baldwin and Rankin 1995), which hinders attempts to drill wells into the formation in search of a groundwater resource. Attempts to measure hydraulic conductivity in the Abo and Yeso formations have resulted in estimates that range from 1×10^{-4} to 0.01 ft/day (Baldwin and Anderholm 1992).

4.2.7 Precambrian Rocks

The Precambrian rocks underlying Permian formations contain very limited amounts of groundwater. In the Zuni Mountains, groundwater in these rocks is occasionally encountered in saturated faults or fracture zones (Baldwin and Rankin 1995). Alternatively, limited amounts of subsurface water are sometimes present in weathered material within the uppermost 200 to 300 ft of Precambrian rock. In areas that are not faulted or fractured, the hydraulic conductivity of the rocks is very small, and virtually no water is transmitted.

4.3 Regional Groundwater Flow System

4.3.1 Recharge and Discharge

4.3.1.1 Alluvial Aquifer

Under natural conditions, recharge to the alluvial aquifer is from direct precipitation on the alluvium, direct precipitation on the Bluewater Basalt that quickly seeps through the basalt to underlying alluvium, seepage losses from streams and other surface water features, infiltration of occasional surface water flow during and after storm events, and upward leakage from the San Andres aquifer where its hydraulic heads are larger than those in overlying alluvium. Additional sources of recharge were created when settlers began to populate the Grants-Bluewater Valley. The anthropogenic sources of subsurface water included seepage of water from irrigation canals and infiltration of irrigation water applied to the land surface.

Though mill-related forms of recharge, such as downward seepage of water from the main tailings impoundment, appeared to occur in earlier years at the Bluewater site, this form of recharge appears to have declined greatly since injection of tailings waste fluid began in 1960. Recharge from downward seepage of tailings fluids has decreased even more since site decommissioning in the 1990s.

Groundwater levels in the alluvial aquifer suggest that direct recharge to the aquifer from stream seepage occurs along a reach of Bluewater Creek that extends about 0.5 mi south from the mouth of Bluewater Canyon to the irrigation diversion structure (Figure 3). When flows in Bluewater Creek are sufficiently large to allow flow in the creek channel downstream of the diversion structure, recharge to the alluvial aquifer from creek seepage losses also likely takes place. This also holds true for the Rio San Jose channel downstream of the confluence of Bluewater Creek and Mitchell Draw. Occasionally, streamflow downstream of the diversion structure is large enough to deliver surface water to an abandoned borrow pit located directly south of the Bluewater site (Figure 3), in an area just south of Highway 122 and directly west of Bluewater production wells Anaconda #3 and Anaconda #4 (Figure 4 and Figure 16). The borrow pit is considered a recharge source (Hydro-Search 1981a, Frenzel 1992), as are reaches of the Rio San Jose downstream of the pit when flows in the river are high enough to deliver water that far downstream. In addition to seepage from Bluewater Creek and the Rio San Jose, surface water losses from irrigation canals contribute substantially to the alluvial aquifer downstream of the major diversion structure on Bluewater Creek.

Under natural conditions, recharge to the alluvial aquifer due to upward leakage from the San Andres aquifer tends to occur in an irregularly shaped area extending from about 1 mile north of Toltec to Grants. Upward flow from the bedrock aquifer is possible here because the Chinle Formation is absent, so that the alluvial aquifer directly overlies the San Andres Limestone.

Upward hydraulic gradients from the bedrock aquifer to the alluvium are created in this area because of accumulating recharge to the San Andres aquifer from precipitation on the nearby Zuni Mountains.

Recharge to the alluvium on the east end of the Grants-Bluewater Valley can be attributed to injection wells and trenches used by HMC on the south end of the Homestake site. In addition, irrigation conducted by HMC on land south and west of the large tailings disposal cell as part of the GRP contributes recharge to the alluvial aquifer.

Though not specifically called recharge, a large amount of alluvial aquifer flow in the Grants-Bluewater Valley is attributed to groundwater inflow from areas bordering the study area. Such subsurface inflow occurs along a 3-mile stretch of the study area's north boundary that lies north-northwest of the Bluewater site. Subsurface inflow to the alluvial aquifer also occurs in the northeast corner of the study area via south-southwestward-migrating groundwater in San Mateo Creek alluvium.

Discharge from the alluvial aquifer takes place through various mechanisms. Much of it is attributed to evapotranspiration in agricultural areas and groundwater withdrawal by wells. Downward leakage of alluvial aquifer groundwater to the San Andres aquifer is also possible in areas where hydraulic heads in the former are larger than underlying heads in the San Andres aquifer. Such downward gradients occur in the recent Rio San Jose alluvium between the mouth of Bluewater Canyon and about 4 mi downstream of the irrigation diversion structure. In addition, downward groundwater migration from the alluvial aquifer to the San Andres aquifer via a branch of the San Mateo Fault has been mentioned as a possibility at the GRP (EPA 2011) despite the local presence of 500 ft or more of the Chinle Formation between the two aquifers. Downward seepage of groundwater into the San Andres aquifer appears to occur in the vicinity of Milan's northernmost municipal wells because pumping of the wells caused a reversal of the local vertical hydraulic gradient.

Discharge of groundwater from the alluvial aquifer to streams in the Grants-Bluewater Valley is minimal to nonexistent. An area where such discharge is known to occur is the Rio San Jose at Horace Springs, which is east of Grants and beyond the east boundary of the study area.

4.3.1.2 San Andres Aquifer

Recharge to the San Andres aquifer occurs on outcrops of sandstone and limestone in the Zuni Mountains southwest of the Grants-Bluewater Valley, by either direct precipitation on or surface water flow across rock outcrops. This type of recharge also occurs along the east side of the Zuni Mountains, above San Rafael. Frenzel (1992) identified five different recharge zones in the Zuni Mountains, three of which affect the San Andres aquifer in the study area. Two of the recharge zones lie within the study area, and the third is located west of the study area's west boundary, in an area south of Bluewater Lake. As part of a groundwater modeling study, Frenzel (1992) developed temporally varied recharge rates for the recharge zones for the water years 1932 to 1985. The method employed for this purpose was quite detailed and involved cumulative precipitation totals for each 6-month period during the 54 water years. The methods employed to estimate these time-varying recharge quantities on the Zuni Mountains are beyond the scope of this conceptual modeling study. The average recharge flux from this recharge source was about 0.1 cfs, or 44.8 gpm, per mile of mountain front.

Another major source of recharge to the San Andres aquifer originates as leakage of water from Bluewater Lake (Frenzel 1992), which enters outcrops of San Andres aquifer rock. This recharge first occurred around the start of the 20th century due to the presence of an earthen dam that created the lake, and it has occurred regularly since 1927, when a concrete dam was constructed to hold the lake water. The manner in which the leaked lake water ends up as recharged groundwater in the aquifer is complex, as some of the leakage flows back into Bluewater Creek just downstream from the dam (Frenzel 1992). Despite this return flow to the creek, net inflow to the San Andres aquifer from Bluewater Lake leakage is large and a major source of recharge in the Grants-Bluewater Valley.

In addition to the recharge from sources on the Zuni Mountains, subsurface inflow along the north boundary of the study area likely contributes to groundwater flow in the San Andres aquifer. It is difficult to assess this groundwater source, however, because most equipotentials for the aquifer trend north-south in the vicinity of the north boundary, indicating that flow here is directly to the east rather than to the southeast.

A large amount of the discharge from the San Andres aquifer occurs in the form of groundwater extraction for agricultural, municipal, and commercial purposes. Additional outflow is attributed to spring discharge and upward leakage into the alluvial aquifer, particularly in areas where the Chinle Formation is absent. Historically, a large amount of discharge from the San Andres aquifer was attributed to spring discharge at Ojo del Gallo near the San Rafael Fault.

Evapotranspiration from the San Andres aquifer is considered to be a minor form of aquifer discharge in this study. Equipotentials for the aquifer in the easternmost third of the Grants-Bluewater Valley suggest that subsurface outflow across the east boundary of the study area constitutes a large amount of aquifer discharge. A lesser amount of subsurface outflow appears to take place across the south boundary of the study area south of Grants.

4.3.2 Information Sources Relevant to Groundwater Flow

Groundwater flow in the alluvial and San Andres aquifers was analyzed using water level data from wells screened in each of the aquifers. Several different information sources were accessed to gather these data, beginning with consultant reports on the hydrology of the Bluewater site in the late 1970s (Hydro-Search 1977, 1978, 1981a). More recent water level data were derived from monitoring reports by additional consultants and ARCO through the mid-1990s. DOE has been collecting groundwater level data at multiple locations since 1997. Additional water level data for wells monitored by HMC in the east half of the Grant-Bluewater Valley have been tabulated in annual monitoring reports for the Homestake site (e.g., HMC and Hydro-Engineering 2013). Historical water level data dating back to the 1940s are also available for 13 wells in the Grants-Bluewater Valley that USGS has monitored and continues to monitor.

Data from the above-mentioned information sources were used to establish a network of wells in the Grants-Bluewater Valley in this study for the purpose of compiling water level and water chemistry data that assist in developing a regional conceptual model. The locations of the wells that make up the network are shown in Figure 16 through Figure 19 for four sub-areas within the entire study area. Plate 7 presents a single map showing all well locations. Because the monitoring locations were drawn from a variety of studies, several of the wells are identified by more than one label. Appendix B presents a list of all monitoring locations, their spatial coordinates, and a cross-reference of all the labels used to identify the wells.

4.3.3 Potentiometric Surfaces

Groundwater flow in the ancestral and recent river deposits within the alluvial aquifer is generally in the same direction as surface water flow in the Rio San Jose drainage. Water moves southward in the alluvium from where the aquifer crosses the north boundary of the study area, then turns to the southeast and east-southeast in the area where Bluewater Creek discharges from Bluewater Canyon and contributes recharge to the aquifer. Groundwater in the San Mateo Creek alluvium, migrating southwest, merges with Rio San Jose alluvial groundwater at multiple locations north of Milan. As part of a study of regional groundwater flow, Hydro-Search (1981a) developed a potentiometric surface for the alluvial aquifer based on water level data collected at several wells in 1980. A slightly modified version of the surface, presented in Figure 20, illustrates flow directions in the alluvial aquifer under hydrologic conditions that existed more than 30 years ago.

A more recent illustration of groundwater levels in the alluvial aquifer was developed by coupling water elevation data collected by DOE at monitoring wells on and near the Bluewater site with alluvial aquifer water level data published by HMC for the GRP in 2012 (HMC and Hydro-Engineering 2013). The results of this latter effort, presented in Figure 21, suggest that groundwater levels in 2012 in the vicinity of the Bluewater site were, on average, slightly lower than those observed in 1980. In contrast, groundwater levels in the vicinity of the GRP appear to have been slightly higher in 2012 than in 1980.

The use of water elevation data from the GRP to prepare Figure 21 provides insight into groundwater flow in ancestral Rio San Jose alluvium in areas outside the Bluewater site. Water level data from seven wells monitored by HMC assist in discerning the flow direction in offsite areas as well as the location of a distinct paleochannel in the ancestral river alluvium. The interpretation resulting from the combined data sets, as expressed by water elevation contours in Figure 21, suggests that the paleochannel extends about 1 mi southeastward from the southeast corner of the Bluewater site before merging with San Mateo Creek alluvium. Bluewater-site wells T(M), 22(M), X(M), and 21(M) appear to lie within the paleochannel, as do GRP wells 636, 637, and 686 in offsite areas (Figure 21).

In addition to providing information regarding flows in the ancestral river alluvium, Figure 21 reveals that conceptualization of groundwater pathways and flow directions in the San Mateo Creek alluvium has changed somewhat over the past 30 years. To better illustrate those changes, a separate map showing measured hydraulic heads in the alluvial aquifer in the vicinity of the Homestake site, as modified from a map included in an annual GRP report (HMC and Hydro-Engineering 2013), is reproduced in Figure 22. This figure shows that the most obvious change in the alluvial aquifer potentiometric surface in recent years is observed in an area about 1.5 mi southwest of the Homestake site's large tailings disposal cell. Monitoring data from this area indicate that groundwater flows around either end of a 2 mi long, buried bedrock ridge of the Chinle Formation, or bedrock high, in the base of the aquifer. This observation in turn signifies that flow in the San Mateo Creek alluvium merges with flow in Rio San Jose alluvium at two separate locations (Figure 21 and Figure 22). The first location is about 1 mi southeast of the Bluewater site, as discussed in the previous paragraph. The second location is about 2 mi south-southwest of the large tailings disposal cell at the Homestake site and approximately 1.5 mi directly east of Toltec. This updated conceptualization affects the interpretation of how contaminant plumes in the ancestral Rio San Jose alluvium originating at the Bluewater site merge with those migrating from the Homestake site.

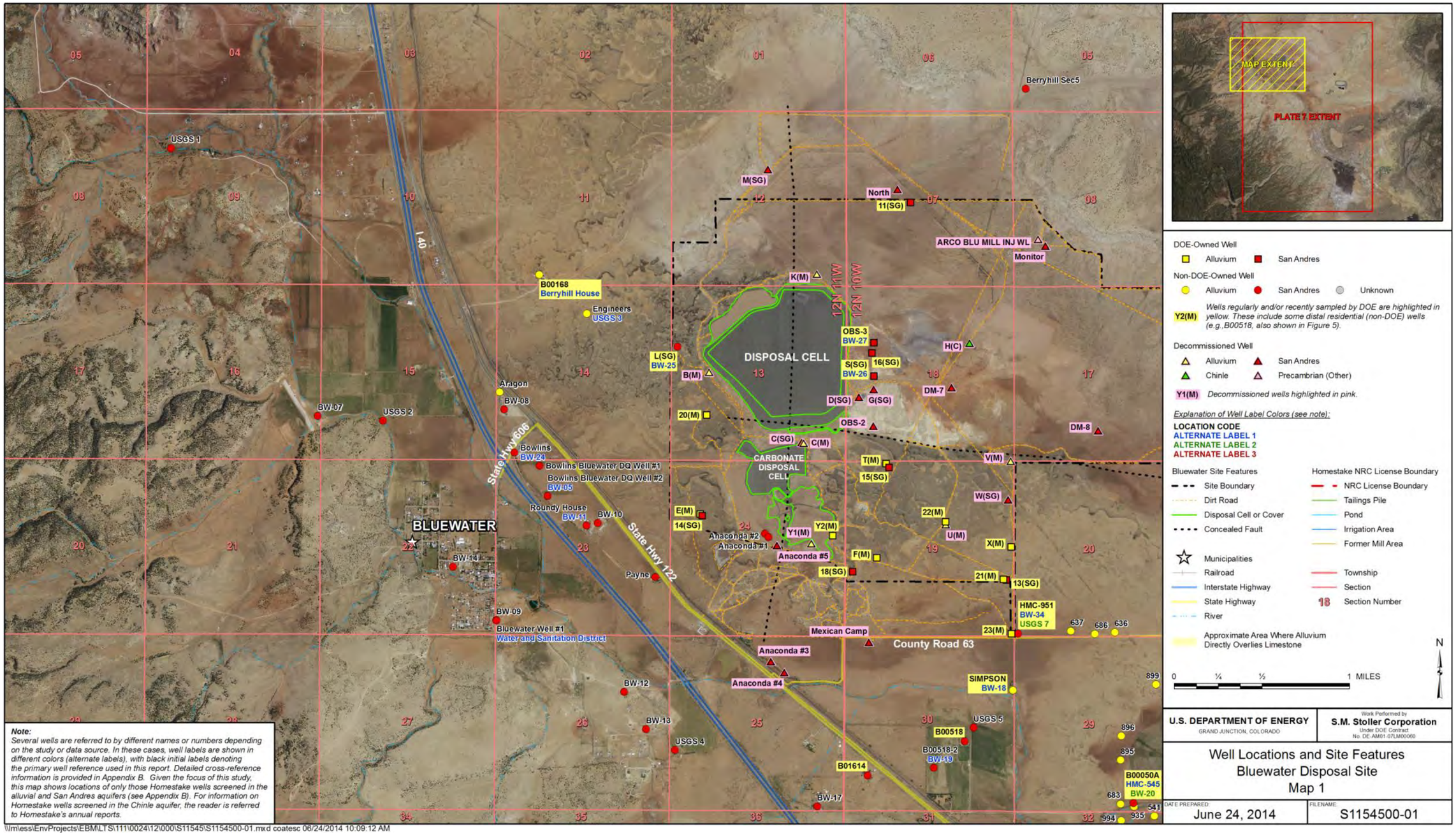

Figure 16. Monitoring Wells in the Study Area, Map 1 of 4

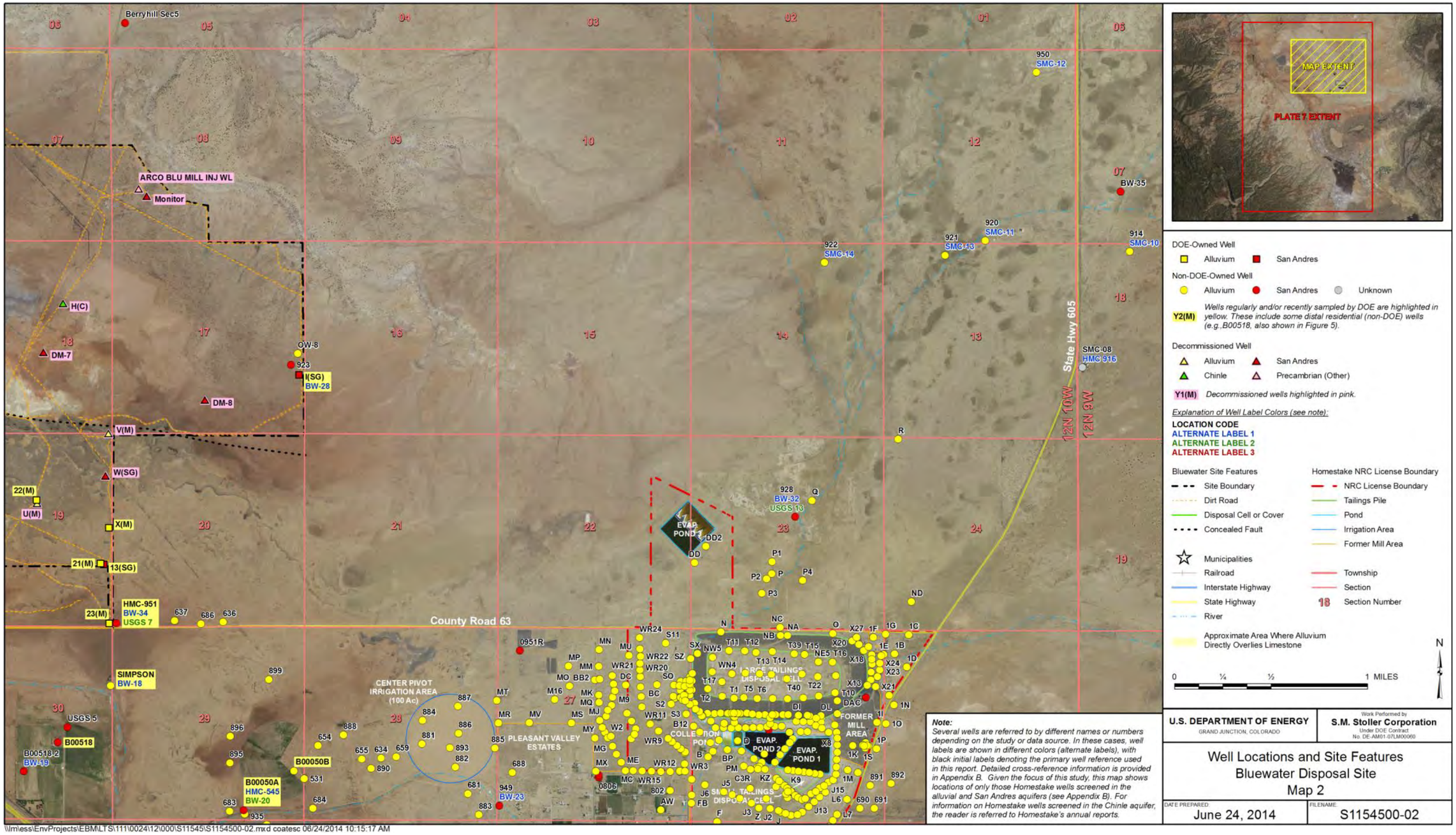

DOE-Owned Well
- Alluvium
- San Andres

Non-DOE-Owned Well
- Alluvium
- San Andres
- Unknown

Y2(M) *Wells regularly and/or recently sampled by DOE are highlighted in yellow. These include some distal residential (non-DOE) wells (e.g.,B00518, also shown in Figure 5).*

Decommissioned Well
- Alluvium
- San Andres
- Chinle
- Precambrian (Other)

Y1(M) *Decommissioned wells highlighted in pink.*

Explanation of Well Label Colors (see note):

LOCATION CODE
ALTERNATE LABEL 1
ALTERNATE LABEL 2
ALTERNATE LABEL 3

Bluewater Site Features
- Site Boundary
- Dirt Road
- Disposal Cell or Cover
- Concealed Fault
- Municipalities
- Railroad
- Interstate Highway
- State Highway
- River
- Approximate Area Where Alluvium Directly Overlies Limestone

Homestake NRC License Boundary
- NRC License Boundary
- Tailings Pile
- Pond
- Irrigation Area
- Former Mill Area
- Township
- Section
- 18 Section Number

N

0 ¼ ½ 1 MILES

Note:
Several wells are referred to by different names or numbers depending on the study or data source. In these cases, well labels are shown in different colors (alternate labels), with black initial labels denoting the primary well reference used in this report. Detailed cross-reference information is provided in Appendix B. Given the focus of this study, this map shows locations of only those Homestake wells screened in the alluvial and San Andres aquifers (see Appendix B). For information on Homestake wells screened in the Chinle aquifer, the reader is referred to Homestake's annual reports.

U.S. DEPARTMENT OF ENERGY
GRAND JUNCTION, COLORADO

Work Performed by
S.M. Stoller Corporation
Under DOE Contract No. DE-AM01-07LM00060

Well Locations and Site Features
Bluewater Disposal Site
Map 2

DATE PREPARED: June 24, 2014
FILENAME: S1154500-02

Figure 17. Monitoring Wells in the Study Area, Map 2 of 4

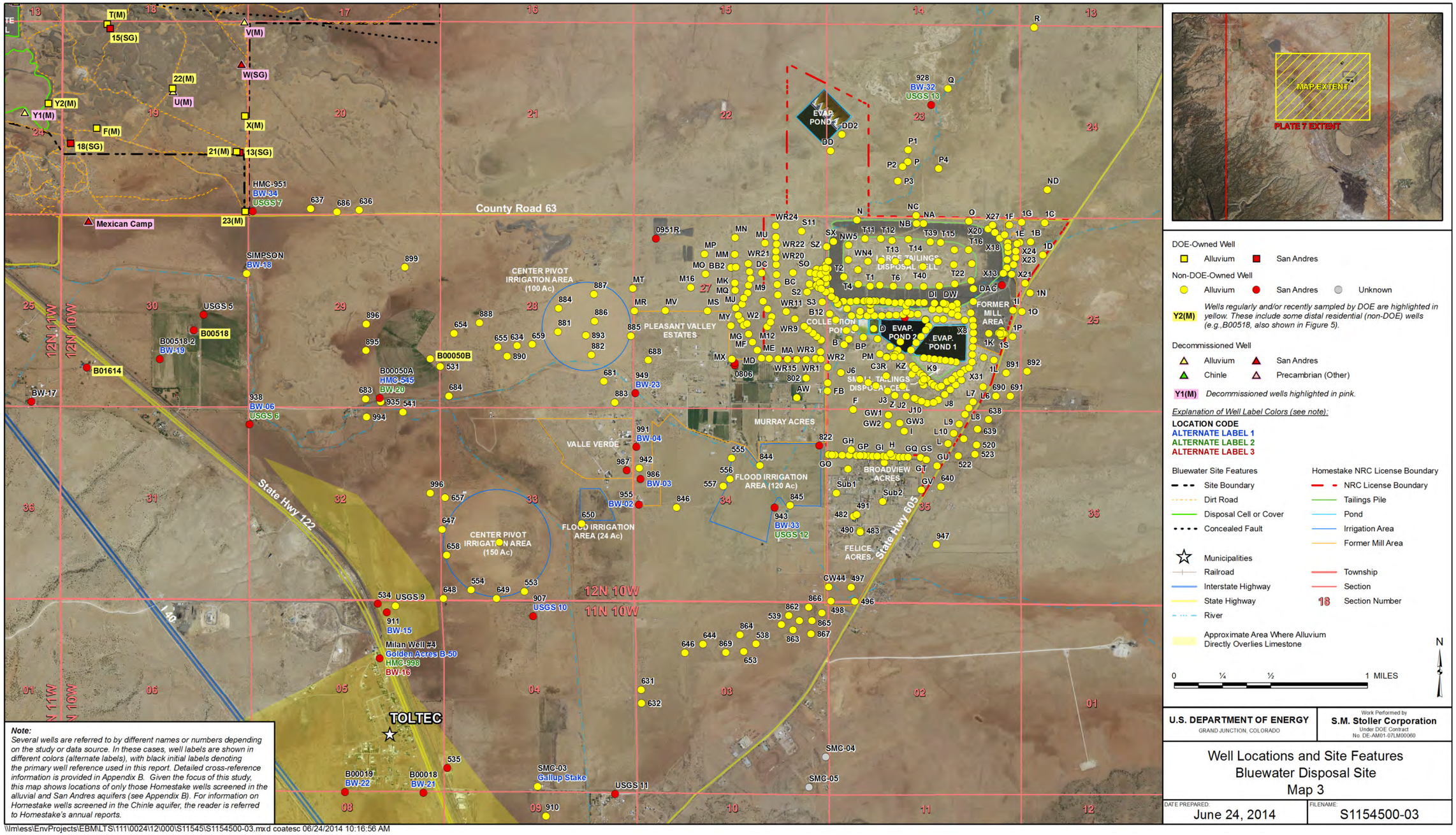

Figure 18. Monitoring Wells in the Study Area, Map 3 of 4

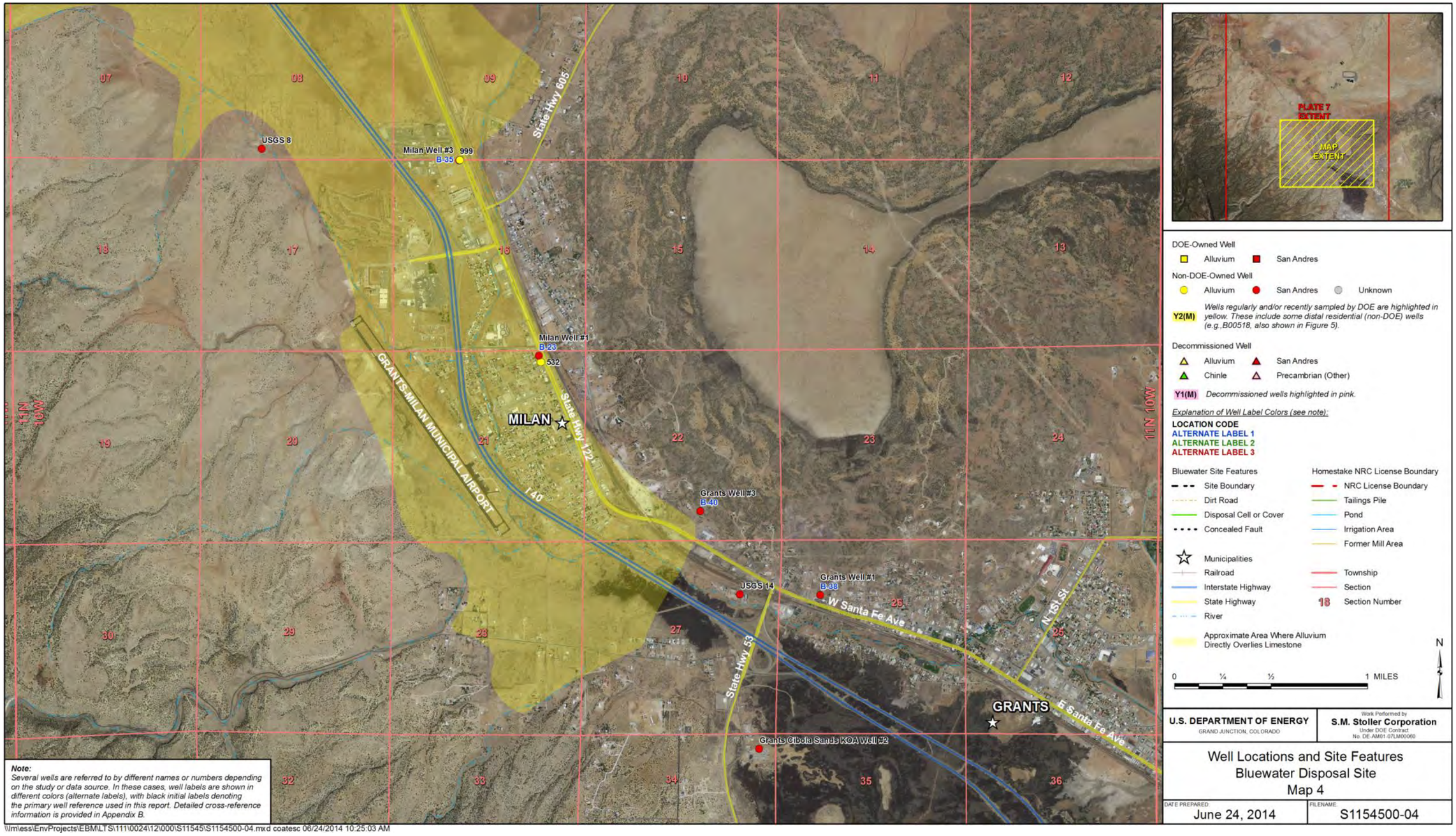

Figure 19. Monitoring Wells in the Study Area, Map 4 of 4

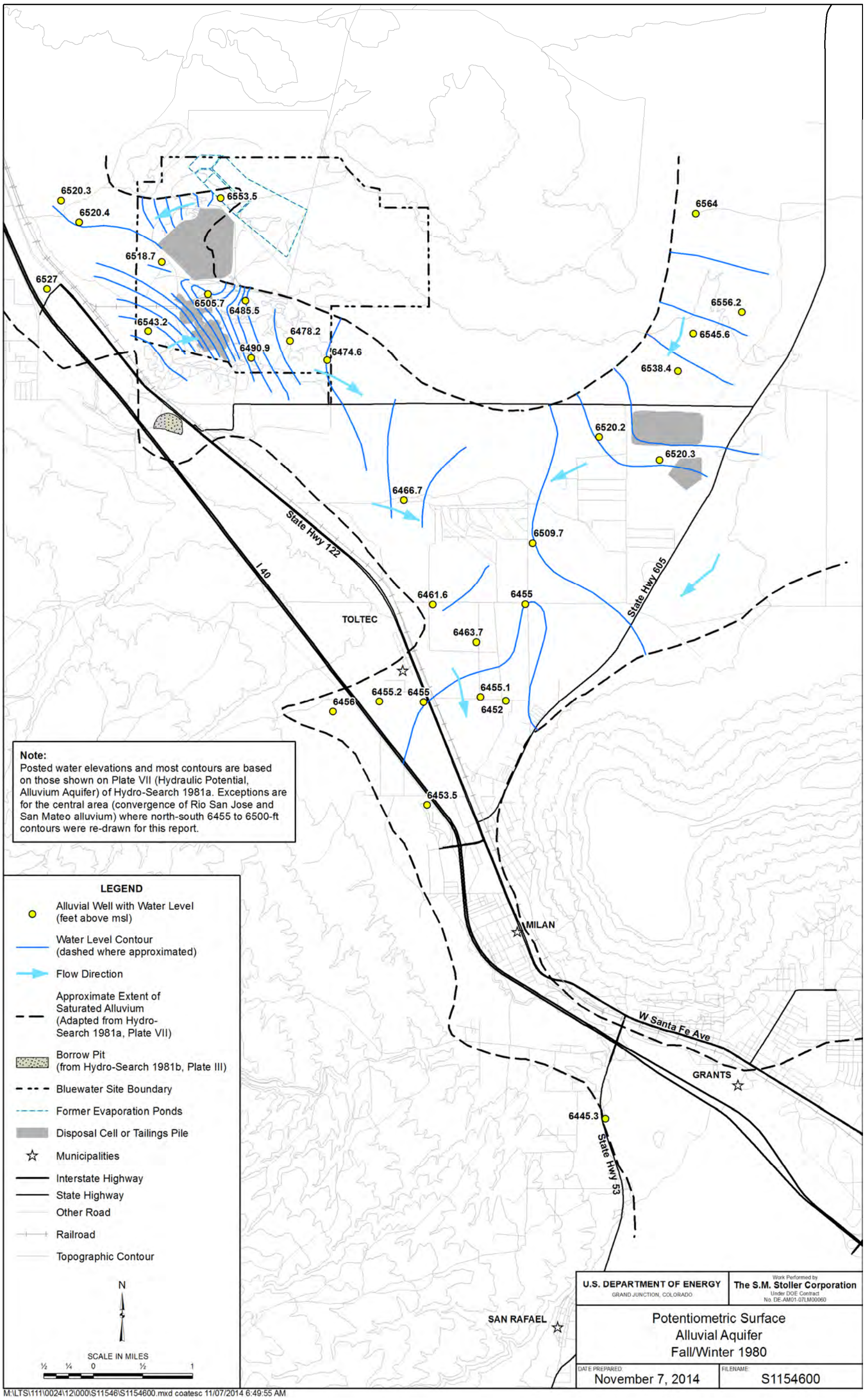

Figure 20. Hydraulic Heads in the Alluvial Aquifer in 1980

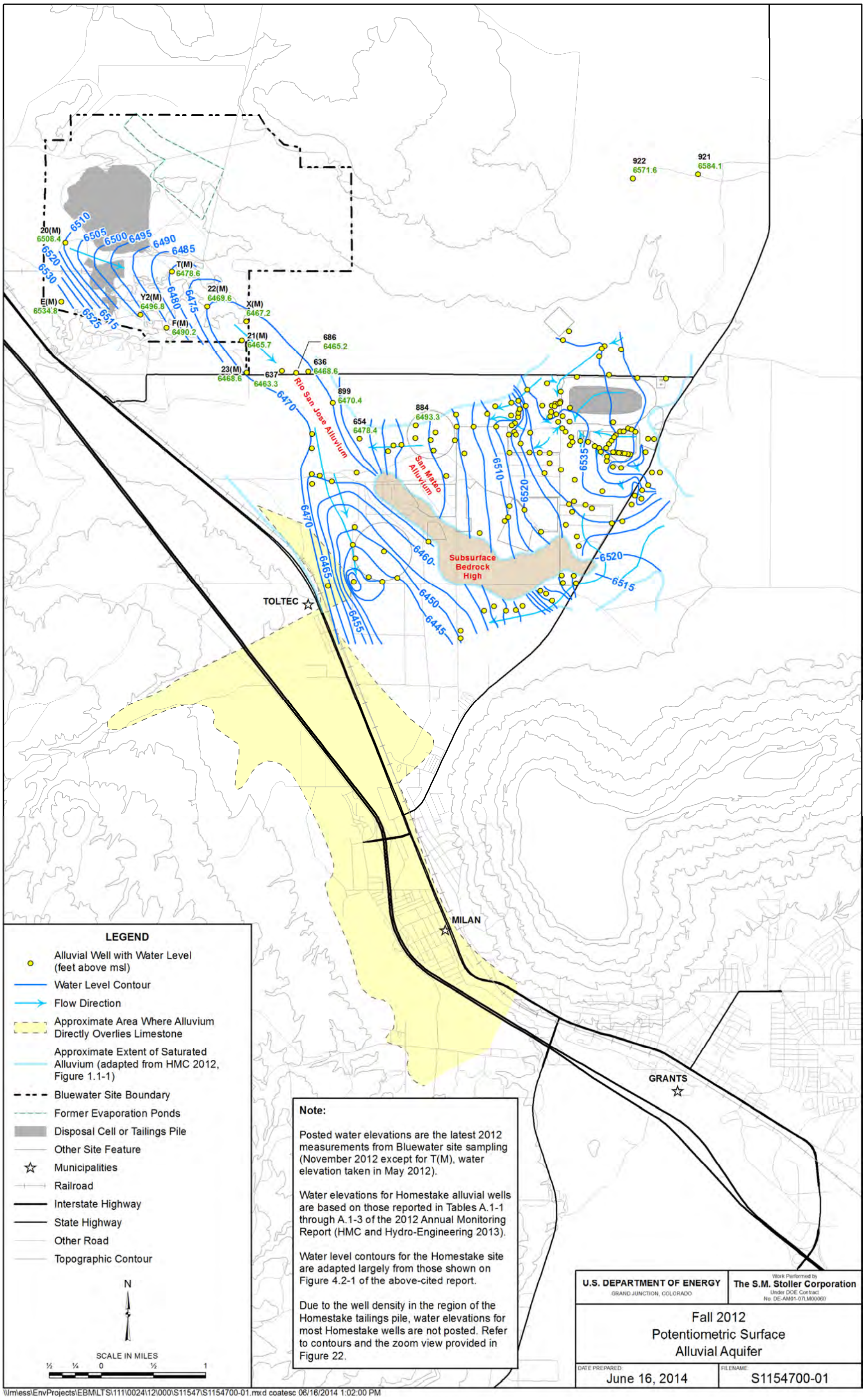

Figure 21. Hydraulic Heads in the Alluvial Aquifer in 2012

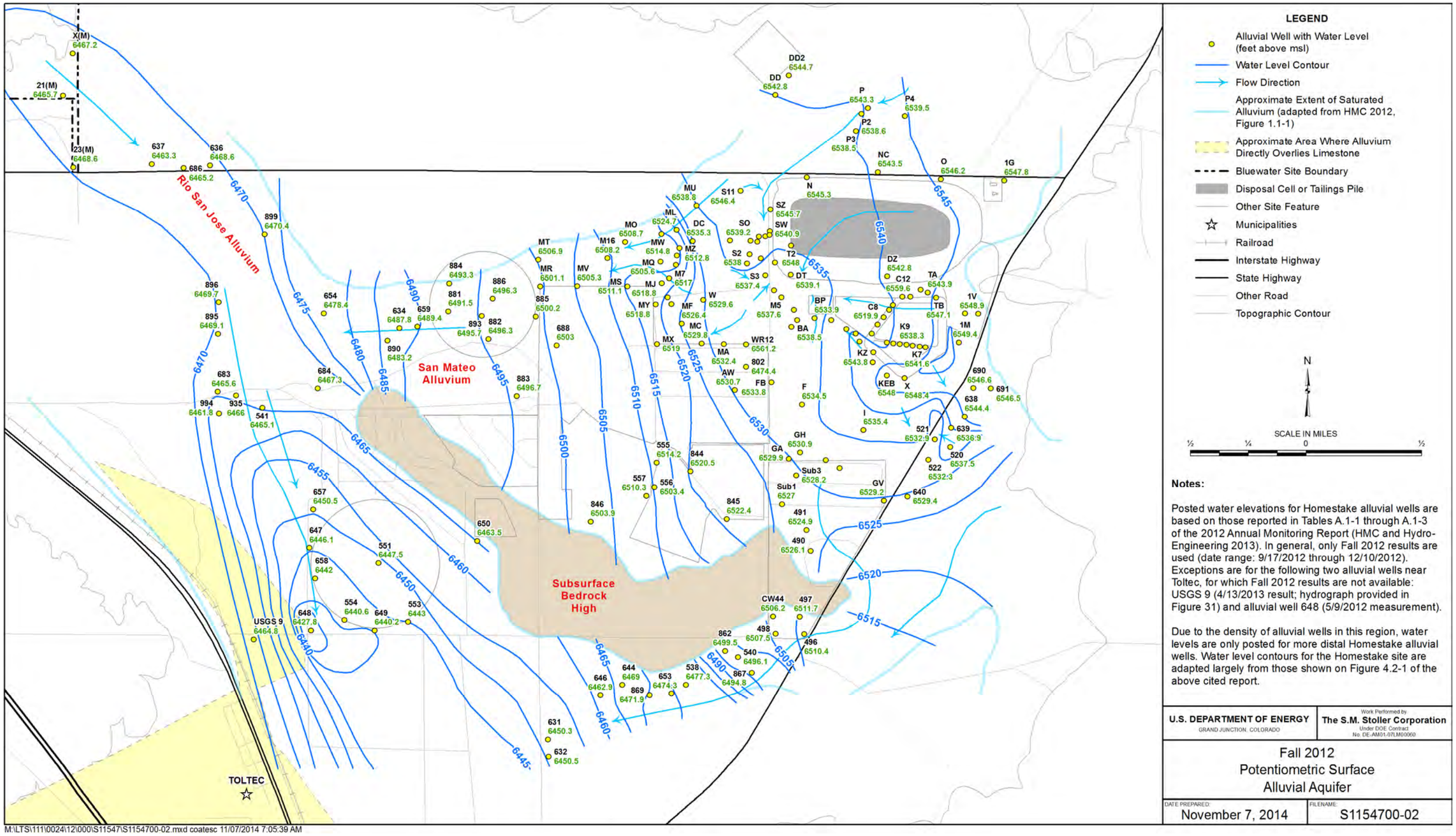

Figure 22. Hydraulic Heads and Flow Directions in the Alluvial Aquifer in 2012

This page intentionally left blank

As part of its investigation of regional hydrology features in the Grants-Bluewater Valley, Hydro-Search (1981a) also produced a map of the potentiometric surface in the San Andres aquifer as perceived in the late 1970s and early 1980s. Figure 23 presents a reproduction of that map. In general, the 1980 potentiometric surface in the San Andres aquifer showed groundwater migrating almost directly to the east in areas west of the main tailings impoundment and then heading in more of a southeast direction in areas east of the pile. This indicated that groundwater in the aquifer east of the Bluewater site was migrating in a direction transverse to the north-northeast dip of the San Andres Limestone and the Glorieta Sandstone. A particularly notable feature of the mapped surface in Figure 23 is the spatial variation in hydraulic gradients. The hydraulic gradient is relatively large in the area west of the main tailings impoundment, where estimates based on the mapped contours have values of 20 to 25 ft/mi, or 0.0038 to 0.0047 in dimensionless units. In contrast, the gradient flattens out considerably in areas east of the tailings impoundment, where estimated slopes of the potentiometric surface range from about 6.5 ft/mi (0.0012 dimensionless) immediately east of the impoundment to as little as 1 ft/mi (0.0002 dimensionless) in an area about 1.5 mi northwest of the large tailings disposal cell at the Homestake site. This general trend toward a flatter gradient east and southeast of the Bluewater site is a reflection of the large transmissivity zone between the Bluewater site and the San Rafael Fault (Section 4.2.4), which was assigned an average transmissivity of 50,000 ft^2/day by Baldwin and Anderholm (1992).

Comparison of the hydraulic heads in Figure 23 with measured groundwater levels in the alluvial aquifer in 1980 (Figure 20) indicates that heads in the ancestral river alluvium at the time were typically about 20 to 40 ft higher than those measured in the underlying bedrock aquifer. This meant that groundwater in the alluvium had the capacity to migrate downward to the San Andres aquifer where a hydraulic connection between the two aquifers occurs. For instance, downward migration of water from the alluvium to the San Andres in fault zones was a possibility, as was lateral movement of alluvial aquifer groundwater from south of the main tailings impoundment to the uplifted San Andres Limestone and Glorieta Sandstone just north of the East-West Fault.

Another notable feature of the potentiometric surface in Figure 23 was the difference in hydraulic heads between areas north and south of the East-West Fault at the Bluewater site. Heads north of the fault were generally about 5 to 10 ft higher than equivalent values south of the fault. Hydro-Search (1981a) identified this phenomenon as an indicator of the East-West Fault's capacity to act as a partial barrier to groundwater flow in the bedrock aquifer. Another notable feature of the potentiometric surface is the curvature of equipotentials south of the East-West Fault. Though a reason for this curvature was not given in the regional study of flow conditions (Hydro-Search 1981a), it was identified in an earlier assessment (Hydro-Search 1978) to represent the east and west edges of a pumping cone of influence centered in the area of the production wells Anaconda #1, Anaconda #3, and Anaconda #4. In the late 1970s and early 1980s, these wells were used to extract San Andres aquifer groundwater to support the milling activity.

Figure 24 presents a more recent depiction of the potentiometric surface in the San Andres aquifer. Because hydraulic head data were only available for a limited number of wells, the number of head contours used in this figure is considerably fewer than the number of contours used to illustrate the potentiometric surface in the aquifer in 1980 (Figure 23). Based on measured hydraulic heads in 2012, this surface shows that groundwater levels in the aquifer have, in more recent times, been considerably less than those observed in 1980. Despite the

obvious disparity in groundwater elevations between time periods, the general shape of the recent potentiometric surface and the groundwater flow direction implied by it are about the same as observed some 30 year earlier.

4.3.3.1 Flow Patterns in the San Andres Aquifer

Using hydraulic head data for the San Andres aquifer, Applied Hydrology Associates Inc. (1990) developed map views of general groundwater flow patterns in the aquifer. This conceptual model study built upon the earlier work to develop an updated map of flow directions in the aquifer (Figure 25). The flow vectors presented in this figure represent the flow paths taken by San Andres aquifer groundwater that originates beneath the Zuni Mountains in the vicinity of Bluewater Lake, and then migrates downgradient in eastward and east-southeastward directions, toward areas north of Milan and Grants. With a few minor exceptions, the flow directions shown in the updated figure are virtually identical to those identified by Applied Hydrology Associates Inc. (1990). Given that the flow directions in the San Andres aquifer appear to have changed little over the past 30 years, it is likely that the arcuate flow pattern pieced together from the vectors (Figure 25) has been present in the Grants-Bluewater Valley since the start of Bluewater mill operations in the 1950s.

Several features of the flow patterns map in Figure 25 have a bearing on contaminant transport. For example, groundwater flowing in the San Andres aquifer underneath the Bluewater site south of the East-West Fault appears to bypass the municipal wells for Milan, taking on a flow path that is about 1.5 to 2 mi north of the Milan public supply wells. Moreover, groundwater following this path appears to be heading for Grants as it passes under Black Mesa. Similarly, the flow path taken by water migrating beneath the Bluewater site north of the East-West Fault intersects the Homestake site both north and south of the large tailings disposal cell. Included in this wide flow path is groundwater that migrates east-southeastward from the northernmost boundary of the site, in the vicinity of the waste-injection well used between 1960 and 1977. The flow paths from Figure 25 imply that groundwater originating at the Bluewater site in areas north of the East-West Fault will pass beneath the Homestake site and continue flowing to the southeast to areas north of Grants.

The flow patterns map for the San Andres aquifer also indicates that recharge on the Zuni Mountains affects southeastward flow in the Grants-Bluewater Valley by pushing it farther to the north than would occur if this type of recharge were not present. This observation is important because it implies that recharge in the mountains is the primary reason that flow paths emanating from the Bluewater site pass well north of the Milan municipal wells.

4.3.3.2 Average Linear Velocities

The average linear velocity of groundwater in the alluvial and San Andres aquifers can be estimated using representative values of hydraulic conductivity, hydraulic gradient, and effective porosity for the two aquifers. Computed velocities based on estimates for these parameters in past investigations have varied widely. Similarly, estimated average linear velocities stemming from transport modeling studies of groundwater in different parts of the Grants-Bluewater Valley have covered a wide range. This report section attempts to develop general estimates of average linear velocity in the two aquifers, values that apply to the study area as a whole. Summaries of past studies and separate calculations based on Darcy's law are used to develop the estimates.

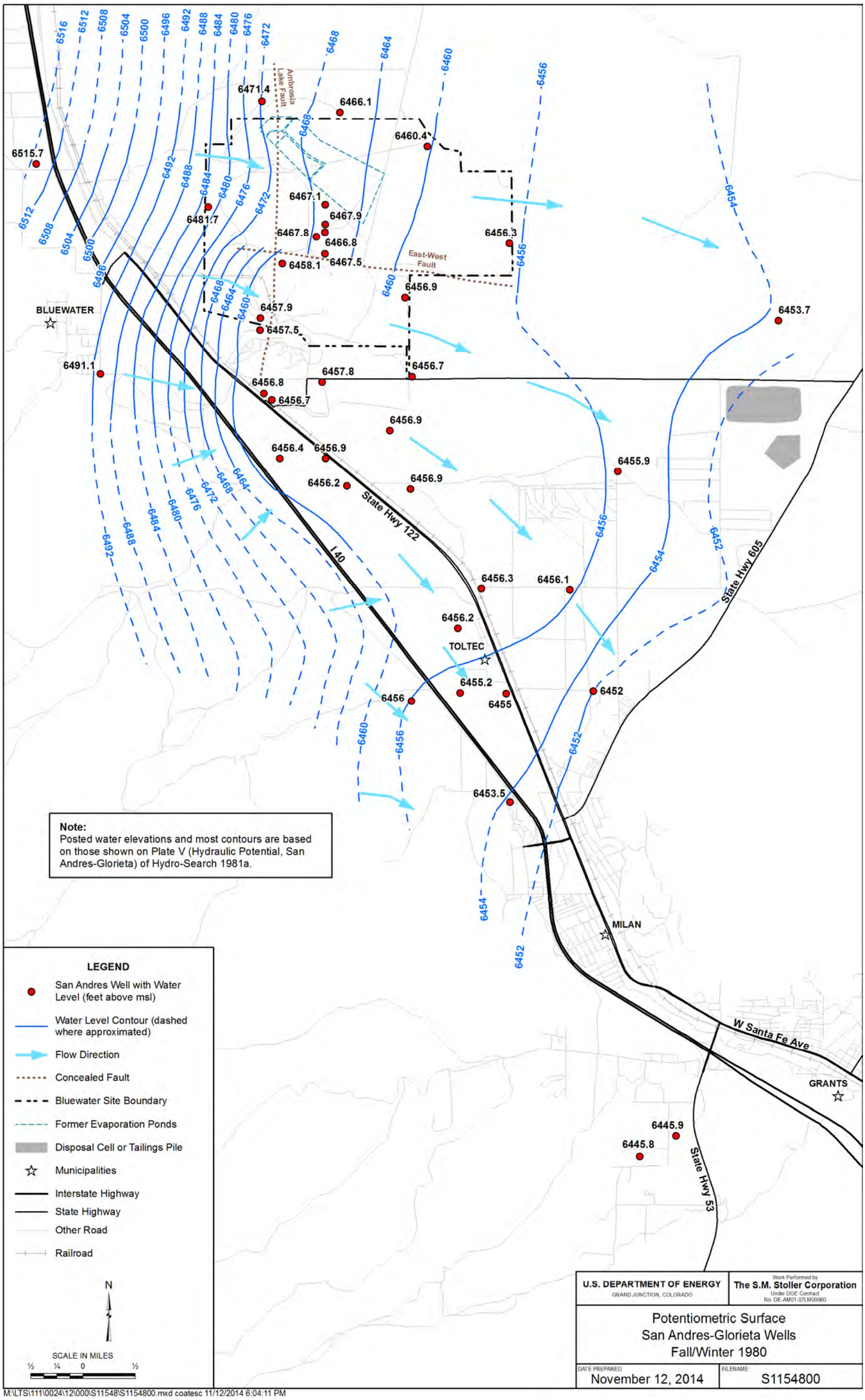

Figure 23. Potentiometric Surface in the San Andres Aquifer in 1980

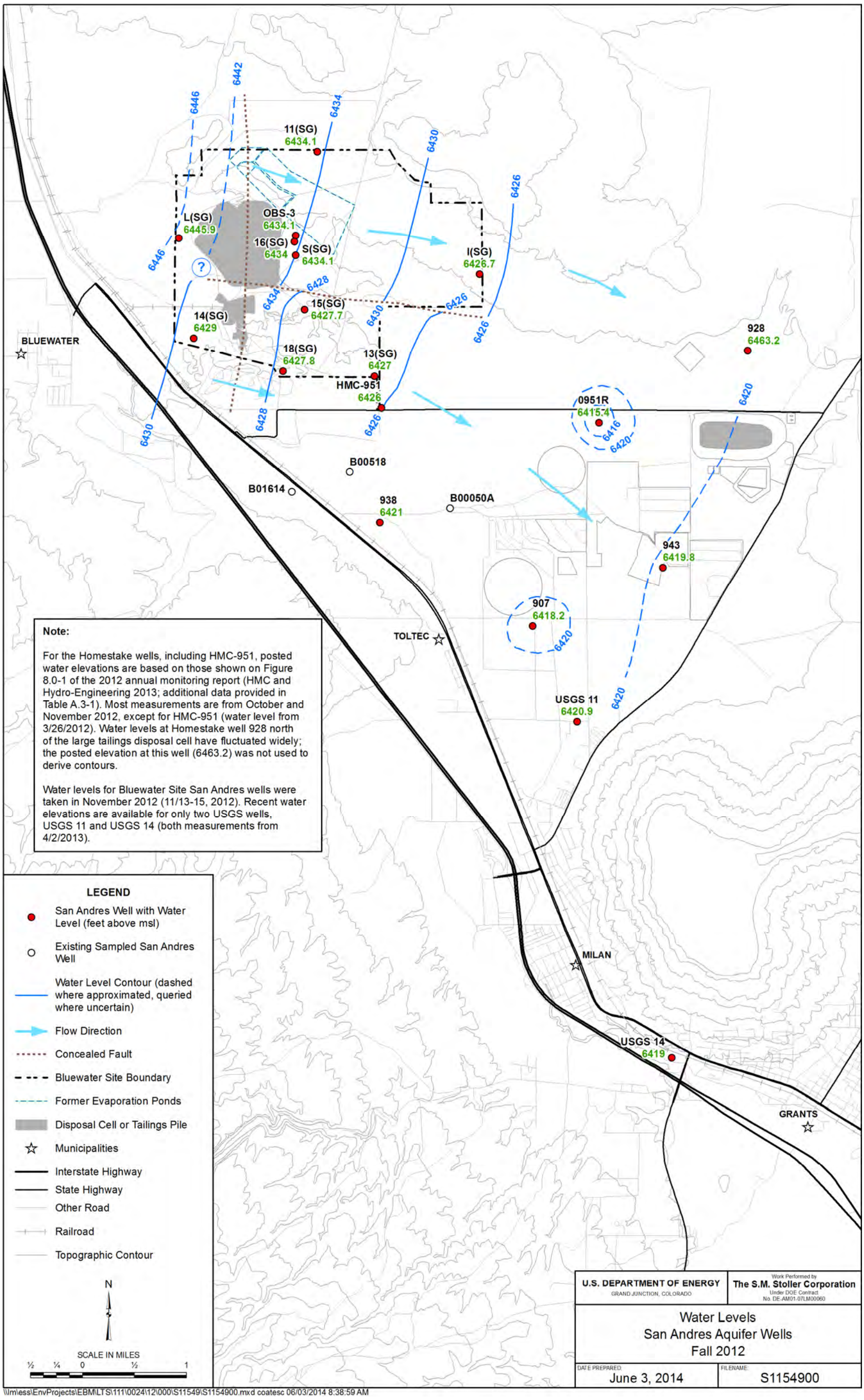

Figure 24. Potentiometric Surface in the San Andres Aquifer in 2012

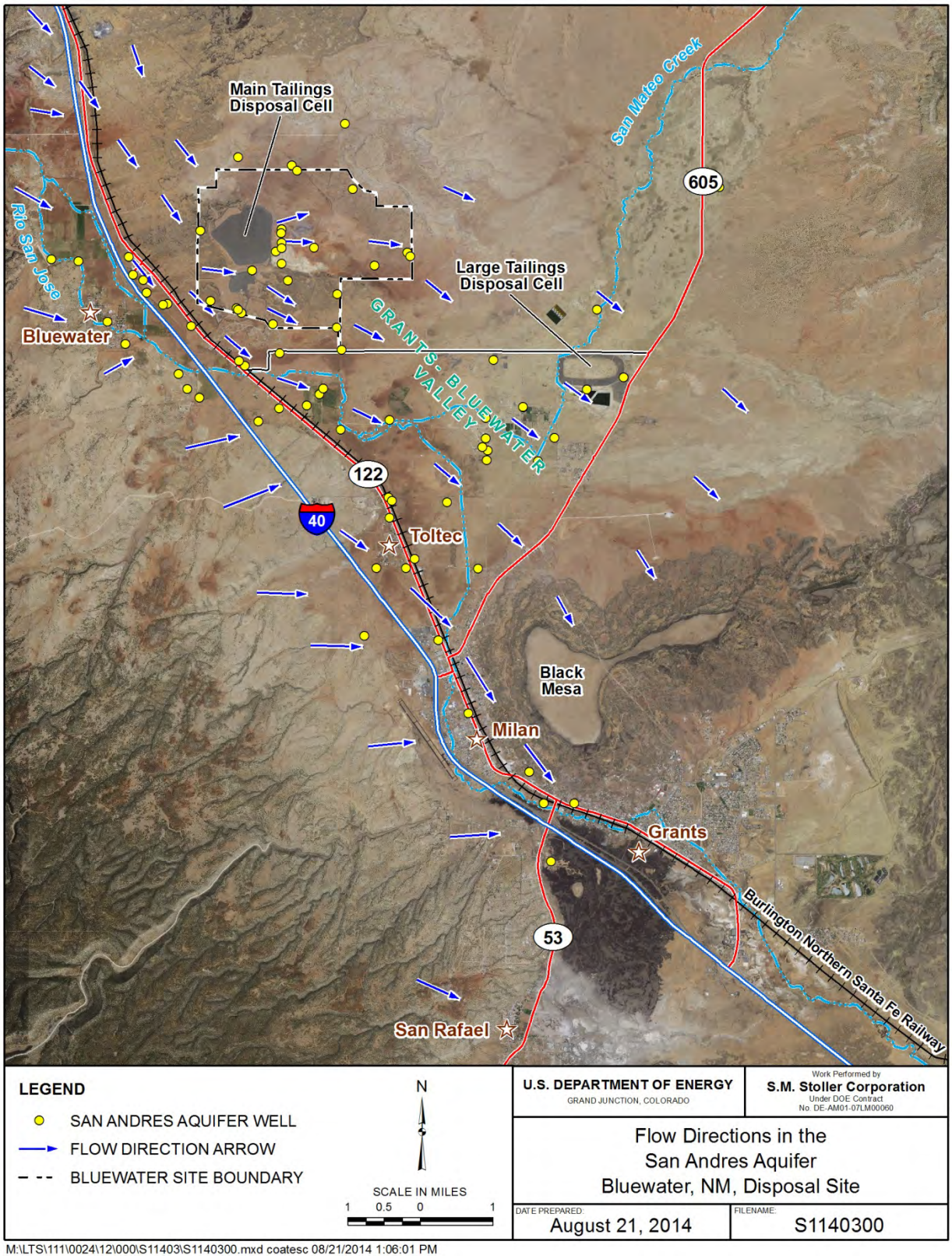

Figure 25. Ambient Flow Directions in the San Andres Aquifer

Hydro-Search (1977) estimated that the average linear velocity of groundwater flowing in ancestral river deposits within the alluvial aquifer at the Bluewater site could be as low as 300 feet per year (ft/yr [0.8 ft/day]) and as high as 1,000 ft/yr (2.75 ft/day). The corresponding estimated velocity for groundwater in the San Andres aquifer east of the main tailings impoundment was limited to 410 ft/yr (1.1 ft/day). All of the estimates by Hydro-Search (1977) were based on an assumed effective porosity of 0.25 in both the alluvial and San Andres aquifers.

In the course of calibrating transport models for groundwater in the Grants-Bluewater Valley, Dames & Moore (1986a) indicated that average linear velocity in the alluvial aquifer at the Bluewater site ranged from 4,500 to 9,000 ft/yr (12.3 to 24.6 ft/day). In the same study, the velocity of water migrating southeastward in the San Andres aquifer south of the East-West Fault at the Bluewater site was estimated to range from 1,800 to 6,000 ft/yr (4.9 to 16.4 ft/day). In comparison, Dames & Moore (1986a) estimated that groundwater flowing eastward in the San Andres aquifer from beneath the main tailings impoundment and north of the East-West Fault had a much slower velocity, varying from about 1,000 to 1,430 ft/yr (2.7 to 3.9 ft/day). The generally larger velocities estimated by Dames & Moore (1986a) for the San Andres aquifer in comparison to those estimated by Hydro-Search (1977) were attributed to the fact that the former assumed the effective porosity of the aquifer was 0.02. This much smaller porosity was used because it was considered more representative of flow in secondary permeability features in limestone, such as fractures, solution channels, and cavities.

Using the above-mentioned velocity estimates by others and information regarding the hydraulic parameters for the two aquifers (e.g., Sections 4.2.1 and 4.2.4), the conceptual model includes a preliminary summary of average linear velocities that could be expected in the various types of media composing the two aquifers (Table 3). In addition to showing a large range of velocities for the alluvial aquifer, the table also lists ranges for karst limestone media, the San Andres Limestone, and sandstone found in both the San Andres Limestone and the Glorieta Sandstone. The table listings suggest that very large velocities can be associated with conduit flow in karst features (fractures, solution channels, cavities) in the San Andres Limestone. Though the estimated velocities associated with unconsolidated sediments in the alluvial aquifer and sandstone media in the San Andres aquifer are smaller than those expected in karst media, the ranges attributed to alluvium and sandstone are similar in magnitude (Table 3).

Table 3. Estimated Ranges for Average Linear Velocity in Regional Aquifers Based on Previous Studies

Aquifer	Formation	Media Type	Flow Type	Average Linear Velocity Range	
				(ft/yr)	(ft/day)
Alluvial aquifer	Ancestral and Recent Rio San Jose alluvium, San Mateo Creek alluvium	alluvium (clay, silt, sand, gravel)	porous media	10–3,000	0.03–8.2
San Andres aquifer	San Andres Limestone	karst limestone (fractures, solution channels, cavities)	conduit	1,500–7,500	4.1–20.5
San Andres aquifer	San Andres Limestone and Glorieta Sandstone	unfractured and fractured sandstone	porous media and equivalent porous media[a]	250–1,500	0.7–4.1

[a] Equivalent porous media is a concept used to model or simulate the flow of groundwater in fractured rocks. The concept is that if the volume is large enough, the fractured geologic material will behave mathematically like a porous medium.

To further assess how groundwater flow in various types of subsurface media affects advective transport of contaminants, separate calculations of average linear velocity were prepared for parts of the two aquifers located downgradient (east and southeast) of the Bluewater site. The calculations were made using Equation 1.

$$v = q/n_e = KJ/n_e \qquad (1)$$

where v = average linear velocity (length/time)
K = hydraulic conductivity (length/time)
J = horizontal hydraulic gradient (dimensionless)
n_e = effective porosity (dimensionless)

The computed velocities were subsequently used to estimate the times that would be required for a conservative (nonretarded) contaminant to migrate to specific locations downgradient of the Bluewater site. In the case of the alluvial aquifer, these estimates represented the time it would take for a contaminant to migrate from the south border of the main tailings disposal cell to a location near Toltec, and then on to Grants. In the case of the San Andres aquifer, travel times were calculated for a contaminant migrating from the east side of the main tailings disposal cell to the large tailings disposal cell at the Homestake site first, and then on to an area directly north of Grants. The travel times were calculated using Equation 2.

$$t_a = s_a/v \qquad (2)$$

where t_a = travel time (days)
s_a = travel distance (ft)

One set of calculations based on equations 1 and 2 was made for the alluvial aquifer, whereas three different sets of computations were made to assess advection in the San Andres aquifer via (1) conduit flow in karst limestone, (2) equivalent porous media flow in fractured sandstone, and (3) porous media flow in unfractured sandstone. Multiple values of hydraulic conductivity and effective porosity considered representative of the various media in the aquifers were used in the calculations. Assumed hydraulic gradient values in the calculations were based on the potentiometric surface maps shown in Figure 20, Figure 21, Figure 23, and Figure 24.

The average linear-velocity and travel-time calculations for the alluvial aquifer, presented in Table 4, show a wide range in computed results. Of some interest is the fact that the minimum computed velocity for the alluvial aquifer is larger than the comparable minimum velocity shown in Table 3 for the alluvial aquifer, and the largest computed velocity in the alluvial aquifer is less than the comparable high end of the range listed in Table 3. The shortest travel time listed in Table 4 for the path between the south border of the main tailings disposal cell and a point immediately east of Toltec is 17 years (Velocity Calculation 4), which results from using a hydraulic conductivity of 180 ft/day and an effective porosity of 0.10. This result suggests that a contaminant such as uranium might have traveled as far as the Toltec area from the main tailings disposal cell as early as 1980, the first year of a comprehensive study of regional groundwater flow by Hydro-Search (1981a). In addition, the Table 4 calculations suggest that a conservative or mildly retarded contaminant could have reached the Toltec area well before the mid-1990s and easily by 2013, even if the effective porosity of the alluvial aquifer was as large as 0.25 (see Calculation 8).

It is less clear from the Table 4 calculations whether a conservative contaminant migrating in the alluvial aquifer from the main tailings disposal cell has presently traveled by advection as far downgradient as Grants. The shortest travel time for this route is 64 years (Velocity Calculation 12), which assumes a hydraulic conductivity of 180 ft/day and an effective porosity of 0.1. In comparison, about 60 years has passed between 1953, when milling at the Bluewater site started, and the year 2013. The comparable alluvial aquifer calculations based on an effective porosity of 0.25 (Calculations 13–16) suggest that at least 150 years would be required for the contamination originating at the main tailings disposal cell to migrate in the alluvial aquifer to as far as Grants (Table 4).

Table 5 shows the velocity and travel-time calculations for the San Andres aquifer. The calculations dealing with flow through secondary permeability features in the aquifer were based on the general observation that representative hydraulic conductivities for this type of flow tend to be high, and corresponding effective porosities are low (Worthington and Ford 2009). The range of hydraulic conductivities used to calculate travel times via conduits in karst limestone comported with the range of values compiled in Huntoon (1995) from tracer tests covering thousands to tens of thousands of feet of travel distance. Somewhat lower values of both hydraulic conductivity and effective porosity were used to represent equivalent porous medium flow in fractured sandstone.

As expected, the highest average linear velocities and shortest travel times are associated with conduit flow in karst limestone within the aquifer (Table 5), as these calculations are based on the very high hydraulic conductivities measured in solution-enlarged joints, solution channels, and cavities. Using hydraulic conductivities that range from 100 to 1,000 ft/day and effective porosities of 0.02 and 0.05, 7 of the 8 calculated travel times for the path between the east border of the main tailings disposal cell at the Bluewater site and the large tailings disposal cell at the Homestake site (4.5 miles) are 21 years or less (Table 5). This suggests a high probability that a conservative or mildly retarded contaminant migrating from the main tailings disposal cell solely through karst features reached the Homestake site by as early as 1980, when the regional hydrogeologic study by Hydro-Search (1981a) was initiated. The longest computed travel time via conduit flow between the two disposal cells, 57 years (Calculation 9), indicates that conservative contaminants would be present in the vicinity of the Homestake site today, if not as early as 1980. The computed average linear velocities for karst limestone features comport with the range of velocities reported by Huntoon (1995), which were derived from aquifer pumping tests in karst aquifers.

The eight calculations representing conduit flow from the main tailings disposal cell to an area directly north of Grants (Calculations 9 through 16 in Table 5) are of interest because six of the eight indicate that a nonretarded contaminant originating beneath the main tailings disposal cell in the mid- to late-1950s would have reached the area north of Grants before 2013. In general, the conduit-flow calculations suggest that mildly to nonretarded contamination originating in the San Andres aquifer at the Bluewater site in the 1950s probably reached the Homestake site by the early 1980s and has since migrated at least another 3 mi farther to the east and southeast.

Table 4. Average Linear Velocity Calculations for the Alluvial Aquifer

Calculation Number	From	To	Distance (s_a)		Estimated Gradient (J)	Hydraulic Conductivity (K)	Effective Porosity (n_e)	Average Linear Velocity (v)		Travel Time (t_a)
			(mi)	(ft)	(dimensionless)	(ft/day)	(dimensionless)	(ft/day)	(ft/yr)	(years)
1	South border of main tailings disposal cell	3500 ft directly east of Toltec	4.5	23,760	0.0021	20	0.1	0.42	154	155
2	South border of main tailings disposal cell	3500 ft directly east of Toltec	4.5	23,760	0.0021	60	0.1	1.26	461	52
3	South border of main tailings disposal cell	3500 ft directly east of Toltec	4.5	23,760	0.0021	120	0.1	2.53	922	26
4	South border of main tailings disposal cell	3500 ft directly east of Toltec	4.5	23,760	0.0021	180	0.1	3.79	1,383	17
5	South border of main tailings disposal cell	3500 ft directly east of Toltec	4.5	23,760	0.0021	20	0.25	0.17	61	387
6	South border of main tailings disposal cell	3500 ft directly east of Toltec	4.5	23,760	0.0021	60	0.25	0.51	184	129
7	South border of main tailings disposal cell	3500 ft directly east of Toltec	4.5	23,760	0.0021	120	0.25	1.01	369	64
8	South border of main tailings disposal cell	3500 ft directly east of Toltec	4.5	23,760	0.0021	180	0.25	1.52	553	43
9	South border of main tailings disposal cell	Grants	10	52,800	0.0013	20	0.1	0.25	92	573
10	South border of main tailings disposal cell	Grants	10	52,800	0.0013	60	0.1	0.76	277	191
11	South border of main tailings disposal cell	Grants	10	52,800	0.0013	120	0.1	1.52	553	95
12	South border of main tailings disposal cell	Grants	10	52,800	0.0013	180	0.1	2.27	830	64
13	South border of main tailings disposal cell	Grants	10	52,800	0.0013	20	0.25	0.10	37	1432
14	South border of main tailings disposal cell	Grants	10	52,800	0.0013	60	0.25	0.30	111	477
15	South border of main tailings disposal cell	Grants	10	52,800	0.0013	120	0.25	0.61	221	239
16	South border of main tailings disposal cell	Grants	10	52,800	0.0013	180	0.25	0.91	332	159

ft = feet; ft/day = feet per day; ft/yr = feet per year; mi = miles

Table 5. Average Linear Velocity Calculations for the San Andres Aquifer

Calculation Number	From	To	Flow Distance (s_a)		Estimated Gradient (J)	Hydraulic Conductivity (K)	Effective Porosity (n_e)	Average Linear Velocity (v)		Travel Time (t_a)
			(mi)	(ft)	(dimensionless)	(ft/day)	(dimensionless)	(ft/day)	(ft/yr)	(years)
Conduit Flow (fractures, solution channels and cavities in karst limestone)										
1	East Border of Main Tailings Disposal Cell	Homestake Large Tailings Cell	4.5	23,760	0.0006	100	0.02	3.16	1,152	21
2	East Border of Main Tailings Disposal Cell	Homestake Large Tailings Cell	4.5	23,760	0.0006	400	0.02	12.63	4,609	5
3	East Border of Main Tailings Disposal Cell	Homestake Large Tailings Cell	4.5	23,760	0.0006	700	0.02	22.10	8,065	3
4	East Border of Main Tailings Disposal Cell	Homestake Large Tailings Cell	4.5	23,760	0.0006	1000	0.02	31.57	11,521	2
5	East Border of Main Tailings Disposal Cell	Homestake Large Tailings Cell	4.5	23,760	0.0006	100	0.05	1.26	461	52
6	East Border of Main Tailings Disposal Cell	Homestake Large Tailings Cell	4.5	23,760	0.0006	400	0.05	5.05	1,843	13
7	East Border of Main Tailings Disposal Cell	Homestake Large Tailings Cell	4.5	23,760	0.0006	700	0.05	8.84	3,226	7
8	East Border of Main Tailings Disposal Cell	Homestake Large Tailings Cell	4.5	23,760	0.0006	1000	0.05	12.63	4,609	5
9	East Border of Main Tailings Disposal Cell	Directly north of Grants	7.5	39,600	0.0004	100	0.02	1.89	691	57
10	East Border of Main Tailings Disposal Cell	Directly north of Grants	7.5	39,600	0.0004	400	0.02	7.58	2,765	14
11	East Border of Main Tailings Disposal Cell	Directly north of Grants	7.5	39,600	0.0004	700	0.02	13.26	4,839	8
12	East Border of Main Tailings Disposal Cell	Directly north of Grants	7.5	39,600	0.0004	1000	0.02	18.94	6,913	6
13	East Border of Main Tailings Disposal Cell	Directly north of Grants	7.5	39,600	0.0004	100	0.05	0.76	277	143
14	East Border of Main Tailings Disposal Cell	Directly north of Grants	7.5	39,600	0.0004	400	0.05	3.03	1,106	36
15	East Border of Main Tailings Disposal Cell	Directly north of Grants	7.5	39,600	0.0004	700	0.05	5.30	1,936	20
16	East Border of Main Tailings Disposal Cell	Directly north of Grants	7.5	39,600	0.0004	1000	0.05	7.58	2,765	14

Table 5 (continued). Average Linear Velocity Calculations for the San Andres Aquifer

Calculation Number	From	To	Flow Distance (s_a)		Estimated Gradient (J)	Hydraulic Conductivity (K)	Effective Porosity (n_e)	Average Linear Velocity (v)		Travel Time (t_a)
			(mi)	(ft)	(dimensionless)	(ft/day)	(dimensionless)	(ft/day)	(ft/yr)	(years)
Fracture Flow in Sandstone (equivalent porous media)										
17	East Border of Main Tailings Disposal Cell	Homestake Large Tailings Cell	4.5	23,760	0.0006	20	0.01	1.26	461	52
18	East Border of Main Tailings Disposal Cell	Homestake Large Tailings Cell	4.5	23,760	0.0006	50	0.01	3.16	1,152	21
19	East Border of Main Tailings Disposal Cell	Homestake Large Tailings Cell	4.5	23,760	0.0006	100	0.01	6.31	2,304	10
20	East Border of Main Tailings Disposal Cell	Homestake Large Tailings Cell	4.5	23,760	0.0006	150	0.01	9.47	3,456	7
21	East Border of Main Tailings Disposal Cell	Homestake Large Tailings Cell	4.5	23,760	0.0006	20	0.02	0.63	230	103
22	East Border of Main Tailings Disposal Cell	Homestake Large Tailings Cell	4.5	23,760	0.0006	50	0.02	1.58	576	41
23	East Border of Main Tailings Disposal Cell	Homestake Large Tailings Cell	4.5	23,760	0.0006	100	0.02	3.16	1,152	21
24	East Border of Main Tailings Disposal Cell	Homestake Large Tailings Cell	4.5	23,760	0.0006	150	0.02	4.73	1,728	14
25	East Border of Main Tailings Disposal Cell	Directly north of Grants	7.5	39,600	0.0004	20	0.01	0.76	277	143
26	East Border of Main Tailings Disposal Cell	Directly north of Grants	7.5	39,600	0.0004	50	0.01	1.89	691	57
27	East Border of Main Tailings Disposal Cell	Directly north of Grants	7.5	39,600	0.0004	100	0.01	3.79	1,383	29
28	East Border of Main Tailings Disposal Cell	Directly north of Grants	7.5	39,600	0.0004	150	0.01	5.68	2,074	19
29	East Border of Main Tailings Disposal Cell	Directly north of Grants	7.5	39,600	0.0004	20	0.02	0.38	138	286
30	East Border of Main Tailings Disposal Cell	Directly north of Grants	7.5	39,600	0.0004	50	0.02	0.95	346	115
31	East Border of Main Tailings Disposal Cell	Directly north of Grants	7.5	39,600	0.0004	100	0.02	1.89	691	57
32	East Border of Main Tailings Disposal Cell	Directly north of Grants	7.5	39,600	0.0004	150	0.02	2.84	1,037	38

Table 5 (continued). Average Linear Velocity Calculations for the San Andres Aquifer

Calculation Number	From	To	Flow Distance (s_a)		Estimated Gradient (J)	Hydraulic Conductivity (K)	Effective Porosity (n_e)	Average Linear Velocity (v)		Travel Time (t_a)
			(mi)	(ft)	(dimensionless)	(ft/day)	(dimensionless)	(ft/day)	(ft/yr)	(years)
Sandstone (porous media flow)										
33	East Border of Main Tailings Disposal Cell	Homestake Large Tailings Cell	4.5	23,760	0.0006	0.1	0.075	0.001	0.3	85,927
34	East Border of Main Tailings Disposal Cell	Homestake Large Tailings Cell	4.5	23,760	0.0006	1	0.075	0.01	3	8,593
35	East Border of Main Tailings Disposal Cell	Homestake Large Tailings Cell	4.5	23,760	0.0006	5	0.075	0.04	14	1,719
36	East Border of Main Tailings Disposal Cell	Homestake Large Tailings Cell	4.5	23,760	0.0006	20	0.075	0.15	55	430
37	East Border of Main Tailings Disposal Cell	Homestake Large Tailings Cell	4.5	23,760	0.0006	0.1	0.125	0.0005	0.2	143,211
38	East Border of Main Tailings Disposal Cell	Homestake Large Tailings Cell	4.5	23,760	0.0006	1	0.125	0.005	2	14,321
39	East Border of Main Tailings Disposal Cell	Homestake Large Tailings Cell	4.5	23,760	0.0006	5	0.125	0.02	8	2,864
40	East Border of Main Tailings Disposal Cell	Homestake Large Tailings Cell	4.5	23,760	0.0006	20	0.125	0.09	33	716
41	East Border of Main Tailings Disposal Cell	Directly north of Grants	7.5	39,600	0.0005	0.1	0.075	0.001	0.2	214,816
42	East Border of Main Tailings Disposal Cell	Directly north of Grants	7.5	39,600	0.0005	1	0.075	0.01	2	21,482
43	East Border of Main Tailings Disposal Cell	Directly north of Grants	7.5	39,600	0.0005	5	0.075	0.03	11	4,296
44	East Border of Main Tailings Disposal Cell	Directly north of Grants	7.5	39,600	0.0005	20	0.075	0.12	44	1,074
45	East Border of Main Tailings Disposal Cell	Directly north of Grants	7.5	39,600	0.0005	0.1	0.125	0.0004	0.1	358,027
46	East Border of Main Tailings Disposal Cell	Directly north of Grants	7.5	39,600	0.0005	1	0.125	0.004	1	35,803
47	East Border of Main Tailings Disposal Cell	Directly north of Grants	7.5	39,600	0.0005	5	0.125	0.02	7	7,161
48	East Border of Main Tailings Disposal Cell	Directly north of Grants	7.5	39,600	0.0005	20	0.125	0.07	27	1,790

ft = feet; ft/day = feet per day; ft/yr = feet per year; mi = miles

The average linear velocity calculations representing equivalent porous media flow in fractured sandstone in the San Andres aquifer (Calculations 17 through 32 in Table 5) were based on estimated hydraulic conductivities that were smaller than those used to represent conduit flow and effective porosities that were equal to or smaller than those assigned to karst conduits. The two effective porosities adopted for these calculations, 0.01 and 0.02, were based on the assumption that the percentage of bulk cross-sectional area of sandstone represented by fractures was very small. Under these assumptions, the resulting calculations suggest that average linear velocities in fractured sandstone are not much smaller than those for conduit flow, and, accordingly, travel times are not much longer. In fact, 5 of the 8 calculated travel times for the 4.5 mi between the main tailings disposal cell and the large tailings disposal cell at the Homestake site are 21 years or less, suggesting that mildly to nonretarded contaminants originating at the Bluewater site reached the Homestake site by 1980. In addition, 7 of the 8 calculations for this path show travel times of 52 years or less, suggesting that conservative contaminants arrived at the Homestake site at least during recent years, if not by as early as 1980. With one exception (Calculation 28), the computed travel times for fractured sandstone flow between the main tailings disposal cell and the area directly north of Grants indicate that contaminants did not migrate the full 7.5 mi distance as of 1980. However, three of the eight calculations for this path suggest that conservative contaminants did cover the full distance by 2013.

Computed travel times for advective transport in fractured sandstone of the San Andres aquifer (Calculations 17 through 32) indicate that this type of transport is close to being as effective as conduit flow in quickly delivering conservative or mildly retarded contamination from the Bluewater site to downgradient locations. However, it is difficult to conceptualize that fracture systems in sandstone within the aquifer are connected over the full 4.5 mi distance between the main tailings disposal cell and the large tailings disposal cell at the Homestake site. Rather, it seems more likely that some combination of conduit flow in limestone and fracture flow in sandstone could facilitate rapid transport of conservative constituents in groundwater between the two sites. Regardless of the specific forms of groundwater flow that govern advection of contaminants between the two sites, the presence of secondary permeability features (fractures, solutions channels, cavities) in the San Andres aquifer enhances the potential for rapid contaminant transport. Given the large span of computed travel times between the two sites under conduit and fractured-sandstone flow (Calculations 1 through 32 in Table 5), influxes of Bluewater-derived contamination at downgradient locations over several decades appears possible.

In contrast to the conduit flow and fractured sandstone assessments, the calculations considered representative of porous media flow in unfractured sandstone (Calculations 33 through 48 in Table 5) suggest that average linear velocities in this type of medium are very low, ranging from 0.3 to 55 ft/yr. This is mostly attributed to the relatively small hydraulic conductivities (0.1 to 20 ft/day) adopted in the calculations for this type of transport, which were based on the assumption that calcareous and silica cements in sandstone pores greatly limit the rock's permeability. Cementation of sandstone pores was also used to justify relatively small effective porosities (0.075 and 0.125) in the porous media calculations (in comparison to porosities of 0.2 to 0.35 in unconsolidated sands). The computed velocities for unfractured sandstone remained very low, and the calculated travel times were on the order of hundreds of years (Table 5). These results strongly suggest that contamination migrating from the Bluewater site in unfractured sandstone is unlikely to ever reach the Homestake site via horizontal transport.

Instead, the non-fractured sandstone is expected to function more like a rock matrix in a fracture-matrix system, with contamination exchanging between the matrix and secondary porosity features such as fractures, solution channels, and cavities via molecular diffusion and very slow advection.

The calculations summarized in Table 4 and Table 5 indicate that estimates of average linear velocity discussed in earlier studies (e.g., Hydro-Search 1977, Dames & Moore 1986a) are reflective of water movement in the most permeable media within each aquifer. This is not surprising given that groundwater flow velocities are often estimated on the basis of first arrival of contaminants at locations downgradient of contaminant sources. However, the presence of lower-permeability sediments in both aquifers (silts and clays in alluvium, unfractured sandstone in the San Andres aquifer) suggests that contamination residing within them will be slowly released to more permeable pathways through diffusion processes (back diffusion), causing contaminants to persist in groundwater much longer (e.g., Chapman et al. 2012) than if transport was limited to high-permeability media. With respect to uranium transport in groundwater, the slow back diffusion would cause long-term "tailing" of uranium concentrations at downgradient locations, even if contaminant sources at the Bluewater site were eventually removed.

4.3.4 Influence of Faults

Faults in the San Andres aquifer affect groundwater flow, partly by blocking flow where vertical offset of the aquifer occurs. Changes in the gradient of the regional potentiometric surface may result from the blockages, such that changes in hydraulic head upgradient and downgradient of fault zones are small, and significant drops in hydraulic heads are observed within the relatively short width of each fault zone (e.g., Frenzel 1992). Faults could also affect the flow of groundwater by providing a preferential flow path for vertical seepage (e.g., Bense and Person 2006).

Faults in the study area can also influence subsurface flow by creating anisotropy in local hydraulic conductivity (variations in hydraulic conductivity with direction of measurement) of the San Andres aquifer. In areas where the amount of offset of faults is slight, hydraulic conductivity in a particular direction may be enhanced by development of solution channels along the fault in the San Andres Limestone and by fracturing in the Glorieta Sandstone. Joint sets in the aquifer framework also may result in anisotropy of hydraulic conductivity.

North- to northeast-trending faults or fault zones have the capacity to block the regional flow of water in the San Andres aquifer within the study area. The impacts vary from mild to significant depending on the magnitude of offset of the aquifer provided by the fault. The south end of Big Draw Fault impacts groundwater flow near the mouth of Bluewater Canyon. However, the offset of the fault is less than the thickness of the San Andres aquifer, and groundwater flow does not appear to be severely blocked by the fault.

The Ambrosia Lake Fault, which traverses the Bluewater site in a north-south direction, appears to act as a partial barrier to eastward-flowing groundwater in the San Andres aquifer. Local offset at the fault in the vicinity of the main tailings impoundment is at least 300 ft. Inspection of hydraulic head data collected from San Andres aquifer wells at the site over the past 3 years suggests that the drop in head across the fault in areas north of the East-West Fault is about 8 ft. In areas south of the East-West Fault, hydraulic head drops across the Ambrosia Lake Fault appear to be minimal to nonexistent due to insignificant displacement along the fault in that area.

The San Rafael Fault near Grants blocks west-to-east flow from Ojo del Gallo northeastward to a point near the Cibola-McKinley county line. Southwest from Ojo del Gallo, the offset of the San Rafael Fault may not exceed the thickness of the San Andres aquifer. At Ojo del Gallo, the San Rafael Fault forces the water table to rise above the land surface, causing the spring. The head difference across the fault, estimated at about 30 ft in Frenzel (1992), indicates that the fault is a major barrier to groundwater flow.

4.3.5 Regional Hydrographs

Regional groundwater levels have changed significantly over the past 65 years, depending on varying annual precipitation quantities and groundwater withdrawals from wells in the Grants-Bluewater Valley. The magnitude and duration of those changes can be seen by examining hydrographs from USGS monitoring wells in the study area.

Figure 26 is a map showing the locations of 14 USGS wells in the region and the geologic units that the wells are screened in. Hydrographs for the wells are presented here to illustrate the duration and magnitude of the changes observed in sub-areas of Grants-Bluewater Valley. The hydrographs show measured water levels in San Andres aquifer wells dating back to as early as the mid-1940s.

Figure 27 presents historical hydrographs for two wells screened in the San Andres aquifer in an area that represents groundwater-level changes in the vicinity of the Bluewater site and Bluewater Village (Bluewater Area). Figure 28 contains hydrographs for four wells located farther to the south, southeast of the Bluewater site (Mid-Valley Area), and Figure 29 shows hydrographs for four wells near the south end of the Grants-Bluewater Valley (South Valley Area). Hydraulic head changes since 1946 in each of these groups of wells illustrate that the San Andres aquifer has experienced regional head variations on the order of 70 ft or more. Some of the more notable changes were observed from the mid-1940s through the late 1950s, a period during which pumping for agricultural irrigation increased greatly. Some of the regional head declines in the late 1950s were also attributed to groundwater withdrawals for uranium-milling purposes. From the early 1960s until the early 1980s, measured water elevations in San Andres aquifer wells fluctuated but did not show any major increases or declines. Water elevations in most San Andres aquifer wells then increased steadily until the late 1980s (Figure 27 through Figure 29), and in some wells achieved water levels that exceeded those initially observed in the mid-1940s. As shown in Figure 28 and Figure 29, hydraulic heads in the bedrock aquifer have declined substantially since the late 1990s, in some cases as much as 50 to 60 ft.

Two additional hydrographs are illustrated in Figure 30 for wells screened in the San Andres aquifer in the vicinity of the Homestake site. Though trends in hydraulic head at one of these locations (USGS 13 [HMC-928]) prior to the early 1980s were similar to those discussed earlier for wells in the Bluewater, Mid-Valley, and South Valley Areas, anomalous changes have been observed at this location (north of the large tailings disposal cell) since the early 2000s. Specifically, heads have increased at this well during the past 10 years (2004–2013) instead of declining as observed at other San Andres aquifer wells during the same period. Though the reason for this increase is unknown, EPA (2011) has speculated that the groundwater remedy at the GRP creates conditions that promote downward leakage of alluvial aquifer groundwater across the Chinle Formation within branches of the San Mateo Fault, thus increasing hydraulic head in the underlying San Andres aquifer.

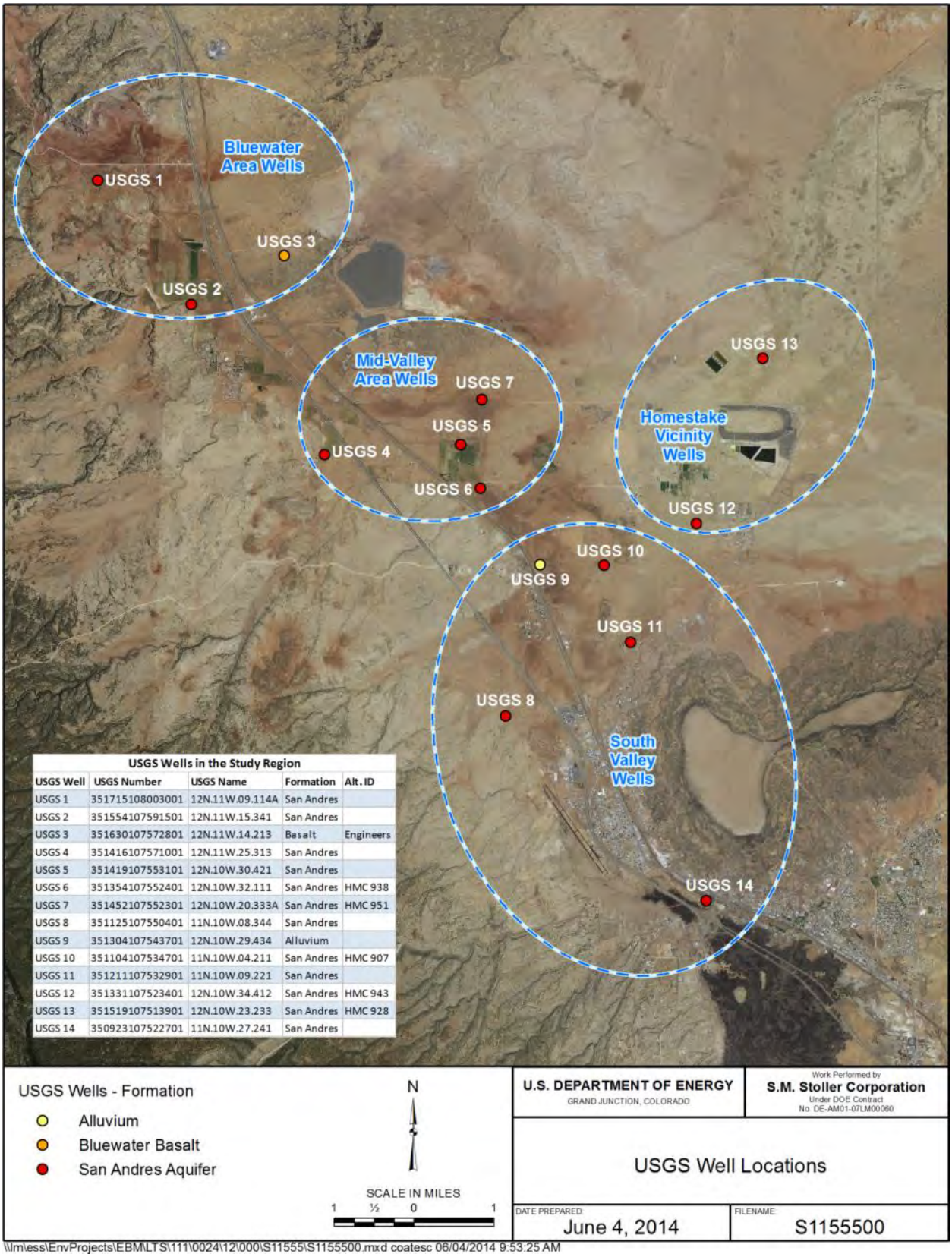

USGS Wells in the Study Region

USGS Well	USGS Number	USGS Name	Formation	Alt. ID
USGS 1	351715108003001	12N.11W.09.114A	San Andres	
USGS 2	351554107591501	12N.11W.15.341	San Andres	
USGS 3	351630107572801	12N.11W.14.213	Basalt	Engineers
USGS 4	351416107571001	12N.11W.25.313	San Andres	
USGS 5	351419107553101	12N.10W.30.421	San Andres	
USGS 6	351354107552401	12N.10W.32.111	San Andres	HMC 938
USGS 7	351452107552301	12N.10W.20.333A	San Andres	HMC 951
USGS 8	351125107550401	11N.10W.08.344	San Andres	
USGS 9	351304107543701	12N.10W.29.434	Alluvium	
USGS 10	351104107534701	11N.10W.04.211	San Andres	HMC 907
USGS 11	351211107532901	11N.10W.09.221	San Andres	
USGS 12	351331107523401	12N.10W.34.412	San Andres	HMC 943
USGS 13	351519107513901	12N.10W.23.233	San Andres	HMC 928
USGS 14	350923107522701	11N.10W.27.241	San Andres	

Figure 26. USGS Monitoring Wells in the Study Area

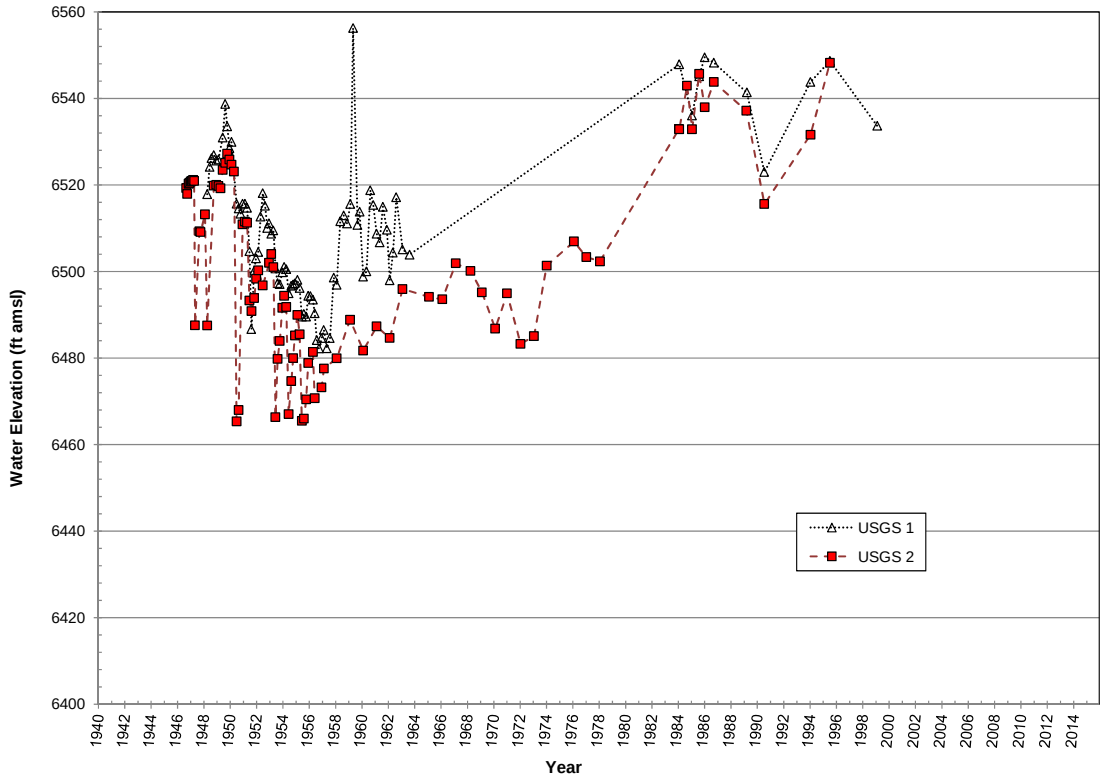

Figure 27. Hydrographs for USGS Wells Screened in the San Andres Aquifer in the Bluewater Area

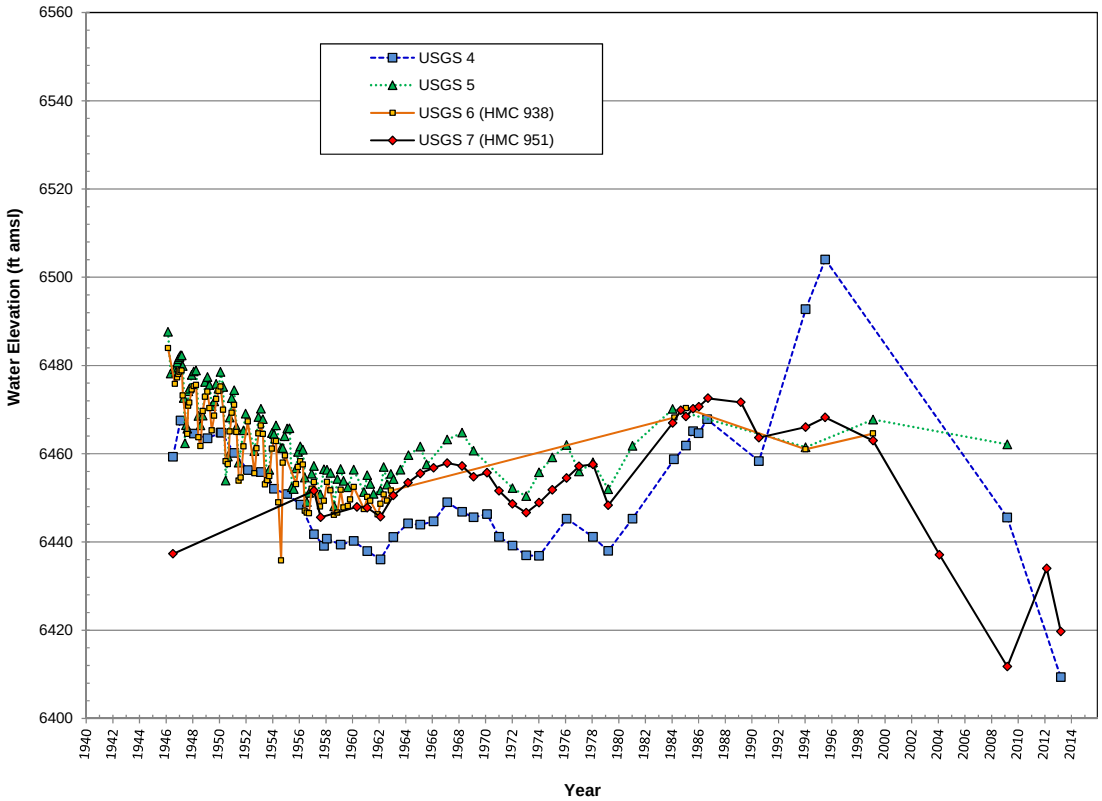

Figure 28. Hydrographs for USGS Wells Screened in the San Andres Aquifer in the Mid-Valley Area

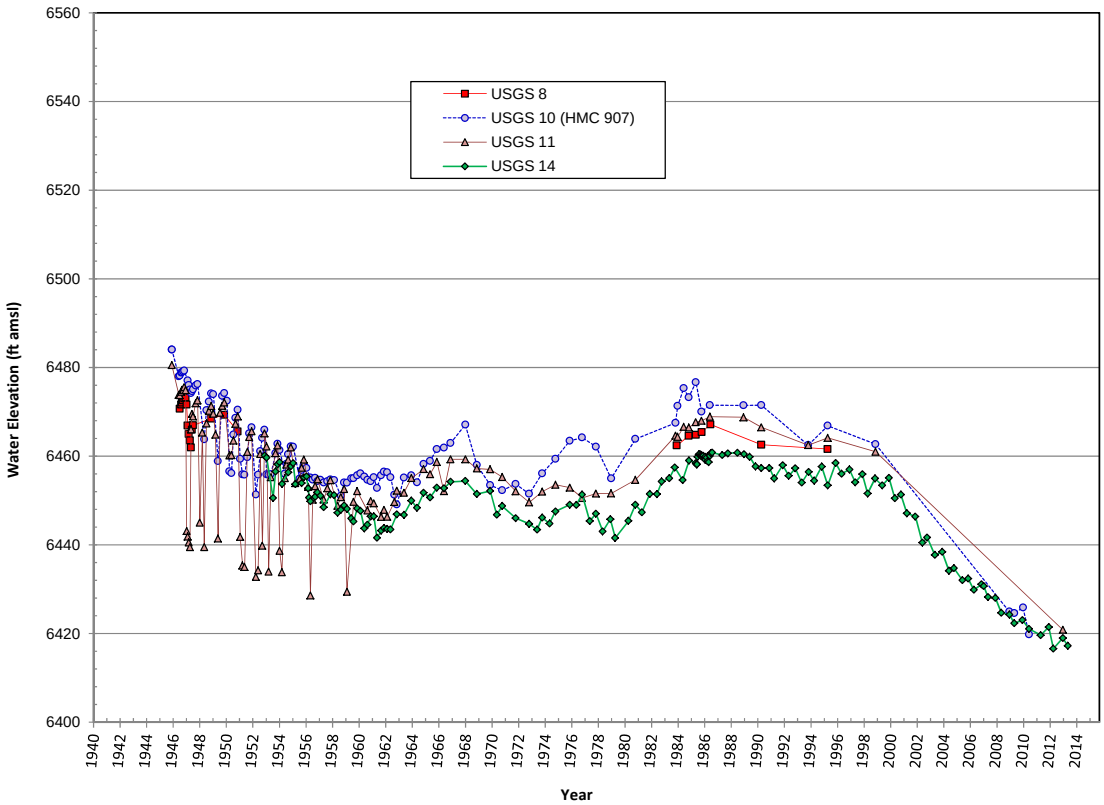

Figure 29. Hydrographs for USGS Wells Screened in the San Andres Aquifer in the South Valley Area

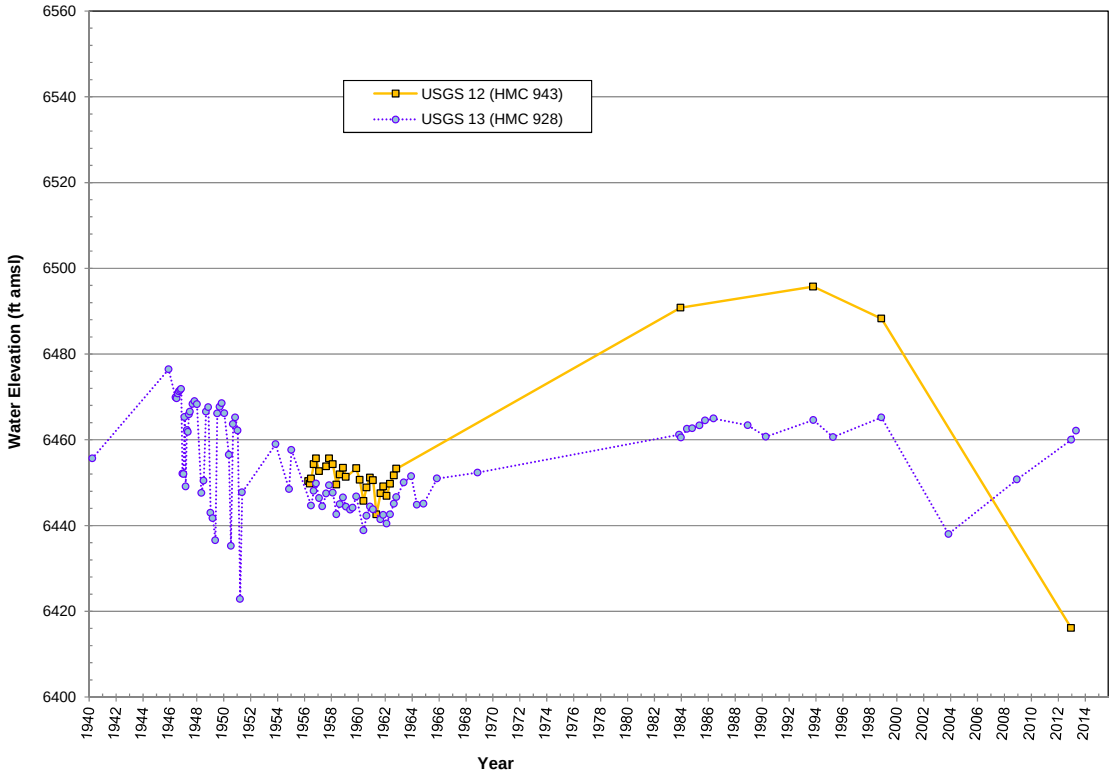

Figure 30. Hydrographs for USGS Wells Screened in the San Andres Aquifer near the Homestake Site

The reason for an increase in hydraulic head at USGS well 12 of about 40 ft between the early 1960s and the mid-1990s is unclear. As with USGS well 13, it is possible that the groundwater remedy at the GRP, which produces a downward gradient and potential downward flow between the alluvial aquifer and the San Andres aquifer played a role in the observed increase in the 1990s. However, the reason hydraulic head at USGS 12 increased in the mid-1980s, prior to implementation of the groundwater remedy, is not understood.

In contrast to the numerous wells monitored in the San Andres aquifer, USGS monitored historical hydraulic heads at only two wells that could be considered representative of the alluvial aquifer within the study area. Figure 31 shows the hydrograph for an alluvial aquifer well about 1 mi north of Milan (USGS 11) and another hydrograph for a well screened in Bluewater Basalt (USGS 5), about 1 mile west of the main tailings disposal cell at the Bluewater site. The ranges in measured hydraulic head at these monitoring locations over the past 65 years are limited to about 20 to 30 ft, as opposed to 50 to 70 ft in the San Andres aquifer wells. Though these two hydrographs are not necessarily representative of the Grants-Bluewater Valley in general, they do suggest that water level variations in the alluvial aquifer are moderated by groundwater responding to hydraulic stresses (e.g., pumping, recharge) under water table conditions. In contrast, hydraulic heads in the San Andres aquifer respond to hydrologic stresses under confined conditions, which reflect the effects of formation compressibility and minor water compressibility. It is likely that recharge of the alluvial aquifer by infiltration of precipitation, streambed seepage, irrigation canal losses, and application of irrigation water to the land surface has helped to minimize water level declines in the aquifer during dry years and periods of heavy regional pumping. Also, the ancestral Rio San Jose alluvium at the Bluewater site ranges from about 0 to 25 ft thick, thus limiting the potential variation in hydraulic head to about 25 ft in that area.

Figure 31. Hydrographs for USGS Wells Screened in the Alluvial Aquifer and the Bluewater Basalt

This page intentionally left blank

5.0 Regional Water Chemistry

This chapter discusses the background chemistry of water resources in the study area. Background water chemistry is considered important because it can influence whether a contaminant stays in solution. In addition, background water chemistry affects the chemical form of the contaminant as it is transported from contaminant sources to downgradient monitoring wells. Much of this chapter focuses on aqueous chemical parameters that influence the transport and retardation properties of uranium, the main contaminant of concern. The chemistry of major ions dissolved in regional water resources is also discussed, partly because it can be used for characterizing the chemical signatures of water in different aqueous environments.

The transport and retardation properties of uranium are typically influenced by the pH, bicarbonate concentration, and oxidation potential of an aqueous system. Uranium is mobile in the oxidized U(VI) state and becomes immobile if chemically reduced to U(IV). Bicarbonate ions complex with U(VI), favoring partitioning into the dissolved, mobile phase. U(VI) is least mobile at near-neutral pH with low bicarbonate concentration. At pH values less than about 4.5, and at pH values above 8 with elevated bicarbonate, U(VI) is most mobile. U(VI) immobility is often caused by its adsorption to mineral particles, particularly hydrous iron oxides. Clay minerals can also adsorb U(VI), but quartz, feldspar, and other major silicate minerals are less adsorptive. Since adsorption is an interaction with mineral surfaces, minerals with high surface area (e.g., clays and iron oxyhydroxide) are more adsorptive than those with low surface area (e.g., quartz).

As previously mentioned, major ion chemistry can be examined for chemical signatures that help distinguish one aqueous environment from another. Changes in major ion chemistry are also useful for constraining mass transfers between the mobile aqueous phase and immobile mineral phases. For example, if water samples are collected at two locations along a known flow path, the change in chemistry can be used to determine the chemical processes (e.g., ion exchange, adsorption, mineral precipitation, mixing) that might have occurred to account for the changes.

Mineral saturation indexes in regional water resources are also calculated in this chapter using the geochemical speciation program PHREEQC (Parkhurst and Appelo 2013). The saturation indexes of calcite ($CaCO_3$) and gypsum ($CaSO_4 \cdot 2H_2O$) provide information on aquifer-mineral interactions.

Data used in this chapter are presented in tabular and graphical forms. Abbreviations are used to denote waters from specific media. The abbreviation “Qb” denotes groundwater in basalt. “SA” denotes groundwater samples collected from wells screened in the San Andres aquifer, and additional abbreviations are used to identify whether each San Andres aquifer well is specifically screened in Glorieta Sandstone (GSS) only or San Andres Limestone (SAL) only. “Qal” signifies groundwater from wells screened in the alluvial aquifer, and “SW” is used to identify surface water chemistry.

5.1 Surface Water

The quality of surface water in the region is useful for understanding the chemical nature of groundwater recharge caused by seepage losses from streams and other surface water bodies. Because surface water is scarce within the region, data from only four background sampling

locations (SW-01 through SW-04) were found to support this analysis, and all of the locations are outside and hydraulically upgradient of the study area. Sampling dates for the four surface water locations varied from 1980 to 2010.

Two surface water sites are in the Bluewater Creek drainage, with one location at Bluewater Lake and the other on the creek itself. The chemistry at these sites is significant because they collectively constitute a major recharge source for both the alluvial and San Andres aquifers upgradient of the Bluewater site. Groundwater fed by this recharge flows beneath the Bluewater site and mobilizes remnant contamination in the subsurface. The remaining two surface water locations are in the San Mateo Creek drainage (Figure 32), several miles northeast of the Homestake site. The water chemistries at these latter locations are not representative of infrequent floodwaters in San Mateo Creek that reach as far south as the Homestake site. However, they do represent the chemistry of recharge water for the San Mateo Creek alluvium upgradient of the Homestake site.

Although stagnant areas of streams or lakes can produce reducing conditions, it is likely that most of the flowing streams in the area are oxidized, and any uranium in them would be in the U(VI) oxidation state. In fresh water, dissolved oxygen (DO) concentrations in equilibrium with the atmosphere range from about 7.5 mg/L at 30 ^{o}C to 12.8 mg/L at 5 ^{o}C (Hem 1986). DO concentrations, measured on three of the four samples collected from surface water, were 7.83, 9.84, and 13.8 mg/L, consistent with oxidized conditions (Table 6).

High iron concentrations generally indicate reduced conditions in natural groundwater, because oxidized iron readily forms low-solubility minerals. The oxidation state for a particular iron concentration is dependent on many solution parameters. Generally, iron concentrations less than about 0.05 mg/L are likely to represent oxidation states higher than the stability field for reduced uranium minerals. Because iron is a common rock-forming mineral, it can be easily included in a groundwater sample as a colloid or particulate. In these cases, an elevated iron concentration does not provide information about oxidation state. Dissolved iron concentrations were measured in three surface water samples with results of 0.004, 0.052, and 0.068 mg/L, values likely representing oxidized conditions.

The pH values for the surface water samples were slightly basic, ranging from 7.80 to 8.70 (Table 6). Specific conductivity values, ranging from 134 to 500 microsiemens per centimeter (µS/cm), indicated relatively low to moderate salinity in these samples. The higher specific conductivity value of the Bluewater Lake sample (SW-02) may indicate evaporation effects.

Most of the major ion concentrations in the surface water samples are relatively low (Table 7), with bicarbonate dominating the anion composition (Figure 33a). The sample collected from Bluewater Creek (SW-01) had chemistry similar to that of Bluewater Lake but was more dilute than the lake sample (SW-02). Cations in Bluewater Lake and Bluewater Creek are dominated by calcium. In contrast, sodium accounts for approximately half of the cation equivalents in San Mateo Creek (SW-03) and El Rito Creek (SW-04) samples in the San Mateo Creek drainage.

The surface water samples are near saturation with calcite, as indicated by saturation indexes near zero (Figure 35). These indexes indicate that the surface water has dissolved calcite from the rocks in the region. All surface water samples are undersaturated (large negative saturation indexes) with gypsum, indicating less interaction with gypsum. Gypsum would be dissolved in these waters.

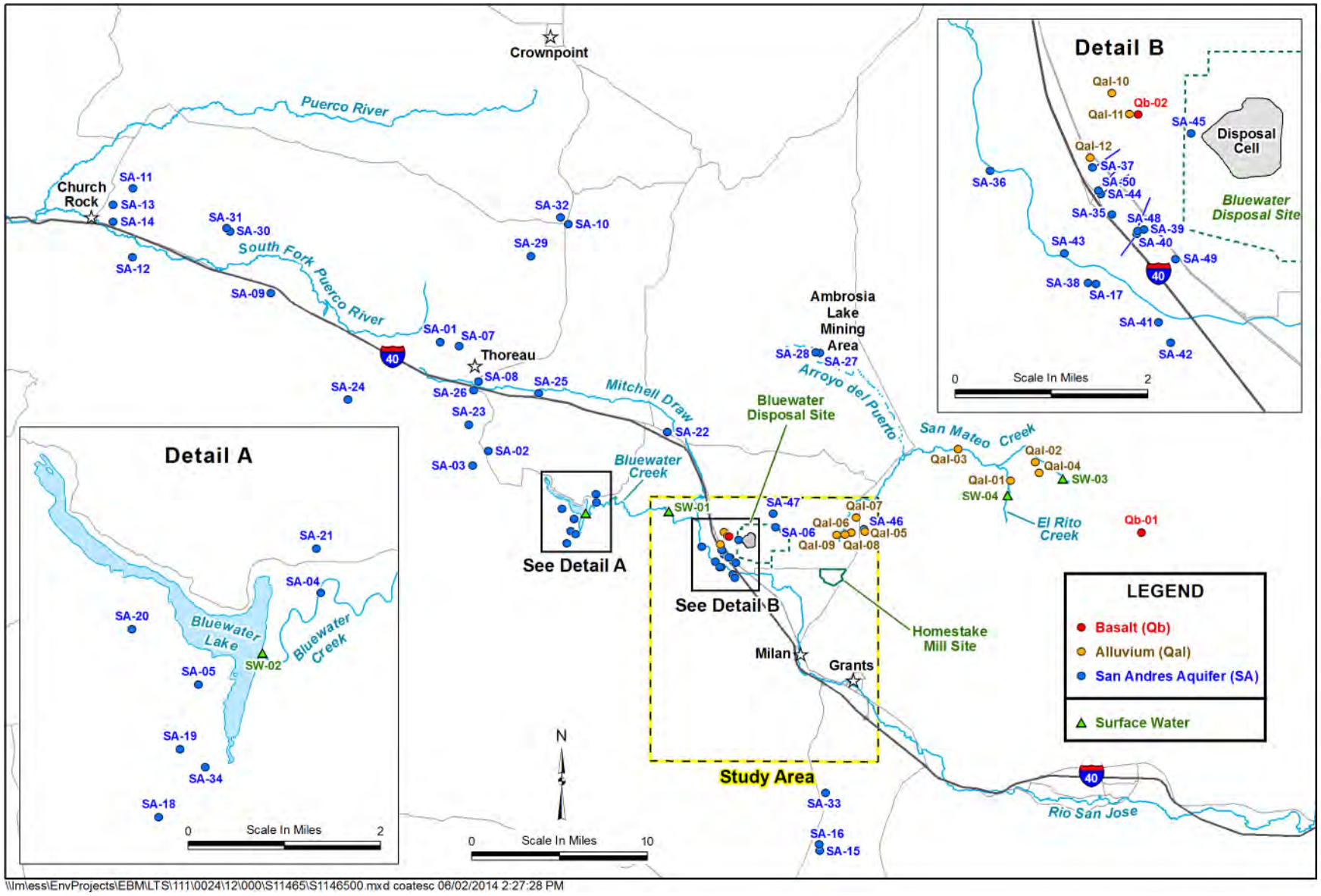

Figure 32. Background Sample Locations

Table 6. Field Parameters

Sample Identifier	Type	Source of Data	Date Sampled	Temperature (°C)	Dissolved Oxygen (mg/L)	pE[a]	pH	Specific Conductivity (µS/cm)
SW-01	SW	USGS	4/18/1980	6			7.80	310
SW-02	SW	USGS	2/19/1992	10	13.6		8.70	500
SW-03	SW	Lang	May-2010	15.8	7.83		8.09	134
SW-04	SW	Lang	May-2010	5.4	9.84		8.19	178
Qb-01	GW	B&R	8/29/1962	7.0			6.60	257
Qb-02[b]	GW	USGS	6/7/1957	19			7.50	1020
Qal-01	GW	Lang	8/21/2008				7.00	
Qal-02	GW	Lang	11/17/2008				7.50	
Qal-03	GW	Lang	2/18/2009				9.30	
Qal-04	GW	Lang	10/24/1961				8.00	
Qal-05	GW	NMED	3/30/2009	12.98	0.16	0.08	7.94	2341
Qal-06	GW	NMED	3/31/2009	13.05	0.2	7.19	6.92	3590
Qal-07	GW	NMED	3/31/2009	12.43	4.1	7.10	7.70	3206
Qal-08	GW	NMED	4/2/2009	13.52	1.52	3.77	6.83	2922
Qal-09	GW	NMED	4/2/2009	11.8	0.17	−0.40	8.76	1643
Qal-10	GW	DOE	4/11/1988	14			7.41	1050
Qal-11[b]	GW	DOE	4/11/1988	14			7.59	1020
Qal-12	GW	DOE	4/11/1988	14			7.24	1150
SA-01 (GSS-01)	GW	B&A	7/14/1970				8.50	1000
SA-02 (GSS-02)	GW	B&A	7/25/1986	12.5			7.48	725
SA-03 (GSS-03)	GW	B&A	12/11/1962	11.5			8.00	476
SA-04 (GSS-04)	GW	B&A	8/17/1963	13			7.60	770
SA-05 (GSS-05)	GW	B&A	8/19/1962				7.40	755
SA-06 (GSS-06)	GW	B&A	4/22/1959	24			7.20	4360
SA-07 (SAL-01)	GW	Lang	7/14/1970				8.50	
SA-08 (SAL-02)	GW	Lang	3/13/1975				7.30	

Table 6 (continued). Field Parameters

Sample Identifier	Type	Source of Data	Date Sampled	Temperature (°C)	Dissolved Oxygen (mg/L)	pE[a]	pH	Specific Conductivity (µS/cm)
SA-09 (SAL-03)	GW	Lang	7/19/1961				7.40	
SA-10 (SAL-04)	GW	Lang	1/26/1975				7.70	
SA-11 (SAL-05)	GW	Lang	3/16/1972				7.90	
SA-12(SAL-06)	GW	Lang	3/23/1972				8.40	
SA-13 (SAL-07)	GW	Lang	10/2/1968				7.30	
SA-14 (SAL-08)	GW	Lang	1/1/1967				8.20	
SA-15	GW	B&A	3/5/1986	15.5			7.40	420
SA-16	GW	B&A	3/5/1986	16.0			7.26	575
SA-17	GW	B&A	3/10/1965				7.20	1460
SA-18	GW	B&A	8/30/1964				7.40	647
SA-19	GW	B&A	8/19/1962				7.20	1110
SA-20	GW	B&A	8/9/1962	16.0			7.40	1390
SA-21	GW	B&A	9/4/1962	13.0			7.80	1120
SA-22	GW	B&A	3/7/1986	18.5			7.10	1330
SA-23	GW	B&A	7/19/1961	17.0			7.30	529
SA-24	GW	B&A	5/29/1963				7.30	490
SA-25	GW	B&A	8/20/1963	19.5			7.70	903
SA-26	GW	B&A	7/19/1961	19.0			7.40	563
SA-27	GW	B&A	8/8/1962	20.5			7.40	1030
SA-28	GW	B&A	3/5/1986	40.0			6.50	2850
SA-29	GW	B&A	2/24/1982	20.0			7.40	470
SA-30	GW	B&A	3/16/1972				7.90	1170
SA-31	GW	B&A	6/22/1955	15.5			7.30	1190
SA-32	GW	B&A	12/6/1975				7.70	960
SA-33	GW	B&R	10/13/1964	17.0			7.40	1180

Table 6 (continued). Field Parameters

Sample Identifier	Type	Source of Data	Date Sampled	Temperature (°C)	Dissolved Oxygen (mg/L)	pE[a]	pH	Specific Conductivity (µS/cm)
SA-34	GW	B&R	8/30/1964				7.40	647
SA-35	GW	NMED	8/25/2008	18.51	1.98	5.52	6.69	1613
SA-36	GW	NMED	8/26/2008	15.29	1.84	6.09	6.34	3231
SA-37	GW	NMED	8/26/2008	14.9	4.86	5.54	6.98	847
SA-38	GW	NMED	8/26/2008	13.94	15.87	5.90	6.66	1068
SA-39	GW	NMED	8/26/2008	14.43	9.67	6.33	6.55	962
SA-40	GW	NMED	8/26/2008	14.58	8.62	6.50	6.55	910
SA-41	GW	NMED	8/27/2008	13.52	3.9	6.22	6.84	1474
SA-42	GW	NMED	8/27/2008	13.67	3.89	6.90	6.82	1446
SA-43	GW	NMED	8/27/2008	15.01	5.32	5.83	6.58	1688
SA-44	GW	NMED	8/25/2008	15.42	1.53	5.70	6.72	2101
SA-45	GW	NMED	8/27/2008	17.16	0.81	−0.57	10.2	1344
SA-46	GW	NMED	8/25/2008	22.99	3.8	4.52	8.48	3857
SA-47	GW	DOE	4/4/1988	18			7.15	2800
SA-48	GW	DOE	4/11/1988	14			7.02	1050
SA-49	GW	DOE	4/11/1988	14			7.23	850
SA-50	GW	DOE	4/11/1988	16			6.94	2000

B&A = Baldwin and Anderholm (1992); B&R = Baldwin and Rankin (1995); DOE = DOE's environmental database; GSS = Glorieta Sandstone; GW = groundwater; Lang = Langman et al. (2012); µS/cm = microsiemens per centimeter; NMED = NMED (2010); Qal = Quaternary alluvium; Qb = basalt; SA = San Andres aquifer; SAL = San Andres Limestone; SW = surface water; USGS = USGS (2014)

[a] pE values based on measured oxidation-reduction potential.
[b] Samples Qb-02 and Qal-11 are probably from the same well. USGS considers sample Qb-02 to be from a well screened in Bluewater Basalt, whereas others investigating the Bluewater site (e.g., Hydro-Search [1977, 1981a]; Dames & Moore [1986b]) have traditionally considered a well at the same location to be an alluvial aquifer well known as Engineers.

Table 7. Major Ion Concentrations (mg/L)

Location	Calcium	Magnesium	Sodium	Potassium	Chloride	Bicarbonate	Carbonate	Sulfate
SW-01	47	9.4	5.5	1.7	2.2	98.9	0.22	50
SW-02	79	18	10	2.9	5.7	146	0	150
SW-03	10	2.8	9.8	3.7	2.2	76.6	0.40	2.6
SW-04	16	4.4	12	3.8	2.7	101.7	0.51	2
Qb-01	26	6.1	6.2	1.4	45	33.2	0.0	5.2
Qb-02[a]								
Qal-01	54	16	78	1.0	7	312.3	0.19	22
Qal-02	71	17	264	2.0	34	473.4	1.02	264
Qal-03	10	4	313	4.0	34	399.3	53.97	273
Qal-04	10	2.4	10	3.0	1.6	65.8	0.35	1
Qal-05	567	149	261	7	47	186.3	1.04	2110
Qal-06	479	88.5	269	10.1	55	173.2	0.09	1580
Qal-07	59	10.3	628	0.5	125	240.2	0.68	955
Qal-08	389	73.7	355	8.4	59	159.8	0.07	1610
Qal-09	4.94	0.84	434	1.1	58	286.9	8.44	535
Qal-10	130	37	57	5	41	242.3	0.32	296
Qal-11[a]	130	34	66	6	42	267.3	0.54	299
Qal-12	170	40	26	6	57	248.0	0.23	325
SA-01 (GSS-01)	31	14	170	0	150	208.4	4.17	72
SA-02 (GSS-02)	62	20	79	1.7	6.5	254.3	0.36	150
SA-03 (GSS-03)	76	14	8	0.9	9.6	256.4	1.11	33
SA-04 (GSS-04)	100	37	12	0	8	211.0	0.40	220
SA-05 (GSS-05)	110	35	8.1	1	14	260.3	0.42	170
SA-06 (GSS-06)	600	140	430	0	300	243.0	0.33	2200
SA-07 (SAL-01)	31	14	170		150	208.4	4.17	72
SA-08 (SAL-02)	150	28	11	1.8	4.8	156.0	0.20	350

Table 7 (continued). Major Ion Concentrations (mg/L)

Location	Calcium	Magnesium	Sodium	Potassium	Chloride	Bicarbonate	Carbonate	Sulfate
SA-09 (SAL-03)	90	15	10	1.2	4.8	252.7	0.39	72
SA-10 (SAL-04)	54	18	130		1.8	169.5	0.55	300
SA-11 (SAL-05)	190	37	25		9.9	222.2	1.21	460
SA-12(SAL-06)	170	82	27	5.0	6.4	171.0	3.01	590
SA-13 (SAL-07)	260	59	1100	21.0	63	97.4	0.18	3000
SA-14 (SAL-08)	120	15	200	3.0	23	188.5	2.09	610
SA-15	39	13	37	2.8	14	193.7	0.23	19
SA-16	52	18	40	3.3	19	231.1	0.21	48
SA-17	180	48	88		69	309.0	0.34	400
SA-18	82	29	14	1.0	13	261.3	0.41	87
SA-19	180	48	9.9	1.0	12	257.3	0.28	390
SA-20	260	45	12		13	264.6	0.38	580
SA-21	160	60	20	2.0	8.1	259.1	0.84	420
SA-22	180	76	40	3.1	3.8	188.7	0.15	680
SA-23	78	19	9.5	0.8	8.0	228.5	0.23	63
SA-24	67	14	20	1.0	4.6	231.2	0.28	48
SA-25	120	38	23		4.8	231.7	0.67	290
SA-26	90	15	10	1.2	4.8	251.6	0.34	72
SA-27	73	33	120		15	288.6	0.43	280
SA-28	260	79	370	14	240	367.8	0.12	1000
SA-29	50	18	13	2.9	2.9	171.7	0.23	84
SA-30	190	37	25		9.9	222.2	1.21	460
SA-31	180	55	14		6.0	208.4	0.23	490
SA-32	54	18	130		1.8	169.5	0.55	300
SA-33	120	41	75	5	80	267.7	0.38	270

Table 7 (continued). Major Ion Concentrations (mg/L)

Location	Calcium	Magnesium	Sodium	Potassium	Chloride	Bicarbonate	Carbonate	Sulfate
SA-34	82	29	14	1	13	261.3	0.41	87
SA-35	170	52.7	178	6.32	101	295.7	0.09	475
SA-36	422	96.1	420	13.7	262	287.0	0.04	1440
SA-37	138	35.2	37.3	3.38	25	238.5	0.12	245
SA-38	164	43.3	71.1	5.46	40	231.4	0.06	345
SA-39	165	35.3	34.9	2.69	17	241.6	0.04	241
SA-40	147	33.6	26.5	2.97	14	225.1	0.04	222
SA-41	143	47	95.7	7.83	45	256.1	0.09	352
SA-42	149	44.8	83.7	6.1	39	251.4	0.09	342
SA-43	196	59.4	56.1	3.99	48	211.7	0.04	451
SA-44	167	53.5	191	5.34	107	302.4	0.09	478
SA-45	0.6	1.9	332	5.47	217	110.4	98.14	2.5
SA-46	159	47.1	106	6.19	65	299.1	6.03	434
SA-47	200	62	350	14	236	586.9	0.54	666
SA-48	170	31	43	2	21	352.4	0.19	242
SA-49	120	31	38	4	30	227.0	0.19	228
SA-50	190	58	190	5	158	293.9	0.15	574

GSS = Glorieta Sandstone; mg/L = milligrams per liter; Qal = Quaternary alluvium; Qb = basalt; SA = San Andres aquifer; SAL = San Andres Limestone; SW = surface water

[a] Samples Qb-02 and Qal-11 are probably from the same well. USGS considers Qb-02 to be from a well screened in basalt, whereas others investigating the Bluewater site (e.g., Hydro-Search [1977, 1981a]; Dames & Moore [1986b]) have traditionally considered a well at the same location to be an alluvial aquifer well known as Engineers.

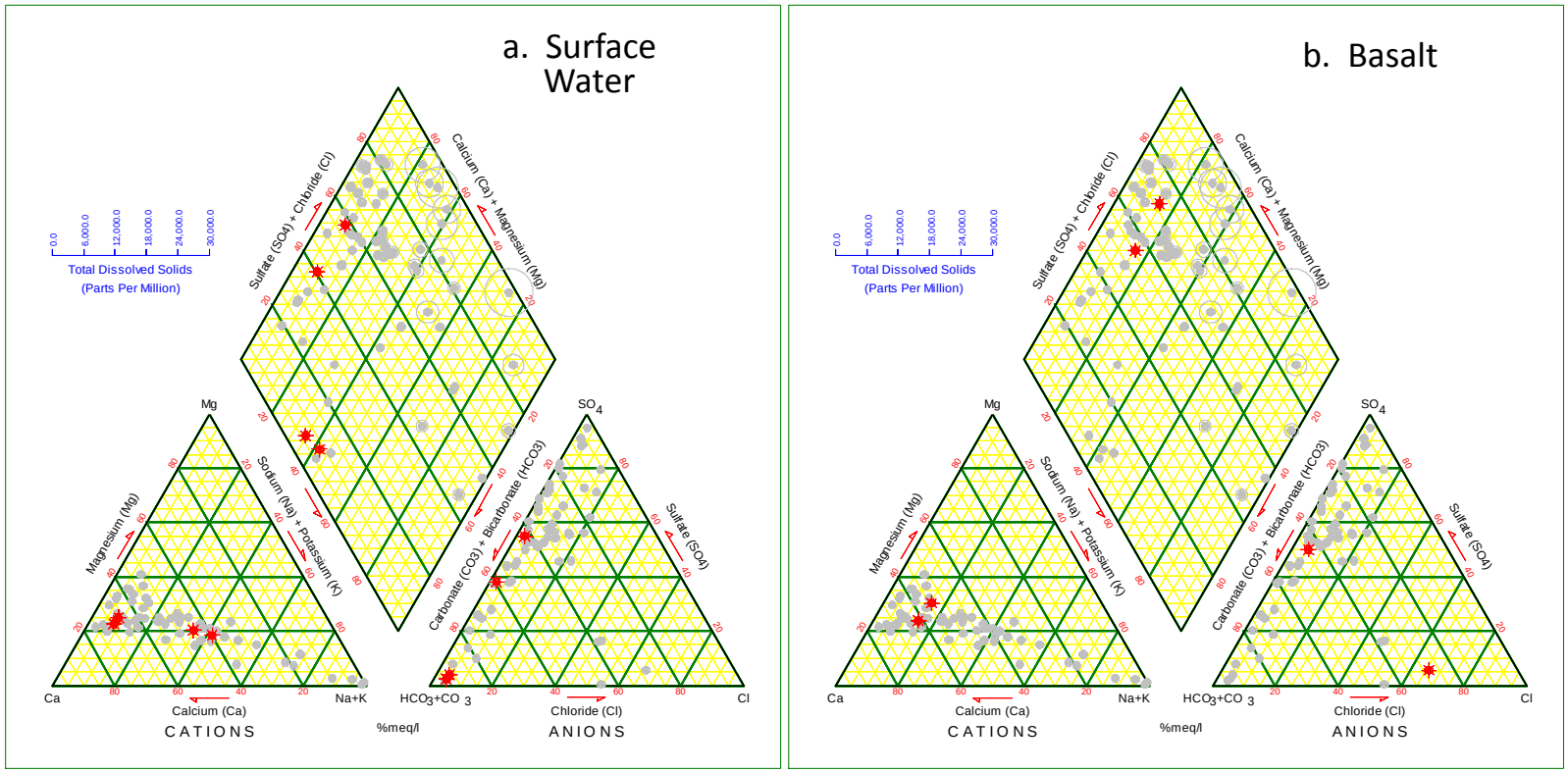

Figure 33. Piper Diagrams for (a) Surface Water and (b) Basalt Background Samples
(Gray symbols are the complete set of background samples used in this study. Red symbols are the designated subgroups.)

Data on contaminant concentrations in surface water were available only from San Mateo Creek and El Rito Creek samples. Arsenic, molybdenum, and selenium concentrations were less than their respective detection limits, and uranium concentrations were less than 0.001 mg/L. These results suggest that surface watercourses in the San Mateo Creek drainage are not receiving high fluxes of these contaminants from natural sources.

5.2 Hydrogeologic Units

5.2.1 Quaternary Alluvium

Concentrations of dissolved constituents in alluvial aquifer groundwater samples from 12 wells were found in three different information sources (Table 6). Locations Qal-01 through Qal-09 are in San Mateo Creek alluvium, with Qal-l through Qal-04 in the upper reaches of the creek drainage and Qal-05 through Qal-09 in the area directly north of the Homestake large tailings disposal cell. Locations Qal-10 through Qal-12 are in the Rio San Jose drainage, about 1 mi west of the Bluewater site main tailings disposal cell.

Oxidation states were measured on five of the alluvial groundwater samples. These were reported as values of pE, which is a dimensionless quantity defined as the negative logarithm (to the base 10) of the electron activity in a solution; the larger the pE value, the more oxidized the solution. The pE results indicated that oxidation states in the alluvial aquifer are variable. However, most water samples collected at alluvial aquifer wells are relatively oxidized, such that reduced uranium minerals would not precipitate even in the sample with the lowest oxidation state (pE = −0.40). There are difficulties in getting measurements of oxidation state representative of in situ conditions. Oxygenation of samples prior to or during measurements of DO can affect results. DO concentrations are consistent with variable oxidation states and generally correlate with pE values. Even the lowest DO concentration of 0.16 mg/L would correlate to a pE value of more than 12.

Dissolved iron concentrations were measured in nine alluvial aquifer samples. Iron concentrations were relatively low, ranging from 0.020 to 0.080 mg/L, consistent with oxidized conditions.

Cation equivalents in the alluvial groundwater are dominated by sodium and calcium, with less than 30 percent magnesium (Figure 34a). The samples from the recent and ancestral Rio San Jose alluvium have higher calcium and lower sodium equivalents than those from the San Mateo Creek alluvium. Anions in the alluvial groundwater are dominated by bicarbonate and sulfate with relatively low equivalents of chloride (Figure 34a). The samples from Rio San Jose alluvium are nearly equivalent in bicarbonate and sulfate. Samples collected from alluvium near the upper reaches of San Mateo Creek are dominated by bicarbonate, whereas those from alluvium directly north of the Homestake site are dominated by sulfate. The anion distribution for groundwater from alluvium in the upper San Mateo Creek drainage suggests that the groundwater is derived from seepage through carbonate-rich bedrock, while the alluvium associated with the reach of the creek north of the Homestake site is more likely representative of surface water infiltrating and seeping through gypsiferous soils or contaminated soils. Contaminated soils in the San Mateo Creek drainage in areas north of the Homestake site are generally attributed to mining and milling activities in the Ambrosia Lake Valley.

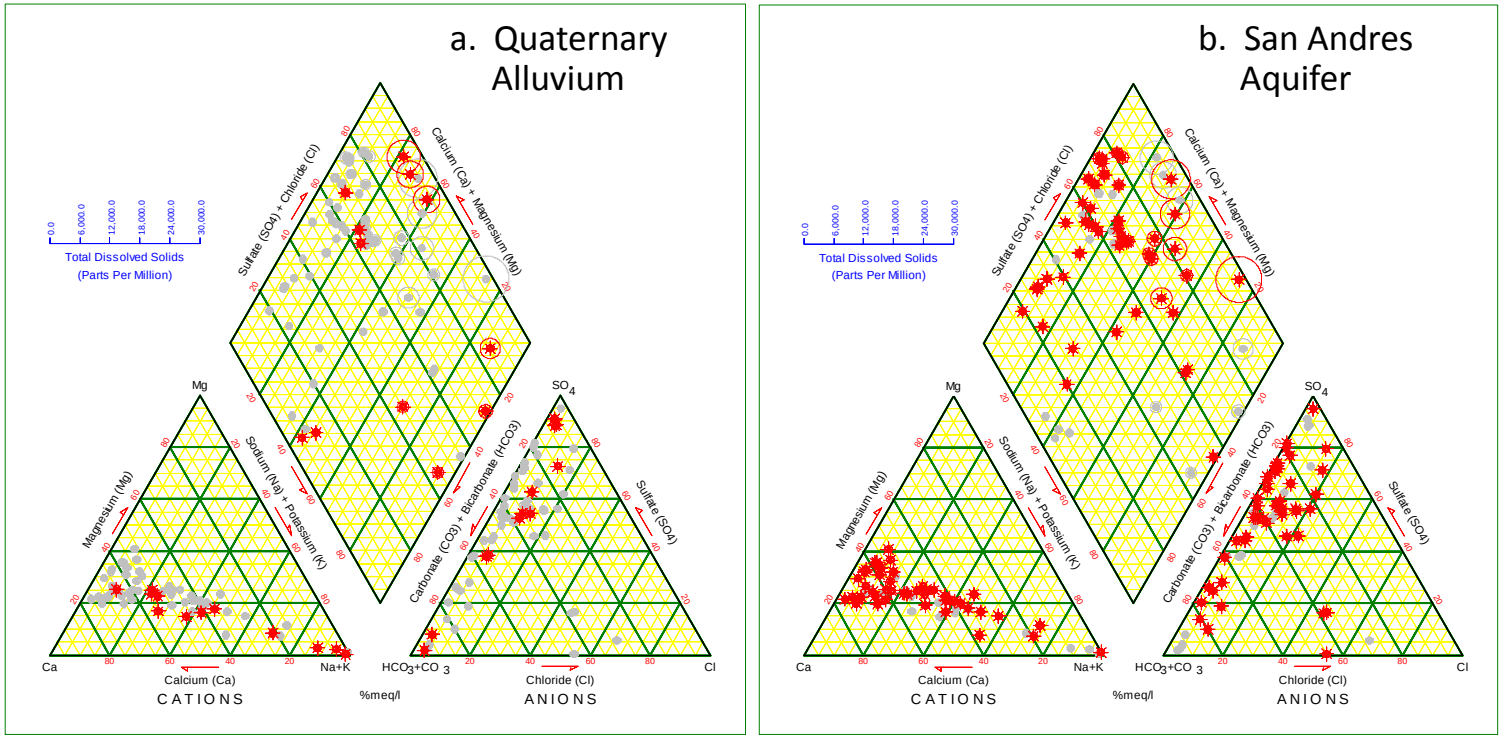

Figure 34. Piper Diagrams for (a) Quaternary Alluvium and (b) San Andres Aquifer Background Samples
(Gray symbols are the complete set of background samples used in this study. Red symbols are the designated subgroups.)

Many of the alluvial groundwater samples are oversaturated with calcite, and the rest are only slightly undersaturated (Figure 35). The saturation indexes suggest that groundwater in alluvium is in contact with calcite, likely derived from abundant limestone in the region. Samples Qal-05, Qal-06, and Qal-08, which are from San Mateo Creek alluvium north of the Homestake site, have the highest salinities, as indicated by the specific conductivities for these locations (Table 6). These three samples also have the highest gypsum saturation indexes (Figure 35), supporting the possible origin of infiltration and seepage through gypsiferous soils.

Alluvial groundwater samples from the San Mateo Creek alluvium north of the Homestake site had elevated concentrations of uranium, with three of the five samples showing uranium concentrations greater than 0.1 mg/L. The three samples with elevated uranium also had selenium concentrations exceeding 0.3 mg/L. These results indicate that alluvial groundwater in this area is contaminated, presumably due to an influx of contaminated waters derived from mining activity in Ambrosia Lake Valley.

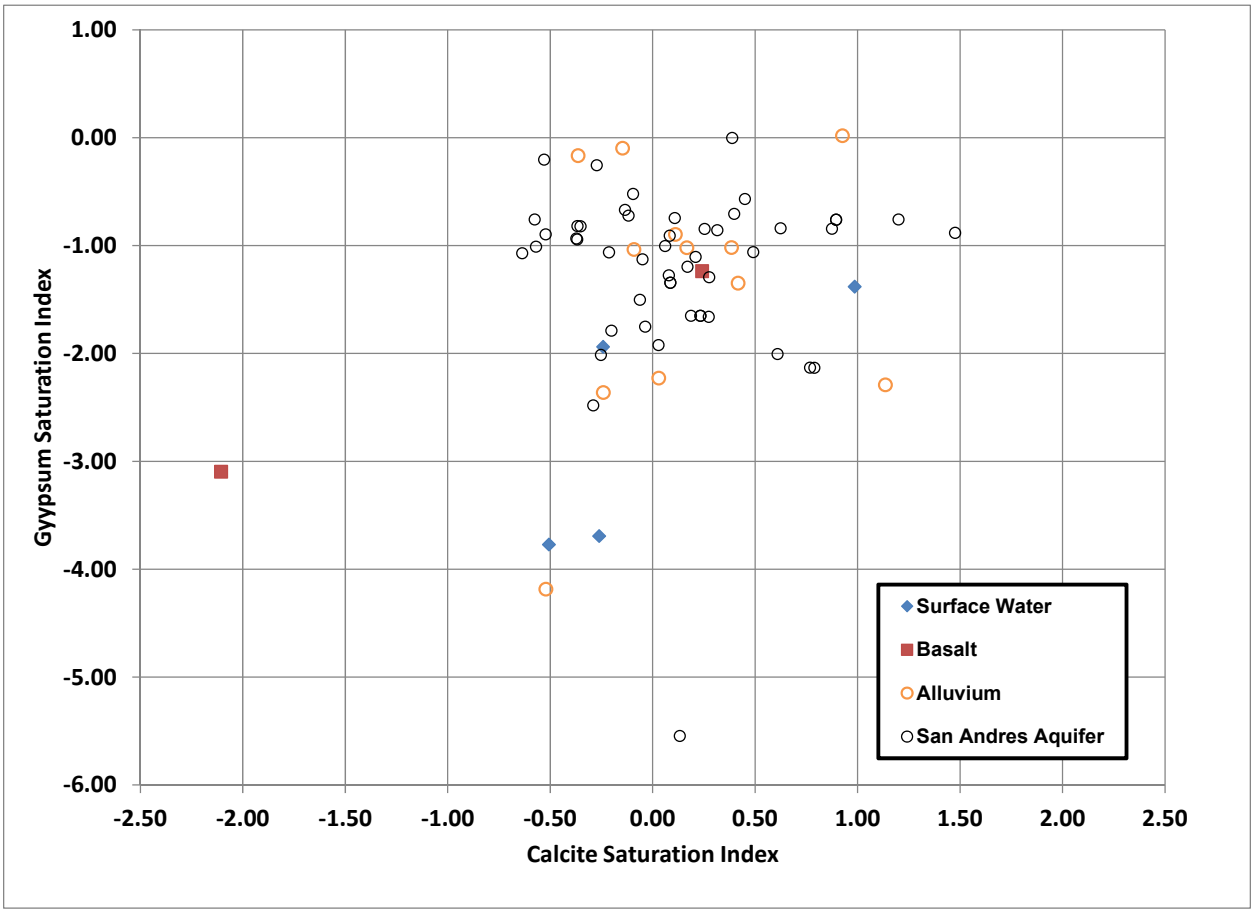

Figure 35. Saturation Indexes for Calcite and Gypsum in Background Samples

5.2.2 Basalts

Groundwater chemistry data from only two wells completed in basalt were located for this analysis. Sample Qb-01 is from basalt in the San Mateo Mountains, and Qb-02 is from Bluewater Basalt about 0.6 mi west of the main tailings disposal cell (Figure 32). No oxidation-

Bluewater Basalt about 0.6 mi west of the main tailings disposal cell (Figure 32). No oxidation-reduction values were available for these waters; however, the groundwater was likely oxidized, based on the shallow depth of each well and a lack of reduced solid matter in these rocks. One sample was analyzed for iron with a result of 0.05 mg/L, consistent with oxidized conditions.

Recharge of water in mountains above the Qb-01 location resulted in low salinity (specific conductivity) and a calcium-chloride composition (Figure 33b). The sample from the Bluewater Basalt had higher salinity, similar cation composition, but an anion composition dominated by sulfate and bicarbonate rather than chloride.

5.2.3 Chinle Formation

Limited data are available regarding the chemistry of groundwater in the Chinle Formation. As a consequence, no specific chemical data for Chinle Formation wells are reported in Table 6 and Table 7. Instead, a brief description of the water chemistry in the Chinle Formation is presented here based on information presented in Baldwin and Anderholm (1992) and Baldwin and Rankin (1995).

Groundwater in the Chinle Formation is generally a sodium-bicarbonate or a sodium-bicarbonate-sulfate water that has small calcium and chloride percentages. The increased sodium concentrations in the Chinle Formation groundwater are probably due to ion-exchange reactions that occur in interbedded shales and clays. Water from wells screened in the Chinle Formation tends to have relatively large TDS concentrations, reflecting long residence times. TDS levels vary from approximately 500 to about 18,000 mg/L. This wide range reflects the complex and highly varied nature of flow systems in Chinle Formation strata. In contrast to the alluvial and San Andres aquifers in the study area, sodium concentrations in Chinle Formation groundwater typically account for 83 to 97 percent of total cations (Baldwin and Rankin 1995).

5.2.4 San Andres Aquifer

Groundwater chemistry in the geologic formations of the San Andres aquifer (San Andres Limestone and Glorieta Sandstone) is largely controlled by lithologies represented in these formations. The dominant lithology is sandstone that contains calcareous cement (mostly calcite with dolomite) and fine-grained pyrite. Most of the pyrite is presumably in fine-grained sandstone found near the top of the San Andres Limestone, as observed in the vicinity of the Bluewater site (Section 3.3.2.4). In addition, beds of gypsum and anhydrite are in the sandstone-dominated formations (Baldwin and Rankin 1995).

Background groundwater chemistry data for the San Andres aquifer are available from the USGS study by Baldwin and Anderholm (1992), specifically for an area near the town of Thoreau, which is located about 19 mi northwest of the Bluewater site. According to Baldwin and Anderholm (1992), the chemistry of the groundwater in the San Andres aquifer is less variable in the Thoreau area than in the Bluewater area.

The presence of pyrite in sandstones of the San Andres aquifer suggests that groundwater in the aquifer may occur under a low oxidation state. However, all pE values for 12 water samples collected from the aquifer were greater than 5, indicating that much of the groundwater in the aquifer is oxidized. Low concentrations of dissolved iron were also observed in most of the

samples, consistent with oxidized conditions. Four groundwater samples from wells screened in the San Andres aquifer had iron concentrations exceeding 1 mg/L. These high iron concentrations could be representative of localized reduced conditions, or the water containing the high iron levels may have been compromised by inadvertent incorporation of particulate iron during sampling. The mineral uraninite is about 6 orders-of-magnitude undersaturated in the San Andres aquifer samples, including in the sample with the lowest pE, which suggests relatively oxidized conditions.

Specific conductivity values in the San Andres aquifer are mostly less than 1,000 µS/cm, indicating moderately high salinity. As indicated in Figure 34b, cation chemistry in most of the San Andres aquifer samples is dominated by calcium, while a few of the samples are dominated by sodium. This variation between calcium dominance in some locations and sodium dominance in others might be the result of cation exchange processes in the aquifer. Anions are spread between bicarbonate and sulfate with little chloride. Molar ratios of bicarbonate to sulfate range from about 1 to 12, with most ratios around 5. The samples with the highest concentrations of dissolved solids are typically high in sulfate. All San Andres aquifer samples were undersaturated with gypsum, indicating that the groundwater has a tendency to dissolve gypsum (Figure 35). Gypsum dissolution is a potential cause of the high salinity in bedrock groundwater. The San Andres aquifer samples are mostly near saturation with calcite, but saturation levels span a broad range from −0.64 to 1.48, reflecting varying amounts of water interaction with carbonate minerals.

Twelve samples of San Andres aquifer groundwater had analytical results for contaminants. In all 12 samples, molybdenum concentrations were less than the instrument detection limit for this constituent. The samples were also low in uranium and nitrate, with the highest-concentration samples showing about 0.011 mg/L uranium and 10.9 mg/L nitrate (as NO_3).

5.3 Background Uranium Concentration

Detailed information regarding the background concentrations of uranium in the alluvial and San Andres aquifers would be beneficial for evaluating the spatial extent of uranium contamination in groundwater due to milling activity in the Grants-Bluewater Valley. Unfortunately, no detailed quantitative assessment of background concentrations for this constituent has ever been conducted. This problem stems from a variety of issues, including (1) a scarcity of dissolved uranium concentration data for wells installed in uncontaminated portions of the two aquifers; (2) the fact that groundwater quality tends to degrade with flow distance and, therefore, residence time in each aquifer; (3) local natural variations in water quality; and (4) leakage of lower-quality water from adjacent formations (e.g., Chinle Formation, Yeso Formation). Nonetheless, a report to ARCO by Applied Hydrology Associates, Inc. (1990) aimed at selecting a corrective action program and establishing alternate concentration limits for selected contaminants at the Bluewater site provides data from which useful approximations of background uranium concentration can be deduced.

Using water chemistry data for samples collected from wells E(M), Aragon, Berryhill House, and Engineers (see Figure 16 and Plate 7), Applied Hydrology Associates, Inc. (1990) reported that the background uranium concentration in the alluvial aquifer varied from 0.003 to 0.04 mg/L. Similarly, concentration data from bedrock wells Bowlins, L(SG), M(SG), and Berryhill Section 5 were used to identify a background uranium concentration range of 0.003 to

0.013 mg/L for the San Andres aquifer. With these findings, Applied Hydrology Associates, Inc. (1990) concluded that there was no significant difference in background uranium concentration between the two aquifers.

On the basis of the above-mentioned concentration ranges, it is assumed in this study that a uranium concentration of 0.01 mg/L is representative of background conditions in both aquifers. Though slightly lower and higher concentrations could probably be identified in uncontaminated wells in the Grants-Bluewater Valley, this value appears reasonable for preliminarily assessing the spatial extent of the uranium plumes in the two aquifers. As discussed in later chapters, a concentration of 0.01 mg/L is used in this report to delineate the lateral boundaries and the leading edge of the uranium plumes emanating from the Bluewater site in the alluvial and San Andres aquifers. It is possible that additional chemical characterization methods (e.g., uranium isotope concentrations) would be helpful for identifying uranium contamination if concentrations slightly larger than 0.01 mg/L are measured at wells located far from the plumes originating at the Bluewater and Homestake sites.

6.0 Disposal Cell Performance

Most of the tailings generated during the 30-year history of milling operations were deposited in the main tailings impoundment. During site reclamation, this impoundment was enclosed with an engineered cover consisting of a clay layer and rock to prevent radon emissions and erosion of the encapsulated tailings (Figure 36). Seepage of tailings fluids from the tailings impoundment and subsequent disposal cell is addressed in this section.

Figure 36. Site Marker near the Southwest Corner of the Main Tailings Disposal Cell

6.1 Tailings Disposal History

Initial deposition of tailings in the main tailings impoundment began in 1956 in a basalt depression that was located in what is now the middle of the main tailings disposal cell. A limited quantity of carbonate tailings was deposited in this depression, followed thereafter by acidic tailings. After initial depositions began to fill the depression, a series of soil starter dikes were constructed to control the surface area of the pond. At this point, the footprint of the tailings pond covered not only basalt surfaces but also windblown sand deposits and an outcrop of San Andres Limestone.

Tailings were conveyed in a slurry and discharged continuously from three movable spigots along the south side of the impoundment. Coarser sands settled near the spigots, and mixed fine sand, silt, and clay settled in the middle portion of the impoundment, with silt and clay (referred to as "slimes") settling out in the north end, where tailings fluid formed a pond. Figure 37 shows the approximate distribution of these materials.

As tailings deposition continued, dikes were periodically raised to contain the tailings and tailings pond. By 1957, the main tailings impoundment attained a footprint similar to that of the final impoundment (and disposal cell). By 1981, the elevation on the south side was 56 ft higher than the north side because of the buildup of sand tailings in that area.

6.2 Main Tailings Impoundment Seepage

ARCO recognized that substantial quantities of tailings fluids seeped through the bottom of the main tailings impoundment, through the underlying unsaturated materials, and into the alluvial and San Andres aquifers. Various estimates of seepage losses through the bottom of the main tailings impoundment were made by Anaconda and ARCO hydrology subcontractors (Arlin et al. 1978, Dames & Moore 1984a, ARCO 1990, Applied Hydrology Associates Inc. 1995). All agreed that high seepage losses of at least 1,000 gpm occurred in the 1950s. To reduce the amount of seepage, Anaconda constructed a deep injection well in 1960.

The injection well, located more than a mile northeast of the tailings impoundment (Figure 4), was completed in the Yeso Formation that underlies the Glorieta Sandstone. Tailings fluid decanted from the pond that persisted at the north (lowest elevation) end of the main tailings impoundment was injected into the well from 1960 through 1977. The injection rate was regulated to ensure only gravity flow within the well (i.e., injection was not under pressure). Approximately 501 million gallons of decanted fluid had been injected by the end of 1965 (West 1972), which is an average rate of approximately 190 gpm. Assuming this rate continued, a total of approximately 1.7 billion gallons of decanted fluids were injected during the operation of the well. In their evaluation of the Bluewater site injection process, USGS considered it to be the most satisfactory and economically feasible method of effluent disposal (West 1972).

After 1977, tailings fluids were evaporated in lined evaporation ponds constructed north of the impoundment. Use of the evaporation ponds removed approximately 525 million gallons of liquid that otherwise would have infiltrated into the tailings. During the years 1977 through 1982, much of the uranium in the decanted water was recovered by recycling the evaporation pond water through the mill (ARCO 1995).

Ore-milling operations and tailings deposition ceased in March 1982. Subsequently, ARCO installed 58 extraction wells in the sand portion of the tailings impoundment. These wells removed approximately 122 million gallons of interstitial fluids from the tailings as part of a program to dewater the impoundment and recover uranium. The extracted fluids were treated at the mill, and most of the barren solution was pumped to the evaporation ponds. The remaining unreported amount of treated water was sprayed on the tailings for dust control during interim tailings impoundment stabilization activities. Pumping from these wells ceased in 1985 when water levels and well yields dropped to levels at which pumping was no longer practical (ARCO 1995).

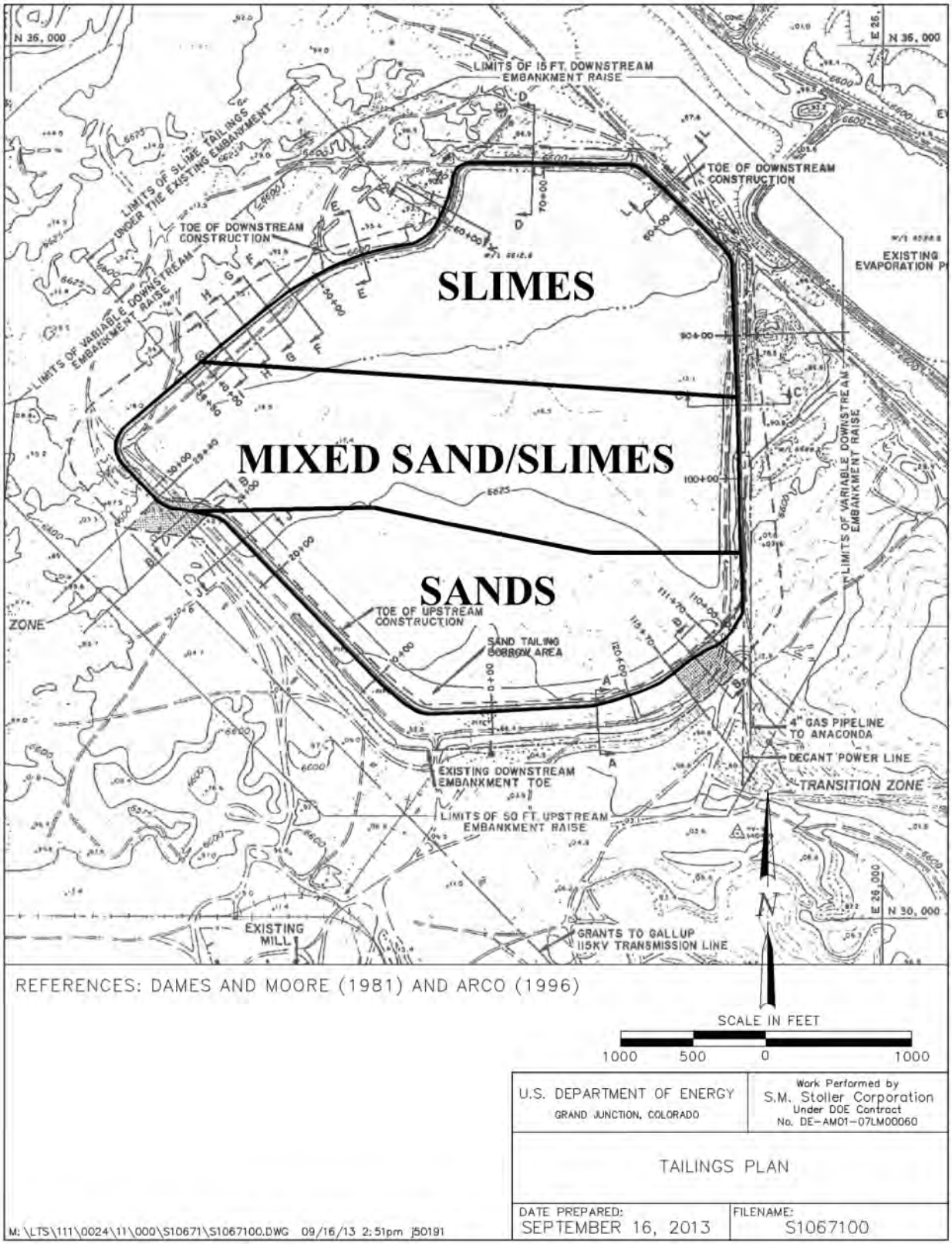

Figure 37. Approximate Distribution of Materials Within the Main Tailings Impoundment

Prior to placement of the radon barrier, ARCO installed vertical band drains to wick fluids out of the slimes. The purposes of this procedure were to reduce the quantity of tailings fluids available for seepage and to consolidate the slimes. Tailings were loaded with a consolidation layer of windblown silty and sandy clay materials (the same type of material used to construct the radon barrier) to squeeze fluid out of the slimes and into the drains.

The wicks drew approximately 24 million gallons of tailings fluids to the surface of the impoundment, where the fluids ponded and evaporated. ARCO calculated that up to 16 million gallons of fluids moved into unsaturated materials of the consolidation layer, thus removing a total of approximately 40 million gallons from potential seepage (Applied Hydrology Associates Inc. 1993). Approximately 7.4 million gallons of fluids were assumed to have been forced through the bottom of the impoundment during the consolidation process (derived from Appendix A, Table A-1). Monitoring results from wells adjacent to the impoundment, however, did not show any increase in contaminant concentrations in either the alluvial or San Andres aquifers as a result of this activity. The band drains were removed when 90 percent consolidation of the slimes had been attained and flow from the band drains ceased. The final cover materials (radon barrier and rock) were installed at that time.

Estimated seepage rates from the tailings impoundment into underlying materials and aquifers were based on mill water-balance calculations, including fluid discharge to the tailings impoundment, decantation of the ponded fluids to the injection well and later to the evaporation ponds, cell dewatering activities, tailings fluid reprocessing, and precipitation. However, ARCO did not account for evaporation of the tailings fluid and precipitation runoff that ponded at the north end of the impoundment prior to decantation activities; these processes may have essentially cancelled each other out, thus not significantly affecting ARCO's seepage rate calculations. Evaporation of the ponded fluids following the start of decantation for deep-well injection (and later disposal in the evaporation ponds) was assumed to have been minimal because most of the ponded water was decanted (Dames & Moore 1981a). A schematic of the Bluewater mill impoundment water cycle is shown in Figure 38.

Cumulative seepage rates from the main tailings impoundment, based on ARCO's last estimates (Applied Hydrology Associates Inc. 1995), are plotted in Figure 39. ARCO estimated that approximately 2.7 billion gallons of tailings fluid seeped from the main tailings impoundment by the time deep-well injection commenced in 1960. Thereafter, seepage continued at a reduced rate. By the time construction of the disposal cell and placement of the rock cover was completed in 1995, ARCO estimated that approximately 5.7 billion gallons of fluid had seeped through the bottom of the impoundment (Appendix A, Table A-1). Although evaporation of tailings pond fluid would have removed some water from the cycle, ARCO's estimate of 5.7 billion gallons of seeped fluid through 1995 is considered to be the best available estimate and is used in this assessment.

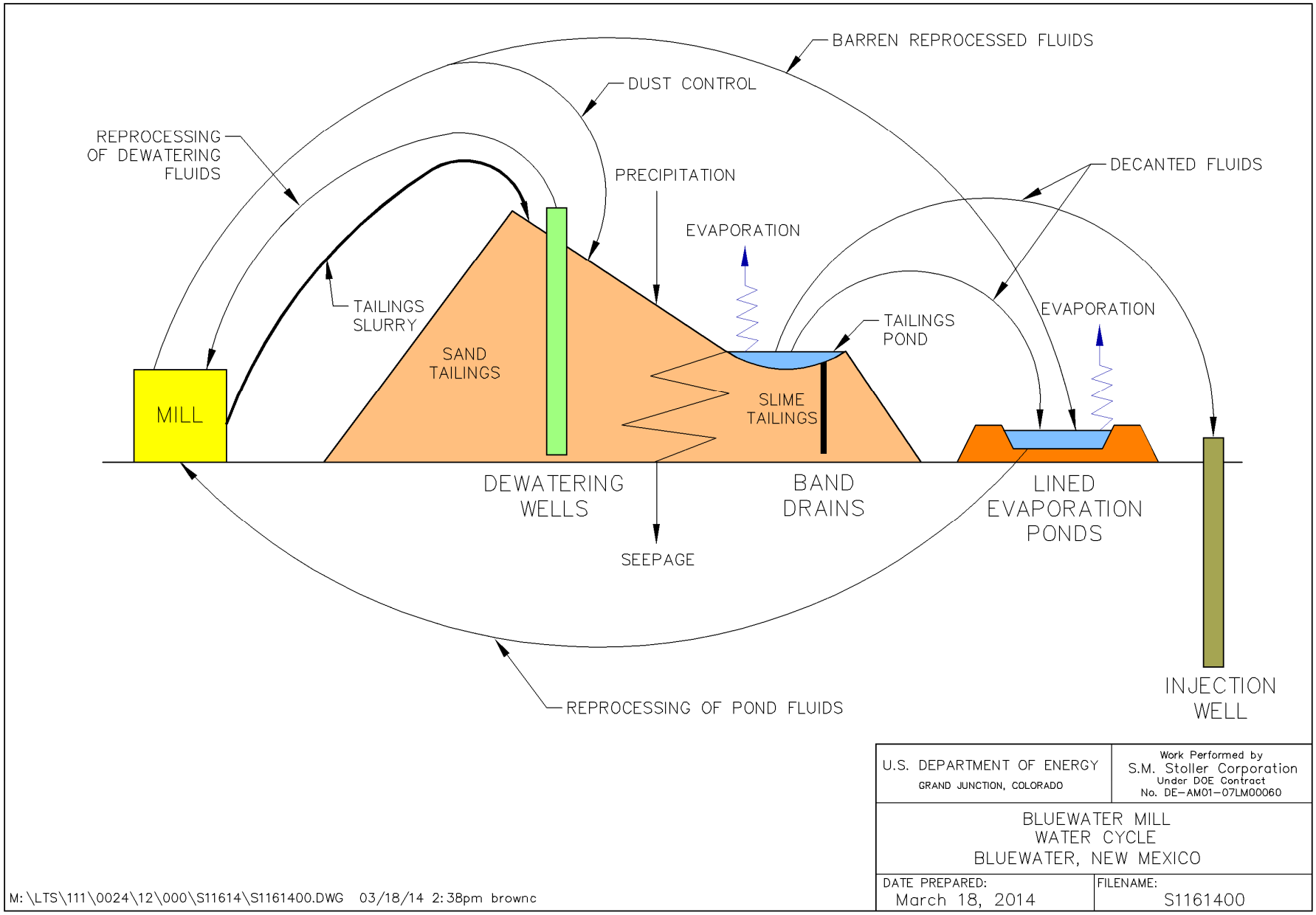

Figure 38. Schematic of the Tailings Impoundment Water Cycle

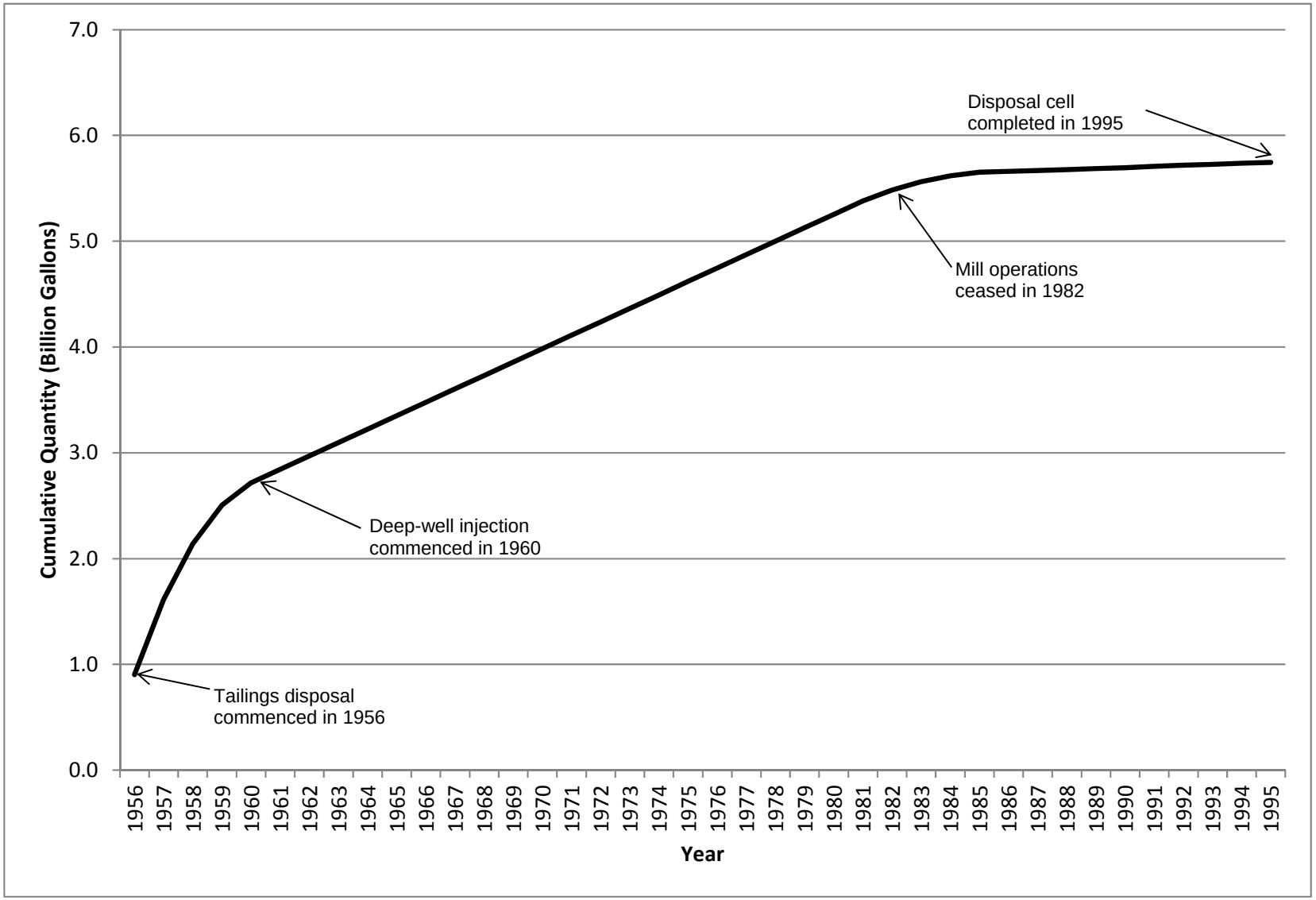

Figure 39. Estimated Cumulative Seepage from the Main Tailings Impoundment Through 1995

6.3 Disposal Cell Performance

A liner was not installed prior to tailings placement, and the tailings were encapsulated in place. Therefore, tailings fluids remaining in the disposal cell, and additional fluids from infiltration of precipitation through the cover, could continue to seep through the bottom of the disposal cell. This assumption of continuing seepage is considered to apply to other rock-covered UMTRCA disposal cells where the tailings were stabilized in place.

A key component of understanding how much fluid could seep out of the disposal cell is evaluating how much precipitation is entering the cell. Therefore, an understanding of how the disposal cell cover was designed and constructed, and how it may change over time, helps characterize the potential hydraulic performance of the cover.

6.3.1 Cell Cover Design and Construction

The main tailings disposal cell cover, completed in December 1995, was designed primarily to satisfy federal regulations and standards for radon attenuation and erosion protection as directed by UMTRCA. Federal regulations and NRC guidelines require groundwater protection but do not include standards or criteria for cover permeability or percolation. Nor was the potential for plant encroachment, root intrusion, or animal burrowing in the cover evaluated. The assumption, however, was that the engineered cover would prevent infiltration of precipitation into the encapsulated tailings, thus eventually eliminating the disposal cell as a continuing source of contamination (after seepage of residual fluids).

Designers used NRC guidelines to calculate radon barrier thicknesses for different surfaces of the main tailings disposal cell to limit radon flux, as required, to less than the 20 picocuries per square meter per second (pCi/m^{2}s) standard (Title 10 *Code of Federal Regulations* Part 40, Appendix A). The radon barrier, consisting of sandy-clay material from the site, ranged in thicknesses from 1.0 to 4.2 ft, with the greatest thickness over the sand tailings (ARCO 1996). Prior to placement of the radon barrier, the tailings surface was graded and covered by up to 15 ft of compacted relocated materials derived from natural windblown deposits and evaporation pond dike materials from the site (primarily sandy-clay material identical to the radon barrier material). The greatest thicknesses of relocated materials were placed over the slimes portion of the tailings, most of which were placed for dewatering through the band drains. Some of these materials contained low levels of windblown radioactive contamination.

The radon barrier was compacted to 100 percent of maximum dry density based on Standard Proctor density. As-built permeability values were not reported. However, a common construction assumption at the time was that laboratory permeability (saturated hydraulic conductivity [*Ks*]) results could be achieved in the field. Designers likely assumed, based on their laboratory results, that by compacting the radon barrier to 100 percent of Standard Proctor density, they had achieved an as-built permeability in the range of 1×10^{-7} to 1×10^{-8} centimeters per second (cm/s).

NRC guidelines (NRC 1990) were used to calculate runoff discharge and velocity from the top and side slopes of the cell and the size of basalt rock necessary to control erosion of these slopes. The NRC procedure is based on calculations of the probable maximum precipitation event and resulting probable maximum flood event.

Cover slopes were designed to shed runoff water primarily to the north. However, the north top slope was designed at a 0.5 percent slope, leaving little latitude for construction irregularities or settlement. The final constructed surface in this area had a 0.45 percent slope (ARCO 1996). The as-built surface topography and cross sections of the main tailings disposal cell are shown in Appendix A, Figures B-2 through B-4.

The condition of vegetation along the north toe slope indicates that runoff is not shedding off of the north edge of the cover as intended. If runoff was occurring, more abundant plant growth would be present along the flat north toe slope where runoff water would accumulate. However, plant growth along the north toe slope appears to be no greater than in surrounding areas, and moist areas have not been observed in this area.

6.3.2 Existing Conditions of the Cell Cover

Depressions have formed on the north end of the disposal cell cover, which is over the portion of the cell containing slimes. These depressions collect runoff water after storm events of sufficient magnitude or intensity (Figure 40). They were first observed by DOE inspectors during the first annual inspection in 1998. Satellite imagery taken in 1997 verifies that they had already started developing before DOE acquired the site. The depressions apparently formed as the slimes continued to consolidate after completion of the cover, which occurred soon after removal of the band drains.

In 2012, DOE conducted a high-resolution topographic survey of the main tailings disposal cell using a light detection and ranging (LiDAR) method to provide a baseline to determine if differential settlement in the depression area is ongoing (DOE intends to conduct another LiDAR survey in 2015). No standing water was present on the cover at the time of the survey. The digital LiDAR survey data were used to develop 6-inch contour intervals for the disposal cell surfaces (Appendix A, Figure 9) and to calculate the areas, depths, and volumes of the depressions. Based on light-colored evaporite minerals that form as ponded water evaporates from the depressions and corresponding elevations determined by the survey, the maximum ponded area has been approximately 15.3 acres. The maximum depth of ponded water has been 2.5 ft in the deepest depression, and the maximum quantity of ponded water has been approximately 4.3 million gallons (Appendix A, Figure 10). This maximum ponded area appears to have occurred during spring 2012 following melting of unusually high snowfall amounts during the previous December. No significant precipitation occurred during the spring, but standing water persisted until mid-June.

Observations of differential settlement and ponding of water have raised concerns about water percolation through the cover, leaching of tailings constituents, and the stability of the north end of the disposal cell. Field observations of the persistence of ponded water suggest that most of it dissipates by evaporation rather than percolation through the cover. Evapotranspiration plays an insignificant role on this portion of the cover because very little vegetation is present.

Figure 40. Ponds in Depressions on the Main Tailings Disposal Cell in August 2012, Following a Summer Storm Event

To determine if the depressions are having an adverse effect on the performance of the radon barrier, radon flux measurements were collected on the uncovered surface of the radon barrier over the area encompassing the depressions (Appendix A, Figure 11). The measurements were collected in early July 2013, after a dry spring and prior to the annual monsoon season; no ponded water was present on the cover. The cell cover materials were at their driest condition of the year, which would be when the highest radon emissions would be expected to occur. Moisture attenuates radon, so radon emission would not occur through wet materials or standing water. A typical measurement location is shown in Figure 41.

Figure 41. Radon Measurement Location RF-05 in the Area of Cell Cover Depressions

Radon flux was below the laboratory detection limit of 0.5 pCi/m^{2}s at all of the locations (the design limit is 20 pCi/m^{2}s). These results suggest that the deformation of the cover in this area has not opened pathways (i.e., cracks or soil fissures through the radon barrier) for radon emission from the underlying tailings materials; therefore, the radon barrier is performing as designed. These results may also imply that the permeability of the radon barrier has not increased by development of the depressions and associated deformation of the surface, or by any other changes that may have occurred since the cover was constructed.

6.3.3 Cell Cover Evolution

Research has shown that surface layers of rock on covers create a favorable habitat for deep-rooted plants in all climates, even in the desert. Depending on climatic conditions and cover design, the rock layer may act as a mulch, effectively reducing soil evaporation (increasing soil water storage) and trapping windblown dust, thereby providing the water and nutrients needed for the germination and establishment of vegetation. Vegetation is sparse but is beginning to establish on the main tailings cell cover. It consists primarily of annual weeds, but populations of perennial grasses, forbs, and deep-rooted woody plants are also establishing. An understanding of the ecology of these plant species provides clues about past and possible future changes in the condition of the disposal cell cover.

Currently, deep-rooted Siberian elm saplings and some robust fourwing saltbush shrubs grow on the cell cover, primarily on the south two-thirds of the cover (DOE controls the elm saplings with herbicide to avoid the establishment of mature trees). Their presence suggests that the underlying relocated materials and tailings are moist, particularly in that area. The sparsity of deep-rooted plants on the north portion of the cover may be because the thick layer of compacted relocated materials over the slimes is inhibiting root penetration.

The long-term consequences of changes in the ecology of covers, including the encroachment and establishment of populations of deep-rooted plant species, can be either detrimental or beneficial depending on the cover design and management practices (Link et al. 1994). A key issue is whether deep-rooted plants that establish on the cover will increase or decrease the likelihood of precipitation percolation through the cover and into the tailings. Detrimental effects are related to root growth through covers and into tailings; plants can increase percolation flux by accelerating soil development, which increases permeability by creating fissures or planes of weakness in the soil structure. Beneficial effects are related to the extraction of soil water by plants (transpiration) and erosion protection; consequently, plant encroachment could actually enhance the performance of the cover. Some studies have shown that vegetation significantly decreases percolation of precipitation (Benson et al. 2011, Waugh et al. 2009). Transpiration can greatly limit percolation if habitat characteristics favor the establishment and resilience of a diverse plant community. Therefore, a combination of high transpiration rates and erosion protection can be achieved.

Ecological succession and natural soil-forming processes alter engineered soil covers over relatively short time periods regardless of climate, cover design, or service life. Studies of disposal cell and landfill covers across the country have shown that compacted soil layers (similar to the main tailings radon barrier) typically fall short of low-permeability targets, often during or shortly after construction, and sometimes by several orders of magnitude (NRC 2011). For example, if compaction of the radon barrier achieved a permeability of 1×10^{-7} cm/s as designed, the current permeability may be closer to 1×10^{-5} cm/s.

6.3.4 Cell Cover Hydraulic Performance

The Reclamation Plan (ARCO 1990) did not reference soil physical or hydraulic property criteria for the cover. Apparently there were no criteria for the permeability of the cover or for percolation flux through the cover. However, it did provide results of grain-size analyses and *Ks* tests for samples of materials specified for use in constructing the radon barrier. Test

materials were low-plasticity clay and sandy clay. Geometric means of permeability tests were 1.7×10^{-8} cm/s for the clay and 2.4×10^{-7} cm/s for sandy clay, with all samples compacted to the specified 100 percent of Standard Proctor dry density. Although the as-built permeability of the radon barrier was not measured directly, it was likely assumed that the as-built *Ks* was between 1×10^{-7} and 1×10^{-8} cm/s as noted in Section 6.3.1.

It would seem likely that percolation into tailings is potentially greatest where water ponds in depressions. However, as noted previously, evaporation appears to be the dominant factor in reducing the ponds (rather than percolation through the cover). ARCO also believed evaporation to be the dominant factor, as this was the method used to eliminate ponded fluids during the wicking procedure (Applied Hydrology Associates Inc. 1993). Even if the permeability of the radon barrier is increasing as expected, the permeability of the underlying thick layer of relocated material likely remains close to the presumed original permeability of 1×10^{-7} cm/s because those materials would not be impacted by the environmental forces affecting the surface materials.

Radon barrier permeability measurements conducted at several UMTRCA Title I sites (Waugh et al. 1999, Waugh et al. 2007, Glenn and Waugh 2001) suggest that the permeability of the radon barrier at the Bluewater site may be on the order of 1×10^{-5} cm/s. However, because of the area of the cover and expected variability of hydraulic performance of the radon barrier (due to variable thicknesses of the barrier and non-uniformity of plant growth), extensive field permeability tests would be necessary to determine the actual permeability of the radon barrier of the main tailings disposal cell. These tests are not considered to be necessary at this time because the performance criterion for radon emission is being met.

6.4 Disposal Cell Seepage

6.4.1 Conditions for Seepage

ARCO assumed that seepage of fluids remaining within the disposal cell would continue to occur after closure of the cell but did not predict the rate or quantity of seepage (ARCO 1990). The cover design was intended to control emanation of radon from the encapsulated tailings and shed precipitation runoff without causing erosion of the cover; percolation of precipitation through the cover and into the cell was not a factor in the design requirements.

Seepage from the disposal cell is controlled by a difference in total hydraulic head. Total hydraulic head is the sum of hydraulic pressure head and elevation head above a reference datum, which in this case is the bottom of the disposal cell. Because the total hydraulic head within the final disposal cell is greater than the total hydraulic head underlying the disposal cell, fluid seepage from the tailings into the underlying foundation material is expected to persist in both saturated and unsaturated conditions.

The degree of saturation within the disposal cell is a key component in evaluating unsaturated seepage. However, actual saturation within the disposal cell is unknown. Cell material saturation was not measured or estimated by ARCO and has not been measured since DOE acquired the site. For the purposes of this assessment and based on studies conducted on the Shiprock, New Mexico, Disposal Site cell (DOE 2012), it is assumed that the sand tailings are moist but unsaturated and the slimes are saturated. Although ARCO attempted to dewater the sand tailings,

pumping likely did not completely drain the tailings, and precipitation would have recharged the tailings to some degree after pumping ceased in 1985.

6.4.2 Seepage Rate

The rate of seepage, or tailings fluid flow through the tailings into underlying foundation material, is governed by the hydraulic conductivity of each material composing the disposal cell. The main tailings disposal cell can be described as a layer-cake type of arrangement with the cover materials (i.e., the radon barrier and underlying soil placed to attain the final construction grade) overlying the tailings mass (sands and slimes), which in turn overlie foundation materials (alluvium, basalt, and limestone). Under saturated conditions, when the largest volume of tailings fluid flow would occur, hydraulic conductivity of the overall system is controlled by the lowest hydraulic conductivity of the materials in the layer-cake arrangement.

Table 8 provides estimates for saturated hydraulic conductivities of materials existing in and under the disposal cell that are used in this analysis. Assuming that tailings fluid seepage is controlled by natural flow, values provided in Table 8 indicate that moisture will percolate through the cover, will flow at a slower rate through the tailings, and will eventually discharge into the underlying foundation materials (which have the highest *Ks*).

Table 8. Estimated Saturated Hydraulic Conductivities for the Bluewater Disposal Cell

Layer	Vertical *Ks* (cm/s)
Cover	10^{-5}–10^{-4} [a]
Tailings: Sand[b]	10^{-6}–10^{-5}
Slimes-Sand[b]	10^{-6}–10^{-5} [c]
Slimes[b]	10^{-7}–10^{-6}
Foundation Materials: Alluvium	10^{-4}–10^{-3}
Basalt	10^{-2}–10^{-1}

cm/s = centimeters per second; *Ks* = saturated hydraulic conductivity
[a] Long-term value after soil development effects have occurred (NRC 2011)
[b] Licensing Documentation, Volume 22, Page 7 (Dames & Moore 1984b)
[c] Conservatively assumed to be controlled by interbedded sand layers

Because of the presence of sand in the slimes-sand portion of the disposal cell, that portion is conservatively assumed to have the same hydraulic conductivity as the sand portion. Therefore, the sand and slimes-sand portions are hereafter included together as “coarse tailings.” The slimes portion of the cell is considered to be “fine tailings.”

6.4.3 Estimated Seepage Quantity

6.4.3.1 Water-Balance Equation

For this assessment, the following basic water-balance equation is used to estimate seepage amount after construction of the cover in 1995.

$$I - O = \Delta S$$

where I = inflow
O = outflow
ΔS = change in storage

6.4.3.2 Inflow

Inflow quantity to the disposal cell is governed by site-specific climatic parameters, which are unavailable. However, average monthly precipitation quantities are available for the Grants, New Mexico, airport, and average monthly evaporation quantities are available for the region (Appendix A, Table 2). Due to the proximity of the site to the data sources, it is assumed that these quantities are representative of precipitation and evaporation at the Bluewater site. Based on these data, the Bluewater disposal cell cover receives an annual average of approximately 10.3 inches of precipitation, with an average free-surface evaporation of 45.9 inches per year.

Yearly free-surface evaporation rates are about 4.5 times greater than yearly precipitation. Evaporation exceeds precipitation in 9 months of the year. During the wettest months of July through September, evaporation rates range from 3.3 to 4.6 times greater than monthly precipitation. Not all precipitation evaporates, however; the water cycle includes infiltration into the ground (some of which recharges aquifers), uptake by vegetation, and diversion into surface water systems. Also, evaporation is an ongoing phenomenon averaged over time, whereas about half of the annual precipitation at the site occurs from July through September as high-intensity, short-duration convective storms. During such storm events, the rate of precipitation far exceeds the rate of evaporation. Regardless, evaporation in the region and at the site is a significant factor in reducing precipitated moisture.

Runoff on the disposal cell cover occurs only during rainfall events of sufficient magnitude and intensity, and after melting of significant snow accumulations. However, there is no evidence that runoff has spilled over the edge of the cell cover. Instead, cell cover runoff accumulates as ponds in depressions that have formed over the slimes area on the north portion of the cover. These ponds persist for long periods of time that correlate to the quantity of accumulated water, indicating that percolation through the cover is minimal at this location. Evaporation, therefore, is the primary cause for loss of ponded water in the depressions.

Shallow- and deep-rooted vegetation is beginning to establish on the disposal cell cover, as noted in Section 6.3.3. It can be assumed, therefore, that some percentage of precipitation percolates through the cover; apparently more over the sand tailings area than the slimes area because that is where most of the vegetation occurs. The vegetation also indicates that evapotranspiration is occurring.

There are no site-specific data to estimate the actual amount of precipitation that percolates through the cover and into the tailings. Studies performed on other covers are not directly applicable to the Bluewater site because of differences in designs, cover materials, and climate. However, percolation rates that have been measured at other sites have ranged up to 18 percent in studies by Albright et al. (2004) and up to 42 percent by Abichou el al. (1998). Rock covers such as on the Bluewater cell may act as mulch and retain moisture, which would tend to decrease evaporation and increase percolation. In the absence of site-specific data, therefore, it is reasonable to assume that between 25 and 50 percent of precipitation currently percolates through the cover. For the purposes of this assessment to estimate a range of potential seepage from the disposal cell after construction, tailings storage and outflow are calculated based on inflow quantities of 50 percent and 25 percent of precipitation.

6.4.3.3 Change in Storage

Moisture in the tailings is stored in voids within the tailings mass. A saturated volumetric moisture content is defined when all void space is occupied by moisture, and 50 percent saturation is when half the void space is occupied by moisture. Porosity is defined as the ratio of void space to the total volume of mass. Therefore, when soil is fully saturated, the volume of moisture is equal to the porosity of the soil mass.

As tailings voids drain from a saturated condition to a lower degree of saturation, negative pore pressures develop within the tailings materials. The relationship between the volumetric moisture content and negative pore pressures is provided on soil moisture characteristic curves. There are no data for moisture-holding properties of the Bluewater site tailings, nor detailed gradation data for the tailings. Therefore, tailings characteristics from the Shiprock disposal cell are used to represent Bluewater site tailings characteristics. Although mined from different geographic locations, the uranium ore processed at both sites was derived from sandstone in the Saltwash Member of the Jurassic Morrison Formation (Merritt 1971). Change in storage calculations are provided in Appendix A, Section 5.3.3.

6.4.3.4 Outflow

Assumptions and calculations to estimate outflow, or seepage, from the disposal cell are provided in Appendix A, Section 5.3.4. When moisture infiltration exceeds available storage, outflow will equal inflow. The rate of discharge will asymptotically approach the cover infiltration rate. Estimates of the volume of moisture that can potentially seep through the base of the disposal cell can be calculated using storage estimates and assumptions taken from the impoundment geometry provided in Figure 37. The approximate areas of the two types of materials covering the bottom of the disposal cell are provided in Table 9.

Table 9. Footprint of Tailings Materials

Material	Percentage of 260-Acre Footprint	Area (ft^2)
Coarse tailings	67	7,588,152
Fine tailings	33	3,737,448

ft^2 = square feet

If the tailings become saturated, drainage will occur at the influx rate if the saturated hydraulic conductivity of the tailings is greater than or equal to the influx rate. If the saturated hydraulic conductivity of the tailings is less than the influx rate, the tailings will store much of the moisture until full saturation occurs. Table 10 provides the potential annual seepage that could occur if the tailings become saturated and outflow equals inflow.

Table 10. Potential Annual Outflow if the Tailings Become Saturated

Material	Infiltration Percentage	Infiltration Rate[a]	Area[b]	Outflow Volume		Outflow Rate
		(ft/yr)	(ft^2)	(ft^3)	(gallons)	(gpm)
Coarse Tailings	50	0.430	7,588,152	3,262,906	24,178,134	46.0
	25	0.215	7,588,152	1,631,453	12,089,067	23.0
Fine Tailings	50	0.430	3,737,448	1,607,102	11,908,626	22.7
	25	0.215	3,737,448	803,551	5,954,313	11.3
Total	50	0.430			36,086,760	68.7
	25	0.215			18,043,380	34.3

ft/yr = feet per year; ft^2 = square feet; ft^3 = cubic feet; gpm = gallons per minute
[a] Derived from an average annual precipitation rate of 10.3 inches per year
[b] Cell cover area is approximately equal to the tailings footprint (Table 9)

Based on the results of Table 10, the extreme scenario would suggest that approximately 36 million gallons of tailings fluid could seep from the disposal cell annually if the tailings become saturated and if 50 percent of precipitation percolates into the tailings. Until the tailings become saturated, the annual seepage rate would be less and would gradually approach the saturated tailings seepage rate.

The estimated 36-million-gallon annual seepage rate is based on an assumed upper limit of precipitation percolation through the cover. As noted in Section 6.4.3.2, increasing vegetation on the cover reduces percolation of precipitation into the tailings because of evapotranspiration. As vegetation is allowed to establish (or is enhanced to accelerate establishment) on the Bluewater cell cover, the precipitation inflow could reduce to substantially less than 25 percent of annual precipitation. And, it is possible that the tailings would not become fully saturated and that seepage would remain minimal as unsaturated drainage.

6.4.4 Estimated Seepage Contaminant Mass

Constituents of concern with respect to ARCO's groundwater corrective action program, and subsequently included in the LTSP, are molybdenum, selenium, and uranium because concentrations were above background levels in monitoring wells near the disposal cell. Therefore, the evaluation of contaminant mass that seeped from the main tailings impoundment, and continues to seep from the disposal cell, addresses these constituents.

As noted previously, an estimated 5.7 billion gallons of tailings fluids seeped through the bottom of the main tailings impoundment prior to encapsulation in 1995. Contaminant concentrations in the raw tailings water, or tailings liquor, varied due to changes in milling processes and ore characteristics, but ARCO considered the concentrations listed in Table A-2 of Appendix A,

Table A-2 as representative of the tailings liquor. According to Table A-2, the liquor had a pH of 1.2 and the following concentrations for contaminants of concern: 1.33 mg/L molybdenum, 4.0 mg/L selenium, and 19.5 mg/L uranium (Dames & Moore 1981b). Contaminant concentrations in seepage from the disposal cell are expected to be less than those in the tailings liquor because of tailings dewatering activities conducted by ARCO in the 1980s and due to mixing with precipitation that is percolating through the cover and into the tailings.

The estimated mass for each constituent of concern that seeped through the bottom of the tailings impoundment prior to completion of the disposal cell cover in 1995 is provided in Table 11. Assuming the seepage volume and contaminant concentrations are representative of actual conditions, nearly 1 million pounds of uranium would have been in the fluids that seeped from the tailings impoundment.

Table 11. Estimated Seeped Contaminant Mass Prior to Disposal Cell Completion

Contaminant	Concentration	Seeped Volume		Contaminant Mass	
	(mg/L)	(billion gallons)	(billion liters)	(mg)[a]	(pounds)
Molybdenum	1.33	5.7	21.6	2.87×10^{10}	63,300
Selenium	4.0	5.7	21.6	8.64×10^{10}	190,500
Uranium	19.5	5.7	21.6	4.21×10^{11}	928,300

mg = milligrams; mg/L = milligrams per liter
[a] Concentration times seeped liters

The mass of uranium in seepage since the cover was completed cannot be estimated because seepage rates and contaminant concentrations in the tailings fluids are unknown. However, the estimated potential seepage under saturated conditions is significantly less than the seepage that occurred prior to completion of the cell cover. Likewise, although seepage may be occurring, the contribution of contaminant mass to the underlying aquifers is also significantly less than occurred prior to completion of the cell cover. The greatest contribution to groundwater contamination, therefore, occurred prior to 1995.

6.5 Disposal Cell Performance Summary

ARCO estimated that approximately 5.7 billion gallons of tailings fluid seeped through the bottom of the main tailings impoundment prior to construction of the disposal cell cover in 1995; about half of that total was projected to have occurred prior to 1960. These fluids entered the two uppermost aquifers at the site.

Tailings fluids may continue to seep from the disposal cell indefinitely. Estimated annual disposal cell seepage volumes, which are less than 1 percent of the total seepage that occurred prior to completion of the cover in 1995, assume saturated moisture conditions within the cell. However, ARCO essentially dewatered the coarse tailings between 1982 and 1985. This large volume of material would need to refill with infiltrated precipitation before saturated discharge begins. Therefore, seepage is probably occurring under unsaturated conditions and would be minimal. If vegetation is allowed to establish on the cover, evapotranspiration will reduce the volume of precipitation entering the tailings, and saturation likely would be delayed or may not occur.

The band drains that ARCO installed in the north portion of the tailings impoundment did not completely dewater the slimes—they only reduced the water content to facilitate consolidation of the slimes. Up to 15 ft of relocated sandy-clay material, similar to the material used for the radon barrier, was placed over the slimes prior to installation of the radon barrier. This thick, low-permeability layer would significantly reduce infiltration of precipitation into the slimes and keep the seepage rate low.

Depressions have formed on the disposal cell cover because the slimes portion of the tailings impoundment continued to consolidate after the cover was completed. Precipitation runoff water forms ponds in these depressions, potentially introducing a second source of fluids infiltrating through the disposal cell. Observations of the persistence of the ponds and the results of radon flux measurements, however, indicate that there has been no reduction in the performance of the radon barrier and that the ponds are reduced primarily through evaporation rather than infiltration. Therefore, the depressions and associated ponds are not indicative of additional seepage from the cell.

Considerable uncertainties are associated with the water balance and mass estimates presented in this assessment. Nevertheless, they do not negate the primary conclusion that the volume of fluid and mass of contaminants seeping from the cell since it was constructed are very small compared to the corresponding volume and mass that seeped through the bottom of the tailings impoundment prior to cell construction.

7.0 Site Hydrogeology and Water Chemistry

Though several features of the groundwater system at the Bluewater site were discussed in the assessment of regional hydrogeology in Chapter 4 and in the summary of regional water chemistry in Chapter 5, examining findings from historical and recent studies focused on the site itself can provide additional insights regarding groundwater flow and contaminant transport in the Grants-Bluewater Valley. This chapter augments the conceptual model of the study area by presenting site characterization data from investigations of the Bluewater site conducted between the late 1970s and the late 1990s. In addition to describing historical conditions that have bearing on current observations regarding uranium concentrations in the alluvial and San Andres aquifers, the earlier reports help lay the groundwork for projecting how uranium originating at the site can be expected to behave in coming years.

This chapter also includes an assessment of the water chemistry in samples DOE collected from Bluewater site wells during a recent sampling event. The water chemistry assessment helps illustrate how some of the impacts of milling processes at the site continue to influence local groundwater quality. To a large degree, the chemical impacts are similar to those previously identified by Longmire et al. (1984) as the common legacy effects of acid- and carbonate-leach milling of uranium ores in the Grants Mineral Belt. The summary of the water chemistry monitoring results is followed by an examination of chemical phenomena that influence the mobility of uranium in site groundwater. The chapter concludes with an assessment of uranium isotope data collected at both onsite wells and wells located in areas hydraulically downgradient of the site.

7.1 Local Groundwater Flow System

Geologic formations that have affected and continue to influence groundwater processes at and near the Bluewater site are the same as those identified in the regional hydrogeology chapter, including the ancestral and recent river alluvium (the alluvial aquifer), Bluewater Basalt, the Chinle Formation, San Andres Limestone and the Glorieta Sandstone (the San Andres aquifer). The Permian Yeso and Abo Formations are also present at the Bluewater site beneath the Glorieta Sandstone.

7.1.1 Aquifer Characterization

7.1.1.1 Aquifer Hydraulic Properties

Several consulting reports dealing specifically with the hydrology of the Bluewater site prior to the site being transferred to DOE contained information on hydraulic properties of geologic units underlying the site. The hydraulic properties were mostly derived from aquifer pumping tests conducted at wells tapping either the alluvial aquifer or the San Andres aquifer. Table 12 provides a summary of the results from those tests. Background information regarding several of the tests and some of the more salient test results are discussed in the following paragraphs.

Table 12. Hydraulic Properties for the Alluvial and San Andres Aquifers Derived from Aquifer Tests

Test	Pumping Well	Drawdown Data from This Well	Flow Rate (gpm)	Duration of Pumping (minutes)	Radial Distance of Observation Well (ft)	Method of Analysis or Aquifer Type	Pumping or Recovery Data	Transmissivity (ft^2/day)	Pumped Thickness (ft)	Estimated Hydraulic Conductivity[a] (ft/day)	Storativity (dimensionless)
San Andres Aquifer Tests											
SA1	Unknown[c]	USGS 5	1,740	1,500	495	Theis Solution	Pumping	414,000	150 (assumed)	2,760	0.00052
		USGS 6			2,970	Theis Solution	Pumping	307,000	150 (assumed)	2,050	0.0014
SA2	Anaconda #1	Anaconda #1	600	1,560	NA	Theis Recovery	Recovery	55,000	150 (assumed)	370	NA
		Anaconda #1	775	2,970	NA	Theis Recovery	Recovery	57,000	150 (assumed)	380	NA
SA3	Anaconda #2	Anaconda #2	1,559	1,440	0	Specific Capacity	Pumping	13,400	123	109	NA
		Anaconda #1			426	Leaky Artesian	Pumping & Recovery	26,200		213	1.3×10^{-4}
SA4	Anaconda #5	Anaconda #5	2,000	4,620	0	Specific Capacity	Pumping	8,700	173	50	NA
		Pilot Hole			33.5	Leaky Artesian	Pumping	19,900		115	3.2×10^{-4}
					33.5	Leaky Artesian	Recovery	20,200		117	6.0×10^{-5}
		Anaconda #2			135	Leaky Artesian	Pumping	66,600		385	1.2×10^{-2}
					135	Leaky Artesian	Recovery	65,200		377	1.2×10^{-2}
		Anaconda #1			514	Leaky Artesian	Pumping	54,700		316	1.3×10^{-3}
					514	Leaky Artesian	Recovery	54,700		316	8.1×10^{-4}
SA5	928	928	2,300	2,610	0	Jacob & Lohman	Pumping	50,800	61	833	NA
SA6	S(SG) GSS[b]	G(SG)	160	2816	401.5	Leaky Artesian	Recovery	3,250	124	26	5.3×10^{-5}

Table 12 (continued). Hydraulic Properties for the Alluvial and San Andres Aquifers Derived from Aquifer Tests

Test	Pumping Well	Drawdown Data from This Well	Flow Rate	Duration of Pumping	Radial Distance of Observation Well	Method of Analysis or Aquifer Type	Pumping or Recovery Data	Transmissivity	Pumped Thickness	Estimated Hydraulic Conductivity[a]	Storativity
			(gpm)	(minutes)	(ft)			(ft^2/day)	(ft)	(ft/day)	(dimensionless)
		D(SG)			597.5	Leaky Artesian	Pumping	3,890		31	8.9×10^{-5}
		D(SG)			597.5	Leaky Artesian	Recovery	4,530		37	2.8×10^{-4}
SA7	OBS-3	OBS-3	NA	NA	NA	NA	NA	1,700	80 (estimated)	21	NA
SA8	D(SG)	D(SG)	NA	NA	NA	NA	NA	4,200	NA	NA	1.8×10^{-4}
SA9	G(SG)	G(SG)	NA	NA	NA	NA	NA	3,260	51 (estimated)	64	5.3×10^{-5}
Alluvial Aquifer Tests											
AL1	B(M)	B(M)	82	1,440	NA	Specific Capacity	Pumping	2,000	27	74	NA
		B(M) Obs			72.5	Leaky Artesian	Recovery	3,200	27	119	1×10^{-3}
AL2	C(M)	C(M)	72	380	NA	Specific Capacity	Pumping	3,200	22	145	NA
AL3	C(M)	C(M)	NA	NA	NA	NA	NA	8195	NA	NA	NA
AL4	F(M)	F(M)	NA	NA	NA	NA	NA	1780	8	223	NA
AL5	T(M)	T(M)	NA	NA	NA	NA	NA	5310	19	287	NA

ft = feet; ft/day = feet per day; ft^2/day = square feet per day; gpm = gallons per minute; NA = not available or not applicable
[a] Hydraulic Conductivity = Transmissivity/Pumped Thickness
[b] GSS—Aquifer test results represent the Glorieta Sandstone
[c] Gordon (1961) reported that the pumping well for test SA1 was located in the southeast corner of Section 30, T12N, R10W; location given was near the current location of well B00518.

Hydro-Search (1977) summarized the results of aquifer tests performed in earlier years at near-site wells screened in the San Andres aquifer, as previously reported in Gordon (1961). A 25-hour test in 1950 using a 1,745 gpm discharge rate at well B00518, about 2 mi south-southeast of the main tailings impoundment (Figure 18, Plate 7), resulted in estimated transmissivities that ranged from 267,00 to 455,000 ft^2/day. Two of the computed transmissivities are listed under Test SA1 in Table 12. Computed storativities using the test data varied from 5.2×10^{-4} to 1.4×10^{-3}, which are within the expected range for confined conditions. These results suggest that the San Andres aquifer south of the site and closer to the Zuni Mountains is quite productive, most likely due to the presence of fractures and solution features in limestone.

It was surmised at the time of the SA1 test pumping that well penetration was about one-third to one-half of the local total aquifer thickness. Assuming that the aquifer thickness was 300 ft, division of the transmissivities listed in Table 12 by half that length results in estimated hydraulic conductivities of 2,760 and 2,050 ft/day, values that comport with the magnitude of hydraulic conductivities associated with karst limestone in Section 4.2.4.

The production well Anaconda #1, screened in the San Andres aquifer south of the main tailings impoundment (Figure 17, Plate 7), was tested in 1951 at two different pumping rates without the benefit of observation wells (test SA2 in Table 12). Using analyses of water-level recovery data after pumping stopped resulted in derived transmissivities for the well that exceeded 50,000 ft^2/day. The pumping well penetrated about 150 vertical feet of the estimated 270 to 280 ft total thickness of the San Andres aquifer in the tested area. Division of the two transmissivities listed in Table 12 by this length produced estimated hydraulic conductivities of 370 and 380 ft/day.

Hydro-Search (1977) conducted test SA3 (Table 12) as part of its initial hydrologic investigation of the Bluewater site. The test consisted of pumping well Anaconda #2 for 24 hours at a constant rate of 1,559 gpm. Using drawdown data from both the pumping well and an observation well (Anaconda #1) about 425 ft south of the pumping well resulted in derived transmissivities of 13,400 and 26,200 ft^2/day, the latter of which Hydro-Search (1977) assumed to be most representative of the San Andres aquifer at the Bluewater site. The aquifer storativity derived from analysis of the test data was 1.34×10^{-4}, a value that was again representative of a confined aquifer. Hydro-Search (1977) concluded that the transmissivity and storativity values resulting from the test were generally representative of the San Andres aquifer in the vicinity of the Bluewater site. Estimated hydraulic conductivities from the test are 109 and 213 ft/day (Table 12).

Two additional tests conducted at wells screened in the San Andres aquifer with pumping durations of more than a day (test SA4 and SA5) resulted in estimated hydraulic properties for the aquifer that were similar in magnitude to those mentioned above for the aquifer. Test SA4 was based on pumping well Anaconda #5 for more than 3 days and made use of drawdown data collected at 3 observation wells (Dames & Moore 1981c). Estimated hydraulic conductivities for the aquifer using seven different analyses of the test data varied from 50 to 385 ft/day (Table 12). Test SA5 is of particular interest in this study because it was conducted a few miles east and downgradient of the east border of the Bluewater site, along a flow path extending east-southeast from site property directly north of the main tailings disposal cell (Figure 18). The test pumping, conducted at well 928, about 0.6 mi north of the large tailings disposal cell at the Homestake site,

resulted in a derived transmissivity of 50,800 ft^2/day and an estimated hydraulic conductivity of 833 ft/day. These latter results suggest that karst features are present in the San Andres aquifer in the vicinity of the Homestake site as well as at the Bluewater site and support the possibility of relatively short travel times (<20 years) between the two sites (see Section 4.3.3.2).

Aquifer hydraulic properties derived from aquifer test SA6 (Figure 17, Plate 7), which used well S(SG) east of the main tailings disposal cell as the pumping well, are of special interest to this study because they are considered representative of the Glorieta Sandstone specifically (Applied Hydrology Associates Inc. 1990). Barrier boundary effects were observed during this test, presumably due to the presence of formation offsets at the Ambrosia Lake and East-West Faults. The data were analyzed by Dames & Moore (1981c), resulting in estimated transmissivities from 3,200 to 4,500 ft^2/day and storativities varying from 5.3×10^{-5} to 2.8×10^{-4} (Table 12). In addition to producing transmissivities for the sandstone that were lower than those considered representative of shallower, fractured limestone, assessment of the test data indicated that fully unconfined conditions were not locally present, at least not in the Glorieta Sandstone.

Applied Hydrology Associates Inc. (1990) also estimated aquifer parameters for the San Andres aquifer using data from short-duration, single-well hydraulic tests performed by ARCO in well OBS-3, and two additional, now-abandoned wells D(SG) and G(SG) just east of the main tailings impoundment (tests SA7, SA8, SA9). The transmissivities resulting from the test analyses (1,700 to 4,200 ft^2/day) were lower than most of the transmissivities derived from long-duration tests (e.g., Tests SA1 through SA5) in the San Andres aquifer. It is possible that the relatively low transmissivities stemming from the singe-well tests were also representative of the lower hydraulic conductivities expected in the Glorieta Sandstone in comparison to those reflective of karst limestone.

All of the hydraulic conductivities listed in Table 12 stemming from aquifer testing in the San Andres aquifer fall into the range of conductivities reported by Huntoon (1995) for the results of numerous pumping tests in karst aquifers. In addition to giving credence to the transmissivity values presented in the table, this result lends support to the travel time calculations discussed in Section 4.3.3.2 regarding the San Andres aquifer.

Hydro-Search (1977, 1978) posited that a wide range of hydraulic properties derived for the San Andres aquifer from multiple aquifer tests near the Bluewater site was an indicator of significant aquifer heterogeneity. Transmissivities were expected to vary spatially depending on a number of factors, including (1) the degree of fracturing or limestone dissolution in the aquifer, (2) the continuity of solution openings in limestone, and (3) the proportion of sandstone within the vertical domain occupied by the San Andres Limestone and Glorieta Sandstone. In general, transmissivity was expected to increase as the proportional amount of sandstone decreased.

To develop estimates of the hydraulic properties of the alluvial aquifer at the site, Dames & Moore (1981c) analyzed drawdown data from a day of pumping at B(M) (test AL1), a well just southwest of the main tailings impoundment (Figure 17 and Plate 7) and that is now abandoned. The collected data showed evidence of leaky-confined conditions, and the computed storativity was 1×10^{-3} (Table 12), which is smaller than expected if the alluvial aquifer was releasing groundwater under unconfined conditions. A hydraulic conductivity of about 120 ft/day was derived for the aquifer, and additional analyses of the data resulted in an estimated vertical

hydraulic conductivity for the overlying Bluewater Basalt of about 13 ft/day. This latter value suggested that fractures in the basalt rendered it moderately permeable and capable of conveying significant quantities of downward seepage due to infiltration of water in shallow surface alluvium above the basalt.

A second aquifer test conducted in the alluvial aquifer and analyzed by Dames & Moore (1981c) was based on pumping from alluvial well C(M) (Test AL2), which was about 500 ft south of the main tailings impoundment (Figure 17 and Plate 7) but is now abandoned. The well was pumped at a constant rate of 72 gpm, but groundwater withdrawal was stopped after a relatively short duration of 6 hours because the well could no longer sustain the pumping rate. An estimated transmissivity of 3,200 ft^2/day was derived from drawdown data, suggesting that well C(M) was screened in coarse-grained, highly permeable alluvial materials deposited in an ancestral Rio San Jose paleochannel. Both barrier and recharge boundary conditions were observed in the drawdown curves generated by the testing. The barrier effects were likely created by the pumping cone-of-depression contacting the north boundary of the ancestral river alluvium north of well C(M). It was impossible to tell whether unconfined flow conditions were present during the testing because no observation well data were available for calculating aquifer storage parameters.

Transmissivities derived by Applied Hydrology Associates Inc. (1990) from individual well, short-duration tests at alluvial aquifer wells F(M), T(M), and the now-abandoned C(M) (tests AL3, AL4, AL5) ranged from about 1,800 to 8,200 ft^2/day. These latter values were of the same general magnitude as those mentioned above for earlier tests at alluvial wells B(M) and C(M), and were considered indicative of highly permeable sands and gravels in paleochannels of the ancestral Rio San Jose.

In general, the transmissivity, hydraulic conductivity, and storativity values derived from testing of the alluvial and San Andres aquifers in the vicinity of the Bluewater site comported with values for these parameters discussed in Chapter 4.

7.1.1.2 Effects of Pumping Anaconda Production Wells

The high pumping rates from the San Andres aquifer achieved during the aquifer tests at wells Anaconda #1, Anaconda #2, and Anaconda #5 (Tests SA2, SA3, and SA4 in Table 12) suggest that all of the Anaconda production wells were pumped at relatively high rates (600 to 2,000 gpm) during milling years at the Bluewater site. As mentioned in Section 4.3.3, the high rates of groundwater removal produced a wide (>1 mi) cone of influence that appeared to be centered on the Anaconda production wells. The general dimensions of the cone of influence during milling years are shown in Figure 42, which presents a map view of the potentiometric surface in the San Andres aquifer based on water-level measurements in August 1978 at wells screened in the aquifer in the vicinity of the Bluewater site. As indicated in the figure, the drawdowns created by the pumping in August 1978, in comparison to the ambient potentiometric surface, appeared to be about 2.5 to 3 ft. Though the actual pumping rates at the Anaconda production wells at the time were unknown, this relatively low amount of drawdown, in comparison to the total aquifer thickness south of the East-West Fault, suggested that the aquifer is very prolific in areas that were tapped by the Anaconda wells.

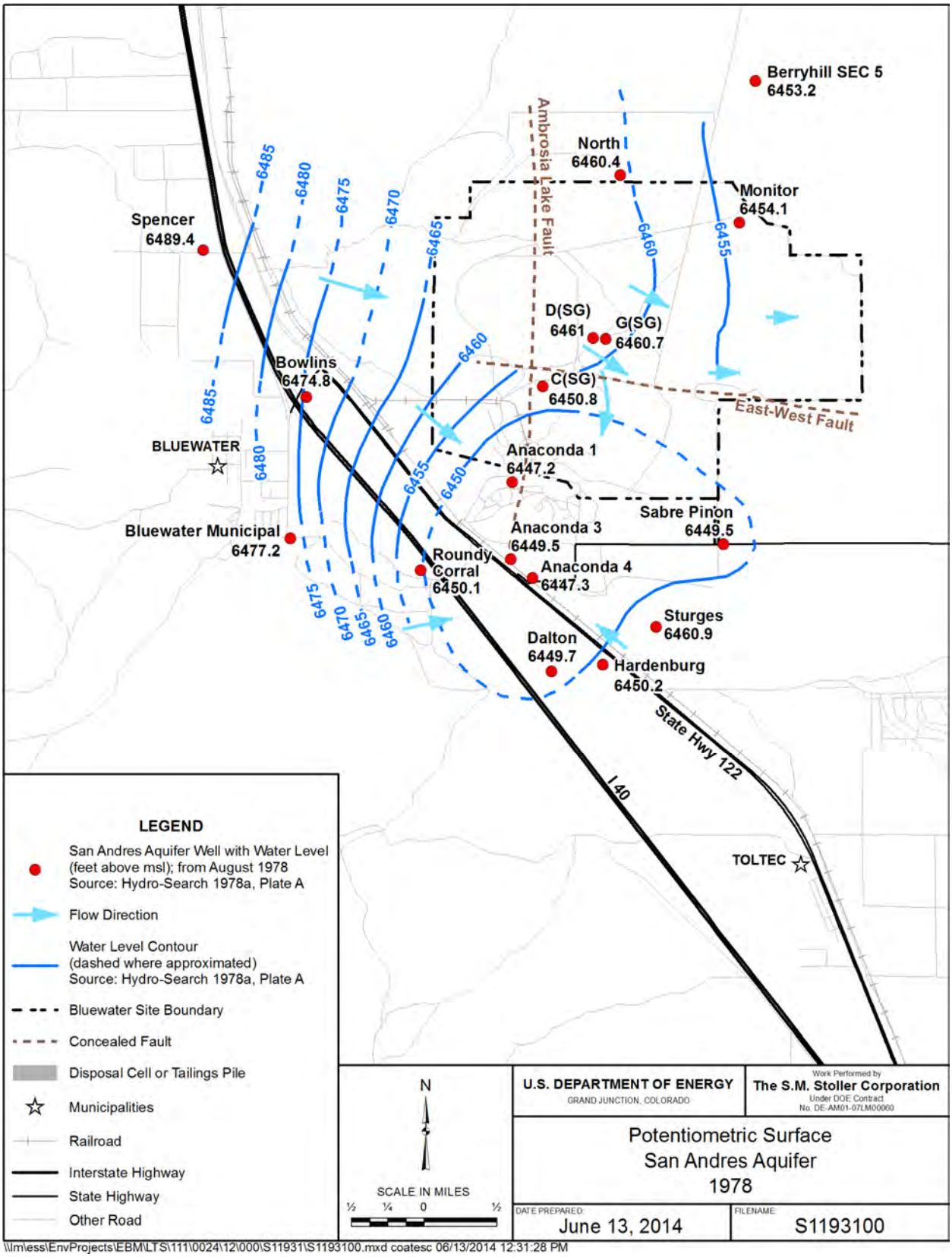

Source: Hydro-Search 1978

Figure 42. Potentiometric Surface in the San Andres Aquifer in August 1978

Hydro-Search (1978) developed the flow arrows shown in Figure 42 on the basis of the observed water levels in local wells and a general understanding of how the groundwater system responded to pumping from the San Andres aquifer at and near the Bluewater site. In addition to showing convergent flow toward the area containing the Anaconda production wells, the arrows indicated southward groundwater movement across the East-West Fault, providing a mechanism for contaminant migration from beneath the main tailings impoundment to areas several hundred feet south of the East-West Fault. The detection of uranium at wells Anaconda #1 and Anaconda #5 at concentrations on the order of 0.2 to 0.35 mg/L in 1980–1981 (Hydro-Search 1981a) indicated that the southward migration of uranium contamination across the fault, via downward conduit flow in the fault zone, was possible. Similarly, the detection of uranium at production well Anaconda #1 in August 2013 at a concentration of about 0.09 mg/L suggested that the contamination that had migrated to the area containing this well as early as 1980 was continuing to reside in local portions of the San Andres aquifer some 33 years later. This latter uranium detection combined with a measured uranium concentration of about 0.13 mg/L at well 18(SG) (Figure 16) in 2013 suggested a possibility that uranium contamination originating at the main tailings impoundment had, in the past, migrated at least 0.8 mi south of the East-West Fault and persists in this general area today.

Inspection of geologic cross section A-A' in Figure 10 indicates that the vertical offset at the East-West Fault just east of the main tailings disposal cell is about 370 ft. The resulting juxtaposition of the San Andres aquifer north of the fault with the mostly impermeable Chinle Formation on the south side suggests that the fault provides a significant partial barrier to southward contaminant migration to areas containing production wells Anaconda #1 and Anaconda #5 (see Figure 17, Figure 42). Nevertheless, southward groundwater flow and concomitant contaminant migration across the East-West Fault appears to have occurred in the past, presumably due to the increased hydraulic gradient across the fault induced by pumping at the Anaconda production wells. Because hydraulic heads in the San Andres aquifer north of the East-West Fault continue to be about 5 to 10 ft higher than comparable heads just south of the fault (Section 4.3.3, Figure 23), long after pumping from the Anaconda production wells ceased, continued southward migration of contamination across the fault appears possible.

Further inspection of geologic cross section A-A' in Figure 10 suggests that, for southward groundwater flow across the East-West Fault in the San Andres aquifer to occur, downward, conduit flow within the fault zone is required. This finding comports with observations by Bense and Person (2006) that faults frequently influence groundwater flow by acting as both partial barriers and conduits. Downward groundwater flow and contaminant migration in the East-West Fault on the west side of the Ambrosia Lake Fault also appears possible. This can be seen in geologic cross section D-D' in Figure 11, which shows the fault providing a connection between ancestral river alluvium and the San Andres Limestone south of the fault. In this latter case, conduit flow within the fault zone would have provided a pathway for contamination that historically originated as downward percolation of tailings fluids into the Bluewater Basalt, to subsequently migrate to alluvium and then deeper to the San Andres aquifer.

It is possible that the relatively high uranium concentrations at wells Anaconda #1 and Anaconda #5 in 1980–1981 were mostly caused by southward conduit flow along the Ambrosia Lake Fault, as opposed to flow across the East-West Fault via downward conduit flow in the East-West Fault zone. If this were the case, the presence of a relatively high uranium concentration in 2013 about 2,000 ft east of the southern end of the Ambrosia Lake Fault, at

well 18(SG) (Figure 16), would have been caused by gradual eastward migration of uranium from the Ambrosia Lake Fault. Further investigation of flow phenomena in the vicinity of the intersection of the two faults and areas south of the East-West Fault may someday reveal the actual processes involved.

7.1.1.3 Aquifer Flow Conditions

Applied Hydrology Associates Inc. (1990) surmised that virtually all groundwater flow in the San Andres aquifer at the site occurs under dual-domain, or fracture-matrix, conditions (e.g., Zimmerman et al. 1993) associated with karst features in the San Andres Limestone. This position assumes that all horizontal groundwater movement takes place in preferential pathways consisting of solution channels and fractures in limestone, and that all remaining groundwater in the adjacent rock matrix, consisting of limestone and sandstone, is effectively immobile. In such a flow system, exchange of dissolved contamination between the fractures and the matrix takes place either through molecular diffusion in the matrix or very slow advection (movement with moving water). Though such dual-domain processes undoubtedly occur in the San Andres Limestone portion of the aquifer, it is unlikely that they govern all significant transport processes in the aquifer. Given that the San Andres Limestone and Glorieta Sandstone have a combined thickness of about 250 to 350 ft in the vicinity of the site, and that fractured sandstones in the aquifer are sufficiently permeable to facilitate relatively rapid advection of contaminants in a horizontal direction, the conceptual model in this study assumes that San Andres aquifer groundwater migrates horizontally in fractured sandstone (Section 4.3.3.2) as well as in karst features in limestone. Additionally, the groundwater migrates horizontally at variable rates that both increase and decrease with depth in the aquifer. Average linear velocity calculations in Table 5 suggest that the advective travel times in fractured sandstone between the Bluewater site and areas hydraulically downgradient of the site are only moderately longer than those attributed to advective transport in karst limestone features (e.g., solution channels). A wide range of estimated groundwater velocities in these two types of media suggests that the arrival times at downgradient sites for contaminants migrating eastward and southeastward in the San Andres aquifer could span decades if not hundreds of years.

While investigating contaminant plumes at the Bluewater site, Hydro-Search (1977, 1978) concluded that the groundwater velocities controlling contaminant migration in both the alluvial and San Andres aquifers were on the order of hundreds of feet per year. In comparison, Dames & Moore (1986a, 1986b) concluded that groundwater velocities in the two aquifers were greater than 1,000 ft/yr and could be higher than 5,000 ft/yr in some locations. In addition, Dames & Moore deduced that relatively stable concentrations of constituents observed at locations on the Bluewater site were caused mostly, if not entirely, by transverse dispersion. This finding suggested that the rate at which contamination was being released to the plumes was relatively constant, and that the leading portions of contaminant plumes had migrated rapidly offsite. Both Hydro-Search (1977, 1978) and Dames & Moore (1986a, 1986b) identified transverse dispersion as the primary mechanism for attenuating onsite concentrations with transport distance in the alluvial and San Andres aquifers. Applied Hydrology Associates Inc. (1990) attributed contaminant attenuation on and downgradient of the Bluewater site to several possible processes, including transverse dispersion.

Assuming that average linear velocities in both aquifers were high, Dames & Moore (1986a) calculated that the leading portion of Bluewater site–related contaminant plumes would migrate

offsite within periods of less than 10 years after initial contaminant mobilization. This conclusion was supported by their transport modeling of the relatively conservative (nonreactive) anions chloride and sulfate, as well as TDS. The high velocities simulated in the Dames & Moore models were achieved by assuming that the effective porosity of the San Andres aquifer was 0.02, a value that is much smaller than the porosities of true porous media. Without using such a low effective porosity, Dames & Moore found that the transport models were incapable of matching elevated concentrations of chloride, sulfate, and TDS observed at San Andres aquifer wells along the east border of the Bluewater site in the 1980s.

Hydro-Search (1977, 1978) and Dames & Moore (1986a) concluded that downward seepage of tailings fluid from the base of the main tailings impoundment provided the primary source of contamination that was transported east and southeast from the Bluewater site in the alluvial and San Andres aquifers. Downward seepage of tailings fluids west of the Ambrosia Lake Fault through Bluewater Basalt and subsequently to underlying ancestral Rio San Jose alluvium provided the source of contamination transported within the alluvial aquifer. Because hydraulic heads in the alluvial aquifer were generally about 20 to 40 ft higher than equivalent heads in the San Andres aquifer east of the tailings impoundment, it was also likely that some alluvial contamination migrated eastward across the Ambrosia Lake Fault and north-northeastward across the East-West Fault into the San Andres aquifer in the vicinity of San Andres hill (where the San Andres Limestone/Glorieta Sandstone sequence is in contact with the alluvium because of the uplifted fault block). In addition, downward seepage of tailings fluids directly to the San Andres aquifer appeared to occur where the base of the tailings in the southeast corner of the main tailings impoundment was either in direct contact with the underlying San Andres Limestone or separated from the San Andres Limestone by a thin layer of jointed (porous) basalt.

Downward flow of tailings fluids to the alluvial and San Andres aquifers is estimated to have declined significantly since milling operations ceased (Chapter 6). Nonetheless, mechanisms for steadily feeding contamination to plumes migrating from the Bluewater site in the alluvial and San Andres aquifers are apparently still present (Appendix A).

7.2 Groundwater Chemistry in the Vicinity of the Bluewater Site

7.2.1 General Water Chemistry

The water chemistry at wells on the Bluewater site was examined partly to identify how the presence of onsite contaminant sources affects water quality. This was largely accomplished by comparing the chemistry of onsite groundwater samples with the samples used to evaluate regional water chemistry in Chapter 4. All onsite wells (background, contaminated, uncontaminated) were included in the onsite groundwater geochemistry evaluation. Samples used in this analysis were collected from May 14 through May 16, 2013, at the locations shown in Figure 43 (wells T(M) and X(M) were dry).

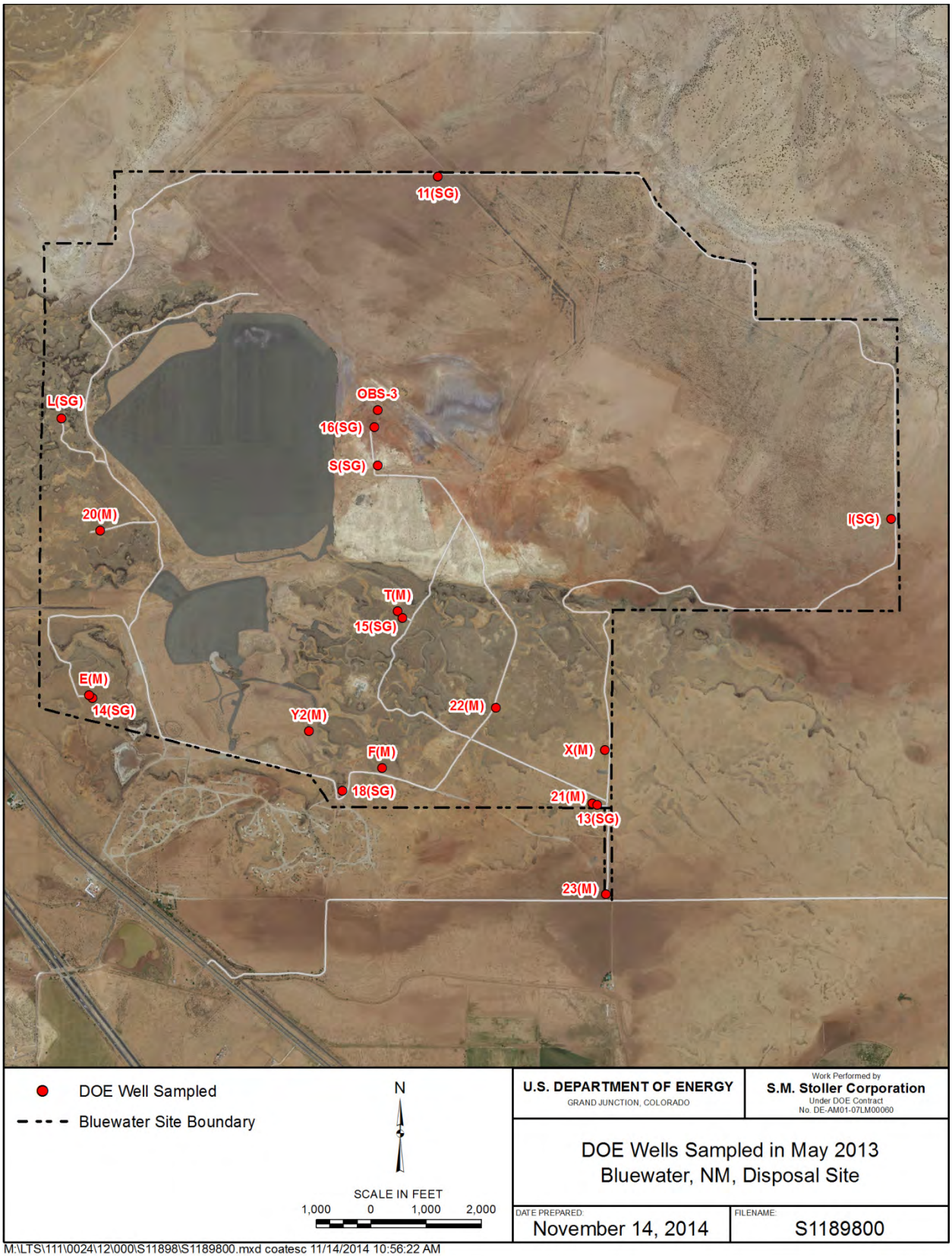

Figure 43. Locations of Bluewater Site Wells Sampled in May 2013

7.2.1.1 Alluvial Aquifer

Oxidation states measured in the groundwater samples collected from alluvial aquifer wells were relatively high, with all but one of the pE values falling above 4.6. The calculated pE value at well E(M) was 0.7. DO concentrations in alluvial groundwater samples ranged from 1.6 to 6.5 mg/L, except in the sample from well E(M), which had a DO concentration of 0.1 mg/L. Thus, the combination of DO concentrations and pE values indicate that groundwater in the vicinity of well E(M) has a lower oxidation state than the groundwater monitored at other alluvial wells.

Water samples collected from all but one of the alluvial aquifer wells showed nearly neutral pH values, ranging from 7.02 to 7.40; the pH at well E(M) was 8.05. The salinity of alluvial aquifer groundwater was moderate, with measured specific conductivity values ranging from 547 to 1,859 µS/cm.

A Piper diagram for the alluvial well samples, shown in Figure 44a, shows that cation equivalents in the cation triangle form a linear trend along a line extending from the sodium (plus potassium) corner to the calcium-magnesium border. The calcium-to-magnesium ratio is about 4 to 1. Most of the anion compositions are about midway between sulfate and bicarbonate, with one sample containing nearly all sulfate. Chloride is low in all onsite alluvial aquifer samples (Figure 44a). Both cation and anion compositions are similar to those for alluvial aquifer groundwater samples collected at most offsite wells in the region. Exceptions to this general finding occur at regional wells in San Mateo Creek alluvium north of the Homestake site, which are noticeably higher in salinity and sulfate than any onsite alluvial aquifer samples. This is because the alluvial aquifer north of the Homestake site has been impacted by contaminated water from the Ambrosia Lake Valley area. The mining and milling activities that generated contamination in the Ambrosia Lake Valley were separate from the uranium milling that took place at the Bluewater site.

The alluvial aquifer groundwater samples group tightly on a plot of calcite versus gypsum saturation indexes, with the exception of the sample from E(M) (Figure 45). Most of the samples are slightly undersaturated with respect to calcite but are undersaturated by about 1 to 2 orders of magnitude with respect to gypsum. In contrast, the sample from well E(M) is far undersaturated with calcite and close to saturation with gypsum. These results suggest that most of the alluvium contains calcite, probably in the form of limestone grains or carbonate cements, whereas the alluvium is devoid of gypsum.

The uranium concentrations in two samples of alluvial groundwater, from wells 21(M) and 22(M), were relatively high at 148 and 380 micrograms per liter (µg/L), respectively. These concentrations comport with monitoring results from previous sampling events, as both wells have shown site-related uranium contamination since their installation in summer 2011. Water in the samples from the two wells also had the highest relative sodium equivalents, suggesting that site-related groundwater contamination elevates sodium concentrations in comparison to inflowing groundwater from offsite areas.

Molybdenum concentrations in all alluvial aquifer samples were low, ranging from 0.3 to 8.4 µg/L. Nitrate (as NO_3) concentrations at all but two wells were also relatively low, ranging from less than 0.1 to 15.3 mg/L. Nitrate concentrations in the water samples from 21(M) and 22(M) were 43.4 and 161.2 mg/L, respectively, indicating that alluvial aquifer groundwater that has been impacted by contamination contains elevated levels of this constituent as well.

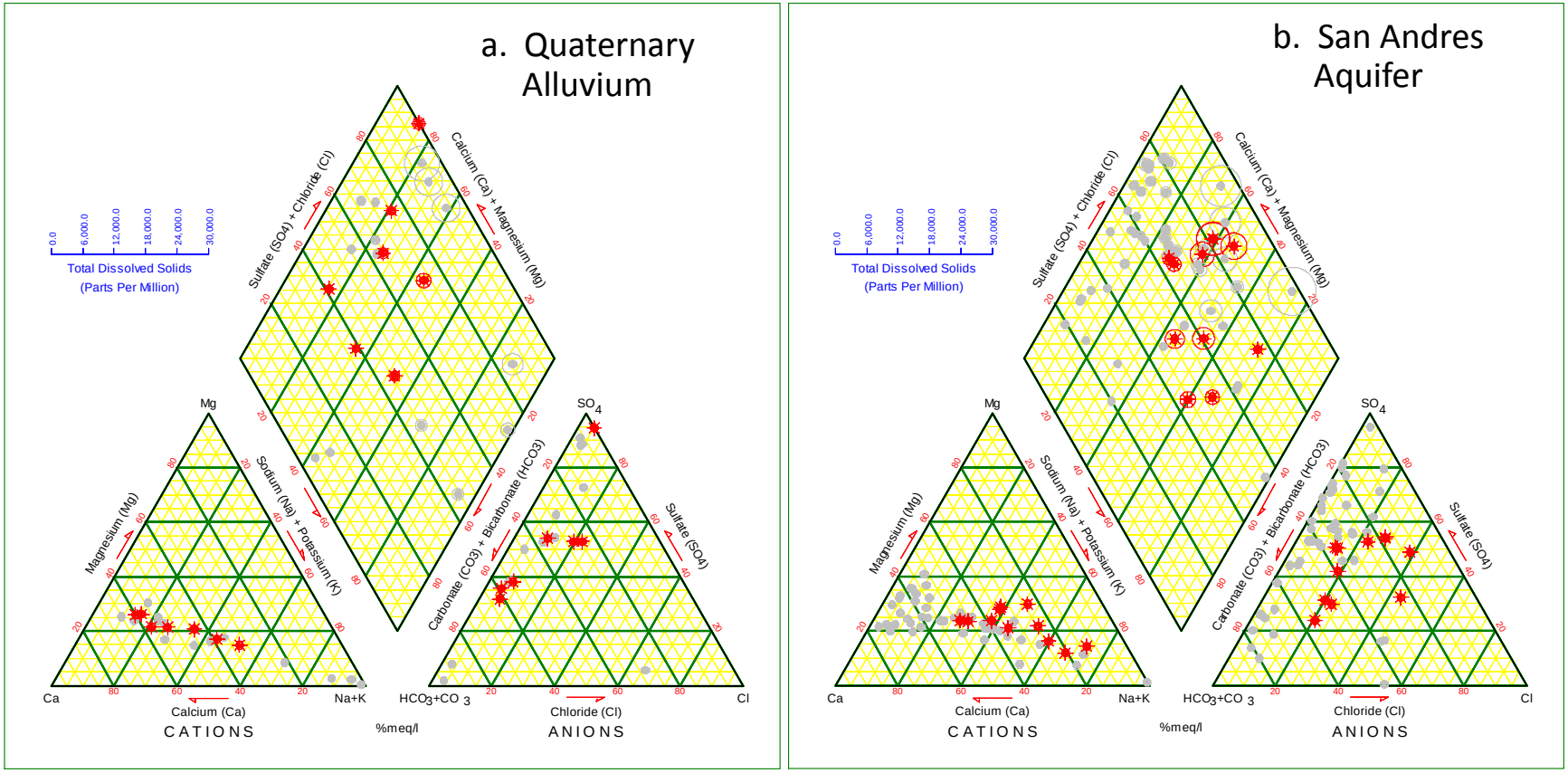

Figure 44. Piper Diagrams for Onsite Groundwater Samples: (a) Alluvial Aquifer and (b) San Andres Aquifer (Gray symbols represent the regional background chemistry from samples collected at offsite well locations, and red symbols represent samples collected from onsite wells.)

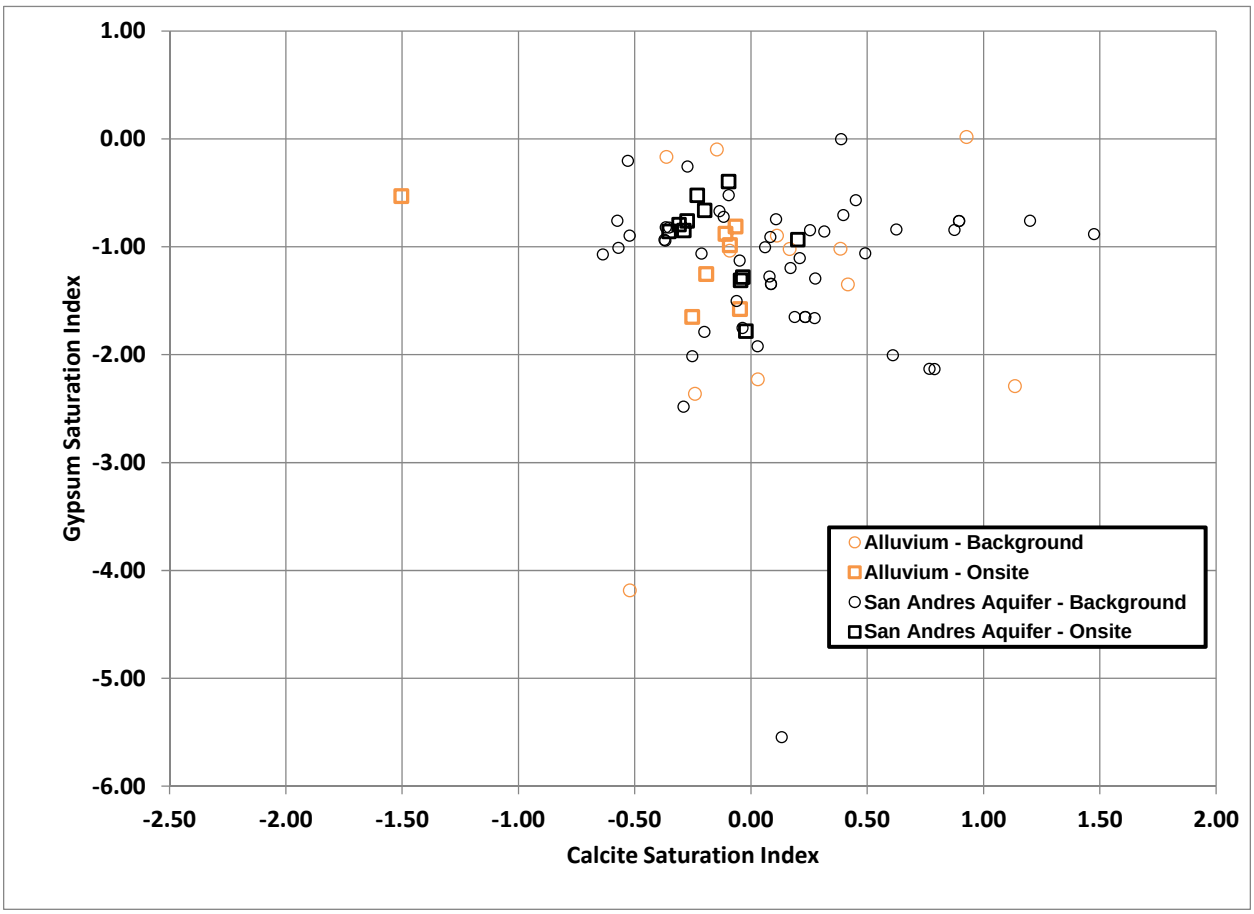

Figure 45. Saturation Indexes for Calcite and Gypsum in Onsite Alluvial Aquifer and San Andres Aquifer Samples

7.2.1.2 San Andres Aquifer

Analytical results from the May 2013 sampling of 10 San Andres aquifer wells on the Bluewater site indicated that the aquifer has moderate to relatively high salinity. Values of specific conductivity varied from 1,204 to 4,065 µS/cm, with the lowest value observed at a depth of about 235 ft below the top of casing in well I(SG), on the east border of the site (Figure 43). In comparison, specific conductivities in regional, background groundwater hydraulically upgradient of the Bluewater site range from less than 1,000 to 2,000 µS/cm (Table 6, Section 5.2.4).

With the exception of well I(SG), the pH values at the San Andres aquifer wells were near neutral, ranging from 6.53 to 7.01. A pH of 7.97 was measured at the 235 ft depth in this well.

The above-mentioned, unique chemical signatures of salinity and pH at well I(SG) reflect the fact that chemical stratification has been identified in this well. Specific conductivities have been shown to vary widely in the well depending on the depth below ground surface at which samples

are collected (Section 10.2.2). Uranium concentrations measured in three samples collected at different depths in well I(SG) in May 2013 also show evidence of chemical stratification. The shallowest sample, collected near the top of the water column in the well at a depth of about 235 ft below the top of casing, had a uranium concentration of about 0.005 mg/L. Another sample, collected at a depth of about 255 ft below the top of casing, had a uranium concentration of 0.350 mg/L. The third sample, collected at a depth of about 300 ft below top of casing, had a uranium concentration of 0.344 mg/L. These results suggested that it is very important to collect multiple samples at different depths from well I(SG) if the data are being used to assess the rate at which site-related contamination might be attenuating.

Uranium concentrations at the onsite San Andres aquifer wells ranged from 0.003 to 1.450 mg/L. Water collected from six wells (13(SG), 16(SG), 18(SG), I(SG), OBS-3, and S(SG)) had uranium concentrations greater than 0.1 mg/L, which are indicative of site-related contamination. Molybdenum concentrations were low in all 10 San Andres wells, ranging from less than 0.2 to 3.8 µg/L. Nitrate concentrations were also relatively low, ranging from less than 0.08 to 20.3 mg/L (as NO_3).

In a Piper diagram of anion and cation concentrations at the onsite San Andres wells (Figure 44b), cations were shown to vary from near the sodium (plus potassium) corner to about 20 percent sodium. Sodium equivalents in the onsite samples were higher than comparable values in the regional offsite wells (Figure 33d). The calcium-to-magnesium ratio in the San Andres aquifer samples was about 4 to 1. The anion distribution in the onsite San Andres aquifer wells (Figure 44b) indicated that chloride was present in higher proportions than observed in regional background wells, suggesting that a sodium-chloride component was added to onsite groundwater in the San Andres aquifer. The logical source for this apparent addition was the former tailings impoundment at the Bluewater site.

As mentioned in Chapter 5, fine-grained pyrite is present in the sandstones within the San Andres aquifer. As a reduced sulfide mineral, pyrite has the capacity to lower the oxidation state of groundwater in the bedrock aquifer. It is possible that pyrite in the aquifer is limited to the top of the San Andres Limestone (see Section 3.3.2.4). If so, groundwater in wells completed in the middle and lower portions of the aquifer is likely to be oxidized. The pE values in onsite groundwater samples collected in May 2013 varied from 2.0 to 5.5, indicating relatively oxidized conditions. DO concentrations in the May 2013 samples ranged from 0.35 to 6.57 mg/L, values that are consistent with oxidizing conditions.

Calcite was undersaturated in several San Andres aquifer samples, but most samples were close to saturation (Figure 45). These results indicate that onsite groundwater in the aquifer is nearly saturated with calcite, which is likely caused by contact with limestone and with calcite cementation in the sandstones. The May 2013 samples were are also slightly undersaturated with respect to gypsum, but were closer to saturation than indicated in the regional background waters of the San Andres aquifer (Figure 45).

7.2.2 Uranium Mobility in Site Groundwater

Many chemical and biochemical processes affect the transport of uranium by groundwater. Uranium is immobile and not available to enter groundwater when it is attached firmly to

mineral phases in the aquifer. While in the aqueous phase, uranium is mobile and can be transported long distances. Uranium can also migrate into less mobile water contained in low-permeability sediments and micropores that are separated from the preferential flow paths in an aquifer. This uranium can "bleed" back out into the groundwater and cause later contamination through a process commonly referred to as back-diffusion.

Uranium can be transferred from the aqueous phase to solid mineral phases via adsorption or mineral precipitation. Transfer to the aqueous phase is usually favored by high pH values with abundant dissolved inorganic carbon or at low pH values without dissolved carbon. Uranium forms soluble complexes with carbonate ions. Under oxidized conditions, it is least soluble at near-neutral pH. Aqueous uranium complexes can also form from dissolved organic species, although the effect of uranium complexation in most natural groundwater is less than the effects of dissolved inorganic carbon.

Uranium is sensitive to changes in the oxidation-reduction (redox) state in an aquifer because it can form oxidized U(VI) species, referred to as uranyl, and reduced U(IV) species, referred to as uranous. A special case of mineral precipitation is the formation of low-solubility uranous minerals if the oxidation state is lowered sufficiently. Uranium can also be incorporated as a trace component in alkaline-earth-bearing minerals, such as calcite that may precipitate in the aquifer.

7.2.2.1 Uranium Adsorption

Adsorption of uranium occurs at mineral surfaces. Adsorption is likely to be a dominant mechanism for uranium retardation in oxidized aquifers. Minerals with high surface area are more adsorbent than those with lower surface area. Thus, clay minerals and hydrous ferric oxide ($Fe(OH)_3$) typically bind more uranium than detrital silicate minerals such as quartz or feldspar. These fine-grained minerals often compose the matrix material that binds detrital grains together. They also commonly occur as grain coatings. Sediments sometimes contain organic particles that can also adsorb uranium.

Many studies of uranium adsorption to mineral surfaces have been conducted. In particular, adsorption to $Fe(OH)_3$ is well understood. Most research indicates that uranium forms chemical complexes with negatively charged hydroxide sites at the surface of $Fe(OH)_3$. The ability to attach to the mineral surface is largely a function of the pH and the concentration of dissolved inorganic carbon. Hydrous ferric oxide is one of the most adsorptive minerals for uranyl in nature. In rocks with little hydrous ferric oxide, other minerals such as clays may dominate uranium adsorption. Although other minerals are less adsorptive than hydrous ferric oxide, they tend to respond to pH and aqueous carbonate concentrations in patterns similar to those observed for $Fe(OH)_3$.

Geochemical modeling was used to help evaluate the potential for adsorption processes to affect the mobility of uranium. The modeling was conducted with the geochemical computer code PHREEQC (Parkhurst and Appelo 2013). The WATEQ4F thermodynamic database supplied with the PHREEQC code was used, with uranyl surface complexation constants from Mahoney et al. (2009), and calcium-magnesium uranyl carbonate complexes from Dong and

Brooks (2006). This database was selected because Mahoney et al. (2009) found that it provided the best fit to all available uranyl surface complexation data for $Fe(OH)_3$. As a check, Mahoney et al. (2009) substituted the aqueous uranyl species stability constants published by the Nuclear Energy Agency (Guillaumont et al. 2003) and found that they produced similar results.

Figure 46 shows aqueous uranium concentrations in micrograms per liter in the presence of a system containing 1 gram (g) of $Fe(OH)_3$ for each liter of water and 2,380 µg of uranium per liter of water. As shown in this figure, the uranium concentrations are also a function of the aqueous dissolved inorganic carbon concentration, which is reflective of the amount of dissolved calcite ($CaCO_3$) in groundwater. When all of the uranium mass is dissolved in the water, the aqueous-phase concentration of the uranium is 1 millimol per liter. The concentration of $Fe(OH)_3$ used in this exercise is equivalent to about 100 parts per million (ppm) of iron in the rock. For comparison, the average crustal abundance of iron is 50,000 ppm (Mason and Moore 1982).

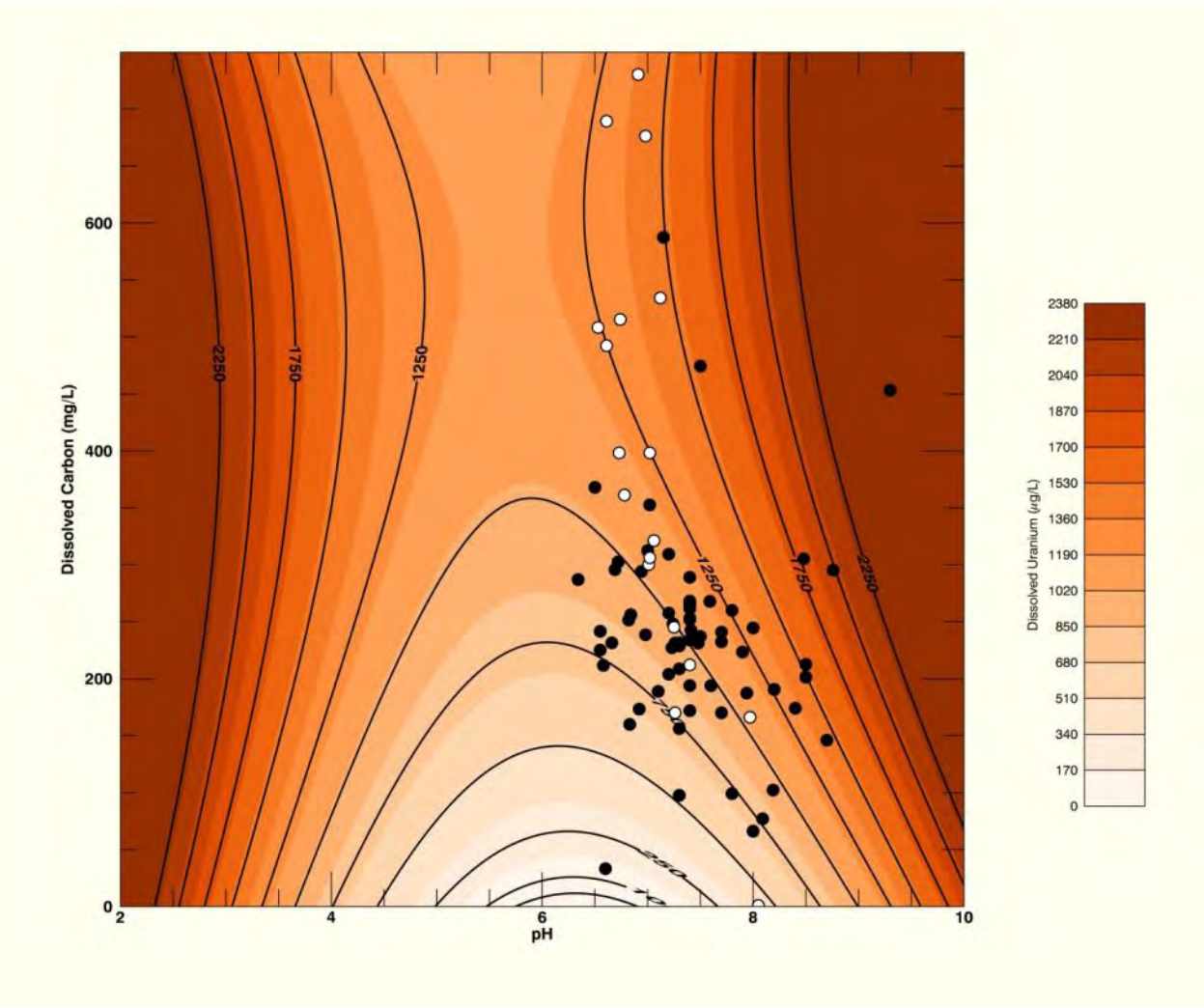

Figure 46. Variation in Uranium Concentrations (µg/L) in Equilibrium with 1 g/L of Hydrous Ferric Oxide and Variable pH and Varying Dissolved Inorganic Carbon Concentrations. Black and White *dots* Represent Background *and* Onsite *Bluewater* Groundwater Compositions, Respectively.

The diagram in Figure 46 shows uranyl strongly adsorbed at pH values ranging from about 5 to 7.5 with low dissolved carbonate. At pH values less than 4.5, uranium is mostly in the dissolved state regardless of the carbonate concentration. At pH values more than about 8 and modest dissolved carbonate, uranyl is mostly in the dissolved phase. The groundwater samples representing background conditions (background samples) cluster around an area in which about half of the uranium is adsorbed. There are a few groundwater samples that have sufficiently high pH and carbonate concentration that would cause uranyl to strongly partition to the aqueous phase. The onsite samples (white dots on Figure 46) generally have higher dissolved carbonate than the background samples and adsorb less uranyl.

Although Figure 46 was developed specifically for $Fe(OH)_3$, it can be used to generalize the degree to which uranyl adsorption will occur in either the alluvial or San Andres aquifers in response to changes in pH and carbonate concentration. These geochemical modeling results indicate that, if adsorbent minerals are present in the aquifers, uranyl will likely be partially adsorbed. However, short of having information regarding the actual concentrations of adsorptive minerals in the subsurface within the Grants-Bluewater Valley, it is difficult to conclude whether significant adsorption of uranyl is occurring in site and regional groundwater.

7.2.2.2 Mineral Saturation

Saturation indexes for uranium minerals were calculated using the PHREEQC code (Parkhurst and Appelo 2013) for groundwater samples collected from six onsite wells in May 2013. The samples examined were of particular interest because they had the highest uranium concentrations out of all the samples collected at the time of the sampling. The resulting saturation indexes were used to determine if a mineral would dissolve in site groundwater or precipitate from it. As previously stated, a negative index indicated that the mineral would dissolve, whereas a positive saturation index indicated that the mineral would precipitate.

Saturation indexes are logarithmic such that a value of −1 indicates that the groundwater is an order-of-magnitude undersaturated with respect to that mineral. Due to analytical uncertainties, and uncertainties in thermodynamic data, saturation indexes are not exact. As a general rule, saturation indexes are likely accurate to about 0.5, or half an order-of-magnitude. Both dissolution and precipitation can be rate-limited. Thus, if a groundwater sample has a negative saturation index for a particular mineral, the mineral may be present but dissolving too slowly to reach an equilibrium state.

Because silicon is a common rock-forming element and is universally present in groundwater, saturation indexes were determined for uranophane, a uranium silicate mineral. Dissolved silica was not measured in the groundwater samples, so the silica concentration was set at saturation with respect to amorphous silica (SiO_2). The resulting saturation indexes suggested that all six groundwater samples were undersaturated with uranophane by more than 10 orders-of-magnitude (Table 13), indicating that uranophane (and likely all uranyl silicate minerals) is not affecting uranium mobility at the Bluewater site. If equilibrated with quartz instead of amorphous SiO_2, uranophane saturation indexes are about 2 orders-of-magnitude lower.

Table 13. Uranium Mineral Saturation Indexes for Groundwater Samples from Six Bluewater Site Wells That Had the Highest Uranium Concentrations in May 2013

Uranium Mineral	16(SG) [1450][a]	18(SG) [232][a]	I(SG) [334][a]	OBS-3 [228][a]	S(SG) [639][a]	22(M) [380][a]
Gummite UO_3	–9.93	–10.65	–10.58	–10.57	–10.68	–10.57
$Na_4UO_2(CO_3)_3$	–21.92	–24.33	–23.03	–22.39	–22.28	–23.26
Rutherfordine UO_2CO_3	–3.99	–4.90	–4.84	–5.17	–4.87	–4.98
Schoepite $UO_2(OH)_2{\cdot}H_2O$	–4.72	–5.43	–5.47	–5.34	–5.48	–5.31
$U(OH)_2SO_4$	–27.42	–26.90	–23.57	–27.88	–20.99	–26.79
U_3O_8	–16.67	–16.89	–13.83	–17.38	–11.33	–15.82
U_4O_9	–33.36	–30.49	–21.26	–32.36	–13.59	–27.81
UO_2(amor)[b]	–15.25	–14.02	–11.12	–14.66	–8.40	–13.11
UO_3(gamma)	–7.18	–7.89	–7.86	–7.81	–7.93	–7.80
Uraninite UO_2(c)[c]	–10.70	–9.51	–6.41	–10.15	–3.85	–8.65
Uranophane $Ca(UO_2)_2(SiO_3OH)_2$	–10.71	–11.80	–12.21	–11.16	–11.80	–11.17

[a] Uranium concentration in micrograms per liter
[b] UO_2(amor) = amorphous UO_2
[c] UO_2(c) = crystalline uraninite

All uranium minerals were undersaturated in all of the groundwater samples (Table 13). In fact, all were undersaturated by at least 3 orders of magnitude, indicating that uranium minerals are not currently precipitating from the groundwater at these locations. These results suggest that uranium mineral precipitation is not an important mechanism affecting transport of uranium in the Bluewater groundwater plumes.

7.2.2.3 Oxidation-Reduction Analysis

Mineral saturation indexes presented in the previous section suggest that chemical reduction potentials sufficient to precipitate reduced uranium minerals are not present at the six sampling locations displayed in Table 13. Because chemical reduction can have a significant effect on uranium mobility, further assessment of possible redox mechanisms was conducted by preparing a compilation of all redox data listed in the DOE environmental database for Bluewater site wells, and then using the data to prepare pE-pH diagrams relative to the speciation of uranium.

Uranium dissolved in groundwater can precipitate low-solubility minerals in water containing chemical reductants, such as organic carbon. Even in a reduced state, uranium contains 2 moles of oxygen per mole of uranium and forms the crystalline mineral uraninite, with the formula UO_2(c). A less crystalline form, amorphous uraninite, with the formula UO_2(amor), is more soluble and more likely to form at shallow groundwater temperatures than its crystalline counterpart. Reducing conditions formed by oxidation of naturally occurring organic carbon can be sufficient to cause precipitation of UO_2(amor). At near-earth-surface temperatures the rate of precipitation of UO_2(amor) by carbon oxidation is increased by microbial respiration.

The stability field of UO_2(amor) is colored medium blue in the pE-pH diagram presented in Figure 47. The predominance fields for dissolved uranium species are shown in lighter color shades. To compile this diagram, the dissolved inorganic carbon concentration was fixed at 120 mg/L.

The pE and pH values for all samples included in the redox analysis are above the stability field for UO_2(amor) (Figure 47). Thus, there is no evidence in the May 2013 samples to suggest that reductive minerals are currently precipitating in the aquifers. Though existing data do not support the presence of redox states low enough to precipitate uranous minerals, redox measurements are problematic due to possible influx of atmospheric oxygen during sampling and analysis. Accordingly, chemically reduced uranium-precipitation zones may be present despite lack of confirmatory data.

Dissolved iron (Fe) concentrations in groundwater were also examined using data from the DOE environmental database. Elevated concentration of dissolved Fe at near-neutral pH is an indicator of chemical reduction because oxidized Fe minerals have a low solubility. Figure 48, which shows the stability fields for amorphous $Fe(OH)_3$ and ferrous carbonate (siderite) at a dissolved Fe concentration of 1 mg/L, indicates that most of the Bluewater groundwater pH-pE measurements fall within the stability fields for these minerals.

Few data were available for dissolved Fe, and only eight samples had data for both redox parameters and Fe concentrations (Table 14). Of the eight measured Fe concentrations, five were higher than 1 mg/L. The Fe concentrations at E(M), OBS-3, and S(SG) are more than an order of magnitude higher than 1 mg/L. The higher Fe concentrations could indicate that groundwater at the site is not at redox equilibrium, or, alternatively, they could reflect errors in the redox measurements. If the redox measurements are in error, the high Fe concentrations signal a more reduced condition that could affect uranium mobility. It is more likely, however, that some of the elevated Fe concentrations are due to particulate or colloidal Fe that inadvertently was included in the respective groundwater samples. In this case, the Fe results would not be useful for evaluating redox conditions.

Collectively, the analyses of existing redox and Fe concentration data in this section, based on samples of groundwater collected from wells in the vicinity of the Bluewater site, provide little evidence of uranium immobility caused by reductive precipitation.

7.2.3 Uranium Isotopes

The activity ratio (AR) of uranium-234 to uranium-238 (^{234}U to ^{238}U) was used in this study to help identify sources of uranium in groundwater. Values of AR in groundwater at a uranium mill site near Cañon City, Colorado, were used by Zielinski et al. (1997) to help distinguish between dissolved uranium resulting from mill site contamination and naturally occurring background uranium. Samples with AR values more than about 1.3 were attributed to background conditions, and lower values were thought to be from the uranium mill. Other studies provide confirmation that groundwater uranium derived from uranium milling operations has an AR value near 1.0 (e.g., Otton et al. 2010; Kamp and Morrison 2014).

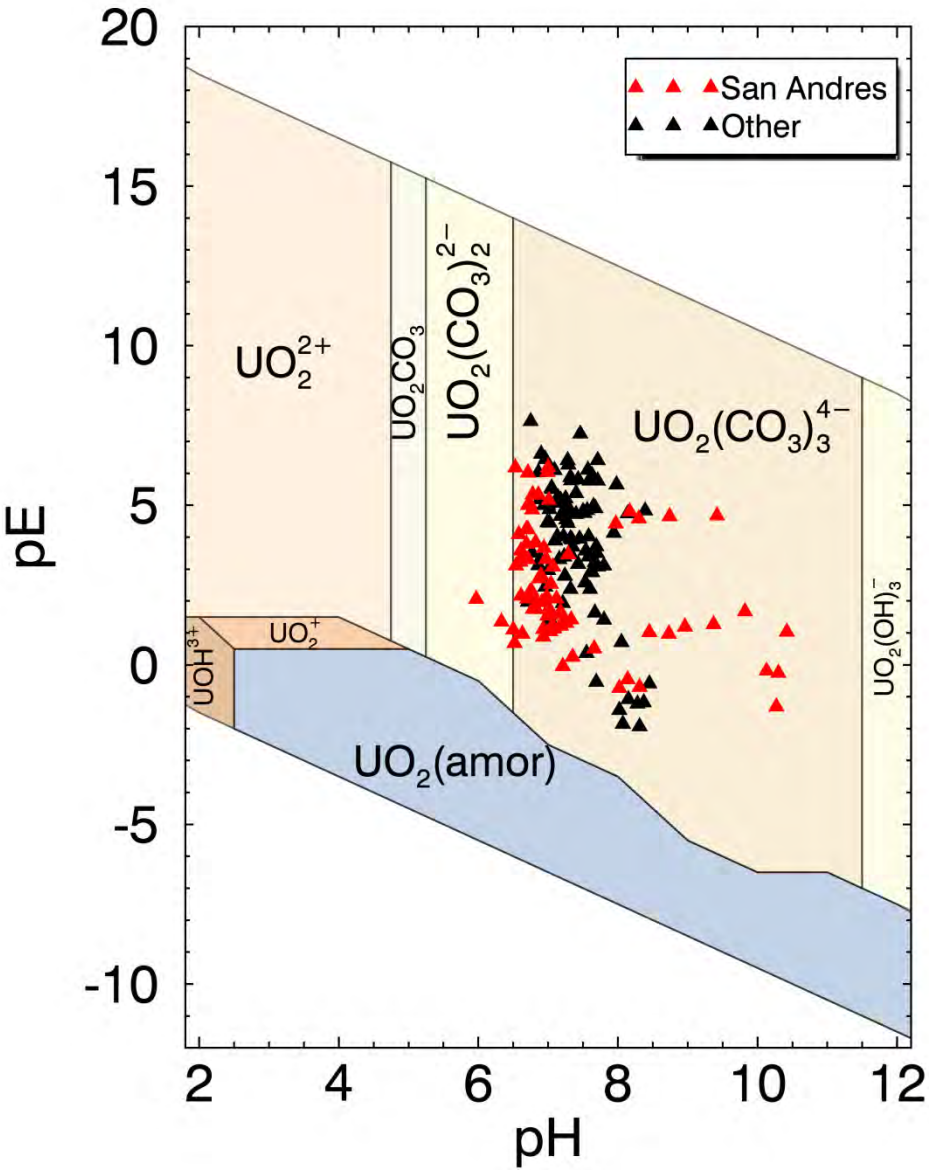

Figure 47. pH-pE Diagram of the U-CO_2 System

System conditions: dissolved carbon = 0.01 mol (120 mg/L), iron = 1.79×10^{-5} mol (1 mg/L), temperature = 25 °C. Sodium nitrate concentrations were held at 0.1 mol for ionic strength control, and sodium concentrations were allowed to fluctuate slightly to maintain charge balance. The mineral stability boundary shown for UO_2(amor) is based on dissolved uranium concentration of 1.85×10^{-7} mol (44 µg/L). The triangles represent individual groundwater samples.

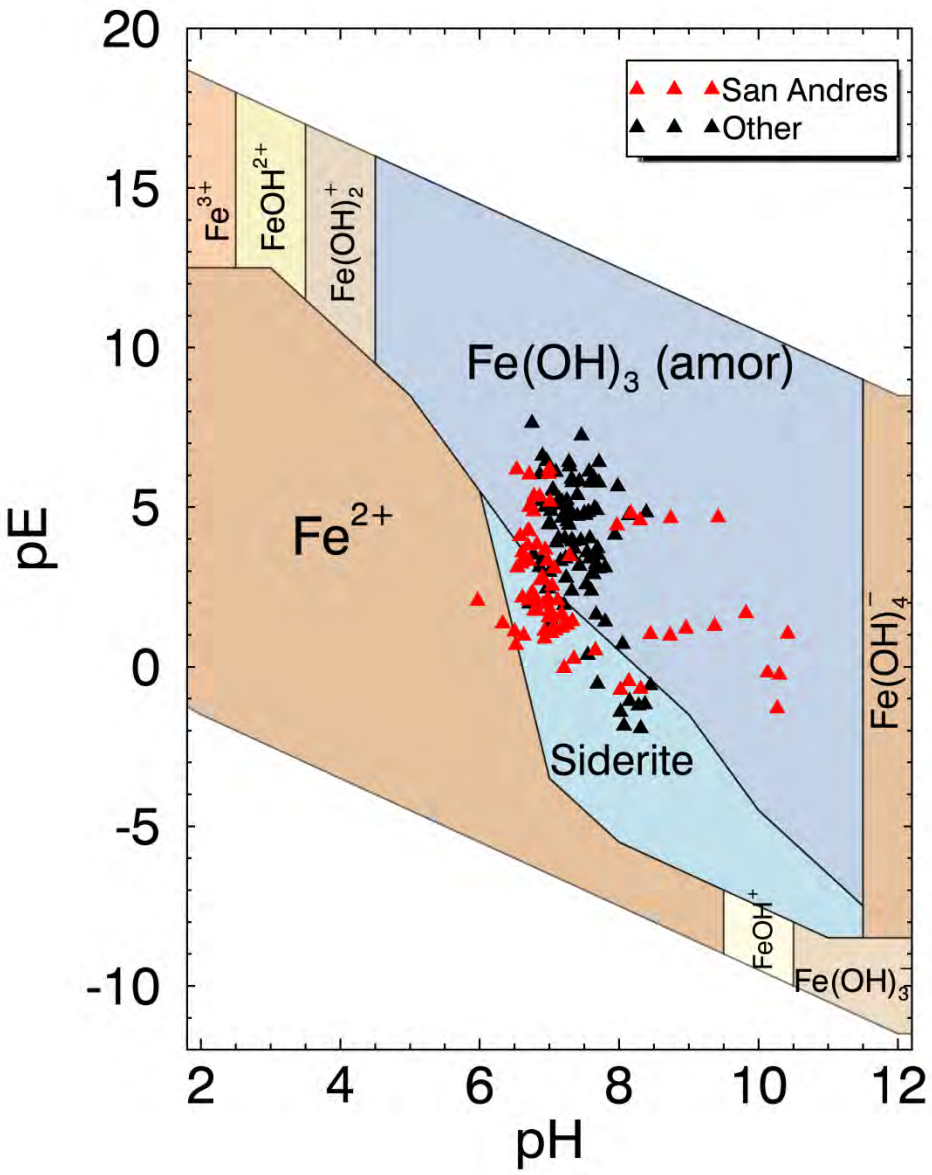

Figure 48. pH-pE Diagram of the Iron System

Conditions are the same as those used to prepare Figure 47. The mineral stability boundaries shown for $Fe(OH)_3$(amor) and siderite are based on a dissolved Fe concentration of 1 mg/L. The triangles represent individual samples of groundwater.

Table 14. Data from DOE Environmental Database for Samples with Reported Concentrations of Dissolved Iron and Redox Parameters

Well	Screened Formation/Aquifer	pH	pE[a]	Iron Concentration (mg/L)[b]
Y2(M)	Quaternary Alluvium	8.14	4.74	0.075
F(M)	Quaternary Alluvium	8.39	4.83	0.44
L(SG)	San Andres Aquifer	9.42	4.67	0.82
I(SG)	San Andres Aquifer	8.74	4.65	1.7
T(M)	Quaternary Alluvium	6.88	5.18	1.7
E(M)	Quaternary Alluvium	7.00	5.01	12
OBS-3	San Andres Aquifer	8.17	4.80	13
S(SG)	San Andres Aquifer	8.30	4.58	570

[a] pE values based on measured oxidation-reduction potential.
[b] All samples were collected on November 10, 2009.

Uranium-234 is produced by the alpha decay of ^{238}U. In a closed system, such as a tight rock matrix, ^{234}U and ^{238}U reach secular equilibrium in a period of about a million years. At secular equilibrium, ^{234}U production from ^{238}U decay is equivalent to its loss through subsequent decay. Under this condition, the AR is 1.0. The uranium in ore deposits, such as those processed at uranium mills like the Bluewater mill, was formed millions of years ago and is near secular equilibrium. Because the milling process uses harsh chemicals to digest the mill feed, the uranium in the mill liquors also has an AR value of near 1.0. In contrast, ^{234}U is preferentially released from uranium-bearing minerals in groundwater aquifers. The preferential release is caused by the disruption of the atomic crystalline structure as ^{234}U is recoiled during the expulsion of an alpha particle from ^{238}U (Cherdyntsev et al. 1955; Kigoshi 1971). The recoiled ^{234}U atom can pass directly into a groundwater pore or may be preferentially leached from its crystalline dislocation. This preferential release of ^{234}U is the cause of elevated AR values that are observed in most natural groundwater.

Uranium isotope data for groundwater wells on the Bluewater site were examined along with isotope information from several other wells in the Grants-Bluewater Valley. In all, 19 samples were collected from 12 wells screened in the alluvial aquifer (Table 15), and 32 samples were collected from 20 wells screened in the San Andres aquifer (Table 16). Data for four municipal wells near Milan, which draw water from the San Andres aquifer, were also included; completion information on the Milan wells was not available. Uranium concentrations measured using chemical methods closely matched concentrations derived from radiometric analyses, confirming the high quality of these data (Table 15 and Table 16). The range in results from chemical analysis of uranium concentrations was 1.1 to 1400 µg/L.

Table 15. $^{234}U/^{238}U$ Activity Ratios (ARs) in Groundwater Samples Collected from Alluvial Aquifer Wells at the Bluewater Site and Surrounding Areas

Well	Alternate Name	Regional Location	Sample Date	Uranium Concentration		Uranium Activity Concentration		Activity Ratio	Data Source
				Chemical (µg/L)	Radiometric (µg/L)	U-234 (pCi/L)	U-238 (pCi/L)		
20(M)		Bluewater Site	11/19/2013	13.9		6.58	4.66	1.41	DOE
21(M)		Bluewater Site	7/27/2011	130	128.5	46.5	43	1.08	DOE
21(M)		Bluewater Site	11/19/2013	137		46.1	40.4	1.14	DOE
22(M)		Bluewater Site	7/27/2011	330	346.7	117	116	1.01	DOE
22(M)		Bluewater Site	11/19/2013	388		122	118	1.03	DOE
23(M)		Bluewater Site	11/19/2013	20.9		8.95	6.24	1.43	DOE
F(M)		Bluewater Site	11/10/2010	8.06	8.8	4.19	2.95	1.42	DOE
F(M)		Bluewater Site	7/28/2011	7.4	7.3	3.4	2.44	1.39	DOE
F(M)		Bluewater Site	11/19/2013	7.34		3.2	2.53	1.26	DOE
T(M)		Bluewater Site	11/9/2010	557	505.2	161	169	0.95	DOE
T(M)		Bluewater Site	7/26/2011	530	544.0	176	182	0.97	DOE
X(M)		Bluewater Site	11/19/2013	145		47.8	44.8	1.07	DOE
Y2(M)		Bluewater Site	11/11/2010	5.19	5.1	2.56	1.7	1.51	DOE
Y2(M)		Bluewater Site	7/28/2011	4.8	4.9	2.61	1.63	1.60	DOE
Y2(M)		Bluewater Site	11/19/2013	5.3		2.97	1.94	1.53	DOE
914	SMC-10	Northeast of Homestake site	3/30/2009	30.9	0.1	0.1	0.04	2.50	NMED
920	SMC-11	Northeast of Homestake site	3/31/2009	228	233.5	78.1	63	1.24	NMED
921	SMC-13	Northeast of Homestake site	4/2/2009	240	192.2	75.8	64.3	1.18	NMED
950	SMC-12	Northeast of Homestake site	3/31/2009	163	155.4	61.9	52	1.19	NMED

µg/L = micrograms per liter; pCi/L = picocuries per liter; DOE = DOE environmental database; NMED = NMED (2010)

Table 16. $^{234}U/^{238}U$ Activity Ratios (ARs) in Groundwater Samples Collected from San Andres Aquifer Wells at the Bluewater Site and Surrounding Areas

Well	Alternate Name	Regional Location	Sample Date	Uranium Concentration		Uranium Activity Concentration		Activity Ratio	Data Source
				Chemical (µg/L)	Radiometric (µg/L)	U-234 (pCi/L)	U-238 (pCi/L)		
11(SG)		Bluewater Site	11/19/2013	11.7		5.73	3.61	1.59	DOE
13(SG)		Bluewater Site	11/19/2013	98.5		37.8	35.4	1.07	DOE
14(SG)		Bluewater Site	11/19/2013	74.1		26.9	23.8	1.13	DOE
15(SG)		Bluewater Site	11/19/2013	174		60.2	55.8	1.08	DOE
16(SG)		Bluewater Site	11/19/2013	1400		381.0	401.0	0.95	DOE
18(SG)		Bluewater Site	11/19/2013	127		44.7	44.1	1.01	DOE
I(SG) (235 ft)		Bluewater Site	11/11/2010	2.7	4.2	1.48	1.4	1.06	DOE
I(SG) (235 t)		Bluewater Site	7/27/2011	1.1	1.3	0.476	0.449	1.06	DOE
I(SG) (210 ft)		Bluewater Site	11/19/2013	346		53.4	54.0	0.99	DOE
I(SG) (240 ft)		Bluewater Site	11/19/2013	149		49.9	49.1	1.02	DOE
I(SG) (265 ft)		Bluewater Site	11/19/2013	334		110	106	1.04	DOE
I(SG) (300 ft)		Bluewater Site	11/19/2013	324		105	103	1.02	DOE
L(SG)		Bluewater Site	7/27/2011	3.2	3.3	1.85	1.11	1.67	DOE
L(SG)		Bluewater Site	11/19/2013	2.94		1.33	1.2	1.11	DOE
S(SG)		Bluewater Site	7/26/2011	260	231.4	71	77.4	0.92	DOE
S(SG)		Bluewater Site	11/20/2013	525		163	176	0.93	DOE
OBS-3 (255 ft)		Bluewater Site	11/10/2010	1.1	1.4	0.422	0.456	0.93	DOE
OBS-3 (325 ft)		Bluewater Site	11/10/2010	0.648	1.7	0.526	0.558	0.94	DOE
OBS-3 (152 ft)		Bluewater Site	7/28/2011	120	119.0	37.2	39.8	0.93	DOE
OBS-3		Bluewater Site	11/20/2013	9.31		3.05	2.56	1.19	DOE
HMC-951	BW-34	Bluewater Site	8/27/2008	53.3	36.8	13.5	12.3	1.10	NMED
HMC-951	BW-34	Bluewater Site	11/20/2013	31.3		12.0	11.0	1.09	DOE
Bowlins DQ #2	BW-05	West of Bluewater Site	8/25/2008	10.5	9.0	6.4	3	2.13	NMED
BW-14		West of Bluewater Site	8/27/2008	10.5	10.2	13.8	3.4	4.06	NMED
Bowlins	BW-24	West of Bluewater Site	8/25/2008	10.9	9.6	14.4	3.2	4.50	NMED
911	BW-15	Southeast of Bluewater Site	8/25/2008	12	8.4	4.5	2.8	1.61	NMED
949	BW-23	Southeast of Bluewater Site	8/25/2008	13.8	12.9	7.1	4.3	1.65	NMED
928	BW-32	North of Bluewater Site	9/16/2008	29	32.9	22.9	11	2.08	NMED
B-23	Milan Well #1	Milan Municipal Well	12/2/2009	4	3.9	3.07	1.3	2.36	NMDWB
B-35	Milan Well #3	Milan Municipal Well	6/19/1996	13	11.0	6.26	3.69	1.70	NMDWB
B-35	Milan Well #3	Milan Municipal Well	12/2/2009	4	3.7	2.6	1.25	2.08	NMDWB
B-50	Golden Acres, Milan Well #4	Milan Municipal Well	12/2/2009	12	11.4	5.79	3.81	1.52	NMDWB

µg/L = micrograms per liter; pCi/L = picocuries per liter; DOE = DOE environmental database; NMDWB = New Mexico Drinking Water Bureau; NMED = NMED (2010)

Figure 49 contains posted values of AR and uranium concentration for the most recent samples collected at wells in the alluvial aquifer. The ARs for at least four alluvial aquifer wells at the Bluewater site (T(M), X(M), 21(M), and 22(M)) are likely impacted by tailings-related uranium contamination. These four wells, with posted uranium concentrations varying between 130 and about 560 µg/L and posted ARs ranging from 0.95 to 1.08 (Figure 49), appear to lie along the flow path following the ancestral Rio San Jose paleochannel extending southeast from the southeast corner of the Bluewater site (Section 4.3.3 and Figure 21). It is also likely that the sample collected from alluvial aquifer well 23(M) at the Bluewater site contained some mill-related uranium contamination. Though the AR for this well is 1.43, the corresponding uranium concentration is about 21 µg/L, about double the adopted background uranium concentration of 10 µg/L (Section 5.3). In addition, inspection of mapped hydraulic heads and flow directions in the alluvial aquifer in 2012 (Figure 21 and Figure 22) indicates that well 23(M) also lies within the paleochannel extending southeast from the Bluewater site. The combination of an elevated uranium concentration with an AR distinctly larger than 1 suggests that mill-related uranium contamination is present in groundwater at this well location, but its impact has been diluted by mixing with uncontaminated water.

Wells F(M) and Y2(M) at the Bluewater site do not appear to be impacted by mill-related uranium. ARs at these locations range from 1.26 to 1.6, and corresponding uranium concentrations are all less than 10 µg/L (Table 15 and Figure 49). Interpretation of the uranium isotope data for well 20(M) is less clear. Though the single calculated AR for the well is 1.41, the corresponding uranium concentration is about 14 µg/L.

Three of the four wells with uranium isotope data in the alluvial aquifer north-northeast of the Homestake site (Figure 49) have computed ARs ranging from 1.18 to 1.24. These values, when combined with corresponding uranium concentrations between 163 and 240 µg/L, suggest that tailings-related uranium contamination is present in the San Mateo Creek alluvium upgradient of the Homestake site. The source of this contamination is presumably mining- and milling-impacted water from Ambrosia Lake Valley. Well 914, with an AR of 2.5, also appears to be impacted by mill-related uranium contamination. The corresponding uranium concentration at this location is about 31 µg/L, which is greater than the assumed background concentration for uranium of 10 µg/L.

A map with posted uranium isotope ARs for San Andres aquifer wells (Figure 50) further illustrates how the activity ratios can be used to help distinguish tailings-related uranium contamination at the Bluewater site from either uncontaminated groundwater or groundwater that represents a mixture of mill-related, dissolved uranium and background water. The posted ARs at four site wells directly east of, and hydraulically downgradient of, the main tailings disposal cell (OBS-3, S(SG), 16(SG), and I(SG)) range from 0.93 to 0.99, and corresponding concentrations range from 346 to 1400 µg/L. Uranium isotope data for onsite San Andres aquifer wells located south of the main tailings disposal cell (13(SG), 14(SG), 15(SG), 18(SG)) are also representative of mill-related impacts. AR values at these locations vary from 1.01 to 1.13, and corresponding uranium concentrations range from about 74 to 174 µg/L (Table 16). Mill-derived uranium contamination also appears to be present at Homestake well HMC-951, which is just east of the Bluewater site's southeast corner. The computed AR at this well is 1.1, and the posted uranium concentration is about 31 µg/L (Figure 50).

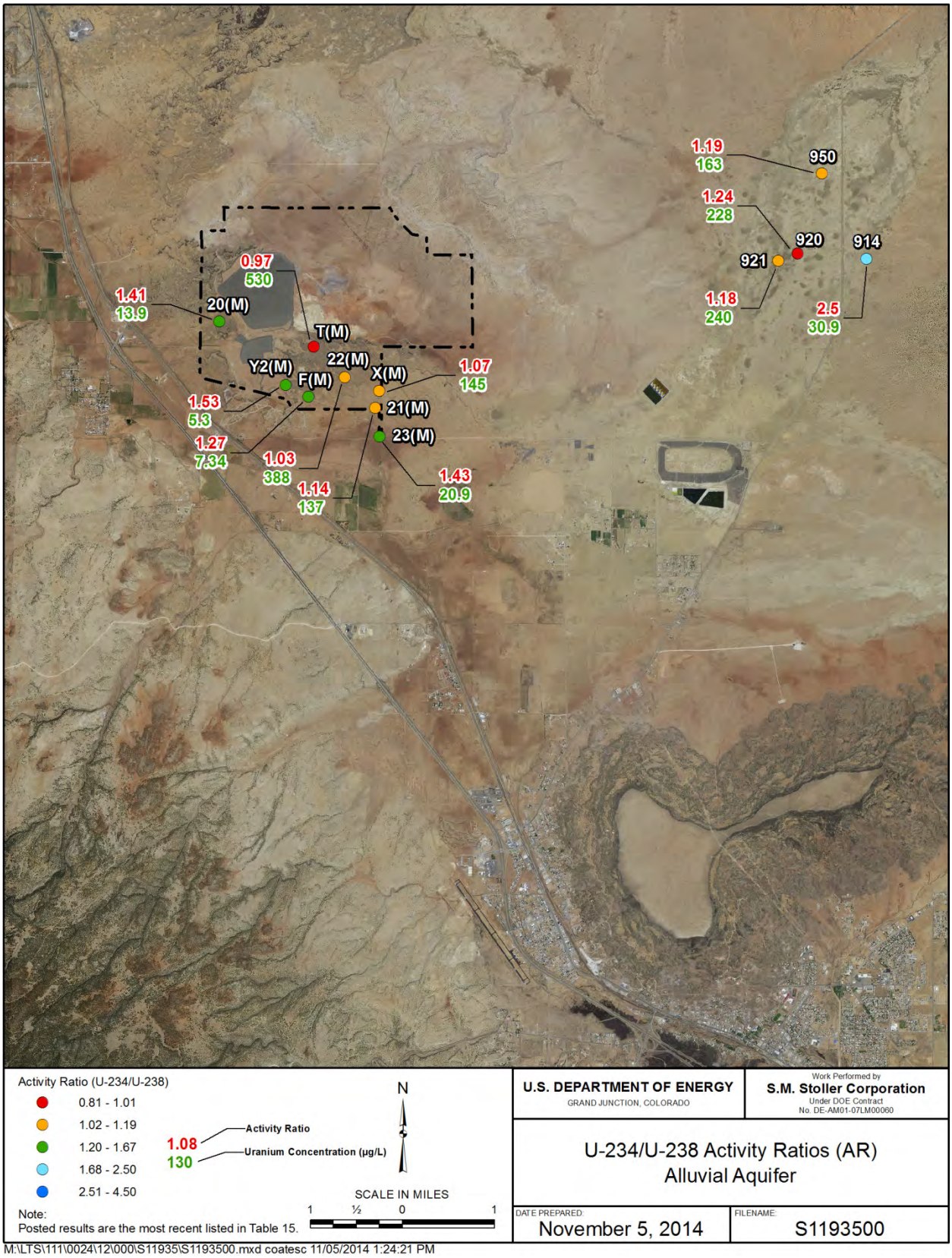

Figure 49. Uranium Isotope Activity Ratios (ARs) for Alluvial Aquifer Wells at the Bluewater Site and in Surrounding Areas

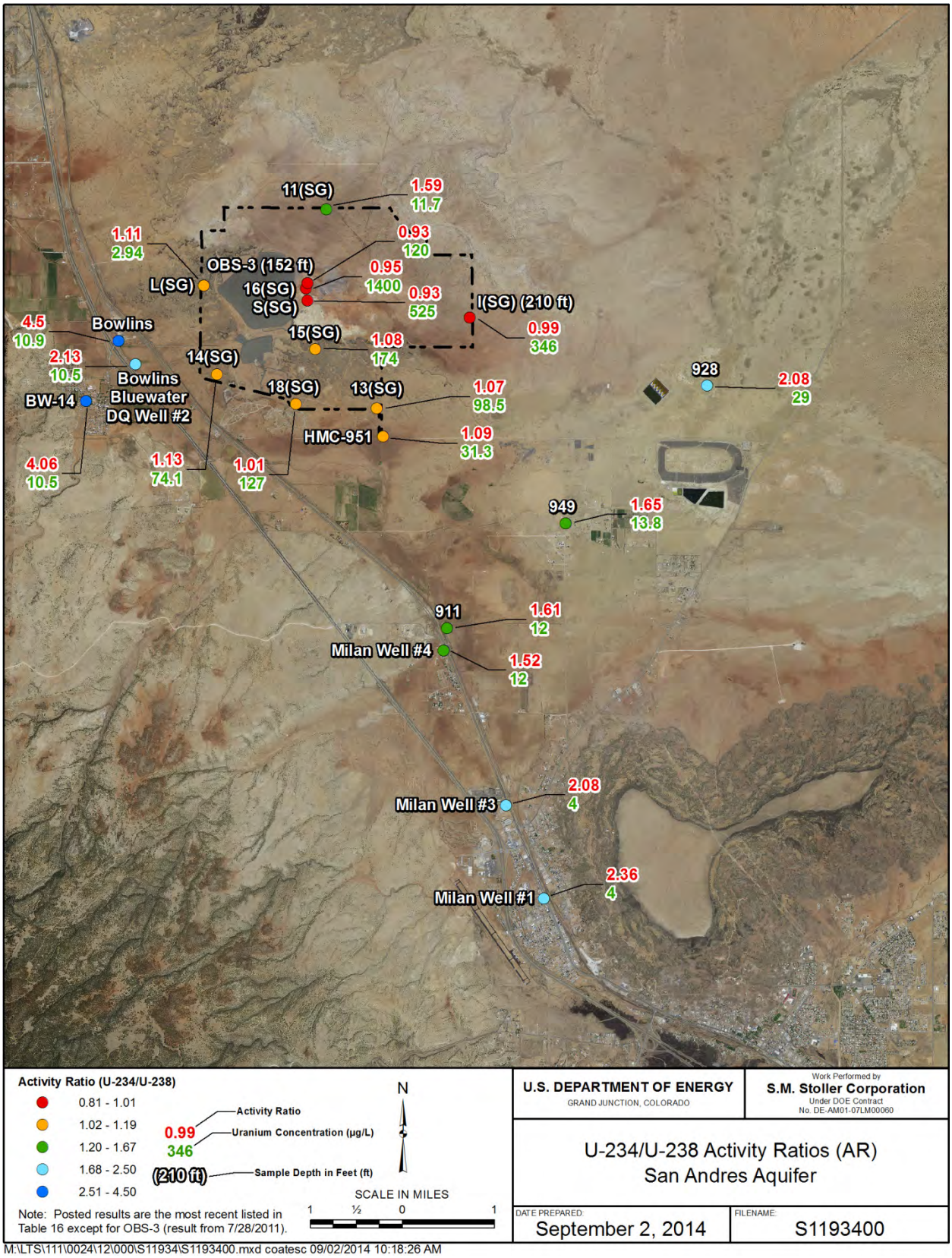

Figure 50. Uranium Isotope Activity Ratios (ARs) for San Andres Aquifer Wells at the Bluewater Site and in Surrounding Areas

Well 11(SG), located north of the main tailings disposal cell and near the Bluewater site's north border, appears to be unaffected by tailings-derived uranium. The single AR value for the well is 1.59, and the associated uranium concentration is about 12 µg/L, which could be representative of background uranium levels farther north in the aquifer. Similarly, no evidence of uranium contamination is observed at onsite well L(SG), with a calculated AR of 1.11 and a uranium concentration of about 3 µg/L. L(SG) is the background well for the San Andres aquifer at the Bluewater site (Figure 50).

The ARs at three wells west of and upgradient of the Bluewater site (Bowlins, Bowlins DQ#2, and BW-14) range from 2.13 to 4.5 (Figure 50), which are considered representative of groundwater that contains naturally occurring uranium. Of some interest is the fact that the corresponding uranium concentrations at these three wells, varying from 10.5 to 10.9 µg/L, are all essentially equal to the adopted background concentration of 10 µg/L.

The results presented in Table 16 for two I(SG) samples merit further analysis. Both of the I(SG) samples, collected at a depth of 235 ft in 2010 and 2011, had low uranium concentrations (2.7 and 1.1 µg/L, respectively), yet the associated ARs were near a value of unity, indicating the presence of tailings-related contamination. This set of illogical results can be explained by the fact that low-flow sampling techniques were employed to collect samples at the well in 2010 and 2011 and that concentrations in the well bore vary with depth, a topic that was briefly addressed in Section 7.2.1.2. Chapter 8 provides further discussion of the effects of low-flow sampling at well I(SG).

Two OBS-3 samples, collected at depths of 255 and 325 ft in 2010, also exhibit the illogical combination of low uranium concentration and low ARs near the value of unity (Table 16). Because uranium contamination stemming from leached tailings at the main disposal cell has historically been detected at this well and at other wells directly east of the disposal cell, an AR of about 1 is feasible, but the low uranium concentrations are probably attributable to other phenomena that influence this well. As discussed later in Chapter 8, the illogical results seen at this well can be attributed to a combination of severe corrosion of the well screen in well OBS-3 and the use of low-flow sampling techniques.

Two San Andres aquifer wells in the general vicinity of the Homestake site (928 and 949 in Figure 50) show computed ARs of 1.65 and 2.08. These results, suggesting that neither well is directly impacted by tailings-related uranium, could be representative of San Andres aquifer groundwater that is a mixture of uranium-contaminated and uncontaminated waters. This possibility is supported by corresponding uranium concentrations at wells 928 and 949 of 29 and 13.8 µg/L, respectively (Table 16). Though these concentrations are not particularly high, they are, nevertheless, higher than the adopted background uranium concentration.

The northernmost drinking-water supply well for Milan (Milan Well B-50) and nearby well 911 have computed ARs of 1.52 and 1.61, respectively. These values suggest that neither well is directly impacted by tailings-related contamination. However, the corresponding uranium concentrations of 12 µg/L at both wells (Table 16) are slightly higher than the background concentration of 10 µg/L. Thus, the possibility that the water sampled at these two wells represents a mixture of uranium-contaminated and uncontaminated groundwater cannot be completely discounted. A discussion of regional groundwater flow directions in the San Andres aquifer in Section 4.3.3.1 indicates that the two wells lie far south of the flow paths for

groundwater that might be contaminated at the Bluewater site and that subsequently migrates to the east-southeast in the direction of Grants. As discussed later in the next chapter, alternative mechanisms of delivering uranium-impacted groundwater to this part of the San Andres aquifer are worthy of examination.

The combination of a computed AR of 2.36 and an associated uranium concentration of 4 µg/L at Milan well B-23 (Figure 50 and Table 16) suggests that this southernmost San Andres aquifer well for Milan remains unaffected by uranium-contaminated groundwater in the Grants-Bluewater Valley. However, the results for Milan well B-35 are somewhat mixed. The combination of a computed AR of 1.70 and a uranium concentration of 13 µg/L in a sample collected in 1996 leave open the possibility that San Andres-aquifer groundwater in the vicinity of the well may have at one time been slightly impacted by uranium contamination. Alternatively, a uranium concentration of 4 µg/L and a computed AR of 2.08 in a sample collected in 2009 imply that the well was not impacted. Such temporally variable results suggest that possible mechanisms for delivering uranium-contaminated groundwater to municipal wells in the Milan area should be examined.

8.0 Groundwater Contamination and Uranium Transport

8.1 Contaminant Source History

8.1.1 Main Tailings Impoundment

Past investigations of contaminant source loading to the alluvial and San Andres aquifers at the Bluewater site have considered a variety of factors that potentially influenced contamination in the subsurface. Estimates have been made of the rates at which tailings fluids seeped from the bottom of the main tailings impoundment, beginning in 1956 and extending through the mid-1990s (e.g., Applied Hydrology Associates Inc. 1990). Estimates have also been made of the inorganic chemical makeup of source material underlying the impoundment that supplied contaminant mass to groundwater migrating beneath the site (e.g., Hydro-Search 1977). Findings from these assessments indicated that acidic tailings fluids seeping downward from the main tailings impoundment were neutralized, causing contaminants to chemically precipitate and adsorb to aquifer media. This process apparently resulted in a mineralized zone in the geologic materials underlying the disposal cell (basalt, alluvium, limestone, and sandstone).

Temporal plots of contaminant concentrations at key wells located hydraulically downgradient of the impoundment have shown that constituent concentrations in the subsurface have remained relatively constant since the early 1980s. This suggests that the rate of contaminant mass loading to the aquifers has remained relatively constant or has been decreasing at a very slow rate over the past 30 years. There is no evidence in the temporal histories to indicate that a new pulse of contamination from the disposal cell has taken place (DOE 2014).

Applied Hydrology Associates Inc. (1995) suggested that contaminant concentrations at downgradient wells were gradually declining prior to decommissioning of the Bluewater site in the 1990s. Trend analyses of the data they examined indicated that, if concentrations were declining, the rate of decrease was extremely slow. Unfortunately, much of the concentration data collected at the site between the mid-1990s and 2011 were largely insufficient for detecting trends. However, a limited quantity of uranium concentration data collected at new wells installed in 2011 and 2012 indicate that rates of contaminant mass loading to the aquifers are either constant or slightly decreasing.

Multiple processes have been proposed for how contaminant mass is mobilized in groundwater beneath the main tailings disposal cell. These include desorption of contaminants from the surfaces of grains that compose alluvial aquifer and San Andres aquifer media and dissolution of contaminants co-precipitated with minerals formed during neutralization of tailings fluids. Alternatively, it is possible that some aqueous-phase contamination continues to reside in low-permeability materials in the alluvial and San Andres aquifers, and it is slowly being released to more-permeable media. Though the nature of the contaminant mobilization is not thoroughly understood, the phenomena involved appear to be uninterrupted.

8.1.2 Anaconda Injection Well

As discussed in Chapters 2 and 6, sandstone strata within the Yeso Formation were used for injection of Bluewater-mill waste fluids from 1960 to 1977, when Anaconda delivered the fluids to a disposal well about 1 mile northeast of the main tailings impoundment. It has been

speculated that some of the injected fluid leaked upward to the San Andres aquifer and has been responsible for uranium contamination observed both historically and currently in San Andres aquifer wells north and east of the main tailing impoundment. San Andres aquifer groundwater in the areas containing these wells migrates offsite in an east-southeast direction toward parts of the GRP north of the large tailings disposal cell at the Homestake site.

The potential for the injection well to be a source of contamination in the San Andres aquifer in areas north of the main tailings impoundment was investigated further by examining historical concentrations of dissolved constituents at the San Andres aquifer well referred to as Monitor, which was located near the injection well (Figure 16, Plate 7). Data included in the DOE environmental database show that, while the well was monitored between the mid-1980s and 1990, uranium concentrations at the Monitor well generally fell in the range of 0.25 to 0.35 mg/L, and TDS concentrations varied from 2,000 to about 2,600 mg/L. The last uranium concentration measured at the Monitor well, from a sample collected in April 1990, was 0.32 mg/L. These values support the assumption that the injection well was a source of contamination in the San Andres aquifer in areas north of the main tailings disposal cell.

Because ARCO decommissioned the Monitor well, it is difficult to discern whether contamination stemming from the injected fluids has continued to feed the uranium plume that originated at the injection well. However, because uranium concentrations at the Monitor well were as high as 0.32 mg/L in 1990, some 13 years after waste injection ceased, it is plausible that uranium concentrations exceeding the MCL (0.03 mg/L) are still present in the San Andres aquifer near the Anaconda injection well.

8.2 Uranium Contamination in the Alluvial Aquifer

The spatial extent of uranium contamination originating at the Bluewater site can be partly assessed by comparing historical and recent uranium plume maps in onsite and offsite areas. In addition, examination of the multi-year histories of uranium concentration at the wells used to create the plume maps aerial views of plumes assists in discerning whether contaminant mass is changing or remaining relatively constant in portions of the contamination located hydraulically downgradient of contaminant source areas.

8.2.1 Uranium Plume Maps

To assess how uranium contamination in the alluvial aquifer has evolved over the past 35 years, maps showing uranium concentrations at selected wells and concentration contours in the aquifer were developed for three separate time periods. In addition, a temporal plot of measured uranium concentrations was prepared for five alluvial aquifer wells on the Bluewater site to assess the degree to which steady-state concentrations have been maintained in onsite wells.

Figure 51 shows measured uranium concentrations in 1980–1981 at alluvial aquifer wells that were included in the regional hydrologic study performed by Hydro-Search (1981a). Data coverage at the time was sparse due to a limited number of monitoring wells at both the Bluewater site and the Homestake site. The contoured concentrations in ancestral Rio San Jose alluvium at the Bluewater site are similar to those shown in a comparable map of uranium concentrations prepared by Applied Hydrology Associates Inc. (1990) for conditions in 1982.

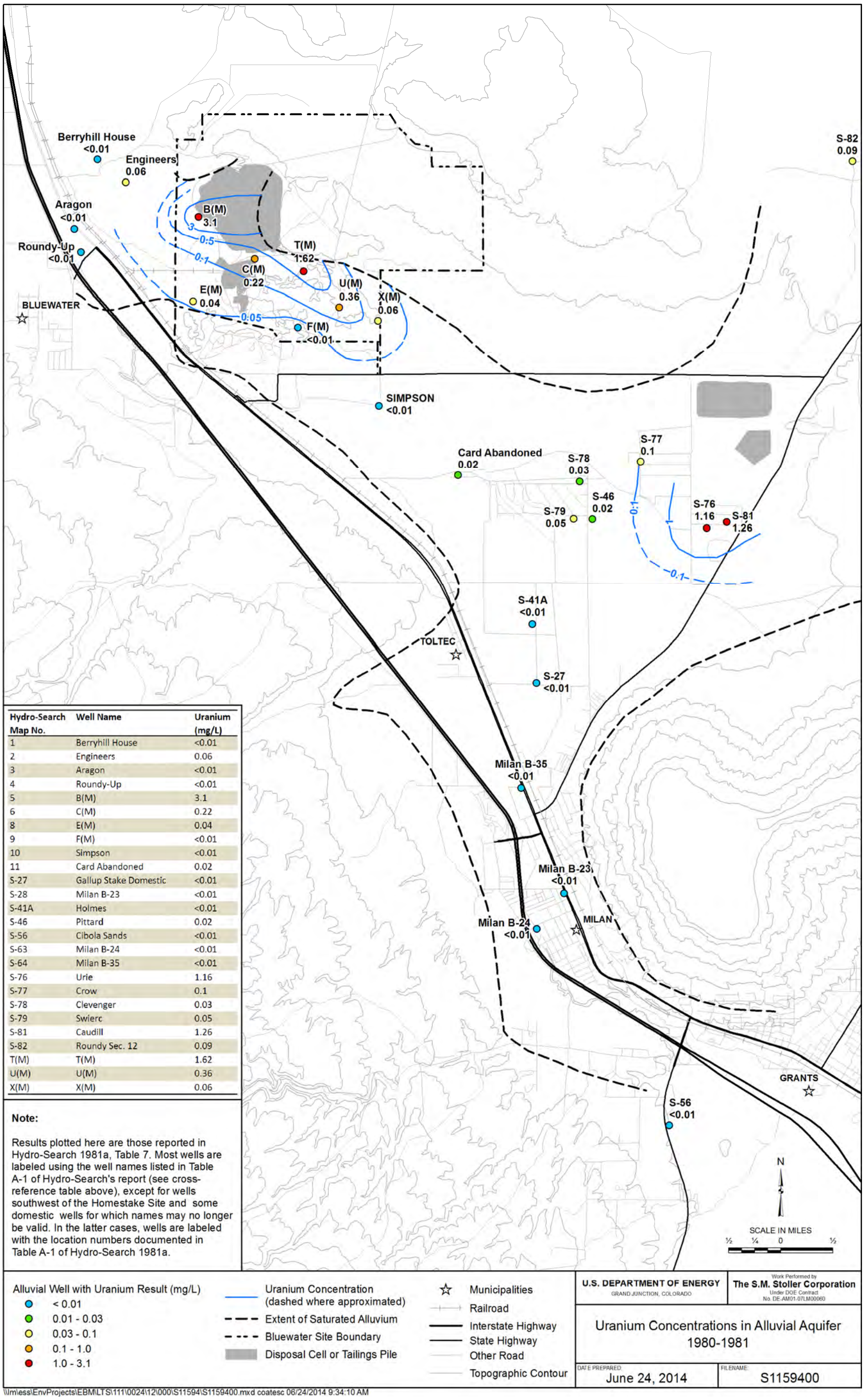

Hydro-Search Map No.	Well Name	Uranium (mg/L)
1	Berryhill House	<0.01
2	Engineers	0.06
3	Aragon	<0.01
4	Roundy-Up	<0.01
5	B(M)	3.1
6	C(M)	0.22
8	E(M)	0.04
9	F(M)	<0.01
10	Simpson	<0.01
11	Card Abandoned	0.02
S-27	Gallup Stake Domestic	<0.01
S-28	Milan B-23	<0.01
S-41A	Holmes	<0.01
S-46	Pittard	0.02
S-56	Cibola Sands	<0.01
S-63	Milan B-24	<0.01
S-64	Milan B-35	<0.01
S-76	Urie	1.16
S-77	Crow	0.1
S-78	Clevenger	0.03
S-79	Swierc	0.05
S-81	Caudill	1.26
S-82	Roundy Sec. 12	0.09
T(M)	T(M)	1.62
U(M)	U(M)	0.36
X(M)	X(M)	0.06

Note:

Results plotted here are those reported in Hydro-Search 1981a, Table 7. Most wells are labeled using the well names listed in Table A-1 of Hydro-Search's report (see cross-reference table above), except for wells southwest of the Homestake Site and some domestic wells for which names may no longer be valid. In the latter cases, wells are labeled with the location numbers documented in Table A-1 of Hydro-Search 1981a.

Figure 51. Regional Uranium Concentrations in the Alluvial Aquifer in 1980–1981

This page intentionally left blank

However, it is difficult to discern from the map the extent of uranium contamination at the time in San Mateo Creek alluvium at the Homestake site. It is very likely that the maximum concentrations in the alluvial aquifer at the Homestake site in 1980 were much larger than the uranium concentrations of 1.16 to 1.26 mg/L posted on Figure 51 for wells directly south of the main tailings disposal cell.

Figure 52 presents a map view of reported uranium concentrations for alluvial aquifer wells in the Grants-Bluewater Valley in 1996–1997. This figure was prepared by combining posted and contoured uranium concentrations from relevant annual GRP reports with concentrations measured at Bluewater site wells during the same time period. Comparison of uranium concentrations in this figure with the uranium concentrations from the 1980–1981 period (Figure 51) reveals that uranium levels in the alluvial aquifer at the Homestake site have indeed been much larger than 1.26 mg/L in past years, and in some cases greater than 50 mg/L. It is difficult to tell from comparing the two maps whether uranium concentrations at the Bluewater site changed significantly between 1980 and 1997. Though concentrations decreased at wells C(M), T(M), U(M), and E(M), apparent increases in concentration were seen at wells B(M) and X(M).

Figure 52 shows two lobes of uranium contamination extending to the south toward Milan, with the uranium concentration in one of the lobes approaching 1 mg/L. The west lobe represents the combined uranium input from the alluvial aquifer plume originating at the Bluewater site and the Homestake plume extending westward from the large tailings disposal cell. It is impossible to tell from this figure whether the location of the leading edge of each of the contaminant lobes, as defined by a concentration of 0.01 mg/L, may have extended as far south as the Milan municipal wells in years preceding 1996–1997. However, this possibility cannot be entirely dismissed given the assessment of uranium concentrations and uranium isotope ratios for Milan Wells B-35 and B-50 in Section 7.2.3.

The potential for uranium contamination in the alluvial aquifer extending as far south as some of the Milan municipal wells at some time in the past can be further assessed by examining the potentiometric surface for the alluvial aquifer in fall 2012 (see Figure 21 and Figure 22), which indicates that a hydraulic sink has occurred in the aquifer during recent years in an area just to the east and northeast of Toltec. This finding, combined with the observation in this study that the alluvial aquifer directly overlies the San Andres Limestone in an area extending from about a mile north of Toltec to Grants (see Figures 18, 19, and 52), suggests that downward migration of groundwater from the alluvial aquifer to the San Andres aquifer in response to pumping at Milan Wells B-35 and B-50 is feasible. This is especially true given that the groundwater sink has been observed near the southern tip of the west lobe of uranium contamination formed by merging of uranium plumes from the Bluewater and Homestake sites (Figure 52).

Figure 53 presents a map view of uranium concentrations in the alluvial aquifer in 2012–2013. Comparison of this figure with the 1996–1998 sampling results in Figure 52 indicates a sharp decline in uranium concentration near the large tailings disposal cell at the Homestake site over the 16-year span separating the two periods. In addition, an overall decline in uranium concentrations is observed between 1996–1998 and 2012–2013. However, it is difficult to tell from comparing the two maps whether uranium concentrations in the alluvial aquifer at the Bluewater site decreased between the two periods.

Preparation of the uranium plume maps in Figures 52 and 53 revealed the importance of including concentration data from offsite locations in developing the conceptual model for the Bluewater site. Identification of the downgradient extent of the uranium plumes in 1996–1997 and 2012–2013 would not have been possible without using uranium-concentration data from downgradient wells and including plume maps prepared for annual reports on the GRP. This finding suggests that it may be advisable to include offsite data when evaluating the conceptual models for other LM sites.

8.2.2 Uranium Concentration Histories

Figure 54 shows the temporal plot of uranium concentrations at alluvial aquifer wells T(M), U(M), X(M), 21(M), and 22(M) between 1984 and 2013. Though the concentrations fluctuate considerably with time, the data, for the most part, suggest that uranium levels in the alluvial aquifer at onsite locations have either remained stable for the past 30 years or have been slowly declining. With the exception of well T(M), the concentration data do not suggest that a pulse of uranium contamination has been migrating from contaminant source areas beneath the Bluewater site.

Prior to 2000, uranium concentrations at well T(M) were relatively steady, remaining within a range of 0.1 to 0.3 mg/L (Figure 54). This was followed by a steady increase in uranium concentration at the well between 2000 and 2010, suggesting that a pulse of uranium contaminant mass had affected the alluvial aquifer. However, analysis of water chemistry data at T(M) and inspection of water levels in the well in recent years indicate that the water being sampled at this location was increasingly from the Chinle Formation and was not representative of the alluvium.

The Savannah River National Laboratory (SRNL 2014) studied the aqueous-phase chemistry of groundwater at well T(M) and concluded that the increase in uranium concentration between 2000 and 2010 was unlikely to have been caused by a pulse release of tailings fluids. SRNL notes that, beginning in the late 1990s, the water table elevation in the alluvial aquifer steadily decreased, and that the water level at well T(M) dropped to the bottom of the 5 ft screened interval in the well in 2008. The bottom of the screen is at the contact between the alluvial aquifer and the Chinle Formation, and the open borehole beneath the screen extends another 9 ft into the Chinle. Thus, virtually all of the water sampled from the well from 2008 to 2012 was from the upper 9 ft of the Chinle, which apparently contained large uranium concentrations.

SRNL (2014) states that the cause of the large uranium concentration in the uppermost part of the Chinle is unclear, but the study provides a possible hypothesis for the responsible chemical processes. The hypothesis is based on assumed diffusion of uranium-impacted groundwater from the alluvial aquifer to the uppermost layers of Chinle Formation over a 30-year period and concomitant interaction of the uranium with minerals in the formation. The diffusion caused either ion exchange of dissolved uranium for other constituents in Chinle Formation rock or precipitation of U(IV) minerals under chemically reducing conditions. Observations made by SRNL supporting the latter mechanism (redox-driven precipitation) include color changes in the uppermost Chinle Formation rock that are considered representative of reducing conditions. In following years, slow remobilization of the uranium in the Chinle Formation rock, perhaps due to the onset of oxidized conditions, led to back diffusion of the contaminant into the formation's pore water. The relatively high concentrations of uranium detected at well T(M) between 2008

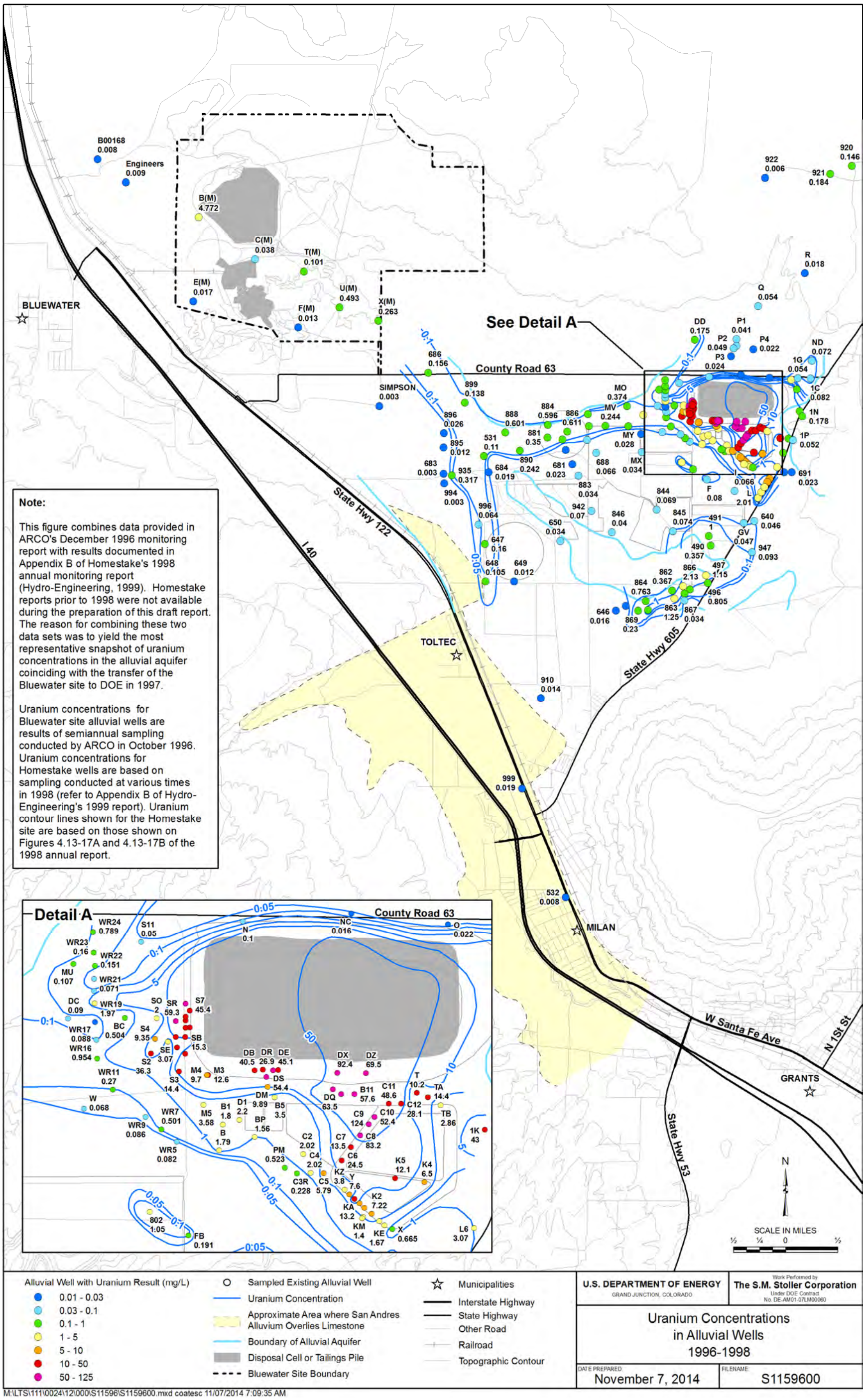

Figure 52. Regional Uranium Concentrations in the Alluvial Aquifer in 1996–1997

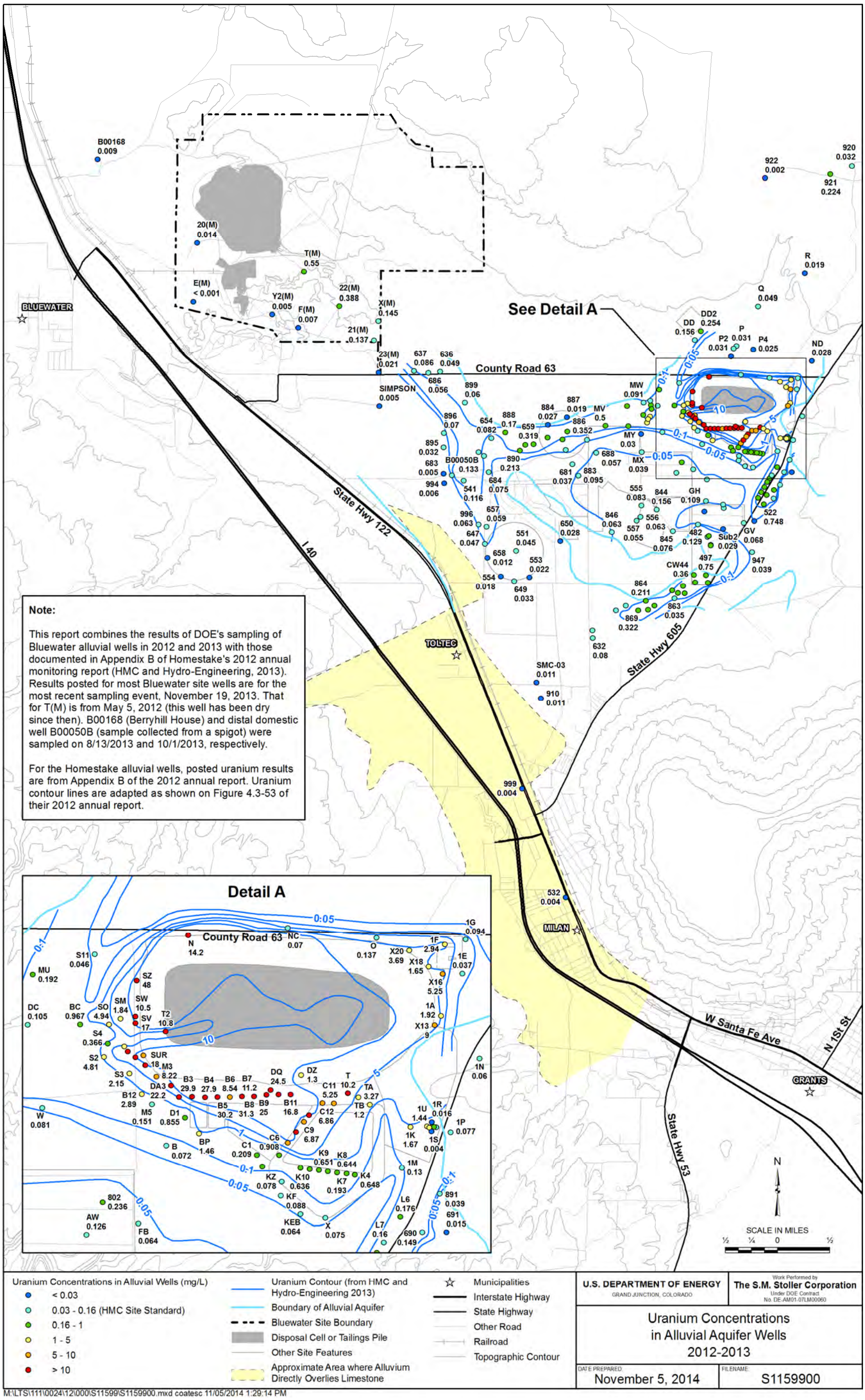

Figure 53. Regional Uranium Concentrations in the Alluvial Aquifer in 2012–2013

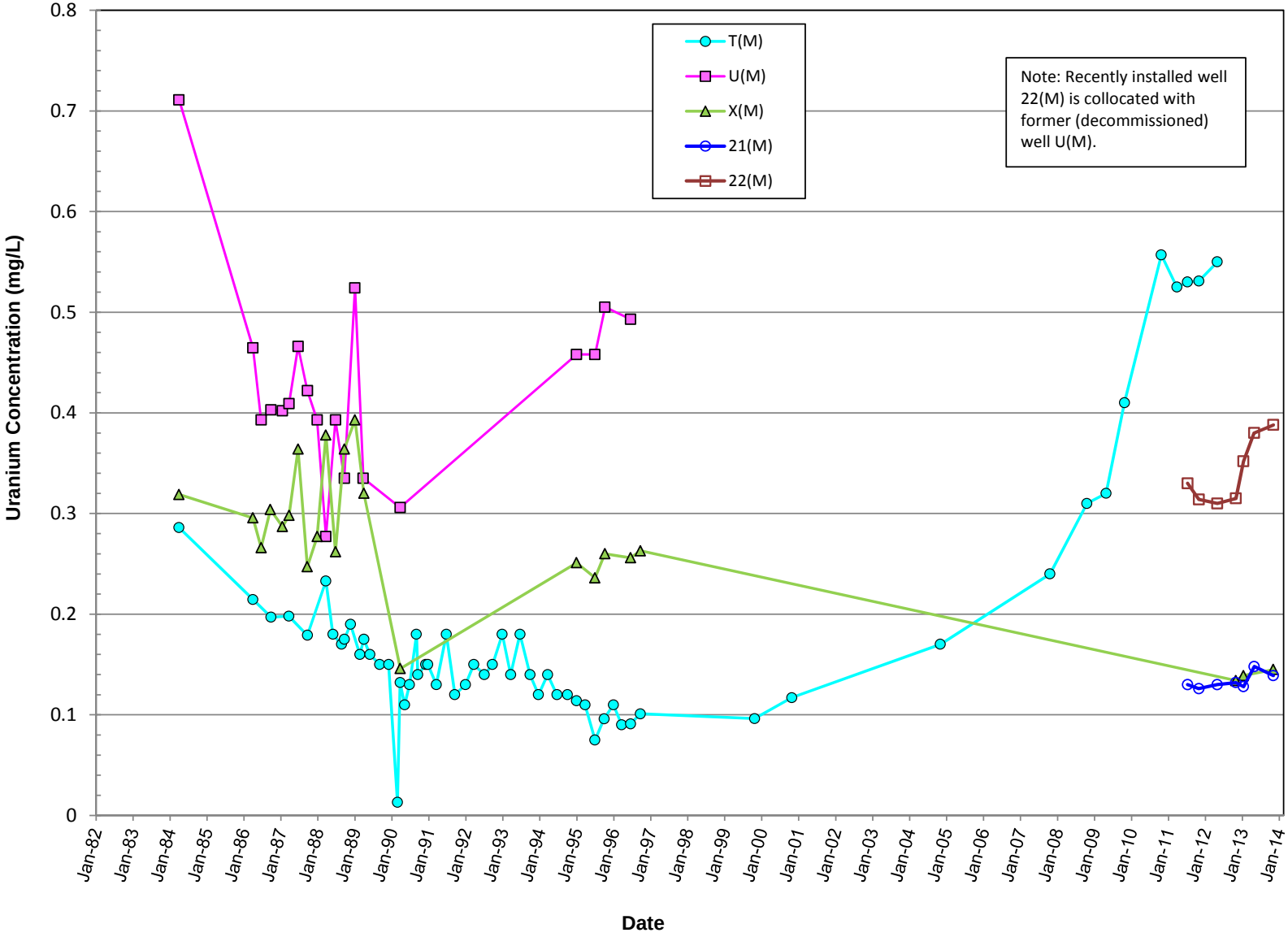

Figure 54. Temporal Plot of Uranium Concentrations in Alluvial Aquifer Wells at the Bluewater Site

and 2012 are attributed to the back diffusion (SRNL 2014). The combination of steadily decreasing water levels at T(M) since the late 1990s, increasing proportions of Chinle Formation water in samples collected from the well beginning in 2000, and the findings and hypothesis by SRNL (2014) suggests that increasing uranium concentrations in well T(M) between 2000 and 2010 were not caused by a pulse of uranium contamination migrating southeastward in the alluvial aquifer. Instead, the uranium increases are attributed to increasing amounts of Chinle pore water in samples collected at the well.

Critical assessment of the uranium concentration data at well T(M), as presented above, provides a possible lesson regarding the annual reporting that is performed for many LM sites. Specifically, it may be helpful to further investigate potential causes of increasing and decreasing concentration trends at LM sites, since simple reporting of the concentrations by themselves may fail to capture difficulties with the wells included in the annual monitoring.

8.3 Uranium Contamination in the San Andres Aquifer

8.3.1 Uranium Plume Maps

Figure 55 presents a map of uranium concentrations measured in 1980 and 1981 at several San Andres aquifer wells in the Grants-Bluewater Valley as part of the Hydro-Search (1981a) assessment of regional hydrogeology and water chemistry. As shown in this figure, the largest uranium concentrations at the time were observed at Bluewater site wells on the east side of the main tailings impoundment, and somewhat elevated concentrations were also observed at the production wells, Anaconda #2 and Anaconda #5.

Of some interest was the relatively high uranium concentration of 0.05 mg/L at well 928 (Roundy Sec. 23 in Figure 55), about 2.5 mi hydraulically downgradient of the Bluewater site and 0.5 mile north of the large tailings disposal cell at the Homestake site. Hydro-Search (1981a) made no attempt to distinguish this latter concentration in its regional assessment, perhaps because the regulatory standard for uranium in 1981 was 5 mg/L, a value that was an order of magnitude higher than the observed concentration at well 928 at the time. It is also possible that the well 928 concentration was considered to be unrelated to the uranium plume at the Bluewater site because Hydro-Search (1977) had estimated that the velocity of groundwater in the San Andres aquifer east of the main tailings impoundment was limited to about 400 ft/yr. If the much higher velocities derived from models by Dames & Moore (1986a) (see Section 4.3.3.2) had been taken into account, arrival of uranium contamination at well 928 from the Bluewater site as of 1980 would have been considered plausible. Such a conclusion would have been supported by the map of ambient flow directions in the San Andres aquifer presented in Figure 24, which indicates that groundwater from various parts of the Bluewater site migrates to multiple locations north and south of the large tailings disposal cell at the Homestake site.

To detect possible changes in the areal extent of uranium contamination since 1980, maps of measured uranium concentrations in the San Andres aquifer were also prepared for three additional periods. Figure 56 through Figure 58 show the maps, which represent the time periods 1996–1997, 2008, and 2012–2013, respectively. As each figure illustrates, the uranium concentrations at Bluewater site wells and areas east of the site were relatively close to concentrations shown for 1980–1981. Similarly, the range of uranium levels (0.03 to 0.07 mg/L) measured in well 928 at the Homestake site was close to the concentration of 0.05 mg/L

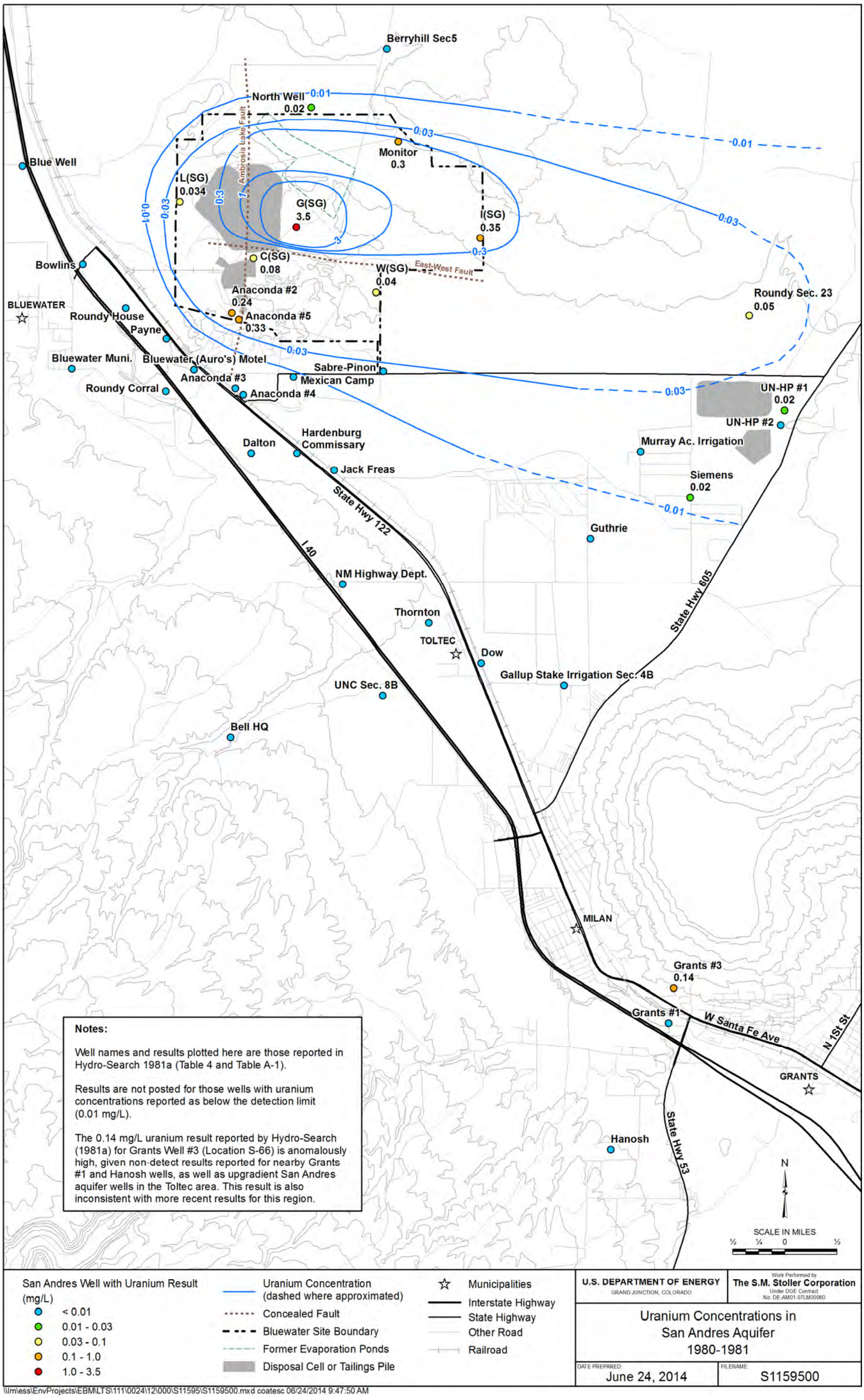

Figure 55. Regional Uranium Concentrations in the San Andres Aquifer in 1980–1981

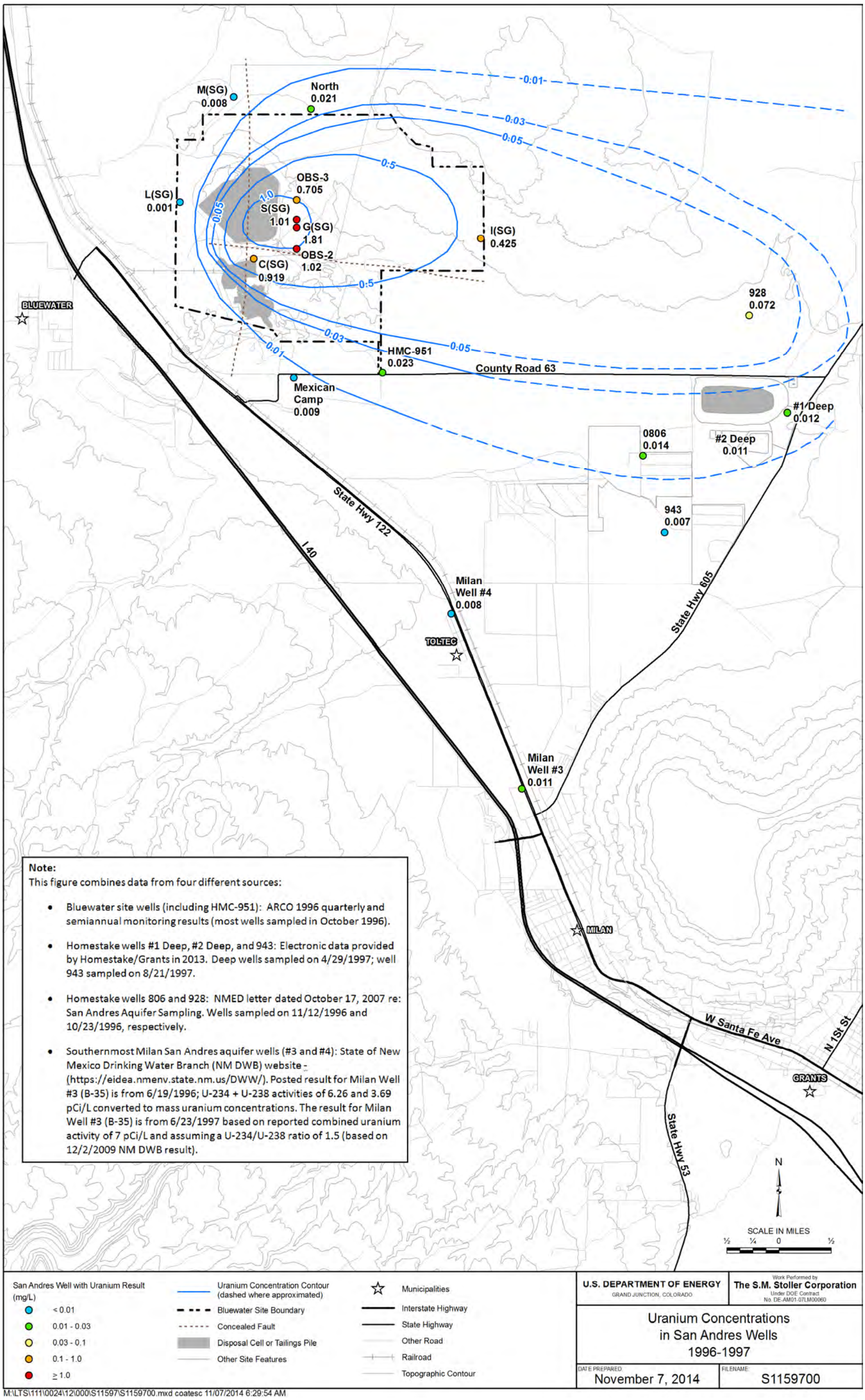

Figure 56. Regional Uranium Concentrations in the San Andres Aquifer in 1996–1997

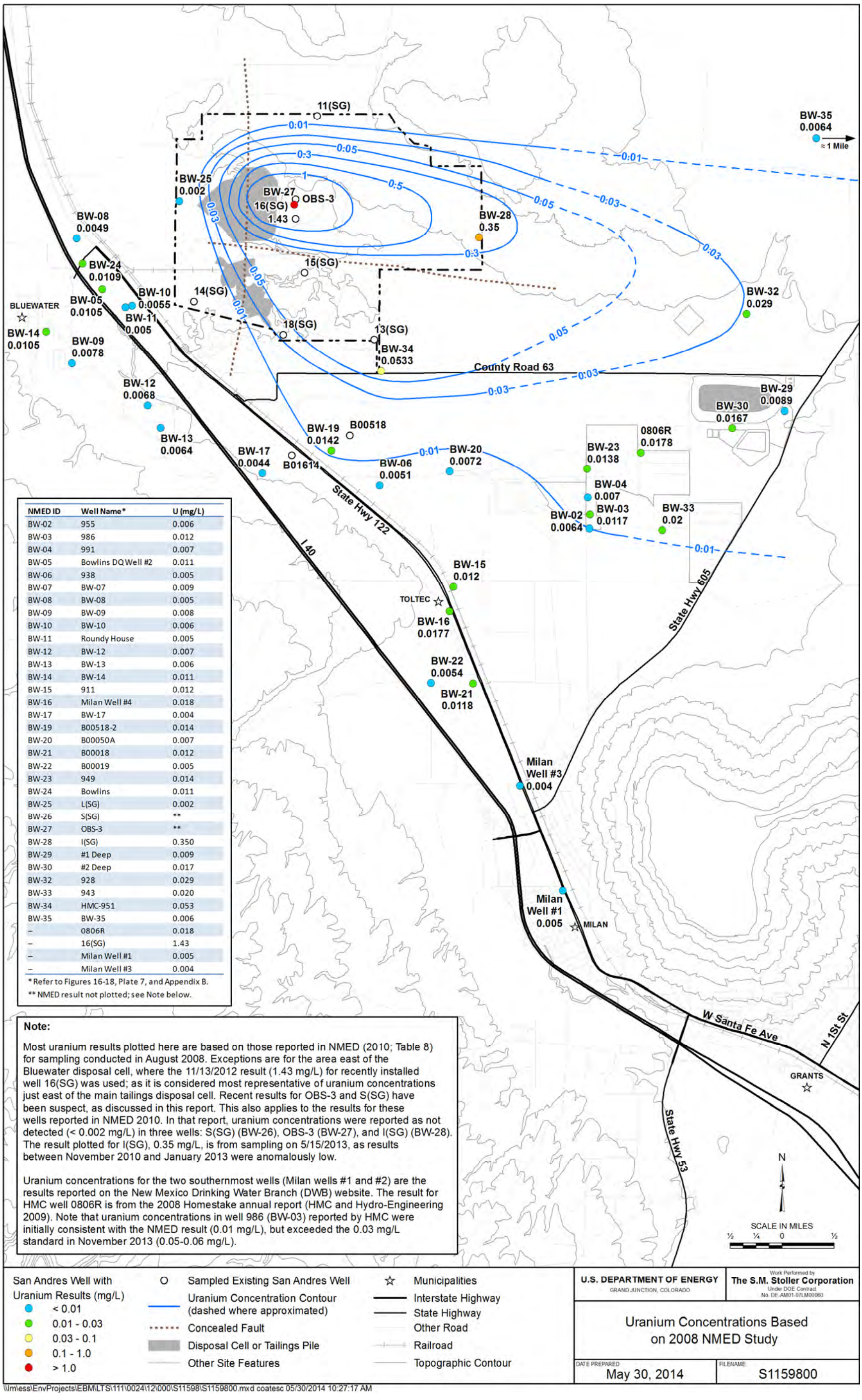

NMED ID	Well Name*	U (mg/L)
BW-02	955	0.006
BW-03	986	0.012
BW-04	991	0.007
BW-05	Bowlins DQ Well #2	0.011
BW-06	938	0.005
BW-07	BW-07	0.009
BW-08	BW-08	0.005
BW-09	BW-09	0.008
BW-10	BW-10	0.006
BW-11	Roundy House	0.005
BW-12	BW-12	0.007
BW-13	BW-13	0.006
BW-14	BW-14	0.011
BW-15	911	0.012
BW-16	Milan Well #4	0.018
BW-17	BW-17	0.004
BW-19	B00518-2	0.014
BW-20	B00050A	0.007
BW-21	B00018	0.012
BW-22	B00019	0.005
BW-23	949	0.014
BW-24	Bowlins	0.011
BW-25	L(SG)	0.002
BW-26	S(SG)	**
BW-27	OBS-3	**
BW-28	I(SG)	0.350
BW-29	#1 Deep	0.009
BW-30	#2 Deep	0.017
BW-32	928	0.029
BW-33	943	0.020
BW-34	HMC-951	0.053
BW-35	BW-35	0.006
–	0806R	0.018
–	16(SG)	1.43
–	Milan Well #1	0.005
–	Milan Well #3	0.004

* Refer to Figures 16-18, Plate 7, and Appendix B.
** NMED result not plotted; see Note below.

Note:

Most uranium results plotted here are based on those reported in NMED (2010; Table 8) for sampling conducted in August 2008. Exceptions are for the area east of the Bluewater disposal cell, where the 11/13/2012 result (1.43 mg/L) for recently installed well 16(SG) was used; as it is considered most representative of uranium concentrations just east of the main tailings disposal cell. Recent results for OBS-3 and S(SG) have been suspect, as discussed in this report. This also applies to the results for these wells reported in NMED 2010. In that report, uranium concentrations were reported as not detected (< 0.002 mg/L) in three wells: S(SG) (BW-26), OBS-3 (BW-27), and I(SG) (BW-28). The result plotted for I(SG), 0.35 mg/L, is from sampling on 5/15/2013, as results between November 2010 and January 2013 were anomalously low.

Uranium concentrations for the two southernmost wells (Milan wells #1 and #2) are the results reported on the New Mexico Drinking Water Branch (DWB) website. The result for HMC well 0806R is from the 2008 Homestake annual report (HMC and Hydro-Engineering 2009). Note that uranium concentrations in well 986 (BW-03) reported by HMC were initially consistent with the NMED result (0.01 mg/L), but exceeded the 0.03 mg/L standard in November 2013 (0.05-0.06 mg/L).

San Andres Well with Uranium Results (mg/L)
- < 0.01
- 0.01 - 0.03
- 0.03 - 0.1
- 0.1 - 1.0
- > 1.0

Sampled Existing San Andres Well
Uranium Concentration Contour (dashed where approximated)
Concealed Fault
Disposal Cell or Tailings Pile
Other Site Features

Municipalities
Interstate Highway
State Highway
Other Road
Railroad
Topographic Contour

U.S. DEPARTMENT OF ENERGY
GRAND JUNCTION, COLORADO

Work Performed by
The S.M. Stoller Corporation
Under DOE Contract No. DE-AM01-07LM00060

Uranium Concentrations Based on 2008 NMED Study

DATE PREPARED: May 30, 2014
FILENAME: S1159800

\\lm\ess\EnvProjects\EBM\LTS\111\0024\12\000\S11598\S1159800.mxd coatesc 05/30/2014 10:27:17 AM

Figure 57. Regional Uranium Concentrations in the San Andres Aquifer in 2008

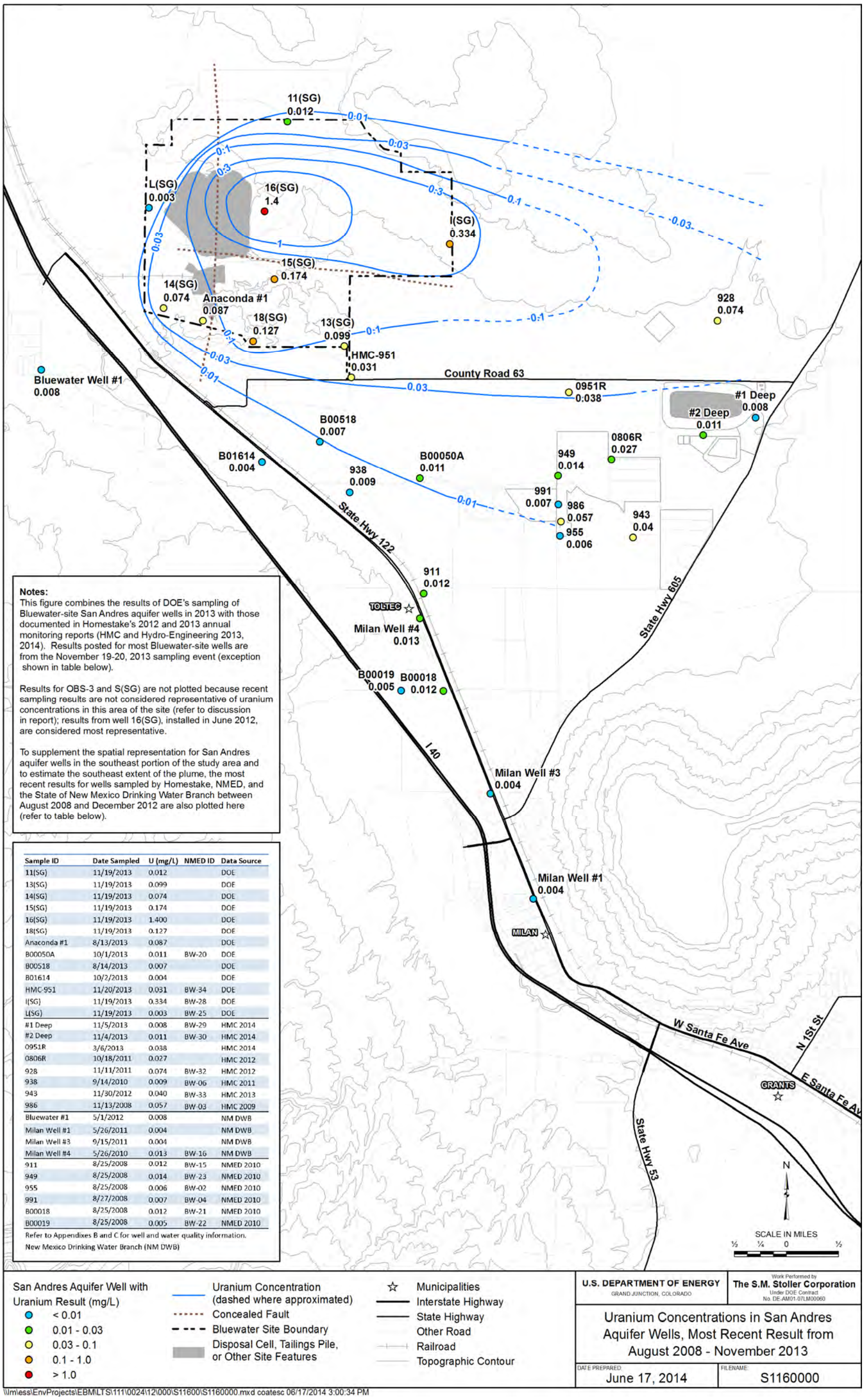

Notes:
This figure combines the results of DOE's sampling of Bluewater-site San Andres aquifer wells in 2013 with those documented in Homestake's 2012 and 2013 annual monitoring reports (HMC and Hydro-Engineering 2013, 2014). Results posted for most Bluewater-site wells are from the November 19-20, 2013 sampling event (exception shown in table below).

Results for OBS-3 and S(SG) are not plotted because recent sampling results are not considered representative of uranium concentrations in this area of the site (refer to discussion in report); results from well 16(SG), installed in June 2012, are considered most representative.

To supplement the spatial representation for San Andres aquifer wells in the southeast portion of the study area and to estimate the southeast extent of the plume, the most recent results for wells sampled by Homestake, NMED, and the State of New Mexico Drinking Water Branch between August 2008 and December 2012 are also plotted here (refer to table below).

Sample ID	Date Sampled	U (mg/L)	NMED ID	Data Source
11(SG)	11/19/2013	0.012		DOE
13(SG)	11/19/2013	0.099		DOE
14(SG)	11/19/2013	0.074		DOE
15(SG)	11/19/2013	0.174		DOE
16(SG)	11/19/2013	1.400		DOE
18(SG)	11/19/2013	0.127		DOE
Anaconda #1	8/13/2013	0.087		DOE
B00050A	10/1/2013	0.011	BW-20	DOE
B00518	8/14/2013	0.007		DOE
B01614	10/2/2013	0.004		DOE
HMC-951	11/20/2013	0.031	BW-34	DOE
I(SG)	11/19/2013	0.334	BW-28	DOE
L(SG)	11/19/2013	0.003	BW-25	DOE
#1 Deep	11/5/2013	0.008	BW-29	HMC 2014
#2 Deep	11/4/2013	0.011	BW-30	HMC 2014
0951R	3/6/2013	0.038		HMC 2014
0806R	10/18/2011	0.027		HMC 2012
928	11/11/2011	0.074	BW-32	HMC 2012
938	9/14/2010	0.009	BW-06	HMC 2011
943	11/30/2012	0.040	BW-33	HMC 2013
986	11/13/2008	0.057	BW-03	HMC 2009
Bluewater #1	5/1/2012	0.008		NM DWB
Milan Well #1	5/26/2011	0.004		NM DWB
Milan Well #3	9/15/2011	0.004		NM DWB
Milan Well #4	5/26/2010	0.013	BW-16	NM DWB
911	8/25/2008	0.012	BW-15	NMED 2010
949	8/25/2008	0.014	BW-23	NMED 2010
955	8/25/2008	0.006	BW-02	NMED 2010
991	8/27/2008	0.007	BW-04	NMED 2010
B00018	8/25/2008	0.012	BW-21	NMED 2010
B00019	8/25/2008	0.005	BW-22	NMED 2010

Refer to Appendixes B and C for well and water quality information.
New Mexico Drinking Water Branch (NM DWB)

Figure 58. Regional Uranium Concentrations in the San Andres Aquifer for the Period 2008–2013

observed at this location in 1980–1981. Moreover, uranium concentrations ranging from 0.007 to 0.05 mg/L were detected at additional wells in the San Andres aquifer (Figure 56 through Figure 58) in the vicinity of the Homestake site, supporting the possibility that dissolved uranium from the Bluewater site had migrated as far as the Homestake site as of 1980. With this possibility, it could be hypothesized that uranium concentrations measured at Homestake site wells screened in the San Andres aquifer after the mid-1990s were representative of steady-state concentrations that form upgradient of a contaminant plume's leading edge. Such a hypothesis implies that the leading edge of the Bluewater site uranium plume, as defined by a concentration of 1 mg/L, has been, for many years, east and east-southeast of the Homestake site, in the direction of areas north of Grants.

In contrast to the above-given finding that the dissolved uranium originating in San Andres aquifer groundwater at the Bluewater site migrated to the Homestake site as early as 1980, alternative arguments have occasionally been made to explain the presence of slightly elevated uranium levels in the aquifer at the Homestake site. In recent years, EPA has posited that uranium at bedrock aquifer wells in the vicinity of the Homestake site are the result of unintended effects of the groundwater remedy at the GRP. EPA (2011) implies that HMC has created a steep downward gradient between local San Mateo Creek alluvium and the underlying San Andres aquifer, which causes uranium contamination to migrate downward to the deeper aquifer along fault zones present at the Homestake site.

As with the alluvial aquifer, preparation of the uranium plume maps in Figure 55 through Figure 58 revealed the importance of including offsite data in this study. This exercise also suggests that it may be helpful to consider information from nearby sites when developing conceptual models for other LM sites. Without such additional information, the effects of historical contaminant processes at sites may go unnoticed.

8.3.2 Uranium Concentration Histories

Prior to development of multiyear, temporal plots of uranium concentration at wells in the study area, the quality of the concentration data was reviewed to identify measured uranium concentrations that might be considered erroneous or not fully representative of the San Andres aquifer. The review indicated that uranium concentrations from Bluewater site wells OBS-3 and S(SG) in samples collected after 1996 were likely to misrepresent uranium contamination in areas just east of the main tailings disposal cell. Specifically, in 1997, samples from the two wells began to yield uranium concentrations that were anomalously low in comparison to concentrations from samples collected over the previous 13 years. This was not known at the time, however, because DOE did not have possession of historical monitoring data collected by ARCO. Because of this, the lower post-1996 concentrations at the two wells were considered signs that uranium contamination in the San Andres aquifer was attenuating in areas downgradient of the main tailings disposal cell. However, in-well video logs of the two wells in 2011 revealed that well screens in the two wells had been severely compromised by corrosion products. Subsequent data collected from the two wells indicated that the corrosion products were likely adsorbing much of the aqueous-phase uranium that had entered the casings of the wells. This observation, combined with the fact that low-flow sampling techniques had largely been used to monitor uranium in the wells since 2004, indicated that measured uranium concentrations at the two locations between 1997 and 2011 could not be trusted to represent contaminant levels in the surrounding aquifer. The effects of the well corrosion on uranium

concentrations in samples collected from wells S(SG) and OBS-3 and corresponding uranium isotope activity ratios (ARs) were discussed in Section 7.2.3.

In response to the discovery of groundwater sampling issues stemming from corrosion in wells OBS-3 and S(SG), new well 16(SG) was installed in the San Andres aquifer just east of the main tailings disposal cell in summer 2012. Uranium concentrations measured in water samples collected from the new well since its installation have generally fallen in the range of concentrations seen at wells OBS-3 and S(SG) during the early 1990s (1.2 to 1.7 mg/L), suggesting that the aquifer east of the main tailings disposal cell continues to be impacted by steady mass loading of uranium from a mineralized zone beneath the cell.

Concentrations of uranium and other groundwater constituents monitored at well I(SG) have also been called into question. Well I(SG) has solid steel casing to a depth within the upper portion of the San Andres Limestone and then is uncased open borehole through the remainder of the San Andres Limestone and the Glorieta Sandstone. ARCO last sampled the well in 1996, using a high-flow casing purge method, and observed a uranium concentration of 0.42 mg/L; this result was consistent with results since 1984. DOE did not begin monitoring the well until 2008 because monitoring the well was not required by the LTSP; monitoring was initiated to support NMED's regional groundwater investigation. DOE collected samples from within the casing just above the open borehole using the low-flow method. Low uranium levels in DOE's samples were thought to be caused by natural attenuation processes in the San Andres aquifer. However, specific conductivities and uranium concentrations measured over the full water column in the well in 2013 revealed that contaminant levels are stratified within the aquifer, with higher conductivities and uranium concentrations observed at depth in the well. This finding indicated that the use of low-flow sampling techniques to collect water from the cased portion of the well resulted in uranium concentrations that were distinctly lower than those within the uncased portion. Sampling at the well since then, using techniques designed to capture water representative of groundwater in the limestone and sandstone surrounding the well, has yielded uranium concentrations only slightly lower than results observed by ARCO.

Upon completing the above-discussed review of sampling challenges at San Andres aquifer wells on the Bluewater site, a temporal plot of historical uranium concentrations at wells OBS-3, S(SG), 16(SG), I(SG), and 13(SG) was prepared (Figure 59). Because of the corrosion problems at wells OBS-3 and S(SG), and contaminant stratification issues in well I(SG), concentration data from 1997 through 2012 at these wells were omitted from the graph. Despite this shortcoming, the available data do indicate that uranium concentrations in onsite San Andres aquifer wells are remaining relatively stable. This finding is supported by measured uranium concentrations at well 16(SG) (1.3 to 1.5 mg/L), the well that is now used to monitor contaminant concentrations just east of the main tailings disposal cell. In addition, measured concentrations at well I(SG) in 2013 (0.35 mg/L) are at the low end of the range of concentrations recorded for this well from 1984 to 1996 (0.35 to 0.65 mg/L). Though constituent concentration data have only been collected at well 13(SG) since late 2012, uranium at this well in the southeast corner of the site has maintained a relatively constant concentration of about 0.1 mg/L. Taken together, the data plotted in Figure 59 suggest that mass loading rates to the San Andres aquifer for uranium residing in the mineralized zone beneath the main tailings disposal cell have been relatively stable, and that relatively steady or slowly decreasing uranium concentrations at onsite wells are reflective of portions of the uranium plume upgradient of the plume's leading edge.

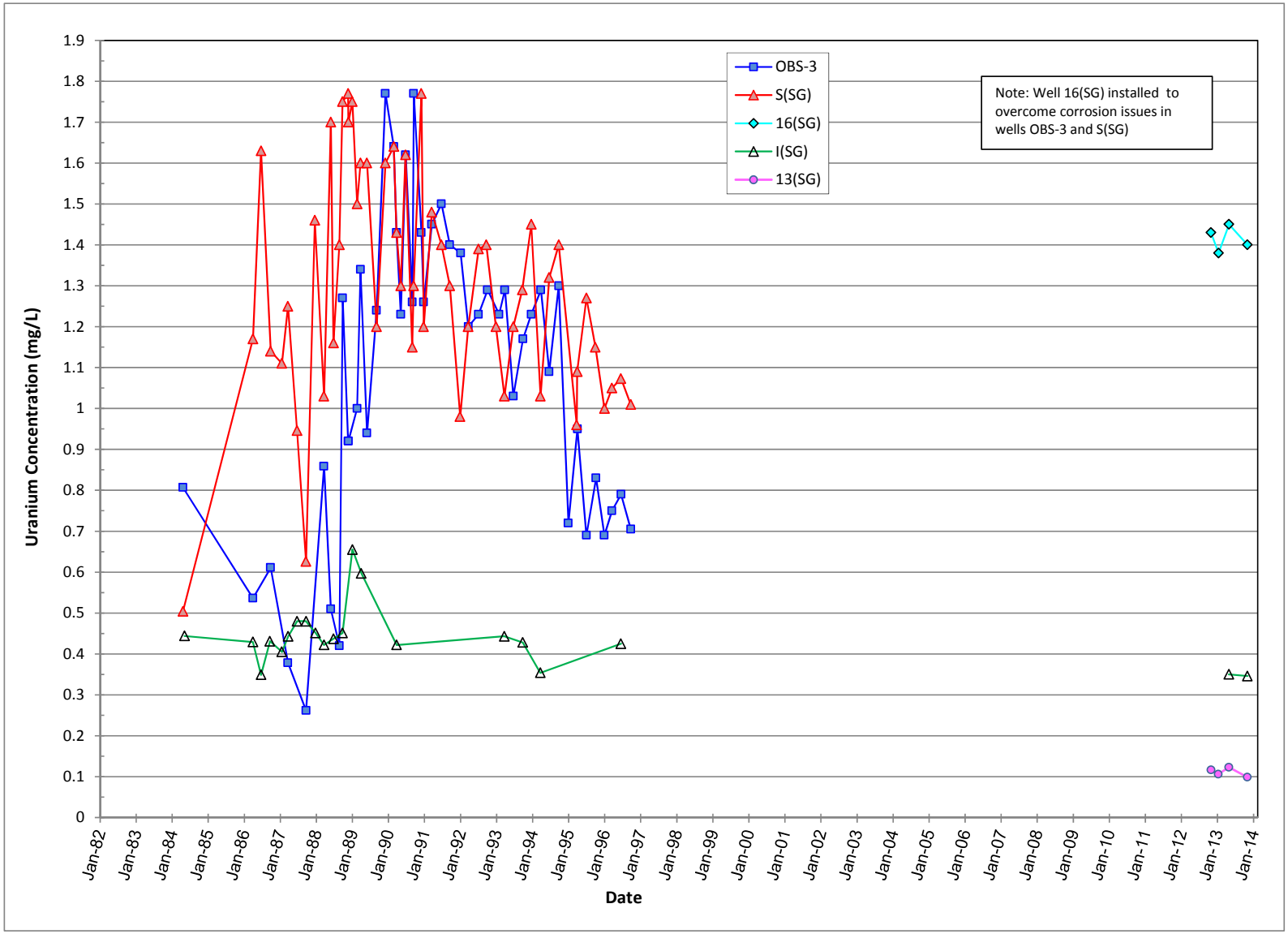

Figure 59. Temporal Plot of Uranium Concentrations in San Andres Aquifer Wells at the Bluewater Site

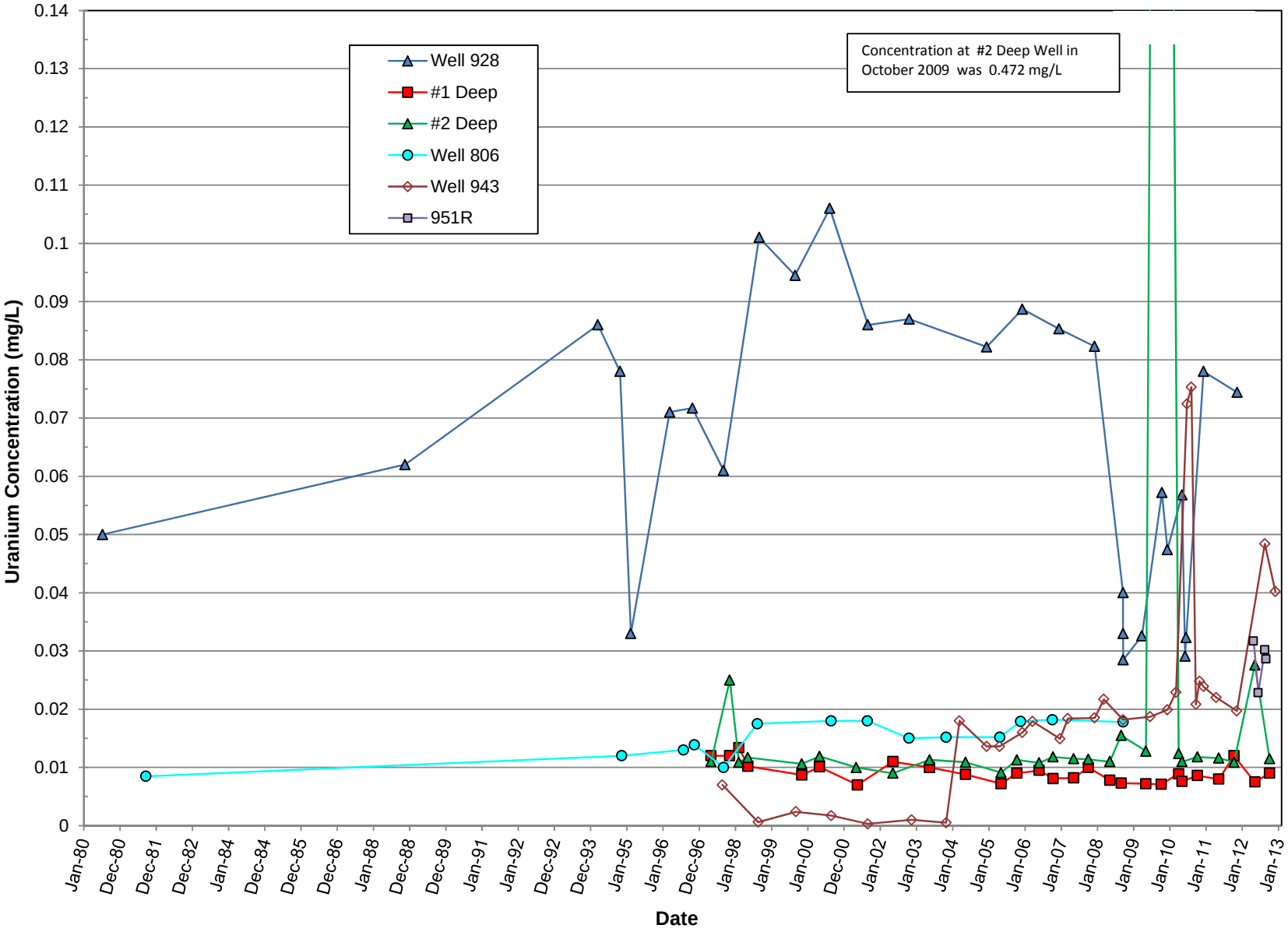

Figure 60. Temporal Plot of Uranium Concentrations in San Andres Aquifer Wells near the Homestake Site

To assess the history of uranium concentrations at wells screened in the San Andres aquifer near the Homestake site, a temporal plot of concentrations at Homestake well locations 928, #1 Deep Well, #2 Deep Well, well 806, well 943, and well 951R was prepared (Figure 60). This graph suggests that the uranium concentration at well 928 has fluctuated between 0.035 and 0.105 mg/L since 1980. In contrast, concentrations in #1 Deep Well have been steady at about 0.01 mg/L, and uranium levels in well 806 have also remained steady, between about 0.01 and 0.02 mg/L. Other than an anomalously high concentration of 0.47 mg/L in 2009, uranium levels at #2 Deep Well have stayed within a range of about 0.01 to 0.03 mg/L (Figure 60). Uranium concentrations in well 943 have occasionally increased as high as 0.07 mg/L in recent years. Collectively, the historical concentrations could be considered relatively stable and representative of attenuated uranium contamination in portions of a plume that originates at the Bluewater site and extends some distance east of the Homestake site. With such a conceptualization, the leading edge of the uranium plume, as defined by a concentration of 0.01 mg/L is expected to be hydraulically downgradient of the Homestake site, in the direction of areas north of Grants.

The difficulties mentioned above concerning obstacles to acquiring contaminant concentrations representative of groundwater conditions in the San Andres aquifer serve as lessons that can potentially be applied to the monitoring of wells at other LM sites. Specifically, it important to examine all historical monitoring data for a site before LM takes responsibility for the long-term surveillance activities at the site. Periodic inspection of the variation in contaminant concentrations with depth in each monitoring well could also be beneficial, as would occasional video logs of the wells. It would also be helpful to compare the results of low-flow sampling with those from well purge sampling to ensure that the most representative concentration data are being collected. Finally, occasional critical assessments of the temporal concentration histories at individual wells, as discussed above, would help confirm the validity of data presented in annual monitoring reports.

8.3.3 Uranium Concentrations at Municipal Wells

Though the uranium plume maps shown in Figure 55 through Figure 58 indicate that uranium contamination in the San Andres aquifer has migrated eastward from the Bluewater site to the Homestake site, none of the maps imply that uranium has migrated west-southwest to Bluewater Village, or directly within the San Andres aquifer to Milan. However, Section 8.2.1 discussed the possibility that uranium-contaminated alluvial groundwater had migrated to an area near Toltec and was subsequently transported downward to parts of the aquifer tapped by Milan Well #4. To assess whether uranium contamination has affected groundwater withdrawn by the municipal wells, this study examined the full suite of historical uranium concentrations measured at drinking-water supply wells in the Grants-Bluewater Valley. Figure 61 illustrates these data, as published in databases maintained by the New Mexico Drinking Water Bureau.

As Figure 61 shows, uranium concentration data are available for community water-supply wells from various samples collected between 1997 and 2011. None of the posted concentrations exceed the uranium MCL of 0.03 mg/L, and most of the measured concentrations are less than 0.01 mg/L. The few cases in which the uranium concentration exceeds 0.01 mg/L are for samples collected from Milan Well B-50 (Milan Well #4) and Milan Well B-35 (Milan Well #3) during the 1990s. In general, the results shown in Figure 61 suggest that uranium contamination has not

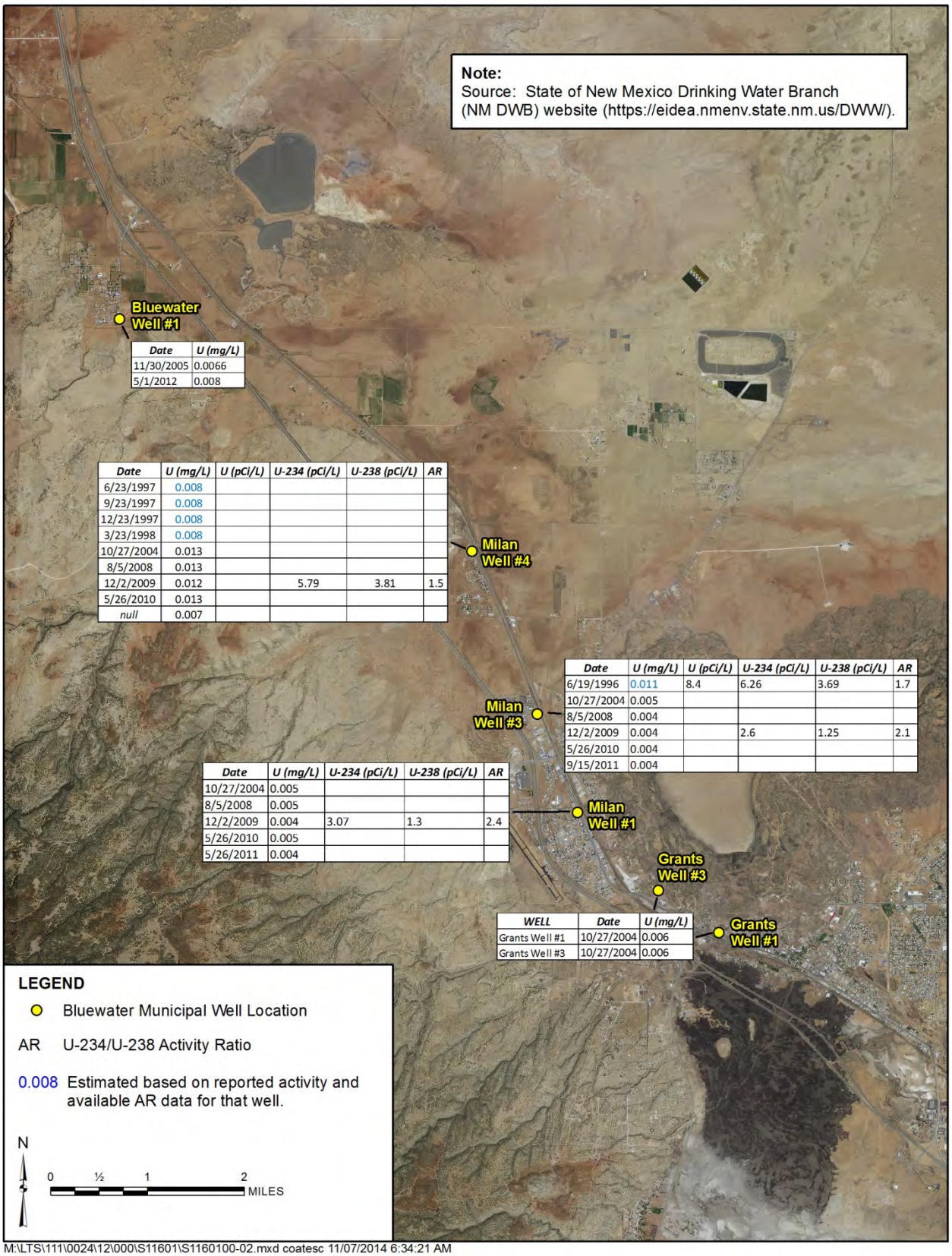

Figure 61. Uranium Concentration Data for Municipal Wells in the Grants-Bluewater Valley

detrimentally affected municipal wells in the Grants-Bluewater Valley such that concentrations approaching the MCL of 0.03 are observed. However, it cannot be firmly concluded that uranium contamination originating in the alluvial aquifer has never reached groundwater that is pumped by one or more Milan municipal wells.

Figure 61 also lists the activity concentrations for the isotopes U-234 and U-238 at Milan Well #1, Milan Well #3, and Milan Well #4, which were addressed in Section 7.2.3. The corresponding AR values, also listed in Figure 61, are all greater than or equal to 1.5. The combination of these AR values with the full suite of uranium concentrations posted on the figure suggest that, if tailings-related uranium contamination reached any of the municipal wells at any time in the past, it was diluted by mixing with uncontaminated groundwater.

8.4 Uranium Transport Processes

The analyses and findings in this and preceding chapters suggest that multiple transport processes have affected uranium contamination in the alluvial and San Andres aquifers, as summarized in the following sections. Much of the following summary builds upon information presented in Appendix F, which comprises a general description of advective-dispersive transport phenomena in the subsurface. This appendix and the glossary in Appendix E provide a better understanding of the fate of uranium contamination originating in groundwater at the Bluewater site.

8.4.1 Advection

High groundwater velocities within secondary permeability features (fractures, solution channels, cavities) in the San Andres aquifer have historically facilitated and continue to promote rapid advection of uranium contamination originating at the Bluewater site (Section 4.3.3.2). Advective transport caused the uranium plume in the aquifer to migrate beyond the site's east boundary in less than 10 years. Moreover, this study concludes that the leading portion of the uranium plume had migrated as far as the Homestake site by 1980, more than 30 years ago. It is also likely that the plume in 1980 had migrated beyond the Homestake site, to the east-southeast in the direction of areas north of Grants (Section 8.3.1).

Though the average linear velocities associated with porous media flow of groundwater in the alluvial aquifer were generally lower than those attributed to secondary permeability features in the San Andres aquifer, they were nevertheless high enough to rapidly convey Bluewater site uranium contamination to offsite areas located southeast of the main tailings disposal cell. Consequently, the estimated travel times for alluvial aquifer groundwater between the site and downgradient areas of interest are relatively short. The travel-time estimates between the main tailings disposal cell and Toltec are generally on the order of 20 to 60 years (Section 4.3.3.2), providing sufficient time for uranium contamination mobilized in the alluvial aquifer in the mid-1950s to reach areas near Milan in recent years.

8.4.2 Dispersion

Relatively stable or slowly-decreasing uranium concentrations observed at onsite monitoring wells (Sections 8.2.2 and 8.3.2) suggest that a relatively continuous contaminant source at the Bluewater site is feeding uranium to plumes in the alluvial and San Andres aquifers. The mostly

stable uranium concentrations in the plumes attenuate with flow distance between the main tailings disposal cell and the east boundary of the site (Sections 8.2.1 and 8.3.1).

As discussed in Chapter 7, transverse dispersion has historically been considered the primary mechanism for attenuating onsite uranium concentrations in the San Andres aquifer with flow distance, and for the relatively stable concentrations observed in site wells (Section 7.1.1.3). The analyses conducted in this study also indicate that transverse dispersion is a significant contributor, if not the most important contributor, to contaminant attenuation with flow distance, and is the primary cause of the uranium plume stability. Though most of this dispersion is assumed to occur in areas lateral to the centerline of the plume in the San Andres aquifer, transverse vertical dispersion is also likely contributing to the uranium attenuation.

A uranium plume influenced by mechanical dispersion is unlikely to maintain a perfectly symmetrical shape. Rather, an irregularly shaped plume is considered more likely in the San Andres aquifer because of groundwater flow through fractures, solution-enlarged joints, solution channels, and cavities. As a consequence, non-contaminated zones within the so-called plume boundaries are possible. It is also possible that the uranium plume in the San Andres aquifer bifurcates in some locations along preferential flow paths, such that uranium migration takes place in relatively thin, isolated plumes as opposed to a single, spatially continuous and wide plume. If this is the case, the capacity of transverse dispersion to attenuate plume concentrations would be enhanced, given that there is more plume surface area along which dispersion can take place with a bifurcated plume than is available with a single connected plume.

Mechanical dispersion of contaminants in site- and regional-scale plumes is generally attributed to aquifer heterogeneity (Domenico and Schwartz 1998). However, it has also been shown that transient flow effects in aquifers can lead to a form of apparent dispersion. This is because transient flow phenomena often cause changes in ambient flow direction over time, which in turn increases lateral spreading of a plume (e.g., Goode and Konikow 2000, Cirpka and Attinger 2003) beyond the spreading that would occur without such transient effects. Though difficult to discern given limited information on uranium transport in the vicinity of the Bluewater site, it is possible that apparent dispersion has also been promoted by decreasing groundwater elevations in the San Andres aquifer over the past 15 years. This is particularly true given that major changes in regional groundwater levels can alter flow directions in fractured-bedrock and karst aquifers (e.g., Huntoon 1995). With this perspective, temporally variable hydraulic heads in the region have the potential to enhance attenuation of the uranium plume in the San Andres aquifer in areas east and east-southeast from the Bluewater site.

Transverse dispersion is potentially increased in fractures and solution channels in the San Andres Limestone because these secondary permeability features act as conduits that are capable of conveying water at very high velocities (see Section 4.3.3.2). If the velocities increase to the extent that turbulent flow, as opposed to laminar flow, takes place, the degree to which contaminated groundwater mixes with fresh water is enhanced. Though it is unlikely that turbulent flow occurs throughout most of the karst-limestone portions of the San Andres Limestone, turbulent flow could occur in areas of rapid, convergent groundwater flow surrounding large-production pumping wells in the San Andres aquifer, such as the San Andres aquifer wells used to support groundwater remediation at the GRP.

Transverse dispersion has also influenced, and likely continues to influence, contaminant transport in the alluvial aquifer at the Bluewater site. The observed decrease in uranium concentration in ancestral river alluvium with distance from the contaminant source is consistent with advective transport in a downstream direction that is modified by transverse dispersion. As in the case of the San Andres aquifer, transient flow phenomena in the alluvial aquifer have the potential to alter groundwater flow directions, thereby inducing apparent transverse dispersion and enhanced attenuation of uranium concentrations.

8.4.3 Plume Stability

The development of a uranium plume in the San Andres aquifer fed by a continuous source and characterized by relatively stable concentrations due solely to the effects of transverse dispersion may seem counterintuitive. However, as discussed in Appendix F and textbooks on contaminant transport (e.g., Domenico and Schwartz 1998), virtually steady conditions can result from transverse dispersion alone. As a plume evolves, transverse spreading of contaminant mass causes concentrations to progressively decrease with flow distance, eventually leading to contaminant levels at the plume front that are indistinguishable from the background concentration. In effect, enough time has elapsed and the plume has migrated sufficiently far downgradient that concentrations outside the zone of constant concentration (i.e., along the plume edges) are so low as to be considered inconsequential. At this later time, loss of contaminant mass along the plume's border, as defined by the background concentration, occurs at the same rate contaminant mass is being added to the aquifer from the plume source area.

Figure 62 illustrates conceptually how steady conditions gradually evolve in a plume that is supplied by a continuous source with concentration C_o and is affected by both longitudinal and transverse dispersion. This graph shows resulting concentration-versus-distance profiles along the centerline of the plume at six different times (t_1 through t_6), with each successive profile indicating that a larger portion of the plume has stabilized (i.e., reached a steady state). Steady concentrations first occur on the downstream edge of the source, and are observed upon the initial onset of contamination in the groundwater. As time progresses, the steady-state portion of the profile constantly expands in the downgradient direction. This process continues until time t_6, when all concentrations in the plume greater than the background concentration no longer change.

The graph in Figure 62 can be used to describe the evolution of the uranium plume in the San Andres aquifer that originates at the main tailings disposal cell on the Bluewater site and extends east-southeastward to the Homestake site and areas north of Grants. This is accomplished by assuming that location S_0 in the figure represents the east edge of the main tailings disposal cell, location S_s represents the east boundary of the Bluewater site, location S_h represents the Homestake site, and location S_b represents an area downgradient of the Homestake site. Under these assumptions, the concentration-versus-distance profiles indicate that steady-state concentrations are achieved between the plume source and the east boundary of the Bluewater site at time t_2, and the steady concentration at the site boundary is C_s. This in turn indicates that, at time t_2, the onsite portion of the plume has stabilized, and all plume areas downgradient of the site are in a transient state. Similarly, steady-state concentrations are observed in all areas of the plume upgradient of the Homestake site as of the later time t_4, with a stable concentration of C_h at this site. Figure 62 shows contaminant levels stabilizing at the background concentration C_b as of time t_5 at location S_b, which is downgradient of the Homestake site.

Current conditions within the uranium plume in the San Andres aquifer correlate with the concentration profile shown for time t_6. This curve indicates that concentrations downgradient of location S_b will remain less than the background concentration C_b, even though the plume front can continue to migrate downgradient of location S_b. This makes it difficult to distinguish uranium contamination, if any, in areas north of Grants from naturally derived uranium in the aquifer.

A background concentration was used here to demonstrate the progression of steady-state conditions during plume evolution in the San Andres aquifer because uranium levels above the regional background concentration (0.01 mg/L) are of greatest interest to this investigation. However, an alternative concentration, such as the New Mexico drinking water standard for uranium (0.030 mg/L) could just as easily be used to delineate the steady plume border. The conceptual model described in this report implies that relatively stable concentrations equal to the standard occur somewhere east of the Bluewater site and perhaps in the vicinity of the Homestake site.

The discussion above regarding plume stability is strictly theoretical in the sense that steady-state concentrations are rarely, if ever, observed in groundwater plumes. In real groundwater systems, fluctuations of measured concentration at each location in space are a natural consequence of hydrologic and transport processes and measurement error (see, for example, Figures 55, 60, and 61). Nonetheless, the concentrations at each point within a so-called stable plume tend to fluctuate around an average, representative value for that point, instead of showing an increasing or decreasing trend. These average concentrations are, in effect, representative of the steady concentrations that would be observed in a theoretical system.

The concentration profiles in Figure 62 for conditions along the plume centerline can be generated using a transient model of advective-dispersive transport that accounts for one-dimensional advection and three-dimensional dispersion. Any of several numerical models, such as those based on finite-difference or finite-element techniques, could be employed for this purpose, eventually producing an effectively stable plume. By using a more simplified approach, the plume evolution could be approximated with an analytical mathematical solution to the governing transport equation. Examples of applicable analytical models include those described in Leij and Bradford (1994), Falta et al. (2007), and Karanovic et al. (2007). Domenico (1987) used an analytical solution to the transient advection-dispersion equation to illustrate that the steady concentrations produced solely by transverse dispersion occur in areas some distance upgradient of the plume's advective front, which is defined as the product of average linear velocity and the time since the onset of contamination in the groundwater. The distance separating the downgradient extent of steady concentrations from the advective front is small in cases where the influence of longitudinal dispersion is relatively minor in comparison to the influence of advection (Domenico 1987).

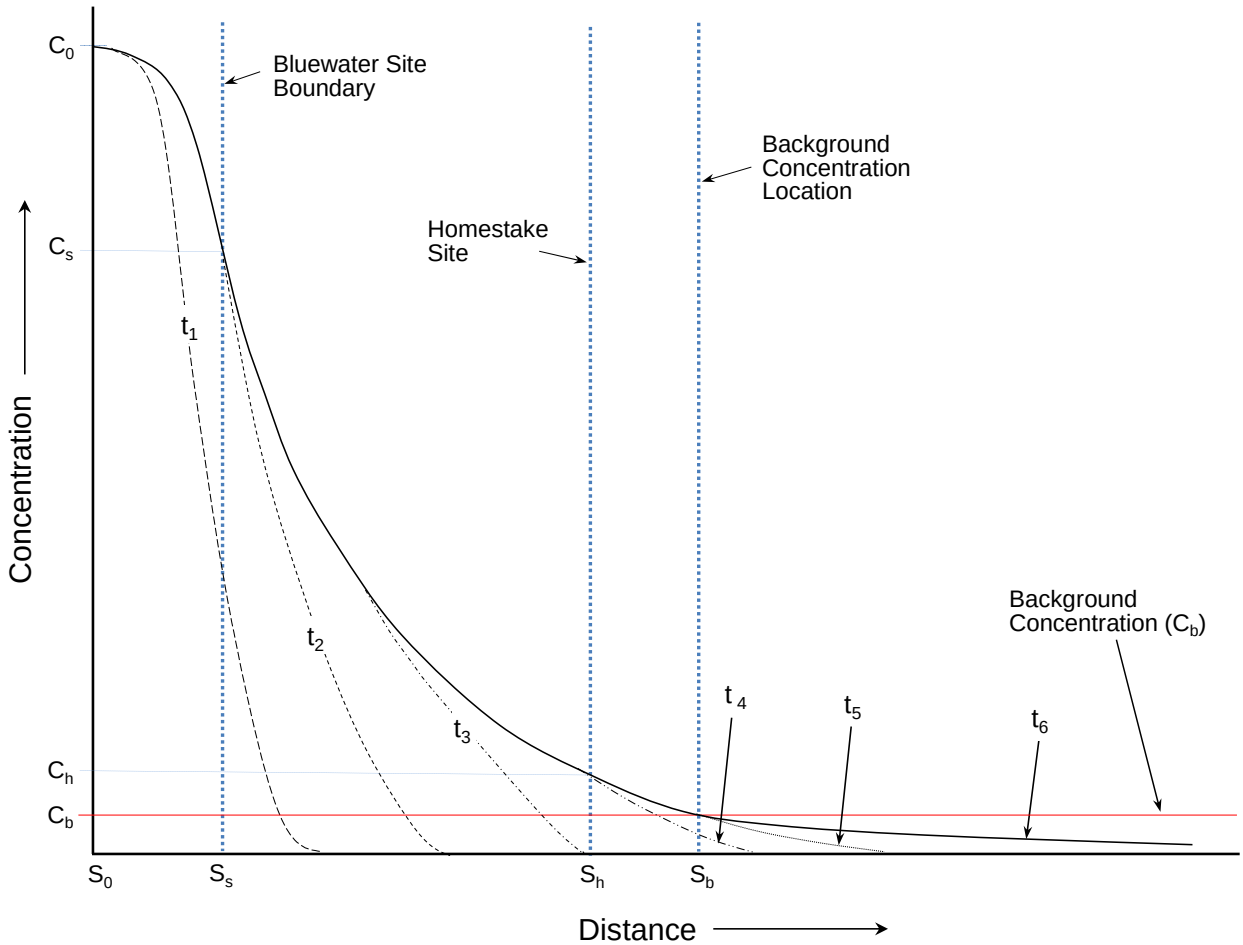

Figure 62. Graphical Depiction of Contaminant Plume Evolution—Concentration Profiles Along the Plume Centerline at Successive Times t_1 Through t_6

For groundwater systems dominated by advective transport in the direction of flow and contaminant spreading normal to the flow direction, the concentrations in a stable plume caused solely by transverse mixing can be calculated directly using analytical solutions to the steady-state version of the transport equation (e.g., Domenico and Palciauskus 1982, Domenico and Robbins 1985, Leij and Bradford 1994). The mathematical derivations under this category assume that transverse concentration gradients determine the ultimate width of the plume and that longitudinal dispersion is an insignificant process. In some cases, this assumption is made on the basis of experimental findings by Harleman and Rumer (1963) during a laboratory investigation of the relative effects of longitudinal and transverse dispersion. An analytical steady-state model could be used to estimate the downgradient extent of the stable uranium plume that originates at the Bluewater site and extends east-southeast of the Homestake site.

8.4.4 Merged Plumes

Concentrations of uranium in the alluvial aquifer plume originating at the Bluewater site appear to decrease with flow distance in areas immediately southeast of the site's east boundary. However, the uranium concentrations in the plume start to increase about a mile southeast of the Bluewater site property. This is attributed to the merging of the Bluewater plume with a separate plume migrating westward from the Homestake site (Section 8.2.1). Though the relative

contributions of the individual plumes to the combined plume have not been quantified, both the volumetric flow rate and the uranium concentrations associated with the Homestake-related plume appear, in recent years, to be larger than the flow and concentrations associated with the Bluewater site plume. Thus, the apparent increase in uranium concentrations about a mile southeast of the Bluewater site's east border can be attributed to mass discharge of uranium from the Homestake site. Continued groundwater remediation at the GRP has the potential to reduce the Homestake site's contribution to the merged plume in the alluvial aquifer.

8.4.5 Geochemical Reactions

The chemical data used to characterize the oxidation state of the alluvial and San Andres aquifers indicate that mostly oxidized conditions are prevalent (Sections 7.2.1.1 and Sections 7.2.1.2). Under such conditions, most of the uranium migrating in the aquifers is expected to occur as highly mobile uranyl species (Section 7.2.2.3). Assessment of whether uranium in groundwater at the Bluewater site could precipitate in mineral form indicates that all uranium minerals are undersaturated by at least 3 orders of magnitude (Section 7.2.2.2). Thus, it is unlikely that uranium minerals are chemically precipitating in the plumes originating at the Bluewater site.

8.4.6 Uranium Adsorption

Adsorption of uranium on mineral surfaces within the alluvial and San Andres aquifers is potentially an effective mechanism for retarding the migration of the uranium plumes originating at the Bluewater site. Though hydrous ferric oxide is expected to be present in the alluvial and San Andres aquifers, limited information regarding its abundance makes it difficult to predict how adsorption of uranium will impact the Bluewater site plumes (Section 7.2.2.1).

8.4.7 Dual-Domain Effects

Groundwater migrating through limestone and fractured sandstone in the San Andres aquifer is subject to contaminant transport processes associated with a coupled fracture-matrix flow system (Zimmerman et al. 1993). The dual-domain transport occurring in such a flow system acts to slow, or retard, the migration of uranium to downgradient areas, in a manner similar to the plume retardation caused by uranium adsorption. If the mechanisms by which uranium contamination was released from the Bluewater site constituted a finite-mass, pulse source, dual-domain transport could provide an effective means of attenuating the uranium plume in the aquifer during future years (Appendix F). However, this type of attenuation is unlikely to take place, given that uranium appears to be released to the San Andres aquifer by a continuous, constant-concentration source. As a result, uranium contamination is expected to persist in the aquifer for at least decades and perhaps hundreds of years.

Dual-domain transport processes also likely affect uranium contamination in the alluvial aquifer. The coarse-grained sands and gravels in paleochannel portions of ancestral Rio San Jose alluvium act as preferential pathways for mobile-phase contamination, whereas finer-grained deposits in non-channel parts of the alluvium retain and slowly release relatively immobile contamination to the preferential pathways. As with the San Andres aquifer, the heterogeneous fluvial deposits in the alluvial aquifer will cause uranium contamination in the aquifer to persist for many years.

8.5 Projected Fate of Uranium Contamination

The analyses presented in this and preceding chapters suggest that dissolved uranium contamination originating at the Bluewater site will persist indefinitely in the alluvial and San Andres aquifers. Moreover, uranium concentrations in groundwater in areas immediately downgradient of contaminant sources at the site are expected to either remain constant or decrease very slowly (Sections 8.2.2 and 8.3.2) in coming years.

Natural attenuation processes have apparently caused uranium concentrations in the San Andres aquifer in the vicinity of the Homestake site to remain relatively low since 1980, though some concentrations exceeding the uranium MCL (0.03 mg/L) have been observed in San Andres aquifer wells at the Homestake site since that time (Section 8.3.2). Given the history of uranium measurements at San Andres aquifer wells at the Homestake site and the apparently stable nature of uranium contamination in the aquifer at the Bluewater site (Section 8.4.2), relatively constant uranium concentrations similar to those measured between 1980 and 2013 (Section 8.3.2) at Homestake site wells are expected for the indefinite future. Large, permanent increases or decreases in uranium concentration are not expected.

The conceptual model in this study suggests that uranium concentrations in the San Andres aquifer downgradient of the Homestake site, in areas directly north of Grants, are less than the assumed background uranium concentration of 0.01 mg/L. Because the conceptual model indicates that uranium concentrations in the vicinity of the Homestake site will remain relatively constant, uranium concentrations above the background level are not expected in the areas directly north of Grants.

8.6 Potential Effects of Increasing Regional Groundwater Levels

It is possible that uranium concentrations in the aquifers will show temporary increases if and when regional groundwater levels begin to recover from the observed decreases in hydraulic head seen over the past 15 years (Section 4.3.5). At the Bluewater site, such increases in concentration could be caused by the upward incursion of groundwater into, and enhanced mobilization of uranium from, parts of the mineralized zone that have been dominated by unsaturated conditions during the past several years. The magnitude and duration of the temporary increases in uranium concentration, if they do occur, are difficult impossible to predict.

8.7 Potential for Source Removal

Because dissolved uranium in the alluvial and San Andres aquifers at the Bluewater site is sourced by dissolution of solid-phase uranium in a thick mineralized zone beneath the main tailings disposal cell and to a lesser extent the carbonate tailings disposal cell, removal of the contaminant source is considered unfeasible. The mineralized zone likely extends more than 100 ft deep below the base elevation of the cells and laterally along fault zones.

Assessing the extent of the mineralized zone would require numerous characterization boreholes beneath the disposal cells and in areas downgradient of the cells. Physical methods of source removal would likely require relocation of the cells and would require considerable excavation to remove the mineralized materials. Dewatering the deeper portions of the excavation to allow

material extraction from the contaminated San Andres Limestone and Glorieta Sandstone may be impossible because of the hydraulic characteristics of the San Andres aquifer.

Source removal through hydraulic means, such as groundwater pumping, is also expected to be unsuccessful. The groundwater withdrawn by pumping would mostly migrate through preferential flow paths that do not come in direct contact with much of the solid-phase contamination in the mineralized zone beneath the main tailings disposal cell. After periods of non-pumping, contaminant rebound due to back diffusion of contamination from the less permeable portions of the mineralized zone would likely occur.

9.0 Groundwater Conceptual Model

The primary purpose of this study was to develop a groundwater conceptual model that describes the aquifers associated with the Bluewater site and the potential exposure of downgradient groundwater users to mill-related contamination. A study area encompassing approximately 195 square miles was used to incorporate the contaminant source areas, the hydrogeologic features that most directly influence groundwater flow and contaminant transport in the Grants-Bluewater Valley, and the points of groundwater use, particularly the communities of Milan and Grants.

The conceptual model is based on work performed to meet the study objectives listed in Section 1.3 of this report. The activities involved in developing the model revealed numerous uncertainties that affect interpretations of groundwater flow and contaminant transport in the study area, which are addressed in Chapter 10. Despite such uncertainties, the following observations and conclusions have been drawn from this study.

9.1 Sources of Groundwater Contamination

The Anaconda/ARCO Bluewater uranium mill operations contaminated the two uppermost aquifers at the site: an aquifer in the ancestral Rio San Jose alluvial system, and the San Andres aquifer composed of the hydraulically connected San Andres Limestone and Glorieta Sandstone formations. Fluids from the mill's tailings impoundments seeped into the two aquifers, and contaminants in the fluids were apparently left in solid form within a mineralized zone in the geologic strata (basalt, alluvium, limestone, and sandstone) and fault zones under the impoundments (Section 8.1.1). This apparent mineralized zone is considered to be a continuing source of groundwater contamination in both aquifers.

Operations at the Homestake uranium mill contaminated the San Mateo Creek alluvial aquifer underlying the site's tailings piles as well as sandstone units of the underlying Chinle Formation (Section 2.4). Contamination at the Homestake site is affected by inflowing alluvial groundwater that is contaminated by processes occurring in areas north of the former mill site, including natural dissolution of uranium-bearing rock within the San Mateo Creek basin and decades of uranium mining and milling in a portion of the basin upgradient of the Homestake site. HMC is in the process of remediating site-derived contamination in the alluvial and affected Chinle aquifers.

9.2 Geological Features that Affect Groundwater Flow

Alluvium of the ancestral Rio San Jose at the Bluewater site is buried by multiple flows of Bluewater Basalt. The alluvial materials are in a former river valley that existed in the south portion of the site, including under a substantial portion of the main tailings disposal cell. The alluvial sediments within this paleochannel combine with San Mateo Creek alluvium about a mile southeast of the Bluewater site. Paleochannels in the two alluvial systems merged to form one channel that coursed southeastward in the direction of Milan. Alluvial groundwater flow paths follow these paleochannels (Section 4.2.1).

Two major faults intersect the Bluewater site under the south portion of the main tailings disposal cell and result in four fault blocks at the site. Movement along the faults and subsequent

erosion caused the surface exposure of the San Andres Limestone under and adjacent to the southeast corner of the main tailings disposal cell. Vertical displacement along portions of the faults resulted in the faults acting as partial hydraulic barriers to horizontal groundwater flow at some site locations (Section 4.3.4). The fault zones are also apparently capable of acting as vertical and horizontal conduits of groundwater flow.

Two major faults that influenced the formation of the San Mateo Creek valley underlie the Homestake site. It is unclear whether the faults act as partial hydraulic barriers in the San Andres aquifer in the vicinity of the Homestake site. Neither the USGS (Baldwin and Anderholm 1992, Frenzel 1992, Gordon et al. 1960) nor HMC (e.g., HMC [2012] and HMC and Hydro-Engineering [2014]) discuss the potential influence of the faults on regional groundwater flow in the aquifer.

The geology of the San Andres Limestone and Glorieta Sandstone provides an environment for a highly productive aquifer. Pumping rates from wells completed in karst features (i.e., solution-enlarged joints, channels, and cavities) in the upper portion of the San Andres Limestone can be 1,000 gpm or higher, and pumping usually creates minimal drawdown. Faults and fracture zones within both formations enhance the productivity of the aquifer and can also serve as conduits for localized high groundwater flow rates. Groundwater also flows through the unfractured, porous sandstone strata within the aquifer.

9.3 Groundwater Sources and Flow

9.3.1 Alluvial Aquifer

The alluvial aquifer in the Grants-Bluewater Valley consists of three different types of alluvium that are distinguished by their respective fluvial sources: ancestral Rio San Jose alluvium underlying the Bluewater Basalt; recent Rio San Jose alluvium along the west and southwest edges of the Bluewater Basalt; and San Mateo Creek alluvium in the east end of the valley. The three alluvium types blend together in the vicinity of Milan. The alluvial aquifer downgradient of Milan is associated with the southeast-coursing Rio San Jose downstream from its confluence with San Mateo Creek. The point of confluence for the river and creek appear to have varied, both over geologic time and during the 19th and 20th centuries.

The ancestral Rio San Jose alluvium is recharged by precipitation on and subsequent downward seepage through the overlying Bluewater Basalt; subsurface inflow from the recent Rio San Jose alluvium in areas west and northwest of the Bluewater site; seepage losses from the current Rio San Jose channel; and infiltration of irrigation water. The ancestral alluvium was also recharged by seepage of tailings fluids during milling operations at the Bluewater site. Groundwater in the ancestral river system flows southeastward within channel sediments buried beneath the south half of the site. This groundwater subsequently merges with westward-flowing groundwater in the San Mateo Creek alluvium, beginning about a mile southeast of the Bluewater site. The combined flows continue to the southeast toward Milan and Grants.

ARCO's hydrology consultants estimated transmissivity, hydraulic conductivity, and storativity values for the ancestral alluvium based on aquifer pumping tests conducted at the Bluewater site. The calculated hydraulic conductivity values are indicative of highly permeable sands and gravels deposited in paleochannels of the ancestral Rio San Jose. Flow patterns and velocities in

the buried alluvium are assumed to be variable because of an apparent complex distribution of channel sediments and associated floodplain deposits. Nonetheless, alluvial aquifer water levels suggest that a main paleochannel traverses the south half of the site. This is assumed to be the river channel that existed when the first lava flow of the Bluewater Basalt filled the alluvial valley. Groundwater flow velocities (and associated contaminant transport by advection) would be highest in this channel (Section 4.2.1).

A variety of water sources recharge the recent Rio San Jose alluvium. Sources include seepage losses from perennial Bluewater Creek where it emerges from Bluewater Canyon in the Zuni Mountains; infiltration of precipitation on the alluvium; downward seepage of surface water flows in irrigation canals fed by Bluewater Creek; seepage from the current channel of the ephemeral river; seepage of surface water diverted from the river into a borrow pit about a half-mile south of the Bluewater site; infiltration of applied irrigation water; and occasional seepage losses from tributary drainages at their outlets at the base of the Zuni Mountains. Groundwater flow directions in the recent alluvium vary from northeastward to eastward and southeastward depending on location. The recent river alluvium is not impacted by contamination originating at the Bluewater site.

San Mateo Creek alluvium in the Grants-Bluewater Valley is recharged by precipitation within the drainage basin, infiltration of applied irrigation water in areas south and west of the Homestake site, and subsurface alluvial inflow from upgradient areas. Historically, much of the subsurface inflow was derived from mining and milling operations (e.g., mine dewatering, seepage from tailings) in upgradient portions of the basin, primarily in the Ambrosia Lake area. Recharge also occurred as tailings fluids seeped from the Homestake tailings piles. Groundwater in San Mateo Creek alluvium generally flows southward toward Milan, but a component of flow is directed west from the former mill area within a paleochannel that terminates at the paleochannel containing ancestral river alluvium and extending southeastward from the Bluewater site.

9.3.2 San Andres Aquifer

The San Andres aquifer is recharged from Bluewater Lake and Bluewater Creek west of the Bluewater site and from precipitation on exposed outcrops of the San Andres Limestone and Glorieta Sandstone on the north slope of the Zuni Mountains. Groundwater flow in the aquifer beneath the site is in the east-southeast direction. Groundwater flows from the Bluewater site toward the Homestake site, and then continues in an east-southeast to southeast direction toward areas north of Grants (Section 4.3.3.1).

Prior to the start of large-scale groundwater extraction activity in the 1940s, groundwater elevations (hydraulic heads) in the aquifer in the Milan/Grants region were high enough to cause upward flow into overlying alluvial deposits as well as discharge to a large spring (Ojo del Gallo) on the southeast end of the Zuni Mountains. Since then the spring has ceased flowing, and the potentiometric surface for the aquifer in the Grants-Bluewater Valley has varied greatly in response to temporal variations in regional pumping and aquifer recharge in the Zuni Mountains.

Flow paths for the groundwater migrating in the San Andres aquifer from the Bluewater site do not intersect the locations of water supply wells for the municipalities of Bluewater and Milan (Section 4.3.3.1). The municipal well for the Village of Bluewater is upgradient of the Bluewater

site, and recharge to that well is primarily from the west and northwest. South of the village, northeastward- and eastward-moving fresh groundwater derived from recharge on the north slopes of the Zuni Mountains pushes groundwater in the Grants-Bluewater Valley about 1.5 mi farther to the north than would occur if this type of recharge were not present. Consequently, San Andres aquifer flow paths from the Bluewater site pass well north of the Milan municipal wells.

Darcy's Law calculations suggest that average linear velocities of groundwater in the San Andres aquifer cover a wide range (Section 4.3.3.2). The highest velocities appear to be associated with conduit flow in the karst portions of the San Andres Limestone. Estimated velocities in secondary permeability features (fractures) in sandstones are somewhat lower than those in karst features, but they appear to be sufficiently high for conveying contaminants significant horizontal distances via advection. In contrast, estimated average linear velocities associated with porous media flow in unfractured sandstone are low, suggesting that contaminant migration in the sandstone is mostly vertical, occurring as either molecular diffusion or very slow advection away from or into the secondary permeability features consisting of karst solution channels or sandstone fractures.

As a result of the widely varying velocity estimates, horizontal flow velocities are expected to vary greatly over the vertical sequence of limestones and sandstones that compose the aquifer. Estimated groundwater travel times between the Bluewater main tailings disposal cell and the Homestake large tailings cell via conduit flow in the karst system, the uppermost and most used portion of the aquifer, vary from 2 years to 52 years, depending on hydraulic conductivity and effective porosity values used in the flow calculations (Table 5). Uranium concentrations in water samples collected from San Andres aquifer wells in the vicinity of the Homestake site suggest that groundwater impacted by milling activity at the Bluewater site had already reached the Homestake area as early as 1980, which is about 24 years since seepage from the main tailings impoundment began.

Groundwater withdrawals from the San Andres aquifer influence local flow directions and hydraulic gradients. Historical pumping of the Anaconda production wells, located south (cross-gradient) of the tailings impoundments at the Bluewater site, produced a cone of depression that drew contaminated groundwater toward the well field (Section 7.1.1.2). Historical withdrawals from the San Andres aquifer in the Milan/Grants area helped contribute to large decreases in hydraulic head that eventually led to the drying up of Ojo del Gallo spring.

Hydraulic head changes in the aquifer in the Toltec/Milan area appear to have caused a local reversal of the vertical gradient between the alluvial and San Andres aquifers (Section 8.2.1). Whereas upward flows from the bedrock aquifer to the alluvial aquifer occurred under natural conditions, the flow direction is mostly downward today due to groundwater pumping from the San Andres aquifer at the Milan municipal wells. Although undetermined at this time, it is possible that pumping from the San Andres aquifer in support of groundwater remediation at the Homestake site may have changed the vertical hydraulic gradient between the alluvial and San Andres aquifers from upward, under natural conditions, to downward under current conditions. EPA has suggested that such a gradient reversal may cause downward migration of contaminants from shallow alluvium to the bedrock aquifer along portions of the San Mateo fault system in the Homestake site area (EPA 2011).

9.4 Ambient Chemistry of Water Resources

Ambient, or background, water chemistry in the study area is important because it affects how contaminants dissolved in groundwater, particularly uranium, are transported from contaminant sources to downgradient monitoring wells.

9.4.1 Surface Water

Surface water features in the study area include Bluewater Lake, Bluewater Creek, Rio San Jose, and San Mateo Creek. Water quality information for these features is limited. Water quality data are available for Bluewater Lake and Bluewater Creek, the only perennial surface water sources on the north slope of the Zuni Mountains. These data are germane to this study because both the lake and the creek provide recharge to parts of the San Andres aquifer that flow beneath the Bluewater site. The Rio San Jose and San Mateo Creek in the Grants-Bluewater Valley only flow when high-intensity rainfall events produce sufficient runoff. Two perennial flow locations in the San Mateo Creek drainage several miles upgradient of the Homestake site (and upgradient of uranium mining and milling) have water quality data.

The dissolved oxygen and dissolved iron concentrations in streams in the area indicate that the water is oxidized, and any uranium in them would be in the U(VI) oxidation state (Section 5.1). The water is slightly basic and has relatively low to moderate salinity. All surface water samples are undersaturated with gypsum, so gypsum would be dissolved in these waters. Contaminant concentrations are unknown for surface water samples upgradient of the Bluewater site, but sample results suggest that surface watercourses in the upper San Mateo Creek drainage are not receiving high fluxes of arsenic, molybdenum, or selenium.

9.4.2 Alluvial Aquifer

Water quality data were evaluated from wells located in Rio San Jose alluvium upgradient of the Bluewater site and from wells completed in San Mateo Creek alluvium in two areas upgradient of the Homestake site. One of the alluvial aquifer wells in the San Mateo Creek drainage is directly north of the Homestake site, and the other is in the upper reaches of the drainage basin upgradient of mining and milling activity.

The chemical signatures of alluvial aquifer groundwater are indicative of the rock types or alluvial materials that the groundwater passes through. The available chemical data for the aquifer show differences between well locations, but most water samples collected from the wells are relatively oxidized, suggesting that precipitation of reduced uranium minerals does not occur (Section 5.2.1).

Samples from the background Rio San Jose alluvial aquifer wells are nearly equivalent in bicarbonate and sulfate, and have higher calcium and lower sodium equivalents than samples collected from wells in the San Mateo Creek alluvium. There was no uranium mining or milling upgradient of the Bluewater site. Correspondingly, no contamination is detected in the background wells for the Rio San Jose alluvial aquifer.

The alluvial groundwater with the highest salinity and highest concentrations of uranium and selenium is in the area directly north of the Homestake site. Groundwater in the alluvium in this

area represents the dissolution product of gypsiferous and uranium-bearing formations in the San Mateo Creek drainage basin, as well as contamination from mining and milling in the basin. Consequently, the ambient quality of the San Mateo Creek alluvial groundwater entering the Homestake site is degraded by elevated contaminant concentrations, with uranium and selenium concentrations exceeding the drinking water standard in some of the alluvial aquifer wells (Section 5.2.1). A background uranium concentration for groundwater unaffected by mining and milling operations has not been determined for the San Mateo Creek alluvial aquifer.

Applied Hydrology Associates, Inc. (1990) reported that uranium concentrations in several alluvial aquifer wells upgradient of the Bluewater site varied from 0.003 to 0.04 mg/L. For the purposes of this study, the background uranium concentration in the Rio San Jose alluvial aquifer is assumed to be approximately 0.01 mg/L (Section 5.3).

9.4.3 San Andres Aquifer

Ambient water quality of the San Andres aquifer was evaluated using groundwater sample results reported by the USGS (Baldwin and Anderholm 1992) for 12 wells near Thoreau, New Mexico, approximately 19 mi northwest (upgradient) of the Bluewater site. Much of the groundwater in the aquifer is oxidized, and specific conductivity values indicate moderately high salinity. All of the samples were undersaturated with gypsum, indicating that the groundwater has a tendency to dissolve gypsum; gypsum dissolution is a potential cause of the moderately high salinity.

The San Andres aquifer upgradient of the Bluewater site is not impacted by contaminants, as no uranium mining or milling activity occurred in upgradient areas. Molybdenum was not detectable at the wells near Thoreau, and background uranium concentrations in the bedrock aquifer were no greater than 0.011 mg/L. For the purposes of this study, the background uranium concentration in the San Andres aquifer is assumed to be approximately 0.01 mg/L, which is the same value estimated to represent background concentration in the alluvial aquifer (Section 5.3).

9.5 Performance of the Bluewater Disposal Cell

Increasing uranium concentrations in DOE alluvial aquifer well T(M) between 2001 and 2010 raised a concern about whether a pulse of contaminated fluids was leaking from the main tailings disposal cell. The performance of the disposal cell was investigated to determine if such a pulse had occurred. Anaconda and ARCO documents were examined to characterize the history of tailings and leachate disposal at the main tailings disposal cell, and to better understand its design and construction. A combination of site observations, radon measurements, and review of studies on other disposal cells and landfills was used to evaluate the performance of the cell and its cover.

The historical characterization revealed that several billion gallons of tailings fluid (leachate) seeped through the bottom of the main tailings impoundment and into the underlying alluvial and San Andres aquifers prior to construction of the disposal cell cover in 1995 (Section 6.2). ARCO expended considerable effort to dewater the tailings prior to placement of the cell cover, but expected seepage to continue until the tailings completely drained. ARCO assumed that the cell cover would prevent infiltration of precipitation.

Other cell and landfill cover studies indicate that precipitation typically infiltrates and percolates through the covers of rock-covered cells. This finding suggested that infiltration of precipitation on the main tailings disposal cell provided a continuous source of recharge. The rates of seepage into the cell as a result of precipitation were estimated using estimated hydraulic properties for cell cover materials, the tailings, and strata underlying the tailings (Section 6.4). It appears that an undetermined portion of the tailings remains unsaturated and is considered available for storage of water derived from precipitation on the cell cover. The calculations used to derive estimated cell inflows and available storage indicated that seepage through the base of the cell is likely occurring, but at very low rates at this time. Additionally, the calculations indicated that downward seepage from tailings into underlying strata would increase as the depth of saturation in the tailings increases. It was assumed that current seepage losses from the cell are contributing to the underlying mineralized zone that apparently acts as a continuing source of groundwater contamination. However, the volume of tailings fluid and contaminant mass leaving the cell under current conditions are estimated to be very small, especially in comparison to the volume and mass that seeped through the bottom of the tailings impoundment during milling operations (Section 6.5).

Depressions have formed on the disposal cell cover because the slimes portion of the tailings impoundment continued to consolidate after the cover was completed. Runoff produced by precipitation on the cover forms ponds in these depressions, potentially introducing a second source of fluids that can infiltrate the disposal cell. However, the persistence of the ponds and the results of radon flux measurements indicate that there has been no reduction in the performance of the radon barrier and that the ponded water is reduced primarily through evaporation rather than infiltration. Therefore, the depressions and associated ponds are not considered a source of fluids that could seep from the cell (Section 6.5).

Vegetation is gradually establishing on the disposal cell cover, including deep-rooted shrubs that indicate the presence of moisture in the tailings. If the vegetation establishment is allowed to continue, evapotranspiration will reduce the volume of precipitation seeping into the tailings, thus delaying or completely preventing saturation of the full thickness of the tailings (Section 6.3.3). Accordingly, seepage losses from the tailings to underlying strata would be expected to remain minimal. However, it is possible that deep-rooted vegetation may degrade the performance of the cell's radon barrier.

Because no unusual seepage from the disposal cell appears to be occurring, other causes were considered to explain the increasing uranium concentrations in alluvial aquifer well T(M). Uranium concentrations in the other alluvial wells downgradient of the cell have exhibited uranium concentrations that have remained steady or are slightly declining. SRNL (2014) evaluated the aqueous-phase chemistry of the groundwater sampled at well T(M) and concluded that the increasing uranium concentrations at the well were not related to a pulse release of fluid from the disposal cell. The bottom of the well screen is at the contact between the alluvium and the underlying Chinle Formation, and the bottom of the well's borehole is 9 ft below the contact. SRNL reasoned that, as the water level dropped in the well to elevations near the base of the screen, most the sampled water was probably drawn from the Chinle Formation instead of the alluvial aquifer. Though the reason for high uranium concentrations in Chinle Formation water has not been verified, SRNL presented a plausible geochemical explanation. It is concluded in this conceptual model that the increasing uranium concentrations in well T(M) were not caused by a pulse release of contaminated water from the main tailings disposal cell (Section 8.2.2).

9.6 Mechanisms for Mobilization of Uranium and Other Constituents

Uranium is mobilized in the alluvial and San Andres aquifers primarily via dissolution by groundwater of solid-phase uranium in the mineralized zone beneath the Bluewater site's main tailings disposal cell (Section 8.1.1). Some of the solids are assumed to be uranium-bearing minerals that precipitated out of solution from downward-seeping tailings fluids as the acidity of the fluids was progressively neutralized with seepage depth. Additional solid-phase uranium may be adsorbed to rock and alluvium beneath the cell. The solid-phase uranium is likely present in basalt, ancestral alluvium, and the San Andres Limestone.

Though uranium and other constituents might be released to groundwater by downward-seeping water from the cell into underlying unsaturated sediments, contaminant contributions from such a source are likely minor in comparison to available contaminant mass in the mineralized zone. The mineralized zone appears to be a continuous contaminant source that produces uranium concentrations in onsite monitoring wells that are either relatively constant or decreasing very slowly (Section 8.1.1). It is assumed that this source will remain indefinitely.

9.7 Migration and Distribution of Uranium Contamination

9.7.1 Alluvial Aquifer

Examination of potential groundwater velocities in the ancestral river alluvium and uranium concentrations in onsite alluvial aquifer wells leads to the conclusion that uranium transport in this aquifer was rapid. This conclusion comports with previous studies of the Bluewater site that focused on characterization of groundwater flow and transport, which found that the plumes for conservative (nonreactive) constituents reached the east boundary of the site just a few years after initial construction of the main tailings impoundment. The rapid movement of uranium is attributed to fast advective transport in coarse sands and gravels.

Much of the rapid contaminant transport appears to occur in the main paleochannel that has been identified in ancestral river alluvium beneath the south half of the Bluewater site. Under the assumption that the first lava flows of the Bluewater Basalt preserved the channel of the Rio San Jose as it existed just prior to the lava incursion, the mostly coarse deposits in the channel were prevented from being redistributed by temporally varying locations of the river and its floodplain across the river valley. In contrast, former overbank areas likely contain a mixture of coarse- and fine-grained materials due to reworking of those sediments by river flows in years preceding the lava incursion. Comparatively low velocities are expected in these floodplain deposits due to the presence of abundant silts and clays.

The resulting groundwater movement and contaminant transport in the ancestral river alluvium can be characterized as a dual-domain system, wherein the paleochannel is a preferential flow path conveying groundwater and contamination downstream at a high velocity, and remaining groundwater contamination in overbank areas migrates much more slowly, converging on the channel from both of its sides (Section 8.4.7). Accordingly, contamination in the overbank deposits flushes much more slowly from the groundwater system, at rates that are similar to those caused by molecular diffusion. This process of "back diffusion" leads to an overall

retardation of contaminant transport from the ancestral river portion of the alluvial aquifer, such that complete flushing of the aquifer is potentially delayed by tens to hundreds of years.

As previously discussed, uranium migrating southeastward in the ancestral alluvium paleochannel from the Bluewater site merges with westward-moving uranium contamination from the Homestake site about 1 mile southeast of the Bluewater site. The historical and current effects of the merged plumes on groundwater in areas farther downgradient of the Bluewater site, such as in the vicinity of Milan, are unclear. Very little information exists for historical concentrations of uranium and other constituents in that portion of the alluvial aquifer underlying Milan. However, it can be deduced that the volume of flow and the amount of contaminant mass contributed by the alluvial paleochannel passing under the Homestake site has historically been much greater than the flow and contaminant mass contributed by the Rio San Jose paleochannel (Section 8.4.4). Uranium concentrations exceeding the drinking water standard of 0.03 mg/L have been reported for alluvial aquifer wells as far south as Toltec, but the processes leading to these concentrations have not been evaluated.

A large portion of the alluvial aquifer from about a mile north of Toltec to Grants appears to directly overlie the San Andres Limestone. If historical groundwater pumping from the San Andres aquifer in this region reversed the vertical hydraulic gradient from upward to downward, as discussed in preceding sections on the conceptual model, it is possible that contaminated alluvial groundwater reached the bedrock aquifer in earlier years. Though uranium concentrations in samples collected from the Milan municipal wells have been safely below the drinking water standard of 0.03 mg/L, groundwater from the northernmost well has exhibited concentrations of 0.013 mg/L, which is slightly above the adopted background concentration of 0.01 mg/L.

9.7.2 San Andres Aquifer

The apparent presence of Bluewater site-derived uranium at wells in the vicinity of the Homestake site as of 1980 is indicative of rapid east-southeastward advective transport in the San Andres aquifer from the main tailings disposal cell. This is attributed to high average linear velocities associated with conduit flow in karst features in the San Andres Limestone and possibly to quick groundwater migration through fractures within sandstone strata. The much slower velocities and mostly vertical transport in unfractured rock are reflective of dual-domain transport (Section 8.4.7), with advection dominating in the mobile domain (secondary permeability features) and mostly diffusive transport dominating the immobile domain (unfractured rock). Accordingly, the uranium that diffuses into the aquifer matrix during early stages of plume development can be expected to back-diffuse into secondary permeability features as uranium concentrations in the aquifer gradually decline. The exchange between domains effectively retards uranium transport in the aquifer, resulting in a plume that persists much longer than would occur if transport took place solely within fractures, solution channels, and cavities.

Figure 63 shows the current estimated uranium plume and associated flow paths in the San Andres aquifer. This graphic is an idealized representation of the plume based on recent hydraulic head and uranium concentration data. In contrast to the smooth concentration contours used to depict the plume, the spatial distribution of uranium in the aquifer is more likely to be irregular, particularly because most of the groundwater flow takes place in secondary

permeability features as opposed to a porous medium. Correspondingly, the plume has the potential to bifurcate in some locations, such that uranium migration takes place in relatively thin, isolated plumes as opposed to a single, spatially continuous plume. Nonetheless, as illustrated Figure 63, the leading and lateral edges of the uranium plume, as defined by a background concentration of 0.01 mg/L, are estimated to be more than a mile north of Milan and Grants.

9.8 Physicochemical Phenomena that Influence Contaminant Transport

Because groundwater in the alluvial and San Andres aquifers is oxidized, precipitation of solid-phase uranium via microbially mediated reduction is not expected to impact the migration and spatial distribution of the contaminant. This signifies that attenuation of the uranium plumes in the respective aquifers via chemical reduction cannot be relied upon either as a groundwater remedy or a mechanism for containing the uranium within Bluewater site boundaries.

It does appear that adsorption of uranium to mineral surfaces in both the alluvial and San Andres aquifers is occurring. However, the degree to which adsorption retards the migration of uranium in the two groundwater systems is not known. It is likely that hydrous ferric oxide is present as a potential sorbent in both aquifers, but virtually no information is available regarding its abundance. The same holds true for additional sorbent minerals, such as those composing clays in the alluvial aquifer. Though retardation of uranium due to sorption processes has not been adequately characterized, it is likely that dual-domain transport phenomena in both aquifers are causing some contaminant retardation.

Though the effects of chemical reactions, adsorption, and dual-domain processes cannot be fully characterized at this time, sampling results from wells located downgradient of the main tailings disposal cell at the Bluewater site indicate that uranium effectively attenuates with transport distance in both the alluvial and San Andres aquifers (Sections 8.2 and 8.3). This attenuation is currently attributed to transverse dispersion (transverse mixing) processes in both horizontal and vertical directions (Section 8.4.2). Highly irregular flow patterns in karst features in the San Andres aquifer are expected to enhance transverse dispersion in that aquifer, whereas substantial heterogeneity of fluvial deposits is assumed to be the primary cause of horizontal transverse dispersion in ancestral Rio San Jose alluvium. It is also possible that transient flow phenomena in either aquifer lead to a form of “apparent” transverse dispersion. In addition to transverse mixing processes, apparent attenuation in the alluvial aquifer can also be attributed to dilution of the uranium plume by recharge from uncontaminated sources, such as inflow of fresh groundwater, seepage from surface-water features, and infiltration of applied irrigation water.

Inspection of uranium concentration histories at onsite alluvial aquifer wells reveals that, in addition to concentrations decreasing with transport distance, the concentrations have tended to either remain constant or slowly decrease with time (Section 8.2.2). Similar observations are made regarding the San Andres aquifer by examining temporal plots of uranium contamination at onsite wells east of the main tailing disposal cell and wells in the vicinity of the Homestake site (Section 8.2.3). These findings support the observation that the mineralized zone beneath the main tailings disposal cell represents a continuous, constant-concentration source of tailings-related contaminants.

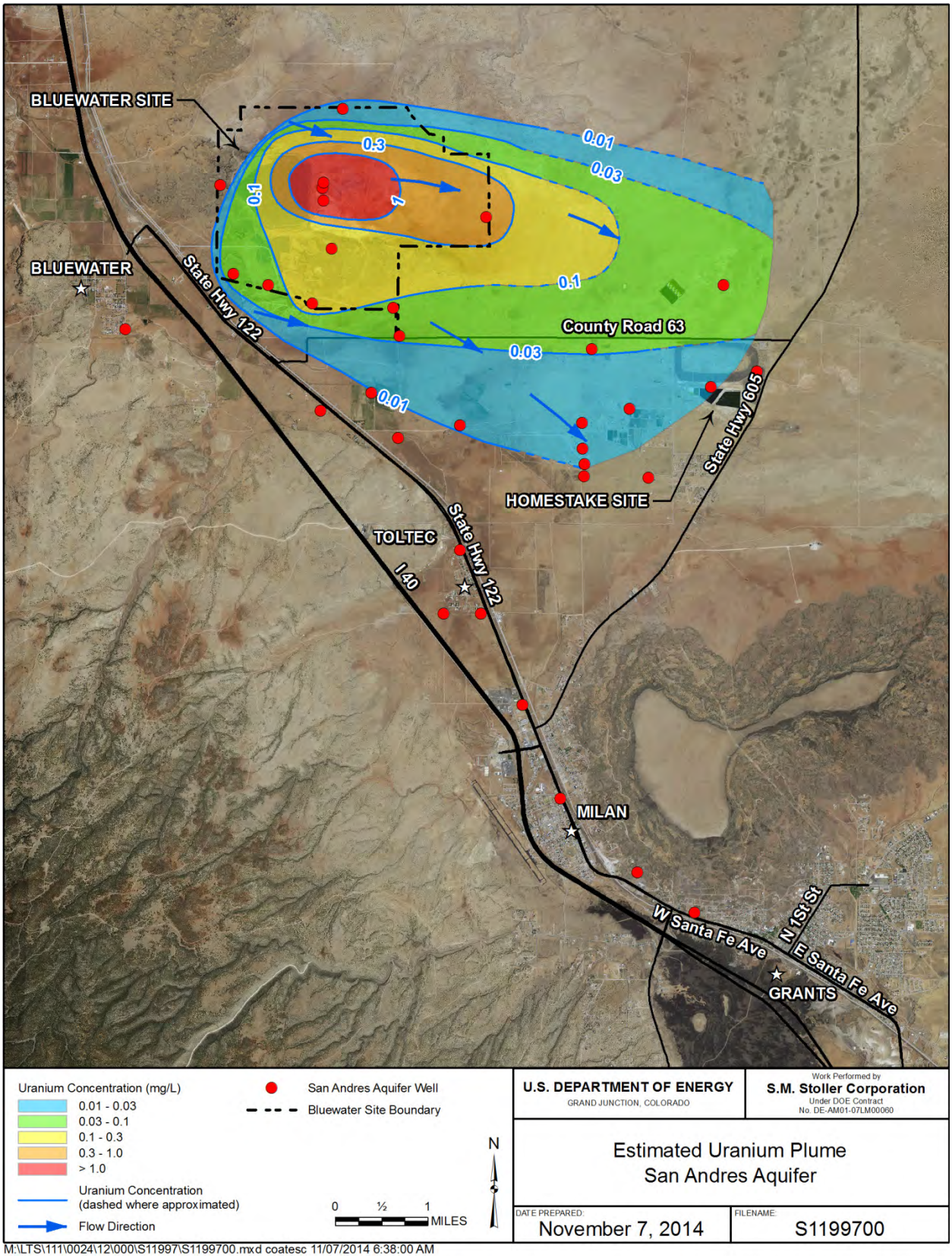

Figure 63. Current Estimated Uranium Plume in the San Andres Aquifer

9.9 Fate of Uranium

The combination of a continuous, constant-concentration contaminant source, rapid advective transport, and attenuated concentrations with transport distance has produced a uranium plume in the San Andres aquifer that has remained relatively stable since at least 1980. Comparison of mapped uranium plumes in the aquifer for four different time periods (1980–1981, 1996–1997, 2008, 2008–2014) reveals a plume whose length and width have remained virtually constant for more than 30 years (Section 8.3.1). Extending from the main tailings disposal cell to areas in the vicinity of the Homestake site, the leading edge of this plume, as defined by a uranium concentration of 0.01 mg/L, is estimated to lie in an area east-southeast of the Homestake site and north of Grants.

The development of a uranium plume in the San Andres aquifer fed by a continuous source and characterized by mostly steady concentrations due solely to the effects of transverse mixing may seem counterintuitive. However, such a plume becomes possible when it migrates sufficiently far downgradient that uranium concentrations continually produced along the leading and lateral plume edges are at background levels (0.01 mg/L).

Uranium concentration histories at San Andres aquifer wells east of the main tailings disposal cell suggest that the mineralized zone beneath the cell will remain a continuous, constant-concentration source for the foreseeable future. Consequently, the uranium plume in the aquifer is not expected to change significantly for at least several decades, if not hundreds of years. This signifies that uranium contamination originating at the Bluewater site will not affect municipal water supplies in Milan and Grants. Nor is it likely that a pulse of contamination from the disposal cell will affect the uranium plume in future years.

9.10 Potential Risk to Downgradient Groundwater Users

Samples from alluvial aquifer wells monitored by HMC downgradient of the location where the ancestral Rio San Jose aquifer merges with the San Mateo Creek aquifer have uranium concentrations that exceed the New Mexico drinking water standard of 0.03 mg/L. However, these concentrations have not been observed in municipal supply wells operated by Milan. Annual reports on the progress of aquifer remediation activities conducted as part of the GRP at the Homestake site suggest that uranium concentrations in the alluvial aquifer are gradually decreasing.

The municipal water supply wells for Bluewater, Milan, and Grants pump groundwater from the San Andres aquifer. Reported concentrations of uranium at those wells since as early as 1996 have all been less than the drinking water standard. These data, combined with the finding that the uranium plume in the San Andres aquifer lies east of Bluewater and more than a mile north of Milan and Grants, indicate that groundwater contamination originating in the aquifer at the Bluewater site does not currently pose a risk for community water systems in the Grants-Bluewater Valley. The relatively stable uranium plume in the aquifer suggests that future impacts on the municipal wells in the region are unlikely.

None of the private drinking water supply wells in the vicinity of the Bluewater site sampled by DOE have uranium concentrations exceeding the drinking water standard. However, not all of the well owners contacted by DOE have allowed their wells to be sampled. Though the

unsampled wells appear to lie outside existing groundwater flow paths emanating from the Bluewater site, it cannot be stated with certainty that no local domestic wells have been adversely impacted by Bluewater-derived contamination.

9.11 Summary of Groundwater Conceptual Model

The major risk-related components of the groundwater conceptual model are summarized below. Figure 64 shows a stylized cross section of the San Andres aquifer uranium contamination and risk.

- Seepage from the carbonate and main tailings impoundments during mill operations contaminated the underlying alluvial and San Andres aquifers. Uranium concentrations exceed the New Mexico drinking water standard in both aquifers at the downgradient site boundary.
- The seeping fluids were neutralized in the materials beneath the cells and apparently formed a mineralized zone in the basalt, alluvium, limestone, and sandstone materials and in fault zones. This mineralized zone is considered to be a continuing source of contamination in both aquifers as groundwater flows through it.
- Minimal seepage from both disposal cells is likely occurring because of residual tailings fluids within the cells and infiltration of precipitation through the cell covers. However, no surge of tailings fluids into the aquifers has occurred since milling operations ceased in the 1980s.
- Contaminated alluvial aquifer groundwater from the Bluewater site merges with contaminated alluvial groundwater from the Homestake site about 1 mi downgradient of the Bluewater site. The combined flow continues in the southeast direction toward Milan.
- San Andres aquifer groundwater beneath the Bluewater site flows in the east-southeast direction toward the Homestake site and areas north of Grants. Contaminated groundwater apparently reached the Homestake site no later than 1980.
- Groundwater remediation by HMC has reduced contaminant concentrations in the alluvial aquifer. However, many alluvial wells downgradient of the Homestake site have uranium concentrations exceeding the drinking water standard.
- The leading edge of the San Andres aquifer uranium plume is apparently downgradient of the Homestake site and has changed little since the early 1980s. The uranium plume in the aquifer is influenced by multiple processes, including a continuous source of uranium contamination in the mineralized zone beneath the main tailings disposal cell and transverse dispersion processes that help maintain essentially stable concentrations upgradient of the leading edge of the plume.
- No alluvial or San Andres aquifer domestic wells solely affected by Bluewater site-derived contamination have uranium concentrations exceeding the drinking water standard.
- Collectively, the direction of groundwater flow in the San Andres aquifer, the apparent stability of the uranium plume in the aquifer, and the locations of municipal supply wells indicate that Bluewater site-derived uranium contamination does not pose a current or future risk for community water systems in the Grants-Bluewater Valley.

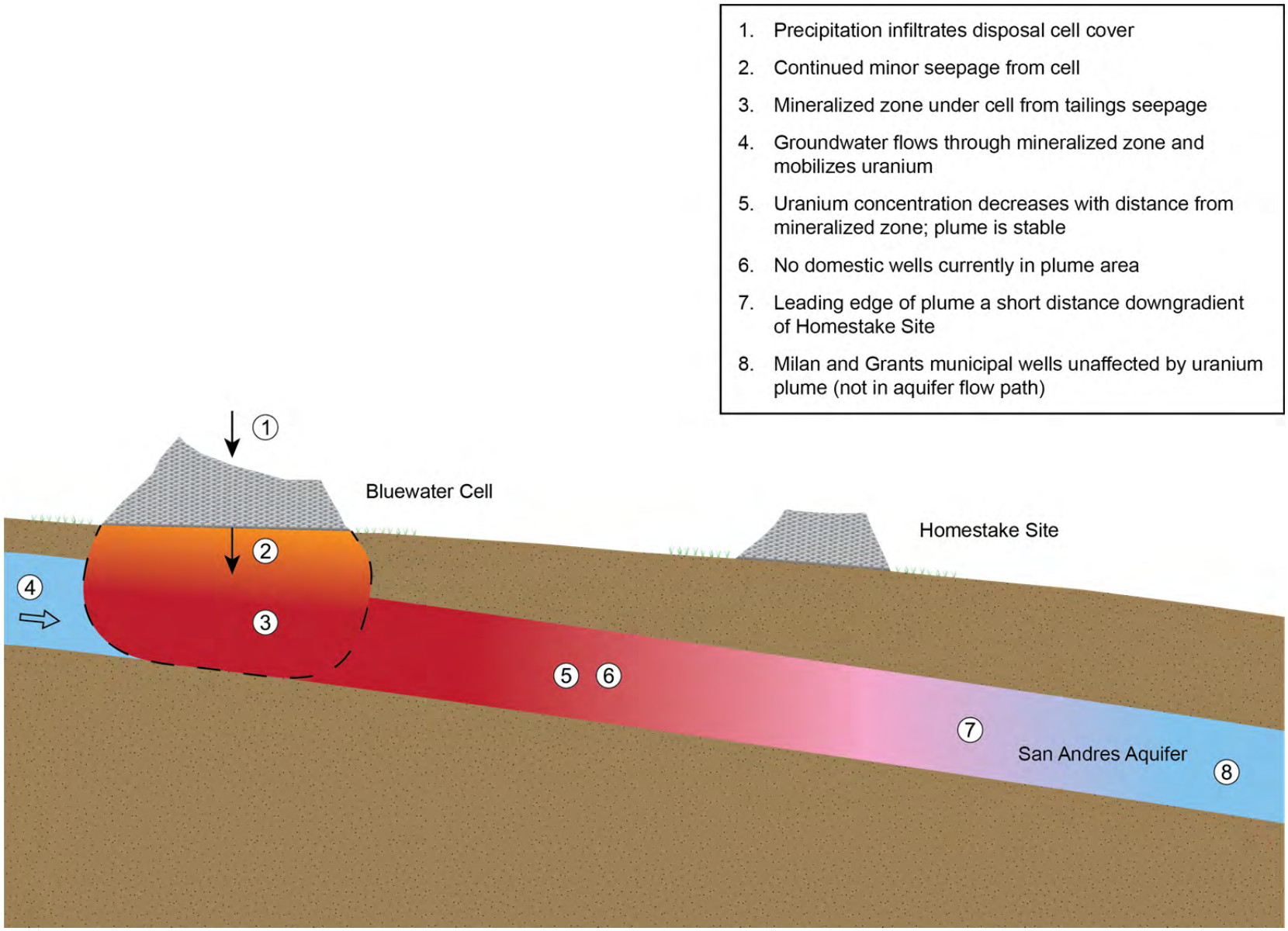

Figure 64. Stylized Cross Section of San Andres Aquifer Uranium Contamination and Risk

10.0 Uncertainties

Uncertainty in the groundwater conceptual model is unavoidable given the sparseness of available data to characterize the hydraulic and chemical properties of the aquifers and the limited amount of information available to corroborate or refute alternative models. Table 17 addresses the major uncertainties associated with the observations and conclusions presented in Chapter 9.

Table 17. Uncertainties and Their Effects on Study Conclusions

Conclusion	Uncertainty	Effect on Conclusion	Significance of Uncertainty
Sources of Contamination			
An estimated 5.7 billion gallons of fluids seeped through the bottom of the Bluewater main tailings impoundment prior to encapsulation. Unknown proportions seeped into the underlying aquifers.	ARCO estimated this quantity based on a water balance analysis of the milling processes. Actual seepage rates and quantities were not measured.	Precipitation and evaporation were not factored into ARCO's estimates. Therefore, actual seepage could have been greater or less than 5.7 billion gallons.	Attempts to more precisely estimate the amount of seepage that occurred would not impact the conclusion that a very large volume of contaminated tailings fluid seeped into the geologic materials and aquifers below the tailings impoundment.
Based on historical groundwater monitoring results near the Bluewater main tailings impoundment, the fluids that seeped through the bottom of the tailings impoundment are assumed to have formed a mineralized zone in the geologic strata and fault zones under the disposal cell.	Sampling of materials under the disposal cells has never been conducted to confirm the presence or extent of the mineralized zone.	Continued elevated uranium concentrations in wells near the disposal cell indicate the presence of a continuing source of contamination. Because ARCO did not observe changes in groundwater chemistry during dewatering activities of the tailings impoundment, there is a high probability that a mineralized zone is present and that it is the primary source of continuing contamination.	Extensive borehole material analysis and groundwater quality measurements under the disposal cells and along the fault zones would be required to define the postulated mineral zone. The characterization most likely would confirm the presence of the mineralized zone and that it should be considered to be a continuing source of contamination to the aquifers. However, it could not completely delineate the extent of the mineralized zone.
The assumed mineralized zone will remain indefinitely as a continuing source of contamination for both aquifers.	It is possible that the source concentrations will decline as inflowing fresh groundwater gradually reduces the contaminant mass. It is also possible that they may increase if groundwater levels rise into the contaminated aquifer matrix materials that are not currently saturated.	If source concentrations decline, then the leading edge of the uranium plume would retreat. Conversely, if source concentrations increase, the leading edge could advance.	With the exception of alluvial well T(M), uranium concentrations in the site wells have remained steady or have declined slightly since the 1980s, after the greatest quantity of seepage from the tailings impoundment occurred. If source contamination declines, it is expected to occur slowly, and a corresponding reduction in the uranium plume would be difficult to discern based on the existing regional well network. It is unlikely that uranium concentrations will increase to levels higher than occurred during milling, so a surge of increased uranium is not expected.

Table 17 (continued). Uncertainties and Their Effects on Study Conclusions

Conclusion	Uncertainty	Effect on Conclusion	Significance of Uncertainty
Seepage continues to occur through the bottom of the Bluewater main tailings disposal cell and is expected to continue indefinitely. However, because of steady or declining uranium concentrations and decreasing water levels in wells near the disposal cell, seepage is assumed to be occurring at a minimal rate. Therefore, the disposal cell is not considered to be a significant source of contamination in the aquifers compared to the source generated and released during milling.	The seepage rate is dependent on the amount of precipitation that percolates through the cell cover, hydraulic characteristics of the tailings materials, and the degree of saturation within the tailings, all of which are unmeasured. Therefore, the current seepage rate is unknown.	Even though the rate is unknown, seepage is most likely occurring. However, the contaminant mass available from present day seepage to impact groundwater contaminant concentrations is extremely small compared to the mass associated with the fluids that seeped during milling.	Measuring precipitation percolation rates, hydraulic properties of the cell materials, and the degree of saturation within the cell would require extensive sampling and testing of the cover and tailings materials. The source term released during milling is much greater than the source term being released from the disposal cell. Therefore, knowing the actual seepage rate would not have a significant bearing on conclusions relating to the behavior of contaminant migration in the aquifers.
Elevated uranium concentrations in DOE's alluvial well T(M) do not represent a new pulse of contamination from the Bluewater disposal cell. The elevated concentrations appear to represent Chinle Formation groundwater.	Although comparisons of historical and current groundwater quality from well T(M) samples suggest that the current uranium concentrations do not represent tailings fluids, the source of the uranium has not been confirmed.	If the elevated uranium in well T(M) is representative of tailings fluid, it may be impossible to determine if it is the result of a new pulse of cell seepage or increased mobilization of uranium from the mineralized zone.	Chemical tests could be conducted in well T(M) that may determine the source of uranium. However, uranium concentrations have not increased in alluvial wells downgradient of well T(M), so fully understanding the cause of increasing uranium in well T(M) would not affect conclusions regarding contaminant transport from the Bluewater site.
Groundwater Flow and Transport			
Groundwater flow and contaminant migration in the San Andres aquifer are influenced by faults to some degree. The faults at the Bluewater site were important conduits for distributing contaminated fluids that leaked from the tailings impoundment into the alluvial and San Andres aquifers at the site.	Because very few faults in the region have a surface expression beyond the foot of the Zuni Mountains, the subsurface locations of the faults are only approximated based on well log information. Therefore, it is difficult to evaluate the degree of their influence on the aquifers. In particular, the effects of pumping for the GRP and by municipal, industrial, and agricultural wells near Milan on flow and contaminant transport through the San Mateo faults are unknown.	Regionally, groundwater flow and contaminant transport in the San Andres aquifer is in the east-southeast direction from the Bluewater site and does not appear to be significantly influenced by faults. Locally, however, faults could direct flow and contaminant transport perpendicular to or vertically from the regional direction. Existing or future San Andres production wells in fault zones could also redirect flow and contaminant transport toward the wells contrary to the regional flow direction, as occurred when the Anaconda production wells were pumping.	Depending on the amount of vertical displacement and the formations involved, faults can behave as conduits or barriers to groundwater flow, or may not influence regional flow. The Milan municipal wells are completed in or near San Mateo fault zones, so additional geochemical analyses or other tests may be useful to help understand potential contaminant migration through the fault zones toward those wells. However, the Milan municipal wells do not show upward trends in uranium concentrations, so additional study may not be warranted at this time.

Table 17 (continued). Uncertainties and Their Effects on Study Conclusions

Conclusion	Uncertainty	Effect on Conclusion	Significance of Uncertainty
Groundwater flow and associated contaminants in the Rio San Jose alluvium merge with flow and contaminants in the San Mateo Creek alluvium about 1 mi downgradient of the Bluewater site. The merged alluvial aquifer flows southeast toward Milan.	The hydrologic and chemical processes that occur in the merge area have not been evaluated, so the contribution of Bluewater-derived contaminant mass to the alluvial system downgradient of the merge area is unknown.	Attenuation of uranium in the Rio San Jose alluvial groundwater appears to be significant by the time its flow merges with contaminated San Mateo Creek alluvial groundwater. Also, uranium concentrations in the Rio San Jose alluvial groundwater are substantially lower than those in the San Mateo Creek alluvial groundwater. Consequently, flow and contaminant transport are likely dominated by the San Mateo Creek alluvial system. Regardless of the contribution of flow and contaminants from the Bluewater site, uranium concentrations exceeding the drinking water standard are present in the alluvial groundwater at least as far as Toltec.	Aquifer tests in both alluvial systems upgradient of the merge zone and a geochemical evaluation of sample data from existing wells in both systems and within the merge zone would be required to evaluate hydrologic and chemical processes occurring in the merge zone. Although this information would be helpful in understanding the alluvial aquifer systems, it would not change the observation that contaminated groundwater has migrated at least as far as Toltec, which is upgradient of Milan. Also, remediation efforts at the GRP are expected to reduce Homestake-derived contaminant concentrations that enter the merge zone.
Uranium concentrations attenuate with distance from the contaminant source. The groundwater in the alluvial and San Andres aquifers is in an oxidized state, so chemical reduction of uranium is not a process influencing attenuation of uranium in the aquifers. Therefore, dispersion is most likely the main process by which attenuation occurs.	Insufficient data are available to characterize the presence of adsorbent minerals (e.g., hydrous ferric oxide) or local reducing environments in the aquifers.	The presence of attenuation processes other than dispersion within the aquifer systems would be advantageous in limiting the extent of the uranium plumes.	Additional analysis of historical and new groundwater sample results, and possibly analysis of core data from new wells along the flow paths, may lead to a better understanding of attenuation processes within the aquifers. However, determining the actual processes of attenuation is not considered critical because the contaminant plumes are stable.
Bluewater-derived contamination in the San Andres aquifer apparently reached the Homestake site by 1980. It is assumed that elevated uranium concentrations in San Andres aquifer wells at and near the Homestake site (including HMC-928 well north of the Homestake site) are attributed to Bluewater-derived contamination, and that the uranium plume between the Bluewater and Homestake sites is continuous.	There is a 2.5-mi gap between the sites without San Andres aquifer wells; therefore, it is difficult to validate the assumptions. ARCO's deep injection well on the Bluewater site contributed to San Andres aquifer contamination, but the magnitude and persistence of the contamination associated with that well are unknown. Also, the contribution of contaminants into the San Andres aquifer resulting from GRP operations and pumping from the Milan municipal wells is unknown.	If elevated uranium concentrations in San Andres aquifer wells near the Homestake site are due partially or wholly to GRP operations, then contaminants have not migrated as far from the Bluewater site as expected.	DOE has an NRC-approved LTSP and is committed to expend resources whenever a clear nexus to radiological safety is established. DOE resources were used to prepare this site status report and groundwater conceptual model, and DOE will maintain a continuing dialog with NRC and NMED for ways to improve our common understanding of the groundwater flow and contaminant transport in the Grants-Bluewater Valley.

Table 17 (continued). Uncertainties and Their Effects on Study Conclusions

Conclusion	Uncertainty	Effect on Conclusion	Significance of Uncertainty
San Andres aquifer flow and uranium transport processes between the Homestake site and Grants are assumed to be similar to those between the Bluewater and Homestake sites.	No San Andres wells are present between the Homestake site and Grants, so flow and uranium transport processes in that region are unknown.	The leading edge of the uranium plume (the 0.01 mg/L contour) could be farther advanced toward areas north of Grants than currently estimated.	Uranium concentrations in the Grants municipal supply wells do not show effects of mill-related contamination. DOE is committed to expend resources whenever a clear nexus to radiological safety is established, and will maintain a continuing dialog with NRC and NMED for ways to improve our common understanding of the groundwater flow and contaminant transport in the Grants-Bluewater Valley.
Potential Risk to Groundwater Users			
Assuming current San Andres aquifer use remains the same, the Milan and Grants municipal water supply wells will continue to have uranium concentrations below the drinking water standard.	Pumping from high-production municipal, industrial, and irrigation wells could influence regional flow patterns in the San Andres aquifer, but the degree to which this pumping could influence flow is unknown.	Pumping from the Anaconda production wells altered San Andres flow patterns; the natural flow direction has recovered since pumping ceased. It is possible that increased pumping south of the estimated uranium plume could draw San Andres aquifer groundwater and its contaminants to the south where it could impact municipal supply wells.	To date, pumping south of the plume appears to have little effect on regional groundwater flows. However, if declines in regional San Andres water levels continue, and/or pumping increases, there is a possibility of an adverse effect on the municipal groundwater supply.
Although uranium concentrations in Milan's municipal wells are expected to remain below the drinking water standard, water in their northwestern-most well appears to be impacted by mill-related contaminants. Uranium concentrations are greater than the adopted background concentration of 0.01 mg/L, and the U-234/U-238 activity ratio may suggest the presence of processed uranium.	Insufficient analyses have been conducted to verify the presence of processed uranium in the Milan well water.	If processed uranium is present in the Milan well water, it would be difficult to determine the source of the uranium. Pumping by the Milan wells and other San Andres aquifer wells in the area appears to have reversed the hydraulic gradient between the alluvial aquifer and the San Andres aquifer in the vicinity of the Milan wells. If this has occurred, then the processed uranium could be derived from the contaminated San Mateo Creek alluvial aquifer as alluvial water is drawn down into the San Andres aquifer by pumping.	Although slightly above background, the uranium concentrations in Milan's water supply wells are well below the drinking water standard and have not shown upward trends; therefore, the water is safe to drink. If the GRP is successful and if uranium concentrations in the Milan municipal wells remain steady or decline, then additional analyses of the hydrology and hydraulics of the aquifers in the vicinity of Milan's wells may be unnecessary.

Table 17 (continued). Uncertainties and Their Effects on Study Conclusions

Conclusion	Uncertainty	Effect on Conclusion	Significance of Uncertainty
Permitted private drinking water wells in the vicinity of the Bluewater site that were sampled by DOE do not have uranium concentrations exceeding the drinking water standard.	DOE did not sample all wells in the immediate downgradient vicinity. Some well owners declined DOE's sampling request, and some owners did not respond to DOE's request. Furthermore, there is a possibility that there are unpermitted wells in the area used for drinking water.	Unsampled private wells could have Bluewater-derived contaminants exceeding the drinking water standard.	No permitted alluvial wells used for drinking water purposes are located between the Bluewater site and the zone where the ancestral Rio San Jose aquifer merges with the San Mateo Creek aquifer. If uranium contamination is present in wells downgradient of that zone, it may be difficult to discern the source of contamination. No known San Andres wells permitted for drinking water use are present within the estimated uranium plume. If a drinking water well were to be installed within the plume area, it would likely encounter Bluewater-derived uranium.

11.0 References

Abichou, T., C.H. Benson, T. Edil, and B. Freber, 1998. "Using waste foundry sand for hydraulic barriers," *Recycled Materials in Geotechnical Applications*, GSP No. 79, American Society of Civil Engineers, p. 86–89.

Albright, W.H., C.H. Benson, G.W. Gee, A.C. Roesler, T. Abichou, P. Apiwantragoon, B.F. Lyles, and S.A. Rock, 2004. "Field water balance of landfill final covers," *J. Environ. Qual.* 33:2317–2332.

Applied Hydrology Associates Inc., 1990. *Corrective Action Program and Alternate Concentration Limits Petition for Uranium, Molybdenum and Selenium, Bluewater Uranium Mill Near Grants, New Mexico*, prepared for the Atlantic Richfield Company, June.

Applied Hydrology Associates Inc., 1993. *Ground Water Corrective Action Program Review, Bluewater Uranium Mill Near Grants, New Mexico*, prepared for the Atlantic Richfield Company, December.

Applied Hydrology Associates Inc., 1995. *Corrective Action Program and Alternate Concentration Limits Petition for Uranium, Molybdenum and Selenium, Bluewater Uranium Mill Near Grants, New Mexico*, prepared for the Atlantic Richfield Company, April.

ARCO (Atlantic Richfield Company), 1990. *Reclamation Plan, Bluewater Mill*, *License Number SUA-1470, Docket Number 40-8902*, March.

ARCO (Atlantic Richfield Company), 1996. *Completion Report for Reclamation of the Bluewater Mill Site,* March.

Arlin, V.E., T.R. Beck, and D.E. Dixon, 1978. *A Study of Seepage Loss from the Mill Tailings Area and an Evaluation of the Adequacy of the Disposal Well: The Anaconda Company*.

Baldwin, J.A., and S.K. Anderholm, 1992. *Hydrogeology and ground-water chemistry of the San Andres-Glorieta aquifer in the Acoma embayment and eastern Zuni uplift, west-central New Mexico*, U.S. Geological Survey Water-Resources Investigations Report WRI 91-4033, 304 pp.

Baldwin, J.A., and D.R. Rankin, 1995. *Hydrogeology of Cibola County, New Mexico* U.S. Geological Survey Water Resources Investigations Report 94-4178, 102 pp.

Bense, V.F., and M.A. Person, 2006. "Faults as conduit-barrier systems to fluid flow in siliciclastic sedimentary aquifers," *Water Resources Research*, 42, W05421.

Benson, C.H., W.J. Waugh, W.H. Albright, G.M. Smith, and R.P. Bush, 2011. "Design and Installation of a Disposal Cell Cover Field Test," *Proceedings of Waste Management 2011 Symposium*, Phoenix, Arizona.

Cather, S., 2011. "Geologic map of the Dos Lomas Quadrangle, Cibola and McKinley Counties, New Mexico," New Mexico Bureau of Geology and Mineral Resources Open-File Geologic Map 219, scale 1:24,000.

Chamberlin, R.M., and O.J. Anderson, 1989. "The Laramide Zuni Uplift, southeastern Colorado Plateau: A microcosm of Eurasian-style indentation-extrusion tectonics?" in *Southeastern Colorado Plateau*, Anderson, O.J. and others, eds., New Mexico Geological Society Guidebook 40, pp 81–90.

Chapin, C.E., and S.M. Cather, 1981. "Eocene tectonics and sedimentation in the Colorado Plateau-Rocky Mountains area," in Dickinson, W.R. and W.D. Payne, eds., "Relations of tectonics to ore deposits in the Southern Cordillera," *Arizona Geological Society Digest*, 14:173-198.

Chapman, S.W., and B.L. Parker, 2005. "Plume persistence due to aquitard back diffusion following dense nonaquieous phase liquid source removal or isolation," *Water Resources Research*, 41, W12411.

Cherdyntsev, V.V., P.I. Chalov, and G.Z. Khaidarov, 1955. *Trans. 3rd Session of Committee for Determination of Absolute Ages of Geologic Formations*, Izv. Akad. Nauk SSSR, 175 pp.

Cirpka, O.A., and S. Attinger, 2003. "Effective dispersion in heterogeneous media under random transient flow conditions," *Water Resources Research*, 39(9), SBH 9-1–9-15.

Dames & Moore, 1981a. Appendix A, "Field Investigations," and Appendix C, "Geologic Data Interpretations," in Volume 10 of *Licensing Documentation Below Grade Seepage, Bluewater Mill Anaconda Copper Company*.

Dames & Moore, 1981b. *Licensing Documentation Volume X—Below-Grade Seepage, Bluewater Mill Near Grants, New Mexico*, prepared for Anaconda Copper Company, August.

Dames & Moore, 1981c. *Licensing Documentation Volume IX—Tailings Management, Bluewater Mill near Grants, New Mexico*, prepared for Anaconda Copper Company, September.

Dames & Moore, 1984a. *Report, Ground Water Study, Above-Tailings Impoundment, Bluewater Mill and Vicinity Near Grants, New Mexico*, prepared for Anaconda Minerals Company, October.

Dames & Moore, 1984b. *Response to Questions Expressed in the Environmental Improvement Division Letter of April 24, 1984, Concerning the Proposed Discharge Plan for the Above-Grade Tailings Impoundment, Bluewater Mill*, Licensing Documentation, Volume 22, prepared for Anaconda Minerals Company, November.

Dames & Moore, 1986a. *Ground Water Model, Above-Grade Tailings Impoundment, Bluewater Mill and Vicinity, Near Grants, New Mexico*, prepared for Anaconda Minerals Company, Job No. 4010-091-06, March.

Dames & Moore, 1986b. *Ground Water Quality Review, Bluewater Mill and Vicinity Near Grants, New Mexico, prepared for Anaconda Minerals Company*, Job No. 4010-096-18.

Dillinger, J.K., 1990. "Geologic map of the Grants 30′ × 60′ Quadrangle, west-central New Mexico," U.S. Geological Survey Coal Investigations Map C-118-A, scale 1:100,000.

DOE (Department of Energy), 1997. *Long-Term Surveillance Plan for the DOE Bluewater (UMTRCA Title II) Disposal Site Near Grants, New Mexico*, Grand Junction Office, Grand Junction, Colorado, July.

DOE (U.S. Department of Energy), 2012. *Shiprock, New Mexico, Disposal Cell Internal Water Balance and Cell Conditions*, LMS/SHP/S08254, Office of Legacy Management, Grand Junction, Colorado, September.

DOE (U.S. Department of Energy), 2014. *Water-Balance Assessment for the Bluewater Main Tailings Impoundment and Disposal Cell, Bluewater, New Mexico*, LMS/BLU/S10666, Office of Legacy Management, Grand Junction, Colorado, June.

Domenico, P.A., 1987. "An analytical model for multidimensional transport of a decaying contaminant species," *Journal of Hydrology,* 91(1-2):49–58.

Domenico, P.A., and V.V. Palciauskas, 1982. "Alternative Boundaries in Solid Waste Management," *Ground Water*, 20(3):303–311.

Domenico, P.A., and G.A. Robbins, 1985. "A New Method of Contaminant Plume Analysis," *Ground Water*, 23(4):476–485.

Domenico, P.A., and F.W. Schwartz, 1998. *Physical and Chemical Hydrogeology*, John Wiley and Sons Inc.

Dong, W., and S.C. Brooks, 2006. "Determination of the formation constants of ternary complexes of uranyl and carbonate with alkaline earth metals (MG^{2+}, Ca^{2+}, Sr^{2+}, and Ba^{2+}) using anion exchange method," *Environmental Science Technology*, 40:4689–4695.

Dunbar, N.W., and F.M. Phillips, 2004. "Cosmogenic ^{36}Cl ages of lava flows in the Zuni-Bandera volcanic field, north-central New Mexico, U.S.A.," in *Tectonics, Geochronology, and Volcanism in the Southern Rocky Mountains and Rio Grande Rift*," Cather, S., W.C. McIntosh, and S.A. Kelly, eds., New Mexico Bureau of Geology and Mineral Resources Bulletin 160, pp 309–317.

EPA (U.S. Environmental Protection Agency), 2011. *Third Five-Year Review Report, Homestake Mining Company Superfund Site (EPA ID: NMD007860935), Cibola County, New Mexico*, September.

Falta, R.W., M.B. Stacy, A.N.M. Ahsanuzzaman, M.Wang, and R.C. Earle, 2007. *REMChlor, Remediation Model for Chlorinated Solvents*, User's Manual, Version 1.0. U.S. Environmental Protection Agency, http://www.epa.gov/ada/csmos/models/remchlor.html, accessed October 31, 2014.

Freeze, R.A., and J.A. Cherry, 1979. *Groundwater*, Prentice-Hall Inc.

Frenzel, P.F., 1992. *Simulation of ground-water flow in the San Andres-Glorieta aquifer in the Acoma embayment and eastern Zuni uplift, west-central New Mexico*, U.S. Geological Survey Water Resources Investigations Report 91-4099, 381 pp.

Glenn, E.D., and W.J. Waugh, 2001. *Disposal Cell Cover Moisture Content and Hydraulic Conductivity, Long-Term Surveillance and Maintenance Program Shiprock, New Mexico, Site*, GJO-2001-204-TAR, U.S. Department of Energy Grand Junction Office, Grand Junction, Colorado.

Goode, D.J., and L.F. Konikow, 2000. "Apparent dispersion in transient groundwater flow," *Water Resources Research*, 26(10): 2339–2351.

Gordon, E.D., H.D. Reeder, and J.L. Kunkler, 1960. *Geology and ground-water resources of the Grants-Bluewater area, Valencia County, New Mexico*, U.S. Geological Survey Open File Report.

Gordon, E.D., 1961. "Geology and ground-water resources of the Grants-Bluewater area, Valencia County, New Mexico," with a section on aquifer characteristics, by H. L. Reeder, and with a section on chemical quality of the ground water, by J. L. Kunkler, New Mexico Office of the State Engineer Technical Report 20, 109 pp.

Guillaumont, R., T. Fanghanel, V. Neck, J. Fuger, D.A. Palmer, I. Grenthe, and M.H. Rand, 2003. *Update on the Chemical Thermodynamics of Uranium, Neptunium, Plutonium, Americium and Technicium*, Mompean, M., and others, eds., Nuclear Energy Agency, Elsevier, Amsterdam, 918 pp.

Hackman, R.J., and A.B. Olson, 1977. "Geology, structure, and uranium deposits of the Gallup 1°× 2° Quadrangle, New Mexico and Arizona," U.S. Geological Survey Map I-981, scale 1:250,000.

Harleman, D.R., and R.R. Rumer, 1963. "Longitudinal and lateral dispersion in an isotropic porous medium," *Journal of Fluid Mechanics*, 16:385–394.

Heckert, A.B., and S.G. Lucas, 2003. "Triassic stratigraphy in the Zuni Mountains, west-central New Mexico," in *Geology of the Zuni Plateau*, Lucas, S.G., and others, eds., New Mexico Geological Society Guidebook 54, pp 245–262.

Hem, J.D., 1986. *Study and Interpretation of the Chemical Characteristics of Natural Water (third edition)*, U.S. Geological Survey Water-Supply Paper 2254, Alexandria, Virginia, 263 pp.

HMC (Homestake Mining Company of California), 2012. *Grants Reclamation Project, Updated Corrective Action Program (CAP)*, prepared for the U.S. Nuclear Regulatory Commission, NRC Radioactive Material License SUA-1471.

HMC and Hydro-Engineering, 2009. *2008 Annual Monitoring Report/Performance Review for Homestake's Grants Project Pursuant to NRC License SUA-1471 and Discharge Plan DP-200*, prepared for the U.S. Nuclear Regulatory Commission and New Mexico Environment Department, March.

HMC and Hydro-Engineering, 2013. *2012 Annual Monitoring Report/Performance Review for Homestake's Grants Project Pursuant to NRC License SUA-1471 and Discharge Plan DP-200*, prepared for U.S. Nuclear Regulatory Commission and New Mexico Environment Department, March.

HMC and Hydro-Engineering, 2014. *2013 Annual Monitoring Report/Performance Review for Homestake's Grants Project Pursuant to NRC License SUA-1471 and Discharge Plan DP-200*, prepared for U.S. Nuclear Regulatory Commission and New Mexico Environment Department, March.

Huntoon, P.W., 1995. "Is it appropriate to apply porous media groundwater circulation models to karstic aquifers?" *Groundwater Models for Resources Analysis and Management,* A.I. El-Kadi, ed., Lewis Publishers, Boca Raton, Florida, pp 339–358.

Hydro-Engineering (Hydro-Engineering LLC), 1999. *Ground-Water Monitoring and Performance Review for Homestake's Grants Project, NRC License SUA-1471 and Discharge Plan DP-200, 1998*, prepared for Homestake Mining Company of California, March.

Hydro-Search (Hydro-Search Inc.), 1977. *Hydrogeology of the Bluewater Mill Tailings Pond Area, Valencia County, New Mexico,* Consultant's report to Anaconda Copper Company, 111 pp.

Hydro-Search (Hydro-Search Inc.), 1978. *Supplement to the hydrogeology report of October 17, 1977, Bluewater Mill area, Valencia County, New Mexico*, consultant's report to Anaconda Copper Company, November, 69 pp.

Hydro-Search (Hydro-Search Inc.), 1981a. *Regional Ground-Water Hydrology and Water Chemistry, Grants- Bluewater Area, Valencia County, New Mexico*, consultant's report to Anaconda Copper Company, June.

Hydro-Search (Hydro-Search Inc.), 1981b. *Licensing Documentation Volume IV—Ground-water Hydrology in the Vicinity of Anaconda Copper Company's Bluewater Mill, Valencia County, New Mexico*.

Kamp, Susan D., and Stan J. Morrison, 2014. "Use of Chemical and Isotopic Signatures to Distinguish Between Uranium Mill-Related and Naturally Occurring Groundwater Constituents," *Groundwater Monitoring and Remediation*, 34(1):68–78, Winter.

Karanovic, M., C.J. Neville, and C.B. Andrews, 2007. "BIOSCREEN-AT: BIOSCREEN with an Exact Analytical Solution," *Ground Water,* 45(2):242–245.

Kigoshi, K., 1971. "Alpha-recoil thorium-234: dissolution into water and the uranium-234/uranium-238 disequilibrium in nature," *Science*, 173:47–48.

Langman, J.B., J.E. Sprague, and R.A. Durall, 2012. *Geologic Framework, Regional Aquifer Properties (1940s–2009), and Spring, Creek, and Seep Properties (2009–2010) of the Upper San Mateo Creek Basin near Mount Taylor, New Mexico*, Scientific Investigations Report 2012-5019.

Laughlin, W.A., F.V. Perry, P.E. Damon, M. Shafiqullah, G. WoldeGabriel, W. McIntosh, C.D. Harrington, S.G. Wells, and P.G. Drakos, 1993. "Geochronology of Mount Taylor, Cebollita Mesa, and Zuni-Bandera volcanic fields, Cibola County, New Mexico," *New Mexico Geology*, 15:81–92.

Leij, F.J., and S.A. Bradford, 1994. *3DADE: A Computer Program for Evaluating Three-Dimensional Equilibrium Solute Transport in Porous Media*, U.S. Salinity Laboratory, Agricultural Research Service, U.S. Department of Agriculture, Research Report No. 134, 81 pp.

Link, S.O., W.J. Waugh, and J.L. Downs, 1994. "The role of plants on isolation barrier systems," in *In-Situ Remediation: Scientific Basis for Current and Future Technologies,* G.W. Gee and N.R. Wing, eds., Battelle Press, Columbus, Ohio.

Longmire, P.A., B.M. Thomson, and D.G. Brookins, 1984. "Uranium industry impacts on groundwater in New Mexico," in *Selected papers on water quality and pollution in New Mexico: proceedings of a symposium on water quality and pollution in New Mexico*, W.J. Stone, compiler, April 12, 1984, Socorro, New Mexico, New Mexico Bureau of Mines and Mineral Resources Hydrologic Report 7, pp 167–183.

Lucas, S.G., and S.N. Hayden, 1989. "Triassic stratigraphy of west-central New Mexico," in *Southeastern Plateau*, O.J. Anderson and others, eds., New Mexico Geological Society Guidebook 40, pp 191–211.

Mahoney, J.J., S.A. Cadle, and R.T. Jakubowski, 2009. "Uranyl adsorption onto hydrous ferric oxide—a reevaluation for the diffuse layer model database," *Environmental Science Technology*, 43(24):9260–9266.

Mason, B., and C.B. Moore, 1982. *Principles of Geochemistry*, Fourth Edition, John Wiley & Sons, New York, 344 pp.

Maxwell, C.H., 1986. "Geologic map of El Malpais lava field and surrounding areas, Cibola County, New Mexico," U.S. Geological Survey Miscellaneous Investigations Series Map I-1595, scale 1:62,500.

Merritt, R.C., 1971. *The Extractive Metallurgy of Uranium*, Colorado School of Mines Research Institute, prepared under contract with the U.S. Atomic Energy Commission, pp. 391 and 422.

NMED (New Mexico Environment Department), 2010. *Geochemical analysis and interpretation of ground water data collected as part of the Anaconda Company Bluewater Uranium Mill Site Investigation and San Mateo Creek Site Legacy Uranium Sites Investigation, McKinley and Cibola County, New Mexico* (Draft for public review released May 2010), Albuquerque, New Mexico, New Mexico Environment Department, 128 pp.

NRC (U.S. Nuclear Regulatory Commission), 1990. *Staff Technical Position Design of Erosion Protection Covers For Stabilization of Uranium Mill Tailings Sites*, Rockville, Maryland.

NRC (U.S. Nuclear Regulatory Commission), 2011. *Engineered Covers for Waste Containment: Changes in Engineering Properties and Implications for Long-Term Performance Assessment*, NUREG CR/7028, Washington, DC.

Otton, J.K., 2011. *Annotated Bibliography of Environmentally Relevant Investigations of Uranium Mining and Milling in the Grants Mineral Belt, Northwestern New Mexico*, U.S. Geological Survey, Open-File Report 2011-1140.

Otton, J.K., R.A. Zielinski, and R.J. Horton, 2010. *Geology, Geochemistry, and Geophysics of the Fry Canyon Uranium/Copper Project Site, Southeastern Utah—Indications of Contaminant Migration*, U.S. Geological Survey, Scientific Investigations Report 2010-5075.

Parkhurst, D.L., and C.A.J. Appelo, 2013. Description of input and examples for PHREEQC version 3—A computer program for speciation, batch-reaction, one-dimensional transport, and inverse geochemical calculations: U.S. Geological Survey Techniques and Methods, book 6, chap. A43, 497 p., available only at http://pubs.usgs.gov/tm/06/a43, accessed October 31, 2014.

Rawling, G.C., 2012. "Geologic map of the Milan Quadrangle, Cibola County, New Mexico," New Mexico Bureau of Geology and Mineral Resources Open-File Geologic Map 231, scale 1:24,000.

Rawling, G.C., 2013. "Geologic map of the Bluewater Quadrangle, McKinley and Cibola Counties, New Mexico," New Mexico Bureau of Geology and Mineral Resources Open-File Geologic Map 236, scale 1:24,000.

Sims, K.W.W., R.P. Ackert Jr., F.C. Ramos, R.A. Sohn, M.T. Murrell, and D.J. DePaolo, 2007. "Determining eruption ages and erosion rates of Quaternary basaltic volcanism from combined U-series disequilibria and cosmogenic exposure ages," *Geology*, 35:471–474.

SRNL (Savannah River National Laboratory), 2014. *Independent Technical Review and Qualitative Risk Assessment of the Department of Energy Office of Legacy Management Bluewater UMTRCA Site*, SRNL-STI-2014-00100, March.

Thaden, R.E., and E.J. Ostling, 1967. "Geologic map of the Bluewater Quadrangle, Valencia and McKinley Counties, New Mexico," U.S. Geological Survey Map GQ-679, scale 1:24,000.

Thaden, R.E., E.S. Santos, and E.J. Ostling, 1967a. "Geologic map of the Dos Lomas Quadrangle, Valencia and McKinley Counties, New Mexico," U.S. Geological Survey Map GC-680, scale 1:24,000.

Thaden, R.E., E.S. Santos, and O.B. Raup, 1967b. "Geologic map of the Grants Quadrangle, Valencia County, New Mexico," U.S. Geological Survey Map GQ-681, scale 1:24,000.

Timmons, J.M., and C.T. Cikoski, 2012. "Geologic map of the San Rafael Quadrangle, Cibola County, New Mexico," New Mexico Bureau of Geology and Mineral Resources Open-File Geologic Map 232, scale 1:24,000.

USGS (U.S. Geological Survey), 2014. "Water Quality Samples for the Nation," National Water Information System, U.S. Geological Survey website, http://nwis.waterdata.usgs.gov/usa/nwis, accessed October 31, 2014.

Waugh, W.J., G.M. Smith, B. Danforth, G.W. Gee, V. Kothari, and T. Pauling, 2007. "Performance Evaluation of the Engineered Cover at the Lakeview, Oregon, Uranium Mill Tailings Site," *Proceedings of Waste Management 2007 Symposium*, Tucson, Arizona.

Waugh, W.J., S.J. Morrison, G.M. Smith, M. Kautsky, T.R. Bartlett, C.E. Carpenter, and C.A. Jones, 1999. *Plant Encroachment on the Burrell, Pennsylvania, Disposal Cell: Evaluation of Long-Term Performance and Risk*, GJO-99-96-TAR, U.S. Department of Energy, Grand Junction, Colorado.

Waugh, W.J., C.H. Benson, and W.H. Albright, 2009. "Sustainable covers for uranium mill tailings, USA: Alternative design, performance, and renovation," *Proceedings of 12th International Conference on Environmental Remediation and Radioactive Waste Management*, Liverpool, United Kingdom.

West, S.W., 1972. *Disposal of Uranium-Mill Effluent by Well Injection in the Grants Area, Valencia County, New Mexico*, prepared in cooperation with the New Mexico Office of the State Engineer and the U.S. Atomic Energy Commission, Geological Survey Professional Paper 386-D.

White, W.D., and T.E. Kelly, 1989. The San Andres-Glorieta Aquifer in West-Central New Mexico, in *New Mexico Geological Society Guidebook, 40th Field Conference, Southeast Colorado Plateau*, pp 331–335.

Worthington, S.R.H., and D.C. Ford, 2009. "Self-Organized Permeability in Carbonate Aquifers," *Ground Water,* 47(3):326–336.

Wyant, D.J., and A. Olson, 1978. "Preliminary geologic map of the Albuquerque 1° × 2° Quadrangle, New Mexico," U.S. Geological Survey Open-File Report 78-467, scale 1:250,000.

Zeiglar, K.E., C.T. Cikowski, P.G. Drakos, and J. Riesterer, 2012. "Geologic map of the Grants Quadrangle, Cibola County, New Mexico," New Mexico Bureau of Geology and Mineral Resources Open-File Geologic Map 224, scale 1:24,000.

Zielinski, R.A., D.T. Chafin, E.R. Banta, and B.J. Szabo, 1997. Use of ^{234}U and ^{238}U isotopes to evaluate contamination of near-surface groundwater with uranium-mill effluent: a case study in south-central Colorado, U.S.A., *Environmental Geology*, 32(2):124–136.

Zimmerman, R.W., G. Chen, and T. Hadgu, 1993. "A numerical dual-porosity model with semianalytical treatment of fracture/matrix flow," *Water Resources Research*, 29:2127–2137.

Appendix A

Water-Balance Assessment for the Bluewater Main Tailings Impoundment and Disposal Cell, Bluewater, New Mexico

This page intentionally left blank

LMS/BLU/S10666

Water-Balance Assessment for the Bluewater Main Tailings Impoundment and Disposal Cell Bluewater, New Mexico

June 2014

U.S. DEPARTMENT OF ENERGY | Legacy Management

This page intentionally left blank

LMS/BLU/S10666

Water-Balance Assessment for the Bluewater Main Tailings Impoundment and Disposal Cell Bluewater, New Mexico

June 2014

This page intentionally left blank

Contents

Abbreviations iii
Executive Summary v
1.0 Purpose of Assessment 1
2.0 Site Description 3
2.1 Site Description and History 3
2.2 Site Hydrogeology 3
2.2.1 Geology 3
2.2.2 Groundwater Hydrology 9
2.3 Historical Groundwater Issues 10
2.4 Groundwater Monitoring by DOE 10
2.4.1 Required Monitoring 10
2.4.2 Alluvial Aquifer 11
2.4.3 San Andres Aquifer 11
2.5 Source of Contamination 12
3.0 Milling History 15
3.1 General Description 15
3.2 Milling Operations 15
3.3 Tailings Disposal History 15
3.4 Main Tailings Impoundment Seepage 17
4.0 Disposal Cell Cover Characteristics 21
4.1 Cell Cover Design and Construction 21
4.2 Depressions on the Disposal Cell Cover 22
4.2.1 Cover Topography 22
4.2.2 Cover Radon Flux 23
4.2.3 Cover Stability 24
4.3 Cell Cover Evolution 24
4.4 Cover Hydraulic Performance 30
5.0 Disposal Cell Seepage 31
5.1 Conditions for Seepage 31
5.2 Seepage Rate 31
5.3 Seepage Quantity 32
5.3.1 Water-Balance Equation 32
5.3.2 Inflow 32
5.3.3 Change in Storage 34
5.3.4 Outflow 36
6.0 Groundwater Contamination 41
6.1 Contaminant Mass 41
6.2 Alluvial Aquifer 42
6.3 San Andres Aquifer 44
6.3.1 Northeast Portion of Site 44
6.3.2 Southeast Portion of Site 45
7.0 Conclusions 47
8.0 Uncertainties 49
9.0 References 53

Figures

Figure 1. Bluewater, New Mexico, UMTRCA Title II Disposal Site 4
Figure 2. Geologic Map of the Bluewater Disposal Site 5
Figure 3. Geologic Cross Section A–A′..... 6
Figure 4. Geologic Cross Section B–B′ 7
Figure 5. Approximate Distribution of Materials Within the Main Tailings Impoundment 16
Figure 6. Schematic of the Tailings Impoundment Water Cycle..... 19
Figure 7. Estimated Cumulative Seepage from the Main Tailings Impoundment Through 1995 20
Figure 8. Ponds in Depressions on the Main Tailings Disposal Cell in August 2012,..... 23
Figure 9. Topographic Map of the Main Tailings Disposal Cell (July 2012 LiDAR Survey Data) 25
Figure 10. Projected Maximum Area to Date of Ponded Water on the Main Tailings Disposal Cell (July 2012 LiDAR Survey Data)..... 26
Figure 11. Radon Flux Measurement Locations in the Area of Depressions (July 2013)..... 27
Figure 12. Radon Measurement Location RF-05 in the Area of Cell Cover Depressions 29
Figure 13. Hydrographs for Alluvial Aquifer Wells T(M) and X(M) 39
Figure 14. Hydrographs for San Andres Aquifer Wells OBS-3 and S(SG) 40

Tables

Table 1. Estimated Saturated Hydraulic Conductivities for the Bluewater Disposal Cell 32
Table 2. Precipitation and Evaporation in the Region of the Bluewater Site 33
Table 3. Unsaturated Tailings Hydraulic Parameters Based on Shiprock, New Mexico, Disposal Cell Data 34
Table 4. Long-Term Volumetric Moisture Contents at Estimated Influx Rates..... 35
Table 5. Estimated Storage Volumetric Moisture Content..... 35
Table 6. Required Tailings Depth Needed for Storage of Infiltration 35
Table 7. Footprint of Tailings Materials 36
Table 8. Estimated Drainable Volume from the Disposal Cell (Low-Permeability Cover)..... 36
Table 9. Estimated Drainable Volume from the Disposal Cell (High-Permeability Cover) 37
Table 10. Potential Annual Outflow if the Tailings Become Saturated 37
Table 11. Estimated Seeped Contaminant Mass Prior to Disposal Cell Completion 41
Table 12. Uncertainties and Their Effects on Conclusions..... 50

Appendixes

Appendix A Bluewater Main Tailings Impoundment Seepage and Fluid Chemistry
Appendix B Bluewater Main Tailings Disposal Cell Configuration
Appendix C Bluewater Main Tailings Disposal Cell Material Hydraulic Properties

Abbreviations

ACL	alternate concentration limit
Anaconda	Anaconda Copper Company
ARCO	Atlantic Richfield Company
cm	centimeters
cm/s	centimeters per second
ΔS	change in storage
DOE	U.S. Department of Energy
ft	feet
gpm	gallons per minute
LiDAR	light detection and ranging
LTSP	Long-Term Surveillance Plan
mg/L	milligrams per liter
NMED	New Mexico Environment Department
NRC	U.S. Nuclear Regulatory Commission
PCBs	polychlorinated biphenyls
pCi/m^2s	picocuries per square meter per second
POC	point of compliance
POE	point of exposure
UMTRCA	Uranium Mill Tailings Radiation Control Act

This page intentionally left blank

Executive Summary

The Bluewater, New Mexico, uranium mill operated from 1953 to 1982. Site reclamation was completed in 1995 and included encapsulating the main tailings impoundment in place in an engineered, rock-covered disposal cell. The U.S. Department of Energy (DOE) acquired the site in 1997. The Bluewater cell is the largest disposal cell currently managed by DOE.

Site groundwater monitoring conducted by DOE has indicated that uranium concentrations exceed groundwater standards in the two uppermost aquifers at the site. DOE is evaluating the source of the contamination and the potential risk to downgradient groundwater users. This assessment is intended to provide an understanding of how much mill processing fluid and contaminant mass drained from the main tailings impoundment prior to completion of the disposal cell, and if the tailings in the disposal cell are a continuing source of contamination.

Atlantic Richfield Company (ARCO), the former licensee, estimated that approximately 5.7 billion gallons of tailings fluid seeped through the bottom of the main tailings impoundment prior to construction of the disposal cell cover in 1995; about half of that total was projected to have occurred prior to 1960. These fluids entered the two uppermost aquifers at the site—an alluvial aquifer beneath basalt lava flows, and the deeper San Andres aquifer. ARCO expended a considerable effort to dewater the tailings before completing the disposal cell, so the volume of tailings liquor available for continued seepage was significantly reduced.

Tailings fluids, consisting of a less-contaminated mixture of the remaining tailings liquor and precipitation that has percolated through the cover materials, are seeping from the disposal cell and may continue to do so indefinitely. Projected maximum estimates for annual seepage, based on saturated conditions within the cell and a potential upper limit of 50 percent of precipitation percolating through the cell cover, are substantially less than 1 percent of the total seepage that occurred prior to 1995. However, current seepage appears to be minimal because decreasing water levels and steady-state contaminant concentrations in the aquifers are not indicative of the maximum estimated rate. It is unlikely, therefore, that the tailings are saturated at this time, and hydraulic properties of the cover materials may not have changed enough to allow the maximum projected precipitation infiltration. An increase in vegetation on the cell cover is expected to keep infiltration rates low due to evapotranspiration, which would keep seepage rates low.

Nearly 1 million pounds of uranium may have been present in the tailings fluids that seeped from the main tailings impoundment. Monitoring of the aquifers by ARCO indicated neutralization of the acidic tailings fluids and substantial reduction of contaminant concentrations in groundwater in the area adjacent to the tailings impoundment. These precipitated and adsorbed contaminants presumably formed a mineralized zone in the aquifer materials under the disposal cell. This assumed mineralized zone, rather than seepage from the cell, is suspected to be the main continuing source of groundwater contamination.

Depressions have formed on the disposal cell cover because the clay-rich (“slimes”) portion of the impounded tailings continued to consolidate after the cover was completed. Precipitation runoff water forms ponds in these depressions, potentially introducing a second source of fluids infiltrating through the disposal cell. However, observations of the persistence of the ponds and the results of radon flux measurements indicate that there has been no reduction in the performance of the radon barrier and that the pond volumes are reduced primarily through evaporation rather than infiltration. Therefore, the ponds are not causing additional seepage from the cell.

This assessment found no evidence to suggest that the elevated uranium concentrations in onsite wells indicate a new pulse of seepage or contamination from within the disposal cell or from ponding on the cell. Uncertainties associated with the water balance and contaminant mass estimates do not negate the primary conclusion that the volume of fluid and mass of contaminants that might seep from within the cell since it was constructed are very small compared to the volume and mass that seeped through the bottom of the tailings impoundment prior to cell construction.

1.0 Purpose of Assessment

The U.S. Department of Energy (DOE) Office of Legacy Management manages the Bluewater, New Mexico, Uranium Mill Tailings Radiation Control Act (UMTRCA) Title II Disposal Site. The site is located in Cibola County (formerly Valencia County) in west-central New Mexico. DOE manages the site in accordance with a Long-Term Surveillance Plan (LTSP), approved by the U.S. Nuclear Regulatory Commission (NRC), to ensure protection of human health and the environment. Requirements of the LTSP (DOE 1997) include verifying that the disposal cell functions as designed and that groundwater meets approved quality standards.

Site groundwater monitoring conducted by DOE has indicated that uranium concentrations exceed groundwater standards in the two uppermost aquifers at the site. DOE is evaluating the source of the contamination and the potential risk to downgradient groundwater users. This assessment is part of that evaluation and is intended to provide an understanding of how much mill processing fluid and contaminant mass entered the aquifers prior to completion of the disposal cell, and if the disposal cell is a continuing source of contamination.

A uranium mill operated at the site for 30 years, processing ore from offsite mines in the region. The site was reclaimed, and the two tailings impoundments at the site were encapsulated as the carbonate tailings and main tailings disposal cells. The two uppermost aquifers at the site have uranium concentrations substantially above background concentrations. It has been assumed that the contamination of the aquifers occurred during milling operations and prior to tailings impoundment encapsulation. However, the performances of the disposal cells have come into question because of increasing uranium concentrations in a site monitoring well and the development of depressions that collect precipitation runoff on the main tailings disposal cell cover.

The former licensee recognized that substantial quantities of tailings fluids leaked through the bottom of the main tailings impoundment and into the underlying aquifers. Therefore, this assessment focuses on the main tailings impoundment and subsequent disposal cell. Most of the tailings generated during mill operations were deposited in this impoundment, and most of the impoundment performance and groundwater-related research conducted by the former licensee dealt with this impoundment.

Although significant quantities of tailings fluids were injected into a deep well in the northeast portion of the site, and later collected in large evaporation ponds north of the main tailings pond, these features are not addressed in this assessment. The injection well was located more than a mile northeast of the main tailings impoundment, and the tailings fluids were injected into a formation underlying the site aquifer of concern (the San Andres aquifer). A former monitoring well that was located near the injection well was sampled by the mill operator and indicated contamination of the San Andres aquifer; however, the magnitude of upward leakage into the San Andres aquifer and the extent of contamination were not evaluated at the time. The potential impacts of the deep-well injection process on the San Andres aquifer will be addressed in a groundwater conceptual model being developed by DOE. The evaporation ponds, constructed northeast of the main tailings impoundment, were lined and therefore were not considered to be a significant source of seepage. Furthermore, the native materials under the pond locations are not in direct contact with the aquifers.

This page intentionally left blank

2.0 Site Description

2.1 Site Description and History

The Bluewater site, approximately 9 miles northwest of Grants, New Mexico, is the location of a former uranium-ore processing site that operated from 1953 to 1982. The uranium mill was constructed and operated by the Anaconda Copper Company (Anaconda). In 1977, Anaconda was acquired by the Atlantic Richfield Company (ARCO).

Milling operations created radioactive mill tailings that were stored in two onsite tailings impoundments. ARCO began decommissioning the mill in 1989 and began site reclamation in accordance to a plan (ARCO 1990) approved by NRC. By 1995, all mill tailings, contaminated soils, demolished mill structures, and contaminated vicinity property materials were encapsulated in six onsite disposal areas (ARCO 1996). Mill tailings were capped in place in two locations, referred to as the carbonate tailings disposal cell and the main tailings disposal cell. Responsibility for the site was transferred to DOE in 1997. The site, shown in Figure 1, is administered under the provisions of an NRC general license.

The most significant site feature is the main tailings disposal cell. The completed disposal cell covers an area of 354 acres, and the enclosed original tailings impoundment has a footprint of approximately 260 acres (two smaller extensions were added during site reclamation). An estimated 22.9 million tons of tailings are in the disposal cell, which makes it the largest disposal cell managed by DOE. The next largest cell is approximately 7.1 million tons at the Falls City, Texas, UMTRCA Title I Disposal Site.

2.2 Site Hydrogeology

2.2.1 Geology

Site geology plays a significant role in the groundwater contamination issues. Figure 2 shows a geologic map of the site. A large portion of the site's surface consists of basalt lava. A series of lava flows eventually filled the former channel of the Rio San Jose. The basalt, which covers alluvial sands and gravels of the former Rio San Jose, has an average thickness of approximately 100 feet (ft) at the site. The buried alluvium, ranging up to 25 ft in thickness, is partially saturated and comprises the uppermost aquifer at the site.

The remainder of the site surface is composed of a small outcrop of the Permian San Andres Limestone; shale, siltstone, and sandstone members of the Triassic Chinle Formation; and Quaternary alluvium consisting primarily of windblown sand, silt, and clay. The Permian Glorieta Sandstone formation underlies the San Andres Limestone and, therefore, does not crop out at the site. These two formations have a combined thickness of approximately 250 ft at the site.

Although deeply buried under most of the site, a portion of the San Andres Limestone is exposed on the surface because of the complex structural geology of the site. Two inactive but significant faults crisscross the site at an approximate 90 degree angle. The north-south fault, referred to regionally as the Ambrosia Lake Fault, tracks under the location of the main tailings disposal cell. The unnamed east-west-tracking fault crosses the Ambrosia Lake Fault beneath the southern end of the main tailings disposal cell. These faults are shown in Figure 2, and their projected subsurface configurations are shown in Figure 3 and Figure 4.

Figure 1. Bluewater, New Mexico, UMTRCA Title II Disposal Site

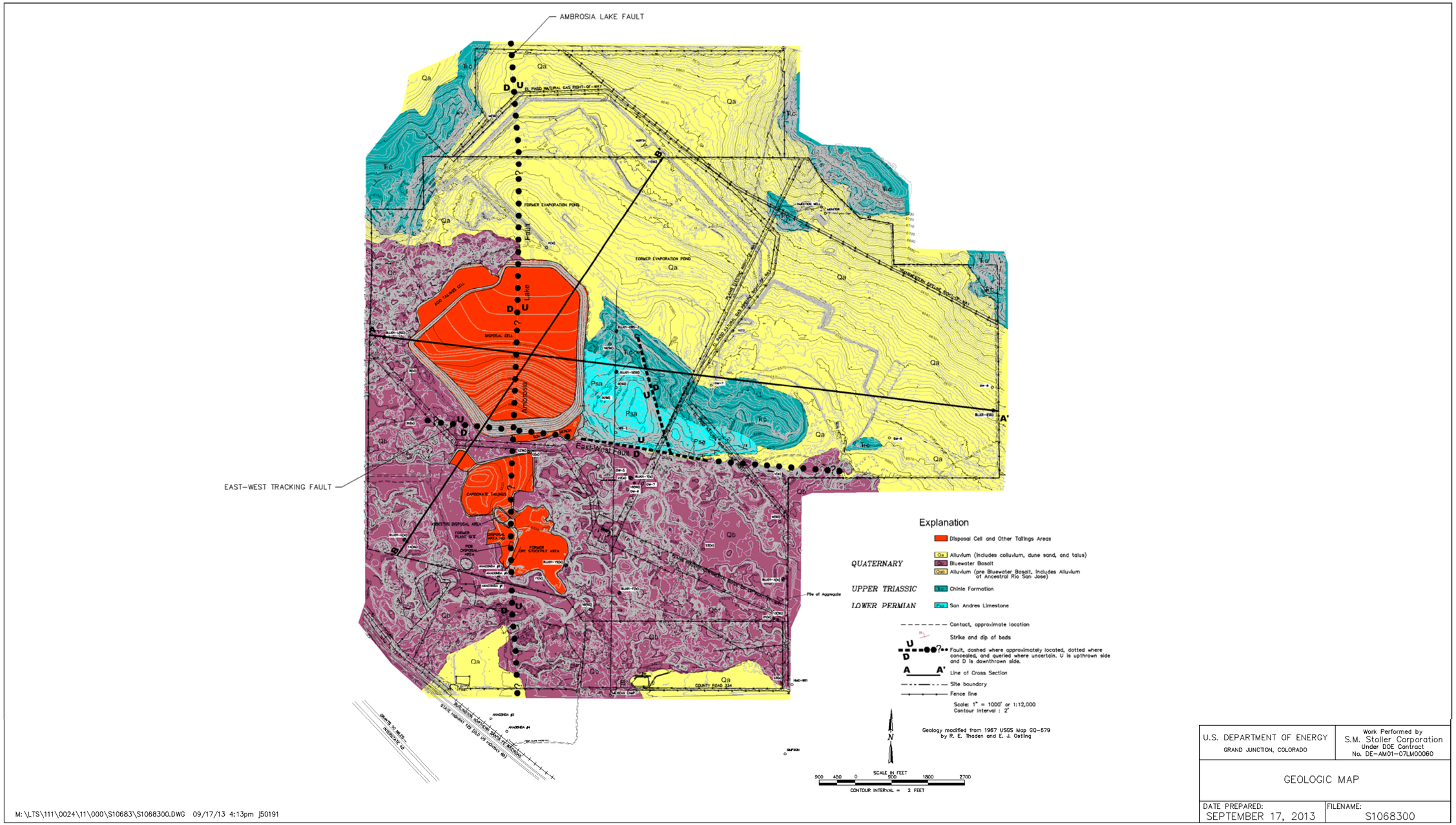

Figure 2. Geologic Map of the Bluewater Disposal Site

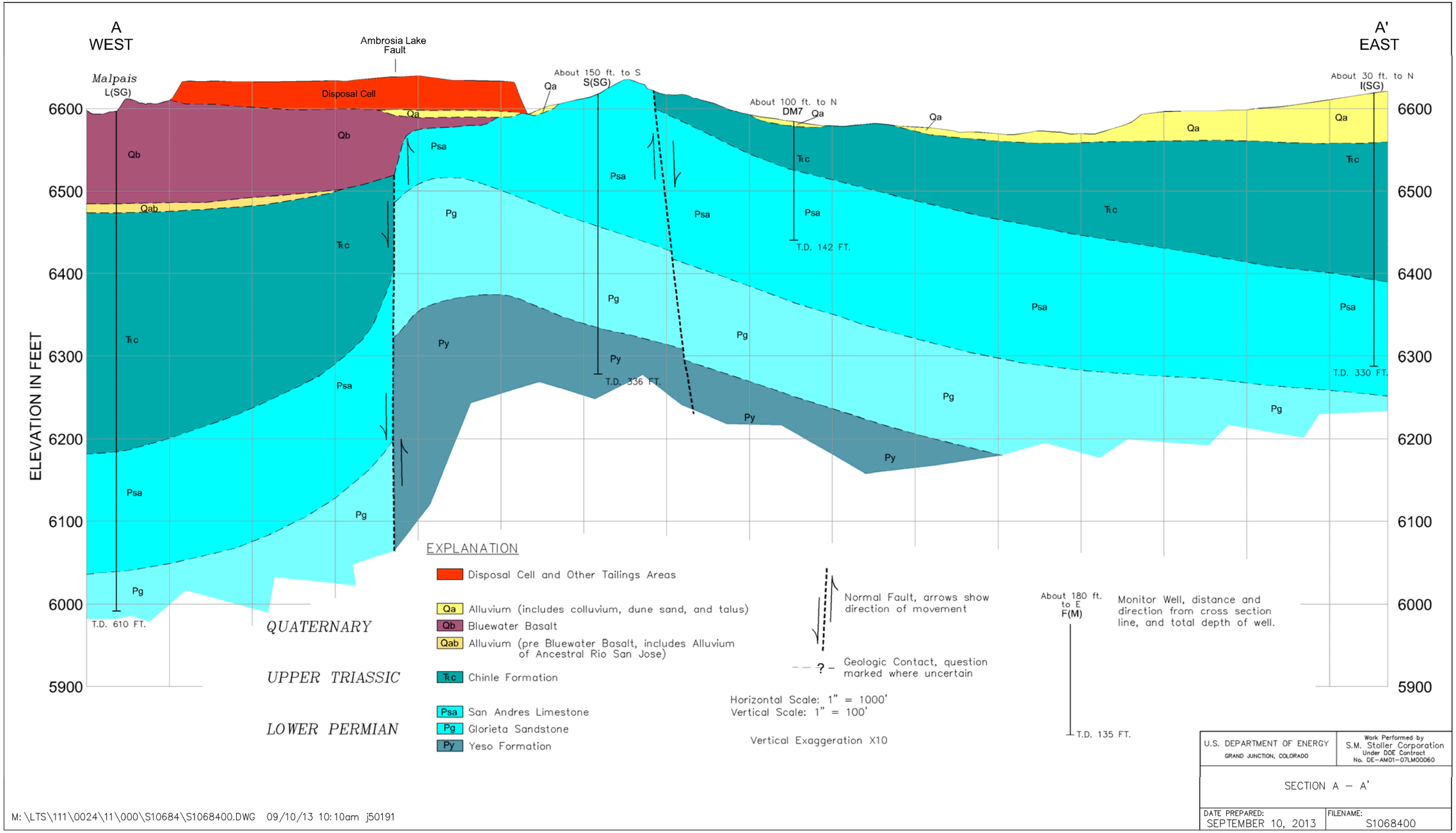

Figure 3. Geologic Cross Section A–A'

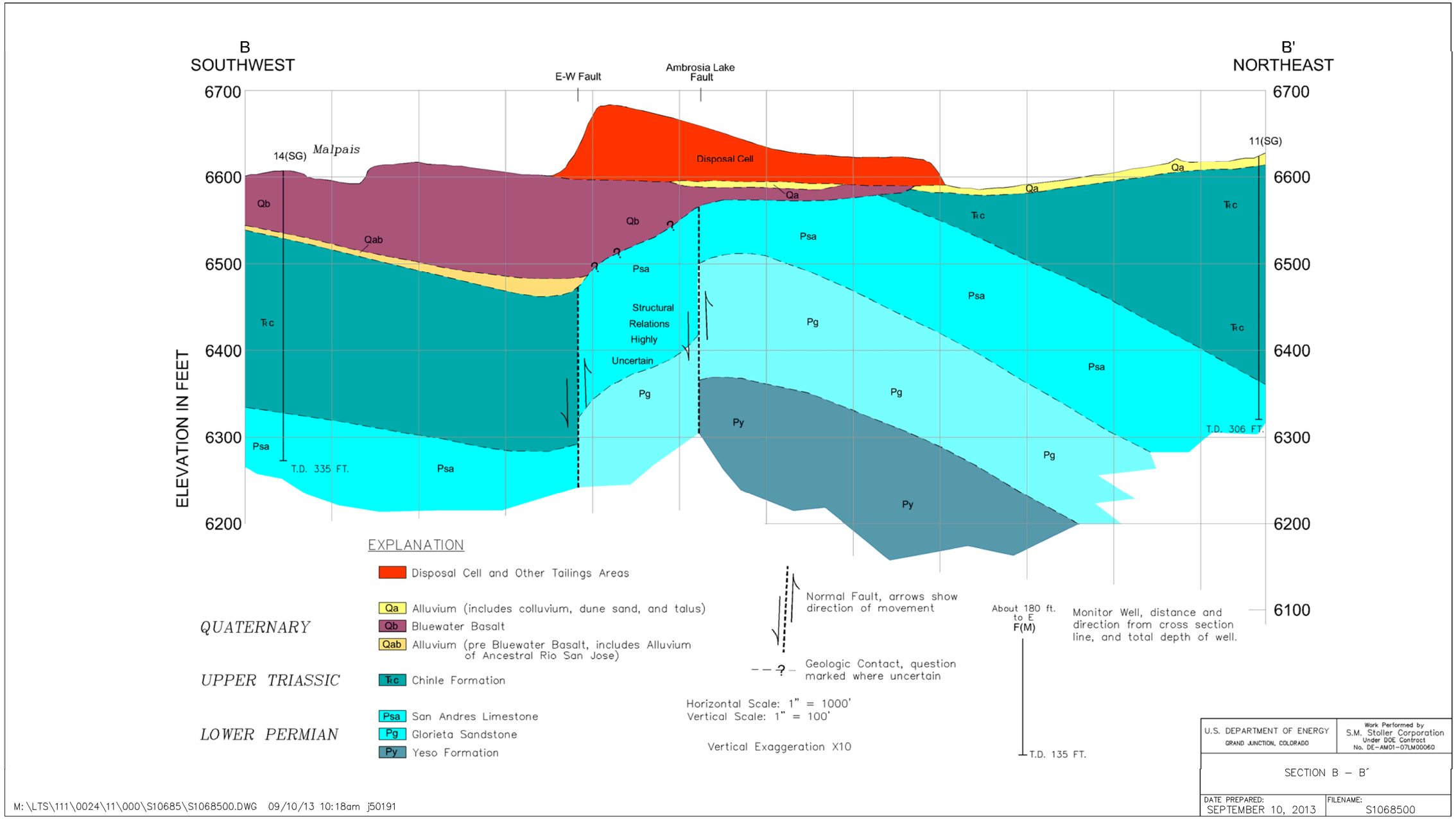

Figure 4. Geologic Cross Section B–B'

This page intentionally left blank

Regionally, the Permian- and Triassic-age formations dip in the northeast direction. This dip, however, is complicated by the faults at the site. The configuration of the faults has resulted in four fault blocks at the site. Surface geology and well completion records indicate that the northeast fault block had the greatest upward displacement, while the northwest block had the greatest downward displacement. Well completion records for wells L(SG) and S(SG) indicate that the relative vertical displacement between these two fault blocks is more than 400 ft. The relative vertical displacement between the northeast fault block and the southeast block is approximately 370 ft. The least displacement, of approximately 50 ft, occurred between the southeast and southwest fault blocks.

The faults do not act as sharp demarcations between the fault blocks. The formations on each side of the faults bent and dragged along the fault as represented in Figure 3 and Figure 4. A characteristic of faulted limestone and sandstone is the resultant zone of shattered rock along the fault (referred to as a fault zone). The shales and siltstones of the Chinle Formation, however, tend to mold like clay along fault zones.

2.2.2 Groundwater Hydrology

The surface Quaternary deposits, located in the northeast portion of the site, are dry and do not behave as an aquifer. Though some thin sandstone members of the lower Chinle Formation are in the subsurface of the site, this formation locally behaves as an aquitard above the underlying San Andres Limestone, and it is not considered to be an aquifer at the site.

The uppermost aquifer at the site is in the basalt-covered sand and gravel alluvium of the ancestral Rio San Jose. This alluvium ranges from dry to fully saturated at the site, depending on location. Because of the difficulty of drilling through the basalt lava and the risk of missing saturated portions of the alluvium, very few wells are completed in this aquifer near the site. The groundwater in this aquifer flows generally southeast across the south portion of the site along the path of the buried river valley.

A deeper aquifer was also contaminated at the site. Regionally and at the Bluewater site, the San Andres Limestone and Glorieta Sandstone formations form a single hydrologic unit referred to as the San Andres aquifer. Although it is confined by the overlying Chinle Formation (and, therefore, exhibits artesian pressure) under most of the site, the exposed portion of San Andres Limestone in the southwest corner of the northeast fault block (adjacent to the main tailings disposal cell) is dry. The San Andres Limestone was partially saturated during milling operations but has become dry at this location because of lowering groundwater elevations. The deeper Glorieta Sandstone portion of the aquifer is saturated at this location. Because of the northeast dip of the formations, the entire San Andres/Glorieta sequence exhibits saturated and artesian pressure conditions between the San Andres Limestone outcrop and the site boundary where the Chinle Formation behaves as a confining layer over the San Andres Limestone. ARCO concluded from San Andres aquifer tests using site wells that the east-west-tracking fault forms a hydraulic boundary that effectively divides the San Andres aquifer into two flow regimes.

The San Andres aquifer is the primary water supply source for municipal, commercial, irrigation, domestic, and livestock use in the region. Although the entire thickness of the aquifer produces groundwater, wells are usually completed in the upper 50 ft because of the high production rates that occur in that portion of the aquifer. The groundwater in this aquifer flows generally

east-southeast from the site. The Village of Milan, which uses groundwater from this aquifer, is the closest downgradient municipality (located about 5 miles southeast of the site). The Village of Bluewater, which also uses San Andres aquifer groundwater, is located southwest and upgradient of the site and would not be affected by site-related contamination.

2.3 Historical Groundwater Issues

As part of its reclamation plan, ARCO attempted to clean up the groundwater to background (upgradient) water quality but was unsuccessful because aquifer pumping did not reduce contaminant concentrations. Consequently, ARCO recommended setting alternate concentration limits (ACLs) for the mill-related contaminants that were showing concentrations higher than background concentrations (Applied Hydrology Associates Inc. 1990). NRC, the site regulator, approved ACLs for uranium of 0.44 milligram per liter (mg/L) for the alluvial aquifer point-of-compliance (POC) wells and 2.15 mg/L for the San Andres aquifer POC wells. The New Mexico drinking water standard for uranium at the time of site reclamation was 5 mg/L, so the approved ACLs were substantially below the state standard. The ACL for selenium is 0.05 mg/L for both aquifers. The alluvial aquifer also has an ACL for molybdenum, which is 0.10 mg/L. The ACLs were not expected to be exceeded at the POC wells.

ARCO's groundwater evaluations indicated that, although alluvial and San Andres aquifer groundwater near the main tailings disposal cell would remain contaminated with mill-related constituents, the contaminants would precipitate or otherwise attenuate to concentrations below New Mexico health-based concentration limits before the groundwater left the mill site boundary. In 2004, however, New Mexico adopted the U.S. Environmental Protection Agency drinking water standard for uranium of 0.03 mg/L, which is significantly below the prior standard of 5 mg/L that was in place when the ACLs were established.

Most of the tailings impoundment is north of the east-west-tracking fault. Because of the apparent hydraulic boundary caused by this fault, ARCO assumed that only the north portion of the San Andres aquifer was significantly affected by mill-related contamination. ARCO knew that contaminated groundwater had been drawn to their production wells south of the tailings impoundment, but assumed that incoming fresh water (from upgradient recharge) would mix with contaminated water and dilute contaminant concentrations to acceptable levels. Low uranium concentrations, ranging from 0.004 to 0.014 mg/L during the 1980s, in a downgradient private well supported this assumption (Sabre-Piñon well, currently known as HMC-951). Consequently, continued monitoring of the San Andres aquifer south of the fault was considered unnecessary, and no monitoring wells were left in that portion of the site.

2.4 Groundwater Monitoring by DOE

2.4.1 Required Monitoring

DOE inherited nine ARCO wells that were to be monitored in accordance with the LTSP. Groundwater is monitored at the site as part of DOE's goal to ensure protection of human health and the environment. When DOE began monitoring at the site in 1998, seven of the wells were to be sampled at specified intervals. Two point-of-exposure (POE) wells—one for each aquifer—located at the site boundary were to be monitored only if ACLs were exceeded in POC

wells. The LTSP does not specify concentration standards to be met at the POE wells. The original site monitoring wells are shown in Figure 1.

2.4.2 Alluvial Aquifer

The original alluvial aquifer monitoring well network consisted of background well E(M), POC wells F(M) and T(M), and POE well X(M). It also included well Y2(M) to monitor for polychlorinated biphenyls (PCBs) because of an upgradient PCB disposal cell. Concentrations of molybdenum and selenium have remained within the regulatory limits and do not show upward trends. However, uranium concentrations in alluvial POC well T(M) soon began to increase. The uranium concentration in this well exceeded the alluvial aquifer ACL of 0.44 mg/L in 2010. DOE notified NRC and the New Mexico Environment Department (NMED) of this occurrence in accordance with LTSP requirements.

DOE tried to sample POE well X(M) in 2008 in anticipation of the ACL being exceeded in well T(M); however, it was dry. Consequently, DOE installed new alluvial wells 21(M) and 22(M) in 2011 (Figure 1). Well 22(M) is located very close to the former location of ARCO well U(M), and 21(M) is located near the site boundary approximately the same distance from T(M) as is X(M). DOE conducted a downhole video examination of X(M) in 2012, which revealed dry sediment at an elevation several feet above the reported bottom of the well. The sediment was removed, and a sufficient volume of alluvial groundwater was present to allow sample collection.

Although uranium concentrations in the new wells were below the ACL, they were above the current drinking water standard of 0.03 mg/L. An additional alluvial well, 23(M), was installed in 2012 near the site entrance, the farthest onsite downgradient distance from the disposal cells. Upgradient well 20(M) was installed near the west site boundary but in an area that could have been impacted by mill-related contamination. Uranium concentrations in those wells are below the drinking water standard, which suggests that the groundwater contaminant plume in the alluvial aquifer has had a minimal impact at those locations. The water quality of the alluvial aquifer is addressed further in Section 6.2.

2.4.3 San Andres Aquifer

The original San Andres aquifer monitoring well network consisted of background well L(SG), POC wells OBS-3 and S(SG), and POE well I(SG). These wells are located north of the east-west-tracking fault.

Uranium concentrations in the monitoring wells were below the ACL of 2.15 mg/L and were not showing upward trends. ARCO and DOE results for background well L(SG) have been consistently low, averaging about 0.003 mg/L. However, DOE became aware that a private industrial production well (HMC-951), located near the site entrance and completed in the San Andres aquifer, was showing increasing uranium concentrations. DOE did not have any San Andres wells in the south portion of the site that could be monitored to understand why uranium was increasing in that well.

At about the same time, NMED notified DOE of its concern regarding suspiciously low uranium concentrations in the POC and POE wells. Subsequent downhole videos of the wells showed that

the slotted well casings in the POC wells were almost completely blocked by iron scale. It is possible that a reducing environment had developed in the wells, and the low concentrations may have been the result of dissolved uranium precipitating onto the iron scale (the cause of low concentrations is still being evaluated). DOE changed from a low-flow sampling method to a higher-flow casing purge method (the method used by ARCO) in these wells; uranium concentrations have increased but still may be affected by the physical and chemical conditions within the corroded well casings.

Uranium concentrations in POE well I(SG) were significantly below ARCO sampling results. The well has solid steel casing down to the top of the San Andres Limestone, and then open borehole into the Glorieta Sandstone. A downhole video indicated that low-flow samples had been inadvertently collected from within the bottom few feet of the casing instead of within the open borehole as intended. Samples are now collected from within the open borehole portion of the well, and uranium concentrations have increased.

Because of a concern that HMC-951 might have been drawing contaminated water from the Bluewater site, and because of the poor condition of the POC wells, DOE installed six new San Andres aquifer wells on the Bluewater site in 2012. Wells 13(SG), 14(SG), 15(SG), and 18(SG) were installed in the south portion of the site. Well 16(SG) was installed between OBS-3 and S(SG). Well 11(SG) was installed near the north property boundary to help DOE understand the groundwater flow direction in the northeast portion of the site.

Sampling of these wells began in November 2012. None of the new wells have contaminant concentrations exceeding ACLs, but downgradient wells 13(SG) and 18(SG) and POE well I(SG) have uranium concentrations exceeding the drinking water standard. Consequently, contaminated San Andres groundwater has migrated beyond the site boundary in the east-southeast direction. The water quality of the San Andres aquifer is addressed further in Section 6.3.

2.5 Source of Contamination

Sand- and clay-rich tailings were pumped in a slurry to the main tailings impoundment during milling operations. ARCO realized that substantial quantities of tailings fluids leaked through the bottom of the impoundment and eventually into the underlying aquifers, especially prior to the use of the deep-injection well and the evaporation ponds.

The alluvial aquifer was contaminated from tailings fluids that seeped through the bottom of the tailings ponds and then through the porous basalt and into the underlying alluvial sand and gravel. The contaminated groundwater would have then flowed in the alluvial aquifer in the southeast direction along the former channel of the Rio San Jose.

Contamination of the San Andres aquifer occurred through more complex conditions. Tailings fluids seeped directly into the San Andres Limestone outcrop that was covered by the southeast portion of the main tailings impoundment. The San Andres Limestone also subcrops under the basalt beneath a portion of the disposal cell (Figure 3 and Figure 4), so tailings fluid in that area would have drained through the basalt and into the limestone. Contaminated alluvial groundwater most likely seeped into the San Andres Limestone where the alluvium and

limestone were in contact. Also, seeping tailings fluids and some contaminated alluvial groundwater would have migrated along the fault zones and into the San Andres aquifer.

A further complicating factor was the southward distribution of contaminated San Andres aquifer groundwater. Anaconda had groundwater production wells south of the site that were used to supply the process water for the mill (Figure 1). The cone of depression resulting from pumping these wells would have drawn contaminated water toward the well field. The Ambrosia Lake Fault zone would have acted as a conduit for rapid southern movement of the contaminated groundwater. Water samples collected by ARCO verified that this occurred; uranium and nitrate concentrations well above background concentrations were observed in the Anaconda #5 production well located along the Ambrosia Lake Fault zone about 1 mile south of the main tailings impoundment. As noted in Section 2.3, however, ARCO did not consider San Andres aquifer contamination south of the east-west-tracking fault to be a significant concern.

This page intentionally left blank

3.0 Milling History

3.1 General Description

The Bluewater mill began operations in 1953, processing both limestone and sandstone ores using a carbonate leach. In 1955, an acid leach circuit was added to process sandstone ore from the Jackpile mine located on the Laguna Reservation about 50 miles east of the site. Only sandstone ores were processed after mid-1959, and the carbonate circuit was phased out. Although some early limestone tailings were initially deposited in the carbonate tailings pond, beginning in 1956, all the tailings were deposited in the main tailings impoundment. Sandstone ore was crushed and leached with sulfuric acid to extract the uranium oxide.

From 1953 to 1977, uranium was removed from the leached solutions by absorption onto resins in ion-exchange vats; the remaining solution and crushed ore and leachate were transported as a slurry to the tailings ponds. Sodium chloride was used in an elutriation process to remove uranium, except for the time period from December 1955 to August 1957 when a nitrate eluent was used. After January 1977, the mill used the solvent extraction method rather than ion-exchange for removing uranium. Solvent extraction resulted in higher concentrations of total dissolved solids and chloride, and higher pH, in the leachate slurry that was pumped to the main tailings impoundment. In 1980, the mill process was again changed to allow for recycling a portion of the tailings liquor from the evaporation ponds and tailings pond.

3.2 Milling Operations

Milling operations were conducted 24 hours per day, 365 days per year. The initial mill rate of 300 tons per day in 1953 was incrementally increased over time, reaching a nominal rate of 6,000 tons per day by 1977. The milling byproduct materials (tailings) were transported in a slurry to tailings impoundments. The solids content of slurry discharged to the main tailings impoundment varied between 30 and 40 percent, so significant quantities of water were needed to convey the slurry to the impoundment. Water for mill operations was supplied by five groundwater production wells completed in the San Andres aquifer south of the mill. These wells, Anaconda #1 through Anaconda #5 (shown in Figure 1), operated at various durations and rates throughout the years of milling operations.

3.3 Tailings Disposal History

Initial deposition of tailings in the main tailings impoundment began in 1956 in a basalt depression that was located in what is now the middle of the main tailings disposal cell. A limited quantity of carbonate tailings was deposited in this depression, followed thereafter by acidic tailings. After initial depositions began to fill the depression, a series of soil starter dikes were constructed along the north, northeastern, and eastern limits of the tailings to control the surface area of the pond. At this point, the footprint of the tailings pond covered not only basalt surfaces, but also windblown sand deposits and an outcrop of San Andres Limestone.

Tailings were discharged continuously from three movable spigots along the south side of the impoundment. Coarser sands settled near the spigots, mixed fine sand, silt, and clay settled in the middle portion of the impoundment, and silt and clay (referred to as “slimes”) settling out in the north end where a tailings pond developed. Figure 5 shows the approximate distribution of these materials.

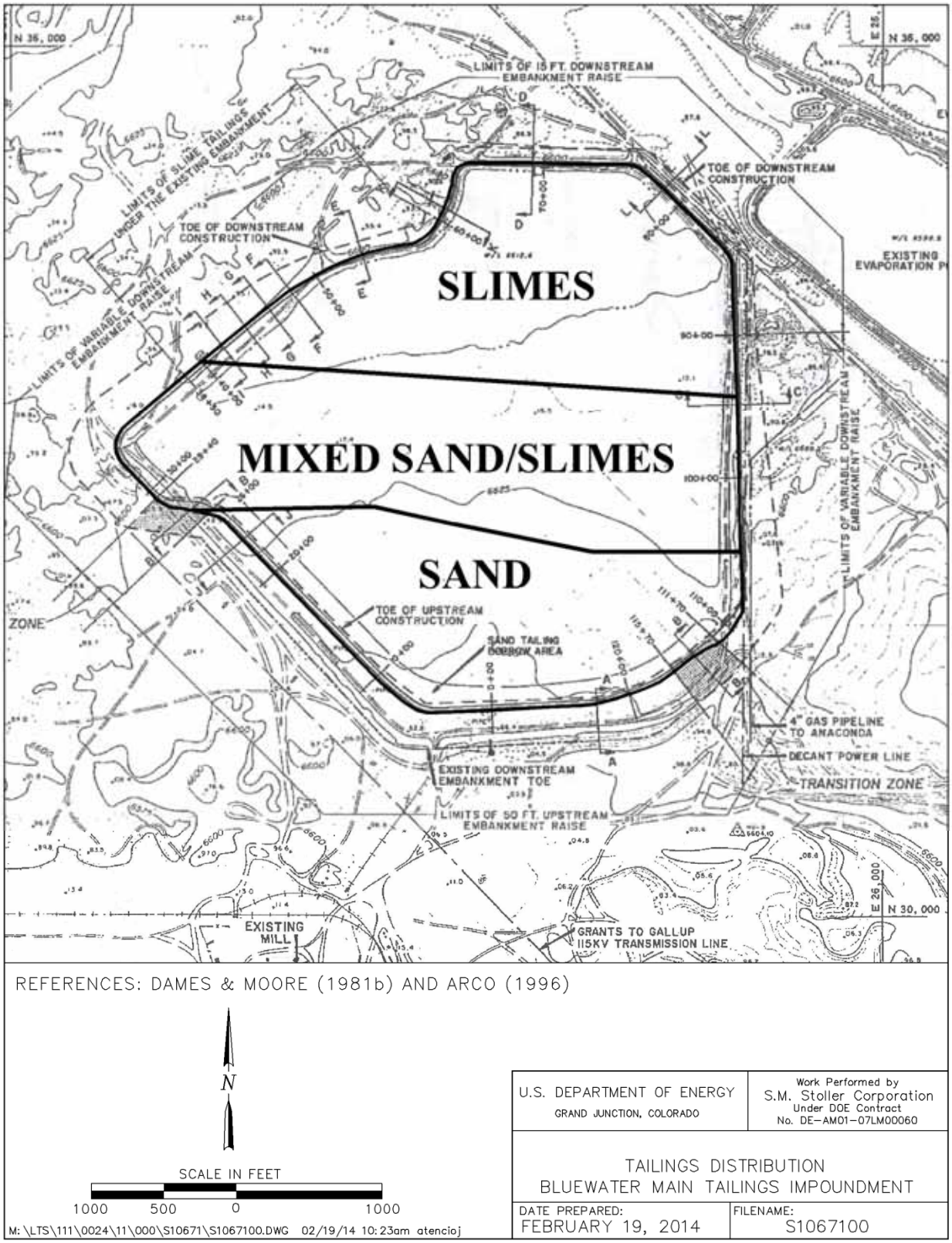

Figure 5. Approximate Distribution of Materials Within the Main Tailings Impoundment

The deposition of slimes toward the north, northwest, and northeast made it necessary to raise the dikes to increase the capacity of the impoundment. A series of crisscrossing, low dikes were pushed up from the tailings, and further deposition occurred in the segmented ponds. During this time, natural soil dikes were compacted on sand tailings at the southeast corner of the impoundment. The main tailings impoundment attained a configuration similar to that of the final impoundment (and disposal cell) except there was no western dike, where the slime tailings were settling directly against higher basalt outcrops.

A western dike was constructed in 1957 over tailings slimes to contain the tailings and effluent. Also at this time, rapid buildup of sand tailings was occurring along the south embankment, and additional dikes were constructed from sand tailings in this area.

In October 1977, tailings impoundment dikes were raised again on the east, west, and north sides to allow for additional ponding of tailings liquor due to a modification in operations. These dikes were constructed from compacted, natural clayey soil. Simultaneously, the sand tailings dikes on the south side were raised. Impoundment dikes continued to be raised to contain the tailings; by 1981, the elevation on the south side was 56 ft higher than the north side because of the buildup of sand tailings in that area.

3.4 Main Tailings Impoundment Seepage

ARCO recognized that substantial quantities of tailings fluids seeped through the bottom of the main tailings impoundment, through the underlying unsaturated materials, and into the alluvial and San Andres aquifers. Anaconda and ARCO hydrology subcontractors made various estimates of seepage losses through the bottom of the main tailings impoundment (Arlin et al. 1978, Dames & Moore 1984a, ARCO 1990, Applied Hydrology Associates Inc. 1995). All agreed that high seepage losses of at least 1,000 gallons per minute (gpm) occurred in the 1950s. To reduce the amount of seepage, Anaconda constructed a deep injection well in 1960.

The injection well, located more than a mile northeast of the tailings impoundment, was completed in the Yeso Formation that underlies the Glorieta Sandstone. Tailings fluid decanted from the pond that persisted at the north (lowest elevation) end of the main tailings impoundment was injected into the well from 1960 through 1977. The injection rate was regulated to ensure only gravity flow within the well (i.e., injection was not under pressure). Approximately 501 million gallons of decanted fluid had been injected by the end of 1965 (West 1972), which is an average rate of approximately 190 gpm. Assuming this rate continued, a total of approximately 1.7 billion gallons of decanted fluids were injected during the operation of the well. In their evaluation of the Bluewater injection process, the U.S. Geological Survey considered it to be the most satisfactory and economically feasible method of effluent disposal (West 1972).

After 1977, tailings fluids were evaporated in lined evaporation ponds constructed north of the impoundment. Use of the evaporation ponds removed approximately 525 million gallons of liquid that otherwise would have infiltrated into the tailings. During the years 1977 through 1982, much of the uranium in the decanted water was recovered by recycling the evaporation pond water through the mill (Applied Hydrology Associates Inc. 1995).

Ore-milling operations and tailings deposition ceased in March 1982. Subsequently, ARCO installed 58 extraction wells in the sand portion of the tailings impoundment. These wells removed approximately 122 million gallons of interstitial fluids from the tailings as part of a program to dewater the impoundment and recover uranium. The extracted fluids were treated at the mill, and most of the barren solution was pumped to the evaporation ponds. The remaining unreported amount of treated water was sprayed on the tailings for dust control during interim tailings impoundment stabilization activities. Pumping from these wells ceased in 1985 when water levels and well yields dropped to levels where pumping was no longer practical (Applied Hydrology Associates Inc. 1995).

Prior to placement of the radon barrier, ARCO installed vertical band drains to wick fluids out of the slimes. The purposes of this procedure were to reduce the quantity of tailings fluids available for seepage and to consolidate the slimes. Tailings were loaded with a consolidation layer of windblown silty and sandy clay materials (the same type of material used to construct the radon barrier) to squeeze fluid out of the slimes and into the drains.

The wicks drew approximately 24 million gallons of tailings fluids to the surface of the impoundment, where the fluids ponded and evaporated. ARCO calculated that up to 16 million gallons of fluids moved into unsaturated materials of the consolidation layer, thus removing a total of approximately 40 million gallons from potential seepage (Applied Hydrology Associates Inc. 1993). Approximately 7.4 million gallons of fluids were estimated to have been forced through the bottom of the impoundment during the consolidation process (derived from Appendix A Table A-1). Monitoring results from wells adjacent to the impoundment, however, did not show any increase in contaminant concentrations in either the alluvial or San Andres aquifers as a result of this activity. The band drains were removed when 90 percent consolidation of the slimes had been attained and flow from the band drains ceased. The final cover materials (radon barrier and rock) were installed at that time.

Estimated seepage rates from the tailings impoundment into underlying materials and aquifers were based on mill water-balance calculations, including fluid discharge to the tailings impoundment, decantation of the ponded fluids to the injection well and later to the evaporation ponds, cell dewatering activities, and tailings fluid reprocessing, and precipitation. However, ARCO did not account for evaporation of the tailings fluid and precipitation runoff that ponded at the north end of the impoundment prior to decantation activities. Evaporation of the ponded fluids following the start of decantation for deep-well injection (and later disposition in the evaporation ponds) was assumed to have been minimal (Dames & Moore 1981a). Figure 6 shows a schematic of the Bluewater mill impoundment water cycle.

Cumulative seepage rates from the main tailings impoundment, based on ARCO's last estimates (Applied Hydrology Associates Inc. 1995), are plotted in Figure 7. ARCO estimated that approximately 2.7 billion gallons of tailings fluid seeped from the main tailings impoundment by the time deep-well injection commenced in 1960. Thereafter, seepage continued at a reduced rate. By the time construction of the disposal cell and placement of the rock cover was completed in 1995, ARCO estimated that approximately 5.7 billion gallons of fluid had seeped through the bottom of the impoundment (Appendix A Table A-1). Although evaporation of tailings pond fluid would have removed some water from the cycle, ARCO's estimate of 5.7 billion gallons of seeped fluid through 1995 is considered to be the best available estimate and is used in this assessment.

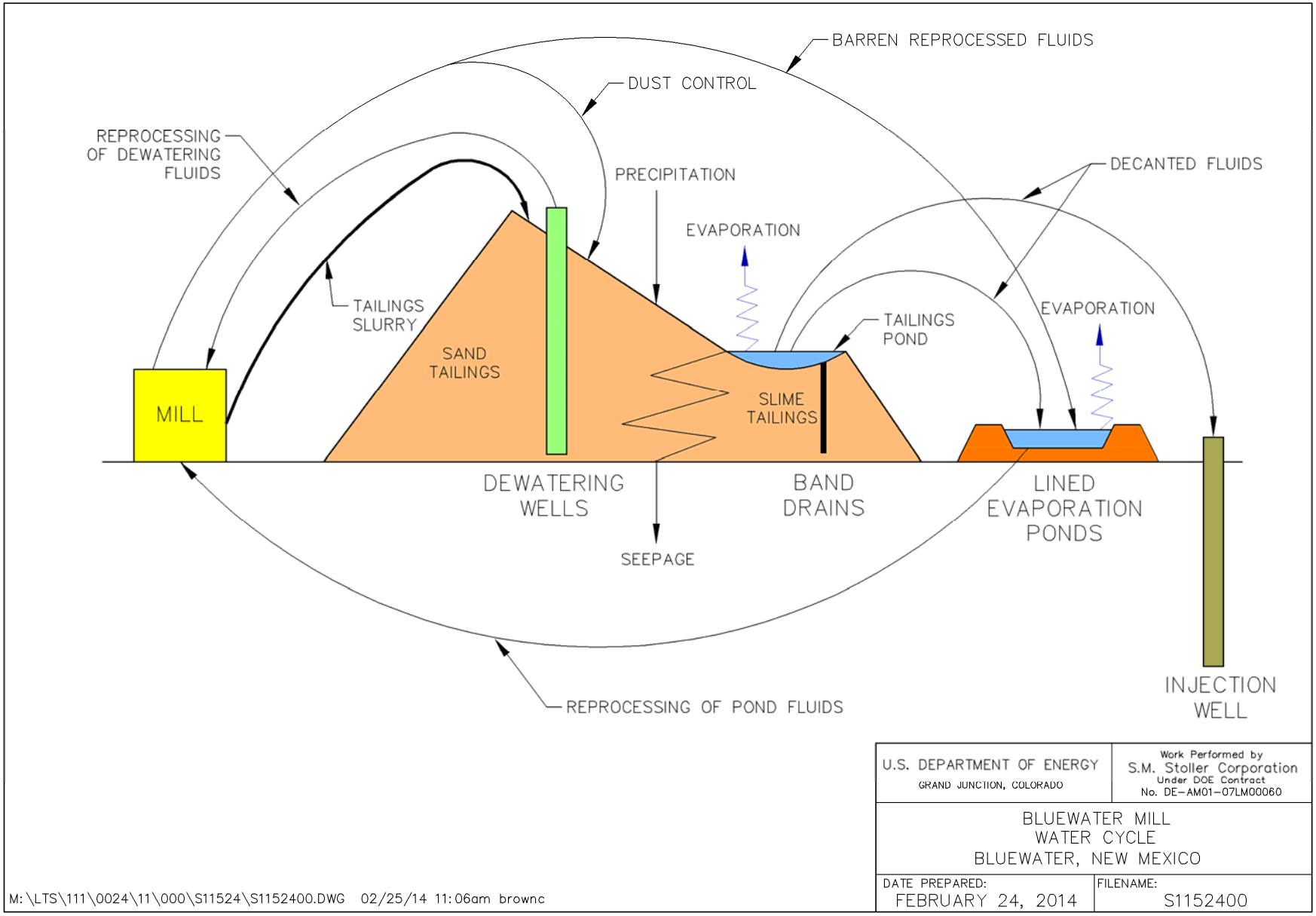

Figure 6. Schematic of the Tailings Impoundment Water Cycle

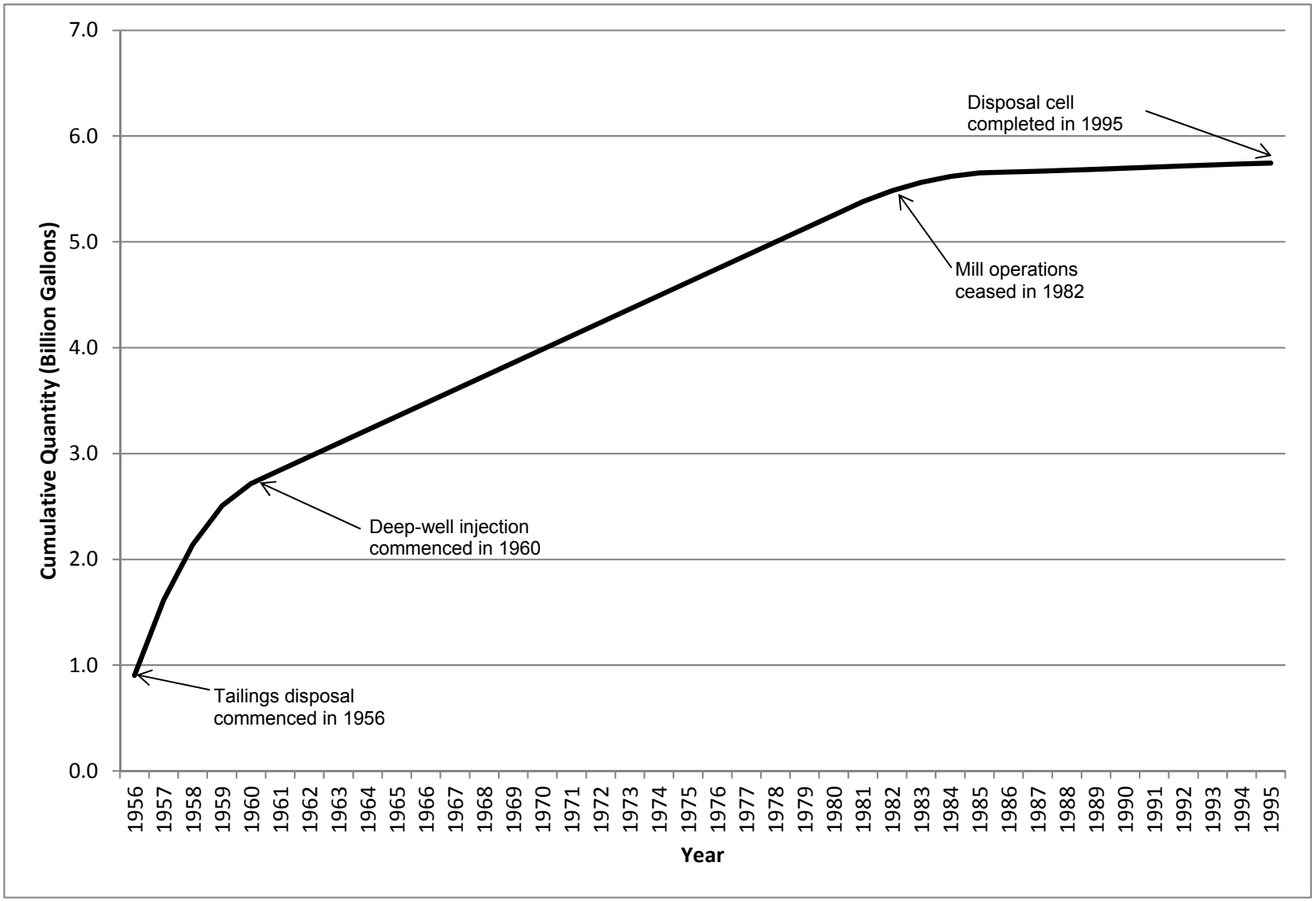

Figure 7. Estimated Cumulative Seepage from the Main Tailings Impoundment Through 1995

4.0 Disposal Cell Cover Characteristics

A liner was not installed prior to tailings placement, and the tailings were encapsulated in place. Therefore, tailings fluids remaining in the main tailings disposal cell, and additional fluids from infiltration of precipitation through the cover, could continue to seep through the bottom of the disposal cell.

A key component of understanding how much fluid could seep out of the disposal cell is evaluating how much precipitation is entering the cell. Therefore, an understanding of how the disposal cell cover was designed and constructed, and how it may change over time, is necessary to characterize the potential hydraulic performance of the cover.

4.1 Cell Cover Design and Construction

The main tailings disposal cell cover, completed in December 1995, was designed primarily to satisfy federal regulations and standards for radon attenuation and erosion protection as promulgated under UMTRCA of 1978. Federal regulations and NRC guidelines require groundwater protection but do not include standards or criteria for cover permeability or percolation. Nor was the potential for plant encroachment, root intrusion, or animal burrowing in the cover evaluated. The assumption, however, was that the engineered cover would prevent infiltration of precipitation into the encapsulated tailings, thus eventually eliminating the disposal cell as a continuing source of contamination (after seepage of residual fluids).

Designers used NRC guidelines and the NRC computer model, RAECOM, to calculate radon barrier thicknesses for different surfaces of the main tailings disposal cell to limit radon flux, as required, to less than the 20 picocuries per square meter per second (pCi/m^2s) standard. The radon barrier, consisting of sandy-clay material from the site, was constructed according to the following thicknesses: 1.0 to 2.2 ft over the slimes tailings, 1.7 to 2.6 ft over the mixed tailings, and 2.3 to 4.2 ft over the sand tailings (ARCO 1996). Prior to placement of the radon barrier, the tailings surface was graded and covered by up to 15 ft of compacted relocated materials derived from natural windblown deposits and evaporation pond dike materials from the site (primarily sandy-clay material similar to the radon barrier material). The greatest thicknesses of relocated materials were placed over the slimes portion of the tailings, most of which were placed for dewatering through the band drains. Some of these materials contained low levels of windblown radioactive contamination.

The radon barrier was compacted to 100 percent of maximum dry density based on Standard Proctor density (ASTM D698). In-place compaction was tested using nuclear gage and sand cone methods. As-built permeability values were not reported. However, a common construction assumption at the time was that laboratory permeability (saturated hydraulic conductivity [*Ks*]) results could be achieved in the field. Designers likely assumed, based on their laboratory results, that by compacting the radon barrier to 100 percent of Standard Proctor density they had achieved an as-built permeability in the range of 1×10^{-7} to 1×10^{-8} centimeters per second (cm/s).

NRC guidelines (NRC 1990) were used to calculate runoff discharge and velocity from the top and side slopes of the cell and the size of basalt rock necessary to control erosion of these slopes.

The NRC procedure is based on calculations of the probable maximum precipitation event and resulting probable maximum flood event.

Cover slopes were designed to shed runoff water primarily to the north. However, the north top slope was designed at a 0.5 percent slope, leaving little latitude for construction irregularities or settlement. The final constructed surface in this area had a 0.45 percent slope (ARCO 1996). The as-built surface topography and cross sections of the main tailings disposal cell are shown in Appendix B Figures B-1 through B-3.

The condition of vegetation along the north toe slope indicates that runoff is not shedding off the north edge of the cover as intended. If the disposal cell were shedding runoff to the north, more abundant plant growth would be present along the flat north toe slope where runoff water would accumulate. However, plant growth along the north toe slope appears to be no greater than in surrounding areas, and moist areas have not been observed in this area.

4.2 Depressions on the Disposal Cell Cover

Depressions have formed on the north end of the disposal cell cover, which is over the portion of the cell containing slimes. These depressions collect runoff water after storm events of sufficient magnitude or intensity (Figure 8). They were first observed by DOE inspectors during the first annual inspection in 1998. Satellite imagery taken in 1997 verifies that they had already started developing before DOE acquired the site. The depressions apparently formed as the slimes continued to consolidate after completion of the cover, which occurred soon after removal of the band drains (see Section 3.4).

Observations of differential settlement and ponding of water have raised concerns about the physical integrity of the disposal cell cover. Specifically, have the depressions degraded the performance of the radon barrier, or have they compromised the stability of the north end of the disposal cell? Field observations of the persistence of ponded water suggest that most of it dissipates by evaporation rather than percolation through the cover. The role of evaporation is addressed further in Section 5.3.2.

4.2.1 Cover Topography

In 2012, DOE conducted a high-resolution topographic survey of the main tailings disposal cell using a light detection and ranging (LiDAR) method to provide a baseline to determine if differential settlement in the depression area is ongoing. No standing water was present on the cover at the time of the survey. The digital LiDAR survey data were used to develop 6-inch contour intervals for the disposal cell surfaces (Figure 9) and to calculate the areas, depths, and volumes of the depressions. It is not known if settlement has stabilized. DOE plans to conduct periodic LiDAR surveys until the data verify that settlement has ceased.

Figure 8. Ponds in Depressions on the Main Tailings Disposal Cell in August 2012, Following a Summer Storm

Based on light-colored evaporite minerals that form as ponded water evaporates from the depressions and corresponding elevations determined by the LiDAR survey, the maximum ponded area has been approximately 15.3 acres. The maximum depth of ponded water has been 2.5 ft in the deepest depression, and the maximum quantity of ponded water has been approximately 4.3 million gallons (Figure 10). This maximum ponded area appears to have occurred during spring 2012 following melting of unusually high snowfall amounts during the previous December. No significant precipitation occurred during the spring, but standing water persisted until mid-June.

4.2.2 Cover Radon Flux

After consultation with NRC, DOE measured radon flux on the uncovered surface of the radon barrier over the area encompassing the depressions (Figure 11). The measurements were taken in early July 2013, after a dry spring and prior to the annual "monsoon" season; no ponded water was present on the cover. The cell cover materials were at their driest condition of the year, which would be when the highest radon emissions would be expected. Moisture attenuates radon, so radon emission would not occur through wet materials or standing water. Figure 12 shows a typical measurement location.

Radon was below the laboratory detection limit of 0.5 pCi/m^{2}s at all of the locations. These results suggest that the deformation of the cover in this area has not opened pathways (i.e., cracks or soil fissures through the radon barrier) for radon emission from the underlying tailings materials. The development of depressions on the cover, therefore, has not had an adverse effect on the performance of the radon barrier. These results may also imply that the permeability of the radon barrier has not been increased by development of the depressions and associated deformation of the surface.

4.2.3 Cover Stability

The depressions and ephemeral ponds that develop within them were evaluated as possible paths of erosion that could destabilize the north portion of the disposal cell. To date, no evidence of erosion has been observed, and the radon flux study confirmed the integrity of the radon barrier.

The cover and side slopes of the disposal cell were designed to shed runoff from the probable maximum precipitation event, primarily over the north side slope. If the depressions developed in a way that provides a preferential flow path for the ponded water, the riprap along the edge of the cover would still protect the cover from erosion. Also, as the depressions fill with water and a large pond develops, the ponded water would greatly dissipate the energy of the runoff from the south portion of the cover, resulting in a lower runoff velocity over the north edge of the cover. Therefore, although the cell cover was designed to shed runoff water, the presence of the depressions and ponds are not expected to compromise the stability of the disposal cell.

4.3 Cell Cover Evolution

Research has shown that surface layers of rock on covers create a favorable habitat for deep-rooted plants in all climates, even in the desert. Depending on climatic conditions and cover design, the rock layer may act as a mulch, effectively reducing soil evaporation (increasing soil water storage) and trapping windblown dust, thereby providing the water and nutrients needed for the germination and establishment of vegetation. Vegetation is establishing on the main tailings cell cover and consists primarily of annual weeds, but populations of perennial grasses, forbs, and deep-rooted woody plants are also establishing. An understanding of the ecology of these plant species provides clues about past and possible future changes in the condition of the disposal cell cover.

Currently, deep-rooted Siberian elm saplings and robust fourwing saltbush shrubs grow on the cell cover, primarily on the south two-thirds of the cover (DOE controls the elm saplings with herbicide to avoid the establishment of mature trees). Their presence suggests that the underlying relocated materials and tailings are moist, particularly in that area. The sparsity of deep-rooted plants on the north portion of the cover may be because the thick layer of compacted relocated materials over the slimes is inhibiting root penetration.

The long-term consequences of changes in the ecology of covers, including the encroachment and establishment of populations of deep-rooted plant species, can be either detrimental or beneficial depending on the cover design and management practices (Link et al. 1994). A key issue is whether deep-rooted plants that establish on the cover will increase or decrease the likelihood of precipitation percolation through the cover and into the tailings. Detrimental effects are related to root growth through covers and into tailings; plants can increase percolation flux

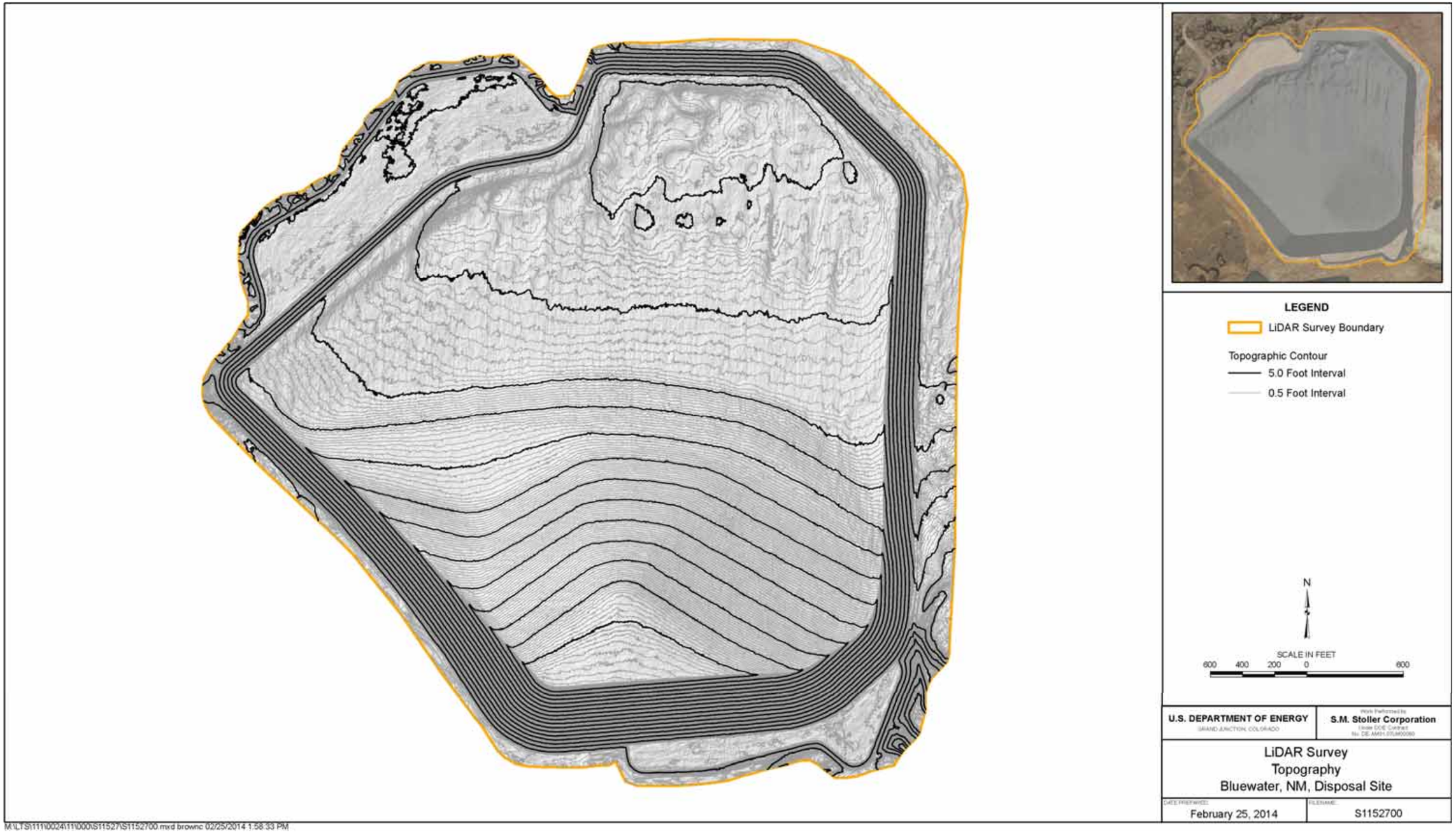

Figure 9. Topographic Map of the Main Tailings Disposal Cell (July 2012 LiDAR Survey Data)

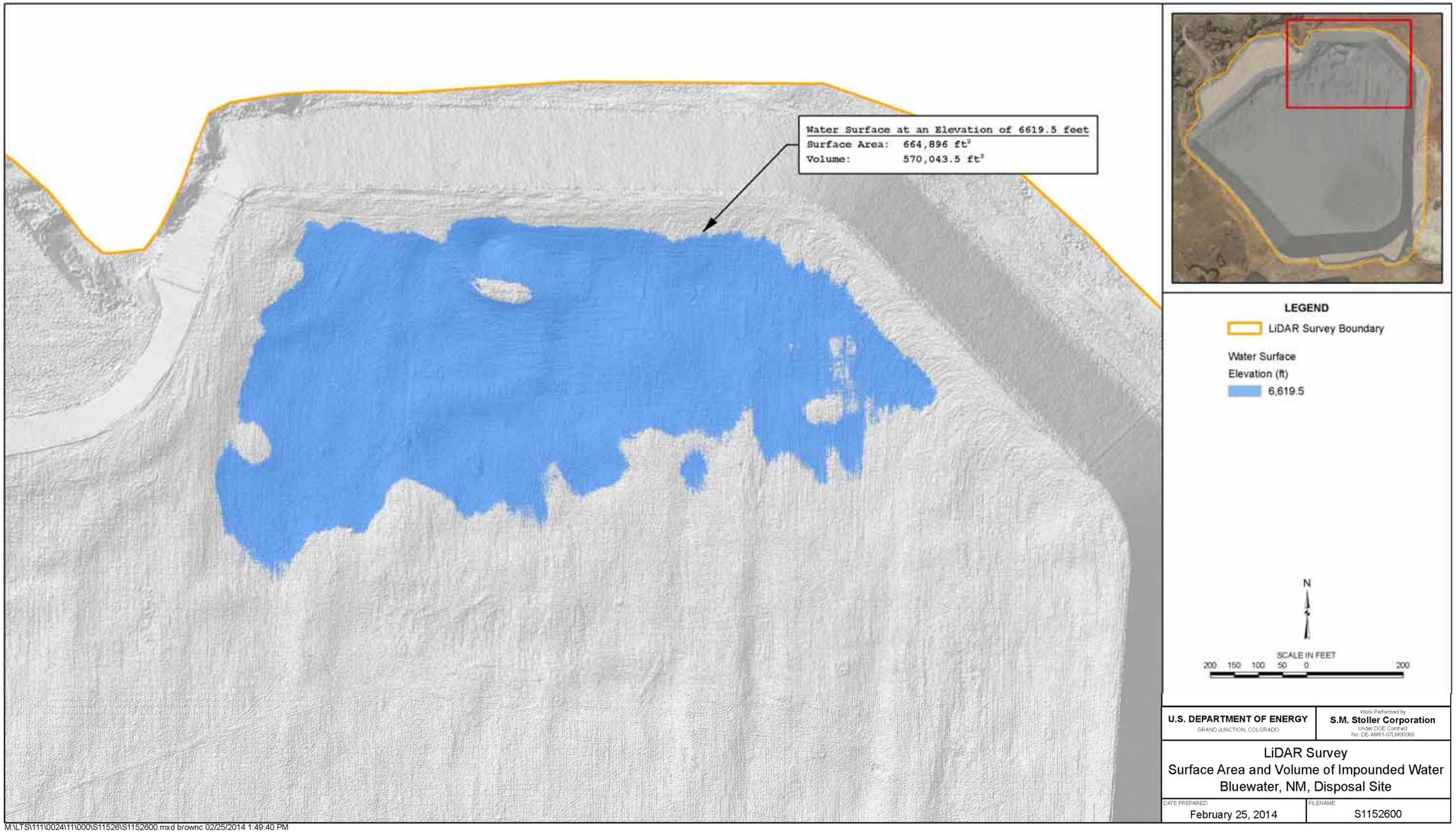

Figure 10. Projected Maximum Area to Date of Ponded Water on the Main Tailings Disposal Cell (July 2012 LiDAR Survey Data)

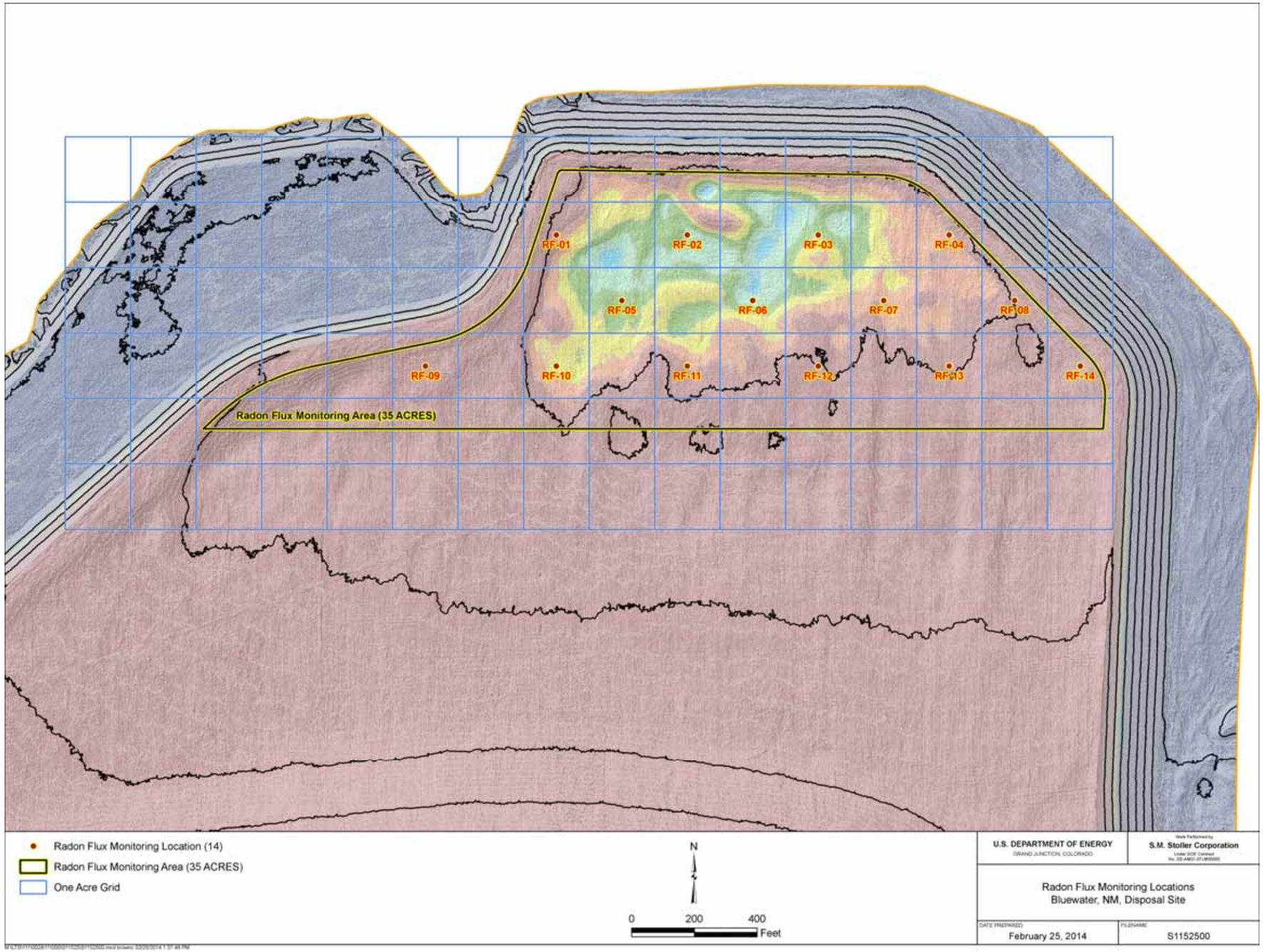

Figure 11. Radon Flux Measurement Locations in the Area of Depressions (July 2013)

This page intentionally left blank

Figure 12. Radon Measurement Location RF-05 in the Area of Cell Cover Depressions

by accelerating soil development, which increases permeability by creating fissures or planes of weakness in the soil structure. Beneficial effects are related to the extraction of soil water by plants (transpiration) and erosion protection; consequently, plant encroachment could actually enhance the performance of the cover. Transpiration can greatly limit percolation if habitat characteristics favor the establishment and resilience of a diverse plant community. A combination of high transpiration rates and erosion protection can be achieved.

Natural soil-forming processes are inevitable and will create fissures in radon barriers, increasing permeability and loosening soil compaction—even in the absence of vegetation. Natural soil-forming processes have likely increased the permeability of the radon barrier by one to several orders of magnitude. Therefore, percolation flux is likely to increase with or without vegetation on the cover.

Ecological succession and soil development processes alter engineered soil covers over relatively short time periods regardless of climate, cover design, or service life. Studies of disposal cell and landfill covers across the country have shown that compacted soil layers (similar to the main tailings radon barrier) often fall short of low-permeability targets, often during or shortly after construction, and sometimes by several orders of magnitude (NRC 2011). For example, if compaction of the radon barrier achieved a permeability of 1×10^{-7} cm/s as designed, the current permeability may be closer to 1×10^{-5} cm/s.

4.4 Cover Hydraulic Performance

The Reclamation Plan (ARCO 1990) did not reference soil physical or hydraulic property criteria for the cover. Apparently there were no criteria for the permeability of the cover or for percolation flux through the cover. However, it did provide results of grain-size analyses and *Ks* tests for samples of materials specified for use in constructing the radon barrier. Test materials were low-plasticity clay and sandy clay. Geometric means of permeability tests were 1.7×10^{-8} cm/s for the clay and 2.4×10^{-7} cm/s for sandy clay, with all samples compacted to the specified 100 percent of Standard Proctor dry density. Although the as-built permeability of the radon barrier was not measured directly, it was likely assumed that the as-built *Ks* was between 1×10^{-7} and 1×10^{-8} cm/s, as noted in Section 4.1.

It would seem likely that percolation into tailings is potentially greatest where water ponds in depressions. However, as noted previously, evaporation appears to be the dominant factor in reducing the pond volumes (rather than percolation through the cover). ARCO also believed evaporation to be the dominant factor, as this was the method used to eliminate ponded fluids during the wicking procedure (Applied Hydrology Associates Inc. 1993). Even if the permeability of the radon barrier is increasing as expected, the permeability of the underlying thick layer of relocated material likely remains close to the presumed original rate of 1×10^{-7} cm/s—those materials would not be impacted by the environmental forces affecting the surface materials.

At the Burrell, Pennsylvania, UMTRCA Title I disposal cell, the mean *Ks* was 3.0×10^{-5} cm/s where Japanese knotweed roots penetrated the radon barrier, compared to 2.9×10^{-7} cm/s at locations with no plants (Waugh et al. 1999). The weighted average *Ks* for the entire cover, calculated using the community leaf area index for Japanese knotweed and the methods of Wells and Norman (1991), was 4.4×10^{-6} cm/s. At the Lakeview, Oregon, Title I Disposal Site, the mean *Ks* for the radon barrier on the cell cover, both with and without sagebrush and bitterbrush roots, was 3.0×10^{-5} cm/s (Waugh et al. 2007). The highest *Ks* values occurred near the top of the radon barrier; the lowest values occurred deeper in the radon barrier. At the Shiprock, New Mexico, Disposal Site, the mean *Ks* in the cell cover radon barrier was 4.4×10^{-5} cm/s (Glenn and Waugh 2001). Results were highly variable and lower where tamarisk and Russian thistle were rooted in the radon barrier. The Shiprock cell radon barrier was nearly saturated at the four locations where measurements were taken. At the Tuba City, Arizona, Title I Disposal Site cell, which is sparsely vegetated, the mean *Ks* of the radon barrier was 8.7×10^{-6} cm/s, and values ranged from a low of 9.8×10^{-9} to a high of 1.18×10^{-4} cm/s.

The radon barrier permeability measurements at the referenced UMTRCA Title I sites suggest that the permeability of the radon barrier at the Bluewater site may be on the order of 1×10^{-5} cm/s. However, because of the area of the cover and expected variability of hydraulic performance of the radon barrier (due to variable thicknesses of the barrier and non-uniformity of plant growth), extensive field permeability tests would be required to determine the actual permeability of the radon barrier of the main tailings disposal cell. Because the performance criterion for radon emission is being met, and because permeability is only one factor affecting the amount of precipitation that percolates through the cover, permeability tests are not considered to be necessary at this time.

5.0 Disposal Cell Seepage

5.1 Conditions for Seepage

ARCO assumed that seepage of fluids remaining within the tailings would continue to occur after closure of the cell but did not predict the rate or quantity of seepage (ARCO 1990). The cover design was intended to control emanation of radon from the encapsulated tailings and shed precipitation runoff without causing erosion of the cover; percolation of precipitation through the cover and into the cell was not a factor in the design requirements.

Seepage from the disposal cell is controlled by a difference in total hydraulic head. Seepage flow occurs from a higher total hydraulic head to a lower total hydraulic head. Total hydraulic head is the sum of hydraulic pressure head and elevation head above a reference datum. Because the elevation of the tailings is greater than the elevation beneath the disposal cell, the total hydraulic head within the final disposal cell is greater than the total hydraulic head underlying the disposal cell. Therefore, fluid seepage from the tailings into the underlying foundation material is expected to persist in both saturated and unsaturated conditions.

The degree of saturation within the disposal cell is a key component in evaluating unsaturated seepage. Actual saturation within the disposal cell is unknown. Cell material saturation was not measured or estimated by ARCO and has not been measured since DOE acquired the site. However, for the purposes of this assessment and based on studies conducted on the Shiprock disposal cell (DOE 2012), it is assumed that the sand tailings are moist but unsaturated. Although ARCO attempted to dewater the sand tailings, pumping likely did not completely drain the tailings, and precipitation would have recharged the tailings to some degree after pumping ceased in 1985.

As found in the Shiprock cell, the slimes in the main tailings disposal cell are assumed to be saturated. Although ARCO's efforts to consolidate the slimes removed a substantial quantity of tailings fluid, clay minerals tend to hold liquid. The overlying silty-clay materials placed to consolidate the slimes are assumed to be unsaturated. However, due to natural soil-forming processes and the heterogeneity of these materials, they could eventually become saturated, allowing precipitation to percolate into the slimes.

5.2 Seepage Rate

The rate of seepage, or tailings fluid flow through the tailings into underlying foundation material, is governed by the hydraulic conductivity of each material within the disposal cell. The main tailings disposal cell can be described as a layer-cake type of arrangement with the cover materials (i.e., the radon barrier and underlying soil placed to attain the final construction grade), which overlie the tailings mass (sands and slimes), which in turn overlie foundation materials (alluvium, basalt, and limestone). Under saturated conditions, when the largest volume of tailings fluid flow would occur, hydraulic conductivity of the overall system is controlled by the lowest hydraulic conductivity of the materials in the layer-cake arrangement.

Table 1 provides estimates for saturated hydraulic conductivities (*Ks*) of materials existing in and under the disposal cell that are used in this analysis. Assuming that tailings fluid seepage is controlled by natural flow, values provided in Table 1 indicate that moisture will percolate

through the cover, flow at a slower rate through the tailings, and eventually discharge into the underlying foundation materials (which have the highest *Ks*).

Because of the presence of sand in the slimes-sand portion of the disposal cell, that portion is conservatively assumed to have the same hydraulic conductivity as the sand portion. Therefore, the sand and slimes-sand portions are hereafter included together as "coarse tailings." The slimes portion of the cell is considered to be "fine tailings."

Table 1. Estimated Saturated Hydraulic Conductivities for the Bluewater Disposal Cell

Layer	Vertical *Ks* (cm/s)
Cover	$10^{-5} – 10^{-4}$ [a]
Tailings: Sand[b]	$10^{-6} – 10^{-5}$
Slimes-Sand[b]	$10^{-6} – 10^{-5}$ [c]
Slimes[b]	$10^{-7} – 10^{-6}$
Foundation Materials: Alluvium	$10^{-4} – 10^{-3}$
Basalt	$10^{-2} – 10^{-1}$

Key: cm/s = centimeters per second; *Ks* = saturated hydraulic conductivity
[a] Long-term value after soil development effects have occurred (NRC 2011)
[b] Licensing Documentation, Volume 22, Page 7 (Dames & Moore 1984b)
[c] Conservatively assumed to be controlled by interbedded sand layers

5.3 Seepage Quantity

5.3.1 Water-Balance Equation

For this assessment, the following basic water-balance equation is used to estimate seepage amount after construction of the cover in 1995.

$$I - O = \Delta S, \quad \text{where:} \quad I = \text{inflow}, \; O = \text{outflow}, \; \Delta S = \text{change in storage}$$

5.3.2 Inflow

Inflow quantity to the disposal cell is governed by site-specific climatic parameters, which are unavailable. However, average monthly precipitation quantities are available for the Grants, New Mexico, airport, and average monthly evaporation quantities are available for the region (Table 2). Due to its proximity, it is assumed that these quantities are representative of precipitation and evaporation at the Bluewater site. From the values in Table 2, the Bluewater disposal cell cover receives an annual average of approximately 10.3 inches of precipitation, with an average free-surface evaporation of 45.9 inches per year.

As presented in Table 2, yearly free-surface evaporation rates are about 4.5 times greater than yearly precipitation. Evaporation exceeds precipitation in 9 months of the year. During the wettest months of July through September, evaporation rates range from 3.3 to 4.6 times greater than monthly precipitation. Not all precipitation evaporates, however; the water cycle includes infiltration into the ground (some of which recharges aquifers), uptake by vegetation, and

diversion into surface water systems. Also, evaporation is an ongoing phenomenon averaged over time, whereas about half of the annual precipitation at the site occurs from July through September as high-intensity, short-duration convective storms. During such storm events, the rate of precipitation far exceeds the rate of evaporation. Regardless, evaporation in the region and at the site is a significant factor in reducing precipitated moisture.

Table 2. Precipitation and Evaporation in the Region of the Bluewater Site

Parameter	Location	Month[a]												Total
		Jan	Feb	Mar	Apr	May	Jun	Jul	Aug	Sep	Oct	Nov	Dec	
Precipitation	Grants, NM[b]	0.50	0.43	0.52	0.45	0.51	0.56	1.72	2.01	1.29	1.09	0.55	0.67	**10.3**
Class A Pan Evaporation	Farmington, NM	0.00	0.00	0.00	7.97	10.06	12.00	12.52	10.70	8.15	5.41	0.00	0.00	66.8
	Gallup, NM	0.00	0.00	0.00	6.61	9.31	12.12	10.50	8.70	7.95	5.07	2.20	0.00	62.5
	Laguna, NM	0.00	0.00	0.00	8.47	9.33	11.98	10.76	8.88	6.83	5.00	1.98	0.00	63.2
	Mt. Taylor, NM	0.00	0.00	3.83	8.09	9.07	12.08	9.70	8.80	6.36	4.65	0.00	0.00	62.6
	Average	0.00	0.00	0.96	7.79	9.44	12.05	10.87	9.27	7.32	5.03	1.05	0.00	63.8
Free-Surface Evaporation[c]	Region	0.00	0.00	0.69	5.61	6.80	8.67	7.83	6.67	5.27	3.62	0.75	0.00	**45.9**

[a] Values in inches
[b] Grants airport meteorological data averaged for the period 1953–2012
[c] Average pan evaporation multiplied by an average pan-to-lake coefficient of 0.72

Runoff on the disposal cell cover occurs only during rainfall events of sufficient magnitude and intensity, and after melting of significant snow accumulations. However, there is no evidence that runoff has spilled over the edge of the cell cover. Instead, cell cover runoff accumulates as ponds in depressions that have formed over the slimes area on the north portion of the cover. These ponds persist for long periods of time that correlate to the quantity of accumulated water, indicating that percolation through the cover is minimal at this location. Evaporation, therefore, is the primary cause for loss of ponded water in the depressions.

Shallow- and deep-rooted vegetation is establishing on the disposal cell cover as noted in Section 4.3. It can be assumed, therefore, that some percentage of precipitation percolates through the cover; apparently more over the sand tailings area than the slimes area because that is where deep-rooted vegetation occurs. The vegetation also indicates that evapotranspiration is occurring.

There are no site-specific data to estimate the actual amount of precipitation that percolates through the cover and into the tailings. Studies performed on other covers are not directly applicable to the Bluewater site because of differences in designs, cover materials, and climate. However, percolation rates that have been measured at other capped landfills have ranged up to 18 percent in studies by Albright et al. (2004) and up to 42 percent by Abichou el al. (1998). Rock covers such as on the Bluewater cell may act as mulch and retain moisture, which would tend to decrease evaporation and increase percolation. However, vegetation, which is gradually establishing on the Bluewater cell cover, has been shown to significantly decrease percolation of precipitation (Benson et al. 2011, Waugh et al. 2009). For the purposes of this assessment to estimate a range of potential seepage from the disposal cell after construction, tailings storage and outflow are calculated based on inflow quantities of 50 percent and 25 percent of precipitation.

5.3.3 Change in Storage

Moisture in the tailings is stored in voids within the tailings mass. A saturated volumetric moisture content is defined as the condition in which all void space is occupied by moisture, and 50 percent saturation is when half the void space is occupied by moisture. Porosity is defined as the ratio of void space to the total volume of mass. Therefore, when soil is fully saturated, the volume of moisture is equal to the porosity of the soil mass.

As tailings voids drain from a saturated condition to a lower degree of saturation, negative pore pressures develop within the tailings materials. The relationship between the volumetric moisture content and negative pore pressures is provided on soil moisture characteristic curves. There are no data for moisture-holding properties of the Bluewater tailings, nor detailed gradation data for the tailings. Therefore, tailings characteristics from the Shiprock disposal cell were used to represent Bluewater cell tailings characteristics. Although mined from different geographic locations, the uranium ore processed at both sites was derived from sandstone in the Saltwash Member of the Jurassic Morrison Formation (Merritt 1971).

Estimated soil moisture characteristic curves (negative pressure head [cm] versus volumetric moisture content [θ]) for coarse-grained tailings (sands and slime-sands) and fine-grained tailings (slimes) are presented in Appendix C Figures C-1 and C-2. These curves are derived from hydraulic parameters developed for the Shiprock cell drainage analysis (DOE 2012), which are provided in Table 3. The *Ks* values for the Shiprock cell are consistent with the estimated *Ks* values for the Bluewater cell (Table 1).

Table 3. Unsaturated Tailings Hydraulic Parameters Based on Shiprock, New Mexico, Disposal Cell Data

Material	θ_r	θ_s	α (1/cm)	n	*Ks* (cm/s)
Coarse tailings	0.127	0.470	0.00035	3.923	5.0×10^{-5}
Fine tailings	0.223	0.640	0.00085	3.857	3.1×10^{-6}

Key: α = curve-fitting parameter; n = curve-fitting parameter; *Ks* = saturated hydraulic conductivity; θ_r = residual volumetric moisture content; θ_s = saturated volumetric moisture content

Appendix C Figures C-3 and C-4 show volumetric moisture content versus log hydraulic conductivity that can be used to relate a moisture content to an unsaturated hydraulic conductivity, or influx value. For example, if the cover functions at a 5×10^{-5} cm/s seepage rate, underlying tailings will also function at a 5×10^{-5} cm/s conductivity.

Table 4 presents volumetric moisture contents related to influx for the range of expected operating values as derived from the figures. The moisture contents are theoretical volumetric contents that can be realized after infinite time for free drainage from the base. The low 1×10^{-7} cm/s influx is provided as the design operating value for radon barrier covers and is used for this assessment. As discussed in NUREG/CR-7028 (NRC 2011), initially low *Ks* values in constructed radon barriers have been shown to increase a few orders of magnitude after being subjected to various climatic forces such as wet-dry cycles, freeze-thaw episodes, and root penetration from plants. Therefore, the maximum cover influx rate is assumed to be 5×10^{-5} cm/s for this assessment.

Table 4. Long-Term Volumetric Moisture Contents at Estimated Influx Rates

Influx Rate	θ (Coarse Tailings)	θ (Fine Tailings)
1×10^{-7} cm/s	0.185	0.385
5×10^{-5} cm/s	0.290	0.640

Key: cm/s = centimeters per second; θ = volumetric moisture content

The volume available to store moisture that will drain from the tailings given an infinite amount of time can be estimated using the information provided in Table 3 and Table 4. The available change in storage value is computed as the difference in porosity (saturated volumetric content from Table 3) and the long-term volumetric moisture content equivalent to the seepage flux (from Table 4). The resulting storage volumes listed in Table 5 represent the theoretical volumetric moisture content in the tailings after infinite time for drainage, assuming free drainage at the base and a consistent upper boundary pressure condition at the surface.

Table 5. Estimated Storage Volumetric Moisture Content

Material	θ_s [a]	ΔS Available [b]	
		1×10^{-7} cm/s influx	5×10^{-5} cm/s influx
Coarse tailings	0.470	0.285	0.180
Fine tailings	0.640	0.255	0.000

Key: cm/s = centimeters per second; θ_s = saturated volumetric moisture content;
ΔS = change in storage
[a] From Table 3
[b] Equals θ_s minus θ from Table 4

According to Table 5, when the cover is operating at 5×10^{-5} cm/s influx, the resulting volumetric moisture content of fine tailings (slimes) equals the saturated volumetric moisture content. In other words, when the cover allows an influx of 5×10^{-5} cm/s, which is equivalent to the saturated hydraulic conductivity of the slimes, the moisture flux that enters the disposal cell will displace existing moisture in the saturated slimes. Therefore, there is no change in storage, and moisture will flow through the slimes at the influx rate.

Based on the estimated annual rainfall of 10.3 inches (26.16 cm) presented in Table 2, inflow would be 13.08 cm if 50 percent of precipitation infiltrated the cover and 6.54 cm if 25 percent infiltrated. The depth of tailings required to store infiltration without outflow is computed by dividing the infiltration amount by ΔS from Table 5. Results are presented Table 6.

Table 6. Required Tailings Depth Needed for Storage of Infiltration

Material	Infiltration Percentage	Infiltration (cm)	1×10^{-7} cm/s Influx		5×10^{-5} cm/s Influx	
			ΔS Available	Depth (cm)	ΔS Available	Depth (cm)
Coarse tailings	50	13.08	0.285	45.89	0.180	72.67
	25	6.54	0.285	22.95	0.180	36.33
Fine tailings	50	13.08	0.255	51.29	0.000	no storage
	25	6.54	0.255	25.65	0.000	no storage

Key: cm = centimeters; cm/s = centimeters per second; ΔS = change in storage

The course tailings (sands and slime-sands) have an average depth of 45 ft (1,372 cm) in the disposal cell. The fine tailings (slimes) have an average depth of 20 ft (610 cm). Therefore, the available storage is greater than the volume of voids that would be filled by precipitation infiltrating the cover. An exception occurs for the fine tailings at an influx rate of 5×10^{-5} cm/s, when no available storage exists in the saturated slimes. Under this condition, outflow equals inflow regardless of the depth of tailings. This creates a steady-state influx/outflow condition when influx equals the saturated hydraulic conductivity of the tailings.

5.3.4 Outflow

When moisture infiltration exceeds available storage, outflow will begin. The rate of discharge will asymptotically approach the cover infiltration rate. Estimates of the volume of moisture that can potentially seep through the base of the disposal cell can be calculated using the storage estimates from the previous section and assumptions taken from the impoundment geometry provided in Figure 5. The approximate areas of the two types of materials covering the bottom of the disposal cell are provided in Table 7.

Table 7. Footprint of Tailings Materials

Material	Percentage of 260-Acre Footprint	Area (ft^2)
Coarse tailings	67	7,588,152
Fine tailings	33	3,737,448

Estimates of stored moisture volumes subject to eventual drainage from the disposal cell (since completion of the cell cover) can be derived from the estimated areas computed in Table 7 and the estimated required storage depths in Table 6. The estimated drainable volumes based on the assumed cover infiltration rates and assumed infiltration percentages of precipitation are provided in Table 8 and Table 9. The estimated drainable volumes, therefore, are a combination of infiltrated precipitation and the unsaturated storage already present in the tailings.

Table 8. Estimated Drainable Volume from the Disposal Cell (Low-Permeability Cover)

Material	Infiltration Percentage	1×10^{-7} cm/s Cover Influx				
		Storage Depth		Area[a]	Drainable Volume	
		(cm)[b]	(ft)	(ft^2)	(ft^3)[c]	(gallons)
Course tailings	50	45.89	1.50	7,588,152	11,382,228	84,342,310
	25	22.95	0.75	7,588,152	5,691,114	42,171,155
Fine tailings	50	51.29	1.68	3,737,448	6,278,912	46,526,738
	25	25.65	0.84	3,737,448	3,139,456	23,263,369

Key: cm = centimeter; cm/s = centimeter per second; ft = feet
[a] From Table 7
[b] From Table 6
[c] Storage depth times area

Assuming the average cover infiltration rate is 1×10^{-7} cm/s and 50 percent of precipitation percolates through the cover (Table 8), then approximately 131 million gallons of tailings fluid would be available for eventual drainage from the coarse and fine tailings storage depths within the disposal cell; more drainable volume would be available if the cover infiltration rate is 5×10^{-5} cm/s. Annual stored volume will decrease as saturation of the tailings increases.

Table 9. Estimated Drainable Volume from the Disposal Cell (High-Permeability Cover)

Material	Infiltration Percentage	5×10^{-5} cm/s Cover Influx				
		Storage Depth		Area[a]	Drainable Volume	
		(cm)[b]	(ft)	(ft^2)	(ft^3)[c]	(gallons)
Course tailings	50	72.67	2.38	7,588,152	18,059,802	133,823,132
	25	36.33	1.19	7,588,152	9,029,901	66,911,566
Fine tailings	50	NS	NS	3,737,448	NC[d]	NC[d]
	25	NS	NS	3,737,448	NC[d]	NC[d]

Key: cm = centimeter; cm/s = centimeter per second; ft = feet; NC = not calculated; NS = no storage
[a] From Table 7
[b] From Table 6
[c] Storage depth times area
[d] Drainage volume will be equal to the cover flux multiplied by the time since cover construction in 1995

Because the hydraulic head will be greater in the tailings than in underlying materials, either saturated or unsaturated drainage will occur. These estimated drainage values are applicable only if the tailings drained below the computed depths provided in Table 6 during and after placement of the final cover. All potential saturation depths are less that the average tailings depth. Since saturated drainage is not expected at this time, drainage will be in an unsaturated condition at very low rates and volumes.

If the tailings become saturated, drainage will occur at the influx rate if the saturated hydraulic conductivity of the tailings is greater than or equal to the influx rate. If the saturated hydraulic conductivity of the tailings is less than the influx rate, the tailings will store much of the moisture until full saturation occurs. Table 10 provides the potential annual seepage that could occur if the tailings become saturated and outflow equals inflow.

Table 10. Potential Annual Outflow if the Tailings Become Saturated

Material	Infiltration Percentage	Infiltration Rate[a]	Area[b]	Outflow Volume		Outflow Rate
		(ft/yr)	(ft^2)	(ft^3)	(gallons)	(gpm)
Coarse Tailings	50	0.430	7,588,152	3,262,906	24,178,134	46.0
	25	0.215	7,588,152	1,631,453	12,089,067	23.0
Fine Tailings	50	0.430	3,737,448	1,607,102	11,908,626	22.7
	25	0.215	3,737,448	803,551	5,954,313	11.3
Total	50	0.430			36,086,760	68.7
	25	0.215			18,043,380	34.3

Key: ft = foot or feet; gpm = gallons per minute; yr = year
[a] Derived from an average annual precipitation rate of 10.3 inches per year
[b] Cell cover area is approximately equal to the tailings footprint (Table 7)

Based on the results of Table 10, the extreme scenario suggests that approximately 36 million gallons of tailings fluid could seep from the disposal cell annually if the tailings become saturated and if 50 percent of precipitation percolates into the tailings. This annual volume equates to approximately 0.6 percent of the total fluids that seeped from the tailings impoundment prior to disposal cell completion. Until the tailings become saturated, the annual seepage rate would be less, and would gradually approach the saturated tailings seepage rate.

The estimated 36-million-gallon annual seepage rate is based on an assumed upper limit of precipitation percolation through the cover and into saturated tailings. As noted in Section 5.3.2, however, studies show that increasing vegetation on the cover reduces percolation of precipitation into the tailings because of evapotranspiration. As vegetation is allowed to establish (or is enhanced to accelerate establishment) on the Bluewater cell cover, the precipitation inflow could reduce to substantially less than 25 percent of annual precipitation. And, it is possible that the tailings would not become saturated and that seepage would remain minimal as unsaturated drainage.

The upper limit seepage rate is equivalent to a rate of approximately 69 gpm (Table 10). This rate is substantially greater than the 1995 seepage rate of approximately 16 gpm estimated by ARCO, prior to closure of the disposal cell (Appendix A Table A-1). If the encapsulated tailings are not saturated, then current actual seepage rates could be closer to ARCO's 1995 estimated rate, or possibly even lower.

Although water levels in both aquifers fluctuated, elevations in 1995, when the cell was closed, were similar to elevations in 1984, near the end of cell dewatering activities (pumping from the sand tailings). However, alluvial aquifer water levels in wells T(M) and X(M), downgradient of the disposal cell, have dropped approximately 13 ft since 1995 (Figure 13). Also, San Andres aquifer levels in wells OBS-3 and S(SG), located adjacent to and downgradient of the disposal cell, have dropped approximately 46 ft since 1995 (Figure 14). These significant drops in water levels can be attributed, at least in part, to a persistent regional drought. However, it seems likely that if seepage is occurring at a rate of 69 gpm, or even 34 gpm (based on a 25 percent precipitation infiltration rate), the declines in water levels would not have been nearly as great near the cell. The declining water levels, therefore, suggest that current seepage from the cell is having a minimal impact on the aquifers.

Continued elevated uranium concentrations in the San Andres POC wells suggest a continuing source of contamination, but the contribution from cell seepage is unknown; however, the greatest contribution is most likely from groundwater flow through the mineralized zone. Groundwater chemistry is being evaluated as part of the groundwater conceptual model to provide a better technical basis for whether there is evidence of continuing seepage.

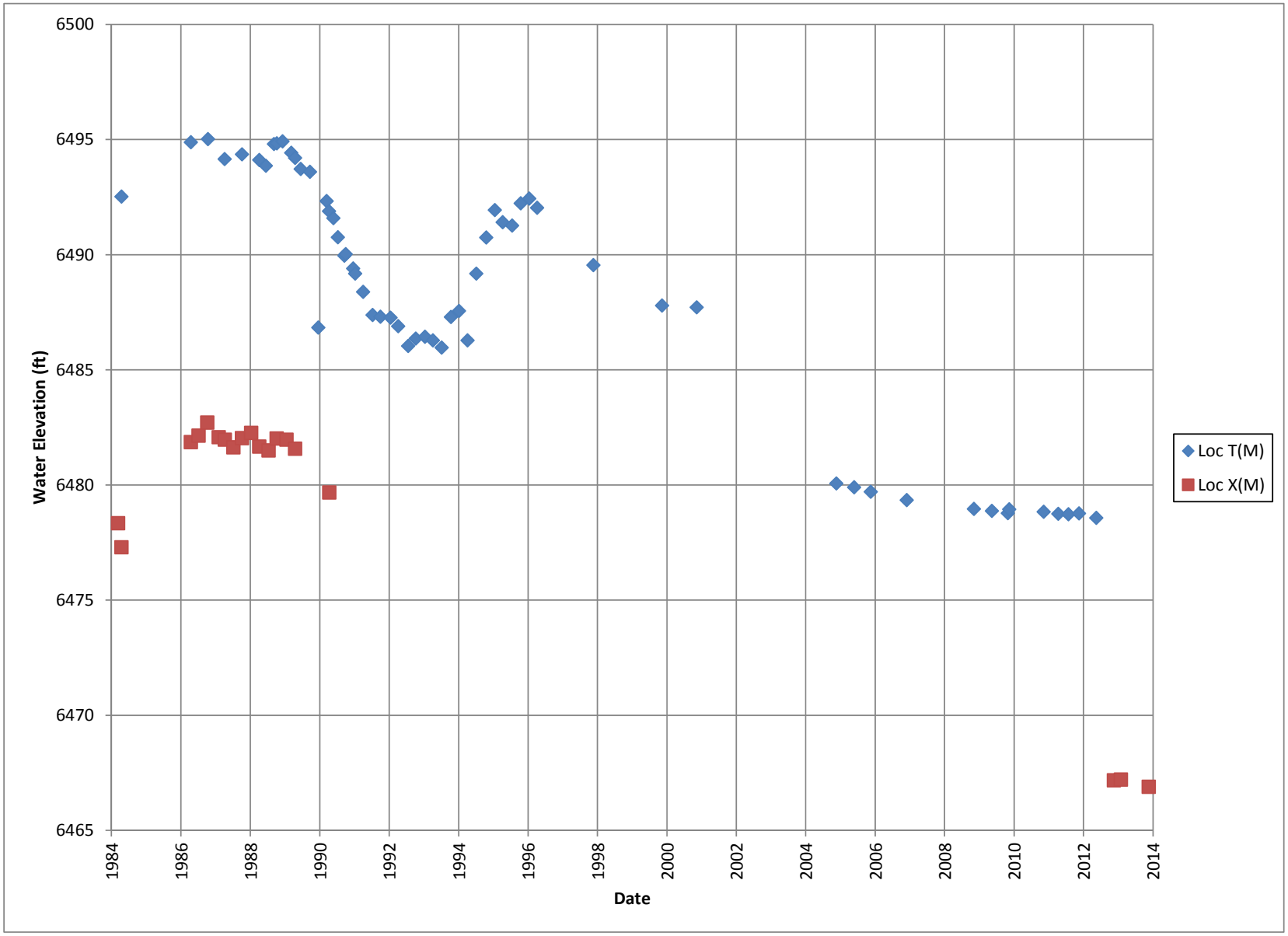

Figure 13. Hydrographs for Alluvial Aquifer Wells T(M) and X(M)

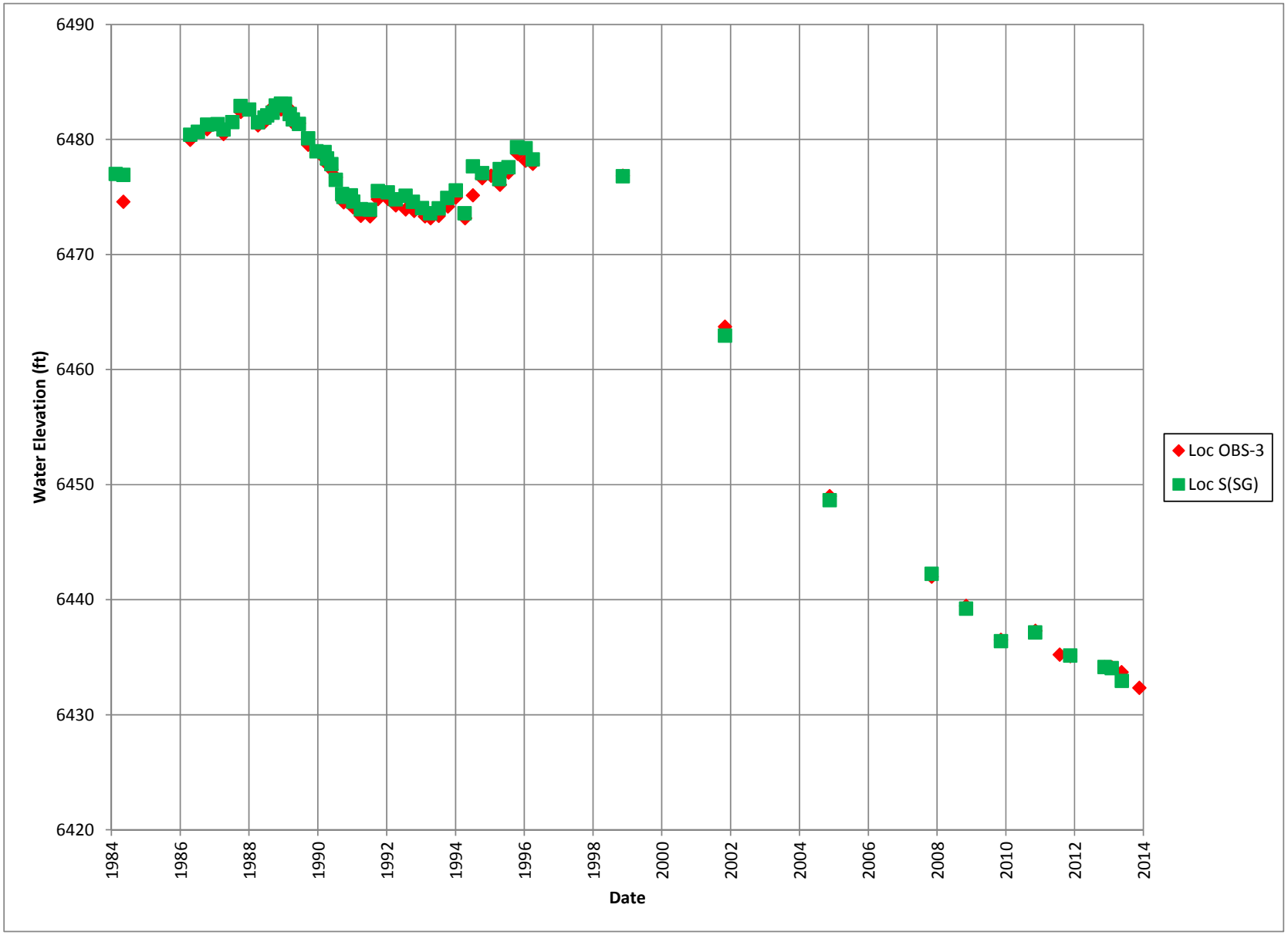

Figure 14. Hydrographs for San Andres Aquifer Wells OBS-3 and S(SG)

6.0 Groundwater Contamination

6.1 Contaminant Mass

Constituents of concern with respect to ARCO's groundwater corrective action program, and subsequently included in the LTSP, are molybdenum, selenium, and uranium because concentrations were above background levels in monitoring wells near the main tailings impoundment. Therefore, the evaluation of contaminant mass that seeped from the tailings impoundment, and continues to seep from the disposal cell, addresses these constituents.

As noted previously, an estimated quantity of 5.7 billion gallons of tailings fluids seeped through the bottom of the main tailings impoundment prior to encapsulation in 1995. Contaminant concentrations in the raw tailings water, or tailings liquor, varied due to changes in milling processes and ore characteristics, but ARCO considered the concentrations listed in Appendix A Table A-2 as representative of the tailings liquor. According to that table, the liquor had a pH of 1.2 and the following concentrations for contaminants of concern: 1.33 mg/L molybdenum, 4.0 mg/L selenium, and 19.5 mg/L uranium (Dames & Moore 1981b).

The estimated mass for each of the constituents of concern that seeped through the bottom of the tailings impoundment prior to completion of the disposal cell cover in 1995 is provided in Table 11. Assuming the seepage volume and contaminant concentrations are representative of actual conditions, nearly 1 million pounds of uranium would have been in the fluids that seeped from the tailings impoundment.

Table 11. Estimated Seeped Contaminant Mass Prior to Disposal Cell Completion

Contaminant	Concentration	Seeped Volume		Contaminant Mass	
	(mg/L)	(billion gallons)	(billion liters)	(mg)[a]	(pounds)
Molybdenum	1.33	5.7	21.6	2.87×10^{10}	63,300
Selenium	4.0	5.7	21.6	8.64×10^{10}	190,500
Uranium	19.5	5.7	21.6	4.21×10^{11}	928,300

Key: mg = milligrams; mg/L = milligrams per liter
[a] Concentration times seeped liters

The mass of uranium in seepage since the cover was completed cannot be estimated because seepage rates and contaminant concentrations in the tailings fluids are unknown. ARCO's efforts to dewater the tailings impoundment means that the fluids currently in the tailings are a mixture of the small amount of remaining leachate and precipitation that has percolated into the tailings since dewatering activities. The current quality of the fluids in the tailings would be better than the original tailings liquor. Regardless, seepage is most likely occurring, and will increase if the tailings become saturated. Therefore, contaminants will continue to enter the aquifers.

Concentrations of hazardous constituents in groundwater beneath the disposal cell are controlled by geochemical reactions between the seeped tailings solution in the geologic formation materials underlying the cell and in the receiving groundwater. The tailings solution with low pH, high reduction potential (Eh), and high sulfate concentrations has high concentrations of trace constituents, including metals, uranium, and molybdenum.

Precipitation of metals, sulfate, molybdenum, and uranium occurs as a result of neutralization of tailings solution. Chloride and selenium are not subject to pH-induced precipitation (Dames & Moore 1981b). Once the ambient pH exceeds about 6.0, further precipitation of sulfate, molybdenum, and uranium is negligible.

Trace components are removed from solution either by precipitation of minerals involving the trace constituent or by coprecipitation and adsorption of trace components on the precipitates. The precipitation process may contribute low concentrations of constituents to groundwater passing through the altered (mineralized) zone. Consequently, constituent concentrations above background levels are expected to persist indefinitely.

ARCO concluded that a neutralizing zone exists in the alluvium and limestone materials beneath the cell (Applied Hydrology Associates Inc. 1995). Their conclusion was based on the geochemistry of groundwater samples from monitoring wells close to the tailings impoundment. The samples had much higher pH values (between 6 and 7 compared to 1.2 in the tailings fluid) and lower constituent concentrations than the seeping tailings fluid. A geochemical analysis of the tailings liquor indicated that it was saturated with respect to metal-carbonates. Therefore, it was implied that uranium, lead, zinc, cadmium, copper, and molybdenum should be precipitated as carbonates in the neutralization zone.

This neutralization zone would be an altered or mineralized zone of constituents that seeped from the tailings impoundment and disposal cell. It would exist under the disposal cell and probably for some distance along the fault zones. If present, it would be an indefinitely continuing source of contamination to the alluvial and San Andres aquifers because groundwater flow through the mineralized zone would mobilize unknown quantities of contaminants. Because of the near-neutral pH of the unaffected inflowing groundwater, however, contaminant mobilization would be expected to be limited.

The actual presence of a mineralized zone cannot be verified without extensive drilling and sampling of the aquifer materials under the disposal cell. However, ARCO's geochemical evaluation of the tailings fluid and the monitoring well samples near the tailings impoundment strongly support its existence.

6.2 Alluvial Aquifer

Anaconda and ARCO sampled wells in the alluvial aquifer from 1980 to 1996. ARCO records indicate that uranium concentrations in POC well T(M) peaked at a concentration of approximately 1.6 mg/L in 1980 and declined rapidly, stabilizing at about 0.1 mg/L in 1995. Uranium concentrations peaked at approximately 0.75 mg/L in 1983 in downgradient well U(M), and peaked at about 0.4 mg/L in POE well X(M) in 1989. ARCO attributed the progressive decline in uranium concentrations from T(M) to U(M) to X(M) to natural attenuation in the alluvial aquifer. The closest offsite downgradient alluvial well (located about 1,400 ft south of the site entrance) indicated negligible uranium concentrations of 0.0031 mg/L in 1989 and 0.0041 mg/L in 1990, supporting ARCO's assessment that uranium in the alluvial aquifer had attenuated to background concentrations near the mill site boundary.

DOE began groundwater monitoring in 1998. Initially, uranium concentrations in POC well T(M) were approximately 0.1 mg/L, which was the same as the lowest results obtained by ARCO. However, uranium concentrations began to increase after the 2000 sampling event. The increasing uranium concentrations coincided with decreasing water levels in that portion of the alluvial aquifer. Before the well dried up, uranium concentrations in well T(M) were averaging 0.54 mg/L, which is less than the peak concentration observed by ARCO. This correlation of increasing uranium and decreasing aquifer water levels has been observed at some UMTRCA Title I sites. Uranium concentrations in POC well F(M) did not change during that period (averaging 0.008 mg/L)—the alluvial aquifer at that location may not have been affected by site contamination—nor did water levels drop significantly (less than 2 ft since 2000).

Although the alluvium at well T(M) has dried up, the aquifer has not dried up because the alluvial sequence is thicker and deeper where the main channel of the former Rio San Jose coursed. For example, the alluvium at well 21(M) is approximately 25 ft thick and is fully saturated. As the volume of water in an aquifer decreases, such as at T(M), it is possible that the contaminant mass is concentrated in the remaining water, resulting in increased concentrations. Uranium is the only contaminant with elevated concentrations to begin with, so its concentration would have increased as the volume of water decreased. As expected under this scenario, total dissolved solids concentrations also increased by approximately 40 percent as water levels in well T(M) dropped. This correlation between reducing water levels and increasing uranium will be addressed further in the conceptual model study.

Whether or not this is the cause for the increasing uranium concentrations in T(M), the increase does not point to a new pulse of contaminated water coming from the disposal cell. The declining water levels are not indicative of additional seepage, and no other mill-related contaminants are showing increasing concentrations in the well. Chloride and sulfate, other indicator constituents of potential cell leakage, had historically low concentrations and decreased slightly in T(M) as water levels dropped.

The uranium concentrations in well 22(M), located about midway between T(M) and 21(M), are averaging 0.33 mg/L, which is nearly equivalent to the last concentration of 0.31 mg/L observed by ARCO for well U(M) in 1990. Wells 21(M) and X(M) are located along downgradient site boundaries, and samples from each well have uranium concentrations of approximately 0.14 mg/L; ARCO's last sample from X(M), collected in 1990, had a uranium concentration of 0.15 mg/L (it averaged 0.31 mg/L during the previous 6 years). Well 23(M), near the site entrance and about 1,600 ft downgradient of well 21(M), has had uranium concentrations averaging 0.02 mg/L, which is below the drinking water standard.

DOE sampled the same offsite alluvial well monitored by ARCO. The bottom of that well apparently is completed in the Chinle Formation (below its contact with the alluvium), but the water is mostly likely from Rio San Jose alluvium because that portion of the Chinle Formation is dry at other nearby well locations (ARCO also considered it to be an alluvial well). Uranium concentrations from two DOE sampling events in 2012 were 0.0033 mg/L and 0.0045 mg/L, which are essentially unchanged from ARCO's results. These results, considered together with DOE's sampling results from 23(M), appear to substantiate ARCO's conclusion regarding the attenuation of uranium in the alluvial aquifer. Although uranium concentrations increased in well T(M), the aquifer at the downgradient wells appears to have reached steady-state conditions because uranium concentrations have remained unchanged since 1990. Fate and transport of

contaminants in the alluvial aquifer will be evaluated further in DOE's groundwater conceptual model.

6.3 San Andres Aquifer

6.3.1 Northeast Portion of Site

Uranium concentrations in the San Andres aquifer groundwater north of the east-west-tracking fault continue to be elevated. Uranium concentrations in POC well S(SG) had been declining since the late 1980s when they peaked at 1.8 mg/L. The uranium concentration in POE well I(SG) peaked at 0.66 mg/L in 1989 and then began to decline. ARCO concluded that this peak in well I(SG) was in response to the high seepage rates that occurred in the 1950s, as supported by results of groundwater velocity and uranium transport analyses (Applied Hydrology Associates Inc. 1995). ARCO considered the decrease in uranium concentrations between the POC and POE wells to represent natural attenuation within the San Andres aquifer.

At the location of new well 16(SG), the San Andres Limestone is dry due to the decline of water levels, but the Glorieta Sandstone is saturated. Therefore, the polyvinyl chloride well screen is in the upper part of the Glorieta Sandstone. Uranium concentrations using the low-flow sampling method have been averaging approximately 1.4 mg/L, which is below the ACL of 2.15 mg/L. This concentration is very similar to ARCO's results for OBS-3 and S(SG) in the mid-1990s, when the wells probably were not exhibiting the current extent of corrosion. Therefore, sample results from 16(SG) appear to be more representative of aquifer conditions at that location than current results from the corroded POC wells.

A downhole conductivity test through the open borehole portion of well I(SG) revealed that the aquifer is stratified into two zones at that location; the upper third of the open borehole had a lower conductivity than the lower two-thirds. Low-flow samples collected in November 2013 showed elevated uranium concentrations in both zones, with a result of 0.15 mg/L in the upper third and results of 0.32 mg/L and 0.33 mg/L in the lower two-thirds of the aquifer. A subsequent high-flow sample (using the casing purge method) had a concentration of 0.35 mg/L, which is less than ARCO's last result of 0.42 mg/L (ARCO also used the casing purge method). For comparison, a conductivity test in background well L(SG) showed no change in conductivity with depth, and samples collected at multiple depths within the open borehole portion of that well averaged 0.003 mg/L uranium during the May 2013 sampling event.

Current uranium, chloride, sulfate, and total dissolved solids concentrations are lower than ARCO's results for OBS-3, S(SG), and I(SG). It appears from a comparison of the ARCO and DOE results, therefore, that San Andres aquifer groundwater quality has improved north of the east-west tracking fault, and there is no obvious indication of a new pulse of contamination from the disposal cell. However, historical and recent groundwater data from San Andres aquifer wells north of the east-west-tracking fault and downgradient of the site are being evaluated in DOE's groundwater conceptual model to estimate the fate and transport of contaminants in that portion of the aquifer.

6.3.2 Southeast Portion of Site

ARCO recognized that the Anaconda #5 production well, located along the Ambrosia Lake Fault more than a mile south of the east-west-tracking fault, was affected by mill-related contaminants. Reported uranium concentrations were as high as 0.18 mg/L in 1989 (the well was not monitored while being used as a production well). Despite the presence of mill-related contaminants in Anaconda #5, ARCO did not consider contamination south of the fault to be of concern. As discussed in Section 2.3, ARCO assumed that incoming fresh water (from upgradient recharge) would mix with contaminated water and dilute contaminant concentrations to acceptable levels in the south portion of the site.

Uranium concentrations in DOE's new San Andres aquifer wells south of the east-west-tracking fault are elevated. Sample results from November 2013 showed a high of 0.18 mg/L in well 15(SG) and a low of 0.074 mg/L in 14(SG). A sample from farthest downgradient well 13(SG) had a concentration of 0.099 mg/L. These results lead to the conclusion that the historical results from Anaconda #5 represent contamination that was drawn south during mill production well pumping and that the contamination has migrated downgradient of the fault zone.

ARCO never had San Andres monitoring wells in the southeastern portion of the site. Based on ARCO's sample results from Anaconda #5 well, the groundwater in this portion of the site probably has had elevated uranium concentrations since the mill was being operated. Therefore, the results from DOE's new wells represent contamination drawn to that area by ARCO's production wells rather than a new pulse of contaminated water from the disposal cell.

The offsite former domestic Sabre-Piñon well (now called HMC-951) had background uranium concentrations when monitored by ARCO in the 1980s (see Section 2.3). However, Homestake Mining Company put HMC-951 into production for their groundwater corrective action plan for its mill site located about 4 miles southeast of the Bluewater site. The well was pumped at an average rate of about 350 gpm from 1999 through 2012. During that time, uranium concentrations ranged from a low of 0.020 mg/L to a high of 0.048 mg/L. It appears likely, therefore, that the pumping drew contaminated groundwater from the southeast portion of the site to HMC-951. DOE has begun sampling this well, and the uranium concentration from the first sampling event in November 2013 was 0.031 mg/L.

A comparison of results from wells on both sides of the east-west tracking fault indicates that uranium concentrations are lower in the southeast portion of the site. Historical and recent groundwater data from San Andres aquifer wells south of the fault and downgradient of the site are being evaluated in DOE's groundwater conceptual model to estimate the fate and transport of contaminants in that portion of the aquifer.

This page intentionally left blank

7.0 Conclusions

ARCO estimated that approximately 5.7 billion gallons of tailings fluid seeped through the bottom of the main tailings impoundment prior to construction of the disposal cell cover in 1995; about half of that total was projected to have occurred prior to 1960. These fluids entered the two uppermost aquifers at the site. ARCO expended a considerable effort to dewater the tailings before completing the disposal cell, so the volume of tailings liquor available for continued seepage was significantly reduced.

Tailings fluids, consisting of a less-contaminated mixture of the remaining tailings liquor and precipitation that has percolated through the cell cover materials, are seeping from the disposal cell and may continue to do so indefinitely. The projected maximum annual seepage estimate of 36 million gallons assumes saturated moisture conditions in the tailings and a potential upper limit of 50 percent of precipitation percolating through the cell cover. Although this maximum estimated annual seepage rate is large, it is substantially less than 1 percent of the total seepage that occurred prior to completion of the cover in 1995. However, current seepage appears to be minimal because decreasing water levels and steady-state contaminant concentrations in the aquifers are not indicative of the maximum estimated rate. It is unlikely, therefore, that the tailings are saturated at this time, and hydraulic properties of the cover materials may not have changed enough to allow the maximum projected precipitation infiltration. An increase in vegetation on the cell cover is expected to keep infiltration rates low due to evapotranspiration, which would keep seepage rates low.

The band drains that ARCO installed in the north portion of the tailings impoundment did not completely dewater the slimes—they only reduced the water content to facilitate consolidation of the slimes. Up to 15 ft of relocated silty-clay material, similar to the material used for the radon barrier, was placed over the slimes prior to installation of the radon barrier. This thick, low-permeability layer would significantly reduce infiltration of precipitation into the slimes and keep the seepage rate low.

Based on groundwater monitoring results that showed higher pH values and lower contaminant concentrations than were present in the tailings fluid, ARCO concluded that the acidic tailings fluids that seeped through the bottom of the tailings impoundment were neutralized, causing contaminants to precipitate and adsorb in the underlying aquifer materials. Consequently, a mineralized zone apparently formed in the aquifer materials under the disposal cell. This mineralized zone is assumed to be the current primary source of groundwater contamination, and it will remain indefinitely.

Depressions have formed on the disposal cell cover because the slimes portion of the tailings impoundment continued to consolidate after the cover was completed. Precipitation runoff water forms ponds in these depressions, potentially introducing a second source of fluids infiltrating through the disposal cell. However, observations of the persistence of the ponds and the results of radon flux measurements indicate that there has been no reduction in the performance of the radon barrier and that the ponds are reduced primarily through evaporation rather than infiltration. Therefore, the depressions and associated ponds are not indicative of additional seepage from the cell.

There is no evidence at this time to suggest that the elevated uranium concentrations in onsite wells indicate a new pulse of contamination from within the disposal cell or recharge from ponds

on top of the cell. An increase in seepage from the disposal cell is not evident because water levels have dropped significantly in both aquifers and continue to decline. Although uranium concentrations increased in alluvium POC well T(M) until the well dried up, the increase appears to be due to decreasing water levels at that location rather than increased seepage from the disposal cell. Also, uranium concentrations at the POE wells in both aquifers are less than those observed by ARCO.

Considerable uncertainties are associated with the water balance and mass estimates presented in this assessment and are addressed in the following chapter. Nevertheless, they do not negate the primary conclusion that the volume of fluid and mass of contaminants seeping from the cell since it was constructed are very small compared to the corresponding volume and mass that seeped through the bottom of the tailings impoundment prior to cell construction.

8.0 Uncertainties

Uncertainty in regards to the performance of the disposal cell is unavoidable given the sparseness of observed data and the limited amount of information available to corroborate or refute alternative models. The major uncertainties and their effects on the conclusions drawn in this study are provided in Table 12.

Table 12. Uncertainties and Their Effects on Conclusions

Conclusion	Uncertainty	Effect on Conclusion	Significance of Uncertainty
An estimated 5.7 billion gallons of fluids seeped through the bottom of the tailings impoundment prior to encapsulation. This quantity was estimated by ARCO based on a water balance analysis of the milling processes. Unknown proportions seeped into the underlying aquifers.	Actual seepage rates and quantities were not measured.	Precipitation and evaporation were not factored into ARCO's estimates. Therefore, actual seepage could have been greater or less than 5.7 billion gallons.	Attempts to more precisely estimate the amount of seepage that occurred would not impact the conclusion that a very large volume of contaminated tailings fluid seeped into the materials and aquifers below the tailings impoundment.
Approximately 1 million pounds of uranium were in the fluids that seeped from the tailings impoundment prior to completion of the disposal cell. This estimated quantity was based on the estimated 5.7 billion gallons of seepage and one sample that was used by ARCO to characterize the tailings fluid.	Contaminant concentrations in the tailings fluids would have varied considerably throughout the period of milling and as distributed within the tailings. Therefore, the actual quantity of uranium that seeped from the tailings is unknown, and the amount remaining for mobilization in the groundwater is unknown.	The actual quantity of uranium that seeped from the tailings impoundment and is potentially available as a continuing contaminant source is greater or less than 1 million pounds.	Data are not available to determine the actual amount of uranium that seeped from the tailings impoundment or how much entered the aquifers. The primary conclusion that a large mass of uranium is available as a continuing source of groundwater contamination is not impacted by the uncertainty associated with this estimate.
Seepage from the tailings impoundment during milling operations affected the aquifer characteristics (potentiometric surface elevations, flow directions, flow rates, and quality) under the site.	Because aquifer monitoring did not begin until near the end of milling operations, the quantitative impacts on the aquifers during the time that the greatest volumes of fluids seeped from the tailings impoundments are unknown.	Due to the absence of data, whatever happened in the aquifers prior to monitoring cannot be recreated. Because monitoring results during the later stages of milling showed that the highest concentrations were near the tailings impoundment and that groundwater and entrained contaminants were drawn to the production wells, the uncertainties have no effect on the conclusion.	Literature and monitoring have shown that the aquifers are contaminated above background concentrations, that water levels have dropped significantly in the past 20 years, and that flow directions have apparently returned to pre-milling conditions. A quantitative understanding of aquifer changes during milling would not add value to our understanding of current or projected conditions.
Seepage continues to occur at an unknown rate through the bottom of the disposal cell, and is expected to continue indefinitely. It is assumed that seepage is occurring at a minimal rate, but will increase as the tailings become more saturated.	Seepage rates are dependent in part on the degree of saturation within the tailings, which is unknown.	Regardless of the degree of tailings saturation or the seepage rate, seepage is still occurring, thus contributing to a continuous source of contamination in the aquifers. However, the contaminant mass available from present day seepage to impact groundwater concentrations is extremely small compared to the mass associated with the fluids that seeped during milling.	Measuring actual saturation and seepage would require extensive sampling and testing of tailings materials. The source term released during milling is much greater than the source term being released from the disposal cell. Therefore, knowing the actual seepage rate would not have a significant bearing on conclusions relating to the behavior of contaminant migration in the aquifers.

Conclusion	Uncertainty	Effect on Conclusion	Significance of Uncertainty
Unless the cell cover develops into an evapotranspiration cover, precipitation will percolate through the cover, and the tailings materials will approach a saturated condition. Under long-term steady state conditions, seepage through the bottom of the cell is expected to equal the rate of precipitation that percolates through the cover. Under those conditions, the rate of seepage is expected to equal 25 to 50 percent of the rate of precipitation. Even using these values, the estimated annual seepage would be much less than the seepage that occurred prior to encapsulation of the disposal cell.	Current and potential percolation rates are unknown because cover soil hydraulic properties have not been tested and will likely continue to change. The potential length of time needed for the full thickness of the cell to become saturated is unknown because the existing depth of saturation in the tailings is unknown, and the rate of precipitation percolating through the cover is unknown.	Regardless of the rate of seepage from the disposal cell, it is estimated to be significantly less than the seepage that occurred during milling operations. Over time, cover percolation and tailings seepage rates would likely continue to decline if vegetation is allowed or encouraged to establish on the cover.	Soil tests of cover materials and the tailings and monitoring of cover percolation rates would be required to refine the estimates. Contaminant concentrations in the aquifers have remained essentially unchanged. Therefore, knowing the actual seepage rate would not have a significant bearing on conclusions relating to the behavior of contaminant migration in the aquifers.
Based on historical groundwater monitoring results near the tailings impoundment, the fluids that seeped through the bottom of the tailings impoundment are assumed to have formed a mineralized zone in the materials under the disposal cell and along fault zones.	Sampling of materials has never been conducted to confirm the presence or extent of the mineralized zone.	Continued elevated uranium concentrations in wells near the disposal cell indicate the presence of a continuing source of contamination. Because ARCO did not observe changes in groundwater chemistry during dewatering activities of the tailings impoundment, there is a high probability that a mineralized zone is present and that it is the primary source of continuing contamination.	Extensive borehole material analysis and groundwater quality measurements under the disposal cell and along the fault zones would be required to define the postulated mineral zone. It is most likely the characterization would confirm the presence of the mineralized zone and that it should be considered to be a continuing source of contamination to the aquifers.
Contaminant concentrations within the fluids currently seeping from the disposal cell were not estimated. However, it is assumed that the quality of the seeping fluid is not as degraded as during milling operations because of dewatering activities conducted by ARCO and infiltration of clean precipitation water (i.e., current disposal cell fluids are a mixture of residual mill fluids and fresh water from precipitation infiltration).	The current chemistry of the tailings fluids is unknown.	Because the current quality of the tailings fluid has not been tested, the conclusion may or may not be valid.	Tailings fluid characterization, which would require numerous monitoring wells completed in the disposal cell, would be required to determine tailings fluid quality. However, if contaminant concentrations in the aquifers were to increase, determination of the source of increased contamination (cell seepage versus mineralized zone) would be difficult, if not impossible, even if the tailings fluid quality was known.

Conclusion	Uncertainty	Effect on Conclusion	Significance of Uncertainty
Based on cell construction, regional evaporation rates, and the lack of radon emission in the area where ponding occurs on the disposal cell cover (over a small area of the slimes portion of the disposal cell), the ponding does not contribute to additional seepage from the disposal cell.	Site-specific evaporation rates and hydraulic properties of the cover and underlying materials in the area of depressions have not been measured. Therefore, actual percolation rates through the approximate 15-ft-thick compacted clay layer over the slimes are unknown.	If some portion of the ponded water is percolating through the thick clay layer, then it would combine with the residual tailings fluids in the slimes and eventually seep through the bottom of the disposal cell.	Evaporation monitoring and characterization of the hydraulic properties of the cover and compacted clay layer materials would be required to determine if or how much precipitation is percolating into and through the slimes. Because seepage is likely occurring through the more permeable sand portions of the tailings, any contribution from the ponded water through the very-low permeability slimes would be insignificant.

9.0 References

Abichou, T., C. H. Benson, T. Edil, and B. Freber, 1998. "Using waste foundry sand for hydraulic barriers," *Recycled Materials in Geotechnical Applications*, GSP No. 79, American Society of Civil Engineers, p. 86–89.

Albright, W.H., C.H. Benson, G.W. Gee, A.C. Roesler, T. Abichou, P. Apiwantragoon, B.F. Lyles, and S.A. Rock, 2004. "Field water balance of landfill final covers," *J. Environ. Qual.* 33:2317–2332.

Applied Hydrology Associates Inc., 1990. *Corrective Action Program and Alternate Concentration Limits Petition for Uranium, Molybdenum and Selenium, Bluewater Uranium Mill Near Grants, New Mexico*, prepared for the Atlantic Richfield Company, June.

Applied Hydrology Associates Inc., 1993. *Ground Water Corrective Action Program Review, Bluewater Uranium Mill Near Grants, New Mexico*, prepared for the Atlantic Richfield Company, December.

Applied Hydrology Associates Inc., 1995. *Corrective Action Program and Alternate Concentration Limits Petition for Uranium, Molybdenum and Selenium, Bluewater Uranium Mill Near Grants, New Mexico*, prepared for the Atlantic Richfield Company, April.

ARCO (Atlantic Richfield Company), 1990. *Reclamation Plan, Bluewater Mill*, License Number SUA-1470, Docket Number 40-8902, 3 Volumes, March.

ARCO (Atlantic Richfield Company), 1996. *Completion Report for Reclamation of the Bluewater Mill Site,* March.

Arlin, V.E., T.R. Beck, and D.E. Dixon, 1978. *A Study of Seepage Loss from the Mill Tailings Area and an Evaluation of the Adequacy of the Disposal Well: The Anaconda Company*.

Benson, C.H., W.J. Waugh, W.H. Albright, G.M. Smith, and R.P. Bush, 2011. "Design and Installation of a Disposal Cell Cover Field Test." *Proceedings of Waste Management 2011 Symposium*, Phoenix, Arizona.

Dames & Moore, 1981a. *Licensing Documentation Volume X—Below-Grade Seepage Bluewater Mill Near Grants, New Mexico*, prepared for Anaconda Copper Company, August.

Dames & Moore, 1981b. *Licensing Documentation Volume IX—Tailings Management, Bluewater Mill near Grants, New Mexico*, prepared for Anaconda Copper Company, September.

Dames & Moore, 1984a. *Report, Ground Water Study, Above-Tailings Impoundment, Bluewater Mill and Vicinity Near Grants, New Mexico*, Prepared for Anaconda Minerals Company, October.

Dames & Moore, 1984b. *Response to Questions Expressed in the Environmental Improvement Division Letter of April 24, 1984 Concerning the Proposed Discharge Plan for the Above-Grade Tailings Impoundment, Bluewater Mill*, Licensing Documentation, Volume 22, prepared for Anaconda Minerals Company, November.

DOE (U.S. Department of Energy), 1997. *Long-Term Surveillance Plan for the DOE Bluewater (UMTRCA Title II) Disposal Site Near Grants, New Mexico*, DE–AC13–96GJ87335, U.S. Department of Energy Grand Junction Office, Grand Junction, Colorado, July.

DOE (U.S. Department of Energy), 2012. *Shiprock, New Mexico, Disposal Cell Internal Water Balance and Cell Conditions*, LMS/SHP/S08254, Office of Legacy Management, Grand Junction, Colorado, September.

Glenn, E.D., and W.J. Waugh, 2001. *Disposal Cell Cover Moisture Content and Hydraulic Conductivity, Long-Term Surveillance and Maintenance Program Shiprock, New Mexico, Site*. GJO-2001-204-TAR, U.S. Department of Energy Grand Junction Office, Grand Junction, Colorado.

Link, S.O., W.J. Waugh, and J.L. Downs, 1994. "The role of plants on isolation barrier systems," in G.W. Gee and N.R. Wing (eds.), *In-Situ Remediation: Scientific Basis for Current and Future Technologies,* Battelle Press, Columbus, Ohio.

Merritt, R.C., 1971. *The Extractive Metallurgy of Uranium*, Colorado School of Mines Research Institute, prepared under contract with the U.S. Atomic Energy Commission, pps 391 and 422.

NRC (U.S. Nuclear Regulatory Commission), 1990. *Staff Technical Position Design of Erosion Protection Covers For Stabilization of Uranium Mill Tailings Sites*, Rockville, Maryland.

NRC (U.S. Nuclear Regulatory Commission), 2011. *Engineered Covers for Waste Containment: Changes in Engineering Properties and Implications for Long-Term Performance Assessment*, NUREG CR/7028, Washington DC.

Waugh, W.J., G.M. Smith, B. Danforth, G.W. Gee, V. Kothari, and T. Pauling, 2007. "Performance Evaluation of the Engineered Cover at the Lakeview, Oregon, Uranium Mill Tailings Site," *Proceedings of Waste Management 2007 Symposium*, Tucson, Arizona.

Waugh, W.J., S.J. Morrison, G.M. Smith, M. Kautsky, T.R. Bartlett, C.E. Carpenter, and C.A. Jones, 1999. *Plant Encroachment on the Burrell, Pennsylvania, Disposal Cell: Evaluation of Long-Term Performance and Risk*, GJO-99-96-TAR, U.S. Department of Energy, Grand Junction, Colorado.

Waugh, W.J., C.H. Benson, and W.H. Albright, 2009. "Sustainable covers for uranium mill tailings, USA: Alternative design, performance, and renovation," *Proceedings of 12th International Conference on Environmental Remediation and Radioactive Waste Management*, Liverpool, United Kingdom.

Wells, J.M., and J.M. Norman, 1991. "Instrument for Indirect Measurement of Canopy Architecture," *Agron. J.*, 83:818–825.

West, S.W., 1972. *Disposal of Uranium-Mill Effluent by Well Injection in the Grants Area, Valencia County, New Mexico*, prepared in cooperation with the New Mexico State Engineer Office and the U.S. Atomic Energy Commission, Geological Survey Professional Paper 386–D.

This page intentionally left blank

Appendix A

Bluewater Main Tailings Impoundment Seepage and Fluid Chemistry

This page intentionally left blank

Table A-1. Estimated Seepage Rates and Quantities from the Main Tailings Impoundment

Year	Estimated Seepage Rates (gpm)[a]			Estimated Seepage Quantities (gallons)	
	Sand Tailings[b]	Slime Tailings[c]	Total	Annual Quantity	Cumulative Quantity
1956	NE	NE	1,717	902,455,200	902,455,200
1957	NE	NE	1,350	709,560,000	1,612,015,200
1958	NE	NE	1,000	525,600,000	2,137,615,200
1959	NE	NE	700	367,920,000	2,505,535,200
1960	NE	NE	400	210,240,000	2,715,775,200
1961	236.8[d]	4.6[e]	241.4	126,879,840	2,842,655,040
1962	236.8	4.6	241.4	126,879,840	2,969,534,880
1963	236.8	4.6	241.4	126,879,840	3,096,414,720
1964	236.8	4.6	241.4	126,879,840	3,223,294,560
1965	236.8	4.6	241.4	126,879,840	3,350,174,400
1966	236.8	4.6	241.4	126,879,840	3,477,054,240
1967	236.8	4.6	241.4	126,879,840	3,603,934,080
1968	236.8	4.6	241.4	126,879,840	3,730,813,920
1969	236.8	4.6	241.4	126,879,840	3,857,693,760
1970	236.8	4.6	241.4	126,879,840	3,984,573,600
1971	236.8	4.6	241.4	126,879,840	4,111,453,440
1972	236.8	4.6	241.4	126,879,840	4,238,333,280
1973	236.8	4.6	241.4	126,879,840	4,365,213,120
1974	236.8	4.6	241.4	126,879,840	4,492,092,960
1975	236.8	4.6	241.4	126,879,840	4,618,972,800
1976	236.8	4.6	241.4	126,879,840	4,745,852,640
1977	236.8	4.6	241.4	126,879,840	4,872,732,480
1978	236.8	4.6	241.4	126,879,840	4,999,612,320
1979	236.8	4.6	241.4	126,879,840	5,126,492,160
1980	236.8	4.6	241.4	126,879,840	5,253,372,000
1981	236.8	4.6	241.4	126,879,840	5,380,251,840
1982	191.8	4.6	196.4	103,227,840	5,483,479,680
1983	146.8	4.6	151.4	79,575,840	5,563,055,520
1984	101.8	4.6	106.4	55,923,840	5,618,979,360
1985	56.8	4.6	61.4	32,271,840	5,651,251,200
1986	11.8[f]	4.6	16.4	8,619,840	5,659,871,040
1987	11.8	4.6	16.4	8,619,840	5,668,490,880
1988	11.8	4.6	16.4	8,619,840	5,677,110,720
1989	11.8	4.6	16.4	8,619,840	5,685,730,560
1990	11.8	4.6	16.4	8,619,840	5,694,350,400
1991	11.8	11.6[g]	23.4	12,299,040	5,706,649,440
1992	11.8	11.6[g]	23.4	12,299,040	5,718,948,480
1993	11.8	4.6	16.4	8,619,840	5,727,568,320
1994	11.8	4.6	16.4	8,619,840	5,736,188,160
1995	11.8	4.6	16.4	8,619,840	5,744,808,000

Key: gpm = gallons per minute; NE = not estimated

[a]Derived from Table 2-2, Applied Hydrology Associates, Inc. (1995).

[b]Area of sand tailings assumed to be 191 acres.

[c]Area of slime tailings assumed to be 74 acres.

[d]Vertical hydraulic conductivity assumed to be 2 ft/yr.

[e]Vertical hydraulic conductivity assumed to be 0.1 ft/yr.

[f]Unsaturated hydraulic conductivity assumed to be 0.1 ft/yr .

[g]Estimated rate due to loading the slimes area with a consolidation layer, totaling approximately 7.4 million gallons.

Table A-2. Tailings Liquor Chemistry

Parameter	Concentration[a,b]
Aluminum	1,020
Arsenic	0.60
Boron	1.7
Barium	< 0.1
Calcium	576
Cadmium	1.03
Cobalt	1.13
Chromium	1.9
Copper	3.17
Iron	2,430
Magnesium	63.3
Manganese	75.1
Molybdenum	1.33
Sodium	1,100
Nickel	1.43
Lead	4.3
Silicon	442
Strontium	16.6
Zinc	5.7
Nitrate (NO_3)	31
Sulfate (SO_4)	24,400
Chloride	1,630
Selenium	4.0
Ammonia (NH_4)	35.67
pH	1.2 standard units
Lead-210	24,224 pCi/L
Uranium-238	6,565 pCi/L[c]
Thorium-230	149,302 pCi/L
Radium-226	3,334 pCi/L

Key: DL = detection limit; pCi/L = picocuries per liter
[a]From Table 3, Dames & Moore (1981b).
[b]Reported in milligrams per liter unless noted otherwise.
[c]Equivalent to 19.54 milligrams per liter.

Appendix B

Bluewater Main Tailings Disposal Cell Configuration

This page intentionally left blank

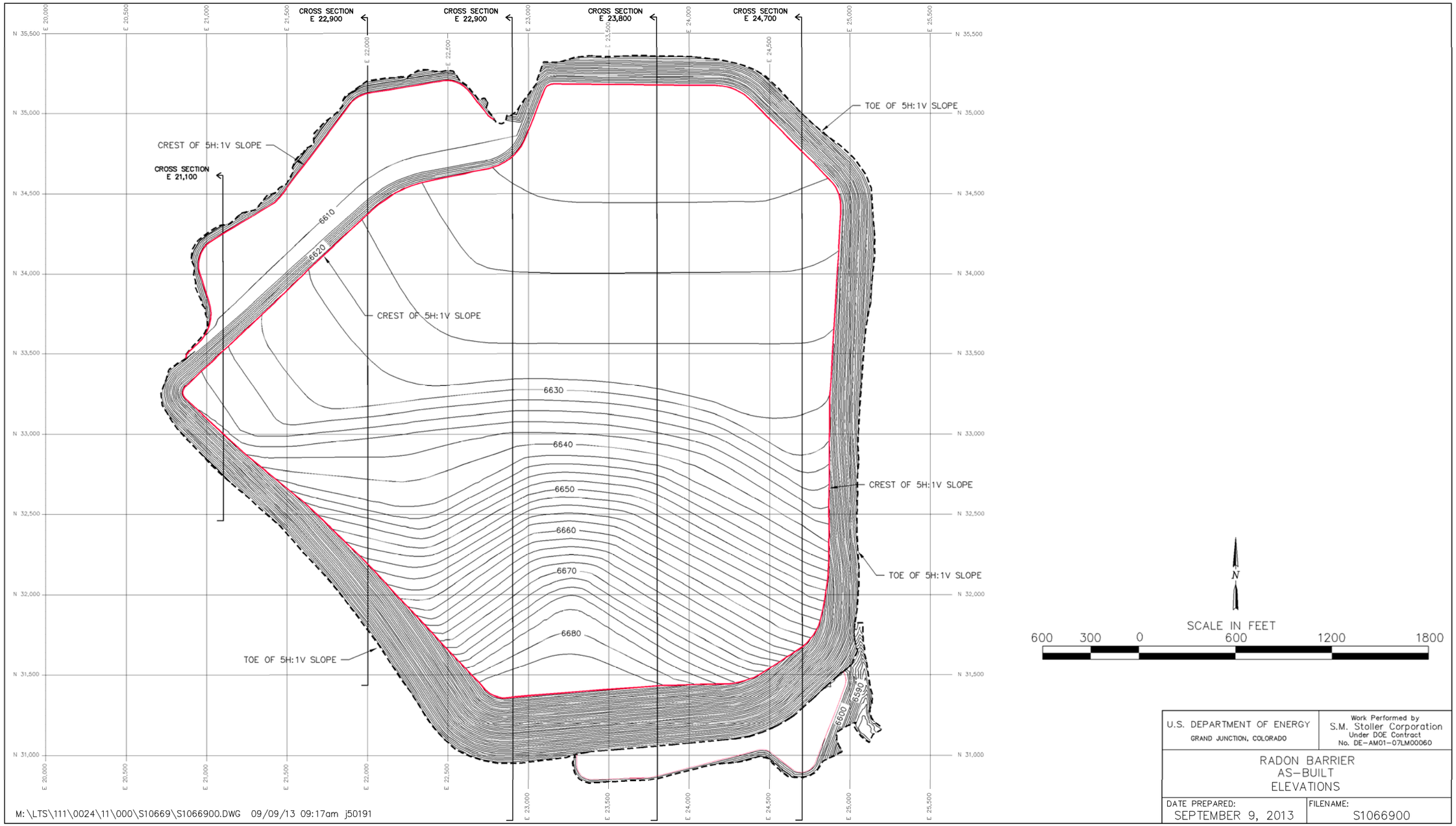

Figure B-1. Main Tailings Disposal Cell Radon Barrier As-Built Surface

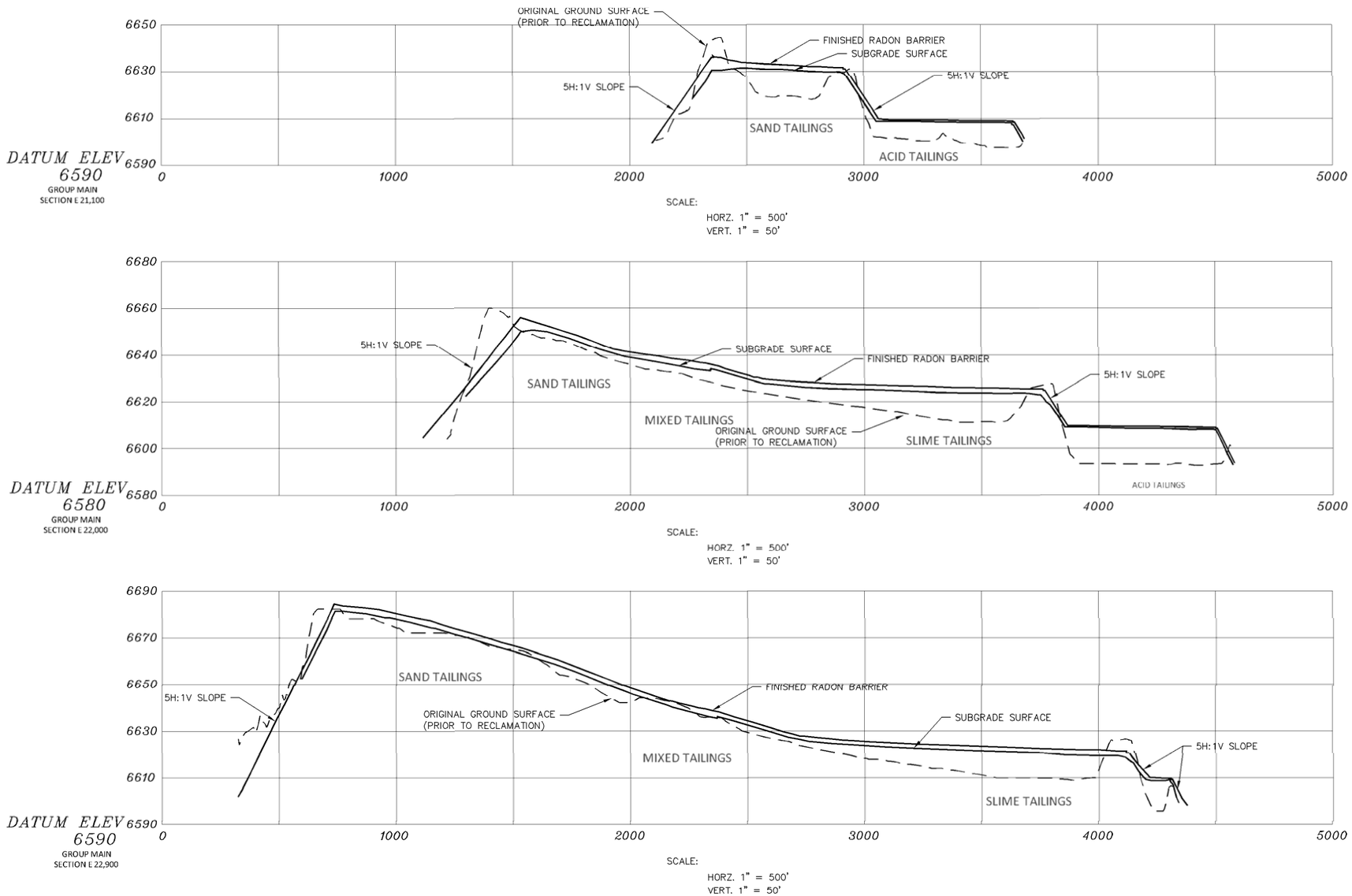

Figure B-2 Main Tailings Disposal Cell As-Built Sections E 21,100, E 22,000, and E 22,900

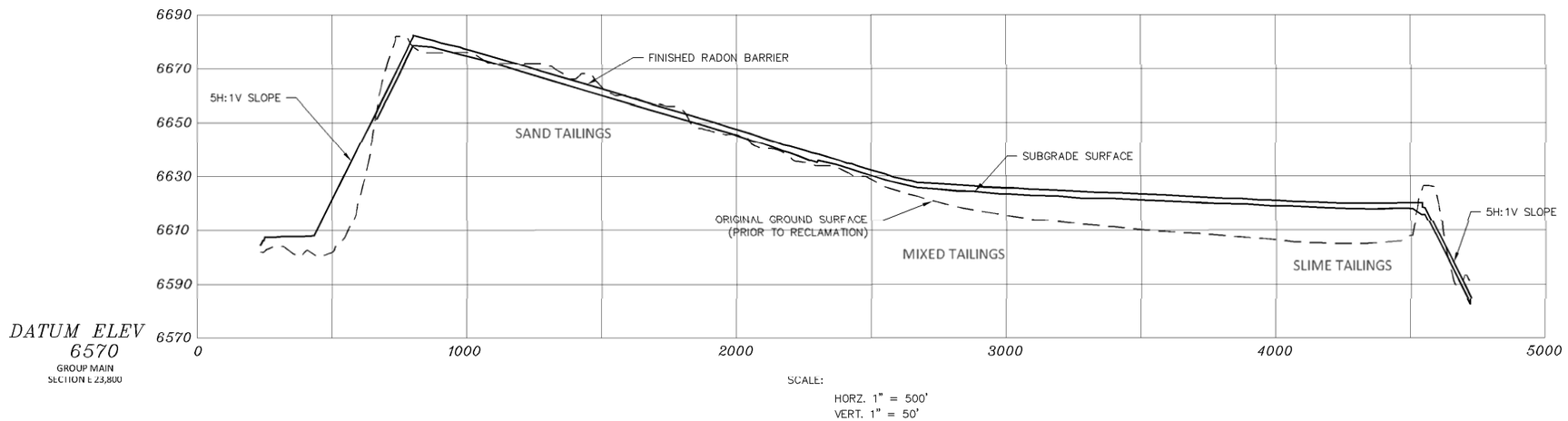

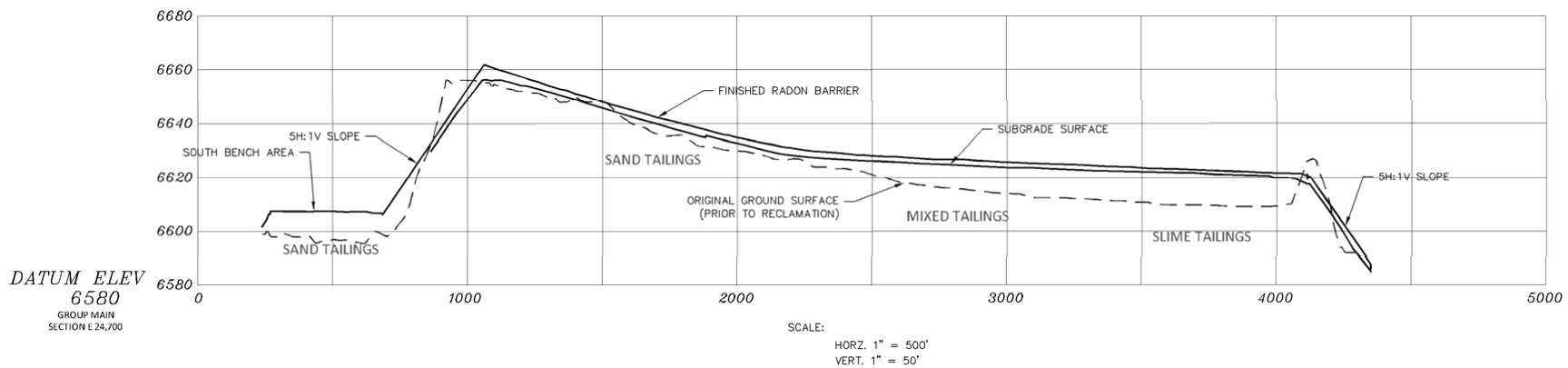

U.S. DEPARTMENT OF ENERGY GRAND JUNCTION, COLORADO	Work Performed by S.M. Stoller Corporation Under DOE Contract No. DE-AM01-07LM00060
SECTIONS E 23,800 AND E 24,700	
DATE PREPARED: SEPTEMBER 9, 2013	FILENAME: S1066800

M:\LTS\111\0024\11\000\S10668\S1066800.DWG 09/09/13 09:11am j50191

Figure B-3. Main Tailings Disposal Cell As-Built Sections E 23,800 and E 24,700

This page intentionally left blank

Appendix C

Bluewater Main Tailings Disposal Cell
Material Hydraulic Properties

This page intentionally left blank

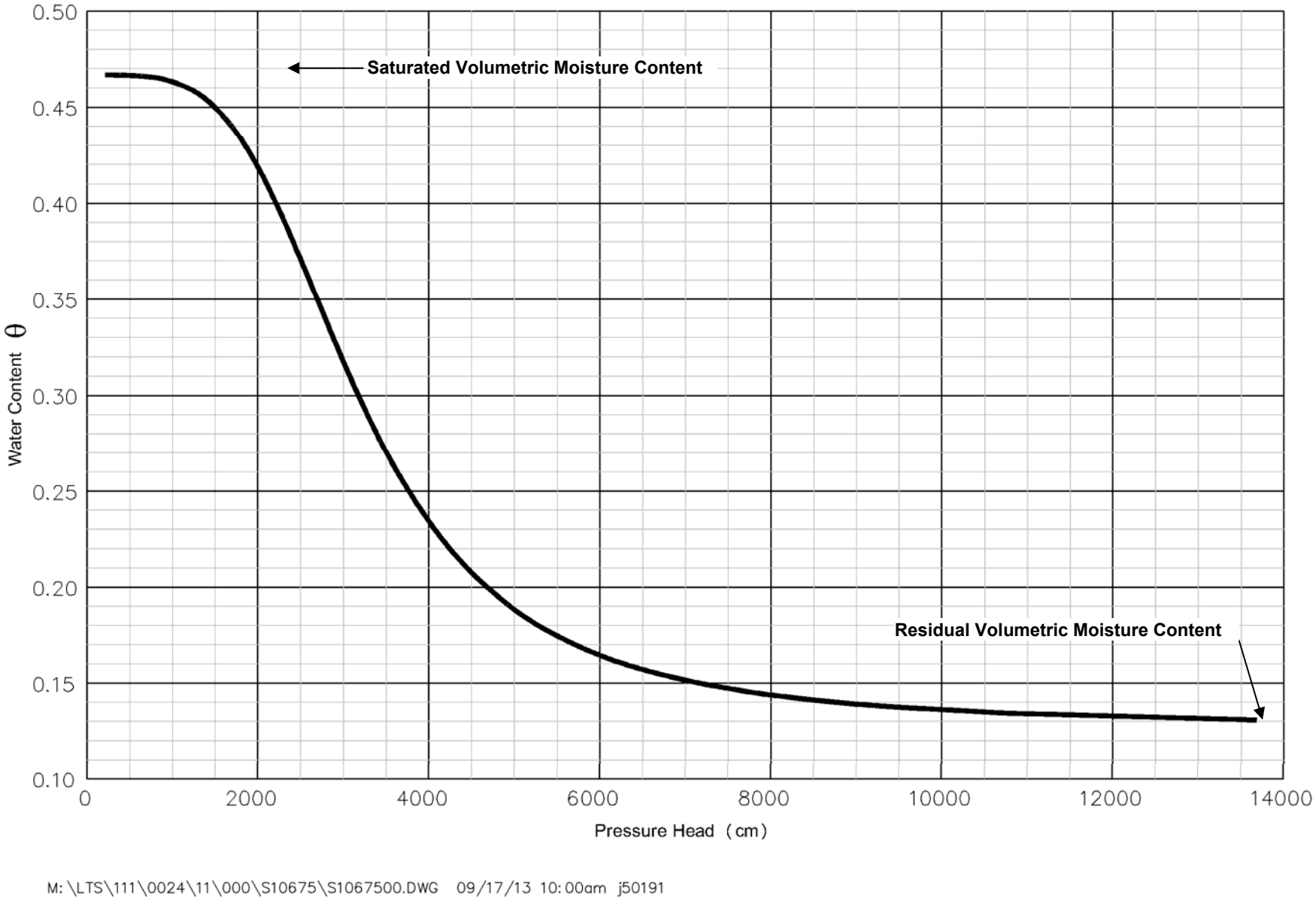

Figure C-1. Water Content Versus Pressure Head for the Coarse Tailings

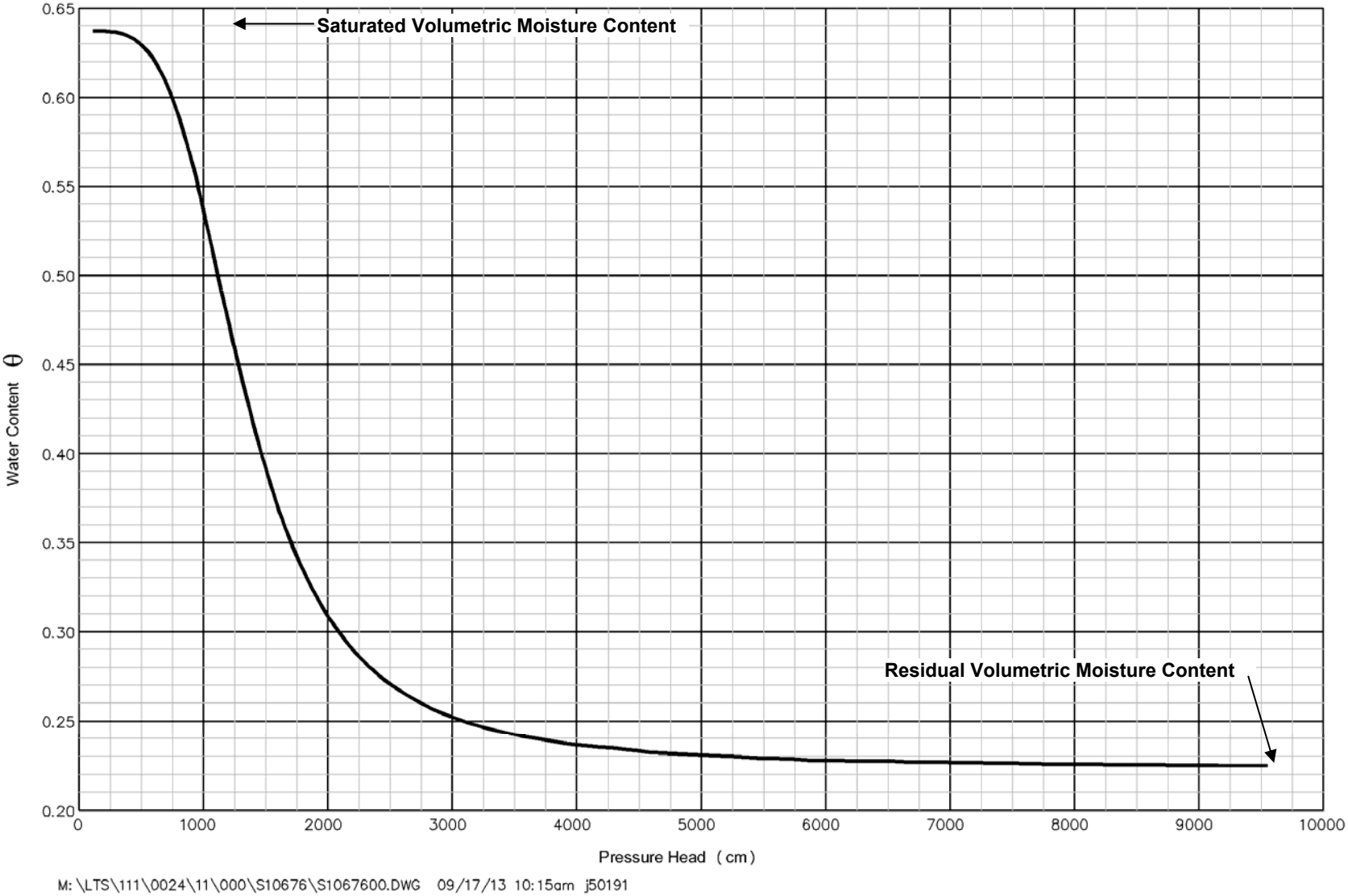

Figure C-2. Water Content Versus Pressure Head for the Fine Tailings

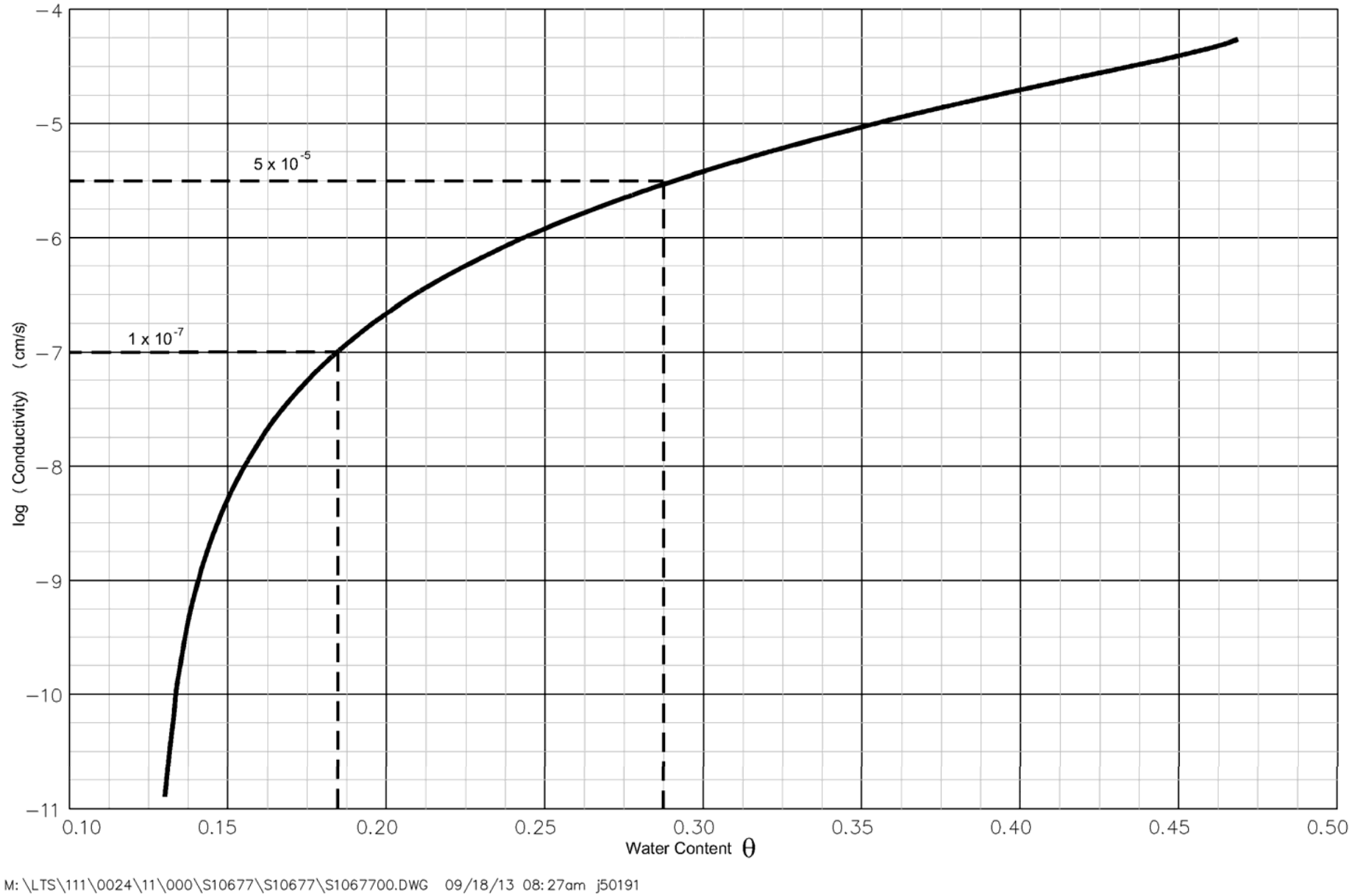

Figure C-3. Hydraulic Conductivity Versus Water Content for the Coarse Tailings

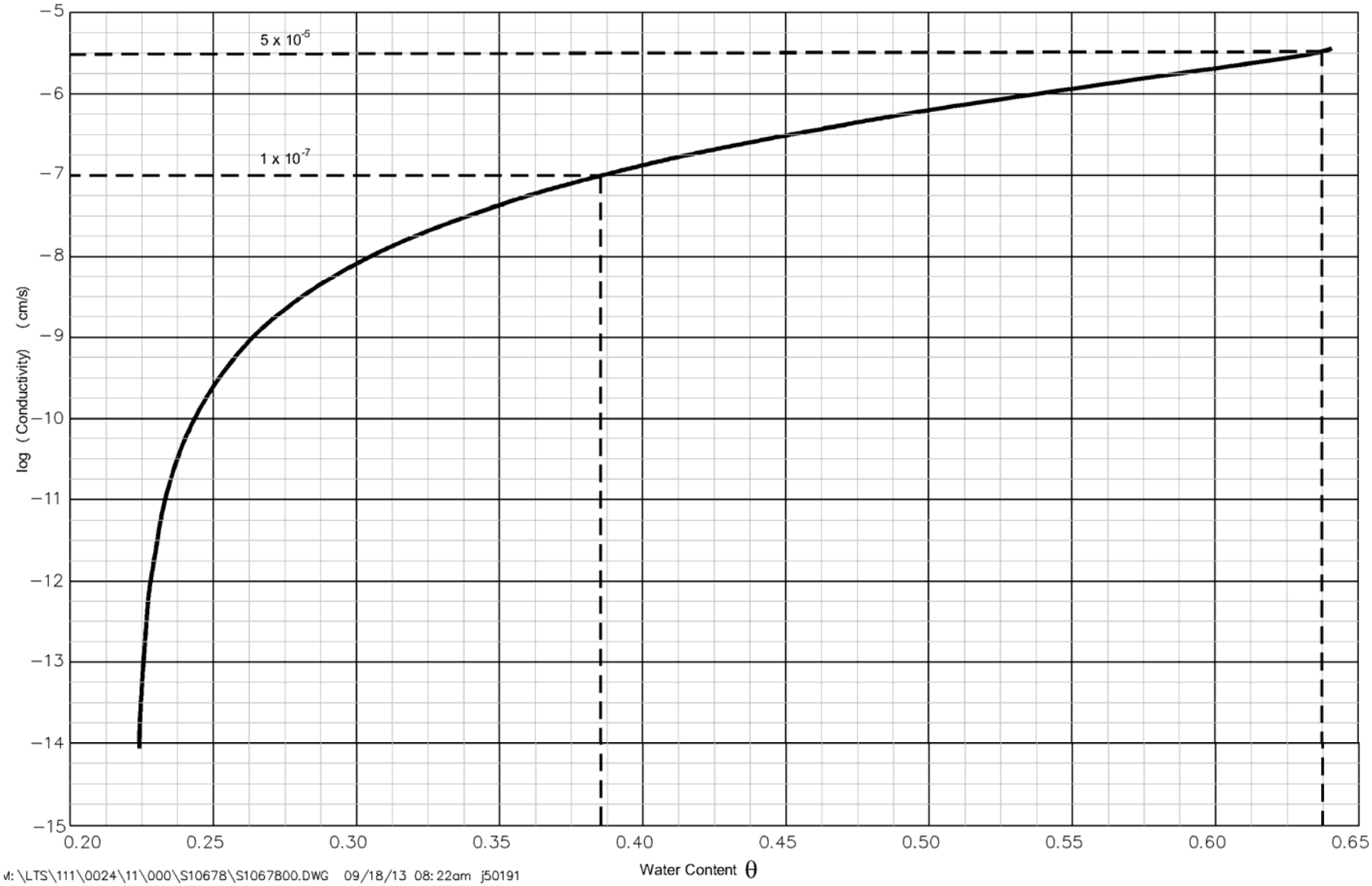

Figure C-4. Hydraulic Conductivity Versus Water Content for the Fine Tailings

Appendix B

Well Information

This page intentionally left blank

Preface

This appendix documents the locations of the wells in the Grants-Bluewater Valley study regionaddressed in the Site Status Report. Well locations are shown on Plate 7 and Figures 16 through 19 of the main report. Because the monitoring locations were drawn from a variety of studies, several of the wells are identified by more than one label. Therefore, cross-reference information is provided where available.

Data sources used to develop these tables include:

- DOE/Bluewater site database
- Homestake annual reports (mainly HMC and Hydro-Engineering 2013)
- Hydro-Search 1981a
- NMED (New Mexico Environment Department) 2010
- State of New Mexico Drinking Water Branch database
- U.S. Geological Survey (USGS) National Water Information System (Mapper)

Well construction information for wells monitored at the Bluewater site is provided in Table 2 of the main report. Well construction information developed by Hydro-Search (1981a), based on their detailed well inventory of the Grants-Bluewater area, is also provided here. Although some of the wells listed in their inventory have since been decommissioned, and some information may no longer apply (e.g., well ownership), the inventory was a fundamental component of the early site characterization work, and much is still relevant today. For wells monitored by Homestake, well construction information is documented in their annual reports; only coordinates and depths (when available) are listed here. For wells not currently monitored at the Bluewater site, some of the well information provided here may need to be verified, and some locations are uncertain. Limited information is available for domestic wells.

Plate 7 includes close to 570 unique locations; the majority consist of Homestake's alluvial wells. Although only a subset of these wells had water level measurements or water chemistry data for the time periods evaluated in this report, location information for all HMC alluvial wells is provided in Tables B-6 and B-7. Because the focus of the site status report is on the San Andres and alluvial aquifers, information for HMC wells screened in the Chinle aquifer is not provided in this appendix.

Only 9 of the 27 unique SMC sample locations referenced in NMED's study were utilized in the Site Status Report: SMC-03, SMC-04, SMC-05, SMC-08, SMC-10, SMC-11, SMC-12, SMC-13, and SMC-14. The remaining SMC locations were not used because they are outside the study region in the report.

Tables

Table B-1 Well Information for Wells Screened in San Andres Aquifer: Bluewater Site Monitoring Wells

Table B-2 Well Information for Homestake, Domestic, and Other San Andres Wells

Table B-3 Well Information for Bluewater Site Alluvial Wells

Table B-4 Information for San Andres Aquifer Wells Adapted from Hydro-Search (1981)

Table B-5 Information for Alluvial Aquifer Wells Adapted from Hydro-Search (1981)

Table B-6 Well Location Information for Homestake Alluvial Tailings Area Wells

Table B-7 Well Location Information for Homestake Alluvial Regional Wells

Abbreviations

amsl	above mean sea level
ARCO	Atlantic Richfield Company
bgs	below ground surface
BW	Bluewater (prefix used by NMED [2010]) for sample IDs)
DOE	U.S. Department of Energy
ft	feet
HMC	Homestake Mining Company
HSI	Hydro-Search Inc.
NM DWB	State of New Mexico Drinking Water Branch (Drinking Water Watch) website
NMED	New Mexico Environment Department
OSE	(New Mexico) Office of State Engineer
SMC	San Mateo Creek
TD	Total Depth
USGS	U.S. Geological Survey

Table B-1. Well Information for Wells Screened in San Andres Aquifer: Bluewater Site Monitoring Wells

Well ID		Easting	Northing	TD (ft bgs)	Well Owner	Alternate Label(s)	OSE ID
11(SG)	*	469874.79	1558335.18	305.7	DOE		B-410-POD31
13(SG)	*	472765.77	1546949.48	314.4	DOE		
14(SG)	*	463598.97	1548886.18	335.2	DOE		
15(SG)	*	469224.43	1550341.01	388	DOE		
16(SG)	*	468714.92	1553798.89	235	DOE		
18(SG)	*	468136.08	1547203.31	305	DOE		
Anaconda #1		465602.60	1548242.67			B00003	
Anaconda #2		465493.49	1548344.17	386			
Anaconda #3	**	465673.99	1544494.28	200	ARCO		
Anaconda #4	**	466076.36	1544171.56	210	ARCO		
Anaconda #5	**	465855.10	1547998.03	440.5	ARCO		
B00050A		476604.01	1540222.92			BW-20, HMC-545	B-50A
B00518		471519.37	1542081.56		non-DOE		
B01614		468584.63	1541060.23				
Berryhill Sec5		473358.86	1561753.67	725			
Bowlins		457941.80	1550791.37	518		BW-24	B-637
C(SG)	**	466600.99	1551103.67	423	ARCO		
D(SG)	**	468324.35	1552464.62	259	ARCO		
DM-7	**	471121.62	1552758.22	142.3	ARCO		
DM-8	**	475535.94	1551456.63	131	ARCO		
G(SG)	**	468771.45	1552696.30	278	ARCO		
HMC-951		473124.09	1545335.99	272	HMC	NMED BW-34, SMC-01 USGS 7 (former Sabre Piñon)	B-28-S-247
I(SG)		478106.06	1552131.20	330	DOE	BW-28	
L(SG)		462856.43	1553977.39	610		BW-25	
M(SG)	**	465579.44	1559328.51	575	ARCO		
Mexican Camp	**	468627.95	1545079.99	280	ARCO		
Monitor	**	473949.24	1557023.81	628	ARCO		
North	**	469489.85	1558726.23	250	ARCO		
OBS-2	**	468766.00	1551594.10	319	ARCO		
OBS-3		468776.17	1554101.25	363	DOE	BW-27	
Payne		462186.79	1547042.46	315			
Roundy House		460119.10	1548590.66	300		BW-11	B-1608
S(SG)		468775.21	1553097.93	336	DOE	BW-26	
W(SG)	**	472820.05	1549373.29	355	ARCO		

* Well installed summer 2012 (see Table 2 of main report)
** Well decommissioned in February 1997
BW Bluewater well location prefix, as referenced in NMED 2010, Tables 6 and 8
OSE New Mexico Office of State Engineer
TD Total depth

Notes:
Domestic wells B00050A, B00518, and B01614 are listed in this table because they were recently sampled by DOE (locations shown on Figure 18 and Plate 7).

Table B-2. Well Information for Homestake, Domestic, and Other San Andres Wells

Well ID	Easting	Northing	TD (ft bgs)	Data Source(s)	NMED ID	Alternate Label(s)	OSE ID
#1 Deepwell	493633.00	1543307.00	1000	HMC	BW-29		B-28
#2 Deepwell	490972.00	1542424.00	870	HMC	BW-30		B-28S
0951R	484163.26	1544589.39		HMC			
0806	486320.00	1541120.00	584	HMC			
0806R	486264.00	1541177.00	600	HMC			
0534	476549.00	1534589.00	1000	HMC			
0535	478450.00	1530100.00	198	HMC			
0545	476600.00	1540200.00					
0822	488630.00	1538920.00	980				
0907	480800.00	1534250.00	360	HMC		USGS 10	
0911	476800.00	1534350.00	188	HMC	BW-15		B-49
0923	477900.00	1552400.00	330	HMC			
0928	491700.00	1548250.00	864	HMC	BW-32	USGS 13	
0938	473040.00	1539500.00	253	HMC	BW-06	USGS 6	
0943	487407.00	1537222.00	978	HMC	BW-33	USGS 12	B-28S-329
0949	483600.00	1540350.00	551	HMC	BW-23		B-44
0955	483699.00	1537338.00	498	HMC	BW-02*	Vasquez	
0986	483690.00	1537894.00	467	HMC	BW-03	Bachman	
0987	483357.00	1538226.00	500	HMC			
0991	483630.00	1538873.00	500	HMC	BW-04	Gebeau	
B00018	477798.96	1529434.73		NMED 2010	BW-21		B-18
B00019	475656.46	1529453.89		NMED 2010	BW-22		B-19
B00518-2	470586.51	1541289.80		NMED 2010	BW-19		B00518-2
BW-07	452010.17	1551895.36		NMED 2010	BW-07		B-1521
BW-08	457637.03	1552088.01		NMED 2010	BW-08		B-1541
BW-09	457395.34	1545737.16		NMED 2010	BW-09		B-1662
BW-10	460452.44	1548662.82		NMED 2010	BW-10	J Elkins-1	
BW-12	461245.55	1543574.28		NMED 2010	BW-12		B-1637
BW-13	461907.28	1542452.78		NMED 2010	BW-13		B-1663
BW-14	456089.10	1547347.44		NMED 2010	BW-14		B-1688
BW-17	467073.80	1540123.75		NMED 2010	BW-17	Anderson	
BW-35	500601.79	1557138.35		NMED 2010	BW-35		B-1458
Bluewater Well #1	457396.82	1545730.98		NM DWB		Water & San. District	
Bowlins Bluewater DQ Well #1	458701.53	1550395.88		NM DWB			
Bowlins Bluewater DQ Well #2	458936.99	1549481.99		NM DWB	BW-05		B-461
Grants Cibola Sands KOA Well #2	488374.91	1508123.63		NM DWB			
Grants Well #1	490053.74	1512328.52		NM DWB		B-38	
Grants Well #3	486771.00	1514626.76		NM DWB		B-40	
Milan Well #1	482352.49	1518873.19		NM DWB		Village of Milan Well B-23	
Milan Well #3	480171.81	1524218.39	214	NM DWB		B-35	
Milan Well #4	476601.36	1533091.41		NM DWB	BW-16	HMC-998, Golden Acres	B-50
USGS 1	447590.18	1559965.42	523	USGS			
USGS 2	453979.00	1551753.83	457	USGS			
USGS 4	462782.49	1541821.20	365	USGS			
USGS 5	471782.90	1542498.68	245	USGS			
USGS 8	474768.99	1524533.55	100	USGS			
USGS 11	483047.57	1529397.54	480	USGS			
USGS 14	487852.60	1512343.18	158	USGS			

Notes:

Wells listed in this table have not been sampled by DOE—data sources include HMC annual reports, NMED (2010), the State of New Mexico Drinking Water Branch website, and the USGS (links provided below). Figure 26 of the main report shows the USGS wells within the Bluewater study region. Well depth listed for HMC 938 is based on USGS' reporting (as this datum not provided in HMC's annual reports). *NMED (2010) Table 6 cross-reference to HMC well 0965 was incorrect (0955 is the correct location).

https://eidea.nmenv.state.nm.us/DWW; http://maps.waterdata.usgs.gov/mapper/index.html

Table B-3. Well Information for Bluewater Site Alluvial Wells

Well ID		Easting	Northing	TD (ft bgs)	Well Owner	Alternate Label(s)
20(M)	*	463734.80	1551924.38	129.5	DOE	
21(M)	*	472680.71	1546974.11	157	DOE	
22(M)	*	470929.88	1548706.26	153	DOE	
23(M)	*	472920.01	1545333.70	121	DOE	
Aragon		457501.92	1552609.66	130	non-DOE	
B(M)	**	463807.78	1553223.79	161	ARCO	
B00050B		477981.74	1541294.26		non-DOE	
B00168		458687.93	1556148.12	150	non-DOE	Berryhill House
C(M)	**	466654.99	1551083.34	356	ARCO	
E(M)		463534.80	1548937.62	100	DOE	
Engineers		460121.05	1554977.95	115	non-DOE	USGS 3
F(M)		468854.40	1547617.57	136	DOE	
K(M)	**	467051.67	1556177.73	67	ARCO	
OW-8		478083.39	1552708.83		ARCO	
SIMPSON		472965.00	1543628.71	160	non-DOE	BW-18; HMC-936
T(M)		469141.12	1550460.89	142	DOE	
U(M)	**	470946.36	1548625.72	150	ARCO	
V(M)	**	472903.82	1550533.80	90	ARCO	
X(M)		472906.86	1547948.81	134.5	DOE	
Y1(M)	**	466892.00	1548053.88		ARCO	
Y2(M)		467531.78	1548289.19	130	DOE	

* Well recently installed: July 2011 or June-July 2012 (see Table 2 of main report)
** Well decommissioned in February 1997
TD Total depth

Additional well construction information for existing Bluewater site wells provided in Table 2 of the main report.

Table B-4. Information for San Andres Aquifer Wells Adapted from Hydro-Search (1981)

HSI Map			TD	Generalized Geologic Log (all depths in ft)						Type of Data	
No. / ID	Well	Source	(ft)	Qal	Qb	QToa	TRc	Psg	Psy	Water Level	Chemistry
12	Berryhill Sec. 5	NMSE	725	--	--	--	0-620	620-TD	--		X
13	Spencer	G	378							X	
14	North Well	G	250							X	X
15	Monitor Well	NMSE	628	0–35	--	--	35–308	308–TD	--	X	X
16	Bowlins	NMSE	518	0–15	15–72	72–110	110–455	455–TD	--	X	X
17	C(SG)	HSI	423	--	0–125	125–146	146–358	358–TD	--	X	X
18	D(SG)	HSI	259	--	--	--	--	0–TD	--	X	
19	G(SG)	HSI	278	--	--	--	--	0–TD	--	X	X
20	Payne (Allen Payne)	NMSE	315	0–1.5	1.5–46	46–100	--	100–TD	--		X
21	Anaconda #1	ACC	356	--	0–91	91–94	94–252	252–TD	--	X	
22	Anaconda #2	ACC	386	--	0–86	86–115	115–263	263–TD	--	X	X
23	Bluewater Municipal										X
24	Roundy Corral	G	199								X
25	Anaconda #3	ACC	200							X	X
26	Anaconda #4	ACC	210							X	X
27	Mexican Camp	G	280							X	X
28	Sabre-Piñon (current HMC-951)	NMSE	275	--	0–96	96–110	110–227	227–TD	--	X	X
29	Sturges Irrigation	G	225							X	X
30	Dalton									X	X
31	Hardenburg Commissary	ACC	238	0–40	--	--	40–118	118–TD	--	X	X
AN-5	Anaconda #5	HSI	440.5	--	0–90	90–106	106–267	267–TD	--	X	X
AN-5 P.H.	Anaconda #5 Pilot Hole	HSI	511	--	0–94	94–110	110–270	270–TD	--	X	
I(SG)	I(SG)	HSI	330	0–60	--	--	60–229	229–TD	--	X	X
L(SG)	L(SG)	HSI	610	--	0–110	110–122	122–412	412–TD	--	X	X
M(SG)	M(SG)	HSI	575	0–15	--	--	15–432	432–TD	--	X	X
S(SG)	S(SG)	HSI	337	--	--	--	--	0–280	280–TD	X	X
W(SG)	W(SG)	HSI	355	--	0–94	94–120	120–252	252–TD	--	X	X
Obs-2	OBS-2	HSI	319	--	--	--	--	0–269	269–TD	X	X
Obs-3	OBS-3	HSI	355	--	--	--	0–50	50–317	317–TD	X	X
S-1	Roundy Sec. 23	G	865	0–138	--	--	138–804	804–TD	--	X	X
S-2	Murray Ac. Irrigation	G	584							X	
S-3	Card Gas	G	551							X	
S-5	Siemons	NMSE	980	0–?	--	--	?–790	790–TD	--		X
S-6	Gallup Stake Irrigation Sec. 4A	G	315							X	
S-8	Dow	NMSE	198	0–30	30–65	65–106	--	106–TD	--		X
S-10	Gallup Stake Irrigation Sec. 5	G	225							X	
S-11	United Nuclear Sec. 8A	G	165							X	
S-12	United Nuclear Sec. 8B	G	150							X	X
S-13	United Nuclear Sec. 8C	G	150							X	
S-14	Gallup Stake Irrigation Sec. 4B	G	480							X	X
S-22	N.M. Highway Department	NMSE	286	0–5.5	--	--	--	5.5–245	245–TD	X	X
S-24	United Nuclear Sec. 17	G	125							X	
S-34	Bell	NMSE	320	0–5	--	--	--	5–TD	--		X
S-35	Jack Freas	G	135								
S-36	Cottonwood Well	G	253							X	
S-39	Dan's Feed Store	NMSE	164	0–16	--	--	--	16–TD	--	X	
S-42	Sturges Irrigation	Same well as #29 above.								X	X
S-43	Harding Irrigation	G	245							X	
S-49	Hanosh		250(?)							X	X
S-50	Thornton	NMSE	195	0–21	--	--	21–75	75–TD	--	X	X
S-51	Guthrie	NMSE	498	0–40	--	--	40–130	130–TD	--		X
S-53	Harding Domestic	NMSE	220	--	--	--	--	0–TD	--		
S-54	Keel	NMSE	165	--	--	--	--	0–TD	--	X	
S-65	Grants #1	NMSE	300	0–11	11–44	44–120	--	120–TD	--		X
S-66	Grants #3	NMSE	367	0–129	--	--	129–192	192–TD	--		X
S-68	Bell HQ		150(?)								X
S-70	Bluewater (Auro's) Motel	G	502								X
S-71	UN-HP #2	NMSE	1000	0–120	--	--	120–955	955–TD	--		X
S-72	UN-HP #1	G	870								X
S-73	Bluewater Cemetary	NMSE	320	0–1	--	--	--	1–270	270–TD	X	
S-74	Roundy (Harmon) House	G	300								X
S-75	Blue Well	G	450								X
DM-7	DM-7	D & M	142.3	0–5	--	--	5–60	60–TD	--	X	
DM-8	DM-8	D & M	131	0–16	--	--	16–82	82–TD	--	X	

Table B-4 (continued). Information for San Andres Aquifer Wells Adapted from Hydro-Search (1981)

Sources of information and notes:

The preceding table was adapted almost entirely from Appendix A (Well Inventory), Table A-1, "Wells in Grants-Bluewater Area Included in Current Investigations" provided in the following Hydro-Search (HSI 1981) report:

> *Regional Ground-Water Hydrology and Water Chemistry, Grants- Bluewater Area, Valencia County, New Mexico*, prepared for Anaconda Copper Company, June 30, 1981.

Corresponding well locations are shown in Figures B-1 and B-2, adapted from Plate IV, "Well Locations" of the above-cited Hydro-Search report. Locations for most existing and decommissioned wells are also shown on Plate 7 and Figures 16 through 19 of the main report. Corresponding water level and uranium data for 1980–1981 are plotted in Figures 23 and 55 of the Site Status Report.

Table B-4 abbreviations:

The following abbreviations regarding sources of information and geological terms are also taken directly from HSI's tables:

HSI	Hydro-Search, Inc., hydrogeologic investigations, 1977-1978 and 1980-1981
ACC	Anaconda Copper Company
NMSE	New Mexico State Engineer
G	Gordon, 1961
UN-HP	United Nuclear-Homestake Partners
D & M	Dames & Moore (1981)

TD	Total depth
Qal	Recent alluvium including eolian and lacustrine deposits
Qb	Quaternary basalt flows from either El Tintero or the Zuni Canyon centers
QToa	Quaternary-Tertiary older alluvium
TRc	Chinle Formation
Psg	San Andres-Glorieta aquifer
Psy	San Ysidro Member of Yeso Formation

Table B-5. Information for Alluvial Aquifer Wells Adapted from Hydro-Search (1981)

HSI Map			Total	Generalized Geologic Log (all depths in ft)						Type of Data	
No. / ID	Well	Source	Depth (ft)	Qal	Qb	QToa	TRc	Psg	Psy	Water Level	Chemistry
1	Berryhill House (now B00168)	G	150							X	X
2	Engineer's Well	G	115							X	X
3	Aragon	HSI	130(?)								X
4	Roundy–Up		134	--	0–72	72–134	134–TD	--	--	X	X
5	B(M)	HSI	161		0–121	121–147	147–TD	--	--	X	X
6	C(M)	HSI	356	--	0–128	128–149	149–353	353– TD	--	X	X
7	OW–5	ACC	71	--	0–65	65–70	70–TD	--	--	X	
8	E(M)	HSI	100	--	0–73	73–82	82–TD	--	--	X	X
9	F(M)	HSI	135	--	0–95	95–112	112–TD	--	--	X	X
10	Simpson	G	160							X	X
11	Card Abandoned	G	152							X	X
J(M)	J(M)	HSI	57	0–11	11–41	41–65	65–TD	--	--	X	X
K(M)	K(M)	HSI	67	0–15	15–37	37–60	60–TD	--	--	X	X
T(M)	T(M)	HSI	142	--	0–128	128–133	133–TD	--	--	X	X
U(M)	U(M)	HSI	150	--	0–125	125–140	140–TD	--	--	X	
V(M)	V(M)	HSI	90	--	0–70	70–73	73– TD	--	--	X	
X(M)	X(M)	HSI	134	--	0–121	121–132	132–TD	--	--	X	X
S–9	Gallup Stake Abandoned	NMSE	100(?)							X	
S–25	Evans Abandoned	NMSE	135	0–14	14–98	98–118	118–TD	--	--	X	
S–27	Gallup Stake Domestic	NMSE	138	0–12	12–95	95–132	132–TD	--	--	X	X
S–28	Milan B–23	NMSE	214	0–179	179–193	193–TD	--	--	--		X
S–41, S–41A	Holmes	NMSE	120	0–8	8–102	102–TD	--	--	--	X	X
S–46	Pittard	NMSE	102	0–70	--	70–TD	--	--	--	X	X
S–47	Roundy Sec. 14	G	105 (?)	0– TD	--	--	--	--	--	X	X
S–56	Cibola Sands	NMSE	90(?)							X	X
S–63	Milan B-24	NMSE	160								X
S–64	Milan B-35	NMSE	180								X
S–76	Urie	NMSE	85	0–TD	--	--	--	--	--		X
S–77	Crow	NMSE	140	0–TD	--	--	--	--	--		X
S–78	Clevenger	NMSE	100 (?)								X
S–79	Swierc	NMSE	110 (?)								X
S–81	Caudill	NMSE	116	0–TD	--	--	--	--	--		X
S–82	Roundy Sec. 12	G	100	0–TD	--	--	--	--	--		X
BC	BC	UN–HP	83	0–TD	--	--	--	--	--	X	
D	D	UN–HP	91	0–TD	--	--	--	--	--	X	
P	P	UN–HP	113	0–TD	--	--	--	--	--	X	
Q	Q	UN–HP	104	0–TD	--	--	--	--	--	X	
R	R	UN–HP	96	0–TD	--	--	--	--	--	X	

Source: Hydro-Search (HSI 1981) Appendix A (Well Inventory), Table A-1, "Wells in Grants-Bluewater Area Included in Current Investigations." Corresponding well locations are shown in Figures B-1 and B-3, adapted from Plate IV, "Well Locations" of HSI's report. Locations for most existing and decommissioned alluvial wells are also shown on Plate 7 and Figures 16 through 19 of the Site Status report. Locations for most existing and decommissioned non-domestic alluvial wells are shown on Plate 7 and Figures 16 through 19 of the main report. Corresponding water level and uranium data for 1980–1981 are plotted in Figures 20 and 51 of the Site Status Report.

See notes and abbreviations following Table B-4.

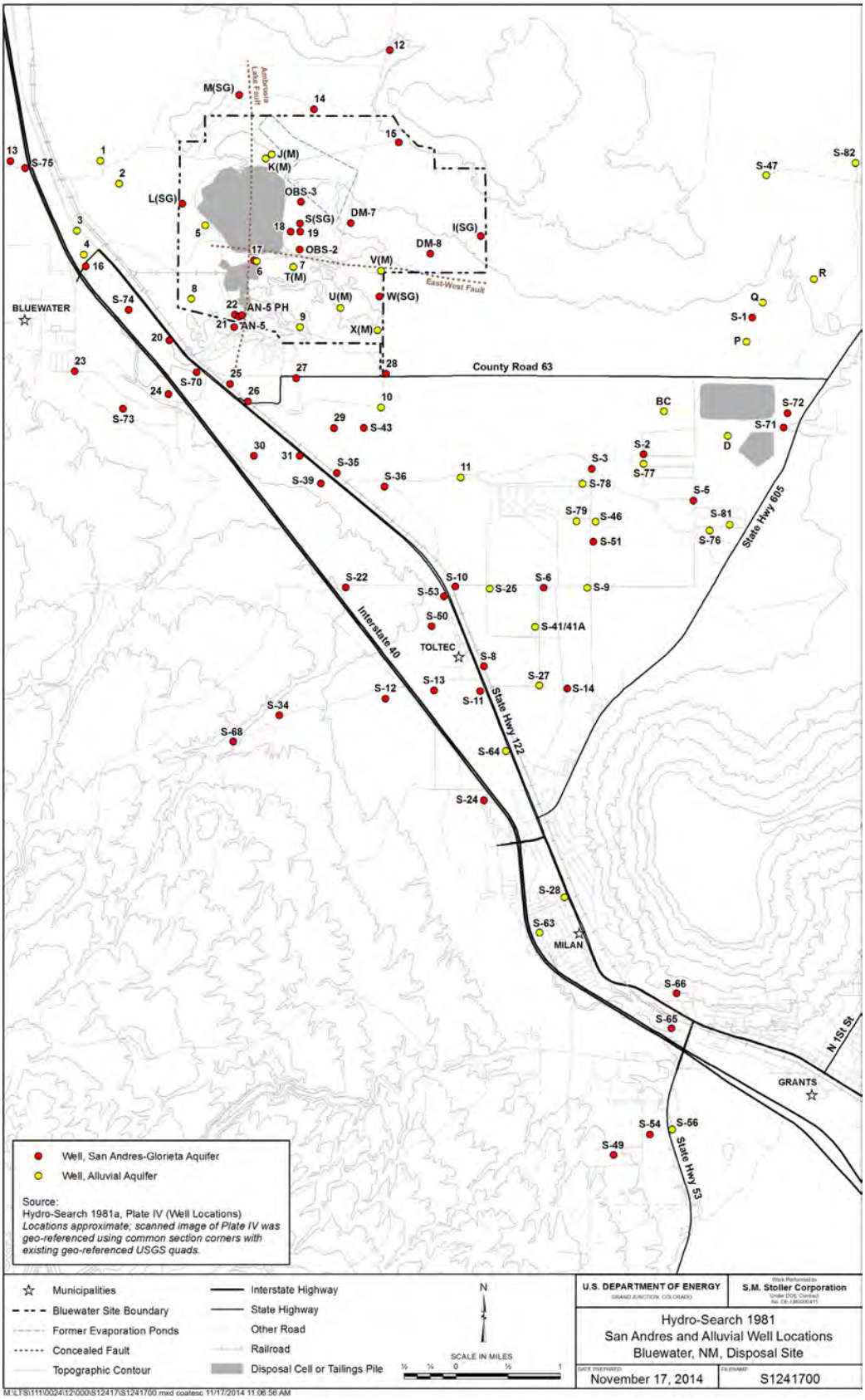

Figure B-1. Hydro-Search 1981 San Andres and Alluvial Well Locations
(Wells labeled with corresponding HSI map number)

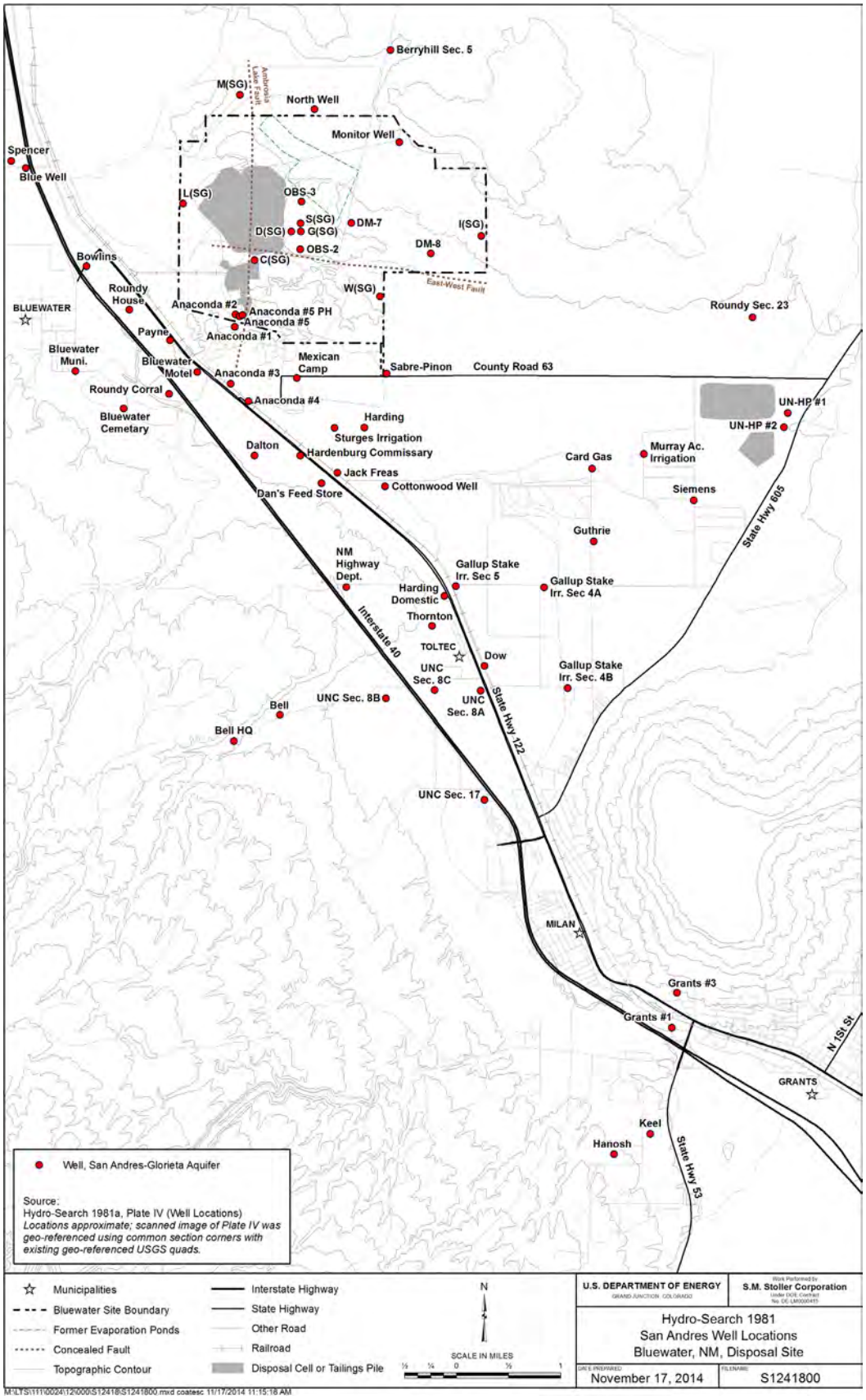

Figure B-2. Hydro-Search 1981 San Andres Well Locations

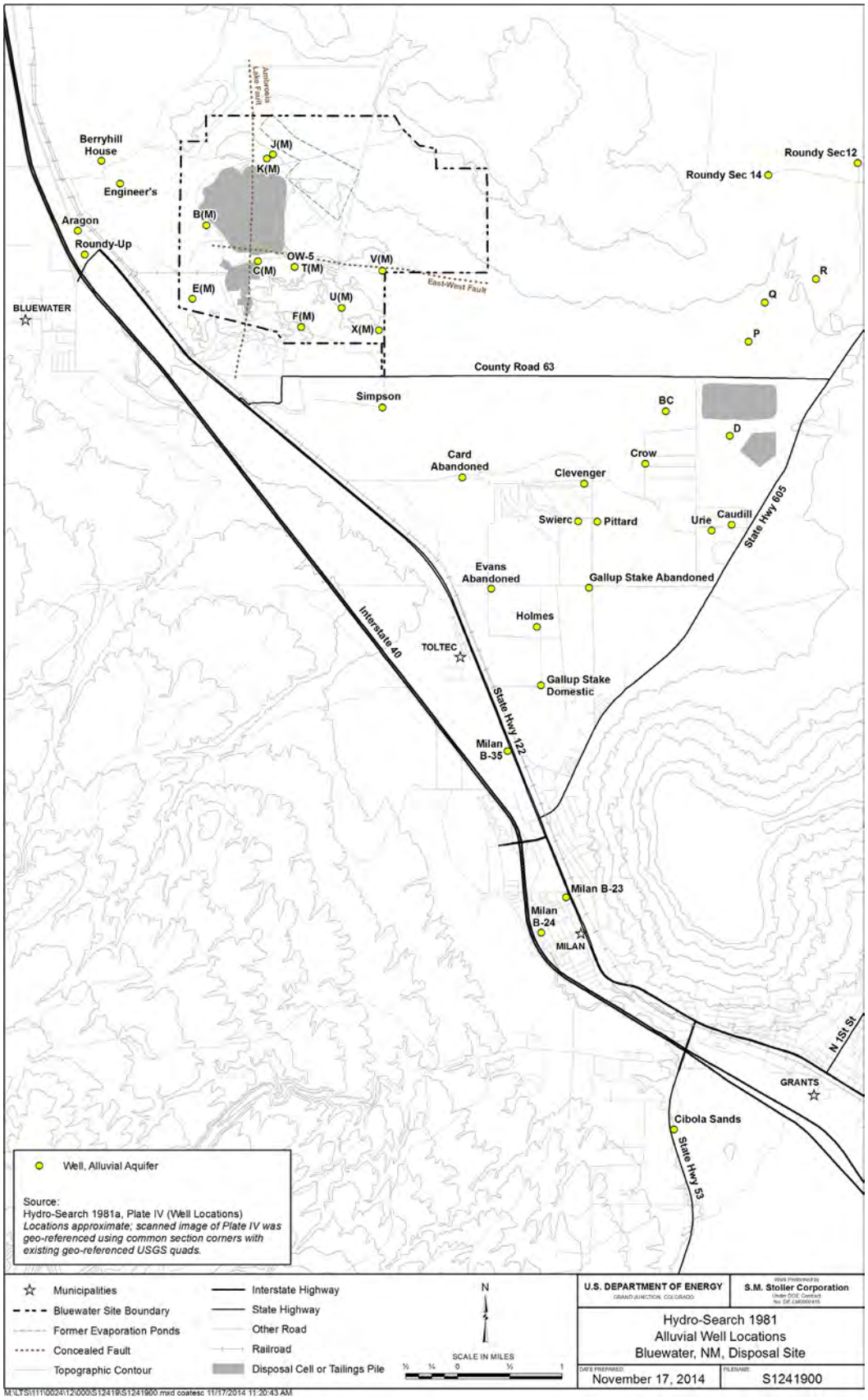

Figure B-3. Hydro-Search 1981 Alluvial Well Locations

Table B-6. Well Location Information for Homestake Alluvial Tailings Area Wells
(Source: 2012 HMC Annual Report, Table 4.1-1)

Well ID	Easting	Northing
1A	493768.00	1543790.00
1B	494412.00	1544502.00
1C	494799.00	1545018.00
1D	494752.00	1544142.00
1E	494116.00	1544481.00
1F	493831.00	1544952.00
1G	494170.00	1545034.00
1H	494266.00	1543363.00
1I	493928.00	1542627.00
1J	493695.00	1541986.00
1K	493275.00	1541992.00
1L	493416.00	1541256.00
1M	493133.00	1541327.00
1N	494396.00	1543100.00
1O	494175.00	1542592.00
1P	493924.00	1541902.00
1Q	493619.00	1541993.00
1R	493623.00	1542071.00
1S	493614.00	1541920.00
1T	493656.00	1541990.00
1U	493542.00	1542001.00
1V	493579.00	1541982.00
690	493465.00	1540279.00
691	493860.00	1540276.00
891	493751.00	1540904.00
892	494317.00	1540954.00
A1	491539.00	1542365.00
A2	491539.00	1542356.00
B	489311.00	1541684.00
B1	489370.00	1542071.00
B10	491133.00	1542517.00
B11	491329.00	1542517.00
B12	488915.00	1542524.00
B13	490223.00	1541841.00
B2	489515.00	1542475.00
B3	489731.00	1542480.00
B4	489942.00	1542471.00
B5	490141.00	1542474.00
B6	490341.00	1542478.00
B7	490540.00	1542488.00
B8	490734.00	1542488.00
B9	490935.00	1542514.00
BA	489440.00	1541835.00
BB2	486213.00	1543791.00
BC	487910.00	1543655.00
BP	489841.00	1541882.00
C	490854.00	1541762.00
C1	490780.00	1541533.00
C10	491629.00	1542182.00
C11	491844.00	1542376.00

Well ID	Easting	Northing
C12	492029.00	1542375.00
C13	490655.00	1541394.00
C14	490713.00	1541413.00
C2	490566.00	1541630.00
C3	490481.00	1541344.00
C3R	490472.00	1541338.00
C4	490675.00	1541348.00
C5	490869.00	1541344.00
C6	491142.00	1541533.00
C7	491280.00	1541734.00
C8	491415.00	1541906.00
C9	491545.00	1542075.00
D	490118.00	1542127.00
D1	489615.00	1542140.00
D2	492107.00	1542641.00
D3	491917.00	1542646.00
D4	491724.00	1542652.00
DA	489488.00	1542864.00
DA2	489656.00	1542881.00
DA3	489390.00	1542664.00
DA4	489756.00	1542598.00
DAA	492411.00	1542733.00
DAB	492399.00	1542633.00
DAC	492851.00	1543218.00
DB	489842.00	1542874.00
DBR	489855.00	1542877.00
DC	487060.00	1543646.00
DD	488943.00	1546989.00
DD2	489251.00	1547439.00
DE	490193.00	1542877.00
DF	490869.00	1542839.00
DG	491157.00	1542839.00
DH	491365.00	1542835.00
DIA	491793.00	1542821.00
DJ	491793.00	1542821.00
DK	492094.00	1542799.00
Dl	491788.00	1542821.00
DL	492398.00	1542813.00
DM	490035.00	1542628.00
DN	490020.00	1542776.00
DNR	490031.00	1542779.00
DO	490049.00	1542874.00
DP	491012.00	1542754.00
DQ	491006.00	1542592.00
DR	489966.00	1542884.00
DS	490118.00	1542876.00
DT	489293.00	1542871.00
DU	490380.00	1542879.00
DV	490702.00	1542826.00
DW	492029.00	1542818.00

Well ID	Easting	Northing
DX	491074.00	1542838.00
DY	492271.00	1542737.00
DZ	491501.00	1542834.00
E	490187.00	1540553.00
EE	490523.00	1542853.00
F	489554.00	1539908.00
FB	488857.00	1540417.00
FF	490017.00	1542878.00
G	488890.00	1538672.00
GA	489255.00	1538657.00
GB	489456.00	1538654.00
GC	489654.00	1538650.00
GE	489972.00	1538637.00
GF	490097.00	1538632.00
GG	489055.00	1538662.00
GH	489509.00	1538807.00
GJ	490382.00	1538629.00
GK	490482.00	1538622.00
Gl	490218.00	1538631.00
GL	490701.00	1538614.00
GM	490824.00	1538605.00
GN	490944.00	1538602.00
GO	489855.00	1538646.00
GO	488973.00	1538663.00
GP	489752.00	1538649.00
GQ	491067.00	1538599.00
GR	490619.00	1538619.00
GS	491408.00	1538597.00
GT	491565.00	1538534.00
GU	491854.00	1538367.00
GV	491428.00	1537701.00
GW1	490530.00	1539755.00
GW2	490497.00	1539471.00
GW3	490835.00	1539532.00
H	490582.00	1538703.00
I	490954.00	1539319.00
J	491302.00	1540174.00
J1	491585.00	1540082.00
J10	491436.00	1540138.00
J11	490909.00	1540545.00
J12	490466.00	1540827.00
J13	492218.00	1540451.00
J14	492367.00	1540585.00
J15	492521.00	1540719.00
J2	491013.00	1540271.00
J3	490499.00	1540414.00
J4	489974.00	1540643.00
J5	489747.00	1540728.00
J6	489221.00	1540919.00
J7	491892.00	1540168.00

Table B-6 (continued). Well Location Information for Homestake Alluvial Tailings Area Wells (Source: 2012 HMC Annual Report, Table 4.1-1)

Well ID	Easting	Northing
J8	492064.00	1540318.00
J9	491759.00	1540101.00
JC	491240.00	1540215.00
K	491590.00	1540730.00
K10	491638.00	1541305.00
K11	491490.00	1541325.00
K2	491587.00	1540736.00
K3	491571.00	1540744.00
K4	492371.00	1541211.00
K5	491935.00	1541269.00
K6	491459.00	1540689.00
K7	492237.00	1541232.00
K8	492081.00	1541250.00
K9	491787.00	1541287.00
KA	491331.00	1540959.00
KB	491406.00	1540893.00
KC	491477.00	1540826.00
KD	491701.00	1540627.00
KE	491776.00	1540566.00
KEB	491487.00	1540570.00
KF	491169.00	1540870.00
KM	491444.00	1540671.00
KN	491492.00	1540734.00
KZ	491183.00	1541100.00
L	492150.00	1538970.00
L10	492310.00	1539250.00
L5	492730.00	1539946.00
L6	493110.00	1540526.00
L7	492842.00	1540113.00
L8	492621.00	1539773.00
L9	492463.00	1539509.00
M1	489157.00	1542797.00
M10	486723.00	1543677.00
M11	486486.00	1542358.00
M12	487209.00	1542174.00
M13	487336.00	1542450.00
M14	487216.00	1542661.00
M15	487094.00	1542872.00
M16	485112.00	1543252.00
M2	489159.00	1542785.00
M3	489151.00	1542805.00
M4	489134.00	1542804.00
M5	489080.00	1542360.00
M6	486674.00	1543097.00
M7	486523.00	1542790.00
M8	486567.00	1542960.00
M9	486699.00	1543310.00
MA	487767.00	1541290.00
MB	487512.00	1541296.00
MC	487264.00	1541304.00

Well ID	Easting	Northing
MD	487050.00	1541311.00
ME	486934.00	1541537.00
MF	486808.00	1541757.00
MG	486694.00	1541972.00
MH	486569.00	1542208.00
MJ	486350.00	1542682.00
MJR	489078.00	1542926.00
MK	486324.00	1543373.00
Ml	486413.00	1542486.00
ML	486691.00	1543902.00
MM	486324.00	1544154.00
MN	486325.00	1544613.00
MO	485518.00	1543620.00
MP	485492.00	1544164.00
MQ	486326.00	1543173.00
MR	483574.00	1542609.00
MS	485570.00	1542607.00
MT	483531.00	1543221.00
MU	487143.00	1544461.00
MV	484418.00	1542618.00
MW	486346.00	1543802.00
MX	486244.00	1541287.00
MY	486213.00	1542200.00
MZ	486757.00	1543485.00
N	489665.00	1545101.00
NA	491488.00	1545000.00
NB	491296.00	1545000.00
NC	491282.00	1545220.00
ND	494872.00	1545927.00
NE5	492332.00	1544279.00
NW5	489433.00	1544408.00
O	492725.00	1545060.00
P	491058.00	1546691.00
P1	491060.00	1547017.00
P2	490912.00	1546555.00
P3	490785.00	1546159.00
P4	491899.00	1546504.00
PM	490292.00	1541426.00
Q	492153.00	1548693.00
R	494514.00	1550372.00
S	488816.00	1543871.00
S1	488401.00	1543288.00
S11	488150.00	1544793.00
S12	488628.00	1543297.00
S2	488299.00	1543127.00
S3	488714.00	1542857.00
S4	488359.00	1543344.00
S5R	488938.00	1543150.00
S6	488874.00	1543515.00
S7	488874.00	1543763.00

Well ID	Easting	Northing
S8	488879.00	1543968.00
SA	488811.00	1543122.00
SB	488811.00	1543371.00
SC	488815.00	1543617.00
SD	488564.00	1543490.00
SD4	488556.00	1543497.00
SE	488550.00	1543301.00
SE4	488560.00	1543308.00
SE6	488615.00	1543244.00
SM	488566.00	1543748.00
SN	488716.00	1543752.00
SO	488381.00	1543652.00
SP	488531.00	1543630.00
SQ	488814.00	1543507.00
SR	488669.00	1543611.00
SS	488666.00	1543374.00
SSR	488650.00	1543370.00
ST	488688.00	1543215.00
SUR	488968.00	1542991.00
SV	488813.00	1543676.00
SW	488812.00	1543783.00
SX	489025.00	1544510.00
SZ	488833.00	1544367.00
T	492260.00	1542536.00
T1	490027.00	1543285.00
T10	492791.00	1543434.00
T11	489887.00	1544585.00
T12	490317.00	1544583.00
T13	490619.00	1544534.00
T14	491071.00	1544565.00
T15	491953.00	1544480.00
T16	492718.00	1544276.00
T17	489430.00	1544008.00
T18	490333.00	1543977.00
T19	490722.00	1543958.00
T2	489303.00	1543538.00
T20	491048.00	1543935.00
T21	491882.00	1543951.00
T22	492311.00	1543876.00
T23	492805.00	1543901.00
T36	489688.00	1543735.00
T39	491669.00	1544498.00
T4	489699.00	1543340.00
T40	491466.00	1543819.00
T41	491079.00	1543278.00
T5	490289.00	1543307.00
T6	490655.00	1543282.00
T7	491484.00	1543272.00
T8	491914.00	1543296.00
T9	492337.00	1543347.00

Table B-6 (continued). Well Location Information for Homestake Alluvial Tailings Area Wells (Source: 2012 HMC Annual Report, Table 4.1-1)

Well ID	Easting	Northing
TA	492426.00	1542471.00
TB	492616.00	1542351.00
W	487297.00	1542302.00
W2	486654.00	1542251.00
WN4	489961.00	1543958.00
WR1	488529.00	1541280.00
WR10	487961.00	1542389.00
WR11	487728.00	1542586.00
WR12	488277.00	1541280.00
WR13	488861.00	1541068.00
WR14	488863.00	1540638.00
WR15	488016.00	1541280.00
WR16	487495.00	1543051.00
WR17	487485.00	1543328.00
WR18	487465.00	1543597.00
WR19	487458.00	1543873.00
WR1R	488536.00	1541302.00
WR2	488678.00	1541290.00
WR20	487449.00	1544059.00
WR21	487449.00	1544241.00
WR22	487462.00	1544434.00
WR23	487445.00	1544632.00
WR24	487438.00	1544938.00
WR3	488671.00	1541490.00
WR4	488678.00	1541788.00
WR5	488683.00	1541813.00
WR6	488566.00	1541902.00
WR7	488456.00	1541997.00
WR8	488328.00	1542095.00
WR9	488217.00	1542185.00
X	491892.00	1540512.00
X1	492129.00	1540671.00

Well ID	Easting	Northing
X10	492835.00	1542352.00
X11	492782.00	1542553.00
X12	492852.00	1542861.00
X13	493665.00	1543640.00
X14	493777.00	1544002.00
X15	493800.00	1544222.00
X16	493795.00	1544473.00
X17	493793.00	1544356.00
X18	493569.00	1544593.00
X19	493437.00	1544753.00
X2	492363.00	1540836.00
X20	493256.00	1544855.00
X21	493894.00	1543606.00
X22	493946.00	1543874.00
X23	494012.00	1544064.00
X24	494011.00	1544244.00
X25	494042.00	1544445.00
X26	493702.00	1544693.00
X27	493374.00	1544953.00
X28	491971.00	1540545.00
X29	492256.00	1540735.00
X3	492599.00	1540992.00
X30	492493.00	1540897.00
X31	492731.00	1541052.00
X4	492814.00	1541210.00
X5	492821.00	1541408.00
X6	492828.00	1541609.00
X7	492851.00	1541808.00
X8	492852.00	1542007.00
X9	492852.00	1542194.00
Y	491256.00	1541025.00
Z	490701.00	1540290.00

Table B-7. Well Location Information for Homestake Alluvial Regional Wells
(Source: 2012 HMC Annual Report, Tables 4.1-2 through 4.1-4)

Well ID	Easting	Northing
427	490410.00	1538450.00
482	489579.00	1536981.00
483	489753.00	1536586.00
490	489752.00	1536553.00
491	489658.00	1537031.00
496	489603.00	1534650.00
497	489503.00	1535039.00
498	488953.00	1534661.00
CW44	488891.00	1535048.00
Sub1	489100.00	1537620.00
Sub2	490370.00	1537392.00
Sub3	489420.00	1538280.00
688	483955.00	1541257.00
802	488277.00	1540765.00
844	487002.00	1538376.00
845	487833.00	1537280.00
AW	488015.00	1540235.00
520	492935.00	1538934.00
521	492588.00	1539104.00
522	492437.00	1538640.00
523	492896.00	1538680.00
531	478262.00	1541086.00
532	482400.00	1518700.00
538	486899.00	1533486.00
539	487596.00	1534014.00
540	488091.00	1534125.00
541	477236.00	1539831.00
551	479881.00	1536272.00
553	480563.00	1534923.00
554	479107.00	1534967.00
555	486236.00	1538572.00
556	486184.00	1538006.00
557	486000.00	1537809.00
631	483756.00	1532234.00
632	483767.00	1531850.00
634	480362.00	1541652.00
636	476038.00	1545374.00
637	474710.00	1545409.00
638	493265.00	1539628.00
639	492961.00	1539370.00
640	491961.00	1537790.00
644	485450.00	1533481.00
646	484953.00	1533246.00
647	478308.00	1536623.00
648	478343.00	1534730.00
649	479798.00	1534730.00

Well ID	Easting	Northing	Alt. ID
650	482135.00	1536779.00	
653	486570.00	1533283.00	
654	478636.00	1541994.00	
655	479830.00	1541620.00	
657	478392.00	1537497.00	
658	478436.00	1535922.00	
659	480772.00	1541689.00	
681	482734.00	1540676.00	
683	476217.00	1540198.00	
684	478499.00	1540273.00	
686	475438.00	1545319.00	
846	484730.00	1537219.00	
861	488702.00	1534332.00	
862	487800.00	1534265.00	
863	487912.00	1533867.00	
864	486464.00	1533735.00	
865	488429.00	1534123.00	
866	488340.00	1534494.00	
867	488409.00	1533762.00	
869	486073.00	1533251.00	
881	481478.00	1542034.00	
882	482396.00	1541404.00	
883	483039.00	1540097.00	
884	481498.00	1542677.00	
885	483474.00	1541919.00	
886	482487.00	1542327.00	
887	482469.00	1543063.00	
888	479335.00	1542285.00	
890	480088.00	1541365.00	
893	482244.00	1541934.00	
895	476222.00	1541521.00	
896	476237.00	1542246.00	
899	477288.00	1543801.00	
910	481150.00	1528800.00	
914	500850.00	1555500.00	SMC-10
920	496900.00	1555800.00	SMC-11
921	495800.00	1555400.00	SMC-13
922	492500.00	1555200.00	SMC-14
935	476629.00	1540115.00	
942	483710.00	1538300.00	
947	491841.00	1536206.00	
950	498300.00	1560400.00	SMC-12
994	476240.00	1539700.00	
996	477989.00	1537621.00	
999	480187.00	1524230.00	

This page intentionally left blank

Appendix C

Water Level and Water Chemistry Data

This page intentionally left blank

Preface

This appendix documents historical water level and water quality data for wells in the Grants-Bluewater Valley study region addressed in the Site Status Report. Data sources used to develop these tables include:

- DOE/Bluewater site database
- Homestake annual reports for years 1996 through 2013
- Hydro-Search 1981a
- NMED (New Mexico Environment Department) 2010
- State of New Mexico Drinking Water Branch (https://eidea.nmenv.state.nm.us/DWW/)

The following tables document historical data for the Bluewater site and conceptual model study region used to develop the Site Status Report. The database is extensive, including not only Bluewater site wells, but Homestake site and other regional wells (see references in Section 11 of the Site Status Report). The site database is being updated and refined and will undergo DOE's quality control and data validation procedures to the extent possible. Because the database is still under development, there may be gaps in the early historical record documented here. Also, this appendix does not include data for all parameters historically analyzed. Rather, the focus is on the key Bluewater site contaminants (e.g., uranium) and water quality parameters. Data for other parameters not regularly monitored or not considered germane to the study are not reported here. Quality assurance/quality control (e.g., duplicate sample) results are also not documented in this appendix.

Investigators evaluated every available Hydro-Engineering report prepared for the Homestake site between 1996 and 2013. All available historical Homestake information and data pertaining to San Andres wells are included here, as this aquifer is the primary focus of the Site Status Report. However, because the data set for HMC alluvial wells is very large (hundreds of wells), only the data supporting the 2012 alluvial potentiometric and uranium plume snapshots are included. The reader is referred to Homestake's annual reports for data and information regarding historical trends in alluvial wells in this region.

LIST OF TABLES

Water Level Data

Table C.1-1 Water Level Data for Bluewater Site San Andres Aquifer Wells

Table C.1-2 Water Level Data for Bluewater Site Alluvial Aquifer Wells

Table C.1-3 Water Level Data for Homestake Site and Distal San Andres Aquifer Wells

Table C.1-4 Water Level Used to Derive 2012 Potentiometric Surface for Alluvial Aquifer

Table C.1-5 Water Level Data for Bluewater Site San Andres Aquifer Wells: Fall/Winter 1980

Table C.1-6 Water Level Data for Bluewater Site Alluvial Aquifer Wells: Fall/Winter 1980

Water Quality Data Tables

Table C.2-1	Water Quality Data for Bluewater Site San Andres Wells
Table C.2-2	Water Quality Data for Bluewater Site Alluvial and Chinle Aquifer Wells
Table C.2-3	Uranium Isotope Results for Bluewater Site Region Based on DOE and NMED Sampling
Table C.2-4	Water Quality Data for San Andres Aquifer Wells from Hydro-Search 1981
Table C.2-5	Water Quality Data for Alluvial Aquifer Wells from Hydro-Search 1981
Table C.2-6	Water Quality Data for Homestake Site and Distal San Andres Aquifer Wells
Table C.2-7	Water Quality Data from NMED 2010
Table C.2-8	Uranium and Uranium Isotope Results from New Mexico Drinking Water Branch

Abbreviations

AL	alluvium or alluvial aquifer
amsl	above mean sea level
AR	activity ratio (U-234/U-238)
ARCO	Atlantic Richfield Company
As	arsenic
bgs	below ground surface
BW	Bluewater (prefix used by NMED [2010]) for sample IDs)
Ca (mg/L)	calcium
$CaCO_3$	calcium carbonate
Cl (mg/L)	chloride
DO (mg/L)	dissolved oxygen
DOE	U.S. Department of Energy
EC	electrical conductivity
Fe	iron
Fm	formation
ft	feet
HMC	Homestake Mining Company
K (mg/L)	potassium
Mg	magnesium

Abbreviations (continued)

mg/L	milligrams per liter
Mo (µg/L)	molybdenum
µg/L	micrograms per liter
µmhos/cm	micromhos per centimeter
µS/cm	microsiemens per centimeter
N	nitrogen
Na (mg/L)	sodium
NM DWB	State of New Mexico Drinking Water Branch (Drinking Water Watch) website
NMED	New Mexico Environment Department
NO_2	nitrite
NO_3	nitrate
ORP (mV)	oxidation-reduction potential (millivolts)
OSE	(New Mexico) Office of State Engineer
pCi/L	picocuries per liter
s.u.	standard units
SA	San Andres
SC	specific conductance
Se (µg/L)	selenium
SMC	San Mateo Creek
SO_4 (mg/L)	sulfate
T (°C)	temperature (degrees Celsius)
U	uranium
U-234	uranium-234
U-238	uranium-238
USGS	U.S. Geological Survey

This page intentionally left blank

Table C.1-1. Water Level Data for Bluewater Site San Andres Aquifer Wells

Well ID	Date	Water Elevation (ft amsl)	TOC Elevation (ft amsl)	Depth from Top of Casing (ft)	Depth from Surface (ft)	Data Source/Comment
11(SG)	11/14/2012	6434.12	6639.19	205.07	202.38	
11(SG)	1/30/2013	6434.08	6639.19	205.11	202.42	
11(SG)	5/14/2013	6433.89	6639.19	205.3	202.61	
11(SG)	11/19/2013	6433.49	6639.19	205.7	203.01	
11(SG)	4/29/2014	6432.18	6639.19	207.01	204.32	
13(SG)	11/15/2012	6427	6593.57	166.57	164.03	
13(SG)	1/28/2013	6427.24	6593.57	166.33	163.79	
13(SG)	5/15/2013	6426.07	6593.57	167.5	164.96	
13(SG)	11/19/2013	6426.49	6593.57	167.08	164.54	
13(SG)	4/29/2014	6426.09	6593.57	167.48	164.94	
14(SG)	11/14/2012	6428.98	6617.2	188.22	185.77	
14(SG)	1/30/2013	6429.14	6617.2	188.06	185.61	
14(SG)	5/14/2013	6428.2	6617.2	189	186.55	
14(SG)	11/19/2013	6428.2	6617.2	189	186.55	
14(SG)	4/30/2014	6427.79	6617.2	189.41	186.96	
15(SG)	11/13/2012	6427.74	6612.53	184.79	182.38	
15(SG)	1/29/2013	6427.9	6612.53	184.63	182.22	
15(SG)	5/14/2013	6425.85	6612.53	186.68	184.27	
15(SG)	11/19/2013	6427.13	6612.53	185.4	182.99	
15(SG)	4/29/2014	6426.71	6612.53	185.82	183.41	
16(SG)	11/13/2012	6433.97	6618.25	184.28	181.58	
16(SG)	1/30/2013	6433.94	6618.25	184.31	181.61	
16(SG)	5/16/2013	6433.67	6618.25	184.58	181.88	
16(SG)	11/19/2013	6432.23	6618.25	186.02	183.32	
16(SG)	4/29/2014	6432	6618.25	186.25	183.55	
18(SG)	11/14/2012	6427.83	6601.32	173.49	170.89	
18(SG)	1/30/2013	6427.96	6601.32	173.36	170.76	
18(SG)	5/14/2013	6426.98	6601.32	174.34	171.74	
18(SG)	11/19/2013	6427.3	6601.32	174.02	171.42	
18(SG)	4/30/2014	6426.74	6601.32	174.58	171.98	
Anaconda #3	4/12/1990	6473.04		-6473.04	-6473.04	
Anaconda #4	4/26/1984	6470.41		-6470.41	-6470.41	
Anaconda #4	4/22/1986	6473.77		-6473.77	-6473.77	
Anaconda #4	10/6/1986	6476.46		-6476.46	-6476.46	
Anaconda #4	4/13/1987	6475.84		-6475.84	-6475.84	
Anaconda #4	10/8/1987	6478.16		-6478.16	-6478.16	
Anaconda #4	4/13/1988	6475.14		-6475.14	-6475.14	
Anaconda #4	10/11/1988	6477.67		-6477.67	-6477.67	
Anaconda #4	4/19/1989	6474.81		-6474.81	-6474.81	
Anaconda #5	5/17/1984	6472.92		-6472.92	-6472.92	
Anaconda #5	4/22/1986	6475.52		-6475.52	-6475.52	
Anaconda #5	10/6/1986	6478.27		-6478.27	-6478.27	
Anaconda #5	11/19/1986	6477.85		-6477.85	-6477.85	
Anaconda #5	4/6/1987	6476.37		-6476.37	-6476.37	
Anaconda #5	10/8/1987	6478.81		-6478.81	-6478.81	
Anaconda #5	4/5/1988	6476.9		-6476.9	-6476.9	
Anaconda #5	10/5/1988	6479.74		-6479.74	-6479.74	
Anaconda #5	4/18/1989	6477.22		-6477.22	-6477.22	
Anaconda #5	4/12/1990	6473.51		-6473.51	-6473.51	
C(SG)	4/16/1984	6471.47		-6471.47	-6471.47	
C(SG)	5/5/1986	6476.14		-6476.14	-6476.14	
C(SG)	4/9/1987	6474.43		-6474.43	-6474.43	
C(SG)	4/13/1988	6476.87		-6476.87	-6476.87	
C(SG)	4/18/1989	6477.24		-6477.24	-6477.24	
C(SG)	4/11/1990	6470.53		-6470.53	-6470.53	
C(SG)	4/16/1990	6473.52		-6473.52	-6473.52	

Table C.1-1. Water Level Data for Bluewater Site San Andres Aquifer Wells

Well ID	Date	Water Elevation (ft amsl)	TOC Elevation (ft amsl)	Depth from Top of Casing (ft)	Depth from Surface (ft)	Data Source/Comment
HMC-951	4/26/1984	6469.54	6576.79	107.25	107.41	
HMC-951	6/20/1986	6473.22	6576.79	103.57	103.73	
HMC-951	4/9/1987	6474.44	6576.79	102.35	102.51	
HMC-951	4/13/1988	6473.42	6576.79	103.37	103.53	
HMC-951	4/19/1989	6473.9	6576.79	102.89	103.05	
HMC-951	8/18/1998	6464.90	6573.7	108.80		HMC 1999 (see Note)
HMC-951	8/19/1999	6466.20	6573.7	107.50		HMC 2000
HMC-951	8/30/1999	6462.85	6573.7	110.85		HMC 2000
HMC-951	9/7/1999	6462.77	6573.7	110.93		HMC 2000
HMC-951	10/5/1999	6462.91	6573.7	110.79		HMC 2000
HMC-951	11/1/1999	6463.78	6573.7	109.92		HMC 2000
HMC-951	11/29/1999	6466.09	6573.7	107.61		HMC 2000
HMC-951	1/3/2000	6463.82	6573.7	109.88		HMC 2001
HMC-951	1/31/2000	6462.72	6573.7	110.98		HMC 2001
HMC-951	3/6/2000	6464.10	6573.7	109.60		HMC 2001
HMC-951	4/3/2000	6463.45	6573.7	110.25		HMC 2001
HMC-951	5/2/2000	6463.50	6573.7	110.20		HMC 2001
HMC-951	8/9/2000	6458.70	6573.7	115.00		HMC 2001
HMC-951	4/12/2001	6457.76	6573.7	115.94		HMC 2002
HMC-951	12/11/2001	6452.38	6573.7	121.32		HMC 2002
HMC-951	3/4/2002	6447.74	6573.7	125.96		HMC 2003
HMC-951	4/1/2002	6450.94	6573.7	122.76		HMC 2003
HMC-951	4/29/2002	6445.2	6573.7	128.5		HMC 2003
HMC-951	6/4/2002	6443.58	6573.7	130.12		HMC 2003
HMC-951	7/1/2002	6442.22	6573.7	131.48		HMC 2003
HMC-951	8/5/2002	6441.09	6573.7	132.61		HMC 2003
HMC-951	9/3/2002	6440.82	6573.7	132.88		HMC 2003
HMC-951	9/30/2002	6440.92	6573.7	132.78		HMC 2003
HMC-951	10/17/2002	6441.34	6573.7	132.36		HMC 2003
HMC-951	11/5/2002	6442.65	6573.7	131.05		HMC 2003
HMC-951	12/2/2002	6442.85	6573.7	130.85		HMC 2003
HMC-951	12/18/2002	6443.16	6573.7	130.54		HMC 2003
HMC-951	12/30/2002	6443.19	6573.7	130.51		HMC 2003
HMC-951	2/3/2003	6442.38	6573.7	131.32		HMC 2004
HMC-951	3/3/2003	6442.42	6573.7	131.28		HMC 2004
HMC-951	3/31/2003	6440.90	6573.7	132.80		HMC 2004
HMC-951	5/5/2003	6439.09	6573.7	134.61		HMC 2004
HMC-951	6/30/2003	6386.26	6573.7	187.44		HMC 2004
HMC-951	8/2/2003	6389.00	6573.7	184.70		HMC 2004
HMC-951	8/14/2003	6437.60	6573.7	136.10		HMC 2004
HMC-951	9/2/2003	6436.10	6573.7	137.60		HMC 2004
HMC-951	9/29/2003	6437.25	6573.7	136.45		HMC 2004
HMC-951	10/27/2003	6437.89	6573.7	135.81		HMC 2004
HMC-951	11/3/2003	6438.20	6573.7	135.50		HMC 2004
HMC-951	12/1/2003	6389.00	6573.7	184.70		HMC 2004
HMC-951	12/29/2003	6403.30	6573.7	170.40		HMC 2004
HMC-951	2/2/2004	6438.39	6573.7	135.31		HMC 2005
HMC-951	3/1/2004	6438.92	6573.7	134.78		HMC 2005
HMC-951	3/29/2004	6437.15	6573.7	136.55		HMC 2005
HMC-951	5/3/2004	6435.76	6573.7	137.94		HMC 2005
HMC-951	6/1/2004	6435.92	6573.7	137.78		HMC 2005
HMC-951	6/28/2004	6434.83	6573.7	138.87		HMC 2005
HMC-951	8/2/2004	6434.70	6573.7	139.00		HMC 2005
HMC-951	8/30/2004	6433.46	6573.7	140.24		HMC 2005
HMC-951	10/4/2004	6433.42	6573.7	140.28		HMC 2005
HMC-951	11/1/2004	6434.46	6573.7	139.24		HMC 2005

Table C.1-1. Water Level Data for Bluewater Site San Andres Aquifer Wells

Well ID	Date	Water Elevation (ft amsl)	TOC Elevation (ft amsl)	Depth from Top of Casing (ft)	Depth from Surface (ft)	Data Source/Comment
HMC-951	11/29/2004	6438.51	6573.7	135.19		HMC 2005
HMC-951	12/8/2004	6438.80	6573.7	134.90		HMC 2005
HMC-951	1/4/2005	6434.62	6573.7	139.08		HMC 2006
HMC-951	1/31/2005	6433.88	6573.7	139.82		HMC 2006
HMC-951	2/28/2005	6434.32	6573.7	139.38		HMC 2006
HMC-951	4/4/2005	6433.85	6573.7	139.85		HMC 2006
HMC-951	4/25/2005	6433.82	6573.7	139.88		HMC 2006
HMC-951	5/2/2005	6433.03	6573.7	140.67		HMC 2006
HMC-951	5/31/2005	6431.78	6573.7	141.92		HMC 2006
HMC-951	7/5/2005	6431.45	6573.7	142.25		HMC 2006
HMC-951	8/1/2005	6436.92	6573.7	136.78		HMC 2006
HMC-951	8/29/2005	6433.35	6573.7	140.35		HMC 2006
HMC-951	10/3/2005	6432.78	6573.7	140.92		HMC 2006
HMC-951	10/31/2005	6432.80	6573.7	140.90		HMC 2006
HMC-951	11/28/2005	6432.79	6573.7	140.91		HMC 2006
HMC-951	12/5/2005	6432.89	6573.7	140.81		HMC 2006
HMC-951	1/3/2006	6432.75	6573.7	140.95		HMC 2006
HMC-951	1/3/2006	6432.75	6573.7	140.95		HMC 2007
HMC-951	1/30/2006	6432.56	6573.7	141.14		HMC 2007
HMC-951	2/27/2006	6432.30	6573.7	141.40		HMC 2007
HMC-951	3/16/2006	6431.34	6573.7	142.36		HMC 2007
HMC-951	4/3/2006	6431.34	6573.7	142.36		HMC 2007
HMC-951	5/1/2006	6431.83	6573.7	141.87		HMC 2007
HMC-951	5/30/2006	6430.90	6573.7	142.80		HMC 2007
HMC-951	6/26/2006	6430.58	6573.7	143.12		HMC 2007
HMC-951	7/31/2006	6429.47	6573.7	144.23		HMC 2007
HMC-951	8/28/2006	6433.80	6573.7	139.90		HMC 2007
HMC-951	9/25/2006	6429.40	6573.7	144.30		HMC 2007
HMC-951	10/30/2006	6430.62	6573.7	143.08		HMC 2007
HMC-951	11/27/2006	6430.55	6573.7	143.15		HMC 2007
HMC-951	12/27/2006	6431.15	6573.7	142.55		HMC 2007
HMC-951	1/29/2007	6435.10	6573.7	138.60		HMC 2008
HMC-951	2/26/2007	6435.10	6573.7	138.60		HMC 2008
HMC-951	3/9/2007	6431.32	6573.7	142.38		HMC 2008
HMC-951	4/2/2007	6430.45	6573.7	143.25		HMC 2008
HMC-951	4/30/2007	6428.78	6573.7	144.92		HMC 2008
HMC-951	5/29/2007	6427.80	6573.7	145.90		HMC 2008
HMC-951	7/2/2007	6426.90	6573.7	146.80		HMC 2008
HMC-951	7/30/2007	6426.80	6573.7	146.90		HMC 2008
HMC-951	9/4/2007	6426.65	6573.7	147.05		HMC 2008
HMC-951	10/1/2007	6425.70	6573.7	148.00		HMC 2008
HMC-951	10/29/2007	6426.40	6573.7	147.30		HMC 2008
HMC-951	12/3/2007	6427.10	6573.7	146.60		HMC 2008
HMC-951	1/2/2008	6427.33	6573.7	146.37		HMC 2009
HMC-951	2/4/2008	6427.04	6573.7	146.66		HMC 2009
HMC-951	3/3/2008	6427.55	6573.7	146.15		HMC 2009
HMC-951	3/5/2008	6427.51	6573.7	146.19		HMC 2009
HMC-951	3/31/2008	6426.60	6573.7	147.10		HMC 2009
HMC-951	5/5/2008	6425.40	6573.7	148.30		HMC 2009
HMC-951	6/2/2008	6424.97	6573.7	148.73		HMC 2009
HMC-951	6/30/2008	6423.40	6573.7	150.30		HMC 2009
HMC-951	9/2/2008	6422.10	6573.7	151.60		HMC 2009
HMC-951	9/4/2008	6422.65	6573.7	151.05		HMC 2009
HMC-951	9/29/2008	6422.90	6573.7	150.80		HMC 2009
HMC-951	10/27/2008	6426.60	6573.7	147.10		HMC 2009
HMC-951	12/1/2008	6421.60	6573.7	152.10		HMC 2009

Table C.1-1. Water Level Data for Bluewater Site San Andres Aquifer Wells

Well ID	Date	Water Elevation (ft amsl)	TOC Elevation (ft amsl)	Depth from Top of Casing (ft)	Depth from Surface (ft)	Data Source/Comment
HMC-951	12/1/2008	6423.70	6573.7	150.00		HMC 2009
HMC-951	12/29/2008	6423.42	6573.7	150.28		HMC 2009
HMC-951	2/2/2009	6424.05	6573.7	149.65		HMC Electronic, prov. to DOE
HMC-951	3/2/2009	6423.75	6573.7	149.95		HMC Electronic, prov. to DOE
HMC-951	3/20/2009	6421.44	6573.7	152.26		HMC Electronic, prov. to DOE
HMC-951	3/30/2009	6422.38	6573.7	151.32		HMC Electronic, prov. to DOE
HMC-951	5/4/2009	6422.6	6573.7	151.1		HMC Electronic, prov. to DOE
HMC-951	6/1/2009	6423.3	6573.7	150.4		HMC Electronic, prov. to DOE
HMC-951	6/29/2009	6419.7	6573.7	154		HMC Electronic, prov. to DOE
HMC-951	8/3/2009	6422.75	6573.7	150.95		HMC Electronic, prov. to DOE
HMC-951	8/31/2009	6420.3	6573.7	153.4		HMC Electronic, prov. to DOE
HMC-951	9/28/2009	6421.95	6573.7	151.75		HMC Electronic, prov. to DOE
HMC-951	11/2/2009	6422.8	6573.7	150.9		HMC Electronic, prov. to DOE
HMC-951	11/30/2009	6422.43	6573.7	151.27		HMC Electronic, prov. to DOE
HMC-951	12/7/2009	6422.7	6573.7	151		HMC Electronic, prov. to DOE
HMC-951	12/28/2009	6423.5	6573.7	150.2		HMC Electronic, prov. to DOE
HMC-951	2/1/2010	6423.25	6573.7	150.45		HMC 2011
HMC-951	3/1/2010	6422.95	6573.7	150.75		HMC 2011
HMC-951	3/3/2010	6424.9	6573.7	148.8		HMC 2011
HMC-951	3/29/2010	6422.87	6573.7	150.83		HMC 2011
HMC-951	5/3/2010	6422.95	6573.7	150.75		HMC 2011
HMC-951	6/1/2010	6421.3	6573.7	152.4		HMC 2011
HMC-951	6/22/2010	6421.17	6573.7	152.53		HMC 2011
HMC-951	6/28/2010	6421.19	6573.7	152.51		HMC 2011
HMC-951	8/2/2010	6420.58	6573.7	153.12		HMC 2011
HMC-951	8/30/2010	6420.8	6573.7	152.9		HMC 2011
HMC-951	9/7/2010	6420.3	6573.7	153.4		HMC 2011
HMC-951	9/13/2010	6420.49	6573.7	153.21		HMC 2011
HMC-951	9/20/2010	6420.77	6573.7	152.93		HMC 2011
HMC-951	9/27/2010	6421.5	6573.7	152.2		HMC 2011
HMC-951	10/11/2010	6422.3	6573.7	151.4		HMC 2011
HMC-951	10/18/2010	6422.72	6573.7	150.98		HMC 2011
HMC-951	10/25/2010	6381.1	6573.7	192.6		HMC 2011
HMC-951	11/1/2010	6423.4	6573.7	150.3		HMC 2011
HMC-951	11/8/2010	6423.4	6573.7	150.3		HMC 2011
HMC-951	11/15/2010	6423.25	6573.7	150.45		HMC 2011
HMC-951	11/29/2010	6423.75	6573.7	149.95		HMC 2011
HMC-951	12/6/2010	6423.8	6573.7	149.9		HMC 2011
HMC-951	12/27/2010	6424.17	6573.7	149.53		HMC 2011
HMC-951	1/31/2011	6423.7	6573.7	150		HMC 2012
HMC-951	2/28/2011	6423.5	6573.7	150.2		HMC 2012
HMC-951	4/13/2011	6421.85	6573.7	151.85		HMC 2012
HMC-951	4/25/2011	6423.21	6573.7	150.49		HMC 2012
HMC-951	5/23/2011	6422.5	6573.7	151.2		HMC 2012
HMC-951	6/27/2011	6420.1	6573.7	153.6		HMC 2012
HMC-951	7/25/2011	6419.73	6573.7	153.97		HMC 2012
HMC-951	8/29/2011	6420.35	6573.7	153.35		HMC 2012
HMC-951	9/26/2011	6420.9	6573.7	152.8		HMC 2012
HMC-951	10/12/2011	6453.7	6573.7	120		HMC 2012
HMC-951	10/24/2011	6421.35	6573.7	152.35		HMC 2012
HMC-951	11/21/2011	6421.1	6573.7	152.6		HMC 2012
HMC-951	12/19/2011	6421.3	6573.7	152.4		HMC 2012
HMC-951	1/23/2012	6386.3	6573.7	187.4		HMC 2013
HMC-951	2/27/2012	6422.72	6573.7	150.98		HMC 2013
HMC-951	3/9/2012	6423.02	6573.7	150.68		HMC 2013
HMC-951	3/26/2012	6426	6573.7	147.7		HMC 2013

Table C.1-1. Water Level Data for Bluewater Site San Andres Aquifer Wells

Well ID	Date	Water Elevation (ft amsl)	TOC Elevation (ft amsl)	Depth from Top of Casing (ft)	Depth from Surface (ft)	Data Source/Comment
HMC-951	11/20/2013	6424.89	6576.79	151.9	152.06	DOE sampling
HMC-951	4/30/2014	6424.5	6576.79	152.29	152.45	DOE sampling
I(SG)	3/12/1984	6467.06	6625.93	158.87	157.78	
I(SG)	5/23/1984	6467.46	6625.93	158.47	157.38	
I(SG)	4/17/1986	6470.61	6625.93	155.32	154.23	
I(SG)	7/7/1986	6471.25	6625.93	154.68	153.59	
I(SG)	10/6/1986	6472.8	6625.93	153.13	152.04	
I(SG)	2/3/1987	6471.66	6625.93	154.27	153.18	
I(SG)	4/8/1987	6470.12	6625.93	155.81	154.72	
I(SG)	7/7/1987	6472.55	6625.93	153.38	152.29	
I(SG)	10/7/1987	6474.52	6625.93	151.41	150.32	
I(SG)	1/11/1988	6472.75	6625.93	153.18	152.09	
I(SG)	4/6/1988	6471.25	6625.93	154.68	153.59	
I(SG)	7/11/1988	6462.42	6625.93	163.51	162.42	
I(SG)	10/10/1988	6473.62	6625.93	152.31	151.22	
I(SG)	1/18/1989	6473.9	6625.93	152.03	150.94	
I(SG)	4/18/1989	6471.78	6625.93	154.15	153.06	
I(SG)	4/11/1990	6478.59	6625.93	147.34	146.25	
I(SG)	11/4/2008	6431.44	6625.93	194.49	193.4	
I(SG)	11/10/2009	6430.22	6625.93	195.71	194.62	
I(SG)	11/11/2010	6430.3	6625.93	195.63	194.54	
I(SG)	7/27/2011	6426.74	6625.93	199.19	198.1	
I(SG)	11/16/2011	6428.23	6625.93	197.7	196.61	
I(SG)	5/15/2012	6429.11	6625.93	196.82	195.73	
I(SG)	11/14/2012	6426.71	6625.93	199.22	198.13	
I(SG)	1/29/2013	6426.74	6625.93	199.19	198.1	
I(SG)	5/15/2013	6425.72	6625.93	200.21	199.12	
I(SG)	5/15/2013	6425.75	6625.93	200.18	199.09	
I(SG)	5/15/2013	6425.72	6625.93	200.21	199.12	
I(SG)	11/19/2013	6426.19	6625.93	199.74	198.65	
I(SG)	11/19/2013	6426.19	6625.93	199.74	198.65	
I(SG)	11/19/2013	6426.19	6625.93	199.74	198.65	
I(SG)	11/19/2013	6426.19	6625.93	199.74	198.65	
I(SG)	4/30/2014	6425.74	6625.93	200.19	199.1	
L(SG)	2/9/1984	6492.8	6606.09	113.29	112.01	
L(SG)	6/7/1984	6494.57	6606.09	111.52	110.24	
L(SG)	4/15/1986	6496.17	6606.09	109.92	108.64	
L(SG)	7/7/1986	6497.75	6606.09	108.34	107.06	
L(SG)	10/13/1986	6498.65	6606.09	107.44	106.16	
L(SG)	2/3/1987	6497.11	6606.09	108.98	107.7	
L(SG)	4/6/1987	6495.27	6606.09	110.82	109.54	
L(SG)	8/31/1987	6499.83	6606.09	106.26	104.98	
L(SG)	10/5/1987	6500.58	6606.09	105.51	104.23	
L(SG)	1/11/1988	6499.07	6606.09	107.02	105.74	
L(SG)	4/5/1988	6497.65	6606.09	108.44	107.16	
L(SG)	6/14/1988	6499.3	6606.09	106.79	105.51	
L(SG)	7/11/1988	6500.84	6606.09	105.25	103.97	
L(SG)	9/8/1988	6500.81	6606.09	105.28	104	
L(SG)	10/10/1988	6500.11	6606.09	105.98	104.7	
L(SG)	12/6/1988	6499.42	6606.09	106.67	105.39	
L(SG)	12/8/1988	6499.42	6606.09	106.67	105.39	
L(SG)	1/18/1989	6499.97	6606.09	106.12	104.84	
L(SG)	3/7/1989	6497.61	6606.09	108.48	107.2	
L(SG)	4/10/1989	6496.84	6606.09	109.25	107.97	
L(SG)	6/15/1989	6497.99	6606.09	108.1	106.82	
L(SG)	9/20/1989	6496.21	6606.09	109.88	108.6	

Table C.1-1. Water Level Data for Bluewater Site San Andres Aquifer Wells

Well ID	Date	Water Elevation (ft amsl)	TOC Elevation (ft amsl)	Depth from Top of Casing (ft)	Depth from Surface (ft)	Data Source/Comment
L(SG)	12/18/1989	6494.35	6606.09	111.74	110.46	
L(SG)	3/13/1990	6493.2	6606.09	112.89	111.61	
L(SG)	4/10/1990	6492.66	6606.09	113.43	112.15	
L(SG)	7/11/1990	6488.98	6606.09	117.11	115.83	
L(SG)	9/18/1990	6487.3	6606.09	118.79	117.51	
L(SG)	10/2/1990	6487.87	6606.09	118.22	116.94	
L(SG)	12/18/1990	6487.16	6606.09	118.93	117.65	
L(SG)	1/9/1991	6487.16	6606.09	118.93	117.65	
L(SG)	4/3/1991	6486.14	6606.09	119.95	118.67	
L(SG)	7/10/1991	6488.46	6606.09	117.63	116.35	
L(SG)	10/2/1991	6491.95	6606.09	114.14	112.86	
L(SG)	1/15/1992	6490.11	6606.09	115.98	114.7	
L(SG)	4/8/1992	6488.95	6606.09	117.14	115.86	
L(SG)	7/21/1992	6490.39	6606.09	115.7	114.42	
L(SG)	10/8/1992	6489.7	6606.09	116.39	115.11	
L(SG)	1/12/1993	6488.57	6606.09	117.52	116.24	
L(SG)	4/5/1993	6487.93	6606.09	118.16	116.88	
L(SG)	7/7/1993	6488.27	6606.09	117.82	116.54	
L(SG)	10/5/1993	6492.15	6606.09	113.94	112.66	
L(SG)	1/5/1994	6491.65	6606.09	114.44	113.16	
L(SG)	4/5/1994	6487.93	6606.09	118.16	116.88	
L(SG)	7/7/1994	6493.8	6606.09	112.29	111.01	
L(SG)	10/13/1994	6494.8	6606.09	111.29	110.01	
L(SG)	1/16/1995	6493.57	6606.09	112.52	111.24	
L(SG)	4/10/1995	6492.69	6606.09	113.4	112.12	
L(SG)	7/18/1995	6496.69	6606.09	109.4	108.12	
L(SG)	10/18/1995	6497.14	6606.09	108.95	107.67	
L(SG)	1/15/1996	6494.78	6606.09	111.31	110.03	
L(SG)	4/3/1996	6493.39	6606.09	112.7	111.42	
L(SG)	11/16/1998	6486.59	6606.09	119.5	118.22	
L(SG)	11/3/2001	6471.89	6606.09	134.2	132.92	
L(SG)	11/18/2004	6455.28	6606.09	150.81	149.53	
L(SG)	11/6/2007	6448.96	6606.09	157.13	155.85	
L(SG)	11/4/2008	6449.35	6606.09	156.74	155.46	
L(SG)	11/10/2009	6444.62	6606.09	161.47	160.19	
L(SG)	11/11/2010	6451.53	6606.09	154.56	153.28	
L(SG)	7/27/2011	6445.27	6606.09	160.82	159.54	
L(SG)	11/17/2011	6446.17	6606.09	159.92	158.64	
L(SG)	5/15/2012	6446.75	6606.09	159.34	158.06	
L(SG)	11/14/2012	6445.94	6606.09	160.15	158.87	
L(SG)	1/30/2013	6445.7	6606.09	160.39	159.11	
L(SG)	5/15/2013	6445.24	6606.09	160.85	159.57	
L(SG)	5/16/2013	6445.24	6606.09	160.85	159.57	
L(SG)	5/16/2013	6445.24	6606.09	160.85	159.57	
L(SG)	11/19/2013	6442.09	6606.09	164	162.72	
L(SG)	4/29/2014	6440.81	6606.09	165.28	164	
M(SG)	6/7/1984	6482.72		-6482.72	-6482.72	
M(SG)	4/15/1986	6484.9		-6484.9	-6484.9	
M(SG)	10/13/1986	6486.8		-6486.8	-6486.8	
M(SG)	4/8/1987	6485.68		-6485.68	-6485.68	
M(SG)	10/8/1987	6487.58		-6487.58	-6487.58	
M(SG)	4/13/1988	6486.41		-6486.41	-6486.41	
M(SG)	10/11/1988	6487.99		-6487.99	-6487.99	
M(SG)	4/19/1989	6486.17		-6486.17	-6486.17	
M(SG)	4/11/1990	6482.9		-6482.9	-6482.9	
Mexican Camp	4/26/1984	6469.31		-6469.31	-6469.31	

Table C.1-1. Water Level Data for Bluewater Site San Andres Aquifer Wells

Well ID	Date	Water Elevation (ft amsl)	TOC Elevation (ft amsl)	Depth from Top of Casing (ft)	Depth from Surface (ft)	Data Source/Comment
Mexican Camp	4/22/1986	6472.72		-6472.72	-6472.72	
Mexican Camp	4/9/1987	6484		-6484	-6484	
Mexican Camp	4/7/1988	6473.65		-6473.65	-6473.65	
Monitor	5/16/1984	6473.17		-6473.17	-6473.17	
Monitor	4/17/1986	6476.36		-6476.36	-6476.36	
Monitor	10/6/1986	6478.91		-6478.91	-6478.91	
Monitor	4/13/1987	6477.51		-6477.51	-6477.51	
Monitor	10/12/1987	6479.04		-6479.04	-6479.04	
Monitor	4/5/1988	6477.39		-6477.39	-6477.39	
Monitor	10/10/1988	6479.06		-6479.06	-6479.06	
Monitor	4/11/1990	6474.62		-6474.62	-6474.62	
North	5/15/1984	6479.65		-6479.65	-6479.65	
North	4/17/1986	6482.68		-6482.68	-6482.68	
North	10/6/1986	6484.13		-6484.13	-6484.13	
North	4/8/1987	6483.14		-6483.14	-6483.14	
North	10/8/1987	6485.51		-6485.51	-6485.51	
North	4/13/1988	6484		-6484	-6484	
North	10/10/1988	6485.32		-6485.32	-6485.32	
North	4/18/1989	6483.88		-6483.88	-6483.88	
North	4/11/1990	6480.84		-6480.84	-6480.84	
OBS-2	4/19/1989	6481.9		-6481.9	-6481.9	
OBS-2	4/10/1990	6478.89		-6478.89	-6478.89	
OBS-3	5/7/1984	6474.56	6617.22	142.66	138.83	
OBS-3	4/17/1986	6479.95	6617.22	137.27	133.44	
OBS-3	10/13/1986	6480.86	6617.22	136.36	132.53	
OBS-3	4/6/1987	6480.45	6617.22	136.77	132.94	
OBS-3	10/7/1987	6482.37	6617.22	134.85	131.02	
OBS-3	4/5/1988	6481.2	6617.22	136.02	132.19	
OBS-3	6/14/1988	6481.5	6617.22	135.72	131.89	
OBS-3	9/8/1988	6482.81	6617.22	134.41	130.58	
OBS-3	10/11/1988	6482.5	6617.22	134.72	130.89	
OBS-3	12/6/1988	6482.61	6617.22	134.61	130.78	
OBS-3	12/8/1988	6482.61	6617.22	134.61	130.78	
OBS-3	3/7/1989	6482.61	6617.22	134.61	130.78	
OBS-3	4/11/1989	6481.44	6617.22	135.78	131.95	
OBS-3	6/15/1989	6481.4	6617.22	135.82	131.99	
OBS-3	9/21/1989	6479.53	6617.22	137.69	133.86	
OBS-3	3/14/1990	6478.33	6617.22	138.89	135.06	
OBS-3	4/10/1990	6477.85	6617.22	139.37	135.54	
OBS-3	5/24/1990	6477.37	6617.22	139.85	136.02	
OBS-3	7/12/1990	6476.69	6617.22	140.53	136.7	
OBS-3	9/18/1990	6474.7	6617.22	142.52	138.69	
OBS-3	10/2/1990	6474.52	6617.22	142.7	138.87	
OBS-3	12/18/1990	6474.3	6617.22	142.92	139.09	
OBS-3	1/10/1991	6474.07	6617.22	143.15	139.32	
OBS-3	4/2/1991	6473.33	6617.22	143.89	140.06	
OBS-3	7/9/1991	6473.29	6617.22	143.93	140.1	
OBS-3	10/2/1991	6474.8	6617.22	142.42	138.59	
OBS-3	1/20/1992	6474.81	6617.22	142.41	138.58	
OBS-3	4/7/1992	6474.25	6617.22	142.97	139.14	
OBS-3	7/20/1992	6473.9	6617.22	143.32	139.49	
OBS-3	10/19/1992	6473.77	6617.22	143.45	139.62	
OBS-3	2/12/1993	6473.3	6617.22	143.92	140.09	
OBS-3	4/12/1993	6473.15	6617.22	144.07	140.24	
OBS-3	7/7/1993	6473.33	6617.22	143.89	140.06	
OBS-3	10/13/1993	6474.16	6617.22	143.06	139.23	

Table C.1-1. Water Level Data for Bluewater Site San Andres Aquifer Wells

Well ID	Date	Water Elevation (ft amsl)	TOC Elevation (ft amsl)	Depth from Top of Casing (ft)	Depth from Surface (ft)	Data Source/Comment
OBS-3	1/5/1994	6474.93	6617.22	142.29	138.46	
OBS-3	4/12/1994	6473.15	6617.22	144.07	140.24	
OBS-3	7/6/1994	6475.13	6617.22	142.09	138.26	
OBS-3	10/11/1994	6476.62	6617.22	140.6	136.77	
OBS-3	1/16/1995	6476.84	6617.22	140.38	136.55	
OBS-3	4/18/1995	6476.06	6617.22	141.16	137.33	
OBS-3	7/18/1995	6477.11	6617.22	140.11	136.28	
OBS-3	10/23/1995	6478.73	6617.22	138.49	134.66	
OBS-3	1/15/1996	6478.13	6617.22	139.09	135.26	
OBS-3	4/2/1996	6477.86	6617.22	139.36	135.53	
OBS-3	11/13/1998	6476.84	6617.22	140.38	136.55	
OBS-3	11/3/2001	6463.72	6617.22	153.5	149.67	
OBS-3	11/18/2004	6448.99	6617.22	168.23	164.4	
OBS-3	11/6/2007	6441.98	6617.22	175.24	171.41	
OBS-3	11/4/2008	6439.45	6617.22	177.77	173.94	
OBS-3	11/10/2009	6436.51	6617.22	180.71	176.88	
OBS-3	11/10/2010	6437.28	6617.22	179.94	176.11	
OBS-3	11/10/2010	6435.5	6617.22	181.72	177.89	
OBS-3	7/28/2011	6435.22	6617.22	182	178.17	
OBS-3	11/16/2011	6435.08	6617.22	182.14	178.31	
OBS-3	11/13/2012	6434.13	6617.22	183.09	179.26	
OBS-3	1/30/2013	6434.12	6617.22	183.1	179.27	
OBS-3	5/14/2013	6433.7	6617.22	183.52	179.69	
OBS-3	11/20/2013	6432.32	6617.22	184.9	181.07	
OBS-3	4/29/2014	6431.23	6617.22	185.99	182.16	
Payne	5/9/1984	6475.1		-6475.1	-6475.1	
Payne	4/24/1986	6478.52		-6478.52	-6478.52	
Payne	11/19/1986	6480.69		-6480.69	-6480.69	
Payne	4/9/1987	6479.56		-6479.56	-6479.56	
Payne	10/12/1987	6482.43		-6482.43	-6482.43	
Payne	4/11/1988	6476.34		-6476.34	-6476.34	
Payne	10/11/1988	6282.99		-6282.99	-6282.99	
S(SG)	2/15/1984	6476.98	6625.25	148.27	146.84	
S(SG)	5/7/1984	6476.9	6625.25	148.35	146.92	
S(SG)	4/17/1986	6480.41	6625.25	144.84	143.41	
S(SG)	7/7/1986	6480.66	6625.25	144.59	143.16	
S(SG)	10/13/1986	6481.28	6625.25	143.97	142.54	
S(SG)	2/3/1987	6481.32	6625.25	143.93	142.5	
S(SG)	4/6/1987	6480.85	6625.25	144.4	142.97	
S(SG)	7/7/1987	6481.49	6625.25	143.76	142.33	
S(SG)	10/5/1987	6482.9	6625.25	142.35	140.92	
S(SG)	1/4/1988	6482.59	6625.25	142.66	141.23	
S(SG)	4/5/1988	6481.47	6625.25	143.78	142.35	
S(SG)	6/14/1988	6481.89	6625.25	143.36	141.93	
S(SG)	7/11/1988	6482.07	6625.25	143.18	141.75	
S(SG)	9/8/1988	6482.32	6625.25	142.93	141.5	
S(SG)	10/10/1988	6482.94	6625.25	142.31	140.88	
S(SG)	12/6/1988	6483.1	6625.25	142.15	140.72	
S(SG)	12/8/1988	6483.1	6625.25	142.15	140.72	
S(SG)	1/17/1989	6483.09	6625.25	142.16	140.73	
S(SG)	3/7/1989	6482.19	6625.25	143.06	141.63	
S(SG)	4/10/1989	6481.72	6625.25	143.53	142.1	
S(SG)	6/15/1989	6481.34	6625.25	143.91	142.48	
S(SG)	9/21/1989	6480.08	6625.25	145.17	143.74	
S(SG)	12/18/1989	6478.95	6625.25	146.3	144.87	
S(SG)	3/14/1990	6478.89	6625.25	146.36	144.93	

Table C.1-1. Water Level Data for Bluewater Site San Andres Aquifer Wells

Well ID	Date	Water Elevation (ft amsl)	TOC Elevation (ft amsl)	Depth from Top of Casing (ft)	Depth from Surface (ft)	Data Source/Comment
S(SG)	4/10/1990	6478.34	6625.25	146.91	145.48	
S(SG)	5/24/1990	6477.84	6625.25	147.41	145.98	
S(SG)	7/11/1990	6476.48	6625.25	148.77	147.34	
S(SG)	9/17/1990	6475.25	6625.25	150	148.57	
S(SG)	10/1/1990	6474.99	6625.25	150.26	148.83	
S(SG)	12/18/1990	6475.14	6625.25	150.11	148.68	
S(SG)	1/10/1991	6474.58	6625.25	150.67	149.24	
S(SG)	4/2/1991	6473.92	6625.25	151.33	149.9	
S(SG)	7/9/1991	6473.89	6625.25	151.36	149.93	
S(SG)	10/2/1991	6475.51	6625.25	149.74	148.31	
S(SG)	1/15/1992	6475.39	6625.25	149.86	148.43	
S(SG)	4/6/1992	6474.79	6625.25	150.46	149.03	
S(SG)	7/20/1992	6475.1	6625.25	150.15	148.72	
S(SG)	10/6/1992	6474.56	6625.25	150.69	149.26	
S(SG)	1/12/1993	6474.02	6625.25	151.23	149.8	
S(SG)	4/8/1993	6473.57	6625.25	151.68	150.25	
S(SG)	7/7/1993	6474.01	6625.25	151.24	149.81	
S(SG)	10/6/1993	6474.89	6625.25	150.36	148.93	
S(SG)	1/5/1994	6475.57	6625.25	149.68	148.25	
S(SG)	4/8/1994	6473.57	6625.25	151.68	150.25	
S(SG)	7/6/1994	6477.65	6625.25	147.6	146.17	
S(SG)	10/11/1994	6477.06	6625.25	148.19	146.76	
S(SG)	4/10/1995	6476.54	6625.25	148.71	147.28	
S(SG)	4/16/1995	6477.42	6625.25	147.83	146.4	
S(SG)	7/18/1995	6477.57	6625.25	147.68	146.25	
S(SG)	10/16/1995	6479.3	6625.25	145.95	144.52	
S(SG)	1/16/1996	6479.23	6625.25	146.02	144.59	
S(SG)	4/2/1996	6478.26	6625.25	146.99	145.56	
S(SG)	11/13/1998	6476.8	6625.25	148.45	147.02	
S(SG)	11/3/2001	6462.94	6625.25	162.31	160.88	
S(SG)	11/18/2004	6448.64	6625.25	176.61	175.18	
S(SG)	11/6/2007	6442.23	6625.25	183.02	181.59	
S(SG)	11/4/2008	6439.22	6625.25	186.03	184.6	
S(SG)	11/10/2009	6436.39	6625.25	188.86	187.43	
S(SG)	11/9/2010	6437.14	6625.25	188.11	186.68	
S(SG)	11/16/2011	6435.14	6625.25	190.11	188.68	
S(SG)	11/13/2012	6434.14	6625.25	191.11	189.68	
S(SG)	1/30/2013	6434.04	6625.25	191.21	189.78	
S(SG)	5/16/2013	6432.94	6625.25	192.31	190.88	
S(SG)	11/20/2013		6625.25			Not enough water to sample
S(SG)	4/29/2014	6432.05	6625.25	193.2	191.77	
W(SG)	6/7/1984	6461.58		-6461.58	-6461.58	
W(SG)	4/17/1986	6472.54		-6472.54	-6472.54	
W(SG)	10/6/1986	6475		-6475	-6475	
W(SG)	4/8/1987	6471.91		-6471.91	-6471.91	
W(SG)	10/5/1987	6476.48		-6476.48	-6476.48	
W(SG)	4/6/1988	6473.45		-6473.45	-6473.45	
W(SG)	10/10/1988	6475.63		-6475.63	-6475.63	
W(SG)	4/17/1989	6473.92		-6473.92	-6473.92	

Note:
Water level data listed here for HMC-951 were obtained mostly from Homestake (HMC) annual reports. For these records, the measuring point (MP) elevation differs slightly from the top of casing (TOC) elevation used in the DOE database.

This page intentionally left blank

Table C.1-2. Water Level Data for Bluewater Site Alluvial Aquifer Wells

Well ID	Date	Water Elevation (ft amsl)	TOC Elevation (ft amsl)	Depth from Top of Casing (ft)	Depth from Surface (ft)	Comment
20(M)	11/14/2012	6508.44	6613.38	104.94	102.1	
20(M)	1/30/2013	6508.37	6613.38	105.01	102.17	
20(M)	5/14/2013	6508.13	6613.38	105.25	102.41	
20(M)	11/19/2013	6507.74	6613.38	105.64	102.8	
20(M)	4/29/2014	6507.23	6613.38	106.15	103.31	
21(M)	7/27/2011	6466.26	6593.8	127.54	124.59	
21(M)	11/15/2011	6466.19	6593.8	127.61	124.66	
21(M)	5/15/2012	6465.87	6593.8	127.93	124.98	
21(M)	11/15/2012	6465.66	6593.8	128.14	125.19	
21(M)	1/29/2013	6465.52	6593.8	128.28	125.33	
21(M)	5/15/2013	6465.71	6593.8	128.09	125.14	
21(M)	11/19/2013	6465.52	6593.8	128.28	125.33	
21(M)	4/29/2014	6465.57	6593.8	128.23	125.28	
22(M)	7/27/2011	6470.02	6606.48	136.46	133.59	
22(M)	11/15/2011	6469.94	6606.48	136.54	133.67	
22(M)	5/15/2012	6470.1	6606.48	136.38	133.51	
22(M)	11/15/2012	6469.57	6606.48	136.91	134.04	
22(M)	1/29/2013	6469.49	6606.48	136.99	134.12	
22(M)	5/14/2013	6469.48	6606.48	137	134.13	
22(M)	11/19/2013	6469.25	6606.48	137.23	134.36	
22(M)	4/29/2014	6469.12	6606.48	137.36	134.49	
23(M)	11/13/2012		6579.22			Dry
23(M)	1/28/2013	6468.61	6579.22	110.61	107.99	
23(M)	5/15/2013	6468.6	6579.22	110.62	108	
23(M)	11/19/2013	6469.02	6579.22	110.2	107.58	
23(M)	4/30/2014	6469.04	6579.22	110.18	107.56	
Aragon	5/9/1984	6531.77		-6531.77	-6531.77	
Aragon	4/24/1986	6534.59		-6534.59	-6534.59	
Aragon	11/19/1986	6535.98		-6535.98	-6535.98	
Aragon	4/13/1987	6531.93		-6531.93	-6531.93	
Aragon	10/12/1987	6533.37		-6533.37	-6533.37	
Aragon	4/11/1988	6534.75		-6534.75	-6534.75	
Aragon	10/11/1988	6538.3		-6538.3	-6538.3	
B(M)	2/13/1984	6520.51		-6520.51	-6520.51	
B(M)	5/7/1984	6519.12		-6519.12	-6519.12	
B(M)	4/15/1986	6522.12		-6522.12	-6522.12	
B(M)	7/7/1986	6522.27		-6522.27	-6522.27	
B(M)	10/13/1986	6523.13		-6523.13	-6523.13	
B(M)	2/3/1987	6521.96		-6521.96	-6521.96	
B(M)	4/6/1987	6521.71		-6521.71	-6521.71	
B(M)	7/7/1987	6521.54		-6521.54	-6521.54	
B(M)	10/5/1987	6521.59		-6521.59	-6521.59	
B(M)	1/4/1988	6521.81		-6521.81	-6521.81	
B(M)	4/5/1988	6521.79		-6521.79	-6521.79	
B(M)	7/11/1988	6521.7		-6521.7	-6521.7	
B(M)	10/6/1988	6522.14		-6522.14	-6522.14	
B(M)	1/17/1989	6522.24		-6522.24	-6522.24	
B(M)	4/10/1989	6521.59		-6521.59	-6521.59	
B(M)	4/12/1990	6520.5		-6520.5	-6520.5	
Berryhill House	5/9/1984	6522.13		-6522.13	-6522.13	
Berryhill House	4/22/1986	6523.68		-6523.68	-6523.68	
Berryhill House	11/19/1986	6523.48		-6523.48	-6523.48	
Berryhill House	4/13/1987	6523.29		-6523.29	-6523.29	
Berryhill House	10/12/1987	6522.36		-6522.36	-6522.36	
Berryhill House	4/11/1988	6522.51		-6522.51	-6522.51	

Table C.1-2. Water Level Data for Bluewater Site Alluvial Aquifer Wells

Well ID	Date	Water Elevation (ft amsl)	TOC Elevation (ft amsl)	Depth from Top of Casing (ft)	Depth from Surface (ft)	Comment
Berryhill House	10/12/1988	6523.32		-6523.32	-6523.32	
C(M)	3/12/1984	6512.61		-6512.61	-6512.61	
C(M)	4/16/1984	6512.24		-6512.24	-6512.24	
C(M)	4/15/1986	6514.11		-6514.11	-6514.11	
C(M)	7/7/1986	6514.29		-6514.29	-6514.29	
C(M)	10/13/1986	6514.44		-6514.44	-6514.44	
C(M)	2/3/1987	6513.96		-6513.96	-6513.96	
C(M)	4/6/1987	6513.64		-6513.64	-6513.64	
C(M)	7/8/1987	6512.96		-6512.96	-6512.96	
C(M)	10/7/1987	6513.57		-6513.57	-6513.57	
C(M)	1/11/1988	6513.84		-6513.84	-6513.84	
C(M)	4/5/1988	6513.47		-6513.47	-6513.47	
C(M)	7/11/1988	6513.44		-6513.44	-6513.44	
C(M)	10/6/1988	6514.22		-6514.22	-6514.22	
C(M)	1/18/1989	6514.36		-6514.36	-6514.36	
C(M)	4/17/1989	6513.35		-6513.35	-6513.35	
C(M)	4/9/1990	6511.72		-6511.72	-6511.72	
E(M)	4/12/1984	6546.44	6616.32	69.88	68.35	
E(M)	4/22/1986	6548.41	6616.32	67.91	66.38	
E(M)	10/13/1986	6547.72	6616.32	68.6	67.07	
E(M)	4/8/1987	6543.32	6616.32	73	71.47	
E(M)	10/8/1987	6543.66	6616.32	72.66	71.13	
E(M)	4/13/1988	6541.53	6616.32	74.79	73.26	
E(M)	6/14/1988	6540.8	6616.32	75.52	73.99	
E(M)	9/7/1988	6541.93	6616.32	74.39	72.86	
E(M)	10/6/1988	6541.94	6616.32	74.38	72.85	
E(M)	12/6/1988	6541.25	6616.32	75.07	73.54	
E(M)	3/7/1989	6540.25	6616.32	76.07	74.54	
E(M)	4/17/1989	6540.04	6616.32	76.28	74.75	
E(M)	6/15/1989	6439.72	6616.32	176.6	175.07	
E(M)	9/20/1989	6539.7	6616.32	76.62	75.09	
E(M)	12/18/1989	6539.13	6616.32	77.19	75.66	
E(M)	3/12/1990	6538.98	6616.32	77.34	75.81	
E(M)	4/9/1990	6538.88	6616.32	77.44	75.91	
E(M)	7/12/1990	6539.58	6616.32	76.74	75.21	
E(M)	9/18/1990	6538.43	6616.32	77.89	76.36	
E(M)	10/3/1990	6538.38	6616.32	77.94	76.41	
E(M)	12/18/1990	6538.18	6616.32	78.14	76.61	
E(M)	1/8/1991	6538.03	6616.32	78.29	76.76	
E(M)	4/3/1991	6537.67	6616.32	78.65	77.12	
E(M)	7/10/1991	6537.63	6616.32	78.69	77.16	
E(M)	10/3/1991	6537.12	6616.32	79.2	77.67	
E(M)	1/14/1992	6536.97	6616.32	79.35	77.82	
E(M)	4/14/1992	6537.27	6616.32	79.05	77.52	
E(M)	7/21/1992	6537.24	6616.32	79.08	77.55	
E(M)	10/6/1992	6537.46	6616.32	78.86	77.33	
E(M)	1/11/1993	6537.78	6616.32	78.54	77.01	
E(M)	4/5/1993	6538.04	6616.32	78.28	76.75	
E(M)	7/8/1993	6538.47	6616.32	77.85	76.32	
E(M)	10/5/1993	6538	6616.32	78.32	76.79	
E(M)	1/6/1994	6538.18	6616.32	78.14	76.61	
E(M)	4/12/1994	6538.43	6616.32	77.89	76.36	
E(M)	7/6/1994	6539.18	6616.32	77.14	75.61	
E(M)	10/6/1994	6541.9	6616.32	74.42	72.89	
E(M)	1/16/1995	6542.31	6616.32	74.01	72.48	

Table C.1-2. Water Level Data for Bluewater Site Alluvial Aquifer Wells

Well ID	Date	Water Elevation (ft amsl)	TOC Elevation (ft amsl)	Depth from Top of Casing (ft)	Depth from Surface (ft)	Comment
E(M)	4/10/1995	6541.11	6616.32	75.21	73.68	
E(M)	7/17/1995	6538.53	6616.32	77.79	76.26	
E(M)	10/23/1995	6538.16	6616.32	78.16	76.63	
E(M)	1/16/1996	6537.84	6616.32	78.48	76.95	
E(M)	4/3/1996	6537.43	6616.32	78.89	77.36	
E(M)	11/19/1997	6538.26	6616.32	78.06	76.53	
E(M)	11/14/1998	6537.41	6616.32	78.91	77.38	
E(M)	12/18/1998	6537.37	6616.32	78.95	77.42	
E(M)	11/11/1999	6537.36	6616.32	78.96	77.43	
E(M)	11/11/2000	6538.2	6616.32	78.12	76.59	
E(M)	11/3/2001	6537.97	6616.32	78.35	76.82	
E(M)	10/17/2002	6536.62	6616.32	79.7	78.17	
E(M)	9/19/2003	6536.23	6616.32	80.09	78.56	
E(M)	11/18/2004	6530.21	6616.32	86.11	84.58	
E(M)	11/15/2005	6535.67	6616.32	80.65	79.12	
E(M)	11/28/2006	6535.43	6616.32	80.89	79.36	
E(M)	11/6/2007	6535.37	6616.32	80.95	79.42	
E(M)	11/4/2008	6535.1	6616.32	81.22	79.69	
E(M)	5/13/2009	6535.16	6616.32	81.16	79.63	
E(M)	11/11/2009	6530.08	6616.32	86.24	84.71	
E(M)	11/11/2010	6534.88	6616.32	81.44	79.91	
E(M)	7/27/2011	6534.86	6616.32	81.46	79.93	
E(M)	11/16/2011	6534.86	6616.32	81.46	79.93	
E(M)	5/15/2012	6534.79	6616.32	81.53	80	
E(M)	11/14/2012	6534.84	6616.32	81.48	79.95	
E(M)	1/30/2013	6534.71	6616.32	81.61	80.08	
E(M)	5/14/2013	6534.77	6616.32	81.55	80.02	
E(M)	11/19/2013	6534.93	6616.32	81.39	79.86	
E(M)	4/30/2014	6534.63	6616.32	81.69	80.16	
Engineers	2/9/1984	6522.17		-6522.17	-6522.17	
Engineers	5/9/1984	6522.13		-6522.13	-6522.13	
Engineers	4/22/1986	6523.68		-6523.68	-6523.68	
Engineers	7/7/1986	6523.46		-6523.46	-6523.46	
Engineers	11/19/1986	6523.55		-6523.55	-6523.55	
Engineers	2/3/1987	6523.14		-6523.14	-6523.14	
Engineers	4/13/1987	6522.89		-6522.89	-6522.89	
Engineers	8/31/1987	6522.69		-6522.69	-6522.69	
Engineers	10/12/1987	6522.79		-6522.79	-6522.79	
Engineers	1/11/1988	6523.11		-6523.11	-6523.11	
Engineers	4/11/1988	6522.77		-6522.77	-6522.77	
Engineers	7/11/1988	6522.73		-6522.73	-6522.73	
Engineers	10/12/1988	6523.24		-6523.24	-6523.24	
Engineers	1/18/1989	6522.56		-6522.56	-6522.56	
F(M)	4/17/1984	6494.29	6603.59	109.3	107.93	
F(M)	4/17/1986	6496.19	6603.59	107.4	106.03	
F(M)	10/6/1986	6496.36	6603.59	107.23	105.86	
F(M)	4/6/1987	6495.88	6603.59	107.71	106.34	
F(M)	10/7/1987	6495.23	6603.59	108.36	106.99	
F(M)	4/6/1988	6495.88	6603.59	107.71	106.34	
F(M)	6/14/1988	6495	6603.59	108.59	107.22	
F(M)	9/7/1988	6494.71	6603.59	108.88	107.51	
F(M)	10/5/1988	6494.8	6603.59	108.79	107.42	
F(M)	12/6/1988	6494.77	6603.59	108.82	107.45	
F(M)	3/7/1989	6494.65	6603.59	108.94	107.57	
F(M)	4/11/1989	6494.59	6603.59	109	107.63	

Table C.1-2. Water Level Data for Bluewater Site Alluvial Aquifer Wells

Well ID	Date	Water Elevation (ft amsl)	TOC Elevation (ft amsl)	Depth from Top of Casing (ft)	Depth from Surface (ft)	Comment
F(M)	6/15/1989	6494.38	6603.59	109.21	107.84	
F(M)	9/20/1989	6494.38	6603.59	109.21	107.84	
F(M)	12/18/1989	6494.1	6603.59	109.49	108.12	
F(M)	3/12/1990	6493.63	6603.59	109.96	108.59	
F(M)	4/9/1990	6493.57	6603.59	110.02	108.65	
F(M)	5/23/1990	6493.36	6603.59	110.23	108.86	
F(M)	9/18/1990	6492.68	6603.59	110.91	109.54	
F(M)	10/2/1990	6492.71	6603.59	110.88	109.51	
F(M)	12/18/1990	6492.19	6603.59	111.4	110.03	
F(M)	1/8/1991	6492.11	6603.59	111.48	110.11	
F(M)	4/3/1991	6491.68	6603.59	111.91	110.54	
F(M)	7/9/1991	6491.27	6603.59	112.32	110.95	
F(M)	10/3/1991	6490.82	6603.59	112.77	111.4	
F(M)	1/15/1992	6490.61	6603.59	112.98	111.61	
F(M)	4/7/1992	6490.54	6603.59	113.05	111.68	
F(M)	7/21/1992	6490.37	6603.59	113.22	111.85	
F(M)	10/5/1992	6490.27	6603.59	113.32	111.95	
F(M)	1/11/1993	6490.25	6603.59	113.34	111.97	
F(M)	4/5/1993	6490.28	6603.59	113.31	111.94	
F(M)	7/6/1993	6490.32	6603.59	113.27	111.9	
F(M)	10/11/1993	6490.36	6603.59	113.23	111.86	
F(M)	1/4/1994	6490.55	6603.59	113.04	111.67	
F(M)	4/5/1994	6490.28	6603.59	113.31	111.94	
F(M)	7/7/1994	6490.92	6603.59	112.67	111.3	
F(M)	10/10/1994	6490.98	6603.59	112.61	111.24	
F(M)	1/17/1995	6491.58	6603.59	112.01	110.64	
F(M)	4/10/1995	6491.92	6603.59	111.67	110.3	
F(M)	7/18/1995	6492.03	6603.59	111.56	110.19	
F(M)	10/23/1995	6492.02	6603.59	111.57	110.2	
F(M)	1/15/1996	6492.38	6603.59	111.21	109.84	
F(M)	4/10/1996	6492.54	6603.59	111.05	109.68	
F(M)	11/19/1997	6493.87	6603.59	109.72	108.35	
F(M)	11/14/1998	6492.78	6603.59	110.81	109.44	
F(M)	12/18/1998	6492.76	6603.59	110.83	109.46	
F(M)	11/11/1999	6492.43	6603.59	111.16	109.79	
F(M)	11/11/2000	6492.23	6603.59	111.36	109.99	
F(M)	11/3/2001	6492.13	6603.59	111.46	110.09	
F(M)	10/17/2002	6491.59	6603.59	112	110.63	
F(M)	9/19/2003	6491.05	6603.59	112.54	111.17	
F(M)	9/26/2003	6491.05	6603.59	112.54	111.17	
F(M)	11/18/2004	6490.77	6603.59	112.82	111.45	
F(M)	5/24/2005	6490.54	6603.59	113.05	111.68	
F(M)	11/15/2005	6490.45	6603.59	113.14	111.77	
F(M)	11/28/2006	6490.26	6603.59	113.33	111.96	
F(M)	11/6/2007	6490.24	6603.59	113.35	111.98	
F(M)	11/4/2008	6490.1	6603.59	113.49	112.12	
F(M)	5/13/2009	6490.2	6603.59	113.39	112.02	
F(M)	11/10/2009	6490.18	6603.59	113.41	112.04	
F(M)	11/10/2010	6490.15	6603.59	113.44	112.07	
F(M)	7/28/2011	6490.12	6603.59	113.47	112.1	
F(M)	11/15/2011	6490.29	6603.59	113.3	111.93	
F(M)	5/15/2012	6490.09	6603.59	113.5	112.13	
F(M)	11/14/2012	6490.17	6603.59	113.42	112.05	
F(M)	1/30/2013	6490.11	6603.59	113.48	112.11	
F(M)	5/14/2013	6489.33	6603.59	114.26	112.89	

Table C.1-2. Water Level Data for Bluewater Site Alluvial Aquifer Wells

Well ID	Date	Water Elevation (ft amsl)	TOC Elevation (ft amsl)	Depth from Top of Casing (ft)	Depth from Surface (ft)	Comment
F(M)	11/19/2013	6490.24	6603.59	113.35	111.98	
F(M)	4/30/2014	6490.14	6603.59	113.45	112.08	
K(M)	5/16/1984	6549.14		-6549.14	-6549.14	
K(M)	4/22/1986	6546.58		-6546.58	-6546.58	
K(M)	10/13/1986	6545.97		-6545.97	-6545.97	
K(M)	4/9/1987	6545.4		-6545.4	-6545.4	
K(M)	10/8/1987	6544.18		-6544.18	-6544.18	
K(M)	4/11/1988	6543.44		-6543.44	-6543.44	
K(M)	10/11/1988	6543.03		-6543.03	-6543.03	
K(M)	4/20/1989	6542.39		-6542.39	-6542.39	
K(M)	4/12/1990	6541.25		-6541.25	-6541.25	
SIMPSON	4/18/1989	6482.23		-6482.23	-6482.23	
SIMPSON	4/12/1990	6478.59		-6478.59	-6478.59	
T(M)	4/17/1984	6492.52	6612.65	120.13	119.58	
T(M)	4/17/1986	6494.88	6612.65	117.77	117.22	
T(M)	10/13/1986	6495.02	6612.65	117.63	117.08	
T(M)	4/6/1987	6494.15	6612.65	118.5	117.95	
T(M)	10/7/1987	6494.35	6612.65	118.3	117.75	
T(M)	4/6/1988	6494.11	6612.65	118.54	117.99	
T(M)	6/14/1988	6493.85	6612.65	118.8	118.25	
T(M)	9/7/1988	6494.8	6612.65	117.85	117.3	
T(M)	10/6/1988	6494.83	6612.65	117.82	117.27	
T(M)	12/6/1988	6494.92	6612.65	117.73	117.18	
T(M)	3/7/1989	6494.42	6612.65	118.23	117.68	
T(M)	4/17/1989	6494.2	6612.65	118.45	117.9	
T(M)	6/15/1989	6493.72	6612.65	118.93	118.38	
T(M)	9/20/1989	6493.59	6612.65	119.06	118.51	
T(M)	12/18/1989	6486.83	6612.65	125.82	125.27	
T(M)	3/14/1990	6492.32	6612.65	120.33	119.78	
T(M)	4/10/1990	6491.88	6612.65	120.77	120.22	
T(M)	5/24/1990	6491.58	6612.65	121.07	120.52	
T(M)	7/11/1990	6490.75	6612.65	121.9	121.35	
T(M)	9/18/1990	6489.95	6612.65	122.7	122.15	
T(M)	10/1/1990	6490.02	6612.65	122.63	122.08	
T(M)	12/18/1990	6489.4	6612.65	123.25	122.7	
T(M)	1/9/1991	6489.17	6612.65	123.48	122.93	
T(M)	4/2/1991	6488.38	6612.65	124.27	123.72	
T(M)	7/10/1991	6487.38	6612.65	125.27	124.72	
T(M)	10/2/1991	6487.3	6612.65	125.35	124.8	
T(M)	1/16/1992	6487.26	6612.65	125.39	124.84	
T(M)	4/6/1992	6486.89	6612.65	125.76	125.21	
T(M)	7/20/1992	6486.03	6612.65	126.62	126.07	
T(M)	10/8/1992	6486.35	6612.65	126.3	125.75	
T(M)	1/12/1993	6486.43	6612.65	126.22	125.67	
T(M)	4/6/1993	6486.27	6612.65	126.38	125.83	
T(M)	7/7/1993	6485.96	6612.65	126.69	126.14	
T(M)	10/13/1993	6487.29	6612.65	125.36	124.81	
T(M)	1/5/1994	6487.55	6612.65	125.1	124.55	
T(M)	4/6/1994	6486.27	6612.65	126.38	125.83	
T(M)	7/6/1994	6489.17	6612.65	123.48	122.93	
T(M)	10/18/1994	6490.74	6612.65	121.91	121.36	
T(M)	1/17/1995	6491.93	6612.65	120.72	120.17	
T(M)	4/10/1995	6491.41	6612.65	121.24	120.69	
T(M)	7/17/1995	6491.26	6612.65	121.39	120.84	
T(M)	10/16/1995	6492.23	6612.65	120.42	119.87	

Table C.1-2. Water Level Data for Bluewater Site Alluvial Aquifer Wells

Well ID	Date	Water Elevation (ft amsl)	TOC Elevation (ft amsl)	Depth from Top of Casing (ft)	Depth from Surface (ft)	Comment
T(M)	1/15/1996	6492.43	6612.65	120.22	119.67	
T(M)	4/6/1996	6492.03	6612.65	120.62	120.07	
T(M)	11/19/1997	6489.54	6612.65	123.11	122.56	
T(M)	11/16/1998		6612.65			
T(M)	11/11/1999	6487.79	6612.65	124.86	124.31	
T(M)	11/11/2000	6487.71	6612.65	124.94	124.39	
T(M)	11/3/2001		6612.65			
T(M)	10/17/2002		6612.65			
T(M)	11/18/2004	6480.06	6612.65	132.59	132.04	
T(M)	5/24/2005	6479.89	6612.65	132.76	132.21	
T(M)	11/15/2005	6479.7	6612.65	132.95	132.4	
T(M)	11/28/2006	6479.34	6612.65	133.31	132.76	
T(M)	11/4/2008	6478.96	6612.65	133.69	133.14	
T(M)	5/13/2009	6478.87	6612.65	133.78	133.23	
T(M)	10/27/2009	6478.77	6612.65	133.88	133.33	
T(M)	11/10/2009	6478.94	6612.65	133.71	133.16	
T(M)	11/9/2010	6478.83	6612.65	133.82	133.27	
T(M)	4/12/2011	6478.74	6612.65	133.91	133.36	
T(M)	7/26/2011	6478.72	6612.65	133.93	133.38	
T(M)	11/16/2011	6478.76	6612.65	133.89	133.34	
T(M)	5/15/2012	6478.57	6612.65	134.08	133.53	
T(M)	11/13/2012		6612.65			Dry
T(M)	5/14/2013		6612.65			Dry
T(M)	11/19/2013		6612.65			Dry
U(M)	3/12/1984	6485.83		-6485.83	-6485.83	
U(M)	4/17/1984	6485.76		-6485.76	-6485.76	
U(M)	4/17/1986	6488.64		-6488.64	-6488.64	
U(M)	7/7/1986	6488.67		-6488.67	-6488.67	
U(M)	10/13/1986	6488.77		-6488.77	-6488.77	
U(M)	2/3/1987	6488.61		-6488.61	-6488.61	
U(M)	4/8/1987	6488.5		-6488.5	-6488.5	
U(M)	7/7/1987	6488.22		-6488.22	-6488.22	
U(M)	10/7/1987	6488.38		-6488.38	-6488.38	
U(M)	1/11/1988	6488.72		-6488.72	-6488.72	
U(M)	4/6/1988	6488.21		-6488.21	-6488.21	
U(M)	7/11/1988	6487.99		-6487.99	-6487.99	
U(M)	10/5/1988	6488.46		-6488.46	-6488.46	
U(M)	1/18/1989	6488.49		-6488.49	-6488.49	
U(M)	4/11/1989	6488.08		-6488.08	-6488.08	
U(M)	4/9/1990	6486.53		-6486.53	-6486.53	
X(M)	3/12/1984	6478.33	6598.91	120.58	118.71	
X(M)	4/17/1984	6477.29	6598.91	121.62	119.75	
X(M)	4/17/1986	6481.86	6598.91	117.05	115.18	
X(M)	7/7/1986	6482.14	6598.91	116.77	114.9	
X(M)	10/6/1986	6482.7	6598.91	116.21	114.34	
X(M)	2/3/1987	6482.07	6598.91	116.84	114.97	
X(M)	4/8/1987	6481.96	6598.91	116.95	115.08	
X(M)	7/7/1987	6481.63	6598.91	117.28	115.41	
X(M)	10/5/1987	6482.03	6598.91	116.88	115.01	
X(M)	1/11/1988	6482.26	6598.91	116.65	114.78	
X(M)	4/6/1988	6481.66	6598.91	117.25	115.38	
X(M)	7/11/1988	6481.49	6598.91	117.42	115.55	
X(M)	10/5/1988	6482.01	6598.91	116.9	115.03	
X(M)	1/18/1989	6481.96	6598.91	116.95	115.08	
X(M)	4/17/1989	6481.57	6598.91	117.34	115.47	

Table C.1-2. Water Level Data for Bluewater Site Alluvial Aquifer Wells

Well ID	Date	Water Elevation (ft amsl)	TOC Elevation (ft amsl)	Depth from Top of Casing (ft)	Depth from Surface (ft)	Comment
X(M)	4/11/1990	6479.67	6598.91	119.24	117.37	
X(M)	11/9/2010		6598.91			Dry
X(M)	7/28/2011		6598.91			Dry
X(M)	11/15/2011		6598.91			Dry
X(M)	5/15/2012		6598.91			Dry
X(M)	11/15/2012	6467.17	6598.91	131.74	129.87	
X(M)	1/29/2013	6467.2	6598.91	131.71	129.84	
X(M)	5/15/2013		6598.91			Dry
X(M)	11/19/2013	6466.89	6598.91	132.02	130.15	
X(M)	4/29/2014	6466.76	6598.91	132.15	130.28	
Y2(M)	11/19/1997	6506.23	6614.13	107.9	105.73	
Y2(M)	11/16/1998		6614.13			
Y2(M)	11/11/1999	6501.67	6614.13	112.46	110.29	
Y2(M)	11/11/2000	6501.55	6614.13	112.58	110.41	
Y2(M)	11/3/2001	6499.95	6614.13	114.18	112.01	
Y2(M)	10/17/2002	6498.54	6614.13	115.59	113.42	
Y2(M)	9/19/2003	6497.35	6614.13	116.78	114.61	
Y2(M)	9/26/2003	6497.65	6614.13	116.48	114.31	
Y2(M)	11/18/2004	6497.08	6614.13	117.05	114.88	
Y2(M)	11/15/2005	6496.77	6614.13	117.36	115.19	
Y2(M)	11/28/2006	6496.55	6614.13	117.58	115.41	
Y2(M)	11/6/2007	6488.13	6614.13	126	123.83	
Y2(M)	11/4/2008	6496.81	6614.13	117.32	115.15	
Y2(M)	5/13/2009	6496.83	6614.13	117.3	115.13	
Y2(M)	11/10/2009	6496.92	6614.13	117.21	115.04	
Y2(M)	11/11/2010	6496.65	6614.13	117.48	115.31	
Y2(M)	7/28/2011	6496.62	6614.13	117.51	115.34	
Y2(M)	11/15/2011	6496.79	6614.13	117.34	115.17	
Y2(M)	5/15/2012	6496.7	6614.13	117.43	115.26	
Y2(M)	11/14/2012	6496.79	6614.13	117.34	115.17	
Y2(M)	1/30/2013	6496.74	6614.13	117.39	115.22	
Y2(M)	5/14/2013	6496.88	6614.13	117.25	115.08	
Y2(M)	11/19/2013	6496.93	6614.13	117.2	115.03	
Y2(M)	4/30/2014	6496.79	6614.13	117.34	115.17	

This page intentionally left blank

Table C.1-3. Water Level Data for Homestake Site and Distal San Andres Aquifer Wells

Well ID	Date	Water Elevation (ft amsl)	Water Level (ft-MP)	MP Elevation (ft amsl)	Data Source
#1 Deepwell	5/13/2003	6441.701	142.06	6583.76	HMC 2004
#1 Deepwell	12/20/2004	6435.58	148.18	6583.76	HMC 2005
#1 Deepwell	5/4/2005	6391.06	192.7	6583.76	HMC 2006
#1 Deepwell	12/1/2005	6388.16	195.6	6583.76	HMC 2006
#1 Deepwell	2/26/2007	6480.76	103	6583.76	HMC 2008
#1 Deepwell	11/13/2007	6485.16	98.6	6583.76	HMC 2008
#1 Deepwell	12/12/2007	6484.68	99.08	6583.76	HMC 2008
#2 Deepwell	5/5/1998	6411.16	164.5	6575.66	HMC 1999
#2 Deepwell	2/3/1999	6407.66	168	6575.66	HMC 2000
#2 Deepwell	2/1/2000	6458.06	117.6	6575.66	HMC 2001
#2 Deepwell	5/2/2001	6397.8	177.86	6575.66	HMC 2002
#2 Deepwell	5/13/2003	6441.6	134.06	6575.66	HMC 2004
#2 Deepwell	5/4/2005	6366.86	208.8	6575.66	HMC 2006
#2 Deepwell	12/12/2009	6423.4	152.26	6575.66	HMC electronic
#2 Deepwell	11/4/2013	6368.55	207.11	6575.66	HMC 2014
534	4/12/2001	6462.81	89.76	6552.57	HMC 2002
534	12/11/2001	6458.78	93.79	6552.57	HMC 2002
534	12/18/2002	6453.67	98.9	6552.57	HMC 2003
534	12/23/2003	6449.47	103.1	6552.57	HMC 2004
534	12/14/2004	6445.87	106.7	6552.57	HMC 2005
534	12/4/2008	6434.45	118.12	6552.57	HMC 2009
534	12/16/2010	6432.56	120.01	6552.57	HMC 2011
535	4/12/2001	6454.76	85.24	6540	HMC 2002
535	12/11/2001	6449.51	90.49	6540	HMC 2002
535	12/18/2002	6444.12	95.88	6540	HMC 2003
535	12/23/2003	6409.9	130.1	6540	HMC 2004
535	12/14/2004	6436.32	103.68	6540	HMC 2005
535	11/13/2007	6429.03	110.97	6540	HMC 2008
535	12/4/2008	6425.2	114.8	6540	HMC 2009
535	12/17/2010	6422.15	117.85	6540	HMC 2011
822	2/13/2008	6432.4	135.6	6568	HMC 2009
907	4/12/2001	6457.9	87.7	6545.6	HMC 2002
907	12/11/2001	6452.52	93.08	6545.6	HMC 2002
907	3/4/2002	6451.94	93.66	6545.6	HMC 2003
907	10/17/2002	6445.4	100.2	6545.6	HMC 2003
907	12/18/2002	6447.5	98.1	6545.6	HMC 2003
907	6/3/2003	6444	101.6	6545.6	HMC 2004
907	10/27/2003	6442.32	103.28	6545.6	HMC 2004
907	12/23/2003	6443.22	102.38	6545.6	HMC 2004
907	3/3/2004	6443.6	102	6545.6	HMC 2005
907	12/14/2004	6439.42	106.18	6545.6	HMC 2005
907	12/14/2004	6439.36	106.24	6545.6	HMC 2005
907	4/12/2005	6438.16	107.44	6545.6	HMC 2006
907	12/1/2005	6437.3	108.3	6545.6	HMC 2006
907	3/16/2006	6435.6	110	6545.6	HMC 2007
907	12/20/2006	6435.7	109.9	6545.6	HMC 2007
907	3/9/2007	6435.1	110.5	6545.6	HMC 2008
907	11/13/2007	6432.37	113.23	6545.6	HMC 2008
907	3/5/2008	6432.44	113.16	6545.6	HMC 2009
907	12/4/2008	6428.7	116.9	6545.6	HMC 2009
907	3/3/2010	6425.97	119.63	6545.6	HMC 2011
907	12/15/2010	6426.9	118.7	6545.6	HMC 2011
907	4/13/2011	6425.7	119.9	6545.6	HMC 2012
907	5/9/2012	6424.6	121	6545.6	HMC 2013

Table C.1-3. Water Level Data for Homestake Site and Distal San Andres Aquifer Wells

Well ID	Date	Water Elevation (ft amsl)	Water Level (ft-MP)	MP Elevation (ft amsl)	Data Source
907	11/20/2012	6418.181	127.42	6545.6	HMC 2013
907	12/11/2013	6423.85	121.75	6545.6	HMC 2014
928	8/27/1998	6462.2	135.4	6597.6	HMC 1999
928	8/9/2000	6458.66	138.94	6597.6	HMC 2001
928	8/29/2001	6453.46	144.14	6597.6	HMC 2002
928	12/11/2001	6451.06	146.54	6597.6	HMC 2002
928	3/4/2002	6452.03	145.57	6597.6	HMC 2003
928	10/21/2002	6444.8	152.8	6597.6	HMC 2003
928	12/18/2002	6445.9	151.7	6597.6	HMC 2003
928	6/3/2003	6443.12	154.48	6597.6	HMC 2004
928	10/27/2003	6440.86	156.74	6597.6	HMC 2004
928	12/23/2003	6442.45	155.15	6597.6	HMC 2004
928	3/3/2004	6442.85	154.75	6597.6	HMC 2005
928	12/9/2004	6438.8	158.8	6597.6	HMC 2005
928	12/14/2004	6438.72	158.88	6597.6	HMC 2005
928	4/12/2005	6438.33	159.27	6597.6	HMC 2006
928	12/1/2005	6436.7	160.9	6597.6	HMC 2006
928	12/5/2005	6436.8	160.8	6597.6	HMC 2006
928	3/16/2006	6436.12	161.48	6597.6	HMC 2007
928	12/10/2006	6434.7	162.9	6597.6	HMC 2007
928	12/20/2006	6434.81	162.79	6597.6	HMC 2007
928	3/9/2007	6435.7	161.9	6597.6	HMC 2008
928	11/13/2007	6432.24	165.36	6597.6	HMC 2008
928	12/3/2007	6432.04	165.56	6597.6	HMC 2008
928	3/5/2008	6433.20	164.40	6597.6	HMC 2009
928	9/17/2008	6425.67	171.93	6597.6	HMC 2009
928	12/4/2008	6442.45	155.15	6597.6	HMC 2009
928	12/22/2008	6428.30	169.30	6597.6	HMC 2009
928	3/20/2009	6427.84	169.76	6597.6	HMC electronic
928	10/12/2009	6457.80	139.80	6597.6	HMC electronic
928	12/7/2009	6427.89	169.71	6597.6	HMC electronic
928	12/9/2009	6427.49	170.11	6597.6	HMC electronic
928	3/3/2010	6428.60	169.00	6597.6	HMC 2011
928	5/3/2010	6430.16	167.44	6597.6	HMC 2011
928	6/14/2010	6423.60	174.00	6597.6	HMC 2011
928	12/6/2010	6455.32	142.28	6597.6	HMC 2011
928	12/16/2010	6432.70	164.90	6597.6	HMC 2011
928	4/13/2011	6441.25	156.35	6597.6	HMC 2012
928	11/11/2011	6455.73	141.87	6597.6	HMC 2012
928	12/6/2011	6447.85	149.75	6597.6	HMC 2012
928	5/30/2012	6459.04	138.56	6597.6	HMC 2013
928	11/14/2012	6463.22	134.38	6597.6	HMC 2013
928	12/11/2013	6467.85	129.75	6597.6	HMC 2014
938	4/12/2001	6458.39	110.41	6568.8	HMC 2002
938	12/11/2001	6453.06	115.74	6568.8	HMC 2002
938	3/4/2002	6452.36	116.44	6568.8	HMC 2003
938	10/17/2002	6445.96	122.84	6568.8	HMC 2003
938	12/18/2002	6447.85	120.95	6568.8	HMC 2003
938	6/3/2003	6443.97	124.83	6568.8	HMC 2004
938	10/27/2003	6442.4	126.4	6568.8	HMC 2004
938	12/23/2003	6443.57	125.23	6568.8	HMC 2004
938	3/4/2004	6443.70	125.10	6568.8	HMC 2005
938	12/14/2004	6439.27	129.53	6568.8	HMC 2005
938	4/12/2005	6438.42	130.38	6568.8	HMC 2006

Table C.1-3. Water Level Data for Homestake Site and Distal San Andres Aquifer Wells

Well ID	Date	Water Elevation (ft amsl)	Water Level (ft-MP)	MP Elevation (ft amsl)	Data Source
938	12/5/2005	6437.69	131.11	6568.8	HMC 2006
938	3/16/2006	6435.80	133.00	6568.8	HMC 2007
938	12/20/2006	6434.89	133.91	6568.8	HMC 2007
938	3/9/2007	6435.80	133.00	6568.8	HMC 2008
938	12/14/2007	6432.30	136.50	6568.8	HMC 2008
938	3/5/2008	6432.50	136.30	6568.8	HMC 2009
938	12/5/2008	6428.34	140.46	6568.8	HMC 2009
938	12/17/2008	6432.30	136.50	6568.8	HMC 2009
938	3/3/2010	6426.17	142.63	6568.8	HMC 2011
938	12/16/2010	6426.91	141.89	6568.8	HMC 2011
938	4/13/2011	6425.92	142.88	6568.8	HMC 2012
938	10/18/2011	6423.62	145.18	6568.8	HMC 2012
938	10/24/2012	6421.04	147.76	6568.8	HMC 2013
938	11/20/2012	6550.20	18.60	6568.8	HMC 2013
938	12/11/2013	6421.15	147.65	6568.8	HMC 2014
943	8/18/1998	6489.11	66.80	6555.91	HMC 1999
943	9/21/1999	6492.71	63.20	6555.91	HMC 2000
943	8/23/2000	6494.98	60.93	6555.91	HMC 2001
943	8/29/2001	6487.91	68.00	6555.91	HMC 2002
943	12/11/2001	6483.91	72.00	6555.91	HMC 2002
943	11/13/2002	6477.91	78.00	6555.91	HMC 2003
943	12/18/2002	6477.51	78.40	6555.91	HMC 2003
943	10/27/2003	6475.93	79.98	6555.91	HMC 2004
943	12/23/2003	6477.03	78.88	6555.91	HMC 2004
943	3/1/2004	6437.27	118.64	6555.91	HMC 2005
943	3/9/2004	6437.41	118.50	6555.91	HMC 2005
943	3/29/2004	6435.76	120.15	6555.91	HMC 2005
943	5/3/2004	6435.13	120.78	6555.91	HMC 2005
943	6/1/2004	6434.29	121.62	6555.91	HMC 2005
943	6/28/2004	6433.01	122.90	6555.91	HMC 2005
943	7/23/2004	6431.81	124.10	6555.91	HMC 2005
943	8/2/2004	6430.43	125.48	6555.91	HMC 2005
943	8/30/2004	6430.21	125.70	6555.91	HMC 2005
943	10/4/2004	6430.33	125.58	6555.91	HMC 2005
943	11/1/2004	6431.37	124.54	6555.91	HMC 2005
943	11/29/2004	6431.40	124.51	6555.91	HMC 2005
943	12/8/2004	6432.17	123.74	6555.91	HMC 2005
943	1/4/2005	6432.69	123.22	6555.91	HMC 2006
943	1/31/2005	6431.73	124.18	6555.91	HMC 2006
943	2/28/2005	6435.81	120.10	6555.91	HMC 2006
943	4/4/2005	6432.26	123.65	6555.91	HMC 2006
943	4/19/2005	6432.41	123.50	6555.91	HMC 2006
943	5/2/2005	6431.08	124.83	6555.91	HMC 2006
943	5/31/2005	6430.96	124.95	6555.91	HMC 2006
943	7/5/2005	6430.61	125.30	6555.91	HMC 2006
943	8/1/2005	6375.91	180.00	6555.91	HMC 2006
943	8/29/2005	6431.81	124.10	6555.91	HMC 2006
943	10/3/2005	6431.66	124.25	6555.91	HMC 2006
943	10/31/2005	6431.41	124.50	6555.91	HMC 2006
943	11/28/2005	6432.05	123.86	6555.91	HMC 2006
943	12/5/2005	6432.08	123.83	6555.91	HMC 2006
943	1/3/2006	6431.31	124.60	6555.91	HMC 2006
943	1/3/2006	6431.31	124.60	6555.91	HMC 2007
943	1/30/2006	6430.91	125.00	6555.91	HMC 2007

Table C.1-3. Water Level Data for Homestake Site and Distal San Andres Aquifer Wells

Well ID	Date	Water Elevation (ft amsl)	Water Level (ft-MP)	MP Elevation (ft amsl)	Data Source
943	2/27/2006	6433.61	122.30	6555.91	HMC 2007
943	3/16/2006	6431.29	124.62	6555.91	HMC 2007
943	4/3/2006	6430.41	125.50	6555.91	HMC 2007
943	5/1/2006	6432.71	123.20	6555.91	HMC 2007
943	5/30/2006	6430.46	125.45	6555.91	HMC 2007
943	6/26/2006	6430.41	125.50	6555.91	HMC 2007
943	7/31/2006	6431.79	124.12	6555.91	HMC 2007
943	8/28/2006	6430.40	125.51	6555.91	HMC 2007
943	9/25/2006	6431.36	124.55	6555.91	HMC 2007
943	10/30/2006	6431.81	124.10	6555.91	HMC 2007
943	11/27/2006	6433.61	122.30	6555.91	HMC 2007
943	1/29/2007	6430.46	125.45	6555.91	HMC 2008
943	2/26/2007	6430.49	125.42	6555.91	HMC 2008
943	3/8/2007	6430.66	125.25	6555.91	HMC 2008
943	4/2/2007	6429.51	126.40	6555.91	HMC 2008
943	4/30/2007	6428.54	127.37	6555.91	HMC 2008
943	5/29/2007	6427.31	128.60	6555.91	HMC 2008
943	7/2/2007	6427.11	128.80	6555.91	HMC 2008
943	7/30/2007	6426.89	129.02	6555.91	HMC 2008
943	9/4/2007	6426.41	129.50	6555.91	HMC 2008
943	10/1/2007	6425.61	130.30	6555.91	HMC 2008
943	10/29/2007	6425.31	130.60	6555.91	HMC 2008
943	12/3/2007	6425.74	130.17	6555.91	HMC 2008
943	1/2/2008	6426.71	129.2	6555.91	HMC 2009
943	2/4/2008	6426.12	129.79	6555.91	HMC 2009
943	3/3/2008	6427.08	128.83	6555.91	HMC 2009
943	3/5/2008	6427.27	128.64	6555.91	HMC 2009
943	3/31/2008	6426.21	129.7	6555.91	HMC 2009
943	5/5/2008	6424.81	131.1	6555.91	HMC 2009
943	6/2/2008	6424.31	131.6	6555.91	HMC 2009
943	6/30/2008	6423.06	132.85	6555.91	HMC 2009
943	8/4/2008	6422.31	133.6	6555.91	HMC 2009
943	9/29/2008	6424.81	131.1	6555.91	HMC 2009
943	10/27/2008	6362.31	193.6	6555.91	HMC 2009
943	12/1/2008	6422.61	133.3	6555.91	HMC 2009
943	12/1/2008	6417.11	138.8	6555.91	HMC 2009
943	12/29/2008	6422.61	133.3	6555.91	HMC 2009
943	2/2/2009	6422.51	133.4	6555.91	HMC electronic
943	3/2/2009	6421.39	134.52	6555.91	HMC electronic
943	3/20/2009	6424.03	131.88	6555.91	HMC electronic
943	3/30/2009	6424.71	131.2	6555.91	HMC electronic
943	4/7/2009	6424.87	131.04	6555.91	HMC electronic
943	5/4/2009	6388.61	167.3	6555.91	HMC electronic
943	6/1/2009	6421.56	134.35	6555.91	HMC electronic
943	6/15/2009	6421.47	134.44	6555.91	HMC electronic
943	6/29/2009	6421.51	134.4	6555.91	HMC electronic
943	8/3/2009	6423.11	132.8	6555.91	HMC electronic
943	8/31/2009	6419.6	136.31	6555.91	HMC electronic
943	9/28/2009	6419.96	135.95	6555.91	HMC electronic
943	11/2/2009	6420.56	135.35	6555.91	HMC electronic
943	11/30/2009	6421.65	134.26	6555.91	HMC electronic
943	12/7/2009	6421.78	134.13	6555.91	HMC electronic
943	12/28/2009	6421.31	134.6	6555.91	HMC electronic
943	2/1/2010	6421.45	134.46	6555.91	HMC 2011

Table C.1-3. Water Level Data for Homestake Site and Distal San Andres Aquifer Wells

Well ID	Date	Water Elevation (ft amsl)	Water Level (ft-MP)	MP Elevation (ft amsl)	Data Source
943	3/1/2010	6421.39	134.52	6555.91	HMC 2011
943	3/3/2010	6421.08	134.83	6555.91	HMC 2011
943	3/29/2010	6423.18	132.73	6555.91	HMC 2011
943	5/3/2010	6421.63	134.28	6555.91	HMC 2011
943	6/1/2010	6420.61	135.3	6555.91	HMC 2011
943	6/22/2010	6421.91	134	6555.91	HMC 2011
943	6/28/2010	6420.36	135.55	6555.91	HMC 2011
943	8/2/2010	6409.31	146.6	6555.91	HMC 2011
943	8/30/2010	6418.91	137	6555.91	HMC 2011
943	9/7/2010	6421.61	134.3	6555.91	HMC 2011
943	9/13/2010	6421.41	134.5	6555.91	HMC 2011
943	9/20/2010	6417.46	138.45	6555.91	HMC 2011
943	9/27/2010	6418.01	137.9	6555.91	HMC 2011
943	10/4/2010	6421.56	134.35	6555.91	HMC 2011
943	10/11/2010	6422.16	133.75	6555.91	HMC 2011
943	10/18/2010	6418.91	137	6555.91	HMC 2011
943	10/25/2010	6419.71	136.2	6555.91	HMC 2011
943	10/27/2010	6419.37	136.54	6555.91	HMC 2011
943	11/1/2010	6419.61	136.3	6555.91	HMC 2011
943	11/8/2010	6418.17	137.74	6555.91	HMC 2011
943	11/15/2010	6420.21	135.7	6555.91	HMC 2011
943	11/29/2010	6420.36	135.55	6555.91	HMC 2011
943	12/6/2010	6420.63	135.28	6555.91	HMC 2011
943	12/27/2010	6420.63	135.28	6555.91	HMC 2011
943	1/31/2011	6420.51	135.4	6555.91	HMC 2012
943	2/28/2011	6420.01	135.9	6555.91	HMC 2012
943	4/4/2011	6419.93	135.98	6555.91	HMC 2012
943	4/13/2011	6420.03	135.88	6555.91	HMC 2012
943	4/25/2011	6419.91	136	6555.91	HMC 2012
943	5/23/2011	6422.27	133.64	6555.91	HMC 2012
943	6/27/2011	6421.01	134.9	6555.91	HMC 2012
943	7/25/2011	6420.5	135.41	6555.91	HMC 2012
943	8/29/2011	6416.01	139.9	6555.91	HMC 2012
943	9/26/2011	6416.31	139.6	6555.91	HMC 2012
943	10/24/2011	6415.51	140.4	6555.91	HMC 2012
943	11/7/2011	6416.61	139.3	6555.91	HMC 2012
943	11/21/2011	6415.91	140	6555.91	HMC 2012
943	12/19/2011	6421.21	134.7	6555.91	HMC 2012
943	1/23/2012	6421.61	134.3	6555.91	HMC 2013
943	2/27/2012	6422.43	133.48	6555.91	HMC 2013
943	3/26/2012	6417.11	138.8	6555.91	HMC 2013
943	4/23/2012	6409.01	146.9	6555.91	HMC 2013
943	5/9/2012	6421.81	134.1	6555.91	HMC 2013
943	5/29/2012	6397.11	158.8	6555.91	HMC 2013
943	6/25/2012	6414.33	141.58	6555.91	HMC 2013
943	7/23/2012	6420.09	135.82	6555.91	HMC 2013
943	9/24/2012	6414.14	141.77	6555.91	HMC 2013
943	10/22/2012	6415.61	140.3	6555.91	HMC 2013
943	11/26/2012	6419.76	136.15	6555.91	HMC 2013
943	12/6/2012	6419.76	136.15	6555.91	HMC 2013
943	1/28/2013	6419.41	136.5	6555.91	HMC 2014
943	2/25/2013	6419.23	136.68	6555.91	HMC 2014
943	3/6/2013	6419.11	136.8	6555.91	HMC 2014
943	3/25/2013	6418.41	137.5	6555.91	HMC 2014

Table C.1-3. Water Level Data for Homestake Site and Distal San Andres Aquifer Wells

Well ID	Date	Water Elevation (ft amsl)	Water Level (ft-MP)	MP Elevation (ft amsl)	Data Source
943	4/29/2013	6413.11	142.8	6555.91	HMC 2014
943	5/28/2013	6412.86	143.05	6555.91	HMC 2014
943	6/24/2013	6411.93	143.98	6555.91	HMC 2014
949	2/13/2008	6431.7	130.6	6562.3	HMC 2009
951	8/18/1998	6464.9	108.8	6573.7	HMC 1999
951	8/30/1999	6462.85	110.85	6573.7	HMC 2000
951	9/7/1999	6462.77	110.93	6573.7	HMC 2000
951	10/5/1999	6462.91	110.79	6573.7	HMC 2000
951	11/1/1999	6463.78	109.92	6573.7	HMC 2000
951	11/29/1999	6466.09	107.61	6573.7	HMC 2000
951	1/3/2000	6463.82	109.88	6573.7	HMC 2001
951	1/31/2000	6462.72	110.98	6573.7	HMC 2001
951	3/6/2000	6464.1	109.6	6573.7	HMC 2001
951	4/3/2000	6463.45	110.25	6573.7	HMC 2001
951	5/2/2000	6463.5	110.2	6573.7	HMC 2001
951	8/9/2000	6458.7	115	6573.7	HMC 2001
951	4/12/2001	6457.76	115.94	6573.7	HMC 2002
951	12/11/2001	6452.38	121.32	6573.7	HMC 2002
951	3/4/2002	6447.74	125.96	6573.7	HMC 2003
951	4/1/2002	6450.94	122.76	6573.7	HMC 2003
951	4/29/2002	6445.2	128.5	6573.7	HMC 2003
951	6/4/2002	6443.58	130.12	6573.7	HMC 2003
951	7/1/2002	6442.22	131.48	6573.7	HMC 2003
951	8/5/2002	6441.09	132.61	6573.7	HMC 2003
951	9/3/2002	6440.82	132.88	6573.7	HMC 2003
951	9/30/2002	6440.92	132.78	6573.7	HMC 2003
951	10/17/2002	6441.34	132.36	6573.7	HMC 2003
951	11/5/2002	6442.65	131.05	6573.7	HMC 2003
951	12/2/2002	6442.85	130.85	6573.7	HMC 2003
951	12/18/2002	6443.16	130.54	6573.7	HMC 2003
951	12/30/2002	6443.19	130.51	6573.7	HMC 2003
951	2/3/2003	6442.38	131.32	6573.7	HMC 2004
951	3/3/2003	6442.42	131.28	6573.7	HMC 2004
951	3/31/2003	6440.9	132.8	6573.7	HMC 2004
951	5/5/2003	6439.09	134.61	6573.7	HMC 2004
951	6/30/2003	6386.26	187.44	6573.7	HMC 2004
951	8/2/2003	6389	184.7	6573.7	HMC 2004
951	8/14/2003	6437.6	136.1	6573.7	HMC 2004
951	9/2/2003	6436.1	137.6	6573.7	HMC 2004
951	9/29/2003	6437.25	136.45	6573.7	HMC 2004
951	10/27/2003	6437.89	135.81	6573.7	HMC 2004
951	11/3/2003	6438.2	135.5	6573.7	HMC 2004
951	12/1/2003	6389	184.7	6573.7	HMC 2004
951	12/29/2003	6403.3	170.4	6573.7	HMC 2004
951	2/2/2004	6438.39	135.31	6573.7	HMC 2005
951	3/1/2004	6438.92	134.78	6573.7	HMC 2005
951	3/29/2004	6437.15	136.55	6573.7	HMC 2005
951	5/3/2004	6435.76	137.94	6573.7	HMC 2005
951	6/1/2004	6435.92	137.78	6573.7	HMC 2005
951	6/28/2004	6434.83	138.87	6573.7	HMC 2005
951	8/2/2004	6434.7	139	6573.7	HMC 2005
951	8/30/2004	6433.46	140.24	6573.7	HMC 2005
951	10/4/2004	6433.42	140.28	6573.7	HMC 2005
951	11/1/2004	6434.46	139.24	6573.7	HMC 2005

Table C.1-3. Water Level Data for Homestake Site and Distal San Andres Aquifer Wells

Well ID	Date	Water Elevation (ft amsl)	Water Level (ft-MP)	MP Elevation (ft amsl)	Data Source
951	11/29/2004	6438.51	135.19	6573.7	HMC 2005
951	12/8/2004	6438.8	134.9	6573.7	HMC 2005
951	1/4/2005	6434.62	139.08	6573.7	HMC 2006
951	1/31/2005	6433.88	139.82	6573.7	HMC 2006
951	2/28/2005	6434.32	139.38	6573.7	HMC 2006
951	4/4/2005	6433.85	139.85	6573.7	HMC 2006
951	4/25/2005	6433.82	139.88	6573.7	HMC 2006
951	5/2/2005	6433.03	140.67	6573.7	HMC 2006
951	5/31/2005	6431.78	141.92	6573.7	HMC 2006
951	7/5/2005	6431.45	142.25	6573.7	HMC 2006
951	8/1/2005	6436.92	136.78	6573.7	HMC 2006
951	8/29/2005	6433.35	140.35	6573.7	HMC 2006
951	10/3/2005	6432.78	140.92	6573.7	HMC 2006
951	10/31/2005	6432.8	140.9	6573.7	HMC 2006
951	11/28/2005	6432.79	140.91	6573.7	HMC 2006
951	12/5/2005	6432.89	140.81	6573.7	HMC 2006
951	1/3/2006	6432.75	140.95	6573.7	HMC 2006
951	1/3/2006	6432.75	140.95	6573.7	HMC 2007
951	1/30/2006	6432.56	141.14	6573.7	HMC 2007
951	2/27/2006	6432.3	141.4	6573.7	HMC 2007
951	3/16/2006	6431.34	142.36	6573.7	HMC 2007
951	4/3/2006	6431.34	142.36	6573.7	HMC 2007
951	5/1/2006	6431.83	141.87	6573.7	HMC 2007
951	5/30/2006	6430.9	142.8	6573.7	HMC 2007
951	6/26/2006	6430.58	143.12	6573.7	HMC 2007
951	7/31/2006	6429.47	144.23	6573.7	HMC 2007
951	8/28/2006	6433.8	139.9	6573.7	HMC 2007
951	9/25/2006	6429.4	144.3	6573.7	HMC 2007
951	10/30/2006	6430.62	143.08	6573.7	HMC 2007
951	11/27/2006	6430.55	143.15	6573.7	HMC 2007
951	12/27/2006	6431.15	142.55	6573.7	HMC 2007
951	1/29/2007	6435.1	138.6	6573.7	HMC 2008
951	2/26/2007	6435.1	138.6	6573.7	HMC 2008
951	3/9/2007	6431.32	142.38	6573.7	HMC 2008
951	4/2/2007	6430.45	143.25	6573.7	HMC 2008
951	4/30/2007	6428.78	144.92	6573.7	HMC 2008
951	5/29/2007	6427.8	145.9	6573.7	HMC 2008
951	7/2/2007	6426.9	146.8	6573.7	HMC 2008
951	7/30/2007	6426.8	146.9	6573.7	HMC 2008
951	9/4/2007	6426.65	147.05	6573.7	HMC 2008
951	10/1/2007	6425.7	148	6573.7	HMC 2008
951	10/29/2007	6426.4	147.3	6573.7	HMC 2008
951	12/3/2007	6427.1	146.6	6573.7	HMC 2008
951	1/2/2008	6427.33	146.37	6573.7	HMC 2009
951	2/4/2008	6427.04	146.66	6573.7	HMC 2009
951	3/3/2008	6427.55	146.15	6573.7	HMC 2009
951	3/5/2008	6427.51	146.19	6573.7	HMC 2009
951	3/31/2008	6426.6	147.1	6573.7	HMC 2009
951	5/5/2008	6425.4	148.3	6573.7	HMC 2009
951	6/2/2008	6424.97	148.73	6573.7	HMC 2009
951	6/30/2008	6423.4	150.3	6573.7	HMC 2009
951	9/2/2008	6422.1	151.6	6573.7	HMC 2009
951	9/4/2008	6422.65	151.05	6573.7	HMC 2009
951	9/29/2008	6422.9	150.8	6573.7	HMC 2009

Table C.1-3. Water Level Data for Homestake Site and Distal San Andres Aquifer Wells

Well ID	Date	Water Elevation (ft amsl)	Water Level (ft-MP)	MP Elevation (ft amsl)	Data Source
951	10/27/2008	6426.6	147.1	6573.7	HMC 2009
951	12/1/2008	6421.6	152.1	6573.7	HMC 2009
951	12/1/2008	6423.7	150	6573.7	HMC 2009
951	12/29/2008	6423.42	150.28	6573.7	HMC 2009
951	2/2/2009	6424.05	149.65	6573.7	HMC electronic
951	3/2/2009	6423.75	149.95	6573.7	HMC electronic
951	3/20/2009	6421.44	152.26	6573.7	HMC electronic
951	3/30/2009	6422.38	151.32	6573.7	HMC electronic
951	5/4/2009	6422.6	151.1	6573.7	HMC electronic
951	6/1/2009	6423.3	150.4	6573.7	HMC electronic
951	6/29/2009	6419.7	154	6573.7	HMC electronic
951	8/3/2009	6422.75	150.95	6573.7	HMC electronic
951	8/31/2009	6420.3	153.4	6573.7	HMC electronic
951	9/28/2009	6421.95	151.75	6573.7	HMC electronic
951	11/2/2009	6422.8	150.9	6573.7	HMC electronic
951	11/30/2009	6422.43	151.27	6573.7	HMC electronic
951	12/7/2009	6422.7	151	6573.7	HMC electronic
951	12/28/2009	6423.5	150.2	6573.7	HMC electronic
951	2/1/2010	6423.25	150.45	6573.7	HMC 2011
951	3/1/2010	6422.95	150.75	6573.7	HMC 2011
951	3/3/2010	6424.9	148.8	6573.7	HMC 2011
951	3/29/2010	6422.87	150.83	6573.7	HMC 2011
951	5/3/2010	6422.95	150.75	6573.7	HMC 2011
951	6/1/2010	6421.3	152.4	6573.7	HMC 2011
951	6/22/2010	6421.17	152.53	6573.7	HMC 2011
951	6/28/2010	6421.19	152.51	6573.7	HMC 2011
951	8/2/2010	6420.58	153.12	6573.7	HMC 2011
951	8/30/2010	6420.8	152.9	6573.7	HMC 2011
951	9/7/2010	6420.3	153.4	6573.7	HMC 2011
951	9/13/2010	6420.49	153.21	6573.7	HMC 2011
951	9/20/2010	6420.77	152.93	6573.7	HMC 2011
951	9/27/2010	6421.5	152.2	6573.7	HMC 2011
951	10/11/2010	6422.3	151.4	6573.7	HMC 2011
951	10/18/2010	6422.72	150.98	6573.7	HMC 2011
951	10/25/2010	6381.1	192.6	6573.7	HMC 2011
951	11/1/2010	6423.4	150.3	6573.7	HMC 2011
951	11/8/2010	6423.4	150.3	6573.7	HMC 2011
951	11/15/2010	6423.25	150.45	6573.7	HMC 2011
951	11/29/2010	6423.75	149.95	6573.7	HMC 2011
951	12/6/2010	6423.8	149.9	6573.7	HMC 2011
951	12/27/2010	6424.17	149.53	6573.7	HMC 2011
951	1/31/2011	6423.7	150	6573.7	HMC 2012
951	2/28/2011	6423.5	150.2	6573.7	HMC 2012
951	4/13/2011	6421.85	151.85	6573.7	HMC 2012
951	4/25/2011	6423.21	150.49	6573.7	HMC 2012
951	5/23/2011	6422.5	151.2	6573.7	HMC 2012
951	6/27/2011	6420.1	153.6	6573.7	HMC 2012
951	7/25/2011	6419.73	153.97	6573.7	HMC 2012
951	8/29/2011	6420.35	153.35	6573.7	HMC 2012
951	9/26/2011	6420.9	152.8	6573.7	HMC 2012
951	10/12/2011	6453.7	120	6573.7	HMC 2012
951	10/24/2011	6421.35	152.35	6573.7	HMC 2012
951	11/21/2011	6421.1	152.6	6573.7	HMC 2012
951	12/19/2011	6421.3	152.4	6573.7	HMC 2012

Table C.1-3. Water Level Data for Homestake Site and Distal San Andres Aquifer Wells

Well ID	Date	Water Elevation (ft amsl)	Water Level (ft-MP)	MP Elevation (ft amsl)	Data Source
951	1/23/2012	6386.3	187.4	6573.7	HMC 2013
951	2/27/2012	6422.72	150.98	6573.7	HMC 2013
951	3/9/2012	6423.02	150.68	6573.7	HMC 2013
951	3/26/2012	6426	147.7	6573.7	HMC 2013
951	8/19/199	6466.2	107.5	6573.7	HMC 2000
986	8/22/2008	6426	124	6550	HMC 2009
986	8/23/2008	6426	124	6550	HMC 2009
991	8/26/2008	6424.18	126.82	6551	HMC 2009
0806R	3/5/2008	6432.29	134.71	6567	HMC 2009
0806R	4/13/2011	6418.4	148.6	6567	HMC 2012
0951R	5/29/2012	6419.13	157.65	6576.78	HMC 2013
0951R	6/25/2012	6416.18	160.6	6576.78	HMC 2013
0951R	7/23/2012	6416.41	160.37	6576.78	HMC 2013
0951R	9/24/2012	6416.92	159.86	6576.78	HMC 2013
0951R	10/22/2012	6416.3	160.48	6576.78	HMC 2013
0951R	11/26/2012	6416.48	160.3	6576.78	HMC 2013
0951R	12/26/2012	6416.03	160.75	6576.78	HMC 2013
0951R	1/28/2013	6422.01	154.77	6576.78	HMC 2014
0951R	2/25/2013	6415.98	160.8	6576.78	HMC 2014
0951R	3/6/2013	6416.78	160	6576.78	HMC 2014
0951R	3/25/2013	6416.11	160.67	6576.78	HMC 2014
0951R	4/29/2013	6417.38	159.4	6576.78	HMC 2014
0951R	5/28/2013	6429.38	147.4	6576.78	HMC 2014
0951R	6/24/2013	6444.03	132.75	6576.78	HMC 2014

MP Measuring Point

Note:
Water level data listed here for HMC-951, also provided in Table C.1-1, are duplicated here, as HMC annual reports have been the primary source for these data. HMC did not issue an annual report in 2010 (reporting data for the year 2009). Water level data from 2009 are from an electronic file provided to DOE.

This page intentionally left blank

Table C.1-4. Water Level Data Used to Derive 2012 Potentiometric Surface for Alluvial Aquifer

Well ID	Date	Water Elevation (ft amsl)	Comment
427	9/20/2012	6536.39	
490	11/14/2012	6526.15	
491	11/15/2012	6524.95	
496	10/9/2012	6510.43	
497	11/14/2012	6511.72	
498	11/14/2012	6507.47	
520	11/13/2012	6537.52	
521	10/15/2012	6532.86	
522	10/16/2012	6532.34	
538	11/13/2012	6477.29	
540	11/13/2012	6496.08	
541	11/14/2012	6465.15	
551	11/13/2012	6447.5	
553	11/13/2012	6443.02	
554	11/13/2012	6440.65	
555	11/27/2012	6514.16	
556	11/27/2012	6503.41	
557	11/27/2012	6510.26	
631	11/13/2012	6450.28	
632	11/13/2012	6450.51	
634	11/19/2012	6487.82	
636	10/17/2012	6468.65	
637	10/17/2012	6463.26	
638	11/13/2012	6544.38	
639	10/18/2012	6536.88	
640	11/13/2012	6529.38	
644	11/13/2012	6468.99	
646	10/22/2012	6462.91	
647	11/13/2012	6446.08	
648	5/9/2012	6427.79	Fall 2012 measurement not taken
649	11/13/2012	6440.24	
650	11/15/2012	6463.53	
653	11/13/2012	6474.32	
654	11/19/2012	6478.4	
657	11/13/2012	6450.46	
658	11/13/2012	6441.99	
659	11/19/2012	6489.37	
683	10/19/2012	6465.63	
684	10/19/2012	6467.33	
686	10/17/2012	6465.19	
688	11/15/2012	6502.97	
690	11/13/2012	6546.59	
691	11/13/2012	6546.46	
802	11/19/2012	6474.44	
844	11/27/2012	6520.47	
845	11/27/2012	6522.43	
846	11/15/2012	6503.9	
862	11/13/2012	6499.53	
867	11/13/2012	6494.79	
869	11/13/2012	6471.85	
881	11/19/2012	6491.54	
882	11/1/2012	6496.32	
883	10/23/2012	6496.66	
884	11/1/2012	6493.34	

Table C.1-4. Water Level Data Used to Derive 2012 Potentiometric Surface for Alluvial Aquifer

Well ID	Date	Water Elevation (ft amsl)	Comment
885	11/19/2012	6500.19	
886	11/19/2012	6496.33	
888	11/19/2012	6482.23	
890	11/19/2012	6483.18	
893	11/19/2012	6495.71	
895	10/19/2012	6469.11	
896	10/19/2012	6469.68	
899	10/19/2012	6470.38	
921	10/17/2012	6584.1	
922	10/17/2012	6571.55	
935	10/19/2012	6466.04	
994	10/1/2012	6461.82	
1G	11/14/2012	6547.79	
1K	11/14/2012	6548.93	
1M	11/14/2012	6549.41	
1V	11/26/2012	6548.87	
20(M)	11/14/2012	6508.44	DOE well/result
21(M)	11/15/2012	6465.66	DOE well/result
22(M)	11/15/2012	6469.57	DOE well/result
23(M)	11/15/2012	6468.61	DOE well/result
AW	11/12/2012	6530.73	
B	11/26/2012	6537.1	
B1	11/13/2012	6536.55	
B12	11/15/2012	6537.42	
B13	11/13/2012	6537.28	
BA	11/26/2012	6538.47	
BC	11/15/2012	6540.84	
BP	11/14/2012	6533.87	
C1	11/13/2012	6540.95	
C10	11/30/2012	6530.48	
C11	11/30/2012	6568.64	
C12	11/30/2012	6559.65	
C2	11/13/2012	6539.34	
C5	11/14/2012	6542.15	
C6	11/30/2012	6533.89	
C7	11/30/2012	6537.04	
C8	11/30/2012	6519.89	
C9	11/30/2012	6525.1	
CW44	11/14/2012	6506.23	
DC	11/15/2012	6535.27	
DD	11/26/2012	6542.77	
DD2	11/26/2012	6544.68	
DT	11/26/2012	6539.12	
DZ	11/26/2012	6542.78	
E(M)	11/14/2012	6534.84	DOE well/result
F	11/14/2012	6534.48	
F(M)	11/14/2012	6490.17	DOE well/result
FB	9/17/2012	6533.76	
GA	11/13/2012	6529.95	
GF	11/13/2012	6531.81	
GH	11/13/2012	6530.91	
GV	11/27/2012	6529.18	
I	10/20/2012	6535.37	
K10	11/30/2012	6542.63	

Table C.1-4. Water Level Data Used to Derive 2012 Potentiometric Surface for Alluvial Aquifer

Well ID	Date	Water Elevation (ft amsl)	Comment
K11	11/30/2012	6539.24	
K4	11/30/2012	6533.72	
K5	11/30/2012	6539.73	
K7	11/30/2012	6541.63	
K8	11/30/2012	6540.39	
K9	11/30/2012	6538.32	
KEB	11/30/2012	6548.01	
KF	11/30/2012	6544.23	
KZ	11/26/2012	6543.75	
M11	11/17/2012	6513.35	
M16	10/22/2012	6508.16	
M5	11/13/2012	6537.59	
M6	11/19/2012	6514.91	
M7	11/19/2012	6517.04	
M9	11/15/2012	6509.81	
MA	11/15/2012	6532.42	
MC	11/15/2012	6529.76	
MF	11/15/2012	6526.43	
MH	11/15/2012	6523.67	
MJ	11/15/2012	6518.84	
ML	11/15/2012	6524.66	
MO	10/2/2012	6508.71	
MQ	11/15/2012	6505.60	
MR	11/19/2012	6501.11	
MS	11/19/2012	6511.12	
MT	10/23/2012	6506.87	
MU	11/15/2012	6538.80	
MV	11/19/2012	6505.34	
MW	11/15/2012	6514.81	
MX	11/27/2012	6519.03	
MY	11/27/2012	6518.78	
MZ	11/19/2012	6512.78	
N	11/20/2012	6545.33	
NC	11/19/2012	6543.48	
O	11/20/2012	6546.19	
P	10/1/2012	6543.33	
P2	11/19/2012	6538.60	
P3	11/19/2012	6538.54	
P4	11/19/2012	6539.50	
S	11/13/2012	6541.57	
S11	11/13/2012	6546.35	
S2	11/19/2012	6538.02	
S3	11/13/2012	6537.39	
S4	11/13/2012	6538.91	
S5R	11/19/2012	6533.20	
SE6	11/19/2012	6537.73	
SM	11/19/2012	6540.51	
SN	11/19/2012	6540.31	
SO	11/19/2012	6539.22	
SP	11/19/2012	6539.51	
Sub1	10/5/2012	6527.00	
Sub3	10/5/2012	6528.21	
SW	12/6/2012	6540.94	
SZ	11/13/2012	6545.72	

Table C.1-4. Water Level Data Used to Derive 2012 Potentiometric Surface for Alluvial Aquifer

Well ID	Date	Water Elevation (ft amsl)	Comment
T	12/10/2012	6510.80	
T(M)	5/5/2012	6478.57	DOE well/result
T2	12/10/2012	6548.02	
TA	10/15/2012	6543.92	
TB	10/18/2012	6547.09	
W	11/13/2012	6529.55	
WR12	11/13/2012	6561.19	
X	11/26/2012	6548.41	
X(M)	11/15/2012	6467.17	DOE well/result
Y2(M)	11/14/2012	6496.79	DOE well/result

Note:
Source: HMC 2013 (annual report for 2012) combined with 2012 water level measurements at Bluewater site alluvial wells. These data are plotted in the figure presenting the Fall 2012 potentiometric surface in the Site Status Report.

Table C.1-5. Water Level Data for Bluewater Site San Andres Aquifer Wells: Fall/Winter 1980 (Source: Hydro-Search 1981)

Well ID	Hydro-Search 1981 Map No.	Water Elevation (ft amsl)	Well Depth (ft)	Easting	Northing
Anaconda #1	21	6457.5	356	465476.78	1547734.58
Anaconda #2	22	6457.9	386	465513.60	1548353.14
Anaconda #3	25	6456.7	200	465276.18	1544848.79
Anaconda #4	26	6456.8	210	466181.82	1543967.85
Bluewater Muni.	23	6491.1		457386.61	1545486.08
C(SG)	17	6458.1	423	466480.31	1551114.60
Card Gas	S-3	6455.9	551	483605.02	1540548.97
Cottonwood Well	S-36	6456.9	253	473098.36	1539641.71
D(SG)	18	6467.8	259	468344.23	1552571.51
Dalton	30	6456.4		466478.21	1541201.52
Dan's Feed Store	S-39	6456.2	164	469880.36	1539803.72
G(SG)	19	6466.8	278	468833.93	1552562.36
Gallup Stake Irrigation Sec 4A	S-6	6456.1	315	481170.74	1534517.07
Gallup Stake Irrigation Sec 5	S-10	6456.3	225	476695.52	1534582.09
Gallup Stake Irrigation Sec. 4B	S-14	6452	480	482359.90	1529411.69
Hanosh	S-49	6445.8	250(?)	484713.42	1505803.90
Hardenburg Commissary	31	6456.9	238	468805.24	1541210.21
Harding	S-43	6456.9	245	472052.69	1542624.07
I(SG)	I(SG)	6456.3	330	477984.38	1552334.88
Keel	S-54	6445.9	165	486549.36	1506845.56
L(SG)	L(SG)	6481.7	610	462856.43	1553977.39
M(SG)	M(SG)	6471.4	575	465741.77	1559495.77
Mexican Camp	27	6457.8	280	468618.83	1545136.95
Monitor	15	6460.4	628	473819.29	1557094.45
North Well	14	6466.1	250	469523.70	1558775.19
OBS-2	OBS-2	6467.5	319	468797.32	1551656.17
OBS-3	OBS-3	6467.1	355	468865.97	1554081.82
Roundy Sec. 23	S-1	6453.7	865	491741.69	1548221.65
S(SG)	S(SG)	6467.9	337	468820.20	1552987.99
Sabre-Piñon (now HMC-951)	28	6456.7	275	473179.36	1545356.06
Spencer	13	6515.7	378	454133.39	1556147.67
Thornton	S-50	6456.2	195	475493.48	1532564.98
UNC Sec. 17	S-24	6453.5	125	478150.92	1523772.65
UNC Sec. 8A	S-11	6455	165	477946.95	1529279.96
UNC Sec. 8B	S-12	6456	150	473150.92	1528902.85
UNC Sec. 8C	S-13	6455.2	150	475616.98	1529312.89
W(SG)	W(SG)	6456.9	355	472847.99	1549280.99

Source:
Hydro-Search (HSI), 1981. *Regional Ground-Water Hydrology and Water Chemistry, Grants- Bluewater area, Valencia County, New Mexico*, prepared for Anaconda Copper Company, June 30.

Note:
Water elevation data for the Fall/Winter 1980 time-frame obtained from Plate V (Hydraulic Potential, San Andres-Glorieta) of HSI's report. Coordinates listed above were georeferenced from Plate V. These results were used to derive the potentiometric surface provided in Figure 23 in the Site Status Report.

Table C.1-6. Water Level Data for Bluewater Site Alluvial Aquifer Wells: Fall/Winter 1980 (Source: Hydro-Search 1981)

Well ID	Hydro-Search 1981 Map ID	Water Elevation (ft amsl)	Note
B(M)	5	6518.7	
BC	BC	6520.2	
Berryhill House (now B00168)	1	6520.3	
C(M)	6	6505.7	
Card Abandoned	11	6466.7	
Cibola Sands	S-56	6445.3	
D	D	6520.3	
E(M)	8	6543.2	
Engineer's Well	2	6520.4	
Evans Abandoned	S-25	6461.6	
F(M)	9	6490.9	
Gallup Stake Abandoned	S-9	6455.0	
Gallup Stake Domestic	S-27	6455.1	
Gallup Stake Irr. Sec. 4B	S-14	6452.0	**
Holmes	S-41A/41A	6463.7	
K(M)	K(M)	6553.5	Could be J(M), not clear from HSI maps
P	P	6538.4	
Pittard	S-46	6509.7	
Q	Q	6545.6	
R	R	6556.2	
Roundy Sec. 14	S-47	6564.0	
Roundy-Up	4	6527.0	
T(M)	T(M)	6485.5	
U(M)	U(M)	6478.2	
United Nuclear Sec. 17	S-24	6453.5	**
United Nuclear Sec. 8A	S-11	6455.0	**
United Nuclear Sec. 8B	S-12	6456.0	**
United Nuclear Sec. 8C	S-13	6455.2	**
X(M)	X(M)	6474.6	

Source:
Hydro-Search (HSI), 1981. *Regional Ground-Water Hydrology and Water Chemistry, Grants- Bluewater area, Valencia County, New Mexico*, prepared for Anaconda Copper Company, June 30.

Note:
Water elevation data for the Fall/Winter 1980 time-frame obtained from Plate VII (Hydraulic Potential, Alluvium Aquifer) of HSI's report. These results were used to derive the potentiometric surface provided in Figure 20 in the Site Status Report.

** Denotes location identified as San Andres well in HSI's report.
The reason data from these wells were used to derive the potentiometric surface for the alluvial aquifer may be explained as follows (Indented language below quoted from page 19 of HSI's 1981 report):

> *In the Milan-Grants area, the San Andres-Glorieta and Alluvium aquifers are interconnected and at the same hydraulic potential. Hydraulic head information and water chemistry data indicate that the San Andres-Glorieta loses a substantial volume of water to the alluvium in this area.*

Table C.2-1. Water Quality Data for Bluewater Site San Andres Aquifer Wells

Sample ID	Date Sampled	U (mg/L)	Se (µg/L)	Mo (µg/L)	As (µg/L)	SO_4 (mg/L)	Cl (mg/L)	NO_3+NO_2 as N (mg/L)	Nitrate as NO_3 (mg/L)	SC (µS/cm)	pH (s.u.)	Alkalinity, Bicarbonate (as $CaCO_3$)	Alkalinity, Carbonate (as $CaCO_3$)	Alkalinity, Total (as $CaCO_3$)	Ca (mg/L)	Mg (mg/L)	Na (mg/L)	K (mg/L)	DO (mg/L)	ORP (mV)
11(SG)	11/14/2012	0.0239	<1.5	0.454	<1.7	461	193	<0.017	<0.08	2590	6.93	544	<0.725		182	66.9	235	11.4	0.51	-134
11(SG)	1/30/2013	0.011	<1.5	0.292	16.3	405	187	<0.017	<0.08	2093	7.03	493	<0.725		161	61.9	251	10.4	0.92	-108.5
11(SG)	5/14/2013	0.00739	<1.5	0.204	22.7	371	177	<0.017	<0.08	2227	6.91	598	<0.725		187	69.3	271	10.8	1.44	-84.2
11(SG)	11/19/2013	0.0117	<1.5	1.88	10.3	744	192	<0.017	<0.08	2634	6.93			568	172	60.8	326	10	1.13	-148.3
13(SG)	11/15/2012	0.116	6.39	1.35	3.11	424	86.5	4.4	19.5	1419	6.86	301	<0.725		168	51	109	6.2	2.24	114.4
13(SG)	1/28/2013	0.106	5.45	1.36	2.8	413	84.9	4.25	18.8	1450	6.99	301	<0.725		149	45.1	101	5.55	2.67	156.2
13(SG)	5/15/2013	0.123	6.79	1.33	3.11	405	81.9	4.45	19.7	1519	6.78	296	<0.725		177	52.7	113	6.3	2.24	115.1
13(SG)	11/19/2013	0.0985	4.96	1.98	<1.7	407	87.7	5.18	22.9	1529	7.04			267	151	43.9	97.7	5.82	3.08	-50.7
14(SG)	11/14/2012	0.0437	<1.5	3	73.4	346	162	<0.017	<0.08	2267	7.08	541	<0.725		118	45	277	5.08	0.78	-130.7
14(SG)	1/30/2013	0.0324	<1.5	2.6	86.6	262	165	<0.017	<0.08	1810	7.18	592	<0.725		103	40.8	296	4.57	2.84	-102.7
14(SG)	5/14/2013	0.0308	<1.5	2.31	54	229	146	<0.017	<0.08	1890	6.98	554	<0.725		104	42.4	294	4.49	0.51	-74.3
14(SG)	11/19/2013	0.0741	<1.5	3.3	6.25	465	153	0.0238	0.11	1947	7.07			451	122	47.3	222	4.82	0.85	-18.3
15(SG)	11/13/2012	0.0743	<1.5	7.1	22.6	339	164	<0.017	<0.08	2085	7.26	421	<0.725		83.7	29	280	5.46	0.62	-123
15(SG)	1/29/2013	0.0553	<1.5	4.76	17.9	307	167	<0.017	<0.08	1695	7.33	429	<0.725		78.9	27.9	295	5.34	0.87	-116
15(SG)	5/14/2013	0.0449	<1.5	3.78	14.6	265	151	<0.017	<0.08	1782	7.12	438	<0.725		80.1	27.9	293	5.36	0.35	-77.6
15(SG)	11/19/2013	0.174	2.27	9.95	2.59	436	185	3.78	16.7	1954	7.29			322	100	34.8	232	5.91	0.96	4.3
16(SG)	11/13/2012	1.43	19.6	2.81	<1.7	1200	455	4.32	19.1	4553	6.58	424	<0.725		301	150	369	12.5	0.84	41.4
16(SG)	1/30/2013	1.38	16	2.57	<1.7	1200	453	4.37	19.4	3769	6.69	431	<0.725		290	145	397	11.6	0.83	23.4
16(SG)	5/16/2013	1.45	18.1	2.4	<1.7	1220	461	4.58	20.3	3967	6.53	416	<0.725		337	170	433	13.1	0.97	164.8
16(SG)	11/19/2013	1.4	14.7	2.88	<1.7	1270	479	4.83	21.4	3970	6.77			378	286	138	358	11.4	1.73	86.9
18(SG)	11/14/2012	0.207	5.1	2.54	<1.7	465	100	3.31	14.7	1904	6.82	332	<0.725		161	51.1	123	6.95	0.99	25.9
18(SG)	1/30/2013	0.212	4.6	2.22	<1.7	445	100	3.11	13.8	1610	6.94	331	<0.725		171	54.9	138	7.39	2.02	15.7
18(SG)	5/14/2013	0.232	5.91	2.02	<1.7	451	96.1	3.39	15.0	1700	6.73	326	<0.725		191	59.4	141	8.09	0.57	99.4
18(SG)	11/19/2013	0.127	1.77	3.93	<1.7	469	101	1.07	4.7	1665	6.97			346	143	40.6	144	6.54	0.81	-4.9
Anaconda #2	1/18/1977	0.5	11	<50	<10															
Anaconda #3	1/18/1977	<0.03	4.0	<50	<10															
Anaconda #3	4/12/1990	0.0277	<5	<5		350	67	3.59	15.9	1200	6.86				150	42	79	6.4		
Anaconda #4	4/26/1984	0.004				217	53.7	2.3	10	850	7.27				120	39.7	55	6.1		
Anaconda #4	4/22/1986	0.0168	<10			302	46	4.3	19	1200	7.1				158	45	60	6		
Anaconda #4	10/6/1986	0.00873				265	36	2.9	13	1050	7.25									
Anaconda #4	4/13/1987	0.0104	<5			290	44	5	22	1100	6.99				140	41	61	4		
Anaconda #4	10/8/1987	0.00597				249	31	3.6	16	1025	7.35									
Anaconda #4	4/13/1988	0.00611	<5			300	41	4.1	18	1100	7.32				140	39	71	5.8		
Anaconda #4	10/11/1988	0.0114				275	38	4.3	19	1050	7.39									
Anaconda #4	4/19/1989	0.00917	<5	<5		310	44	3.79	16.8	1100	7.22				150	42	62	5.2		
Anaconda #5	5/17/1984	0.064				471	129	4.3	19	1300	7.1				191	58	140	7.8		
Anaconda #5	4/22/1986	0.0528	<10			358	90	4.3	19	1400	7.2				168	55	93	10		
Anaconda #5	10/6/1986	0.0924				486	151	4.7	21	1900	6.85									
Anaconda #5	11/19/1986					507	162	3.6	16	2000	6.92									
Anaconda #5	4/6/1987	0.0566	<5			400	100	4.7	21	1550	6.86				160	50	110	1		
Anaconda #5	10/8/1987	0.112				486	172	5.4	24	1800	6.85									
Anaconda #5	4/5/1988	0.125	<5			569	186	6.8	30	2050	6.96				200	59	180	7.7		
Anaconda #5	10/5/1988	0.16				580	178	7.2	32	2050	7.51									
Anaconda #5	4/18/1989	0.175	<5	<5		520	200	5.5	24.3	2000	7.15				170	62	230	11		
Anaconda #5	4/12/1990	0.0815	<5	<5		460	190	4.8	21.2	1925	6.86				190	56	160	8.8		

Table C.2-1. Water Quality Data for Bluewater Site San Andres Aquifer Wells

Sample ID	Date Sampled	U (mg/L)	Se (µg/L)	Mo (µg/L)	As (µg/L)	SO_4 (mg/L)	Cl (mg/L)	NO_3+NO_2 as N (mg/L)	Nitrate as NO_3 (mg/L)	SC (µS/cm)	pH (s.u.)	Alkalinity, Bicarbonate (as $CaCO_3$)	Alkalinity, Carbonate (as $CaCO_3$)	Alkalinity, Total (as $CaCO_3$)	Ca (mg/L)	Mg (mg/L)	Na (mg/L)	K (mg/L)	DO (mg/L)	ORP (mV)
B00003	8/13/2013	0.087	6.3	1.59	3.32	489	101	2.5	10.9	1700	6.86	352	<0.725		179	54.2	139	8.37	5.2	-16
B00050A	10/1/2013	0.0114	11.8	0.936	<1.7	417	49.8	3.9	17.1	1365	7	244	<0.725		189	54.2	62.7	4.37	5.22	165
B00518	8/14/2013	0.00666	4.69	1.02	<1.7	295	31.1	4.6	20.3	1150	6.9	304	<0.725		159	41.9	46.4	3.29	6.39	190
B01614	10/2/2013	0.00403	3.63	1.74	<1.7	196	19.3	4.5	20.1	815	7.09	216	<0.725		89.2	37.9	41.6	2.8	4.4	160
Berryhill Sec5	5/9/1984	0.001				706	242	0.6	2.5	2320	7.06				211	76	367	15.1		
Berryhill Sec5	4/22/1986	0.0108	<10			670	255	<0.2	<1	2800	6.8				250	94	386	23		
Berryhill Sec5	11/19/1986	0.0099				804	249	0.2	1.0	2800										
Berryhill Sec5	4/10/1987	0.0115	<5			690	198	0.2	1.0	2900	6.8				230	76	350	14		
Berryhill Sec5	10/8/1987	0.0131				650	192	<0.2	<1	2900	7.01									
Berryhill Sec5	4/4/1988	0.00393	<5			666	236	0.2	1.0	2800	7.15				200	62	350	14		
Berryhill Sec5	10/11/1988	0.00611				660	220	<0.2	<1	2800	7.05									
Bowlin	5/9/1984	0.01				492	96	2.3	10	1300	7.09				184	51.9	137	9.5		
Bowlin	4/24/1986	0.0113	<10			445	89	2.0	7.0	1600	6.9				172	55	147	10		
Bowlin	11/19/1986	0.0115				442	87	2.0	7.0	1600	7									
Bowlin	4/13/1987	0.0179	<5			570	146	2.0	7.0	2000	6.89				210	72	190	5		
Bowlin	10/12/1987	0.00815				555	141	0.9	4.0	2200	6.89									
Bowlin	4/11/1988	0.00932	<5			574	158	2.0	8.0	2000	6.94				190	58	190	5		
Bowlin	10/11/1988	0.0134				610	151	1.0	6.0	1900	6.98									
C(SG)	3/4/1977	2.5	11	<50	<10															
C(SG)	4/16/1984	0.896	<5			927	345	6.48	28.7	2610	6.98				263	137	272	9.8		
C(SG)	5/5/1986	0.8496	<10			1054	352	4.5	20	3100	6.7				262	140	268	12		
C(SG)	4/9/1987	1.37	9			1020	380	6.1	27	3025	6.82				300	140	300	9		
C(SG)	4/13/1988	0.932	<5			841	256	5	22	2800	6.87				240	110	250	7.8		
C(SG)	4/18/1989	1.24	8	<5		830	280	5.6	24.8	2600	6.94				240	120	270	9		
C(SG)	4/11/1990	0.291	6	5.0		580	290	15	66.3	3100	6.71				160	43	350	6.9		
C(SG)	4/16/1990	1.19	8	9.0		820	290	4.09	18.1	2650	6.7				240	110	270	9		
C(SG)	10/22/1996	0.919	<5	8.0		734	181	3.5	15.5		6.96									
D(SG)	3/13/1977	2.4	23	<50	<10															
G(SG)	10/16/1996	1.81	<5	15.0		1180	511	4.5	19.9		7.0									
HMC-951	4/26/1984	0.014				426	87.4	4	17.7	1060	7.58				150	47.6	91	7.1		
HMC-951	6/20/1986	0.0097	<10			357	66	3.8	17	1250	7.2				161	47	79	7		
HMC-951	4/9/1987	0.00376	<5			287	62	0.2	1	1100	7.73				110	47	81	7		
HMC-951	4/13/1988	0.0083	<5			342	56	0.1	0.5	1210	7.24				140	41	76	4.9		
HMC-951	4/19/1989	0.0132	<5	<5		360	59	5.99	26.5	1150	7.22				160	47	78	5.6		
HMC-951	4/12/1990	0.0204	<5	<5		280	74	4.99	22.1	1125	6.86				140	42	78	6.1		
HMC-951	04/15/1993	0.018																		
HMC-951	10/05/1993	0.022																		
HMC-951	04/05/1994	0.022																		
HMC-951	08/31/1995	0.019																		
HMC-951	03/07/1996	0.017																		
HMC-951	10/22/1996	0.005																		
HMC-951	10/23/1996	0.023	<5	5.0		311	48	4.5	19.9		7.015									
HMC-951	08/21/1997	0.024																		
HMC-951	12/17/1997	0.024																		
HMC-951	8/18/1998	0.025	< 5.0	<30		323	50.3			1478	7.85	342	<1.0		148	43.2	76.5	5.6		

Table C.2-1. Water Quality Data for Bluewater Site San Andres Aquifer Wells

Sample ID	Date Sampled	U (mg/L)	Se (µg/L)	Mo (µg/L)	As (µg/L)	SO_4 (mg/L)	Cl (mg/L)	NO_3+NO_2 as N (mg/L)	Nitrate as NO_3 (mg/L)	SC (µS/cm)	pH (s.u.)	Alkalinity, Bicarbonate (as $CaCO_3$)	Alkalinity, Carbonate (as $CaCO_3$)	Alkalinity, Total (as $CaCO_3$)	Ca (mg/L)	Mg (mg/L)	Na (mg/L)	K (mg/L)	DO (mg/L)	ORP (mV)
HMC-951	8/19/1999	0.025	3.0			333														
HMC-951	9/17/1999	0.026	5.0			313				1185										
HMC-951	10/19/1999	0.025	< 5.0			335				1221										
HMC-951	11/2/1999	0.023	3.0			335				1222										
HMC-951	12/10/1999	0.020	6.0			350				1200										
HMC-951	1/20/2000	0.032	< 5.0	<30		333				1240										
HMC-951	8/9/2000	0.003	< 5.0			270				1226										
HMC-951	10/17/2002	0.028	< 5.0			314				1623										
HMC-951	10/27/2003	0.031	< 5.0			342				1305										
HMC-951	12/8/2004	0.027	8.0			334				1288										
HMC-951	4/25/2005	0.028	< 50	<30		358	68.0			1318	7.78	331	<1.0		145	43.1	80.5	4.90		
HMC-951	12/5/2005	0.033	5.0			316				1350										
HMC-951	3/16/2006	0.037	6.0	<30		356	83.0			1459	7.91	342	<1.0		145	43.4	79.9	5.60		
HMC-951	3/9/2007	0.032	< 5.0	<30		360	62.0			1318	7.79	354	<1.0		154	47.2	83.6	5.30		
HMC-951	12/3/2007	0.041	6.0			325				1346										
HMC-951	3/5/2008	0.040	6.0	<30		349	62.0			1348	7.49	352	<1.0		147	43.5	86.0	5.50		
HMC-951	8/27/2008	0.047	5.0	<30		382	74.0			1421	7.66	339	<1.0		170	50.0	98.0	5.70		
HMC-951	12/1/2008	0.042	6.0			348				1401										
HMC-951	3/20/2009	0.038	5.0	<30		356	64				7.44	347	<1.0		152	44.6	88.8	5.3		
HMC-951	3/24/2009	0.037	5.0	<30		349	63				7.35	348	<1.0		168	46.9	80.6	5.4		
HMC-951	3/31/2009		6.3			353	57				7.3	274	<10		162	42.3	71.2	4.59		
HMC-951	12/7/2009	0.037	6.0	<100		356														
HMC-951	3/3/2010	0.033	7.0	<30		341	61.0			1366	7.39	375	<5.0		148	43.6	81.3	5.10		
HMC-951	6/22/2010	0.045	6.0	<30		37.2	72.0			1429	7.47	372	<5.0		152	44.9	90.3	5.60		
HMC-951	6/24/2010	0.048	7.0	<30		391	100.0			907										
HMC-951	12/6/2010	0.034	<5			359				1005										
HMC-951	4/13/2011	0.033	7.0	<30		356	59.0			1340	7.48	360	<5.0		153	44.0	85.0	5.50		
HMC-951	7/6/2011	0.041	5.0	<30		363	64.0			1379										
HMC-951	10/12/2011	0.037	5.0	<30		360	63.0			1366										
HMC-951	3/9/2012	0.035	6.0	<30		348	61.0			1400	7.47	346	<5.0		146	43.3	87.4	5.40		
HMC-951	11/20/2013	0.0313	<7.5	1.42	<8.5	369	59.4	5.04	22.3272	1215	7				129	37	70.3	4.67	3.75	-25
I(SG) - 210 ft	11/19/2013	0.346	7.7	1.66	<8.5	887	293	1.46	6.47	2705	6.71			404	228	84.1	262	11.8	1.06	50
I(SG) - 234.91 ft	5/15/2013	0.00545	<1.5	0.7	<1.7	176	176	<0.017	<0.08	1204	7.97	136	<0.725		30.5	20.6	195	6.45	0.44	-16.7
I(SG) - 240 ft	11/19/2013	0.149	<7.5	0.898	<8.5	601	238	0.43	1.91	2070	6.9			804	138	56.1	227	9.25	1.18	-35
I(SG) - 261.91 ft	5/15/2013	0.35	9.49	1.28	<1.7	849	272	1.42	6.29	2876	6.54	405	<0.725		288	109	320	13.8	3.44	60.7
I(SG) - 265 ft	11/19/2013	0.334	8.39	1.42	<8.5	948	306	1.53	6.78	2745	6.71			414	231	84.7	262	11.5	1.35	95
I(SG) - 298.91 ft	5/15/2013	0.334	8.82	1.08	<1.7	846	272	1.45	6.42	2929	6.61	404	<0.725		283	106	311	13.9	1.1	11.3
I(SG) - 300 ft	11/19/2013	0.324	8.65	1.53	<8.5	902	288	1.45	6.42	2735	6.71			380	224	82.6	249	10.9	1.46	155
I(SG)	3/12/1984					1155	530	2.44	10.8	2400	6.81									
I(SG)	5/23/1984	0.444				1218	525	5.44	24.1	3300	6.81				350	134	439	16		
I(SG)	4/17/1986	0.4291	<10			1123	456	5	22	3650	6.7				340	148	430	23		
I(SG)	7/7/1986	0.349				1120	442	4.7	21	3600	6.77									
I(SG)	10/6/1986	0.431				1109	438	4.5	20	3750	6.73									
I(SG)	2/3/1987	0.405				1089	426	3.6	16	3650	6.78									
I(SG)	4/8/1987	0.443	12			1070	516	5.9	26	3700	6.81				330	130	380	13		

Table C.2-1. Water Quality Data for Bluewater Site San Andres Aquifer Wells

Sample ID	Date Sampled	U (mg/L)	Se (µg/L)	Mo (µg/L)	As (µg/L)	SO_4 (mg/L)	Cl (mg/L)	NO_3+NO_2 as N (mg/L)	Nitrate as NO_3 (mg/L)	SC (µS/cm)	pH (s.u.)	Alkalinity, Bicarbonate (as $CaCO_3$)	Alkalinity, Carbonate (as $CaCO_3$)	Alkalinity, Total (as $CaCO_3$)	Ca (mg/L)	Mg (mg/L)	Na (mg/L)	K (mg/L)	DO (mg/L)	ORP (mV)
I(SG)	7/7/1987	0.48				1090	426	5.4	24	4000	6.87									
I(SG)	10/7/1987	0.48				976	430	4.7	21	3800	6.73									
I(SG)	1/11/1988	0.451				1080	430	5	22	3600	6.8									
I(SG)	4/6/1988	0.422	<5			974	399	6.1	27	3550	6.86				290	100	360	12		
I(SG)	7/11/1988	0.437				1010	450	4.3	19	3450	6.98									
I(SG)	10/10/1988	0.451				1005	412	5.2	23	3550	6.85									
I(SG)	1/18/1989	0.655				1100	420	4.3	19	3400	6.98									
I(SG)	4/18/1989	0.597	<5	<5		1100	500	4.99	22.1	3200	6.87				340	120	460	17		
I(SG)	4/11/1990	0.422	8.0	6		760	450	6.1	27	3300	6.55				300	110	340	12		
I(SG)	7/2/1996	0.425	10.0	<5		950	342	3.3	14.6		7.03									
I(SG)	11/4/2008	0.0014	<0.11		0.58			<0.05	<0.2	947	9.37									-125
I(SG)	11/10/2009	0.0013	<0.038	<1.3	0.11	87	210	<0.05	<0.2	894	8.74		16		9.2	6.5	140	4.5		74.4
I(SG)	11/11/2010	0.0027	<1.0	0.777	2.24	124	179	<0.05	<0.2	1236	8.45	102	20.2		17.3	12.4	184	5.6	4.86	-139.7
I(SG)	7/27/2011	0.0011	<0.032	0.81	0.35	79	190	<0.01	<0.04	960	8.96		<10		11	8.9	150	6.1		-130
I(SG)	11/16/2011	0.00636	<1.5	0.663	<1.7	200	190	<0.01	<0.04	1267	8.02	161	<0.725		35.4	21.6	209	7.1	0.3	-243.2
I(SG)	5/15/2012	0.0	<0.1	0.78		230	170	<0.01	<0.04	1435	7.87		<20		39	28	180	9.7	0.38	-221.8
I(SG)	5/15/2012							<0.01	<0.04											
I(SG)	11/14/2012	0.00276	<1.5	0.532	<1.7	215	195	<0.017	<0.08	1454	8.14	140	<0.725		24.4	24.4	194	6.98	0.27	-227.4
I(SG)	1/29/2013	0.00202	<1.5	0.58	<1.7	199	195	<0.017	<0.08	1176	8.31	134	<1.05		18.9	20.6	197	6.29	0.45	-241.4
L(SG) - 438.72 ft	5/15/2013	0.003	<1.5	0.419	<1.7	580	192	<0.017	<0.08	2579	6.61	565	<0.725		153	82.3	378	8.57	0.38	-72.7
L(SG) - 508.72 ft	5/16/2013	0.00301	<1.5	0.57	<1.7	585	188	<0.017	<0.08	2531	6.61	565	<0.725		142	78.2	361	8.37	0.78	-9.5
L(SG) - 578.72 ft	5/16/2013	0.00301	<1.5	0.443	<1.7	571	186	<0.017	<0.08	2560	6.6	572	<0.725		153	78.8	362	8.7	0.6	-3.7
L(SG)	2/9/1984					622	238	0.34	1.5	2200	6.99									
L(SG)	6/7/1984	0.005	<5			624	277	0.41	1.8	2230	7.28				183	82	380	10.9		
L(SG)	4/15/1986	0.0053	<10			603	218	<0.2	<1	2590	6.9				156	90	366	14		
L(SG)	7/7/1986	0.00466				609	218	<0.2	<1	2450	7.06									
L(SG)	10/13/1986	0.00611				650	218	<0.2	<1	2700	6.88									
L(SG)	2/3/1987	0.00584				602	200	<0.2	<1	2650	6.88									
L(SG)	4/6/1987	0.00771	<5			560	192	<0.2	<1	2650	6.78				120	82	400	4		
L(SG)	8/31/1987	0.00408				603	223	<0.2	<1	2700	6.96									
L(SG)	10/5/1987	0.00291				645	206	<0.2	<1	2800	6.85									
L(SG)	1/11/1988	0.00291				596	202	<0.2	<1	2650	6.92									
L(SG)	4/5/1988	0.00422	<5			627	171	0.2	1.0	2590	6.9				130	70	380	8		
L(SG)	6/14/1988	0.003	<5								6.97									
L(SG)	7/11/1988	0.0114				629	180	<0.2	<1	2500	6.9									
L(SG)	9/8/1988	0.0047	<5	<5	<5						6.96									
L(SG)	10/10/1988	0.00771				605	189	0.9	4	2620	6.81									
L(SG)	12/6/1988	0.004	<5	<5	<5						6.96									
L(SG)	12/8/1988	0.004	<5								6.96									
L(SG)	1/18/1989	0.00757				610	210	<0.2	<1	2450	7.07									
L(SG)	3/7/1989	0.004	<5								7.2									
L(SG)	4/10/1989	0.00233	<5	<5		580	220	0.05	0.2	2450	7.05				140	70	380	7.9		
L(SG)	6/15/1989	0.003	<5								6.88									
L(SG)	9/20/1989	0.002	<5								6.77									
L(SG)	12/18/1989	0.003	<5								6.6									

Table C.2-1. Water Quality Data for Bluewater Site San Andres Aquifer Wells

Sample ID	Date Sampled	U (mg/L)	Se (µg/L)	Mo (µg/L)	As (µg/L)	SO_4 (mg/L)	Cl (mg/L)	NO_3+NO_2 as N (mg/L)	Nitrate as NO_3 (mg/L)	SC (µS/cm)	pH (s.u.)	Alkalinity, Bicarbonate (as $CaCO_3$)	Alkalinity, Carbonate (as $CaCO_3$)	Alkalinity, Total (as $CaCO_3$)	Ca (mg/L)	Mg (mg/L)	Na (mg/L)	K (mg/L)	DO (mg/L)	ORP (mV)
L(SG)	3/13/1990	0.003	<5								6.62									
L(SG)	4/10/1990	0.002	<5	<5		610	230	0.07	0.3	2600	6.73				130	64	430	9.1		
L(SG)	7/11/1990	0.003	<5								6.78									
L(SG)	9/18/1990	0.003	<5								6.75									
L(SG)	10/2/1990	0.002	<5								6.67									
L(SG)	12/18/1990	0.002	<5								6.79									
L(SG)	1/9/1991	0.002	<5								6.68									
L(SG)	4/3/1991	0.003	<5								6.56									
L(SG)	7/10/1991	0.002	<5								7.01									
L(SG)	10/2/1991	0.005	<5								6.96									
L(SG)	1/15/1992	0.001	<5								7.01									
L(SG)	4/8/1992	0.003	<5								6.85									
L(SG)	7/21/1992	0.003	<5								6.87									
L(SG)	10/8/1992	0.002	<5								6.86									
L(SG)	1/12/1993	0.003	<5								6.72									
L(SG)	4/5/1993	0.003	<5								6.84									
L(SG)	7/7/1993	0.004	<5								6.83									
L(SG)	10/5/1993	0.002	<5								6.9									
L(SG)	1/5/1994	0.003	<5								6.81									
L(SG)	4/5/1994	0.003	<5								6.84									
L(SG)	7/7/1994	0.002	<5								6.81									
L(SG)	10/13/1994	0.003	<5								6.72									
L(SG)	1/16/1995	0.002	<5								6.73									
L(SG)	4/10/1995	0.004	<5								6.7									
L(SG)	7/18/1995	0.002	<5								6.99									
L(SG)	10/18/1995	0.004	2.0								6.73									
L(SG)	1/15/1996	0.003	<1								6.78									
L(SG)	4/3/1996	0.001	<1								6.76									
L(SG)	10/9/1996	0.001	<5	<5		598	216	<0.10	<0.4		7.08									
L(SG)	11/16/1998	0.0024	<2							1774	7.02									
L(SG)	11/3/2001	0.004	<1							2090	6.98									
L(SG)	11/18/2004	<0.000075	0.32							1514	10.27									-277
L(SG)	11/6/2007	<0.00004	<0.028							1467	10.42									-139.3
L(SG)	11/4/2008	<0.00003	<0.081					0.01	0.04	1450	10.3									-215.5
L(SG)	11/10/2009	<0.00003	<0.027	16.0	0.045	3.7	220	<0.02	<0.09	1317	9.42		**280**		0.7	1.4	240	5.7		75.3
L(SG)	11/11/2010	<0.00005	<1	17.6	2.24	1.7	188	<0.05	<0.2	1654	10.13	15.7	**242**		0.876	1.39	314	5.35	0.39	-211.2
L(SG)	7/27/2011	0.0032	<0.032	0.43	0.13	600	210	<0.01	<0.04	2540	6.71		<20		150	77	310	13		-5
L(SG)	11/17/2011	0.00511	<1.5	0.338	<1.7	548	199	<0.01	<0.04	2585	6.69	540	<0.725		157	76.2	333	11	4.14	50.9
L(SG)	5/15/2012	0.0	<0.095	0.41	0.24	560	180	0.025	0.11	2547	6.9		<20		160	72	260	14	3.42	-61.9
L(SG)	5/15/2012							0.025	0.11											
L(SG)	11/14/2012	0.00316	<1.5	0.464	<1.7	613	197	<0.017	<0.08	2913	6.7	563	<0.725		145	77.8	345	8.14	0.97	-77.6
L(SG)	1/30/2013	0.00341	<1.5	0.458	<1.7	581	190	<0.017	<0.08	2413	6.78	565	<0.725		139	76.6	360	7.87	1.21	-96.9
L(SG)	11/19/2013	0.00294	<7.5	0.657	<8.5	630	203	<0.017	<0.08	2531	6.76			557	129	67.1	320	7.53	0.98	-63.5
M(SG)	6/7/1984	0.01	<5			533	117	0.97	4.3	1500	7.39				205	52	159	18.7		
M(SG)	4/15/1986	0.0114	<10			464	98	0.9	4	1700	7				192	55	143	14		

Table C.2-1. Water Quality Data for Bluewater Site San Andres Aquifer Wells

Sample ID	Date Sampled	U (mg/L)	Se (µg/L)	Mo (µg/L)	As (µg/L)	SO_4 (mg/L)	Cl (mg/L)	NO_3+NO_2 as N (mg/L)	Nitrate as NO_3 (mg/L)	SC (µS/cm)	pH (s.u.)	Alkalinity, Bicarbonate (as $CaCO_3$)	Alkalinity, Carbonate (as $CaCO_3$)	Alkalinity, Total (as $CaCO_3$)	Ca (mg/L)	Mg (mg/L)	Na (mg/L)	K (mg/L)	DO (mg/L)	ORP (mV)
M(SG)	10/13/1986	0.0121				516	95	0.7	3	1750	6.98									
M(SG)	4/8/1987	0.0138	<5			380	90	0.9	4	1700	7.1				180	50	130	9		
M(SG)	10/8/1987	0.00655				430	95	0.9	4	1720	7.04									
M(SG)	4/13/1988	0.00568	<5			435	90	0.79	3.5	1650	7.07				180	45	120	9.2		
M(SG)	10/11/1988	0.0146				425	93	0.9	4	1650	7.08									
M(SG)	4/19/1989	0.00655	<5	<5		470	93	0.79	3.5	1600	7.07				190	50	120	9.4		
M(SG)	4/11/1990	0.00713	<5	<5		400	95	0.77	3.4	1550	6.86				170	47	140	11		
M(SG)	10/16/1996	0.008	5.0	<5		422	78	1.0	4.4											
Mexican Camp	1/14/1977		8.0	<50	<10															
Mexican Camp	4/26/1984	0.006				119	17.3	0.32	1.4	490	7.54				81	24.4	37.1	4		
Mexican Camp	4/22/1986	0.0067	<10			181	12	<0.2	<1	750	7.3				78	34	44	4		
Mexican Camp	4/9/1987	0.00563	<5			149	12	<0.2	<1	725	7.26				84	29	46	3		
Mexican Camp	4/7/1988	0.00786	<5			149	13	0.41	1.8	700	7.32				77	26	46	0.06		
Mexican Camp	10/17/1996	0.009	<5	<5		145	19.2	0.9	4.0		6.8									
Monitor	1/14/1977		13	<50	<10															
Monitor	5/16/1984	0.239	<5			971	355	0.79	3.5	2560	6.9				290	105	342	15.5		
Monitor	4/17/1986	0.2643	<10			950	325	0.2	1	3100	6.7				296	122	342	22		
Monitor	10/6/1986	0.284				907	315	0.2	1	3150	6.73									
Monitor	4/13/1987	0.231	<5			790	340	0.7	3	3000	6.69				260	98	310	13		
Monitor	10/12/1987	0.306				796	308	<0.2	<1	3100	6.82									
Monitor	4/5/1988	0.291	<5			840	295	0.9	4	3000	6.88				270	87	290	11		
Monitor	10/10/1988	0.32				865	330	0.7	3	3000	6.89									
Monitor	4/11/1989	0.349	6	<5		920	320	1.1	4.9						280	99	350	16		
Monitor	4/11/1990	0.32	<5	<5		920	330	0.41	1.8	2900	7.09				270	88	350	13		
North	1/14/1977		19	<50	<10															
North	5/15/1984	0.012	<5			499	196	2.1	9.3	1600	6.92				107	61	238	12.4		
North	4/17/1986	0.0155	<10			554	182	<0.2	<1	2000	7				125	75	228	16		
North	10/6/1986	0.021				593	183	0.2	1	2150	6.99									
North	4/8/1987	0.0179	<5			550	164	0.2	1	2050	7.03				120	72	230	11		
North	10/8/1987	0.0083				497	177	0.2	1	2050	7.24									
North	4/13/1988	0.00844	<5			530	171	0.1	0.5	1900	7.13				92	63	220	13		
North	10/10/1988	0.032				525	168	0.2	1	1900	7.15									
North	4/18/1989	0.032	8.0	<5		630	200	0.47	2.1	2000	7.03				190	81	260	14		
North	4/11/1990	0.0105	<5	7		470	200	0.1	0.6	1800	6.92				96	58	250	11		
North	10/16/1996	0.021	9.0	<5		530	178	0.2	0.89		7.07									
OBS-2	4/19/1989	1.75	<5	17		1100	510	9.98	44.2	3500	6.87				280	150	420	10		
OBS-2	4/10/1990	1.34	14.0	33.0		950	400	9.98	44.2	3300	6.71				240	120	420	11		
OBS-2	10/17/1996	1.02	33.0	12.0		672	245	7.1	31.5		6.61									
OBS-3	5/7/1984	0.807				1722	910	5.83	25.8	4260	6.92				406	215	629	16.8		
OBS-3	4/17/1986	0.5362	<10			1676	829	4.5	20	5100	6.9				380	230	620	22		
OBS-3	10/13/1986	0.611				1677	772	4.1	18	5200	6.94									
OBS-3	4/6/1987	0.378	<5			1570	921	2.7	12	5300	6.92				310	210	640	14		
OBS-3	10/7/1987	0.262				1670	934	2.0	8.0	5700	7.03									
OBS-3	4/5/1988	0.859	<10			1490	750	3.4	15	5000	6.98				300	190	580	16		
OBS-3	6/14/1988	0.51	<8								7.11									

Table C.2-1. Water Quality Data for Bluewater Site San Andres Aquifer Wells

Sample ID	Date Sampled	U (mg/L)	Se (µg/L)	Mo (µg/L)	As (µg/L)	SO_4 (mg/L)	Cl (mg/L)	NO_3+NO_2 as N (mg/L)	Nitrate as NO_3 (mg/L)	SC (µS/cm)	pH (s.u.)	Alkalinity, Bicarbonate (as $CaCO_3$)	Alkalinity, Carbonate (as $CaCO_3$)	Alkalinity, Total (as $CaCO_3$)	Ca (mg/L)	Mg (mg/L)	Na (mg/L)	K (mg/L)	DO (mg/L)	ORP (mV)
OBS-3	9/8/1988	0.42	10	<5	<5						6.95									
OBS-3	10/11/1988	1.27				1610	810	4.7	21	5050	6.88									
OBS-3	12/6/1988	0.92	10	<5	<5						6.94									
OBS-3	12/8/1988	0.92	10								6.94									
OBS-3	3/7/1989	1	11								6.88									
OBS-3	4/11/1989	1.34	11	<5		1700	720	6.98	30.9	4750	6.91				600	190	430	10		
OBS-3	6/15/1989	0.94	11								6.67									
OBS-3	9/21/1989	1.24	20								6.64									
OBS-3	12/19/1989	1.77	10								6.44									
OBS-3	3/14/1990	1.64	14								6.54									
OBS-3	4/10/1990	1.43	13	<5		1600	670	6.39	28.3	4400	6.76				420	180	550	15		
OBS-3	5/24/1990	1.23	8								6.66									
OBS-3	7/12/1990	1.62	8								6.67									
OBS-3	9/18/1990	1.26	11								6.77									
OBS-3	10/2/1990	1.77	10								6.66									
OBS-3	12/18/1990	1.43	<5								6.6									
OBS-3	1/10/1991	1.26	11								6.68									
OBS-3	4/2/1991	1.45	16								6.67									
OBS-3	7/9/1991	1.5	<10								6.91									
OBS-3	10/2/1991	1.4	6								6.69									
OBS-3	1/20/1992	1.38	<5								6.8									
OBS-3	4/7/1992	1.2	7								6.85									
OBS-3	7/20/1992	1.23	7								6.87									
OBS-3	10/19/1992	1.29	10								6.77									
OBS-3	2/12/1993	1.23	5								6.68									
OBS-3	4/12/1993	1.29	16								6.84									
OBS-3	7/7/1993	1.03	14								6.85									
OBS-3	10/13/1993	1.17	10								6.78									
OBS-3	1/5/1994	1.23	<5								6.78									
OBS-3	4/12/1994	1.29	16								6.84									
OBS-3	7/6/1994	1.09	20								6.98									
OBS-3	10/11/1994	1.3	18								6.94									
OBS-3	1/16/1995	0.72	<5								6.9									
OBS-3	4/18/1995	0.95	14								6.76									
OBS-3	7/18/1995	0.69	10								7.05									
OBS-3	10/23/1995	0.83	17								6.84									
OBS-3	1/15/1996	0.69	12								7.15									
OBS-3	4/2/1996	0.75	11								6.93									
OBS-3	10/9/1996	0.705	<5	15		1420	658	4.2	18.6		6.98									
OBS-3	11/13/1998	0.532	5							3050	6.36									
OBS-3	11/3/2001	0.745	<1							3530	6.86									
OBS-3	11/18/2004	0.0054	<0.15							3092	8.73									-143
OBS-3	11/6/2007	0.00082	0.071							3890	7.66									-169.8
OBS-3	11/4/2008	0.00048	<0.1					<0.05	<0.2	3917	7.21									-202.2
OBS-3	11/10/2009	0.00022	<0.034	<0.57	0.061	670	1100	<0.2	<0.9	3567	8.17		<5.0		110	150	410	17		83.2

Table C.2-1. Water Quality Data for Bluewater Site San Andres Aquifer Wells

Sample ID	Date Sampled	U (mg/L)	Se (µg/L)	Mo (µg/L)	As (µg/L)	SO_4 (mg/L)	Cl (mg/L)	NO_3+NO_2 as N (mg/L)	Nitrate as NO_3 (mg/L)	SC (µS/cm)	pH (s.u.)	Alkalinity, Bicarbonate (as $CaCO_3$)	Alkalinity, Carbonate (as $CaCO_3$)	Alkalinity, Total (as $CaCO_3$)	Ca (mg/L)	Mg (mg/L)	Na (mg/L)	K (mg/L)	DO (mg/L)	ORP (mV)
OBS-3, 325 ft	11/10/2010	0.000648	<1	<0.167	<1.6	220	871	<0.05	<0.2	3993	6.63	15.2	<0.725		80.7	93.7	475	14.4	0.79	-101.4
OBS-3, 255 ft	11/10/2010	0.0011	<1	0.386	2.19	79.8	821	<0.05	<0.2	3416	9.82	<0.725	<9.1		24	57.5	463	13.8	1.92	-142.7
OBS-3	7/28/2011	0.12	7.9	0.65	0.079	1000	590	1.6	7.09	3877	7.18		<20		210	170	390	22		-127.1
OBS-3	11/16/2011	0.0106	<1.5	0.197	<1.7	844	626	<0.01	<0.04	3623	6.99	20.3	<0.725		118	168	452	16.3	2.93	-109.3
OBS-3	5/15/2012	0.0076	<0.39	<0.32	0.077	790	650	0.044	0.19	3533	7.08		<5.0		110	140	350	20	1.24	-133.3
OBS-3	11/13/2012	0.0106	<1.5	0.191	<1.7	797	616	0.040	0.18	3928	6.81	16	<0.725		106	132	379	12.4	2.62	-77.6
OBS-3	1/30/2013	0.0116	<1.5	0.175	<1.7	865	577	0.061	0.27	3260	7.18	41.8	<0.725		112	143	436	13.1	1.79	-128.2
OBS-3	5/14/2013	0.228	8.32	1.14	<1.7	908	525	1.75	7.75	3589	7.01	246	<0.725		193	146	420	14.5	6.57	104.7
OBS-3	11/20/2013	0.00931	<1.5	0.852	<1.7	999	622	0.0256	0.113	3240	7.35			38	128	136	372	11.9	0.51	-185
Payne	3/5/1977		5	<50	<10															
Payne	5/9/1984	0.006	<5			315	46.5	2.2	9.8	870	7.16				150	39.2	59	4.8		
Payne	4/24/1986	0.0044	<10			230	43	2.3	10	870	7.1				115	34	31	2		
Payne	11/19/1986	0.0048				220	30	2	8	815	7.15									
Payne	4/9/1987	0.00501	<5			212	25	2.7	12	820	7.43				120	28	31	3		
Payne	10/12/1987	0.0048				240	33	2	9	900	7.24									
Payne	4/11/1988	0.00509	<5			228	30	2	9	850	7.23				120	31	38	4		
Payne	10/11/1988	0.00757				230	27	2.3	10	800	7.49									
Roundy House	5/9/1984	0.006				33.2	44.6	1.3	5.6	1000	7.16				182	40.8	439	2.3		
Roundy House	4/24/1986	0.0097	<10			325	38	4.1	18	1300	6.9				198	47	41	2		
Roundy House	4/13/1987	0.0105	<5			301	30	3.8	17	1200	7.04				190	43	38	2		
Roundy House	4/11/1988	0.00684	<5			242	21	2	9	1050	7.02				170	31	43	2		
S(SG)	2/15/1984					1673	970	1.1	4.9	2625	6.81									
S(SG)	5/7/1984	0.504	<5			1854	950	3.03	13.4	4210	6.96				398	260	670	15.1		
S(SG)	4/17/1986	1.17	<10			1737	763	5.4	24	5100	6.8				405	290	560	20		
S(SG)	7/7/1986	1.63				1716	742	4.1	18	4800	6.77									
S(SG)	10/13/1986	1.14				1689	727	4.1	18	5100	6.71									
S(SG)	2/3/1987	1.11				1614	692	2.7	12	5000	6.89									
S(SG)	4/6/1987	1.25	11			1520	670	4.3	19	5000	6.72				340	230	560	9		
S(SG)	7/7/1987	0.946				1690	710	3.8	17	5000	6.82									
S(SG)	10/5/1987	0.626				1610	655	2.9	13	5080	6.86									
S(SG)	1/4/1988	1.46				1610	670	2.7	12	4750	6.96									
S(SG)	4/5/1988	1.03	<5			1530	690	2	9	4700	6.87				310	200	530	12		
S(SG)	6/14/1988	1.7	12								6.95									
S(SG)	7/11/1988	1.16				1460	660	2.5	11	4550	6.92									
S(SG)	9/8/1988	1.4	10	<5	<5						6.91									
S(SG)	10/10/1988	1.75				1510	678	2.7	12	4550	6.84									
S(SG)	12/6/1988	1.77	12	<5	<5						6.84									
S(SG)	12/8/1988	1.7	12								6.84									
S(SG)	1/17/1989	1.75				1500	620	2.5	11	4400	6.9									
S(SG)	3/7/1989	1.5	7								6.79									
S(SG)	4/10/1989	1.6	7	5		1400	620	3.59	15.9	4200	6.92				330	210	490	15		
S(SG)	6/15/1989	1.6	11								6.8									
S(SG)	9/21/1989	1.2	9								6.82									
S(SG)	12/18/1989	1.6	7								6.68									
S(SG)	3/14/1990	1.64	9								6.66									

Table C.2-1. Water Quality Data for Bluewater Site San Andres Aquifer Wells

Sample ID	Date Sampled	U (mg/L)	Se (µg/L)	Mo (µg/L)	As (µg/L)	SO_4 (mg/L)	Cl (mg/L)	NO_3+NO_2 as N (mg/L)	Nitrate as NO_3 (mg/L)	SC (µS/cm)	pH (s.u.)	Alkalinity, Bicarbonate (as $CaCO_3$)	Alkalinity, Carbonate (as $CaCO_3$)	Alkalinity, Total (as $CaCO_3$)	Ca (mg/L)	Mg (mg/L)	Na (mg/L)	K (mg/L)	DO (mg/L)	ORP (mV)
S(SG)	4/10/1990	1.43	10	5		1500	660	4.7	20.8	4400	6.57				380	200	520	14		
S(SG)	5/24/1990	1.3	5								6.65									
S(SG)	7/11/1990	1.62	6								6.72									
S(SG)	9/17/1990	1.15	7								6.79									
S(SG)	10/1/1990	1.3	5								6.66									
S(SG)	12/18/1990	1.77	<5								6.6									
S(SG)	1/10/1991	1.2	5								6.66									
S(SG)	4/2/1991	1.48	<10								6.65									
S(SG)	7/9/1991	1.4	<10								7.03									
S(SG)	10/2/1991	1.3	5								6.93									
S(SG)	1/15/1992	0.98	<5								6.82									
S(SG)	4/6/1992	1.2	6								6.86									
S(SG)	7/20/1992	1.39	6								6.86									
S(SG)	10/6/1992	1.4	10								6.83									
S(SG)	1/12/1993	1.2	12								6.82									
S(SG)	4/8/1993	1.03	10								6.9									
S(SG)	7/7/1993	1.2	9								6.89									
S(SG)	10/6/1993	1.29	11								6.88									
S(SG)	1/5/1994	1.45	<5								6.8									
S(SG)	4/8/1994	1.03	8								6.9									
S(SG)	7/6/1994	1.32	16								6.79									
S(SG)	10/11/1994	1.4	5								6.76									
S(SG)	4/10/1995	0.96	13								6.85									
S(SG)	4/16/1995	1.09	<5								6.81									
S(SG)	7/18/1995	1.27	15								6.9									
S(SG)	10/16/1995	1.15	16								6.97									
S(SG)	1/16/1996	1	14								7									
S(SG)	4/2/1996	1.05	13								7.02									
S(SG)	10/9/1996	1.01	<5	13.0		1200	528	4.0	17.7		7.12									
S(SG)	11/13/1998	0.577	4							2520	7.02									
S(SG)	11/3/2001	0.178	<1							3280	6.98									
S(SG)	11/18/2004	0.00043	<0.029							5194	6.5									-135
S(SG)	11/6/2007	<0.0002	<0.066							6264	6.52									-159.9
S(SG)	11/4/2008	0.00036	<0.1					0.02	0.0886	6991	6.33									-120.4
S(SG)	11/10/2009	<0.00002	<0.034	0.43	0.087	300	2500	<5	<22	6632	8.3		<5.0		860	54	78	1.4		70
S(SG)	11/9/2010	<0.00005	<1	<0.167	<1.6	295	2570	0.056	0.24808	7701	5.97	<0.725	<0.725		897	52.7	105	1.95	0.51	-78.3
S(SG)	7/26/2011	0.26	11	0.73	0.22	1200	800	2.1	9.303	4421	6.83		<20		410	180	390	21		-97.1
S(SG)	11/16/2011	0.312	10.6	0.916	<1.7	1260	609	2.64	11.6952	4289	7.16	325	<0.725		334	177	443	16.5	0.98	-105.6
S(SG)	5/15/2012	0.44	13	1	0.23	1200	520	3.0	13.29	4265	7.03		<20		340	170	360	21	2.69	-138.2
S(SG)	11/13/2012	0.367	12	1.26	<1.7	1160	493	2.64	11.6952	4576	7.01	374	<0.725		287	161	385	13.3	3.57	-95.5
S(SG)	1/30/2013	0.441	11	1.27	<1.7	1200	467	2.91	12.8913	3780	7.05	400	<0.725		310	173	427	13.5	3.96	-129
S(SG)	5/16/2013	0.639	13.7	1.48	<1.7	1210	463	2.66	11.7838	4065	6.74	422	<0.725		326	172	425	14	2.13	-65.2
S(SG)	11/20/2013	0.525	8.97	2.26	<1.7	1190	485	2.61	11.5623	3635	6.87			432	283	160	388	12.7	3.41	-40
W(SG)	6/7/1984	0.06	<5			1098	419	21	91	2850	6.82				370	106	363	15.8		
W(SG)	4/17/1986	0.0885	<10			992	418	18	81	3450	6.8				356	120	386	18		

Table C.2-1. Water Quality Data for Bluewater Site San Andres Aquifer Wells

Sample ID	Date Sampled	U (mg/L)	Se (µg/L)	Mo (µg/L)	As (µg/L)	SO_4 (mg/L)	Cl (mg/L)	NO_3+NO_2 as N (mg/L)	Nitrate as NO_3 (mg/L)	SC (µS/cm)	pH (s.u.)	Alkalinity, Bicarbonate (as $CaCO_3$)	Alkalinity, Carbonate (as $CaCO_3$)	Alkalinity, Total (as $CaCO_3$)	Ca (mg/L)	Mg (mg/L)	Na (mg/L)	K (mg/L)	DO (mg/L)	ORP (mV)
W(SG)	10/6/1986	0.0886				981	406	17	76	3450	6.93									
W(SG)	4/8/1987	0.104	10			910	449	19	84	3400	6.92				310	99	360	11		
W(SG)	10/5/1987	0.0961				926	387	17	75	3400	6.96									
W(SG)	4/6/1988	0.124	<5			859	364	20	88	3200	7.02				270	86	320	9.3		
W(SG)	10/10/1988	0.0917				895	392	18	80	3200	7.03									
W(SG)	4/17/1989	0.146	9	<5		1000	420	18	79.6	3000	7.02				300	93	390	12		

Notes:

Data for S(SG) and OBS-3 from 1996 through the present are suspect for reasons discussed in the Site Status Report. Results for more recently installed well 16(SG) are considered more representative of groundwater quality in this region of the site.

For well HMC-951, refer to Appendix C, Table C.2-6 for the complete historical record.

Table C.2-2. Water Quality Data for Bluewater Site Alluvial and Chinle Aquifer Wells

Sample ID	Date Sampled	U (mg/L)	Se (µg/L)	Mo (µg/L)	As (µg/L)	SO_4 (mg/L)	Cl (mg/L)	NO_3+NO_2 as N (mg/L)	Nitrate as NO_3 (mg/L)	SC (µS/cm)	pH (s.u.)	Alkalinity, Bicarbonate (as $CaCO_3$)	Alkalinity, Carbonate (as $CaCO_3$)	Alkalinity, Total (as $CaCO_3$)	Ca (mg/L)	Mg (mg/L)	Na (mg/L)	K (mg/L)	DO (mg/L)	ORP (mV)
20(M)	11/14/2012	0.0197	4.67	1.86	9.41	394	56.4	3.18	14.1	1511	7.1	258	<0.725		148	38.1	83.7	4.5	6.12	29.4
20(M)	1/30/2013	0.015	3.73	1.9	9.62	391	55.8	3.15	14.0	1267	7.24	257	<0.725		149	38.4	91.8	4.54	7.08	-35.3
20(M)	5/14/2013	0.0155	5.47	1.98	8.54	370	54.8	3.38	15.0	1318	7.02	251	<0.725		166	41.3	92.8	5	6.5	87.1
20(M)	11/19/2013	0.0139	3.81	2.54	<8.5	395	58.3	4.37	19.4	1297	7.23			250	137	33.9	82.9	4.17	7.47	-0.2
21(M)	7/27/2011	0.13	10	1.1	2.4	520	170	7.9	35.0	1885	7.28		<20		160	42	190	7.8		62
21(M)	11/15/2011	0.123	10.5	0.893	1.98	467	154	8.41	37.3	1927	7.33	256	<0.725		162	42.9	214	6.66	6.18	140.8
21(M)	5/15/2012	0.13	9	0.87	2.8	490	150	7.9	35.0	1934	7.28		<20		170	41	180	7.9	4.24	79.1
21(M)	11/15/2012	0.132	10.6	0.937	<1.7	490	150	8.68	38.5	1726	7.14	164	<0.725		151	40.8	196	5.53	4.22	109.6
21(M)	1/29/2013	0.128	9.35	0.865	3.21	483	152	9.46	41.9	1762	7.29	260	<0.725		146	39.4	203	5.52	4.58	87.4
21(M)	5/15/2013	0.148	12	0.918	<1.7	489	135	9.81	43.5	1859	7.06	263	<0.725		168	44.7	216	6.52	4.27	125.3
21(M)	11/19/2013	0.137	10.1	1.45	<1.7	509	150	12	53.2	1874	7.32			261	132	34.4	178	5.13	4.9	33.5
22(M)	7/27/2011	0.33	7.6	3.3	2.7	280	44	26	115.2	1440	7.18		<20		100	29	170	6.7		75
22(M)	11/15/2011	0.314	6.7	0.819	2.78	263	37.6	31.2	138.2	1442	7.32	316	<0.725		102	28.2	181	5.36	0.59	147.1
22(M)	5/15/2012	0.31	6.8	0.73	3.8	240	36	29	128.5	1426	7.29		<20		100	27	150	6.2	0.67	90.9
22(M)	11/15/2012	0.315	5.58	0.783	2.51	239	33.4	32.3	143.1	1251	7.18	327	<0.725		86.2	24.4	157	4.69	1.12	104.3
22(M)	1/29/2013	0.352	4.69	0.796	3.08	231	31.8	30.7	136.0	1276	7.31	323	<0.725		90.1	25.9	176	4.89	1.56	7.9
22(M)	5/14/2013	0.38	5.98	0.711	3.26	221	33.6	36.4	161.3	1332	7.02	326	<0.725		97.6	27	177	5.22	1.58	62.7
22(M)	11/19/2013	0.388	3.72	0.975	3.46	222	32.8	34	150.6	1323	7.34			315	78.4	21.2	151	4.32	2.67	31.2
23(M)	1/28/2013	0.0203	8.86	8.11	<1.7	325	94.2	3.98	17.6	1113	7.29	133	<0.725		134	29.9	53.9	6.56	4.82	170
23(M)	5/15/2013	0.0203	6.91	8.42	<1.7	285	88.8	3.46	15.3	1153	7.26	139	<0.725		152	34.7	60.3	6.76	3.48	68.6
23(M)	11/19/2013	0.0209	2.75	7.47	<1.7	295	91.7	2.35	10.4	970	6.75			150	118	26.1	46.5	5.23	3.03	250
Aragon	1/14/1977		16	<50	<10															
Aragon	5/9/1984	0.005				354	59.8	4.79	21.2	990	7.22				180	48.2	26.2	2.9		
Aragon	4/24/1986	0.0072	10			325	48	4.7	21	1200	7				168	50	24	2		
Aragon	11/19/1986	0.0106				324	58	3.8	17	1200	7.06									
Aragon	4/13/1987	0.00689	<5			310	54	6.1	27	1150	7.12				180	47	25	3		
Aragon	10/12/1987	0.003				316	54	5.2	23	1200	7.22									
Aragon	4/11/1988	0.005	<5			325	57	5.2	23	1150	7.24				170	40	26	5		
Aragon	10/11/1988	0.00742				315	55	5.4	24	1200	7.06									
B(M)	3/3/1977	3.3	34	<50	<10															
B(M)	3/20/1977	1.55	61	<50	<10															
B(M)	2/13/1984					3411	3279	14	61	7400	6.42									
B(M)	5/7/1984	2.504	<5			3654	3009	11.7	51.6	11000	6.42				719	600	1860	29.9		
B(M)	4/15/1986	3.292	50			3449	3030	14	60	14000	6.4				780	620	1810	50		
B(M)	7/7/1986	3.57				3451	3092	12	52	14000	6.42									
B(M)	10/13/1986	4.53				3510	3115	13	58	15000	6.31									
B(M)	2/3/1987	3.67				3438	3059	11	47	14500	6.42									
B(M)	4/6/1987	3.52	57			3200	3050	11	49	15000	6.51				610	580	2000	29		
B(M)	7/7/1987	3.2				3290	3010	9.9	44	15000	6.5									
B(M)	10/5/1987	2.91				3380	3010	14	62	15000	6.4									
B(M)	1/4/1988	3.2				3370	2850	12	53	14500	6.59									
B(M)	4/5/1988	4.22	75			3110	3000	11	50	14200	6.51				670	580	1800	20		
B(M)	7/11/1988	4.66				3122	3020	9.5	42	13500	6.66									
B(M)	10/6/1988	4.66				3174	2982	12	54	14000	6.58									
B(M)	1/17/1989	6.4				3100	2800	14	62	13500	6.57									
B(M)	4/10/1989	3.2	54	<5		3200	3000	15	66	13000	6.65				740	510	1900	30		
B(M)	4/12/1990	4.66	32	<12		3200	3200	14	61.9	13250	6.55				780	480	2200	30		
B00050B	10/1/2013	0.133	25.2	3.37	3.43	697	162	2.73	12.1	2280	6.96	328	<0.725		226	65.5	219	7.19	5.56	180

Table C.2-2. Water Quality Data for Bluewater Site Alluvial and Chinle Aquifer Wells

Sample ID	Date Sampled	U (mg/L)	Se (µg/L)	Mo (µg/L)	As (µg/L)	SO_4 (mg/L)	Cl (mg/L)	NO_3+NO_2 as N (mg/L)	Nitrate as NO_3 (mg/L)	SC (µS/cm)	pH (s.u.)	Alkalinity, Bicarbonate (as $CaCO_3$)	Alkalinity, Carbonate (as $CaCO_3$)	Alkalinity, Total (as $CaCO_3$)	Ca (mg/L)	Mg (mg/L)	Na (mg/L)	K (mg/L)	DO (mg/L)	ORP (mV)
Berryhill House	1/14/1977		7	<50	<10															
Berryhill House	5/9/1984	0.011				349	48.4	6.46	28.6	930	7.57				160	44.6	63	4.3		
Berryhill House	4/22/1986	0.0094	<10			312	48	3.6	16	1150	7.4				142	43	52	4		
Berryhill House	11/19/1986	0.00742				300	43	2.5	11	1100	7.38									
Berryhill House	4/13/1987	0.0067	<5			301	39	4.3	19	1100	7.39				140	38	53	4		
Berryhill House	10/12/1987	0.00597				284	42	3.2	14	1100	7.38									
Berryhill House	4/11/1988	0.00655	<5			296	41	3.2	14	1050	7.41				130	37	57	5		
Berryhill House	10/12/1988	0.0099				298	40	3.6	16	1050	7.49									
B00168	8/13/2013	0.00884	2.85	1.23	1.7	417	68	3.19	14.1	1370	6.77	258	<0.725		184	50	59.6	4.97	6.44	7
C(M)	3/25/1977	0.33	9.0	<50	20															
C(M)	3/12/1984					313	84	2.1	9.4	980	6.77									
C(M)	4/16/1984	0.091				325	100	5.6	24.8	1190	6.73				132	57	99	4.3		
C(M)	4/15/1986	0.073	10			314	61	3.6	16	1200	6.7				141	41	70	5		
C(M)	7/7/1986	0.0547				304	60	3.2	14	1200	6.73									
C(M)	10/13/1986	0.0709				352	58	3.2	14	1200	6.71									
C(M)	2/3/1987	0.0626				305	55	2.3	10	1150	6.81									
C(M)	4/6/1987	0.0738	<5			301	65	3.4	15	1150	6.82				130	38	95	1		
C(M)	7/8/1987	0.0684				320	59	2.5	11	1200	6.9									
C(M)	10/7/1987	0.0757				292	56	3.2	14	1200	6.88									
C(M)	1/11/1988	0.0597				308	51	2.9	13	1150	6.85									
C(M)	4/5/1988	0.0524	<5			299	53	3.2	14	1100	6.95				130	34	69	2.3		
C(M)	7/11/1988	0.0786				315	54	2.7	12	1100	7.18									
C(M)	10/6/1988	0.0801				287	59	3.6	16	1120	7.4									
C(M)	1/18/1989	0.0699				310	51	2.9	13	1100	7.15									
C(M)	4/17/1989	0.0684	<5	<5		300	52	2.89	12.8	1100	7				130	34	76	4.1		
C(M)	4/9/1990	0.0495	<5	<5		300	58	4	17.7	960	6.77				130	38	72	4.2		
E(M)	4/12/1984	0.018				454	159	2.1	9.3	1350	7.19				183	40	123	5		
E(M)	4/22/1986	0.0355	<10			296	48	2	8	1100	7.5				120	34	92	5		
E(M)	10/13/1986	0.0231				342	57	2.3	10	1150	7.4									
E(M)	4/8/1987	0.0185	<5			313	61	2.7	12	1100	7.42				150	34	59	5		
E(M)	10/8/1987	0.0189				292	56	2	9	1150	7.36									
E(M)	4/13/1988	0.0105	<5			305	64	2.1	9.3	1075	7.69				130	30	63	5.4		
E(M)	6/14/1988	0.013	<5	<5							7.72									
E(M)	9/7/1988	0.017	<5	<5	<5						7.73									
E(M)	10/6/1988	0.0291				322	61	2.5	11	1050	7.41									
E(M)	12/6/1988	0.019	<5	<5	<5						7.04									
E(M)	3/7/1989	0.022	<5	<5							7.49									
E(M)	4/17/1989	0.0233	<5	<5		290	60	2	8.8	980	7.14				120	32	77	5		
E(M)	6/15/1989	0.027	<5	<5							7.14									
E(M)	9/20/1989	0.017	<5	<5							7.27									
E(M)	12/18/1989	0.03	<5	<5							7.21									
E(M)	3/12/1990	0.029	<5	<5							7.16									
E(M)	4/9/1990	0.025	<5	<5		300	65	2.3	10.2	910	7.18				130	34	72	5.3		
E(M)	7/12/1990	0.027	<5	<5							7.25									
E(M)	9/18/1990	0.022	<5	<5							6.9									
E(M)	10/3/1990	0.03	<5	<5							7.22									
E(M)	12/18/1990	0.031	<5	<5							7.22									
E(M)	1/8/1991	0.031	<5	<5							7.03									

Table C.2-2. Water Quality Data for Bluewater Site Alluvial and Chinle Aquifer Wells

Sample ID	Date Sampled	U (mg/L)	Se (µg/L)	Mo (µg/L)	As (µg/L)	SO_4 (mg/L)	Cl (mg/L)	NO_3+NO_2 as N (mg/L)	Nitrate as NO_3 (mg/L)	SC (µS/cm)	pH (s.u.)	Alkalinity, Bicarbonate (as $CaCO_3$)	Alkalinity, Carbonate (as $CaCO_3$)	Alkalinity, Total (as $CaCO_3$)	Ca (mg/L)	Mg (mg/L)	Na (mg/L)	K (mg/L)	DO (mg/L)	ORP (mV)
E(M)	4/3/1991	0.024	<5	<5							7.09									
E(M)	7/10/1991	0.027	<5	<5							7.29									
E(M)	10/3/1991	0.019	<5	<5							7.14									
E(M)	1/14/1992	0.024	<5	<5							7.33									
E(M)	4/14/1992	0.021	<5	<5							7.24									
E(M)	7/21/1992	0.022	<5	<5							7.2									
E(M)	10/6/1992	0.031	<5	<5							7.3									
E(M)	1/11/1993	0.025	<5	<5							7.36									
E(M)	4/5/1993	0.024	<5	<5							7.3									
E(M)	7/8/1993	0.032	<5	<5							7.34									
E(M)	10/5/1993	0.032	<5	<5							7.32									
E(M)	1/6/1994	0.024	<5	<5							7.26									
E(M)	4/12/1994	0.024	<5	<5							7.21									
E(M)	7/6/1994	32.0	0.6	<5							7.29									
E(M)	10/6/1994	0.032	<5	<5							7.32									
E(M)	1/16/1995	0.028	<5	<5							7.29									
E(M)	4/10/1995	0.022	<5	<5							7.48									
E(M)	7/17/1995	0.024	<5	<5							7.37									
E(M)	10/23/1995	0.021	1	<5							7.34									
E(M)	1/16/1996	0.023	<1	<3							7.34									
E(M)	4/3/1996	0.025	<1	<3							7.36									
E(M)	11/19/1997									819	7.66									
E(M)	11/14/1998	0.0122	<2	<10						600	7.11									
E(M)	12/18/1998									877	7.75									
E(M)	11/11/1999	0.005	<2	<10						584	7.13									
E(M)	11/11/2000	0.004	<1	4.2						1018	7.14									
E(M)	11/3/2001	<0.001	2	2.0						1043	7.48									
E(M)	10/17/2002	0.001	2	2.0						1089	8.02									
E(M)	9/19/2003									1179	8.65									
E(M)	11/18/2004	<0.0002	<0.055	<0.61						1337	8.45									-235
E(M)	11/15/2005									1592	8.28									-272.2
E(M)	11/28/2006									1742	7.55									-177.9
E(M)	11/6/2007	<0.00004	0.038	0.47						1683	8.37									-269.8
E(M)	11/4/2008	<0.00002	<0.077	0.59				0.019	0.084	1688	8.15									-263.5
E(M)	5/13/2009	<0.00003						<0.01	<0.04	1607	8.07									-309
E(M)	11/11/2009	0.00009	0.39	<1.5	0.046	960	42	<0.1	<0.4	1586	7		<5.0		250	58	51	4.8		95.5
E(M)	11/11/2010	<0.00005	<1	0.18	<1.6	949	37.8	<0.05	<0.2	2042	7.03	16.2	<0.725		262	63.1	63.6	5.43	0.32	-117.1
E(M)	7/27/2011	0.0004	<0.032	0.31	0.063	870	39	<0.01	<0.04	1600	7.32		<5.0		250	61	58	5.4		-60
E(M)	11/16/2011	<0.00007	<1.5	0.294	<1.7	890	31.2	<0.01	<0.04	1591	7.69	8.14	<0.725		233	59.5	56.9	5.56	0.41	-231.7
E(M)	5/15/2012	0.0001	<0.069	0.49	0.07	780	32	<0.01	<0.04	1552	7.62		<5.0		240	56	55	4.9	0.64	-26.6
E(M)	11/14/2012	<0.00007	<1.5	0.404	<1.7	750	32.7	<0.017	<0.08	1701	7.21	11.8	<0.725		195	50.2	50.9	3.99	3.92	-85.9
E(M)	1/30/2013	<0.00007	<1.5	0.416	<1.7	751	32.2	<0.017	<0.08	1411	8.31	2.61	<0.725		202	53.2	57.1	4.11	0.45	-313.6
E(M)	5/14/2013	<0.00007	<1.5	0.345	<1.7	754	31.7	<0.017	<0.08	1445	8.05	<0.725	<0.725		225	58.8	56.6	4.45	0.12	-158
E(M)	11/19/2013	<0.00007	<1.5	0.638	<1.7	747	33	<0.017	<0.08	1338	8.02			15	164	42.1	47.4	3.88	0.35	-284
Engineers	2/9/1984					342	56	3.82	16.9	900	7.78									
Engineers	5/9/1984	0.013	<5			392.5	63.4	17	74	1120	7.59				156.5	51.7	86	5.7		
Engineers	4/22/1986	0.0161	<10			302	48	4.7	21	1150	7.6				142	43	56	4		
Engineers	7/7/1986	0.0127				300	46	6.1	27	1150	7.68									

Table C.2-2. Water Quality Data for Bluewater Site Alluvial and Chinle Aquifer Wells

Sample ID	Date Sampled	U (mg/L)	Se (µg/L)	Mo (µg/L)	As (µg/L)	SO_4 (mg/L)	Cl (mg/L)	NO_3+NO_2 as N (mg/L)	Nitrate as NO_3 (mg/L)	SC (µS/cm)	pH (s.u.)	Alkalinity, Bicarbonate (as $CaCO_3$)	Alkalinity, Carbonate (as $CaCO_3$)	Alkalinity, Total (as $CaCO_3$)	Ca (mg/L)	Mg (mg/L)	Na (mg/L)	K (mg/L)	DO (mg/L)	ORP (mV)
Engineers	11/19/1986	0.0132				299	47	3.2	14	1100	7.54									
Engineers	2/3/1987	0.0131				310	45	2.7	12	1100	7.59									
Engineers	4/13/1987	0.0108	<5			287	38	6.1	27	1100	7.4				130	37	59	4		
Engineers	8/31/1987	0.005				296	46	3.2	14	1100	7.74									
Engineers	10/12/1987	0.006				287	42	3.2	14	1100	7.59									
Engineers	1/11/1988	0.005				300	41	2.9	13	1050	7.52									
Engineers	4/11/1988	0.00771	<5			299	42	3.2	14	1020	7.59				130	34	66	6		
Engineers	7/11/1988	0.00684				283	45	2.3	10	1020	7.79									
Engineers	10/12/1988	0.00742				285	42	2.9	13	1020	7.6									
Engineers	1/18/1989	0.0102				310	46	3.2	14	1000	7.45									
F(M)	4/17/1984	0.006				183	41.5	5.13	22.7	730	7.26				98	39	20.9	3.8		
F(M)	4/17/1986	0.005	<10			181	36	2.3	10	770	7.3				107	34	16	3		
F(M)	10/6/1986	0.00713				200	36	2.5	11	820	7.39									
F(M)	4/6/1987	0.00675	<5			196	33	2.7	12	830	7.27				110	33	30	1		
F(M)	10/7/1987	0.0064				208	37	2.9	13	900	7.36									
F(M)	4/6/1988	0.00713	<5			222	41	3.8	17	900	7.26				120	31	22	3.3		
F(M)	6/14/1988	0.006	<5	<5							7.54									
F(M)	9/7/1988	0.007	<5	<5	<5						7.8									
F(M)	10/5/1988	0.00713				214	44	4.7	21	910	7.32									
F(M)	12/6/1988	0.007	<5	<5	<5						7.46									
F(M)	3/7/1989	0.007	<5	<5							7.53									
F(M)	4/11/1989	0.00568	<5	<5		290	48	3.5	15.5	880	7.42				150	36	31	5.4		
F(M)	6/15/1989	0.006	<5	<5							7.1									
F(M)	9/20/1989	0.005	<5	<5							7.29									
F(M)	12/18/1989	0.006	<5	<5							7.25									
F(M)	3/12/1990	0.007	<5	<5							7.1									
F(M)	4/9/1990	0.00582	<5	<5		260	52	7.5	33.2	815	7.12				150	37	30	4.8		
F(M)	5/23/1990	0.008	<5	<5							7.27									
F(M)	9/18/1990	0.003	<5	<5							7.2									
F(M)	10/2/1990	0.007	<5	<5							7.12									
F(M)	12/18/1990	0.013	<5	<5							7									
F(M)	1/8/1991	0.008	<5	<5							7.08									
F(M)	4/3/1991	0.006	<5	<5							7.14									
F(M)	7/9/1991	0.008	<5	<5							7.19									
F(M)	10/3/1991	0.003	<5	<5							7.22									
F(M)	1/15/1992	0.004	<5	<5							7.15									
F(M)	4/7/1992	0.009	<5	<5							7.2									
F(M)	7/21/1992	0.009	<5	<5							7.24									
F(M)	10/5/1992	0.008	<5	<5							7.25									
F(M)	1/11/1993	0.014	<5	<5							7.24									
F(M)	4/5/1993	0.011	<5	<5							7.32									
F(M)	7/6/1993	0.013	<5	<5							7.33									
F(M)	10/11/1993	0.013	<5	<5							7.32									
F(M)	1/4/1994	0.012	<5	<5							7.3									
F(M)	4/5/1994	0.011	<5	<5							7.32									
F(M)	7/7/1994	0.013	6	<5							7.2									
F(M)	10/10/1994	0.013	<5	<5							7.14									
F(M)	1/17/1995	0.012	<5	<5							7.32									

Table C.2-2. Water Quality Data for Bluewater Site Alluvial and Chinle Aquifer Wells

Sample ID	Date Sampled	U (mg/L)	Se (µg/L)	Mo (µg/L)	As (µg/L)	SO_4 (mg/L)	Cl (mg/L)	NO_3+NO_2 as N (mg/L)	Nitrate as NO_3 (mg/L)	SC (µS/cm)	pH (s.u.)	Alkalinity, Bicarbonate (as $CaCO_3$)	Alkalinity, Carbonate (as $CaCO_3$)	Alkalinity, Total (as $CaCO_3$)	Ca (mg/L)	Mg (mg/L)	Na (mg/L)	K (mg/L)	DO (mg/L)	ORP (mV)
F(M)	4/10/1995	0.014	<5	<5							7.06									
F(M)	7/18/1995	0.011	<5	<5							7.34									
F(M)	10/23/1995	0.01	3	<5							7.24									
F(M)	1/15/1996	0.013	<1	<3							7.32									
F(M)	4/10/1996	0.013	<1	<3							6.99									
F(M)	11/19/1997									730	7.39									
F(M)	11/14/1998	0.0144	<2	<10						438	6.98									
F(M)	12/18/1998									826	7.57									
F(M)	11/11/1999	0.0125	<2	<10						450	7.14									
F(M)	11/11/2000	0.0156	<1	0.8						733	6.92									
F(M)	11/3/2001	0.016	2	<1						677	7.45									
F(M)	10/17/2002	0.015	2	<1						680	7.63									
F(M)	9/19/2003									601	7.73									
F(M)	9/26/2003									601	7.73									
F(M)	11/18/2004	0.011	1	<1						607	7.67									-10
F(M)	5/24/2005									611	7.71									140.7
F(M)	11/15/2005									596	7.53									-47.7
F(M)	11/28/2006									578	7.94									43.6
F(M)	11/6/2007	0.0067	0.97	0.76						573	7.98									133.5
F(M)	11/4/2008	0.0057	0.43	0.71				0.065	0.29	580	7.8									-16.4
F(M)	5/13/2009	0.007						0.75	3.32	548	7.58									0.1
F(M)	11/10/2009	0.0093	1	4	1.1	120	13	0.93	4.12	585	8.39		<20		78	19	17	2.6		85
F(M)	11/10/2010	0.00806	1.22	0.797	1.71	106	12.2	0.765	3.39	672	7.8	173	<0.725		75.2	19.4	22.3	3.59	3.69	-117.1
F(M)	7/28/2011	0.0074	1.2	0.85	1.2	110	13	0.68	3.01	565	7.68		<20		72	19	19	3		89
F(M)	11/15/2011	0.0076	<1.5	0.93	<1.7	102	11.5	0.182	0.81	575	7.65	167	<0.725		76.8	20.1	21.7	3.89	5.78	93.3
F(M)	5/15/2012	0.0073	1.1	1	1.2	99	11	0.7	3.10	569	7.71		<20		74	19	19	2.9	3.05	177.9
F(M)	11/14/2012	0.0086	<1.5	1.03	<1.7	101	11	0.695	3.08	625	7.58	170	<0.725		70.2	19	20.2	3.45	2.67	37.4
F(M)	1/30/2013	0.00808	<1.5	1.03	<1.7	99.1	11.1	0.654	2.90	536	7.7	180	<0.725		70.4	19.2	21.3	3.38	2.65	6.4
F(M)	5/14/2013	0.00753	1.76	0.895	<1.7	101	11	0.665	2.95	547	7.4	174	<0.725		75.4	20.6	21.1	3.49	2.39	78.7
F(M)	11/19/2013	0.00734	<7.5	1.39	<8.5	104	12.2	0.66	2.92	537	7.71			162	60.7	16.1	18.4	3.01	2.96	-18.3
H(C) (Chinle well)	4/15/1986	0.0076	<10			520	100	<0.2	<1	1750	9.6				15	8	342	13		
H(C) (Chinle well)	7/2/1986	0.00568				499	92	<0.2	<1	1500	9.94									
H(C) (Chinle well)	10/1/1986	0.004				330	94	<0.2	<1	1190	10.03									
H(C) (Chinle well)	1/5/1987	0.00722				193	58	<0.2	<1	990	9.95									
H(C) (Chinle well)	4/2/1987	0.004	20			235	61	<0.2	<1	1100	10.16				3	<1	210	4		
H(C) (Chinle well)	7/6/1987	0.004				242	67	<0.2	<1	950	10.07									
H(C) (Chinle well)	10/5/1987	0.00728				463	100	<0.2	<1	1700	9.83									
H(C) (Chinle well)	2/1/1988	0.0009				712	122	<0.2	<1	2150	9.48									
H(C) (Chinle well)	4/4/1988	0.003	<10			1105	133	0.2	1	2750	7.42				36	24	560	10		
H(C) (Chinle well)	7/11/1988	0.001				538	157	<0.2	<1	2650	7.91									
H(C) (Chinle well)	10/4/1988	0.001				1102	145	0.099	0.44	2400	9.74									
H(C) (Chinle well)	1/17/1989	0.005				780	150	<0.2	<1	1700	10.23									
H(C) (Chinle well)	4/16/1990	0.00655	50	34		410	100	2.6	11.5	1575	10.37				10	0.36	330	8.2		
K(M)	5/16/1984	0.37				2432	2099	22	97	7900	6.8				810	210	1350	4.8		
K(M)	4/22/1986	0.0696	20			2262	1710	19	84	7900	6.7				669	256	1175	15		
K(M)	10/13/1986	0.0926				2288	1573	19	84	7700	6.52									
K(M)	4/9/1987	0.0438	22			2000	1500	9	40	7250	6.74				600	140	1100	3		
K(M)	10/8/1987	0.003				2070	1640	2.3	10	7800	6.61									

Table C.2-2. Water Quality Data for Bluewater Site Alluvial and Chinle Aquifer Wells

Sample ID	Date Sampled	U (mg/L)	Se (µg/L)	Mo (µg/L)	As (µg/L)	SO_4 (mg/L)	Cl (mg/L)	NO_3+NO_2 as N (mg/L)	Nitrate as NO_3 (mg/L)	SC (µS/cm)	pH (s.u.)	Alkalinity, Bicarbonate (as $CaCO_3$)	Alkalinity, Carbonate (as $CaCO_3$)	Alkalinity, Total (as $CaCO_3$)	Ca (mg/L)	Mg (mg/L)	Na (mg/L)	K (mg/L)	DO (mg/L)	ORP (mV)
K(M)	4/11/1988	0.118	6.9			1740	1000	14	62	5850	6.74				410	120	790	2		
K(M)	10/11/1988	0.0335				1810	1115	12	52	6000	7.1									
K(M)	4/20/1989	0.0815	<5	<5		870	1200	0.34	1.5	4600	7.41				97	100	920	7.6		
K(M)	4/12/1990	0.121	<5	7		990	840	0.79	3.5	4450	8.16				25	66	1100	3.9		
Raw Tailings Water	3/6/1977	66.0	27	<50	780															
SIMPSON	4/18/1989	0.003	8	<5		300	65	6.69	29.6	1100	7.28				170	37	37	2.6		
SIMPSON	4/12/1990	0.004	16	<5		280	73	0.79	3.5	1125	6.92				180	36	35	2.8		
SIMPSON	5/15/2012	0.003	42	0.6	0.65	570	120	7.9	35.0	1842	7.4		<20		260	47	110	3.6	7.91	117.5
SIMPSON	11/13/2012	0.005	56.4	0.645	<1.7	617	122	8.69	38.5	2097	7.22	205	<0.725		224	46.8	109	3.22		37.4
T(M)	4/17/1984	0.286				435	159	7.48	33.1	1610	7.14				97	42	300	7.4		
T(M)	4/17/1986	0.2146	<10			324	80	4.7	21	1450	7.2				130	52	130	7		
T(M)	10/13/1986	0.197				376	73	4.5	20	1450	6.83									
T(M)	4/6/1987	0.198	10			310	70	5.9	26	1425	7.01				120	42	150	1		
T(M)	10/7/1987	0.179				326	69	5	22	1500	7.12									
T(M)	4/6/1988	0.233	<5			332	72	5.9	26	1500	7.18				110	37	120	5.1		
T(M)	6/14/1988	0.18	13	2.7							7.16									
T(M)	9/7/1988	0.17	8	19	<5						7.46									
T(M)	10/6/1988	0.175				288	64	4.1	18	1300	7.19									
T(M)	12/6/1988	0.19	8	27	<5						7.24									
T(M)	3/7/1989	0.16	7	33							7.19									
T(M)	4/17/1989	0.175	8	35		310	73	5.11	22.6	1200	7.17				120	36	130	4.8		
T(M)	6/15/1989	0.16	8	34							7									
T(M)	9/20/1989	0.15	7	32							7.07									
T(M)	12/18/1989	0.15	<5	45							7.1									
T(M)	3/14/1990	0.013	5	25							7.01									
T(M)	4/10/1990	0.132	6	30		290	66	5.69	25.2	1175	7				140	41	100	5.3		
T(M)	5/24/1990	0.11	12	34							7.01									
T(M)	7/11/1990	0.13	5	32							7.08									
T(M)	9/18/1990	0.18	5	28							7.05									
T(M)	10/1/1990	0.14	5	33							7.02									
T(M)	12/18/1990	0.15	<5	34							6.96									
T(M)	1/9/1991	0.15	5	30							6.95									
T(M)	4/2/1991	0.13	5	37							6.95									
T(M)	7/10/1991	0.18	6	31							7.21									
T(M)	10/2/1991	0.12	<5	33							7.04									
T(M)	1/16/1992	0.13	<5	29							6.99									
T(M)	4/6/1992	0.15	5	29							7.15									
T(M)	7/20/1992	0.14	6	24							7.1									
T(M)	10/8/1992	0.15	8	30							7.12									
T(M)	1/12/1993	0.18	8	34							7.02									
T(M)	4/6/1993	0.14	6	30							6.98									
T(M)	7/7/1993	0.18	8	31							7.06									
T(M)	10/13/1993	0.14	<5	31							7.07									
T(M)	1/5/1994	0.12	6	30							7.04									
T(M)	4/6/1994	0.14	6	30							6.98									
T(M)	7/6/1994	0.12	6	30							7.2									
T(M)	10/18/1994	0.12	<5	38							7.06									
T(M)	1/17/1995	0.11	<5	25							6.96									

Table C.2-2. Water Quality Data for Bluewater Site Alluvial and Chinle Aquifer Wells

Sample ID	Date Sampled	U (mg/L)	Se (µg/L)	Mo (µg/L)	As (µg/L)	SO_4 (mg/L)	Cl (mg/L)	NO_3+NO_2 as N (mg/L)	Nitrate as NO_3 (mg/L)	SC (µS/cm)	pH (s.u.)	Alkalinity, Bicarbonate (as $CaCO_3$)	Alkalinity, Carbonate (as $CaCO_3$)	Alkalinity, Total (as $CaCO_3$)	Ca (mg/L)	Mg (mg/L)	Na (mg/L)	K (mg/L)	DO (mg/L)	ORP (mV)
T(M)	4/10/1995	0.11	8	26							7.07									
T(M)	7/17/1995	0.08	<5	28							7.19									
T(M)	10/16/1995	0.1	4	26							6.86									
T(M)	1/15/1996	0.11	5	<30							7.05									
T(M)	4/6/1996	0.09	2	<30							7.21									
T(M)	11/19/1997									969	7.34									
T(M)	11/11/1999	0.0962	5	<10						974	7.07									
T(M)	11/11/2000	0.117	6	27.6						1307	6.93									
T(M)	11/18/2004	0.17	19	35						1710	7.16									-4.6
T(M)	5/24/2005									1701	7.13									37
T(M)	11/15/2005									1698	6.96									-56
T(M)	11/28/2006									1741	7.25									91.4
T(M)	11/6/2007	0.24	8.5	29						1683	7.28									178
T(M)	11/4/2008	0.31	5.4	29				57	252.5	1689	7.1									99
T(M)	5/13/2009	0.32						48	212.6	1635	6.89									-4.4
T(M)	11/10/2009	0.41	4.1	30	4	290	58	66	292.4	1753	6.88		<20		110	30	210	5.3		105.7
T(M)	11/9/2010	0.557	4.31	26.1	3.08	264	47.9	52	230.4	1738	6.71	388	<0.725		116	31.4	238	4.89	1.28	-84
T(M)	4/12/2011	0.512				275	46.4	59.5	263.6	1725	6.86									155.8
T(M)	7/26/2011	0.53	2.6	24	3.4	250	46	49	217.1	1679	6.94		<20		120	32	200	5.9		95.2
T(M)	11/16/2011	0.531	2.79	24.9	2.16	241	37.7	53.5	237.0	1718	7.05	405	<0.725		120	32.7	222	5.15	1.24	127.5
T(M)	5/15/2012	0.55	3.7	23	3	220	36	47	208.2	1673	6.99		<20		120	30	180	5.5	1.21	63.3
U(M)	3/12/1984					1203	675	5.35	23.7	2680	7.24									
U(M)	4/17/1984	0.711				1192	870	15.4	68.2	3850	6.93				395	84	680	13		
U(M)	4/17/1986	0.4645	<10			689	298	10	45	2800	7.2				189	60	455	16		
U(M)	7/7/1986	0.393				674	268	10	45	2600	7.15									
U(M)	10/13/1986	0.403				674	255	9	40	2600	7.18									
U(M)	2/3/1987	0.402				588	222	7.7	34	2450	7.35									
U(M)	4/8/1987	0.409	6			570	194	9.7	43	2400	7.3				150	39	370	7		
U(M)	7/7/1987	0.466				540	216	8.8	39	2600	7.36									
U(M)	10/7/1987	0.422				497	192	9	40	2580	7.31									
U(M)	1/11/1988	0.393				540	184	9	40	2200	7.41									
U(M)	4/6/1988	0.277	11			510	162	10	46	2050	7.31				120	33	300	6.7		
U(M)	7/11/1988	0.393				463	150	11	50	1900	7.44									
U(M)	10/5/1988	0.335				526	157	9.7	43	1900	7.43									
U(M)	1/18/1989	0.524				470	140	7.7	34	1850	7.57									
U(M)	4/11/1989	0.335	9	12.0		430	130	7.88	34.9	1700	7.35				110	27	300	6.3		
U(M)	4/9/1990	0.306	13	19.0		430	130	9.19	40.7	1420	7.08				100	28	270	9		
X(M)	3/12/1984					1332	1160	34.3	152	2980	7.21									
X(M)	4/17/1984	0.319				1448	995	34.3	152	4470	7.18				485	146	630	11.3		
X(M)	4/17/1986	0.2957	<10			1073	762	20	87.0	3950	7.2				393	117	577	18		
X(M)	7/7/1986	0.266				1029	774	22	96.0	3650	7.22									
X(M)	10/6/1986	0.304				952	475	19	84.0	3650	7.22									
X(M)	2/3/1987	0.287				871	409	14	64.0	3350	7.34									
X(M)	4/8/1987	0.298	<5			850	350	19	84.0	3300	7.29				350	64	430	7		
X(M)	7/7/1987	0.364				786	376	16	71.0	3350	7.35									
X(M)	10/5/1987	0.247				779	344	16	71.0	3300	7.39									
X(M)	1/11/1988	0.277				722	340	16	71.0	2950	7.45									
X(M)	4/6/1988	0.378	<5			666	310	17	75.0	2800	7.21				190	47	370	6		

Table C.2-2. Water Quality Data for Bluewater Site Alluvial and Chinle Aquifer Wells

Sample ID	Date Sampled	U (mg/L)	Se (µg/L)	Mo (µg/L)	As (µg/L)	SO_4 (mg/L)	Cl (mg/L)	NO_3+NO_2 as N (mg/L)	Nitrate as NO_3 (mg/L)	SC (µS/cm)	pH (s.u.)	Alkalinity, Bicarbonate (as $CaCO_3$)	Alkalinity, Carbonate (as $CaCO_3$)	Alkalinity, Total (as $CaCO_3$)	Ca (mg/L)	Mg (mg/L)	Na (mg/L)	K (mg/L)	DO (mg/L)	ORP (mV)
X(M)	7/11/1988	0.262				672	320	12	52.0	2700	7.35									
X(M)	10/5/1988	0.364				678	330	17	74.0	2650	7.57									
X(M)	1/18/1989	0.393				680	280	13	57.0	2500	7.55									
X(M)	4/17/1989	0.32	5	<5		620	280	14	61.8	2400	7.33				190	38	360	6.6		
X(M)	4/11/1990	0.146	11	<5		950	380	17	75	2400	7.23				270	82	370	11		
X(M)	11/15/2012	0.134	7.32	0.702	<1.7	499	192	9.8	43.4	1795	7.43	230	<0.725		163	45.9	186	5.49	4.22	142.8
X(M)	1/29/2013	0.139	6.35	0.754	2.03	495	199	11.1	49.2	1836	7.56	224	<0.725		159	44.5	197	5.41	2.99	85.4
X(M)	11/19/2013	0.145	6.59	1.81	<1.7	504	195	8.71	38.6	1920	7.69			200	165	46.7	183	5.49	3.07	18.9
Y2(M)	11/19/1997									678	7.14									
Y2(M)	11/11/1999									700	7.84									
Y2(M)	11/11/2000									724	7.01									
Y2(M)	11/3/2001									681	7.6									
Y2(M)	10/17/2002									734	7.61									
Y2(M)	9/19/2003									588	7.43									
Y2(M)	9/26/2003									586	7.42									
Y2(M)	11/18/2004									620	7.46									227
Y2(M)	11/15/2005									635	7.43									-13.4
Y2(M)	11/28/2006									641	7.6									-60.4
Y2(M)	11/6/2007									599	7.63									150.3
Y2(M)	11/4/2008							1.2	5.3	641	7.5									83.5
Y2(M)	5/13/2009	0.005						1.1	4.9	587	7.35									18.1
Y2(M)	11/10/2009	0.005	0.64	3	1.2	110	7	0.62	2.7	552	8.14		<20		77	18	14	2.6		79.4
Y2(M)	11/11/2010	0.005	1.31	1.57	3.64	96.1	15.8	1.42	6.3	740	7.67	194	<0.725		59.3	16.2	56.5	3.33	5.48	-104
Y2(M)	7/28/2011	0.005	1.2	1.6	1.5	98	17	1.4	6.2	630	7.52		<20		61	17	47	3.1		80
Y2(M)	11/15/2011	0.005	1.75	1.68	<1.7	92.2	13.6	0.494	2.2	642	7.59	201	<0.725		65	17.8	53	3.67	5.57	140.5
Y2(M)	5/15/2012	0.005	1.0	1.6	1.3	92	14	1.3	5.8	648	7.57		<20		62	17	48	3.1	5.61	160.6
Y2(M)	11/14/2012	0.005	<1.5	1.71	<1.7	99.9	15.2	1.52	6.7	718	7.45	206	<0.725		58.2	16.6	52.3	3.21	5	33.3
Y2(M)	1/30/2013	0.005	<1.5	1.61	<1.7	97	14.4	1.39	6.2	617	7.54	208	<0.725		62.1	17.8	55	3.24	6.23	11.1
Y2(M)	5/14/2013	0.005	2.17	1.76	<1.7	100	15.6	1.54	6.8	640	7.25	201	<0.725		63.1	18	55.8	3.17	5.42	107.1
Y2(M)	11/19/2013	0.005	<1.5	2.55	<1.7	101	17.3	1.66	7.4	643	7.63			205	56.5	16.6	54.1	2.92	5.89	-29

Note:
Berryhill House and location B00168 correspond to the same location; original nomenclature used in historical records.

Table C.2-3. Uranium Isotope Results for Bluewater Site Region Based on DOE and NMED Sampling

Bluewater Site Wells

Fm	Well ID	NMED ID	Data Source	Date Sampled	Uranium (mg/L)	U-234 (pCi/L)	U-235/236 (pCi/L)	U-238 (pCi/L)	U-234/U-238 Activity Ratio
AL	20(M)		DOE	11/19/2013	0.0139	6.58	0.418	4.66	1.41
AL	21(M)		DOE	7/27/2011	0.13	46.5	2	43	1.08
AL	21(M)		DOE	11/19/2013	0.137	46.1	1.9	40.4	1.14
AL	22(M)		DOE	7/27/2011	0.33	117	5.4	116	1.01
AL	22(M)		DOE	11/19/2013	0.388	122	4.77	118	1.03
AL	23(M)		DOE	11/19/2013	0.0209	8.95	0.587	6.24	1.43
AL	E(M)		DOE	11/11/2010	<0.00005	<0.234	<0.0647	<0.167	--
AL	E(M)		DOE	7/27/2011	0.00038	<0.0673	<0.034	<0.045	--
AL	E(M)		DOE	11/19/2013	<0.000067	<0.113	<0.139	<0.113	--
AL	F(M)		DOE	11/10/2010	0.00806	4.19	<0.15	2.95	1.42
AL	F(M)		DOE	7/28/2011	0.0074	3.4	0.123	2.44	1.39
AL	F(M)		DOE	11/19/2013	0.00734	3.2	<0.189	2.53	1.26
AL	T(M)		DOE	11/9/2010	0.557	161	7.61	169	0.95
AL	T(M)		DOE	7/26/2011	0.53	176	9.7	182	0.97
AL	X(M)		DOE	11/19/2013	0.145	47.8	1.77	44.8	1.07
AL	Y2(M)		DOE	11/11/2010	0.00519	2.56	<0.162	1.7	1.51
AL	Y2(M)		DOE	7/28/2011	0.0048	2.61	0.101	1.63	1.60
AL	Y2(M)		DOE	11/19/2013	0.0053	2.97	<0.288	1.94	1.53
SA	11(SG)		DOE	11/19/2013	0.0117	5.73	<0.19	3.61	1.59
SA	13(SG)		DOE	11/19/2013	0.0985	37.8	1.86	35.4	1.07
SA	14(SG)		DOE	11/19/2013	0.0741	26.9	0.971	23.8	1.13
SA	15(SG)		DOE	11/19/2013	0.174	60.2	2.71	55.8	1.08
SA	16(SG)		DOE	11/19/2013	1.4	381	19.6	401	0.95
SA	18(SG)		DOE	11/19/2013	0.127	44.7	1.45	44.1	1.01
SA	HMC-951	BW-34	NMED 2010	8/27/2008	0.053	13.5	0.5	12.3	1.10
SA	HMC-951		DOE	11/20/2013	0.031	12	0.518	11	1.09
SA	I(SG)	BW-28	NMED 2010	8/27/2008	<0.002	0.4	−0.01	0.04	--
SA	I(SG)		DOE	11/11/2010	0.0027	1.48	<0.0682	1.4	1.06
SA	I(SG)		DOE	7/27/2011	0.0011	0.476	<0.054	0.449	1.06
SA	I(SG)		DOE	11/19/2013	0.346	53.4	3.06	54	0.99
SA	I(SG)		DOE	11/19/2013	0.149	49.9	2.48	49.1	1.02
SA	I(SG)		DOE	11/19/2013	0.334	110	4.98	106	1.04
SA	I(SG)		DOE	11/19/2013	0.324	105	5.74	103	1.02
SA	L(SG)	BW-25	NMED 2010	8/27/2008	<0.002	0.01	0.0008	-0.03	--
SA	L(SG)		DOE	11/11/2010	<0.00005	<0.133	<0.165	<0.0523	--
SA	L(SG)		DOE	7/27/2011	0.0032	1.85	0.108	1.11	1.67
SA	L(SG)		DOE	11/19/2013	0.00294	1.33	<0.141	1.2	1.11
SA	OBS-3	BW-27	NMED 2010	8/27/2008	<0.002	0.06	0.08	7.61	
SA	OBS-3 (255-ft)		DOE	11/10/2010	0.0011	0.422	<0.2	0.456	0.93
SA	OBS-3 (325-ft)		DOE	11/10/2010	0.000648	0.526	<0.17	0.558	0.94
SA	OBS-3		DOE	7/28/2011	0.12	37.2	2.35	39.8	0.93
SA	OBS-3		DOE	11/20/2013	0.00931	3.05	<0.273	2.56	1.19
SA	S(SG)	BW-26	NMED 2010	8/27/2008	<0.002	0.4	−0.1	0.2	
SA	S(SG)		DOE	11/9/2010	<0.00005	<0.134	<0.065	<0.0876	
SA	S(SG)		DOE	7/26/2011	0.26	71	4.5	77.4	0.92
SA	S(SG)		DOE	11/20/2013	0.525	163	7.52	176	0.93

Fm Formation
AL Alluvium
SA San Andres

Note:
As discussed in the Site Status Report, uranium concentrations reported for S(SG) (BW-26) , OBS-3 (BW-27), and I(SG) (BW-28) are suspect, as uranium concentrations in San Andres aquifer wells in this region are known to be higher. Results for well 16(SG), averaging ≈ 1 mg/L uranium, are considered more characteristic of this region.

Table C.2-3. Uranium Isotope Results for Bluewater Site Region Based on DOE and NMED Sampling

Other NMED Results

Fm	Well ID	NMED ID	Data Source:	Date Sampled	Uranium (mg/L)	U-234 (pCi/L)	U-235/236 (pCi/L)	U-238 (pCi/L)	U-234/U-238 Activity Ratio
AL	HMC-914	SMC-10	NMED 2010	3/30/2009	0.0309	0.1	0.01	0.04	2.5
AL	HMC-920	SMC-11	NMED 2010	3/31/2009	0.228	78.1	2.8	63	1.24
AL	HMC-950	SMC-12	NMED 2010	3/31/2009	0.163	61.9 [54.6]	2.3	52 [44.8]	1.19
AL	HMC-921	SMC-13	NMED 2010	4/2/2009	0.24	75.8	3.2	64.3	1.18
SA	BW-05	BW-05	NMED 2010	8/25/2008	0.0105	6.4	0.07	3.0	2.13
SA	BW-14	BW-14	NMED 2010	8/27/2008	0.0105	13.8	0.08	3.4	4.06
SA	HMC-911	BW-15	NMED 2010	8/25/2008	0.012	4.5	0.1	2.8	1.61
SA	HMC-949	BW-23	NMED 2010	8/25/2008	0.0138	7.1	0.4	4.3	1.65
SA	BW-24	BW-24	NMED 2010	8/25/2008	0.0109	14.4	0.1	3.2	4.50
SA	HMC #1 Deepwell	BW-29	NMED 2010	8/27/2008	0.0089			0.3	
SA	HMC-928	BW-32	NMED 2010	9/16/2008	0.029	22.9	0.5	11.0	2.08
UNK	SMC-04	SMC-04	NMED 2010	3/31/2009	0.0206	[11.1]		[5.61]	1.98
UNK	SMC-08	SMC-08	NMED 2010	3/30/2009	<0.002	3.9	0.2	2.8	--

Fm Formation
AL Alluvium
SA San Andres
UNK Unknown

NMED results for SMC samples in brackets are SLD radiochemical data (NMED 2010; Table 10)

Table C.2-4. Water Quality Data for San Andres Aquifer Wells from Hydro-Search 1981

Well ID	HS Map No.	Date	U (mg/L)	pH (s.u.)	TDS (mg/L)	EC (mg/L)	HCO_3 (mg/L)	CO_3 (mg/L)	Cl (mg/L)	SO_4 (mg/L)	NO_3 (mg/L)	Na (mg/L)	K (mg/L)	Ca (mg/L)	Mg (mg/L)	As (mg/L)	Fe (mg/L)	Mo (mg/L)	Se (mg/L)
Berryhill Sec. 5	12	10/1/1957							226	621	1.0								
Berryhill Sec. 5	12	5/28/1960		7.7	2269	2500	682	Nil	241	686	4.0	350		230	76.0				
Berryhill Sec. 5	12	7/26/1980	<0.01	7.3	2270	2910	745	Nil	250	625	<0.1	330	17.0	230	62.0	ND	11	ND	ND
North Well	14	Jun-56							126	553	3.0								
North Well	14	May-60			1768														
North Well	14	7/29/1980	0.02	7.2	1871	2460	509	Nil	186	680	0.9	175	11.0	200	95	ND	0.5	ND	ND
Monitor Well	15	7/23/1980	0.30	7.4	2532	3290	510	Nil	350	895	4.0	315	17	330	96	ND	0.14	ND	ND
Bowlins	16	7/17/1980	<0.01	6.9	2207	2530	472	Nil	123	983	3.5	250	12.0	269	80.0	ND	0.03	ND	ND
C(SG)	17	1/10/1981	0.08	7.8	1344	1600	255	Nil	150	530	13.3	180	14	135	55	ND	0.01	ND	ND
G(SG)	19	1/10/1981	3.5	6.9	5734	6550	500	Nil	1050	2400	53.1	840	29.0	560	275	ND	1.4	ND	ND
Allen Payne	20	7/22/1980	<0.01	7.5	926	1140	287	Nil	89	275	8.9	59	3.3	134	44	ND	ND	ND	ND
Anaconda #1	21	Apr-52							70	380	15								
Anaconda #1	21	May-57			1167														
Anaconda #2	22	7/18/1956		7.4	1086	1330	351	Nil	60	351	19		105.0	142	42				
Anaconda #2	22	11/20/1980	0.24	7.2	1776	1960	535	Nil	135	570	37.2	210	10	195	66	ND	0.02	ND	ND
Bluewater Municipal	23	May-61		7.2	1150	1400	320	Nil	57	379	80	80		185	49				
Bluewater Municipal	23	7/23/1980	<0.01	7.4	1007	1210	331	Nil	40	350	14.2	50	3.3	155	45	0.01	ND	ND	ND
Roundy Corral	24	7/25/1980	<0.01	7.4	1087	1310	363	Nil	48	360	14.2	66	3.7	165	49	ND	0.01	ND	ND
Anaconda #3	25	7/11/1946			1100	1320	366	Nil	57	356	29		95	147	49				
Anaconda #3	25	7/22/1980	<0.01	7.6	883	1100	306	Nil	36	280	11.5	63	3.3	125	40	ND	ND	ND	ND
Anaconda #4	26	9/27/1961		7.4	988	1325	340	Nil	48.0	321	27	60		150	42				
Anaconda #4	26	10/22/1980	<0.01	7.5	893	1120	307	Nil	30	287	26.6	60	3.2	126	35	ND	ND	ND	ND
Mexican Camp	27	Jul-56							16	134	32								
Mexican Camp	27	May-60			585														
Mexican Camp	27	10/22/1980	<0.01	7.5	649	798	289	Nil	18	162	7.1	45	2.7	89	26	ND	ND	ND	ND
Sabre-Piñon (now HMC-951)	28	Mar-59							89	232	5								
Sabre-Piñon (now HMC-951)	28	7/25/1980	<0.01	7.5	965	1220	306	Nil	66	300	20.4	52.0	3.0	155	44	ND	ND	ND	ND
Sturges Irrigation	29	1945			997		386	Nil	46	300	26		6	158	75				
Sturges Irrigation	29	11/18/1980		7.6	1053	1200	380	Nil	41	318	36	33	2	180	45				
Dalton	30	7/25/1980	<0.01	7.4	716	864	287	Nil	16	200	21.7	39	2.0	96	38	ND	0.03	ND	ND
Hardenburg Commissary	31	7/23/1980	<0.01	7.6	712	826	268	Nil	12	230	7.5	49	2.0	88	39	ND	ND	ND	ND
AN-5	AN-5	1/9/1981	0.33	7.5	2071	2420	335	Nil	270	790	57.5	275	17.0	240	68	ND	0.14	ND	ND
I(SG)	I(SG)	10/24/1980	0.35	7.1	3066	3730	491	Nil	365	1290	28.8	380	28	320	146	ND	ND	ND	ND
L(SG)	L(SG)	1/20/1981		7.2	1952	2380	600	Nil	180	605	1.3	270	21.0	190	71	ND	0.05	ND	ND
M(SG)	M(SG)	3/26/1981		7.7	1640	1810	420	Nil	105	640	4.4	180	18.0	205	51	ND	0.04	ND	ND
OBS-2	OBS-2	2/6/1981		7.7	5293	6490	450	Nil	1140	2040	41.2	805	28	515	250	ND	0.07	ND	ND
OBS-3	OBS-3	2/7/1981		7.3	4413	6690	415	Nil	810	1880	28.8	540	24	505	190	ND	0.07	ND	ND
S(SG)	S(SG)	1/28/1981		7.8	5077	6270	490	Nil	895	2110	48.7	700	29	560	220	ND	0.06	ND	ND
Roundy Sec. 23	S-1	7/12/1946			2523	3040	702	Nil	270	829	0.6		379	254	88				
Roundy Sec. 23	S-1	7/9/1980	0.05	7.7	1399	1930	333	Nil	49	567	1.3	390	9.0	31	5.4	ND	0.01	ND	0.002
Roundy Sec. 23	S-1	1/12/1981		7.0	2171	2460	520	Nil	180	810	0.4	430	16	155	44	ND	0.06	ND	ND
United Nuclear Sec. 8B	S-12	7/11/1946			468	581	225	Nil	8.0	122	0.7	20		60	32				
United Nuclear Sec. 8B	S-12	7/24/1980	<0.01	7.5	468	556	223	Nil	5.0	115	2.2	23.0	1.7	46	30	ND	ND	ND	ND

Table C.2-4. Water Quality Data for San Andres Aquifer Wells from Hydro-Search 1981

Well ID	HS Map No.	Date	U (mg/L)	pH (s.u.)	TDS (mg/L)	EC (mg/L)	HCO_3 (mg/L)	CO_3 (mg/L)	Cl (mg/L)	SO_4 (mg/L)	NO_3 (mg/L)	Na (mg/L)	K (mg/L)	Ca (mg/L)	Mg (mg/L)	As (mg/L)	Fe (mg/L)	Mo (mg/L)	Se (mg/L)
Gallup Stake Irrigation Sec. 4B	S-14	7/22/1980	<0.01	7.5	1052	1270	299	Nil	39.0	400	14.2	66	3.3	142	54	ND	ND	ND	ND
Murray Ac. Irr.	S-2	7/10/1980	<0.01	7.3	1582	1900	393	Nil	109	600	10.6	190	11	195	57	ND	0.01	ND	0.004
N.M. Highway Department	S-22	7/17/1980	<0.01	7.4	532	671	224	Nil	7.7	153	<0.1	25.0	2.0	67	34	ND	ND	ND	ND
Jack Freas	S-35	7/12/1980	<0.01	7.4	664	836	248	Nil	25	197	9.3	39	2.7	93	35	ND	0.01	ND	0.002
Hanosh	S-49	7/12/1980	<0.01	7.4	471	576	248	Nil	8.4	80	4.4	21	1.7	61	26	ND	0.02	ND	ND
Siemons	S-5	7/12/1980	0.02	7.0	1614	1950	448	Nil	111	575	8.4	190	12	198	55	ND	0.04	ND	0.003
Thornton	S-50	7/16/1980	<0.01	7.6	721	838	254	Nil	19	240	8.4	38	2.7	105	34	ND	0.02	ND	ND
Guthrie	S-51	7/10/1980	<0.01	7.2	1140	1420	333	Nil	61	414	5.8	91	7.0	166	47	ND	0.02	ND	ND
Grants #1	S-65	9/27/1977	<0.01	7.7	816	1068	298	Nil	36.2	260.3	6.1	64.4	4.3	111.2	35.1	0.01	0.01	ND	0.01
Grants #1	S-65	7/24/1980	<0.01	7.5	947	1180	338	Nil	50	280	3.1	80	3.7	130	40	ND	0.01	ND	ND
Grants #3	S-66	11/15/1978		7.7	776	998	291.3	Nil	30.5	241.5	6.1	57.5	3.5	110.4	34.9	0.01	ND	ND	0.03
Grants #3	S-66	7/24/1980	0.14	7.5	820	999	293	Nil	30	260	3.5	59	2.7	110	40	ND	ND	ND	ND
Bell HQ	S-68	7/25/1980	<0.01	7.4	476	552	229	Nil	<3	115	0.9	23	1.7	55	31	ND	ND	ND	ND
Bluewater (Auro's) Motel	S-70	10/23/1980	<0.01	7.6	708	848	327	Nil	10	167	4	39	2	112	21	ND	ND	ND	ND
UN-HP #2	S-71	10/23/1980	<0.01	7.4	1927	2340	558	Nil	139	669	3.5	259	13	207	62	ND	ND	ND	ND
UN-HP #1	S-72	10/23/1980	0.02	7.0	2217	2680	614	Nil	358	569	2.2	330	24	244	59	ND	ND	ND	ND
Roundy (Harmon) House	S-74	6/4/1947			653	794	305	Nil	12	158	18		9.4	121	30				
Roundy (Harmon) House	S-74	10/30/1980	<0.01	7.3	1489	1560	421	Nil	63	490	32.3	63	3.2	251	43	ND	ND	ND	ND
Blue Well	S-75	11/14/1980	<0.01	7.4	1605	1800	414	Nil	91	627	4.4	190	14	215	37	ND	0.05	ND	ND
Dow	S-8	7/16/1980	<0.01	7.3	944	1220	387	Nil	18	261	7.5	39	3.3	169	29	ND	ND	ND	ND
W(SG)	W(SG)	1/17/1981	0.04	7.3	2184	2510	355	Nil	205	940	53.1	265	16	250	82	ND	0.02	ND	ND

ND Not Detected

Source:
Tables 2 through 4 of Hydro-Search (HSI), 1981. *Regional Ground-Water Hydrology and Water Chemistry, Grants- Bluewater area, Valencia County, New Mexico*, prepared for Anaconda Copper Company, June 30. EC units reported by HSI as mg/L but assumed here to be µmhos/cm.
These data are tabulated separetely because they were used as the basis for characterizations of early (1980-1981) contaminant (uranium) distributions in the Site Status Report.

Table C.2-5. Water Quality Data for Alluvial Aquifer Wells from Hydro-Search 1981

Well ID	HS Map No.	Date	U (mg/L)	pH (s.u.)	TDS (mg/L)	EC (mg/L)	HCO_3 (mg/L)	CO_3 (mg/L)	Cl (mg/L)	SO_4 (mg/L)	NO_3 (mg/L)	Na (mg/L)	K (mg/L)	Ca (mg/L)	Mg (mg/L)	As (mg/L)	Fe (mg/L)	Mo (mg/L)	Se (mg/L)
Berryhill House	1	Jun-56							32	258	16								
Berryhill House	1	May-60			949														
Berryhill House	1	7/23/1980	<0.01	7.5	1048	1370	287	Nil	68	375	11.1	65	3.3	150	54	ND	ND	ND	ND
Engineers	2	6/7/1957		7.5	692	1020	264	Nil	17	211	6.6	33		102	34				
Engineers	2	7/23/1980	0.06	7.7	1009	1190	287	Nil	64	350	12	80	3.7	145	35	ND	ND	ND	ND
Aragon	3	7/23/1980	<0.01	7.4	945	1130	312	Nil	54	300	8.9	38	2.7	160	46	ND	ND	ND	ND
Roundy-Up	4	7/17/1980	<0.01	7.4	940	1170	278	Nil	40	346	8.4	43	3.3	159	40	0.01	0.02	ND	ND
B(M)	5	3/3/1977	3.3	7.7	9265	12500	551	Nil	2802	2779	79.3	1710	25.3	790	498	ND	0.01	ND	0.034
B(M)	5	7/22/1980	3.1	7.2	10762	15000	656	Nil	3000	3550	44.3	2000	50	920	512	ND	0.04	ND	ND
C(M)	6	11/20/1980	0.22	7.0	1274	1540	315	Nil	115	450	8.0	140	7	170	37	ND	0.08	ND	0.002
E(M)	8	7/22/1980	0.04	7.5	884	1170	236	Nil	100	280	8.9	56	3.0	115	59	ND	ND	ND	ND
F(M)	9	7/22/1980	<0.01	7.5	707	880	236	Nil	36	220	9.7	20	2.3	110	39	ND	0.2	ND	ND
Simpson	10	Jun-56							24	178	26								
Simpson	10	Nov-56			707														
Simpson	10	10/22/1980	<0.01	7.5	1101	1330	298	Nil	46	419	36.7	43	2.7	197	38	ND	ND	ND	0.003
Card Abandoned	11	10/24/1980	0.02	7.5	1487	1870	231	Nil	58	727	34.5	181	6.5	180	43	ND	ND	ND	ND
K(M)	9	11/6/1980		7.5	5283	8260	245	Nil	1320	1960	79.7	910	18	549	178	ND	0.07	ND	ND
T(M)	T(M)	12/19/1980	1.62	7.0	8264	11500	320	Nil	1620	3450	106.2	1900	100	600	140	0.02	0.12	0.02	0.003
U(M)	U(M)	12/19/1980	0.36	7.5	1495	1740	315	Nil	115	565	62	155	10	215	30	ND	0.02	ND	ND
X(M)	X(M)	1/18/1981	0.06	7.6	2387	3050	300	Nil	390	850	133.0	335	16	280	56	ND	0.03	ND	ND
Gallup Stake Domestic	S-27	7/11/1980	<0.01	7.3	997	1190	303	Nil	32	350	20.4	54	4.0	167	35	ND	ND	ND	ND
Milan B-23	S-28	3/28/1979		7.8	505	652	236	Nil	12	117.4	13.9	28	1.56	68.6	28				
Milan B-23	S-28	7/16/1980	<0.01	7.4	610	730	242	Nil	19	167	8.4	33	2.7	93	26	ND	ND	ND	ND
Holmes	S-41A	7/12/1980	<0.01	7.4	1079	1290	272	Nil	41	437	19	85	6	154	35	ND	0.01	ND	0.003
Pittard	S-46	11/12/1980	0.02	7.5	2230	2670	221	Nil	100.5	1210	30.6	330	8.5	249.5	56	ND	0.02	ND	ND
Cibola Sands	S-56	7/24/1980	<0.01	7.5	1838	2380	586	Nil	180	530	<0.1	220	10	210	77	ND	0.03	ND	ND
Milan B-24	S-63	6/7/1957		7.6	581	898	256	Nil	15	147	8.2	39		39	51				
Milan B-24	S-63	2/1/1978														ND		ND	0.005
Milan B-24	S-63	7/16/1980	<0.01	7.4	556	695	236	Nil	14	138	9.7	28	2.3	77	28	ND	0.03	ND	ND
Milan B-35	S-64	2/1/1978		7.87	701	924	261	Nil	20.3	215	18.3	36.8	3.12	103.6	42				
Milan B-35	S-64	7/16/1980	<0.01	7.4	778	902	260	Nil	23	260	16.8	41	3.0	120	30	ND	0.04	ND	ND
Urie	S-76	11/15/1980	1.16	7.5	3195	3360	414	Nil	144	1660	35.4	460	10	361	87	ND	0.06	ND	0.007
Crow	S-77	11/15/1980	0.10	7.4	2460	3080	315	Nil	140	1240	12.4	430	12	245	46	ND	ND	ND	ND
Clevenger	S-78	11/21/1980	0.03	7.6	1553	1940	315	Nil	55	700	17.3	210	6.5	195	30	ND	ND	ND	ND
Swierc	S-79	11/21/1980	0.05	7.7	1773	2120	325	Nil	69	820	26.6	310	7.0	155	36	ND	ND	ND	ND
Caudill	S-81	11/24/1980	1.26	7.5	2465	3100	365	Nil	120	1240	9.3	390	9.0	255	64	ND	0.02	ND	0.011
Roundy Sec. 12	S-82	May-60		7.7	1847	2000	243	Nil	57	1006	26	200		269	46				
Roundy Sec. 12	S-82	12/11/1980	0.09	7.4	3012	2940	225	Nil	84	1740	106	305	15	440	76	ND	0.04	ND	ND

ND Not Detected

Source:
Tables 2 through 4 of Hydro-Search (HSI), 1981. *Regional Ground-Water Hydrology and Water Chemistry, Grants- Bluewater area, Valencia County, New Mexico*, prepared for Anaconda Copper Company, June 30. EC units reported by HSI as mg/L but assumed here to be µmhos/cm.
These data are tabulated separetely because they were used as the basis for characterizations of early (1980-1981) contaminant (uranium) distributions in the Site Status Report.

This page intentionally left blank

Table C.2-6. Water Quality Data for Homestake Site and Distal San Andres Aquifer Wells

Well ID	Date	U (mg/l)	Mo (mg/l)	Se (mg/l)	SO_4 (mg/l)	NO_3 (mg/l)	pH (s.u.)	TDS (mg/l)	SC (µS/cm)	Ca (mg/l)	Mg (mg/l)	K (mg/l)	Na (mg/l)	HCO_3 (mg/l)	CO_3 (mg/l)	Cl (mg/l)	Ra-226 (pCi/l)
#1 Deepwell	5/22/1958				671	1.2		1790		214	74.0	0.0		617	<0.10	205	
#1 Deepwell	4/20/1979	0.21	0.22	0.03	649	0.86		1500						569		149	
#1 Deepwell	5/8/1980	<0.01	0.02	0.02	801	1.3	7.1	1575								191	1.5
#1 Deepwell	5/8/1980	<0.01	0.02	0.02	734	1.1	7.0	1800								206	0.9
#1 Deepwell	7/2/1980	<0.01	0.02	<0.01	714	<0.1	7.4		1261			0.0		651			1.9
#1 Deepwell	10/23/1980	0.02	<0.05	<0.00	569	2.2	7.0	2217		244	59.0	24.0	330	614		358	0.31
#1 Deepwell	5/11/1983	<0.01	0.01	<0.01	708	0.7	7.0	1920	2273			13.0	315	622		248	0.5
#1 Deepwell	12/20/1983	0.01	0.02	0.01	714	2.5	7.5	1780	2581			0.0		509		191	2.3
#1 Deepwell	3/21/1984	0.01	<0.00	0.01	779	12	7.2	1950	2778	305	61.0	16.0	310	633		213	2.4
#1 Deepwell	7/31/1984				730			2130	2607								
#1 Deepwell	9/28/1984	0.01	0.07	0.01	807	8.4	7.1	1990	2613	301	7.0	15.0	340	511	<0.00	206	0.2
#1 Deepwell	12/29/1984				734			2670									
#1 Deepwell	3/13/1985		<0.01	0.01	755	4.6	7.1	1520		284	31.0	10.0	260	540	<0.00	156	<0.01
#1 Deepwell	6/27/1985				709			3080	2378								
#1 Deepwell	9/13/1985	<0.01	<0.01	<0.01	782	6.0	7.0	1770		271	24.0	14.0	313	566	<0.00	184	1.5
#1 Deepwell	12/20/1985				730			2920									
#1 Deepwell	6/26/1986				742			1170									
#1 Deepwell	9/17/1986	<0.01	0.01	0.01	713	2.9	7.6	1680	2582	269	7.0	12.0	325	523	0.00	191	0.8
#1 Deepwell	1/8/1987				712			2920								149	
#1 Deepwell	3/30/1987	<0.01	0.01	0.01	743	0.9	7.7	1710		297	17.0	16.0	320	547	<10.00	213	1
#1 Deepwell	7/15/1987		0.01		802			1720	2938								
#1 Deepwell	9/30/1987	<0.01	0.01	<0.01	818	1.4	7.0	1890	2744	319	10.0	14.0	335	558	<10.00	206	2.3
#1 Deepwell	12/22/1987				963			3230	2470								
#1 Deepwell	1/21/1988				802			1890									
#1 Deepwell	3/29/1988	0.03	0.01	0.01	777	1.0	7.6	1730		271	6.0	15.0	358	488	<10.0	248	0.2
#1 Deepwell	6/15/1988		0.01		710			3330	2470								
#1 Deepwell	9/27/1988	0.04	0.01	<0.01	771	2.0	7.5	1880		284	10.0	15.0	338	412	<10.0	206	0.2
#1 Deepwell	12/8/1988				754			3300									
#1 Deepwell	6/21/1989				820			3670									
#1 Deepwell	11/29/1989				821			1940	2768								
#1 Deepwell	12/19/1989	0.02	<0.01	<0.01	773	0.2	7.0	1950	2756	318	37.0	14.0	373	650		213	<0.1
#1 Deepwell	2/15/1990				886			2000									
#1 Deepwell	5/9/1990	<0.01	<0.01	0.01	808	1.8	7.3	1990		314	9.0	7.0	352	603		199	0.4
#1 Deepwell	8/7/1990				754			1780									
#1 Deepwell	2/25/1991				1005			2070									
#1 Deepwell	5/22/1991	0.08	<0.01	<0.01	717	2	7.1	1900		297	18.0	14.0	317	561	<0.1	213	
#1 Deepwell	8/22/1991				701			1810									3.1
#1 Deepwell	11/6/1991				753			2010	2673								
#1 Deepwell	2/5/1992				711			2010									
#1 Deepwell	5/4/1992	0.03	0.01	0.01	844	1.7	7.2	1890		310	16.0	18.0	337	620		199	
#1 Deepwell	8/12/1992				708			1860	2572								2.7
#1 Deepwell	11/12/1992				795			1940	2464								
#1 Deepwell	3/2/1993				876			2020	2577								
#1 Deepwell	5/14/1993	0.02	<0.01	<0.01	709	1.7	7.4	1950	2481	269	22.0	14.0	337	575	<0.01	199	0.8
#1 Deepwell	9/1/1993	0.01		<0.00	736			1795	2526								

Table C.2-6. Water Quality Data for Homestake Site and Distal San Andres Aquifer Wells

Well ID	Date	U (mg/l)	Mo (mg/l)	Se (mg/l)	SO_4 (mg/l)	NO_3 (mg/l)	pH (s.u.)	TDS (mg/l)	SC (µS/cm)	Ca (mg/l)	Mg (mg/l)	K (mg/l)	Na (mg/l)	HCO_3 (mg/l)	CO_3 (mg/l)	Cl (mg/l)	Ra-226 (pCi/l)
#1 Deepwell	11/8/1993				660			1940	2552								
#1 Deepwell	2/9/1994				591			1653	2226								
#1 Deepwell	5/5/1994	0.02	<0.03	<0.01	823	<0.1	7.17	1890	2609	209	58.4	10.0	309	529	<0.1	200	1.3
#1 Deepwell	8/1/1994	0.02		<0.01	723			1806	2525								
#1 Deepwell	11/16/1994	0.01		<0.01	696			1948	2631	219	72.0	12.0	317				
#1 Deepwell	2/9/1995	0.01		<0.01	689			1970	2814								
#1 Deepwell	5/10/1995	0.03	<0.1	<0.01	580	<0.1	8.01	1716	2623	165	74.0	11.5	307	459	<0.10	215	<0.2
#1 Deepwell	8/16/1995	<0.01		<0.01	742			999	1822								
#1 Deepwell	11/15/1995	<0.01		0.01	390			1071	1711								
#1 Deepwell	2/15/1996	<0.01	<0.03	0.01	727	0.16	7.67	1999	3203	218	73.2	12.2	310	645	<0.10	222	0.7
#1 Deepwell	5/15/1996	0.014	<0.10	<0.01	751	<0.10	7.98	1720	2497	125	38.6	6.6	393	464	<0.10	148	6.4
#1 Deepwell	8/12/1996	0.011	<0.03	<0.005	733	0.35	7.77	2030		232	73.1	12.3	322	627	<0.10	235	0.3
#1 Deepwell	10/30/1996	0.008	<0.03	<0.005	701	0.24	7.85	1810	2648	207	65.3	10.4	309	582	<0.10	210	1.4
#1 Deepwell	2/27/1997				440			1140	1822								
#1 Deepwell	4/29/1997	0.012	<0.1	<0.001	630	0.19	7.71	1910		193	61.7	10.4	303	608	0	183	0.8
#1 Deepwell	7/24/1997				641			1650	2367								
#1 Deepwell	11/3/1997	0.012			748			2010	2802								
#1 Deepwell	2/4/1998	0.013		<0.005	647			1860	2652								
#1 Deepwell	5/5/1998	0.01	<0.03	<0.005	681	0.33	7.91	1940		206	66.7	11.6	310	605	<1.0	214	0.4
#1 Deepwell	8/3/1998				641			1730	2443								
#1 Deepwell	10/28/1998				755			1970	2709								
#1 Deepwell	2/3/1999				811			1820	3081								
#1 Deepwell	5/11/1999				752			2070	31								
#1 Deepwell	8/17/1999				722			1980	2969								
#1 Deepwell	11/2/1999	0.0087	<0.03	<0.0010	763	0.38	8.25	2040	3160	164	65.9	12.6	267	469	<1.0	224	<0.200
#1 Deepwell	2/1/2000				744			2000	2759								
#1 Deepwell	4/27/2000	0.0101	<0.03	<0.005	716	0.41	7.62	2030	3013	225	74.2	13.1	302	635	<1.0	256	1.3
#1 Deepwell	8/2/2000				736			1780	2850								
#1 Deepwell	11/21/2000				718			1910	2846								
#1 Deepwell	5/16/2001	0.007	<0.03	<0.005	523	0.24	7.88	1660		169	65.6	11.8	232	445	<1.0	182	<0.200
#1 Deepwell	5/7/2002	0.011	<0.03	0.009	706	0.5	8	2000	2958	225	73.8	12.8	300			229	0.6
#1 Deepwell	5/13/2003	0.01	<0.03	0.007	713	0.5	7.87	1800	2898	232	78.5	12.5	281			228	1.4
#1 Deepwell	5/10/2004	0.0088	<0.03	<0.005	809	0.390	7.37	2130	2851	244	82.8	14.5	313			267	0.700
#1 Deepwell	4/5/2005	0.0072	<0.03	0.005	746	0.500	7.48	2000	2821	222	72.8	13.7	309			249	0.800
#1 Deepwell	10/10/2005	0.0090	<0.03	<0.005	703			2040	2815								
#1 Deepwell	5/23/2006	0.0095	<0.03	0.0050	759	0.800	8.19	2140	2870	234	76.0	14.2	320			307	1.50
#1 Deepwell	10/10/2006	0.0081	<0.03	0.0050	726			1950	2852								
#1 Deepwell	5/7/2007	0.0082	<0.03	0.0050	763	0.800	7.16	1980	2755	243	82.0	12.8	304			232	0.500
#1 Deepwell	10/1/2007	0.0100	<0.03	0.0060	682			1950									
#1 Deepwell	5/5/2008	0.0078	<0.03	<0.005	769	0.930	7.22	1900	2689	249	83.7	13.0	320			229	0.280
#1 Deepwell	8/27/2008	0.0073	<0.03	0.0130	738	1.000	7.47	1970	2751	244	80.6	12.8	318	585	<1.0	224	0.0400
#1 Deepwell	5/4/2009	0.0072	<0.03	<0.005	705	1.09	6.99	1980		226	74.1	11.4	293			221	0.41
#1 Deepwell	10/5/2009	0.0071	<0.03	<0.005	744			1990									
#1 Deepwell	3/30/2010	0.0089	<0.03	<0.005	730	1.10		1940	2795							223	
#1 Deepwell	5/3/2010	0.0076	<0.03	0.0070	758	1.10	7.20	1980	2792	229	75.7	13.3	323			238	0.230

Table C.2-6. Water Quality Data for Homestake Site and Distal San Andres Aquifer Wells

Well ID	Date	U (mg/l)	Mo (mg/l)	Se (mg/l)	SO_4 (mg/l)	NO_3 (mg/l)	pH (s.u.)	TDS (mg/l)	SC (µS/cm)	Ca (mg/l)	Mg (mg/l)	K (mg/l)	Na (mg/l)	HCO_3 (mg/l)	CO_3 (mg/l)	Cl (mg/l)	Ra-226 (pCi/l)
#1 Deepwell	10/6/2010	0.0086	<0.03	<0.005	736			2020	2807								
#1 Deepwell	5/9/2011	0.008	<0.03	0.006	747	1.1	7.43	1960	2758	233	75.3	13.1	312			236	0.44
#1 Deepwell	10/10/2011	0.0120	<0.03	<0.005	758			1930	2726								
#1 Deepwell	5/7/2012	0.0075	<0.03	<0.005	744	1.1	7.34	1970	2762	237	74.4	12.8	284			226	0.46
#1 Deepwell	10/2/2012	0.0090	<0.03	0.0050	777			2030	2769								
#1 Deepwell	5/6/2013	0.0095	<0.03	0.005	754	1.1	7.28	2040	2840	241	79.7	12.4	307			238	11
#1 Deepwell	11/5/2013	0.008	<0.03	<0.005	748			1990	2770								
#2 Deepwell	10/15/1956				467	3.2	7.0	1170		65.0	128	0.0		466	<0.10	106	
#2 Deepwell	9/16/1977	0.06	0.07	0.01	634.9	1.6	7.1	1275								141.8	5.6
#2 Deepwell	9/28/1977	0.06	0.08	0.03	644	1.9	7.1	1500								141.8	0.8
#2 Deepwell	10/14/1977	0.03	0.02	<0.01	659	1.6	6.9	1500								127.65	2.1
#2 Deepwell	10/28/1977	0.03	0.01	<0.01	641	1.9	7.5	1350								134.71	0.2
#2 Deepwell	11/10/1977	0.05	<0.10	<0.01	609	1.6	7.5	1275								145	0.6
#2 Deepwell	11/23/1977	0.05	0.05	0.01	621	1.4	7.3	1575								145	1.0
#2 Deepwell	12/8/1977	0.08	0.05	0.01	650	1.1	7.2	1200								135	0.6
#2 Deepwell	12/29/1977	0.08	0.04	0.01	608	1.2	8.2	1350								145	1.2
#2 Deepwell	1/11/1978	0.07	0.03	0.01	634	1.2	7.6	1275								142	2.0
#2 Deepwell	3/20/1978	0.03	0.01	<0.01	609	1.5	7.5	1500		135						163	1.6
#2 Deepwell	5/22/1978	0.19	<0.01	<0.01	614	2.1	7.2	1200				0.0		823.2		135	2.9
#2 Deepwell	7/24/1978	0.04	0.03	0.04	608	1.2	7.35	1350								142	1.6
#2 Deepwell	9/15/1978	0.02	0.03	0.02	652	1.2	7.8	1500								149	1.6
#2 Deepwell	11/10/1978	0.05	0.03	0.01	656	1.8	7.4	1425								92	2.9
#2 Deepwell	1/12/1979	<0.01	0.09	0.01	641	2.1	7.7	1350								142	1.5
#2 Deepwell	3/5/1979	0.06	0.11	0.03	654	1.8	8.2	1425								177	2.2
#2 Deepwell	5/4/1979	0.09	0.08	0.03	541	1.4	8.1	1397						553		135	1.6
#2 Deepwell	7/3/1979	0.10	0.10	0.08	602	1.35	8.0	975								148.9	1.3
#2 Deepwell	9/4/1979	0.08	0.13	0.01	617.7	1.35	7.7	1200								149	1.8
#2 Deepwell	11/2/1979	<0.01	0.06	0.01	642	1.2	7.1									490	0.2
#2 Deepwell	1/3/1980	<0.01	0.09	<0.01	616.8	1.2	7.5	1575								199	0.7
#2 Deepwell	3/3/1980	<0.01	0.05	<0.01	807	1.1	7.75	1500								160	1.1
#2 Deepwell	9/4/1980	<0.01	0.02	0.02	668	1.2	7.9	1050						549		135	0.6
#2 Deepwell	10/23/1980	<0.01	<0.05	<0.00	669	3.5	7.4	1927		207	62	13.0	259	558		139	0.36
#2 Deepwell	11/6/1980	<0.01	0.03	0.02	650	1.1	7.8	1050				0.0		523		156	1.1
#2 Deepwell	1/6/1981	<0.01	0.02	<0.01	659	5.6	7.25									149	1.0
#2 Deepwell	3/16/1981	<0.01	<0.01	0.02	653	1.0	7.7	1640				0.0				149	1.7
#2 Deepwell	5/4/1981	<0.01	0.02	<0.01	646	1.05	7.6	1680				0.0		602		57	1.4
#2 Deepwell	7/1/1981	<0.01	0.02	<0.01	656	1.1	7.4	1600				0.0		561		178	0.5
#2 Deepwell	9/16/1981	<0.01	0.03	<0.01	638	5.4	8.0	1510				0.0		563		170	3.8
#2 Deepwell	12/23/1981	<0.01	0.02	<0.01	662	1.2	8.0	1620				0.0		374		163	1.2
#2 Deepwell	3/1/1982	<0.01	0.03	<0.01	713	1.1	7.8	1690				0.0		553		163	1.3
#2 Deepwell	7/29/1982	<0.01	0.04	<0.01	713	1.0	8.5	1620				0.0		558		156	4.6
#2 Deepwell	1/25/1983	<0.01	<0.01	0.03	650	1.3	7.9	1660		240	26.0	15.4	250	549		92	1.0
#2 Deepwell	4/7/1983	<0.01	0.02	0.03	664	0.7	7.8	1670				0.0		531		104	2.4
#2 Deepwell	6/16/1983	<0.01	<0.01	0.01	666	1.3	7.0	1590				0.0		573		77	0.9
#2 Deepwell	12/21/1983	<0.01	0.02	0.01	670	2.1	7.4	1540	2578			0.0		481		156	0.6

Table C.2-6. Water Quality Data for Homestake Site and Distal San Andres Aquifer Wells

Well ID	Date	U (mg/l)	Mo (mg/l)	Se (mg/l)	SO_4 (mg/l)	NO_3 (mg/l)	pH (s.u.)	TDS (mg/l)	SC (µS/cm)	Ca (mg/l)	Mg (mg/l)	K (mg/l)	Na (mg/l)	HCO_3 (mg/l)	CO_3 (mg/l)	Cl (mg/l)	Ra-226 (pCi/l)
#2 Deepwell	3/22/1984	<0.01	0.01	0.01	669	6.2	7.8	1560	2125	250	49	14.0	245	549		156	0.9
#2 Deepwell	5/25/1984								2086								
#2 Deepwell	7/31/1984				629			1620	2193								
#2 Deepwell	9/24/1984	<0.01	0.02	0.01	702	13.1	7.3	1660	2384	298	6.0	14.0	260	437	<0.00	170	0.3
#2 Deepwell	12/29/1984				779			2430									
#2 Deepwell	3/13/1985	0.02	<0.01	0.02	762	4.1	7.1	1530		318	29.0	10.0	260	551	<0.00	156	0.5
#2 Deepwell	6/27/1985				702			3310	2346								
#2 Deepwell	9/12/1985	<0.01	<0.01	<0.01	682	7.8	7.0	1650		276	10.0	14.0	257	548	<0.00	156	1.8
#2 Deepwell	12/20/1985				675			3030									
#2 Deepwell	6/26/1986				718			1530									
#2 Deepwell	9/17/1986	<0.01	<0.01	0.02	707	5.4	7.7	1180	2384	279	10.0	13.0	275	471	<0.00	163	1.0
#2 Deepwell	1/9/1987				663			3090									
#2 Deepwell	7/15/1987	0.02			772			1730	2630								
#2 Deepwell	8/15/1987	0.02	0.01	0.01	772	2.7	7.0	1730		297	24.0	14.0	303	590	<10.0	203	0.3
#2 Deepwell	9/30/1987	0.01	0.01	0.01	806	2.5	7.3	1670	2360	298	2.0	14.0	295	449	<10.0	156	0.6
#2 Deepwell	12/22/1987				810			2950	2182								
#2 Deepwell	1/21/1988				815												
#2 Deepwell	2/21/1988							2460									
#2 Deepwell	3/29/1988	0.03	0.01		682	1.4	7.7	1440		234	22.0	15.0	287	468	<10.0	177	0.2
#2 Deepwell	6/15/1988				690			3510	2207								
#2 Deepwell	9/27/1988	0.17	0.01	<0.01	721	2.5	7.5	1500		279	15.0	14.0	278	421	<10.0	170	0.2
#2 Deepwell	12/8/1988				665			2820									
#2 Deepwell	6/21/1989				749			3680									
#2 Deepwell	12/19/1989	0.03	<0.01	<0.01	737	0.8	7.2	1850	2575	307	20.0	14.0	333	595	<10.0	191	<0.10
#2 Deepwell	2/15/1990				731			1720									
#2 Deepwell	5/9/1990	<0.01	<0.01	0.01	765	3.1	7.3	177.0		297	7.0	3.0	303	540		177	0.3
#2 Deepwell	8/7/1990				695			1700									
#2 Deepwell	11/27/1990				700			1730									
#2 Deepwell	2/25/1991				927			1820									
#2 Deepwell	5/22/1991	0.04	<0.01	<0.01	716	3.6	7.0	1850		308	22.0	14.0	285	572	<0.10	184	
#2 Deepwell	8/21/1991				711			1870									0.1
#2 Deepwell	11/6/1991				683			1840	2501								
#2 Deepwell	2/5/1992				711			1860									
#2 Deepwell	5/4/1992	0.02	0.01	0.01	831	3.3	7.4	1800		304	20.0	17.0	300	571	<0.10	184	
#2 Deepwell	8/12/1992				698			1830	2446								<0.20
#2 Deepwell	11/12/1992				823			1860	2361.55								
#2 Deepwell	3/3/1993				782			1870	2349.21								
#2 Deepwell	5/14/1993	0.05	<0.01	<0.01	669	3.5	7.5	1800	2308.99	269	26.0	15.0	277.0	536	<0.10	177	0.5
#2 Deepwell	9/1/1993	0.02		0.00	691			1761	2369.97								
#2 Deepwell	11/8/1993				633			1808	2363.58								
#2 Deepwell	2/9/1994				652			1777	2184.55								
#2 Deepwell	5/5/1994	0.05	<0.03	<0.01	768	1.96	7.06	1808	2411.62	222	64.1	10.1	257	487	<0.10	178	0.6
#2 Deepwell	8/1/1994	0.01		0.01	705			1714	2357.41								
#2 Deepwell	11/16/1994	0.01		<0.01	677			1799	2362.69	214	69.8	11.5	256				
#2 Deepwell	2/9/1995	0.01		<0.01	646			1790	2496.87								

Table C.2-6. Water Quality Data for Homestake Site and Distal San Andres Aquifer Wells

Well ID	Date	U (mg/l)	Mo (mg/l)	Se (mg/l)	SO_4 (mg/l)	NO_3 (mg/l)	pH (s.u.)	TDS (mg/l)	SC (µS/cm)	Ca (mg/l)	Mg (mg/l)	K (mg/l)	Na (mg/l)	HCO_3 (mg/l)	CO_3 (mg/l)	Cl (mg/l)	Ra-226 (pCi/l)
#2 Deepwell	5/10/1995	<0.01	<0.10	<0.01	649	1.44	8.02	1817		218	74.0	11.4	250.0	549	<0.10	192	0.6
#2 Deepwell	8/16/1995	0.02		<0.01	679			1813	2553.11								
#2 Deepwell	11/15/1995	0.01		<0.01	704			1869	2525.80								
#2 Deepwell	3/13/1996	0.012	<0.03	<0.01	823	1.73	7.59	1854		267	86.7	12.0	253.0	560	<0.10	244	<0.20
#2 Deepwell	5/14/1996	0.011	<0.10	<0.01	698	1.84	7.47	1836	2739	220	89.8	11.8	263	565	<0.10	196	2.4
#2 Deepwell	8/28/1996	0.019	<0.03	0.009	662			1860									
#2 Deepwell	10/24/1996	0.008	<0.03	0.009	700	1.96	8.01	1830	2647	228	72.6	11.8	264	555	<0.10	206	0.4
#2 Deepwell	2/27/1997				702			1800	2350								
#2 Deepwell	4/29/1997	0.011	<0.1	0.004	627	2.25	7.83	1850		214	67.8	11.2	246	539	0	181	0.8
#2 Deepwell	7/24/1997				1031			1850	2492								
#2 Deepwell	11/3/1997	0.025	0.007	0.006	730			1960	2699								
#2 Deepwell	2/4/1998	0.011		0.008	642			1850	2521								
#2 Deepwell	5/5/1998	0.012	<0.03	0.008	661	1.71	7.8	1850	2597	212	69.3	11.4	257	558	<1.0	195	0.3
#2 Deepwell	8/3/1998				697			1860	2475								
#2 Deepwell	10/28/1998				716			1790	2453								
#2 Deepwell	2/3/1999				732			1780	2619								
#2 Deepwell	5/11/1999				693			1810	2806								
#2 Deepwell	8/17/1999				704			1790									
#2 Deepwell	11/2/1999	0.0106	<0.03	<0.0010	684	2.05	8.16	1800	3055	161	64.4	11.7	226	384	<1.0	197	<0.200
#2 Deepwell	2/1/2000				688			1810	2480								
#2 Deepwell	4/27/2000	0.0119	<0.03	<0.005	654	2.39	7.79	1810	2840	210	69.1	12.1	237	529	<1.0	218	0.4
#2 Deepwell	8/1/2000				678			1920	2721								
#2 Deepwell	11/21/2000				693			1800	2766								
#2 Deepwell	5/2/2001	0.01	<0.03	0.009	603	3.17	7.79	1790		211	69.1	10.7	237	512	<1.0	189	<0.200
#2 Deepwell	5/7/2002	0.009	<0.03	0.01	646	2.58	8.1	1780	2792	215	69.7	11.6	236			198	<0.200
#2 Deepwell	5/13/2003	0.0113	<0.03	0.013	646	2.3	7.86	1770	2628	234	76.3	12	239			198	0.2
#2 Deepwell	5/10/2004	0.0109	<0.03	0.0070	693	2.61	7.53	1790	2449	218	73.5	12.3	230			211	<0.200
#2 Deepwell	4/5/2005	0.0091	<0.03	0.0120	666	2.40	7.71	1730	2395	206	68.4	11.40	230.0			212.0	0.5
#2 Deepwell	10/10/2005	0.0113	<0.03	0.0080	602			1800	2455								
#2 Deepwell	5/23/2006	0.0108	<0.03	0.0090	653	2.60	8.36	1970	2434	206	67.6	12.0	240			237	<0.200
#2 Deepwell	10/10/2006	0.0118	<0.03	0.0090	681			1770	2670								
#2 Deepwell	5/7/2007	0.0115	<0.03	0.0080	706	2.40	7.29	1780	2426	230	75.1	12.0	251			210	<0.200
#2 Deepwell	10/1/2007	0.0114	<0.03	0.0090	612			1720	2389								
#2 Deepwell	5/5/2008	0.0110	<0.03	0.0080	709	2.43	7.38	1660	2412	225	76.6	11.5	256			194	0.230
#2 Deepwell	8/27/2008	0.0155	<0.03	0.0070	719	4.80	7.51	1900	2549	251	81.8	12.1	272	512	<1.0	216	0.0700
#2 Deepwell	5/4/2009	0.0128	<0.03	0.007	720	2.18	7.18	1890		227	76.2	12.3	267			222	0.25
#2 Deepwell	10/5/2009	0.472	0.25	0.006	1050			2180									
#2 Deepwell	3/29/2010	0.0904	0.0400	0.0070	757	1.20		1920	2711							210	
#2 Deepwell	3/30/2010	0.0124	<0.03	0.0070	714	2.00		1860	2659							216	
#2 Deepwell	5/3/2010	0.0110	<0.03	0.0090	736	2.00	7.21	1890	2576	228	76.0	12.7	290			230	0.0800
#2 Deepwell	10/6/2010	0.0118	<0.03	0.0070	684			1890	2600								
#2 Deepwell	5/9/2011	0.0116	<0.03	0.0080	716	2.10	7.74	1820	2586	225	72.5	12.1	281			218	0.1100
#2 Deepwell	10/10/2011	0.0109	<0.03	0.0070	698			1770	2509								
#2 Deepwell	5/7/2012	0.0276	<0.03	0.0060	712	1.50	7.68	1840	2528	224	71.6	11.3	265			198	0.0600
#2 Deepwell	10/2/2012	0.0115	<0.03	0.0080	709			1840	2538								

Table C.2-6. Water Quality Data for Homestake Site and Distal San Andres Aquifer Wells

Well ID	Date	U (mg/l)	Mo (mg/l)	Se (mg/l)	SO_4 (mg/l)	NO_3 (mg/l)	pH (s.u.)	TDS (mg/l)	SC (µS/cm)	Ca (mg/l)	Mg (mg/l)	K (mg/l)	Na (mg/l)	HCO_3 (mg/l)	CO_3 (mg/l)	Cl (mg/l)	Ra-226 (pCi/l)
#2 Deepwell	5/6/2013	0.0122	<0.03	0.008	661	2.5	7.44	1790	2462	219	71.7	10.6	243			197	1.8
#2 Deepwell	11/4/2013	0.0108	<0.03	0.007	695			1800	2566								
534	7/24/1956				252	19.0	8.2					0.00		258	<0.10	28.0	
535	11/8/1995	0.02	<0.03	0.02	301	2.69	7.57	801	1154	143	34.0	3.2	77.0	322	<0.10	35.5	<0.2
545	5/6/2004	0.008	<0.03	0.0090	327	3.94	7.36	857	1178	155	43.4	2.50	56.5	423	<1.0	34.2	<0.200
806	7/25/1956				392	6.9	7.3					0.00		392.0	<0.10	72.0	
806	9/18/1981	<0.01	0.02	<0.01	617	3.6		1330				0.00		398.53			0.5
806	11/9/1994	0.012	<0.03	0.01	581	5.16	7.58	1500	1925	205	63.0	9.3	186	416	<0.10	168	0.3
806	7/24/1996	0.013	<0.03	0.008	578	4.06	8.06	1486	2190	200	62.8	9.1	182	404	<0.10	156	<0.2
806	11/12/1996	0.014	<0.03	0.008	585	4.5	7.79	1440	2217	210	64.1	9.0	176	399	<0.10	165	<0.2
806	9/2/1997	0.01	<0.03	0.007	592	4.42	7.95	1550	2063	212	63.4	9.2	184	406	<0.10	165	<0.2
806	8/10/1998	0.018	0.1	0.009	559	4.3	7.93	1500		197	61.7	8.8	179	406	<1.0	154	0.5
806	8/22/2000	0.018		0.008	498			1480	2304								
806	8/24/2001	0.018		0.011	540			1550	2178								
806	10/17/2002	0.015		0.01	566			1570	2673								
806	10/27/2003	0.015		<0.05	589			1570	2120								
806	4/21/2005	0.015	<0.03	<0.05	607	3.90	7.62	1510	2173	188	63.8	9.30	193	404	<1.0	193	0.300
806	11/18/2005	0.018		0.0090	1190			1460	2118								
806	10/4/2006	0.018	<0.03	0.0110	555	3.80		1530	2259							162	
806	10/2/2007	0.0184		0.0090	605			1570									
0806R	9/24/2008	0.0178	<0.03	0.008	634	4.10	7.13	1630	2258	234	76.8	9.90	211	423	<1.0	189	0.41
0806R	9/13/2010	0.0170		0.009	658			1660	2301								
0806R	4/14/2011	0.0203	<0.03	0.010	636	3.80	7.37	1650	2276	219	69.5	10.8	226	447	<5.0	191	0.33
0806R	10/18/2011	0.0274		0.017	635			1530	2291								
822	11/14/1988	<0.01	<0.01	<0.01	580	19.0	7.1	1400	2217	200	60	9.9	170	430	<0.10	150	0.3
822	8/23/1995	0.01	<0.03	0.01	592	3.18	7.34	1510	2174	185	59	8.9	230	442	<0.10	152	1.3
822	11/20/1996	0.096	<0.03	0.009	604	3.25	7.87	1490	2279	192	58.4	8	222	423	<0.10	149	6.1
907	8/5/1948													296	<0.10	28.0	
907	8/10/1953													296	<0.10	31.0	
907	6/15/1955						7.3							296	<0.10	33.0	
907	7/17/1956				291	14.0	7.5					0.00		286	<0.10	31.0	
907	6/7/1957				277	17.0	7.6							284	<0.10	31.0	
911	7/17/1956				253	15.0	7.5					0.00		261	<0.10	21.0	
911	6/7/1957				255	12.0	7.5					0.00		262	<0.10	22.0	
911	7/17/1996	0.016	<0.03	0.0080	300	5.1	7.61	869	946	134	37.3	3.5	67.6	298	<0.10	44.8	0.4
911	8/25/2008	0.010	<0.03	0.0150	336	4.2	7.80	823	1165	150	41.9	3.70	63.0	280	<1.0	38.0	-0.04
923	4/7/1993	0.44	0.01	0.01	960	15.47	6.78	2500	3729	290	110	14.0	320	480	<0.10	370	
923	10/11/1993	0.43	0.01	0.01	890	15.0	6.71	2300								350	
923	4/6/1994	0.35	<0.01	0.01	910	15.91	6.72	2850		300	120	13.0	340	500	<0.10	490	
928	7/12/1946				829	0.60		2170		254	88.00	0.00		702	<0.10	270	
928	6/4/1947				794									669	<0.10	238	
928	8/4/1948													688	<0.10	250	
928	8/18/1949													686	<0.10	254	
928	10/16/1950													668	<0.10	239	
928	6/25/1952													682	<0.10	245	

Table C.2-6. Water Quality Data for Homestake Site and Distal San Andres Aquifer Wells

Well ID	Date	U (mg/l)	Mo (mg/l)	Se (mg/l)	SO_4 (mg/l)	NO_3 (mg/l)	pH (s.u.)	TDS (mg/l)	SC (µS/cm)	Ca (mg/l)	Mg (mg/l)	K (mg/l)	Na (mg/l)	HCO_3 (mg/l)	CO_3 (mg/l)	Cl (mg/l)	Ra-226 (pCi/l)
928	8/25/1952													675	<0.10	250	
928	10/6/1954				604	<0.1						0.00		360	<0.10	53.0	
928	8/10/1955				772		6.8					0.00		656	<0.10	242	
928	7/12/1976				829	0.60		2520				0.00		702		270	
928	07/09/1980	0.04	<0.05	<0.01	567	1.3	7.7	1400				0.00		333		49	0.86
928	01/12/1981		<0.05	<0.01	810	0.4	7.0	2170				0.00		520		180	
928	11/15/1988	0.062	<0.01	<0.01	630	0.8	8.36	1200	2208	30.0	7.2	1.8	420	330	5.0	43.0	0.2
928	03/14/1994	0.086	<0.03	0.01	818	0.48	7.71	1618	2236	81.5	16.8	2	439	299	<0.10	47.3	<0.2
928	10/24/1994	0.078	<0.03	0.03	835	0.53	8.01	1652	2197	79.6	19.3	2.8	408	316	<0.10	45.7	<0.2
928	02/09/1995	0.033	<0.03	0.01	569	0.15	8.4	1182	1819	18.1	4.9	1.6	372	319	4.5	40.9	<0.2
928	3/8/1996	0.071	<0.03	0.20	861	0.50	8.03	1580	2384	81.4	20.2	2.7	381	317	<0.10	45.5	<0.2
928	10/23/1996	0.072	<0.03	0.02	774	0.62	8.19	1490	2271	67.2	16.2	2.4	403	250	<0.10	43.2	<0.2
928	09/02/1997	0.061	<0.03	0.018	823	0.53	8.12	1500	2271	93.2	21.4	2.9	392	315	<0.10	46.0	<0.2
928	8/27/1998	0.101	<0.03	0.14	826	0.74	8.13	1640	2297	83.4	20.3	3.0	416	307	<1.0	49.2	0.4
928	8/26/1999	0.0945		0.03	836			1640									
928	8/9/2000	0.106		0.034	790			1590	2844								
928	8/29/2001	0.086		0.036	810			1710	2889								
928	10/21/2002	0.087		0.042	799			1740	2973								
928	12/9/2004	0.0822		0.0350	892			1700	2359								
928	12/5/2005	0.0887		0.0390	849			1620	2330								
928	12/10/2006	0.0853		0.032	863			1680	2335								
928	12/3/2007	0.0823		0.0290	806			1650	2321								
928	9/15/2008	0.0400	<0.03	0.0140	599	0.200	8.00	1230		31.7	7.50	1.60	422	319	<1.0	39.0	0.130
928	9/16/2008	0.0330	<0.03	0.0110	585	0.100	8.24	1210	1842	23.0	5.70	1.60	436	318	<1.0	44.0	0.290
928	9/17/2008	0.0285	<0.03	0.0100	556	0.100	8.19	1180	1819	15.6	4.10	1.50	431	317	2.0	44.0	0.720
928	3/24/2009	0.0326	<0.03	0.011	639	0.2	7.96	1320		39	10.2	2.6	396	347	<1.0	57	0.02
928	10/12/2009	0.0572		0.018	742			1390									
928	12/7/2009	0.0474	<0.1	0.015	660			1270									
928	5/3/2010	0.0568		0.016	720			1360	2065								
928	6/3/2010	0.0291	<0.03	0.009	537	<0.100	7.94	1120		12.1	2.80	1.40	434	344	<5.0	40.0	0.0060
928	6/14/2010	0.0323	<0.03	0.008	546	0.100		1180	1804							41.0	
928	12/6/2010	0.0780		0.020	865			1620	1835								
928	11/11/2011	0.0744		0.028	933			1640	2393								
938	7/12/1946				268	21.0		691		126	42.0	0.00		308	<0.10	32.0	
938	6/15/1955					22.0	7.30							295	<0.10	30.0	
938	7/18/1956				295	14.0	7.50					0.00		281	<0.10	23.0	
938	9/14/2010	0.0086		<0.005	316			819	1176								
943	8/28/1956				563	0.6	7.8					0.00		305	<0.10	88	
943	6/15/1995	0.02	<0.03	0.05	1053	8.56	8.04	2095	3108	22.5	4.4	2.3	615	261	<0.10	73.2	<0.2
943	6/15/1995	0.02	<0.03	0.05	1066	8.29	8.04	2012	3108	22.6	4.5	2.3	620	262	<0.10	71.5	
943	6/12/1996	0.029	<0.03	0.062	1189	8.36	8.13	2130		29.6	6.0	2.3	628	249	<0.10	81.0	<0.2
943	10/23/1996	0.025	<0.03	0.069	1170	8.64	8.25	2080	3189	31.4	6.6	2.6	641	320	<0.10	83.5	<0.2
943	8/21/1997	0.007	0.05	<0.005	1180	0.21	8.68	2040	3178	9.2	5.6	2.9	654	215	5.8	91.0	<0.2
943	8/18/1998	0.0006	<0.03	<0.005	1100	<0.10	8.29	1980	3046	8.4	6.5	4.3	623	222	<1.0	83.9	<0.2
943	9/2/1999	0.0024		0.006	1170			2070	3919								

Table C.2-6. Water Quality Data for Homestake Site and Distal San Andres Aquifer Wells

Well ID	Date	U (mg/l)	Mo (mg/l)	Se (mg/l)	SO_4 (mg/l)	NO_3 (mg/l)	pH (s.u.)	TDS (mg/l)	SC (µS/cm)	Ca (mg/l)	Mg (mg/l)	K (mg/l)	Na (mg/l)	HCO_3 (mg/l)	CO_3 (mg/l)	Cl (mg/l)	Ra-226 (pCi/l)
943	8/23/2000	0.0017		<0.005	1070			2010	3832								
943	8/29/2001	<0.00030		<0.005	1000			2040	3822								
943	11/13/2002	0.001		<0.005	1080			2010	3840								
943	10/27/2003	0.0005		<0.005	1090			2030	2899								
943	3/9/2004	0.0180	<0.03	0.029	793	5.25	7.43	1830	2505	166	52.9	8.80	314	391	<1.0	188	0.3
943	12/8/2004	0.0136		0.020	690			1720	2315								
943	4/19/2005	0.0136	<0.03	<0.05	712	4.2	7.66	1680	2365	165	54.3	8.8	282	399	<1.0	181	<0.2
943	12/5/2005	0.0160		0.027	658			1690	2314								
943	3/16/2006	0.0179	<0.03	0.029	695	4.0	7.80	1670	2551	167	54.8	10.2	261	412	<1.0	161	0.400
943	12/19/2006	0.0149	<0.03	0.022	716	3.8	7.12	1710		191	62.4	9.80	282	298	<1.0	188	<0.2
943	3/8/2007	0.0184	<0.03	0.028	753	4.2	7.57	1790	2420	178	58.5	9.20	310	403	<1.0	175	0.600
943	12/3/2007	0.0185		0.023	649			1700	2356								
943	3/5/2008	0.0217	<0.03	0.029	742	4.0	7.48	1640	2411	181	56.2	9.40	288	422	<1.0	177	-0.06
943	9/16/2008	0.0182	<0.03	0.022	689	4.2	7.40	1650	2312	206	64.1	9.20	293	401	<1.0	168	1.20
943	12/1/2008	0.0162		0.022	666			1700	2344								
943	6/15/2009	0.0187	<0.03	0.022	696	4.0	7.26	1670		162	55.4	12.2	263	413	<1.0	182	0.18
943	12/7/2009	0.0199	<0.1	0.024	733			1670									
943	3/3/2010	0.0229	<0.03	0.029	697	5.20	7.52	1710	2494	176	56.0	8.70	302	467	<5.0	171	0.120
943	6/22/2010	0.0724	<0.03	0.087	1150	6.80	7.74	2200	3378	52.0	13.3	3.40	670	330	<5.0	144	-0.0500
943	8/5/2010	0.0753	<0.03	0.087	1330	9.40	8.09	2390	3502	62.0	15.6	3.30	788	347	<5.0	160	0.0900
943	9/21/2010	0.0208	<0.03	0.024	724	4.40		1700	2425							187	
943	10/27/2010	0.0246	<0.03	0.024	725			1740	2446							187	
943	12/6/2010	0.0239		0.022	731			1770	2085								
943	4/13/2011	0.0220	<0.03	0.025	713	4.2	7.46	1750	2497	195	60.6	10.00	316	439	<5.0	185	0.33
943	11/7/2011	0.0197		0.020	686			1620	2384								
943	8/16/2012	0.0484	<0.03	0.047	818	4.30	7.39	1850	2564	133	42.3	7.60	371	403	<5.0	176	0.560
943	11/30/2012	0.0402	<0.03	0.034	784			1810	2480							182	
949	10/6/1954				394	11.0						0.00		377	<0.10	65.0	
949	7/17/1956				407	9.5						0.00		377	<0.10	65.0	
949	5/7/1957				407	9.1						0.00		377	<0.10	65.0	
949	11/14/1988	<0.01	<0.01	0.01	470	16.0	7.21	1000	1725	160	51	7.5	100	310	<0.10	54.0	0.2
949	7/27/1994	0.010	<0.03	0.01	531	5.36	7.67	1151	1626	193	50	6.2	87.4	327	<0.10	89.8	0.6
949	11/20/1996	0.008	<0.03	0.008	464	5.3	7.69	1110	1703	189	51.9	5.87	104	340	<0.10	82	3.7
949	8/25/2008	0.012	<0.03	0.009	512	5.00	7.63	1200	1620	184	56.6	6.80	128	344	<1.0	108	0.170
951	04/15/1993	0.018	<0.01	<0.01	350	22.1	7.13	890	1422	140	42.0	4.7	74.0	260	<0.10	60.0	
951	10/05/1993	0.022	<0.01	<0.01	340	23.0	7.11	830					75.0			55.0	
951	04/05/1994	0.022	<0.01	<0.01	350	20.8	7.08	890	1514	160	46.0	5.2		340	<0.10	57.0	
951	08/31/1995	0.019	<0.03	<0.01	327	0.16	8.27	841	1262	138	44	5.1	77.0	325	<0.10	54.0	<0.2
951	03/07/1996	0.017	<0.03	<0.01	567	0.11	8.21	993	1530	87.2	69	9.8	117	113	<0.10	88.9	<0.2
951	10/22/1996	0.005	<0.03	<0.005	7.4	2.66	7.66	104	213	27.6	3.7	11.7	2.3	94.5	<0.10	3.1	<0.2
951	08/21/1997	0.024	<0.03	<0.005	330	1.48	7.94	872	1388	153	43	5.2	75.6	346	<0.10	50	<0.2
951	12/17/1997	0.024	<0.03	0.005	314	4.52	8.21	867	1243	148	42.3	5.2	73.0	340	<0.10	51	<0.2
951	8/18/1998	0.025	<0.03	<0.005	323	4.57	7.85	872	1478	148	43.2	5.6	76.5	342	<1.0	50.3	<0.200
951	8/19/1999	0.025		0.003	333			842									
951	9/17/1999	0.026		0.005	313			855	1185								

Table C.2-6. Water Quality Data for Homestake Site and Distal San Andres Aquifer Wells

Well ID	Date	U (mg/l)	Mo (mg/l)	Se (mg/l)	SO_4 (mg/l)	NO_3 (mg/l)	pH (s.u.)	TDS (mg/l)	SC (µS/cm)	Ca (mg/l)	Mg (mg/l)	K (mg/l)	Na (mg/l)	HCO_3 (mg/l)	CO_3 (mg/l)	Cl (mg/l)	Ra-226 (pCi/l)
951	10/19/1999	0.025		<0.005	335			838	1221								
951	11/2/1999	0.023		0.003	335			857	1222								
951	12/10/1999	0.020		0.006	350			861	1200								
951	1/20/2000	0.032	<0.03	<0.005	333			824	1240								
951	8/9/2000	0.003		<0.005	270			623	1226								
951	10/17/2002	0.028		<0.005	314			896	1623								
951	10/27/2003	0.031		<0.005	342			942	1305								
951	12/8/2004	0.027		0.0080	334			919	1288								
951	4/25/2005	0.028	<0.03	<0.05	358	4.40	7.78	921	1318	145	43.1	4.90	80.5	331	<1.0	68.0	0.2
951	12/5/2005	0.033		0.0050	316			892	1350								
951	3/16/2006	0.037	<0.03	0.0060	356	4.20	7.91	912	1459	145	43.4	5.60	79.9	342	<1.0	83.0	0.800
951	3/9/2007	0.0317	<0.03	<0.005	360	4.50	7.79	916	1318	154	47.2	5.30	83.6	354	<1.0	62.0	<0.200
951	12/3/2007	0.0406		0.0060	325			932	1346								
951	3/5/2008	0.0400	<0.03	0.0060	349	4.50	7.49	938	1348	147	43.5	5.50	86.0	352	<1.0	62.0	7.60
951	8/27/2008	0.0470	<0.03	0.0050	382	5.00	7.66	976	1421	170	50.0	5.70	98.0	339	<1.0	74.0	-0.200
951	12/1/2008	0.0416		0.0060	348			982	1401								
951	3/20/2009	0.0384	<0.03	0.005	356	4.8	7.44	962		152	44.6	5.3	88.8	347	<1.0	64	0.09
951	3/24/2009	0.0366	<0.03	0.005	349	4.7	7.35	937		168	46.9	5.4	80.6	348	<1.0	63	-0.01
951	3/31/2009			0.0063	353	4.7	7.3	884		162	42.3	4.59	71.2	274	<10	57	
951	12/7/2009	0.0367	<0.1	0.006	356			899									
951	3/3/2010	0.0333	<0.03	0.0070	341	4.40	7.39	872	1366	148	43.6	5.10	81.3	375	<5.0	61.0	0.060
951	6/22/2010	0.0452	<0.03	0.0060	37.2	4.30	7.47	990	1429	152	44.9	5.60	90.3	372	<5.0	72.0	0.008
951	6/24/2010	0.0482	<0.03	0.0070	391	6.30		1040	907							100.0	
951	12/6/2010	0.0339		<0.005	359			985	1005								
951	4/13/2011	0.0325	<0.03	0.007	356	4.50	7.48	966	1340	153	44.0	5.50	85.0	360	<5.0	59.0	0.09
951	7/6/2011	0.0410	<0.03	0.0050	363	4.40		927	1379							64.0	
951	10/12/2011	0.0371	<0.03	0.005	360	4.6		927	1366							63.0	
951	3/9/2012	0.0351	<0.03	0.0060	348	4.50	7.47	960	1400	146	43.3	5.40	87.4	346	<5.0	61.0	0.48
0951R	4/24/2012	0.0317	<0.03	0.009	536			1410								147	
0951R	6/11/2012	0.0228	<0.03	0.009	520			1380	1973							139	
0951R	8/16/2012	0.0302	<0.03	0.0090 .	548	4.00	7.45	1490	2027	182	61.3	9.20	167	438	<5.0	156	0.95
0951R	8/27/2012	0.0286	<0.03	0.007	555	3.20		1420	2045							156	
0951R	3/6/2013	0.0377	0.08	0.009	581	4	7.25	1490	2107	205	67.3	9.6	195	425	<5.0	169	1.7
955	7/10/1980	<0.01	<0.05	<0.01	414	5.80	7.20	1149				0.00		333		61.0	0.3
955	7/21/1994	<0.00	<0.03	0.01	495	3.27	7.73	1082	1468	157	47.1	5.9	106	315	<0.10	64.3	1.0
955	11/3/1995	<0.01	<0.03	0.01	441	3.17	6.84	1031	1443	159	48.0	6.2	107	398	<0.10	63.0	0.3
955	7/18/1996	0.006	<0.03	0.007	433	3.08	7.58	1109	1645	152	48.1	6.2	109	320	<0.10	63.4	0.50
955	10/22/1996	0.019	<0.03	0.0110	454	3.56	7.85	1050	1577	159	48.8	6.2	109	328	<0.10	65.7	0.30
955	5/1/2006	0.0054	<0.001	0.011	461	3.60	7.84	1030	891	164	51.8	6.60	107	336	<1.0	68.0	1.0
955	8/25/2008	0.0054	<0.03	0.011	438	4.20	7.65	1030	1460	165	53.8	6.30	103	320	<1.0	70.0	0.21
986	1/11/1900																
986	11/2/1995	0.01	<0.03	0.010	435	4.53	7.95	1058	1476	170	47.0	5.60	99	331	<0.10	70.0	<0.2
986	11/3/1995								1476								
986	5/2/2006	0.0458	0.0020	0.018	606	2.90	7.92	1330		139	39.5	3.10	268	410	<1.0	48.0	<1.0
986	05/15/2007	0.0514															

Table C.2-6. Water Quality Data for Homestake Site and Distal San Andres Aquifer Wells

Well ID	Date	U (mg/l)	Mo (mg/l)	Se (mg/l)	SO_4 (mg/l)	NO_3 (mg/l)	pH (s.u.)	TDS (mg/l)	SC (µS/cm)	Ca (mg/l)	Mg (mg/l)	K (mg/l)	Na (mg/l)	HCO_3 (mg/l)	CO_3 (mg/l)	Cl (mg/l)	Ra-226 (pCi/l)
986	8/22/2008	0.0111	<0.03	0.01	468	4.30	7.62	1100	1290	166	50.7	5.70	119	328	<1.0	71.0	0.35
986	8/23/2008	0.0094	<0.03	0.01	474	4.90	7.60	1090	1310	178	52.5	5.90	114	328	<1.0	78.0	0.31
986	8/25/2008	0.0087	<0.03	0.01	476	4.60	7.52	1150	1300	173	54.5	6.20	118	337	<1.0	81.0	0.27
986	11/13/2008	0.0534	<0.03	0.024	876	5.10	7.84	1760	2270	192	50.6	3.70	322	384	<1.0	65.0	0.05
986	11/13/2008	0.0573	<0.03	0.024	876	5.10	7.78	1730	1640	196	51.7	3.70	319	385	<1.0	66.0	0.09
987	11/3/1995	0.01	<0.03	0.010	422	4.74	7.61	1054	1487	143	41.0	5.30	139	353	<0.10	61.0	<0.2
987	5/10/2007	0.0091	0.0010	0.011	547	3.60	7.60	1170		172	51.2	6.00	116	366	<1.0	59.0	<0.2
991	11/8/1995	<0.01	<0.03	<0.01	435	4.63	7.67	1064	1476	168	48.0	5.60	101	344	<0.10	70.0	<0.2
991	8/26/2008	0.0062	<0.03	0.010	427	4.40	7.73	1030	1430		52.3	6.10	101	320	<1.0	71.0	0.55
995	6/28/1956					31.0	7.40					0.00					
995	5/14/1958						7.60					0.00					
995	8/23/1995	0.01	<0.03	0.01	423	4.41	7.40	990	1489	169	46.4	4.80	85	315	<0.10	53.0	0.60
Old #1	7/19/1994	0.01	0.2	0.16	12.9	<0.10	9.77	696	1284	1.6	0.2	2.8	296	316	105	135	0.6
Old #1	3/8/1996	0.02	<0.03	<0.01	632	<0.10	8.24	1382		7.6	1.4	1.1	440	351	<0.10	53.7	<0.2

Notes:

Data from tables in HMC's annual reports issued since 1996, "Water Quality Analyses for the San Andres Aquifer" (scan quality was poor in very early reports so some results are uncertain).
HMC did not issue an annual report for the year 2009, so electronic data provided by HMC are used in some cases.
This table is limited to key parameters; some analytes not regularly reported by HMC and/or not monitored in Bluewater site wells are excluded (e.g., chromium, Ra-228, Th-230, vanadium).
Locations for most HMC wells are shown on Plate 7 (and Figures 16-19) of the Site Status Report; a few (e.g., Old #1) are not mapped due to the paucity of data and/or lack of relevance.
Although included in HMC's database, well 923 (three results from 1993−1994) was located at the Bluewater site in the region of San Andres well I(SG).
Results for HMC well 951 are duplicated in Table C.2-1 as it is at the Bluewater site boundary and is currently monitored by DOE.
Results from Bahar 2007 were also consulted to verify and/or supplement uranium results reported by HMC (reference provided below).

Bahar, 2007. Letter from Dana Bahar, Manager, Superfund Oversight Section of New Mexico Environment Department, to Chris Clayton, Office of Long-Term Stewardship, U.S. Department of Energy Office of Environmental Management, and to Ron Linton, Senior Groundwater Hydrologist, U.S. Nuclear Regulatory Commission Office of Federal and State Materials and Environmental Management Programs. Subject: Request for DOE and NRC to sample San Andres aquifer. October 17, 2007.

Uranium data obtained from Figure 6 ("Data from HMC" of this letter. Note that the units for uranium concentrations in this exhibit, listed as ppb (parts per billion) are incorrect. As confirmed by comparison of results with those in Homestake's reports, the units should be as mg/L uranium.

Table C.2-7. Water Quality Data, from NMED 2010 (Tables 8 and 10)

Sample ID	Fm	Alternate IDs (see App. B)	Latitude	Longitude	Date Sampled	U (µg/L)	U-238 (pCi/L)	U-235 (pCi/L)	U-234 (pCi/L)	Se (µg/L)	Mo (µg/L)	SO_4 (mg/L)	HCO_3 (mg/L)	SC (µS/cm)	Ca (mg/L)	Mg (mg/L)	Na (mg/L)	K (mg/L)
BW-02	SA	HMC-965	35.225595	-107.888629	8/25/2008	6.4				10.9	<2	434	267	1289	159	47.1	106	6.19
BW-03	SA	HMC-986	35.224344	-107.888396	8/25/2008	11.7				10.8	<2	463	273	1379	171	49.4	126	6.11
BW-04	SA	HMC-991	35.229749	-107.888762	8/27/2008	7				9.2	<2	434	262	1273	160	50.2	105	6.16
BW-05	SA	BW-05	35.258875	-107.972292	8/25/2008	10.5	3.0	0.07	6.4	4	<2	475	356	1613	170	52.7	178	6.32
BW-06	SA	HMC-938	35.231733	-107.923966	8/25/2008	5.1				3.7	<2	249	230	1115	109	38.5	46.9	2.9
BW-07	SA	BW-07	35.265414	-107.994713	8/26/2008	9.4				2.2	<2	1440	476	3231	422	96.1	420	13.7
BW-08	SA	BW-08	35.265967	-107.975864	8/26/2008	4.9				2.5	<2	245	249	847	138	35.2	37.3	3.38
BW-09	SA	BW-09	35.248517	-107.976643	8/26/2008	7.8				4.8	2.1	345	293	1068	164	43.3	71.1	5.46
BW-10	SA	BW-10	35.256567	-107.966417	8/26/2008	5.5				2	<2	241	335	962	165	35.3	34.9	2.69
BW-11	SA	BW-11	35.25595	-107.967767	8/26/2008	5				<2	<2	222	312	910	147	33.6	26.5	2.97
BW-12	SA	BW-12	35.242589	-107.963738	8/27/2008	6.8				4.7	<2	352	288	1474	143	47	95.7	7.83
BW-13	SA	BW-13	35.23951	-107.961517	8/27/2008	6.4				3.8	<2	342	286	1446	149	44.8	83.7	6.1
BW-14	SA	BW-14	35.252936	-107.981026	8/27/2008	10.5	3.4	0.08	13.8	10	<2	451	284	1688	196	59.4	56.1	3.99
BW-15	SA	HMC-911	35.21802	-107.912511	8/25/2008	12	2.8	0.1	4.5	10.1	<2	341	233	1033	134	39.1	63.5	3.59
BW-16	SA	HMC-998	35.213846	-107.912278	8/27/2008	17.7				18.8	<2	385	230		148	42.3	80.6	3.92
BW-17	SA	BW-17	35.233128	-107.944206	8/28/2008	4.4				3.9	3.3	181	200	7889	79.3	37.7	33.8	2.18
BW-18	AL	Simpson, HMC-936	35.242809	-107.924478	8/28/2008	3.6				31	<2	529	188	1804	228	48.2	116	3.11
BW-19	SA	BW-19	35.236342	-107.932447	8/28/2008	14.2				11.1	3.3	290	242	1113	131	43.7	63.8	3.8
BW-20	SA	HMC-545	35.23341	-107.912254	8/28/2008	7.2				18.7	<2	415	222	1373	185	52.3	56.6	4.39
BW-21	SA	BW-21	35.203787	-107.908264	8/25/2008	11.8				16.3	<2	329	220	995	125	36.5	72.5	3.45
BW-22	SA	BW-22	35.203835	-107.915436	8/25/2008	5.4				7.3	3.4	162	182	644	73.3	29.2	32.5	2.22
BW-23	SA	HMC-949	35.234271	-107.888866	8/25/2008	13.8	4.3	0.4	7.1	8.5	<2	517	280	1624	187	54.5	133	7.02
BW-24	SA	BW-24	35.26193	-107.97442	8/25/2008	10.9	3.2	0.1	14.4	4.1	<2	478	362	2101	167	53.5	191	5.34
BW-25	SA	L(SG)	35.271106	-107.957824	8/27/2008	<2	-0.03	0.0008	0.01	<2	16.5	2.5	102	1344	0.6	1.9	332	5.47
BW-26	SA	S(SG)	35.268777	-107.938559	8/27/2008	<2 *	0.2	−0.1	0.4	<2	<2	357	<5	6753	758	61.6	113	1.84
BW-27	SA	OBS-3	35.271529	-107.938604	8/27/2008	<2 *	7.61	0.08	0.06	<2	<2	567	<5	3727	83.5	132	535	15.3
BW-28	SA	I(SG)	35.266163	-107.907318	8/27/2008	<2 *	0.04	−0.01	0.4	<2	<2	103	80	1175	14.5	10.8	192	5.22
BW-29	SA	HMC #1 Deepwell	35.242032	-107.856229	8/27/2008	8.9	0.3			7.3	<2	749	485	2828	225	77.8	312	13
BW-30	SA	HMC #2 Deepwell	35.239529	-107.864253	8/27/2008	16.7				7.7	3.5	727	426	2530	231	78.1	282	12.6
BW-32	SA	HMC-928	35.255295	-107.86176	9/16/2008	29	11.0	0.5	22.9	5	9.0	555	315	1858	15.2	4.3	423	1.56
BW-33	SA	HMC-943	35.225191	-107.876176	9/16/2008	20				16	1.0	678	400	2079	187	62.2	286	9.36
BW-34	SA	HMC-951	35.24748	-107.923981	8/27/2008	53.3	12.3	0.5	13.5	5.3	<2	383	274	1254	159	47.5	101	5.62
BW-35	SA	BW-35	35.279927	-107.831931	8/25/2008	6.4				10.9	<2	434	267	3857	159	47.1	106	6.19
SMC-03	AL	SMC-03	35.204251	-107.897797	3/31/2009	11				22.1	<50	369	272	1481	172	40.1	54.3	4.1
SMC-04	UNK	SMC-04	35.206449	-107.871402	3/31/2009	20.6 [19]	[5.61]		[11.1]	5.8	<50	200	284	1291	11.2	3.24	208	2.4
SMC-05	UNK	SMC-05	35.204204	-107.872925	3/31/2009	26.2 [26]				4.6	<50	105	308	1126	2.63	0.58	199	0.5
SMC-08	UNK	SMC-08	35.266714	-107.835451	3/30/2009	<2 [9]	2.8	0.2	3.9	3.8	<50	911	10	727	106	23.4	341	2.3
SMC-10	AL	HMC-914	35.277739	-107.830824	3/30/2009	30.9	0.04	0.01	0.1	32.1	<50	2110	170	2341	567	149	261	7
SMC-11	AL	HMC-920	35.276939	-107.84418	3/31/2009	228 [200]	63.0	2.8	78.1	367	<50	1580	188	3590	479	88.5	269	10.1
SMC-12	AL	HMC-950	35.289443	-107.839515	3/31/2009	163 [150]	52 [44.8]	2.3	61.9 [54.6]	382	<50	955	210	3206	59	10.3	628	0.5
SMC-13	AL	HMC-921	35.275482	-107.850652	4/2/2009	240 [220]	64.3	3.2	75.8	618	<50	1610	180	2922	389	73.7	355	8.4
SMC-14	AL	HMC-922	35.275194	-107.859294	4/2/2009	23.2 [21]				52.9	<50	535	246	1643	4.94	0.84	434	1.1

See Notes on following page. Results for SMC- samples in brackets are SLD radiochemical data (as reported in NMED 2010, Table 10).

* Result suspect; see Notes on following page and Figure 57 of Site Status Report.

Table C.2-7. Water Quality Data, from NMED 2010 (Tables 8 and 10)

Sample ID	Fm	Alternate IDs (see App. B)	Latitude	Longitude	Date Sampled	Cl (mg/L)	NO_3+NO_2 (mg/L)	Temp (°C)	DO (mg/L)	ORP (mV)	pH (s.u.)	Fe (µg/L)
BW-02	SA	HMC-965	35.225595	-107.888629	8/25/2008	65	3.83	16.23	2.0	69.4	6.89	<25
BW-03	SA	HMC-986	35.224344	-107.888396	8/25/2008	73	4.28	16.5	2.21	99.8	6.79	<25
BW-04	SA	HMC-991	35.229749	-107.888762	8/27/2008	67	4.13	16.2	3.68	-22	6.9	177
BW-05	SA	BW-05	35.258875	-107.972292	8/25/2008	101	1.75	18.51	1.98	118.6	6.69	<25
BW-06	SA	HMC-938	35.231733	-107.923966	8/25/2008	20	4.39	13.25	4.15	118.5	7.14	<25
BW-07	SA	BW-07	35.265414	-107.994713	8/26/2008	262	0.33	15.29	1.84	147.4	6.34	53.9
BW-08	SA	BW-08	35.265967	-107.975864	8/26/2008	25	2.69	14.9	4.86	115.6	6.98	<25
BW-09	SA	BW-09	35.248517	-107.976643	8/26/2008	40	4.18	13.94	15.87	135.2	6.66	<25
BW-10	SA	BW-10	35.256567	-107.966417	8/26/2008	17	2.79	14.43	9.67	160.1	6.55	<25
BW-11	SA	BW-11	35.25595	-107.967767	8/26/2008	14	2.24	14.58	8.62	170.1	6.55	<25
BW-12	SA	BW-12	35.242589	-107.963738	8/27/2008	45	3.83	13.52	3.9	153	6.84	<25
BW-13	SA	BW-13	35.23951	-107.961517	8/27/2008	39	3.46	13.67	3.89	191.6	6.82	<25
BW-14	SA	BW-14	35.252936	-107.981026	8/27/2008	48	4.79	15.01	5.32	132.3	6.58	<25
BW-15	SA	HMC-911	35.21802	-107.912511	8/25/2008	33	4.13	13.96	13.15	113.9	7.25	<25
BW-16	SA	HMC-998	35.213846	-107.912278	8/27/2008	42	4.2					<25
BW-17	SA	BW-17	35.233128	-107.944206	8/28/2008	11	3.51	15.55	7.89	104.2	7.14	<25
BW-18	AL	Simpson, HMC-936	35.242809	-107.924478	8/28/2008	147	10	16.95	7.76	80.5	6.99	<25
BW-19	SA	BW-19	35.236342	-107.932447	8/28/2008	27	4.65	13.62	4.98	197.3	6.85	<25
BW-20	SA	HMC-545	35.23341	-107.912254	8/28/2008	60	4.77	13.88	5.12	37	7.15	<25
BW-21	SA	BW-21	35.203787	-107.908264	8/25/2008	31	3.36	14.21	10.81	129.7	7.25	<25
BW-22	SA	BW-22	35.203835	-107.915436	8/25/2008	10	1.4	15.31	10.48	134.6	7.52	<25
BW-23	SA	HMC-949	35.234271	-107.888866	8/25/2008	101	4.76	16.35	8.24	135.6	7.06	<25
BW-24	SA	BW-24	35.26193	-107.97442	8/25/2008	107	0.34	15.42	1.53	125.5	6.72	45.4
BW-25	SA	L(SG)	35.271106	-107.957824	8/27/2008	217	0.02	17.16	0.81	-232.8	10.21	<25
BW-26	SA	S(SG)	35.268777	-107.938559	8/27/2008	2380	0.07	17.94	1.03	-75.4	5.4	564000
BW-27	SA	OBS-3	35.271529	-107.938604	8/27/2008	996	0.13	17.7	2.76	-119.6	6.48	1020
BW-28	SA	I(SG)	35.266163	-107.907318	8/27/2008	216	0.07	15.38	0.89	88.6	8.66	68.5
BW-29	SA	HMC #1 Deepwell	35.242032	-107.856229	8/27/2008	219	1.02	20.47	3.97	124.4	6.69	87.2
BW-30	SA	HMC #2 Deepwell	35.239529	-107.864253	8/27/2008	209	2.33	18.13	9	132.2	6.75	<25
BW-32	SA	HMC-928	35.255295	-107.86176	9/16/2008	36.5	0.11	14.95	0.81	74	8.27	<50
BW-33	SA	HMC-943	35.225191	-107.876176	9/16/2008	139	4.8	18.66	0.93	121.6	6.86	<50
BW-34	SA	HMC-951	35.24748	-107.923981	8/27/2008	57	4.61	13.92	8.95	172.8	7.22	33.4
BW-35	SA	BW-35	35.279927	-107.831931	8/25/2008	65	3.83	22.99	3.8	64.9	8.48	<25
SMC-03	AL	SMC-03	35.204251	-107.897797	3/31/2009	32	4.12	13.28	4.55	130.2	7.29	<25
SMC-04	UNK	SMC-04	35.206449	-107.871402	3/31/2009	33	0.82	12.79	1.29	25.2	8.57	<25
SMC-05	UNK	SMC-05	35.204204	-107.872925	3/31/2009	27	0.86	15.09	3.24	93.3	8.81	<25
SMC-08	UNK	SMC-08	35.266714	-107.835451	3/30/2009	78	0.05	12.74	5.01	116.5	8.36	2740
SMC-10	AL	HMC-914	35.277739	-107.830824	3/30/2009	47	21.2	12.98	0.16	-195.3	7.94	<25
SMC-11	AL	HMC-920	35.276939	-107.84418	3/31/2009	55	0.02	13.05	0.2	207.4	6.92	<25
SMC-12	AL	HMC-950	35.289443	-107.839515	3/31/2009	125	11.5	12.43	4.1	201	7.7	<25
SMC-13	AL	HMC-921	35.275482	-107.850652	4/2/2009	59	18.6	13.52	1.52	13.7	6.83	<25
SMC-14	AL	HMC-922	35.275194	-107.859294	4/2/2009	58	2.36	11.8	0.17	-222.5	8.76	28.4

Abbreviations

AL Alluvial Aquifer
Fm Formation
SA San Andres Glorieta (San Andres)
UNK Unknown

Notes

Data taken directly from NMED 2010, Tables 8 and 10 for sampling conducted in 2008 (not all parameters reported by NMED are listed here). For many locations, results are split samples of DOE and Homestake sampling.

Only 9 of the 27 unique SMC sample locations referenced in NMED's study were utilized in the Site Status Report: SMC-03, SMC-04, SMC-05, SMC-08, SMC-10, SMC-11, SMC-12, SMC-13, and SMC-14. The remaining SMC locations were not used because they are outside the study region addressed in the Site Status Report.

Uranium concentrations reported for BW-26 (S(SG)), BW-27 (OBS-3), and BW-28 (I(SG)) are all suspect, as uranium concentrations in San Andres aquifer wells in this region are known to be higher. Results for San Andres well 16(SG), about 1 mg/L uranium, are considered more characteristic

Table C.2-8. Uranium and Uranium Isotope Results from New Mexico Drinking Water Branch

Sample Location (DWB Facility Name)	System Name	Latitude	Longitude	Well Depth (ft)	Sample Date	DWB Hyperlink (= Lab Sample No.)	Result Type	Sampling Point	Combined Uranium (mg/L)	Combined Uranium (pCi/L)	U-234 (pCi/L)	U-238 (units vary)	Activity Ratio	Comment
Grants Well #1 (B-38)	Grants Domestic Water System	35.1568	-107.8672	300	10/27/2004	RC20040452	RAD	SP261330011	0.006			6 µg/L		
Grants Well #3 (B-40)	Grants Domestic Water System	35.1631	-107.8782	388	10/27/2004	RC20040453	RAD	SP261330031	0.006			6 µg/L		
Well #1 (B-23)	Milan Community Water System	35.1748	-107.8930	214	10/27/2004	RC20040449	RAD	SP255330011	0.005			5 µg/L		
Well #1 (B-23)	Milan Community Water System	35.1748	-107.8930	214	8/5/2008	RC200800268	RAD	SP255330011	0.005					
Well #1 (B-23)	Milan Community Water System	35.1748	-107.8930	214	12/2/2009	RC200900327	RAD	SP255330011	0.004		3.07	1.3 pCi/L	2.4	
Well #1 (B-23)	Milan Community Water System	35.1748	-107.8930	214	5/26/2010	RC201000119	RAD	SP255330011	0.005					
Well #1 (B-23)	Milan Community Water System	35.1748	-107.8930	214	5/26/2011	2011019872	RAD	SP255330061	0.004					
Well #1 (B-23)	Milan Community Water System	35.1748	-107.8930	214	7/2/2014	2014021196	RAD	SP255330061	0.005					See Note 1
Well #3 (B-35)	Milan Community Water System	35.2061	-107.9004	185	6/19/1996	RC960292	RAD	SP255330031	0.011	8.4	6.26	3.69 pCi/L	1.7	See Note 2
Well #3 (B-35)	Milan Community Water System	35.2061	-107.9004	185	10/27/2004	RC20040450	RAD	SP255330031	0.005			5 µg/L		
Well #3 (B-35)	Milan Community Water System	35.2061	-107.9004	185	8/5/2008	RC200800270	RAD	SP255330031	0.004					
Well #3 (B-35)	Milan Community Water System	35.2061	-107.9004	185	12/2/2009	RC200900325	RAD	SP255330031	0.004		2.6	1.25 pCi/L	2.1	
Well #3 (B-35)	Milan Community Water System	35.2061	-107.9004	185	5/26/2010	RC201000120	RAD	SP255330031	0.004					
Well #3 (B-35)	Milan Community Water System	35.2061	-107.9004	185	9/15/2011	2011033474	RAD	SP255330051	0.004					
Well #3 (B-35)	Milan Community Water System	35.2061	-107.9004	185	7/2/2014	2014021200	RAD	SP255330051	0.004					See Note 1
Well #4 (Golden Acres)	Milan Community Water System	35.2138	-107.9123	165	6/23/1997	RC980131	RAD	SP255330041	0.008	7				See Note 3
Well #4 (Golden Acres)	Milan Community Water System	35.2138	-107.9123	165	9/23/1997	RC980131	RAD	SP255330041	0.008	7				See Note 3
Well #4 (Golden Acres)	Milan Community Water System	35.2138	-107.9123	165	12/23/1997	RC980131	RAD	SP255330041	0.008	7				See Note 3
Well #4 (Golden Acres)	Milan Community Water System	35.2138	-107.9123	165	3/23/1998	RC980131	RAD	SP255330041	0.008	7				See Note 3
Well #4 (Golden Acres)	Milan Community Water System	35.2138	-107.9123	165	10/27/2004	RC20040451	RAD	SP255330041	0.013			13 µg/L		
Well #4 (Golden Acres)	Milan Community Water System	35.2138	-107.9123	165	8/5/2008	RC200800269	RAD	SP255330041	0.013					
Well #4 (Golden Acres)	Milan Community Water System	35.2138	-107.9123	165	12/2/2009	RC200900326	RAD	SP255330041	0.012		5.79	3.81 pCi/L	1.5	
Well #4 (Golden Acres)	Milan Community Water System	35.2138	-107.9123	165	5/26/2010	RC201000121	RAD	SP255330041	0.013					
Well #4 (Golden Acres)	Milan Community Water System	35.2138	-107.9123	165	null	RC980131	RAD	SP255330041	0.007					
Well #4 (Golden Acres)	Milan Community Water System	35.2138	-107.9123	165	7/2/2014	2014021198	RAD	SP255330071	0.012					See Note 1
Bluewater Well #1	Bluewater Water & Sanitation District	35.2485	-107.9766	345	11/30/2005	10500973	RAD	SP250330011	0.0066					
Bluewater Well #1	Bluewater Water & Sanitation District	35.2485	-107.9766	345	11/30/2005	8290DW1	RAD	SP250330011	0.0066					
Bluewater Well #1	Bluewater Water & Sanitation District	35.2485	-107.9766	345	5/1/2012	2012015919	RAD	SP250330011	0.008					

DWB Drinking Water Branch (State of New Mexico website)
U Uranium
0.011 Mass uranium (in mg/L) calculated based on actual or assumed U isotope concentrations using: (a*2.989) + (b*0.4683) + (c*0.00016), where a = U-238 in pCi/L; b=U-235 (pCi/L), and c=U-234 (pCi/L)
U-235 contribution assumed to be negligible given lack of data for these samples. See Notes below.

Notes

1 Results from July 2014 weren't available at the time the Site Status report was being developed, so these are not included in Figure 61 of the report.
2 Mass uranium calculated using the formula above. The combined uranium result for this record, 8.4 pCi/L, is anomalous given reported activites of U-234 and U-238 isotopes for that sample.
3 Mass uranium calculated using the formula above assuming a U-234/U-238 activity ratio of 1.5 based on the 12/2/2009 result.

This page intentionally left blank

Appendix D

Information Sources

This page intentionally left blank

D1.0 Information Sources

Numerous sources of information were accessed to develop the Bluewater-site components and regional components of the conceptual model. Given the long history of the Bluewater site and widespread interest in how mill-related contaminant plumes have evolved in the study area, groundwater-elevation and water-chemistry data for the alluvial and San Andres aquifers were drawn from a variety of databases, government publications, and consulting reports. This chapter briefly summarizes the content of some of the information sources used for the conceptual model and highlights findings that have bearing on the long-term fate of uranium in the regional groundwater system. More detailed summaries of environmental investigations performed in the Grants-Bluewater Valley are available in the bibliography by Otton (2011).

D1.1 Bluewater Site–Related Reports

From the late-1970s to the mid-1980s, the firm Hydro-Search, Inc. (Hydro-Search) developed several reports describing the hydrogeology of the Bluewater site and surrounding region, and presented water chemistry data collected from numerous wells in the Grants-Bluewater Valley. In the report *Hydrogeology of the Bluewater Mill Tailings Pond Area, Valencia County, New Mexico*, Hydro-Search (1977) summarized the geology of and groundwater conditions in the alluvial and San Andres aquifers at the Bluewater site and developed a conceptual model of contaminant seepage from the main tailings impoundment to the aquifers. The chemistry of tailings fluids was examined along with the chemistry at site wells to develop a contaminant source mechanism for plumes migrating east and southeast of the site. Taking into account the apparent impact of the Ambrosia Lake fault and the East-West fault on local groundwater flow, Hydro-Search (1977) described various flow processes by which contamination originating as tailings waste fluids was distributed between the two aquifers. A follow-up report the next year (Hydro-Search 1978a) refined some of the hydrologic- and transport-process descriptions as well as quantities attributed to the processes.

Hydro-Search (1978b) provided a thorough report on the groundwater-monitoring program at the Bluewater site as of the late 1970s, including construction details for the wells comprising the monitoring network and descriptions of the physical measurements and chemical analyses that facilitated characterization of the ambient and mill-impacted groundwater system. In addition, several recommendations were made in this report regarding monitoring system improvements to better evaluate spatial and temporal trends of site-related contaminant plumes. A detailed history of contaminant concentrations at key wells within the monitoring system was provided in a separate report a few years later (Hydro-Search 1981a).

Hydro-Search (1981b) conducted a study of the groundwater hydrology of the Grants-Bluewater Valley, producing a useful and insightful assessment of the potential impact of contamination stemming from milling at the Bluewater site on regional hydrologic resources. Map views and extensive tabulations of groundwater-elevation and groundwater-chemistry data provided an initial perspective on the extent to which impacted groundwater had, at the time, migrated eastward and southeastward in the alluvial and San Andres aquifers from the mill site.

The consulting firm Dames & Moore (1981c) summarized the activities and results from several aquifer pumping tests performed on wells at the Bluewater site. The report shed light on the wide range of transmissivity, hydraulic conductivity, and storativity values that characterize the San

Andres aquifer. Several of the tests analyzed also provided information on the nature of groundwater flow in ancestral Rio San Jose deposits below basalt flows at the site.

Dames & Moore (1986a) developed a comprehensive model of groundwater flow and transport processes at the Bluewater site and in downgradient areas. In addition to accounting for flow in both the alluvial and San Andres aquifers, the model simulated the transport of chloride, sulfate, and TDS in areas hydraulically downgradient of the Bluewater site. The model report provides detailed descriptions of the geologic units that comprise both the regional and site-specific groundwater flow and transport systems and summarizes numerous subsurface processes that impact the fate of inorganic constituents in the Grants-Bluewater Valley.

Much of the modeling effort by Dames & Moore (1986a) focused on the steps taken to calibrate the regional flow and transport simulator. Multiple calibration targets in the form of measured water levels at regional wells, groundwater discharges at springs, and the concentrations of nitrate and chloride in Bluewater site wells were selected. One of the findings from the modeling was that an effective porosity of 0.02 for the San Andres aquifer was needed to accurately match the plume extents for contaminants transported east and southeast of the site. Dames & Moore confirmed earlier findings from Hydro-Search that the velocities in the two aquifers were large enough to establish mostly steady-state constituent concentrations in onsite plumes within just a few years. Predictions made with the model suggested that both onsite and offsite contaminant concentrations would decrease steadily in following years.

Dames & Moore (1986b) followed up its modeling investigation of the Bluewater site with a lengthy summary of water quality conditions in the alluvial and San Andres aquifers. The assessments of water quality was based on the preparation of plume maps of key contaminants in 1986 and temporal plots of contaminant concentrations at onsite wells over several years.

The consulting company Applied Hydrology Associates Inc. (1990, 1993, 1995) developed a corrective action program for the Bluewater site after assessing the benefits of site remediation steps designed to reduce the amount of contamination loaded into the local groundwater system and remove contamination residing in the subsurface. Several different alternatives were evaluated, all of which took into consideration a list of physicochemical processes that could impact contaminant migration. Though the list of contaminants included in the evaluations comprised uranium, selenium, and molybdenum, most of the technical assessments conducted dealt with uranium because of its relatively high mobility and apparently large extent in areas downgradient of the site. Applied Hydrology Associates, Inc. (1995) provided detailed estimates of the volume of tailings waste fluids and associated uranium contaminant mass that was loaded to the subsurface at the main tailings impoundment, covering the period from 1953 to 2000. Measured uranium levels at key wells were plotted over multi-year periods from the early 1980s through the early 1990s to ascertain the relative stability of uranium concentrations during that period, and to help in projecting future concentration beneath onsite areas.

Applied Hydrology Associates Inc. (1995) summarized the results of previous and recent aquifer pumping tests at the site to characterize hydraulic properties that govern contaminant transport in the alluvial and San Andres aquifers. Assessments of the aquifers' capacity to attenuate uranium transport with flow distance were also conducted. After a thorough evaluation of the various processes that influence long-term fate of contaminants at the Bluewater site, Applied Hydrology Associates, Inc. (1995) proposed ACLs for uranium, selenium, and molybdenum.

D1.2 Homestake Site-Related Reports

The geology, hydrogeology, and groundwater remediation activities at the Homestake site have been documented in a large number of reports that have been prepared by a variety of sources, including HMC, environmental consultants to HMC, and the EPA. Annual reports on the progress of the GRP have been prepared by HMC and their consultants over the past few decades. A few of the more recent examples include HMC and Hydro-Engineering (2010, 2013). These reports provide detailed summaries of the remediation activities carried out each year under the GRP and tabulations and maps of monitoring results. Some map products and accompanying cross sections illustrate the latest understanding of the spatial distribution of hydrogeologic units, which include San Mateo alluvium, several distinct strata within the Chinle Formation, and the underlying San Andres Limestone. Other maps contain posted groundwater levels and concentrations of select contaminants, including uranium and sulfate, in the geologic units present, along with contoured representations of these parameters. Detailed tables provide time-varying values of these parameters over the course of the reporting year and potential explanations for anomalous changes in concentration for monitored contaminants. In recent years, monitoring results from a vast array of wells completed in the alluvial aquifer have made it possible to prepare contour maps of groundwater levels and uranium concentration in the aquifer, including at areas where ancestral Rio San Jose alluvium extends from near the Bluewater site and merges with San Mateo alluvium extending westward from the Homestake site. The annual reports (e.g., HMC and Hydro-Engineering 2010, 2013) also provide maps and tabulated versions of water quality results, including for uranium, from wells screened in the San Andres aquifer at and near the Homestake site.

A corrective action plan for the Homestake site, outlining the various components and procedures of the GRP, has been published a few times. Hydro-Engineering (1989) developed a version of the Homestake corrective action plan that comported with early phases of the GRP. An updated corrective action plan was prepared in 2012 (HMC 2012). The plans provide detailed descriptions of the geologic and hydraulic properties of the hydrogeologic units, including updates that result from new characterization activities. The latest water quality results for the components of the GRP are also reported.

Three five-year review reports have been prepared for the Homestake site, as mandated under Superfund. In addition to reporting on the progress being made by HMC in its attempt to meet prescribed groundwater remediation goals, the five-year reports (CH2M-Hill 2001; EPA 2006, 2011) identify potential problems with site-cleanup efforts and make recommendations for improving the groundwater remediation strategy and remediation activities. In the third and most recent five-year review of the Homestake site, the EPA (2011) expressed concern that the complex groundwater remedy might be contributing to elevated uranium concentrations observed at wells screened in the San Andres aquifer in the vicinity of the site. Specifically, the concern is that the combination of HMC's pumping from the San Andres aquifer and injection of water into shallow alluvium has created about 100 ft of hydraulic-head difference between the two aquifers, which, when combined with the local presence of a major fault zone that can act as conduit, has the potential to convey alluvial groundwater with high levels of uranium contamination to the San Andres aquifer. Elevated uranium concentrations have been observed locally in recent years.

D1.3 USGS Reports

The USGS has published several reports that address the hydrology of the Grants-Bluewater Valley and the Zuni Mountains. The reports shed light on the potential impacts that both surface water and groundwater features in the region can have on contaminant migration from the Bluewater and Homestake sites.

A USGS report by Baldwin and Anderholm (1992) assessed regional groundwater flow in the San Andres Limestone and the underlying Glorieta Sandstone in west-central New Mexico, as well as in the alluvial aquifer in the Grants-Bluewater Valley. The effects that less permeable geologic units have on the regional hydrogeology, including the Triassic-age Chinle Formation and Permian-age formations underlying the Glorieta Sandstone, were also identified. The authors described how a large amount of subsurface flows in the region occurs within secondary permeability features, particularly solution channels, cavernous zones, and fractures in the San Andres Limestone. The presence of these features was identified using aquifer-test results and the rock lithologies reported in well logs for several key wells screened in the San Andres aquifer. In addressing the spatial variability of hydraulic properties for the aquifer, this report identified a wide range of values for transmissivity and hydraulic conductivity derived from aquifer tests at San Andres aquifer wells. The authors used this information to divide the region into seven transmissivity zones. The spatial distribution of the zone helped explain the regional potentiometric surface that is typically observed for the San Andres aquifer in the Grants-Bluewater Valley.

Baldwin and Anderholm (1992) identified multiple recharge zones for the San Andres aquifer on the northeast flanks of the Zuni Mountains where outcrops of limestones and sandstones associated with the aquifer are observed. The importance of recharge from precipitation and surface water features in the region, including Bluewater Lake, Bluewater Creek, Rio San Jose, and several irrigation canals was also identified. A significant finding in the report was that recharge varies substantially from year to year depending on yearly precipitation amounts and the general availability of surface water over multi-year periods. Significant areas of groundwater discharge from the San Andres and alluvial aquifers, such as at springs, were also pointed out along with rough estimates of the discharge quantities. The combination of recharge and discharge features in the region allowed the authors to illustrate general directions of groundwater flow in the Grants-Bluewater Valley and the impact that faults have on regional flow patterns. Baldwin and Anderholm (1992) also described the inorganic chemistry and general quality of water in the alluvial and San Andres aquifers as well as in less permeable geologic units affecting aquifer flows. The chemical data helped in identifying flow patterns in the regional groundwater system.

Baldwin and Rankin (1995) authored a USGS report that summarized the hydrogeology of Cibola County and evaluated occurrence, availability, and quality of groundwater resources. Rocks of Precambrian through Quaternary age were studied. The report focused mostly on the most productive aquifers in the county, including Quaternary alluvium and basalt, sandstones in the Mesaverde Group, the Dakota-Zuni-Bluff aquifer, the Westwater Canyon aquifer, the Todilto-Entrada aquifer, and the San Andres-Glorieta aquifer. The authors described how well yields can vary greatly within the county. Baldwin and Rankin (1995) also described the water quality in the most productive aquifers in the region, characterizing dissolved-solids levels and the concentrations of the major anions and cations in each geologic unit.

Frenzel (1992) developed a numerical model of groundwater flow in the San Andres aquifer and overlying valley fill. The work was performed in cooperation with the New Mexico Office of the State Engineer, two Native American Pueblos east of Grants, and the U.S. Bureau of Indian Affairs. The purpose of the study was to determine the effects of current and projected water development in the region containing the San Andres aquifer on hydraulic heads in the aquifer and flow in the Rio San Jose.

The digital, finite-difference flow model by Frenzel (1992) contained 2 layers, 76 rows, and 43 columns. In addition to simulating groundwater flow in the Grants-Bluewater valley fill, the model accounted for flow to and from Bluewater Lake and flow in Bluewater Creek and the Rio San Jose. A major spring in the region, Ojo del Gallo, was simulated as a stream. The effects of multiple faults in the region were assessed with the model. Historical groundwater withdrawals and recharge were simulated for the period of fall 1899 to fall 1985. Measured hydraulic heads and streamflows were considered to have been matched reasonably well by the simulated values.

A study was conducted by Risser (1983) to estimate the natural streamflow in the Rio San Jose just upstream of two Native American Pueblos east of Grants. The estimates were based on numerous streamflow and precipitation records compiled by the author, along with historical accounts of streamflow, records of irrigated acreage, and empirically derived estimates of the effects of Bluewater Lake, groundwater withdrawals, and irrigation diversions on surface water flows at various locations within the Rio San Jose watershed. The Risser study used 55 years of recorded and reconstructed streamflow data, from water years 1913 to 1972. The report provides historical precipitation data for meteorology stations in the region and streamflow data for several streams in the Rio San Jose drainage.

West (1972) examined the geologic and hydrologic environments in the vicinity of the Bluewater uranium mill to ascertain whether Permian formations older and beneath the Glorieta Sandstone were favorable for disposal of mill effluent via an injection well north of the main tailings impoundment. His investigation specifically evaluated the capacity of beds of sandstone in the Yeso Formation to accept effluent delivered by gravity flow at rates of 200 to 400 gallons per minute (gpm) at depths of 950 to about 1,400 ft below ground surface. It was demonstrated in the study that a thick interval of siltstone, anhydrite, and gypsum of low permeability in the upper part of the Yeso Formation would separate the injection interval from the principal freshwater aquifer in the Glorieta Sandstone and the San Andres Limestone.

An exploratory disposal well was tested thoroughly during and following drilling (West 1972), and borehole core samples were analyzed for porosity and permeability. The water quality of native formation fluids was examined, which showed the injection interval contained 3,900 mg/L of dissolved solids, of which 2,200 mg/L was sulfate. The exploratory well was subjected to various aquifer pumping tests, after which additional casing intervals were perforated and all perforated horizons were fractured hydraulically. A 90-day injection test followed, using intermittent inflow rates varying between 380 and 1,300 gpm. Operational injection began in December 1960, after which additional testing of the Yeso Formation was conducted and the capacity of the well to accept injection water was recorded. Some data from the testing suggested that the Yeso Formation might be leaking effluent to overlying formations. The injected water contained mill waste effluent with TDS concentrations as high as 13,000 mg/L and uranium concentrations considerably higher than regional background values.

D1.4 Regional Studies

Gordon (1961) described the geology and hydrogeology of the Grants-Bluewater area at a time when uranium mining and milling activity in the region was approaching its peak. This work provided a scientific assessment of the aquifers in the region and summarized the development of regional groundwater resources while reporting on the historical importance of both the alluvial and San Andres aquifers to local agricultural, industrial, and municipal needs. Gordon (1961) reported on the physical effects of groundwater withdrawals in the valley and the potential environmental issues stemming from using the groundwater for irrigation and industrial uses, including uranium milling.

In addition to providing detailed descriptions of the physical, lithologic, and hydraulic properties of geologic units in the region, Gordon (1961) characterized the groundwater quality. The author discussed how hydrologic and other processes such as recharge, pumping, chemical weathering, and evapotranspiration might impact water chemistry. The earliest aquifer pumping tests performed on wells in the Grants-Bluewater Valley were discussed in Gordon (1961).

Kaufmann et al. (1975) summarized the degree to which contamination from uranium mining and milling activities in the Grants Mineral Belt affected regional groundwater quality. In their study, radium, selenium, and nitrate were of most value as indicators of contamination. The authors described how effluents from recent mining contained high radioactivity levels and mill-tailing seepage contributed to elevated levels of selenium in local, shallow alluvial aquifers. The study was sponsored by the EPA at the request of the New Mexico Environmental Improvement Agency in 1974. Water sampling and analysis occurred in 1975. Many of the findings in the EPA report were subsequently summarized in a journal paper (Kaufmann et al. 1976).

The New Mexico Environment Department (NMED) (2010) conducted a study in 2008 of the groundwater chemistry at a large number of wells in the Grants-Bluewater Valley to ascertain whether the chemical results could be used to determine the source of mill-related contaminants in the valley. The region included in this investigation extended from the Bluewater site to the Homestake site, and covered areas between the Ambrosia Lake mining district and the Homestake site. A large variety of chemical parameters were measured in 2008 at the wells in the study region, ranging from major ions to TDS, metals and other dissolved inorganic constituents, and both stable and radioactive isotopes.

NMED (2010) examined isotopic ratios of carbon, oxygen, hydrogen, sulfur, and the radioactive uranium series from a limited number of groundwater samples. One of the objectives of this effort was to determine if discrepancies in the isotopic ratios could distinguish background water quality from groundwater impacted by releases from uranium mining and milling operations. Utilization of environmental forensic methods such as these was expected to more accurately define baseline water quality conditions in groundwater sources with and without possible anthropogenic impacts.

D1.5 DOE Reports

DOE (1997) developed a long-term surveillance plan (LTSP) for the Bluewater site. The plan described physical, geological, and hydrological features of the site and addressed how groundwater contamination resulting from the former uranium mill operations would be

monitored by DOE in coming years. Relevant construction features of the main tailings disposal cell and the carbonate tailings disposal cell were described to help facilitate future inspections of remnant features of the milling activities.

DOE (2014) assessed the water balance of the main tailings disposal cell at the Bluewater site (Appendix A). The assessment took into account the history of the cell from its origin as an impoundment for the storage of tailings fluids produced by the Bluewater mill. Technical reviews of previous work performed by various environmental consultants aimed at quantifying the seepage rates and volumes of tailings fluids discharging to the subsurface from the base of the impoundment and disposal cell were also performed. As part of its assessment, DOE (2014) took into consideration some recent geologic characterization work aimed at describing the physical and potential hydraulic relationships between the hydrogeologic units underlying the disposal cell, concentrating a great deal on the impacts of the Ambrosia Lake fault and the East-West fault on local and regional groundwater flow.

Conclusions drawn from the water balance assessment included the recognition that nearly half of the mass loading of uranium contamination from the main tailings impoundment and disposal cell occurred prior to 1960. The water balance report also concluded that most of the acidic tailings fluids that had drained from the impoundment in earlier years of mill operation had been neutralized, such that the contaminants in the fluids remained in the alluvial and San Andres aquifer media as solids, in adsorbed and mineralized phases. As a result of the subsurface neutralization processes, dissolved concentrations of uranium and other tailings-related contaminants had been greatly reduced. DOE (2014) found no evidence that the groundwater beneath and near the main tailings disposal cell had received a pulse of contamination from the cell over the past several years. The mineralized zone beneath the disposal cell was expected to be a continuing source of groundwater contamination for an indefinite period in the future.

D1.6 Miscellaneous Papers

Longmire et al. (1984) authored a paper that described the general impacts of the uranium industry in the Grants Mineral Belt on groundwater quality in the region. The paper described the thermodynamic controls on the geochemistry of the principal contaminants in mill tailings and raffinates, including uranium, iron, selenium, and molybdenum, and some of the controlling mineral reactions. It noted differences in the aqueous geochemistry of raffinates and the seepage from mill tailings, and between the seepage derived from acid-leach mill processes and those derived from alkaline-leach mill processes. Contamination of groundwater from acid-tailings seepage was characterized by sulfate, chloride, nitrate, iron, aluminum, manganese, and other metals (Longmire et al. 1984). Contamination of groundwater from alkaline-tailings seepage was characterized by elevated levels of arsenic, sodium, bicarbonate, nitrate, selenium, molybdenum, sulfate, and uranium.

Zielinski et al. (1997) identified a tool that can sometimes be used to help identify sources of dissolved uranium at mill and mining sites. The method involves the examination of uranium isotope distributions in water samples collected at several monitoring locations. Specifically, the ratio of the activity concentrations for uranium-234 (U-234) and uranium-238 (U-238) are calculated under the hypothesis that mill-related contamination would have a U-234/U-238 value, or uranium activity ratio (AR), that was noticeably different from that of naturally derived uranium. In applying this logic to a former uranium mill site near Cañon City, Colorado, Zielinski et al. (1997) showed that the AR in contaminated groundwater samples exhibited ratios

generally reflective of secular equilibrium (AR ≅ 1), while those of natural waters had ratios greater than 1.3. The Cañon City study built upon previous work by researchers that suggests natural waters tend to show an excess of U-234 activity in comparison to that of U-238 at the mineral/water interface during prolonged mild leaching of subsurface uranium-bearing rock by groundwater. This excess comprises a form of isotopic fractionation related to alpha recoil displacement (Zielinski et al. 1997) of the U-234 atom from its U-238 parent, with the net effect of enhanced leachability of U-234. In contrast, high-grade uranium ores with more recent histories of open-system alteration appear to be mixtures of materials with both AR<1 and AR>1, which, when leached over periods of just a few decades or more, yield waters with an AR of 1.0 ± 0.1. The work by Zielinski et al. (1997) suggests that uranium isotope data can be used in areas on and near the Bluewater site to distinguish mill-related uranium with ARs of about 1.0 with naturally-occurring uranium with ARs higher than 1.1.

Appendix E

Glossary

This page intentionally left blank

Glossary

absorption. The incorporation of a chemical in the interior of a solid.

adsorption. The adhesion of molecules (in a thin layer) to the surfaces of solid bodies or liquids with which they are in contact.

advection. The process by which solutes are transported by the bulk motion of the flowing groundwater.

advection-dispersion equation (ADE). The most widely used equation for simulating solute transport in porous media. Also referred to as the classical advective-dispersive equation.

advective flux. The mass of chemical in a fluid passing through a unit cross-sectional area per unit time due to advection. Advective flux is calculated as the product of Darcy velocity (specific discharge) and the chemical concentration.

advective front. The location downgradient of the source in a contaminant plume that is equal to the product of average linear velocity and time since onset of groundwater contamination.

aerobic. Living, active, or occurring only in the presence of oxygen.

alluvium. General term for deposits of clay, silt, sand, gravel, or other particulate material deposited by a stream or other body of running water in a streambed, on a floodplain, on a delta, or at the base of a mountain.

anaerobic. Living, acting, or occurring in the absence of free oxygen.

analytical model. A mathematical model that uses closed formed solutions of the governing equations applicable to groundwater flow and chemical transport processes.

anion. A negatively charged ion.

anisotropy. The condition of an aquifer in which the value of a material property (such as hydraulic conductivity) varies depending on the direction of measurement.

aquifer. (1) Stratum of permeable rock, sand, or gravel that can store and supply groundwater to wells and springs. (2) A geologic formation, group of formations, or part of a formation that contains sufficient saturated permeable material to yield significant quantities of water to wells and/or springs.

aquitard. A less permeable bed in a stratigraphic sequence that is incapable of yielding significant quantities of water to a pumping well. A semipervious geologic formation transmitting water at a very slow rate compared to the aquifer.

average linear velocity (groundwater). The Darcy velocity divided by aquifer effective porosity. Also known as mean pore water velocity or seepage velocity.

bedrock. A general term for the consolidated (solid) rock that underlies soils or other unconsolidated surficial material.

biodegradation. The chemical alteration of substances through the action of biota.

breakthrough curve. A representation of the concentration of solute in a fluid as a function of time at a selected point.

calibration. The process of refining a model representation of flow and transport in a groundwater system in order to achieve a desired degree of correspondence between the model simulation and observations of the groundwater system.

capillary fringe. Zone of constant water saturation extending upward from the water table, containing water held in capillary tension. Capillarity is the cohesion of water molecules and the adhesion of water to solid materials. The thickness of the capillary fringe depends on the soil properties and the uniformity of pore sizes.

cation. Positively charged ion.

chemical precipitation. The process of removing a substance from solution by chemical reaction.

complex. A type of compound in which a central metal ion is surrounded by a number of ions or molecules, called ligands, that can also exist separately, also known as a coordination compound. A chelate is a type of complex.

complexation. Combination of cations and anions to form a more complex ion.

complexing agent. A dissolved ligand that binds with a simple charged or uncharged molecular species in a liquid solution to form a complex, or coordination compound.

computer code. The assembly of numerical techniques, bookkeeping, and control language that represents a mathematical model of groundwater flow and contaminant transport.

conceptual model. An interpretation or working description of the characteristics and dynamics of a groundwater system.

cone of depression. The depression of hydraulic heads around a pumping well caused by the withdrawal of groundwater.

confined aquifer. A permeable geologic unit located between two saturated, less permeable units (i.e., between confining beds).

confining bed. A geologic unit that will not readily transmit water and which impedes or stops the free movement of water into or out of an aquifer. Confining beds have also been called aquicludes, aquitards, or semi-confining beds.

contaminant. Harmful or hazardous matter introduced into the environment.

continuous release. A contaminant release from a source area that continues indefinitely at a relatively constant rate.

coprecipitation. The incorporation of elements into other compounds, such as metal oxide minerals, as they precipitate from solution.

Darcy velocity. The volumetric flow rate of groundwater per unit cross-sectional area perpendicular to the flow direction. Also known as Darcy flux or specific discharge.

denitrification. Conversion by microorganisms of nitrate or nitrite to more reduced states, ending in nitrogen gas under anaerobic conditions.

deterministic model. A model in which there is an exact mathematical relationship between the independent and dependent variables that characterize a groundwater system.

diffusion. (1) the transport process of a chemical in the direction of decreasing concentration of the chemical due to thermal kinetic energy (and resulting Brownian motion) of the dissolved chemical. (2) The natural tendency of molecules to move out of areas of high concentration into areas of low concentration until a solution or gas has a uniform concentration of the molecules. Also known as molecular diffusion.

diffusion coefficient. The capacity of a specific chemical to migrate through a specific material (e.g., water or air) by the process of molecular diffusion. It is expressed in terms of the mass of chemical that will diffuse through a unit area in a unit time under the influence of a unit concentration gradient.

diffusive flux. The mass of a contaminant or other constituent passing through a unit area per unit time due to molecular diffusion. Diffusive flux is calculated as the product of a diffusion coefficient and a concentration gradient.

discharge. (1) With respect to fluid flow, the rate of flow at a given instance in terms of volume per unit of time; pumping discharge equals pumping rate, usually given in gallons per minute (gpm); stream discharge, usually given in cubic feet per second (cfs). With respect to groundwater, the movement of water out of an aquifer. Discharge may be natural, as from springs, as by seepage, or by evapotranspiration, or it may be artificial as by constructed drains or from wells. (2) With respect to mass movement, the rate of mass movement in terms of mass per unit of time. See also **mass discharge**.

dispersion (in porous media transport). Fluid mixing due to velocity variations at unresolved spatial scales. These velocity variations are often attributed to unresolved heterogeneities in permeability, and other phenomena existing at the pore scale or larger. Dispersion is usually the greatest in the direction parallel to flow (longitudinal direction), and is usually less in the transverse directions. Also known as mechanical dispersion.

dispersion coefficient. Capacity of a specific chemical to migrate through a specific material (e.g., water or air) by the process of hydrodynamic dispersion. It is expressed in terms of

the mass of chemical that will disperse through a unit area in a unit time under the influence of a unit concentration gradient.

dispersive flux. The mass of chemical in a fluid passing through a unit cross-sectional area per unit time due to dispersion. Dispersive flux is calculated as the product of a dispersion coefficient and a concentration gradient.

dispersivity. a parameter representing the spreading potential of a solute-porous medium system.

dissolved constituents. Chemical compounds in solution, also called solutes.

dissolved oxygen. The amount of free (not chemically combined) oxygen in water. Usually expressed in milligrams per liter (mg/L).

drawdown (groundwater). The depression or decline of the hydraulic head or water level in a pumped well or in nearby wells caused by pumping. At the well, it is the vertical distance between the static water level and the water level under pumping conditions.

effective porosity. (1) The percent of the total volume of soil or rock that consists of interconnected pore space. (2) The porosity through which flow can occur.

Eh. Oxidation-reduction potential; the relative susceptibility of a substrate to oxidation or reduction.

equipotential line. A contour line on a map or cross section along which hydraulic heads are the same.

equivalent porous medium. A concept that is used to model or simulate the flow of groundwater in fractured rocks. The concept is that is you take a large enough volume, the fractured geologic material will behave mathematically like a porous medium.

evaporation. Process by which water is changed from the liquid state to the vapor state. See also **evapotranspiration, transpiration**.

evapotranspiration. Process by which water is returned to the air through direct evaporation, or by transpiration from vegetation.

Fickian model. A model that simulates contaminant transport as governed by the classical advection-dispersion equation and linear, equilibrium sorption.

Fickian transport. Contaminant transport that can be simulated with models based on the classical advection-dispersion equation and linear, equilibrium sorption. Also referred to as ideal transport.

finite-difference method. A numerical technique for solving a system of equations using a rectangular mesh representing an aquifer or other hydrostratigraphic unit and solving for the dependent variable in a piece wise manner.

finite-element method. A numerical technique for solving a system of equations using an irregular triangular or quadrilateral mesh representing an aquifer or other hydrogeologic unit and solving for the dependent variable in a continuous manner.

floodplain. Land bordering a stream. The land was built up of sediment from overflow of the stream and is still subject to flooding when the stream is at flood stage.

flow. The movement of a fluid.

flow path. The idealized path followed by particles of water. Also known as a flow line.

flux. Fluid or mass discharge per unit area.

gaining stream. A river, or a reach of a stream or river, that gains in flow from upward groundwater seepage from the streambed, or from springs in, or alongside, the river channel; sometimes called an effluent stream.

groundwater. Water in the saturated zone that is under a pressure equal to or greater than atmospheric pressure. More generally, all subsurface water as distinct from surface water; specifically, the portion of subsurface water within the saturated zone.

groundwater flow model. Application of a mathematical model to represent a site-specific groundwater flow system.

groundwater storage. The amount of water in storage within the defined limit of an aquifer.

half-life. The time required for half of the atoms of a radioactive substance to disintegrate.

heterogeneous. Consisting of diverse or dissimilar constituents.

hydraulic conductivity. The capacity of a rock or soil formation to transmit water through it under hydraulic gradients. It is expressed as the volume of water of a given viscosity that will move in unit time under a unit hydraulic gradient through a unit area, measured at right angles to the direction of flow. It is a combined property of the porous medium and the fluid flowing through it.

hydraulic gradient. Change in hydraulic head per unit of distance measured in the direction of the steepest change. In a three-dimensional coordinate system, the hydraulic gradient consists of three components, with two corresponding to horizontal (x and y) axes, and one corresponding to the vertical (z) axis. A non-zero hydraulic gradient represents the potential for flow to occur.

hydraulic head. (1) The height above a datum plane of a column of water. In a groundwater system, it is the sum of elevation head and pressure head. (2) The height at which water stands in a piezometer or well due to the presence of elevation and pressure forces in groundwater surrounding the well. Also called piezometric head.

hydrodynamic dispersion. Fluid mixing due to the combined effect of mechanical dispersion and molecular diffusion.

hydrograph. A graph showing the stage, flow, velocity, or other property of water with respect to the passage of time. Hydrographs of wells show the changes in water levels during the period of observation.

hydrologic unit. Aquifer or surface water body.

hydrolysis. The splitting of a bond by a reaction with water, specifically the addition of the hydrogen cation and the hydroxide anion of water.

hydrophobic compound. A nonpolar organic compound that tends to exhibit low solubility in water and a preference for sorbing to the organic matter component of a soil matrix porous medium.

hydrostratigraphic unit. A geologic formation, group of formations, or part of a formation that consists of materials with similar hydraulic properties, in contrast to adjacent formations or parts of a formation. Also referred to as a hydrogeologic unit.

immobilization. The precipitation or binding of a substance so that it is no longer able to circulate freely.

inorganic compounds. Chemicals that do not contain carbon; for example, metals are inorganic.

insoluble. Not readily dissolved in a liquid.

ion. An atom or group of atoms that carries a positive or negative electric charge as a result of having lost or gained one or more electrons; a charged subatomic particle (as a free electron).

ion exchange. A reversible reaction in which ions are interchanged. This phenomenon is common in soils.

isotope. Any of two or more species of atoms of a chemical element with the same atomic number (number of protons) and nearly identical chemical behavior but with a different number of neutrons, hence a different atomic weight.

isotropy. Having the same properties in all directions.

karst aquifer. An aquifer in which the flow of groundwater is or can be appreciable through one or more of the following: joints, faults, bedding-plane partings, and cavities—any or all of which have been enlarged by dissolution

leaching. The process of separating the soluble components from some material by percolation.

ligand. A group, ion, or molecule coordinated to a central atom or molecule in a complex.

long-term stewardship. The physical controls, institutions, information, and other mechanisms needed to ensure protection of people and the environment.

losing stream. A river, reach of a stream or river, that loses a portion of its flow to groundwater through seepage in, or alongside, the channel. Sometimes called an influent stream.

mass discharge. The mass of chemical in a fluid that passes from one point to another per unit time. Mass discharge is the product of the fluid discharge rate and the concentration of the contaminant (in units of mass per unit volume) in the fluid.

mass flux. The mass of chemical in a fluid that passes through a unit cross-sectional area per unit time. Mass flux can be caused by advection (advective flux), dispersion (dispersive flux), and molecular diffusion (diffusive flux).

mathematical model. The representation of a physical or chemical system by mathematical expressions from which the behavior of a groundwater system can be simulated.

mechanical dispersion. pore-scale spreading of a chemical caused by flow through a macroscopically tortuous and nonuniform porous medium with nonuniform pore size.

milligrams per liter or mg/L. The mass in milligrams of any substance contained in 1 liter of liquid. (Equivalent to parts per million for values less than about 7,000 mg/L).

non-Fickian model. A model that simulates contaminant transport as governed by the classical advection-dispersion equation and linear, equilibrium transport.

non-Fickian transport. Contaminant transport that does not coincide with that simulated by models governed by the classical advection-dispersion equation as affected by linear, equilibrium sorption. Also referred to as ideal transport.

numerical methods. A set of procedures used to solve the equations of a mathematical model in which the applicable partial differential equations are replaced by a set of algebraic equations written in terms of discrete values of state variables at discrete point in space and time.

oxidation. The reaction of a substance, in the presence of oxygen, with a chemical that causes removal of electrons from the original substance.

pE. A dimensionless measure of the oxidizing or reducing tendency of a solution. By definition, $pE = -\log_{10}[e]$, where [e] is equal to electron activity. pE is analogous to pH, which is used to measure hydrogen-ion activity.

perched groundwater. Water within a saturated zone of material underlain by a relatively impervious stratum which acts as a barrier to downward flow and which is separated from the main groundwater body by a zone of unsaturated material above the main groundwater body.

permeability. The capacity of a material to transmit fluids. Permeability is a material property that is not dependent on the property of the fluid.

phreatophyte. A plant that habitually obtains its water supply from the zone of saturation, either directly or through the capillary fringe.

physicochemical. Of or pertaining to both physical and chemical properties, changes, and reactions.

piezometer. A device or type of well used to measure hydraulic head at a point in the subsurface.s

piezometric head. The height at which water stands in a piezometer or well due to the presence of elevation and pressure forces in groundwater surrounding the well. Also called hydraulic head.

plume. An elongated body of fluid that is used to define the contaminated areas of an environment.

porosity. The ratio of the total volume of pore space (voids) in a rock or soil to its total volume, sometimes stated as a percentage. Effective porosity is the ratio of the volume of interconnected voids to the total volume. Unconnected voids contribute to total porosity but are ineffective in transmitting water through the rock.

porous medium. A multi-phase material consisting of a continuum of solid matrix with some interconnected void space.

potentiometric surface. An imaginary surface representing the static head of groundwater in tightly cased wells that tap a water-bearing rock unit (aquifer); or in the case of unconfined aquifers, the water table.

precipitation. The process whereby a solid settles out of a solution.

pressure head. Fluid pressure expressed as the height of an equivalent column of water. Calculated by dividing the fluid pressure by the product of fluid density and the acceleration due to gravity.

pulse release. A contaminant release from a source area that occurs for a finite period of time. See also **slug release.**

radioactivity. Spontaneous emission by radionuclides of energetic particles through the disintegration of their atomic nuclei; the rays emitted.

radioisotope. An isotope of an element that has an unstable nucleus; it tries to stabilize itself by giving off radioactive particles and undergoes spontaneous decay.

radionuclide. Radioisotope.

reactant. A substance that enters into and is altered in the course of a chemical reaction.

reaction. A process in which one or more substances are changed chemically into one or more different substances. Examples include biotransformation, radioactive decay, and hydrolosis.

recalcitrant. (1) Resistant to degradation/transformation. (2) Resistant to decreases in concentration.

recharge. The addition of water to the saturated zone in an aquifer by infiltration, either directly into the aquifer or indirectly by way of another soil or rock formation. Recharge may be natural, as when precipitation infiltrates to the water table, or artificial, as when water is injected through wells or spread over permeable surfaces for the purpose of recharging an aquifer.

redox reaction. Oxidation-reduction reaction in which electrons are transferred between two or more compounds.

retardation. The slowing of the rate of movement of a solute due to partitioning to and from stationary solid material within the porous media.

retardation factor. a parameter in the advection-dispersion equation that accounts for association of a dissolved chemical with immobile phases in a porous medium (e.g., sorption)

riparian vegetation. Vegetation growing on the banks of a stream or other body of surface water.

rock. Any naturally formed, consolidated or unconsolidated material (but not soil) consisting of two or more minerals.

runoff. The part of the precipitation that appears in surface streams.

saturated zone. The subsurface zone in which all the connected interstices or voids in permeable rock or soil formations are filled with water under pressure equal to, or greater than atmospheric pressure. The saturated zone should not be confused with isolated zones of perched groundwater.

secondary permeability. The increased permeability or hydraulic conductivity due to the presence of secondary porosity.

secondary porosity. Voids and associated hydraulic media that form through physical and chemical processes following deposition, including compaction, fracturing, faulting, dissolution, and mineralization.

sediment. Material in suspension in water or deposited from suspension or precipitation.

seepage. (1) The infiltration or percolation of water through rock or soil to or from the surface. (2) The very slow velocity movement of groundwater.

simulation. One complete execution of groundwater modeling computer program, including input and output.

sink. In groundwater flow modeling, a process whereby, or a feature from which, water is extracted from the groundwater system. In transport modeling, a process whereby, or a feature from which, a contaminant is extracted from the groundwater system.

slug release. A contaminant release from a source area that occurs for a finite period of time. See also **pulse release**.

soil-water distribution coefficient (K_d). The ratio of the mass fraction of a chemical adsorbed to the solid phase to the concentration of the chemical in aqueous solution.

solubility. The relative capacity of a substance to serve as a solute, usually in reference to water as the solvent.

soluble. Able to be dissolved; to pass into solution.

solute. Any material that is dissolved in another, such as salt dissolved in water.

solution. A homogeneous mixture of a solute in a solvent. When a solute is dissolved in a solvent, the solute molecules are separated from one another and dispersed throughout the liquid medium.

solution channel. Tubular or planar channel formed by solution in carbonate rock, usually along joints and bedding planes. It is the main water carrier in carbonate rocks.

sorption. The process by which a chemical partitions between solid and fluid phases. Sorption, exchange, absorption, adsorption and desorption are often used synonymously, although these terms may represent different physical processes.

sorption isotherm. A regression of sorbed-phase concentrations against aqueous-phase concentrations at a given, constant temperature.

source. The process by which a contaminant is released or fed into subsurface water.

specific discharge. Darcy velocity.

specific storage. The volume of water that a unit volume of porous medium releases from storage per unit change in hydraulic head. In confined aquifers, a quantity with units of 1/Length that represents the volume of water released from storage in a unit volume of the aquifer per unit change in hydraulic head.

specific yield. The ratio of the volume of water that will drain under the influence of gravity to the volume of saturated soil or rock. In an unconfined aquifer, a dimensionless quantity

representing the volume of water that is released from storage per unit surface area of aquifer, per unit decline in the water table. Specific yield is relevant only to unconfined aquifers, and is analogous to storativity in a confined aquifer.

stable plume. A contaminant plume, or a portion of a contaminant plume, in which groundwater concentrations are virtually constant with time. Also referred to as a steady-state plume or a steady plume.

static water level. The level at which water stands in a well screened in a confined or unconfined aquifer when no water is being removed from the aquifer either by pumping or free flow to the ground surface.

steady-state flow. A condition where the magnitude and direction of the flow field are constant with time.

stochastic process. A process in which the dependent variable is random, so that prediction of its value depends on a set of underlying probabilities, and the outcome at any instant is not known with certainty.

storativity. The volume of water released from storage in a unit prism of an aquifer when the hydraulic head is lowered a unit distance. In a confined aquifer, a dimensionless quantity representing the volume of water an aquifer releases or takes into storage per unit surface area of the aquifer per unit change in hydraulic head. Storativity, which is equal to the product of specific storage and aquifer thickness, is synonymous with the storage coefficient of a confined aquifer and analogous to the specific yield of an unconfined aquifer.

stratification. The layered structure of sedimentary rocks and alluvium.

stream, ephemeral. A stream or portion of a stream that flows only in direct response to precipitation. Such flow is usually of short duration.

stream, perennial. A stream that normally has water in its channel at all times and flows continuously.

streamflow. The discharge that occurs in a natural channel of a surface stream course.

subsurface. The geologic zone below the surface of the Earth.

surface water. An open body of water, such as a stream, pond or a lake.

total dissolved solids (TDS). An aggregate of anions (carbonates, bicarbonates, chlorides, sulfates, phosphates, nitrates, etc.) and cations (calcium, magnesium, manganese, sodium, potassium, etc.) which form salts. High TDS solutions have the capability of changing the chemical nature of water.

transient flow. A condition that occurs when at some point in a flow field the magnitude or direction of the flow velocity changes with time.

transmissivity (groundwater). The rate at which water at the prevailing water temperature is transmitted through a unit width of the aquifer under a unit hydraulic gradient. It was traditionally expressed as gallons per day through a vertical strip of the aquifer 1 foot wide under a gradient of 1 foot per foot. More recently, it has been expressed as cubic feet per day through a vertical strip of the aquifer 1 foot wide under a gradient of 1 foot per foot.

transpiration. Process by which water is absorbed by plants, usually through the roots. The residual water vapor is emitted into the atmosphere from the plant surface. See also **evaporation, evapotranspiration**.

transport. Conveyance of solutes and particles in flow systems.

unconfined aquifer. A permeable geologic unit with the water table forming its upper boundary; also referred to as a water-table aquifer.

unsaturated zone. Soil or rock partially saturated with water, lying above the capillary fringe. Sometimes used to refer to the vadose zone.

vadose zone. The zone containing both the unsaturated zone and the capillary fringe just above the water table. Sometimes used to refer to the unsaturated zone.

valence. The property of an element that determines the number of other atoms with which an atom of the element can combine.

volumetric moisture content. In porous media, the volume of water divided by the combined volume of solid, liquid, and vapor.

water budget. An accounting of the inflow to, outflow from, and storage changes of water in a hydrologic unit.

water table. The level in the saturated zone at which the pressure is equal to atmospheric pressure; the upper surface of the zone of saturation. Also called the phreatic surface. See also **potentiometric surface**.

withdrawal. Water removed from the ground or diverted from a surface water source for use.

Appendix F

Processes Affecting Contaminant Plumes

This page intentionally left blank

F1.0 Introduction

Physical processes such as advection, mechanical dispersion, and recharge can play significant roles in the attenuation of groundwater contamination at LM sites. These processes by themselves contribute to reductions in contaminant concentration but do not cause net reduction of contaminant mass. Consequently, physical influences on contaminant transport are generally considered "nondestructive." However, mass-reducing, or "destructive," processes at LM sites would not occur to the degree observed were it not for the manner in which processes like advection, dispersion, and recharge facilitate them. Destructive processes such as biodegradation and abiotic chemical transformation rely on groundwater flow and the resulting mixing of contaminants with other reactants to effect significant attenuation. Moreover, additional processes like volatilization and sorption are influenced by the hydraulic transport of contaminants. Most of this appendix discusses the nondestructive contributions of transport processes to contaminant attenuation.

Before a discussion of how attenuation of dissolved constituents occurs in aquifers, it is important to clarify what "concentration" represents. Often, concentration represents the dissolved mass of a contaminant within a limited volume of groundwater that has been collected in a piezometer, which is screened over a small vertical interval (e.g., ≤3 feet). Such a concentration can be considered a point value. Alternatively, concentration can also represent the contaminant mass collected in water pumped at a relatively high rate from a well with a long screen (e.g., >3 feet), which tends to represent a mixture of water from various depths. This latter type of concentration can be considered a vertically averaged, composite value rather than a point concentration.

Point concentrations can be used to assess the three-dimensional distribution of a contaminant in an aquifer. However, complete spatial characterization of a contaminant plume using point concentrations is rarely achieved because the associated costs can be prohibitive. Rather than collecting the entire suite of concentrations necessary for showing the full horizontal and vertical extents of a plume, it is common practice to assume that transport occurs solely within a horizontal plane in a limited-depth aquifer, and that contaminant concentrations do not vary significantly with depth in the groundwater. In such cases, the two-dimensional, horizontal distribution of a contaminant is sometimes described using vertically averaged concentration values measured by purging wells with long screens. Unfortunately, this latter approach to plume delineation can result in poor estimation of flow direction, inaccurate bifurcation of the plume, incorrect identification of contaminant source areas and release mechanisms, and overestimation of natural attenuation impacts (Martin-Hayden and Robbins 1997). The challenges to plume delineation, regardless of the monitoring practices employed, suggest that caution should be applied when attempting to interpret measured contaminant levels and identify influential transport processes.

F2.0 Groundwater Flow and Velocity

F2.1 Darcy's Law

The direction and rate of groundwater flow at a given point in an aquifer is governed by Darcy's law. Several mathematical expressions of this law exist, depending on the number of spatial

dimensions that are used to describe the flow, and the specific hydraulic properties of the porous medium in which the flow is occurring. Discussions of groundwater flow in this appendix focus initially on the more general form of Darcy's law that applies to a three-dimensional domain containing aquifer materials that transmit water more readily in some directions than in others. A simplified form of the law is also given to represent flow in domains that tend to be less complex than those represented by the law's general form.

The general form of Darcy's law is (Bear 1979)

$$\mathbf{q} = [\mathrm{K}]\,\mathbf{J} \qquad \textbf{(1)}$$

where **q** = Darcy velocity (length/time),
[K] = hydraulic conductivity (length/time), and
J = hydraulic gradient (dimensionless).

Boldface lettering is applied to the symbols for Darcy velocity and hydraulic gradient to indicate that each of these variables is a vector. Vectors are used to describe three-dimensional fields. That is, velocity and gradient are each characterized by a direction and three components (Bear 1979), with the components describing the magnitude of the variable parallel to horizontal (*x* and *y*) and vertical (*z*) directions in space. In Equation **(1)**, hydraulic conductivity is placed in brackets to indicate that it is a 3 × 3 matrix consisting of 9 components. The vectors **q** and **J** are sometimes referred to as first-order tensors, and the matrix [K] is sometimes referred to as a second-order tensor (Bear 1972).

Each of the nine components of [K] has subscripts i and j, with the first representing the direction of the Darcy velocity and the second representing the direction of the hydraulic gradient. The three components composing the diagonal of the hydraulic conductivity matrix are symbolized by K_{xx}, K_{yy}, and K_{zz}, wherein i = j. In contrast, the indices i and j are different in each of the off-diagonal components (e.g., K_{xy}). A simple interpretation of each [K] component is that it is the hydraulic conductivity value determining the Darcy velocity in the i direction due to a hydraulic gradient in the j direction.

Equation **(1)** is applicable to an anisotropic domain (Bear 1979), wherein the hydraulic conductivity components in the *x*, *y*, and *z* directions are not equal to each other. If the axes of the 3-dimensional domain are oriented so that *x* and *y* are parallel to the direction of sediment bedding, and *z* is perpendicular to this direction, the off-diagonal components of [K] have zero values. Furthermore, in most alluvial aquifers, it is usually assumed that K_{xx} is equal to K_{yy}, which signifies that the only anisotropy applicable to the aquifer is attributed to differences between K in the horizontal and vertical directions. In cases where Darcy's law is applied to an anisotropic medium, the Darcy velocity (**q**) will not be oriented in the same direction as the hydraulic gradient (**J**) (Bear 1979).

If a porous medium is isotropic, all components of the hydraulic conductivity tensor take on a uniform value, symbolized by K. K in this case is described as a scalar value, or a zero-order tensor (Bear 1972). Darcy's law in this simplified instance can be written

$$q = K\,J \qquad \textbf{(2)}$$

where q = a single value of Darcy velocity in the direction of the hydraulic gradient (length/time), and
J = a single value of the hydraulic gradient (i.e., in the direction of maximum drop in hydraulic head) (dimensionless).

F2.2 Average Linear Velocity

Though the Darcy velocity is useful for describing quantities of water and associated contaminants that move in specific directions, it is not a direct indicator of the rate at which the contaminant is moving through space. This latter rate is estimated using the average linear velocity (Freeze and Cherry 1979), which is the average rate at which water moves through the pores of an aquifer

$$\mathbf{v} = \frac{\mathbf{q}}{n_e} \qquad \textbf{(3)}$$

where $\mathbf{v}$ = average linear velocity (length/time), and
n_e = effective porosity of the aquifer (dimensionless).

Because **q** is a vector, consisting of both a direction and a magnitude, **v** is also a vector with three components, each aligned with the *x*, *y*, and *z* axes. Average linear velocity is more commonly described with a single, scalar value that applies to the direction of groundwater flow.

F3.0 Contaminant Transport in Groundwater

F3.1 Contaminant Mass Balance

The movement and concentration of a chemical in groundwater is affected by four general factors: (1) advection, (2) mechanical dispersion, (3) molecular diffusion, and (4) sources and sinks of the contaminant, such as chemical and biological reactions, or sorption onto the solid materials that compose the porous medium and solid matrix (Domenico and Schwartz 1997). Models of aqueous-phase transport are based on mass-balance equations that describe these factors. In general terms, the contaminant mass balance can be written (Mercer and Waddell 1993):

> Advection by natural flow + advection by pumping or injection + dispersion + diffusion + contaminant sources and sinks = rate of change of mass of aqueous-phase contaminant stored in the medium. **(4)**

The various components of Equation **(4)** are discussed further in the following sections.

F3.2 Advection

Transport by advection consists of the movement of a contaminant caused by the net or average motion or flow of the groundwater (Mercer and Wadell 1993). For a non-reactive contaminant, the rate of transport is equal to the average linear groundwater velocity, v, as defined by Equation **(3)**. The effects of advection on plume behavior can be examined by first considering a plume that emanates from, or is "fed" by, a “continuous contaminant source.” This type of source maintains relatively constant contaminant concentrations along its downgradient edge and remains undepleted (Mercer and Waddell 1993).

Advection, by itself, does not cause attenuation of a contaminant plume fed by a continuous source. The reason for this is seen in the advection of a dissolved contaminant in a hypothetical stream tube located directly downgradient of the source (Domenico and Schwartz 1997). By definition, the stream tube is associated with a steady flow system, and flow does not occur across the stream tube walls. And when only advection is operating, the contaminant front in the stream tube at any given time is a flat surface determined by the average linear velocity along the transport path. Because contaminant mass cannot spread beyond either the stream tube walls or the plume front, the concentration at all points in the stream tube is equal to the concentration observed on the downgradient edge of the source, and no attenuation occurs. This concept is illustrated in Figure F-1a, which shows the effects of processes on flow and transport along a 1-dimensional (1-D) plume originating at a continuous contaminant source in a steady-state flow field. Pure advection, denoted by process A in Figure F-1a, affects the location but not the concentration of a dissolved contaminant in 1-D transport. A continuous source is also referred to as a continuous-release source in this appendix.

In cases where the contaminant source varies in strength over time, it is possible for pure advection to appear as contributing to natural attenuation. This occurs, for instance, when a contaminant source is depleted or removed and uncontaminated water moves in behind the released contaminant. Process A in Figure F-1b illustrates this phenomenon for 1-D flow and transport fed by a “pulse” source. In effect, the clean water has displaced the contaminant pulse through advection, moving the pulse farther down the flow path. Such displacement of contaminated water by uncontaminated water can potentially occur in a vertical direction when recharge to a groundwater system occurs above the dissolved contaminant plume. A pulse source is also referred to in this appendix as a pulse-release source, and in the scientific literature as a slug source.

F3.2.1 Travel Time

The time it takes for a non-reactive contaminant to migrate from one location to another in the direction of groundwater flow is called the travel time. It is defined by

$$t_a = s_a/v \qquad \textbf{(5)}$$

where t_a = advective travel time (time), and
s_a = travel distance (length).

Because it is determined using the average linear velocity v, the parameter t_a represents the average time it would take for a non-reactive contaminant to migrate the travel distance. In a

porous medium, the velocities with which molecules of water travel through the medium's pores vary around the average value. A non-reactive constituent in groundwater is sometimes referred to as a conservative constituent.

F3.2.2 Mass Flux and Mass Discharge

The chemical mass flux due to advection is equal to the product of the Darcy velocity and the aqueous concentration of the chemical. Because Darcy velocity in three-dimensional space has three components, advective mass flux can also have three components. For example, the advective mass flux of a contaminant in the *x*-direction is

$$F_{ax} = q_x C_w \quad \textbf{(6)}$$

where F_{ax} = advective mass flux in the *x*-direction, [(mass/area)/time],
q_x = Darcy velocity in the *x*-direction (length/time), and
C_w = dissolved contaminant concentration (mass/volume).

Typically, mass flux is simply described using a single scalar value representative of the direction of groundwater flow.

Another measure of mass transport brought about by advection is mass discharge, which is equal to the product of volumetric discharge of the groundwater and the aqueous concentration of the dissolved chemical in that discharge, i.e.:

$$M_d = Q C_w \quad \textbf{(7)}$$

Where M_d = mass discharge (mass/time),
Q = volumetric discharge rate (volume/time), and
C_w = dissolved contaminant concentration (mass/volume).

Example units for the parameters in Equation **(7)** are milligrams per liter for C_w, liters per day for Q, and milligrams per day for M_d.

F3.3 Hydrodynamic Dispersion

Advection in real groundwater systems is neither perfectly uniform in space nor steady in time. Water migrates in the direction of flow at variable velocities, and water flowing in individual stream tubes mixes with water in adjacent stream tubes. In addition, some dissolved contamination may move between adjacent stream tubes if contaminant concentrations in the stream tubes differ. The effects of these phenomena are described using the concept of hydrodynamic dispersion.

Hydrodynamic dispersion is a term used to describe the spreading of contaminants in groundwater caused by both mechanical processes (mechanical dispersion) and molecular-scale chemical processes (molecular diffusion). Each of these processes can be considered potential contributors to plume attenuation because they can non-destructively reduce contaminant concentrations compared to the concentration that emanates from the contaminant source.

F3.3.1 Mechanical Dispersion

Mechanical dispersion in porous media flow is water mixing that occurs as a consequence of local variations in velocity around the average, or mean, water velocity (Domenico and Schwartz 1997). Because this mixing occurs in response to groundwater velocity variations, it is the product of advective processes, rather than chemical processes. The net impact of mechanical dispersion on dissolved mass transport is to cause spreading of a contaminant plume beyond the plume extent that would be expected based on bulk advection alone.

The effects of mechanical dispersion have traditionally been represented as if the dispersion process obeyed Fick's first and second laws of diffusion (Anderson 1984). Fick's first law expressed for dispersion in porous media is:

$$F_d = -[D_m]\, i_c \qquad \textbf{(8)}$$

where F_d = the dispersive flux of mass [(mass/length^2)/time, or (mass/area)/time],
D_m = the coefficient of mechanical dispersion (length^2/time), and
i_c = the dissolved concentration gradient [(mass/length^3)/length, or (mass/volume)/length].

Note that the dispersion coefficient D_m can have as many as three or more components depending on the dimensionality of the groundwater system being studied and the manner with which dispersion is characterized (Bear 1979). Mechanical dispersion in a 1-D plume occurs only along the direction of groundwater flow. A plume influenced by mechanical dispersion in two or three spatial dimensions will spread groundwater contamination in directions normal to (perpendicular to) the flow as well as parallel to the flow.

The effects of mechanical dispersion as governed by Fick’s laws in a 1-D plume fed by a continuous source are illustrated in Figure F-1a. The concentration-versus-distance curve reflective of both advection and dispersion (processes A + D) in this graphic shows that contaminant spreading has occurred both downgradient and upgradient of the transport distance associated with advection alone (process A). However, the concentration at the source remains at the same concentration as that attributed solely to advection. Figure F-1b shows the combined influences of advection and mechanical dispersion in a 1-D plume supplied by a pulse source. In this case, contaminant spreading has occurred along both the leading and trailing portions of the plume, resulting in a peak concentration that is less than the concentration associated with pure advection.

Equation **(8)** is based on the assumption that the concentration gradient is a driving force for mechanical dispersion, and the dispersive flux will increase linearly with increasing gradient. This is a mathematical convenience rather than a representation of cause-and-effect. In reality, mechanical dispersion is caused by velocity variations at various spatial scales.

Laboratory-scale experiments in the 1960s designed to identify the relationship between mechanical dispersion coefficients and the velocity of water in a porous medium generally found that, in cases where the effects of longitudinal dispersion overwhelm the effects of molecular diffusion, the dispersion coefficient is proportional to velocity, i.e.:

$$D_{mi} = \alpha_i |\mathbf{v}| \quad \textbf{(9)}$$

where D_{mi} = the mechanical dispersion coefficient in direction i (length^2/time),
α_i = the dispersivity in the direction i (length), and
$|\mathbf{v}|$ = the magnitude of the average linear groundwater velocity (length/time).

On the basis of this relationship, it is typically assumed that a porous medium, at least at a laboratory scale, can be characterized by single values of dispersivity in the longitudinal and transverse directions. Centimeters and feet are commonly used units for dispersivity in the scientific literature. Commonly used units for the dispersion coefficient include centimeters^2/second and feet^2/day.

Many groundwater transport models that simulate advection and dispersion use the linear relationship in Equation **(9)** between the dispersion coefficient and the average linear velocity. Thus, average linear velocities are determined separately from the transport model and the modeler chooses dispersivities for input in the model. The dispersivity values are often finalized through model calibration. Though early column-based experiments that focused on the quantification of dispersion coefficients (e.g., Harleman and Rumer 1963) found the relationship in Equation **(9)** to be accurate, more recent laboratory experiments have shown that it is not always correct (e.g., Olsson and Grathwohl 2007). For problems dealing with dispersive transport at a field scale (e.g., hundreds to thousands of feet), the direct proportionality between the dispersion coefficient and flow velocity is questionable.

Mechanical dispersion in groundwater can be analyzed in terms of the three scales upon which it is observed: microscopic (local scale), macroscopic (local to field scale), and megascopic (field to regional scale). Variations in velocity leading to dispersion at each of these scales are produced by nonidealities in the porous medium. At the microscopic scale, the nonidealities are attributed to pore-size distribution, different pore geometries, and such phenomena as dead-end pore space (Domenico and Schwartz 1997). Macroscopic nonidealities consist of variations in medium properties that occur within a given formation or between neighboring wells. Included in this latter category are nonuniform hydraulic conductivities, permeability trends, directional permeabilities, and variations in aquifer stratification. Dispersion on a macroscopic scale is expected to be larger in a very heterogeneous aquifer than in a less heterogeneous system. Megascopic nonidealities, which occur at the interformational and regional scales, are features such as large changes in geologic structure and the overall stratigraphic framework (Domenico and Schwartz 1997). The multiple scales over which dispersion occurs results in mechanical dispersion coefficients that appear to increase as a function of plume length (e.g., Gelhar et al. 1992).

F3.3.2 Longitudinal and Transverse Mechanical Dispersion

Mechanical dispersion can be characterized as being either longitudinal or transverse. Longitudinal dispersion is the mixing that occurs along the direction of flow, whereas transverse dispersion is the mixing that occurs in directions normal to (perpendicular to) the flow path (Mercer and Waddell 1993). The combined influence of longitudinal and transverse dispersion is seen in 2-dimensional (2-D) and 3-dimensional (3-D) plumes fed by sources with limited, finite dimensions.

Figure F-2a illustrates the relative influences of longitudinal and transverse dispersion on plume-centerline concentrations downgradient of a continuous source of limited width in a 2-D groundwater system with a uniform (non-varying) velocity in the direction of flow. Whereas longitudinal spreading affects concentrations in the leading portion of the plume, transverse dispersion causes spreading laterally from the interior of the plume. As a result, contaminant concentrations at a given time along the plume centerline are less than those resulting solely from combined advection and longitudinal dispersion (Domenico 1987). In effect, the downgradient migration of a plume affected by transverse dispersion is lessened, or retarded, in comparison to a plume subject to dispersion only in the direction of flow. Similar effects from transverse dispersion are observed in a 2-D plume fed by a pulse source (Figure F-2b).

Contaminant spreading in a 3-D plume is governed by three components of dispersivity (longitudinal, transverse horizontal, and transverse vertical). Dispersivities are not amenable to direct measurement, though evaluation of carefully conducted field-scale tracer tests with a high-resolution monitoring network may yield valid site-specific values. Generally, the horizontal transverse dispersivity is less than the longitudinal dispersivity, and the vertical transverse dispersivity is less than the transverse horizontal dispersivity. Vertical dispersivities are strongly influenced by the natural stratification of an aquifer.

In most modeling investigations of contaminated sites, dispersivity values are estimated through model calibration. Models that resolve heterogeneities at smaller spatial scales usually require smaller values of dispersivity to achieve an acceptable calibration to field data. If field concentration data are insufficient for model calibration, empirical relationships between plume length and longitudinal and transverse dispersivities (EPA 1986a, 1986b; ASTM 1995; Xu and Eckstein 1995) can be employed to estimate dispersion parameters. These latter methods are subject to considerable uncertainty.

An increased "apparent dispersion" in directions transverse to groundwater flow may be observed in transient flow systems (e.g., Goode and Konikow 1990, Cirpka and Attinger 2003, Swain and Chin 2003). As illustrated in Figure F-3, changing flow directions in these systems create individual plumes with different orientations, which, when considered together, suggest that the plume is wider than would be observed in a steady-state flow field.

Some field investigations that focus on very detailed characterization of the concentrations in a 3-D plume (e.g., Rivett et al. 2003) have suggested that transverse dispersion is a less important transport process than is frequently assumed. In addition, modeling studies tend to over-represent the magnitude of dispersion (Gelhar et al. 1992, Cirpka et al. 1999). The magnitude of transverse mixing can strongly affect overall plume attenuation (Cirpka et al. 1999). The mixing between contaminated and uncontaminated water along the lateral borders of a plume facilitates chemical reactions that are destructive of contaminant mass. As a consequence, the plume is shorter than it would be if no reactions took place.

Gelhar et al. (1992) compiled and evaluated dispersivity data from 59 separate sites. The data collected in the study indicated a systematic increase of longitudinal dispersivity with the observation scale. On the basis of this and similar work, dispersion in many modeling investigations has been treated as a scale-dependent process (e.g., Falta et al. 2007). At a given scale, Gelhar et al. (1992) found that estimated longitudinal dispersivities tended to vary over 2 to 3 orders of magnitude. In addition to reflecting the propensity for dispersion to increase in

magnitude with increasing heterogeneity in the subsurface media examined, the large variability in derived dispersivities indicated that it is inappropriate to represent longitudinal dispersion using a single, universal relationship between transport scale and dispersivity.

F3.3.3 Molecular Diffusion

Contaminants can migrate in groundwater in response to spatial variations in dissolved concentration, from an area of greater concentration to an area where it is less concentrated. This phenomenon is referred to as molecular diffusion, a mixing process caused by random molecular motions due to the thermal kinetic energy of the dissolved contaminant (Domenico and Schwartz 1997). Molecular diffusion will occur as long as a concentration gradient exists, even if the water is not moving. Aqueous diffusive transport in a subsurface medium obeys a form of Fick's first law for diffusion that has been adapted to porous media:

$$F^* = -D^* i_c \qquad \textbf{(10)}$$

where F^* = the diffusive flux of mass [(mass/area)/time],
D^* = the effective diffusion coefficient (area/time), and
i_c = the dissolved concentration gradient [(mass/volume)/length].

The effective diffusion coefficient in a porous medium is smaller than the bulk diffusion coefficient for a given contaminant in pure water. This reduction in magnitude accounts for a decreased diffusive flux caused by (a) the limited pore space through which diffusion can occur, as represented by the porosity; and (b) the tortuous path that diffusing molecules must follow to transport the chemical around soil grains (Domenico and Schwartz 1997). In relatively permeable groundwater systems, the contributions of molecular diffusion to spreading of contamination are generally regarded as less than those attributed to mechanical dispersion. Diffusion transverse to the ambient flow direction provides another mechanism for mixing contaminated water with uncontaminated water, thus helping to facilitate reactions that are potentially destructive of contamination.

F3.4 Advective-Dispersive Transport

Assessments of aqueous-phase contaminant migration in porous media typically account for the cumulative effects of advection, mechanical dispersion, molecular diffusion, and contaminant sources and sinks, which are the processes listed in the mass balance expression in Equation **(4)**. Appropriately, this combination of processes is called advective-dispersive transport (Cherry et al. 1984). Most models of contaminant transport in groundwater are formulated upon a partial differential equation representative of one form or another of Equation **(4)** (e.g., Bear 1979, Freeze and Cherry 1979, Domenico and Schwartz 1997, Karanovic et al. 2007).

Traditional models of advective-dispersive transport attribute contaminant spreading to the combined influences of mechanical dispersion and molecular diffusion, assuming that both are proportional to the concentration gradient [Equation **(8)** and Equation **(10)**]. The combined process is referred to as hydrodynamic dispersion, with coefficients defined by

$$D_{hi} = D_{mi} + D^*$$

where: D_{hi} = the coefficient of hydrodynamic dispersion in direction i (area/time),
D_{mi} = the coefficient of mechanical dispersion in direction i (area/time), and
D^* = the effective diffusion coefficient (area/time).

Contaminant spreading in 3-D models of transport is simulated using hydrodynamic dispersion coefficients in the longitudinal, transverse horizontal, and transverse vertical directions.

Because hydrodynamic dispersion is assumed to obey Fick's laws (see Section F.3.3.1), advective-dispersive models are commonly referred to as Fickian models. The differential equation upon which the models are based is called the advection-dispersion equation, or simply the ADE. Because it has become tradition over several decades to use models of this kind to simulate contaminant transport in groundwater, the ADE is also sometimes referred to as the classical ADE.

Researchers and practitioners alike have long recognized that Fickian models do not accurately represent transport processes in real groundwater systems. With this recognition, it is not surprising that predictive transport simulations are rarely borne out by subsequent plume monitoring, despite the best efforts of groundwater modelers to calibrate their models. Konikow (2011) describes several characteristics of the Fickian model that do not comport with transport phenomena observed in real groundwater systems. Deviations of the observed transport behavior from that expected by the Fickian model is generally referred to as non-Fickian transport. In response to the fundamental differences between real transport behavior and the results of models based on the classical ADE, Konikow (2011) has called for the development of a better governing equation of transport in groundwater, an equation that captures non-Fickian transport. He is encouraged by recent efforts directed toward that goal, of few of which are briefly mentioned later in Section F3.8.

F3.5 Dispersion Contributions to Plume Stability

A contaminant plume fed by a continuous source could eventually reach a stable, or steady-state, configuration due solely to the effects of transverse dispersion. The development of such a stable plume without the benefit of contaminant degradation processes may seem counterintuitive. However, as discussed in the scientific literature dealing with contaminant transport (e.g., Domenico and Schwartz 1997), virtually steady conditions can result from transverse dispersion alone. As a plume evolves, transverse spreading of contaminant mass across an increasing area causes concentrations to decrease with flow distance, eventually producing contaminant levels at the plume front and margins that are less than the background concentration. In effect, enough time has elapsed and the plume has migrated sufficiently far downgradient that concentrations outside the zone containing constant concentrations (i.e., along the plume edges) are so low as to be considered inconsequential. At this later time, loss of contaminant mass along the plume's border, as defined by the background concentration, occurs at the same rate new contaminant mass is added to the aquifer from the plume source area.

Figure F-4 illustrates conceptually how steady concentrations gradually evolve in a plume that is fed by a continuous source of constant concentration C_0 and is subject to both longitudinal and transverse dispersion. This graph shows concentration-versus-distance profiles along the centerline of the plume for successive times t_1 through t_6. As the plume front migrates, increasing lengths of the plume, extending downgradient from the downstream edge of the source, become

stable. This process continues until all parts of the plume with concentrations greater than or equal to the background concentration C_b have effectively stabilized. In Figure 4, the steady-state concentration equal to the background concentration C_b occurs at location S_b beginning at time t_5. At this time, concentrations upgradient of S_b are stable, ranging between C_0 and C_b, while concentrations downgradient of S_b are less than background and in a transient state. As of time t_6, the plume front has moved even farther downgradient of location S_b (Figure F-4), but it may be a challenge to distinguish the contaminant plume in this area from naturally occurring uranium because contaminant concentrations near the plume front are less than the background value.

The discussion above regarding plume stability is strictly theoretical in the sense that steady-state concentrations are rarely, if ever, observed in groundwater plumes. In real groundwater systems, fluctuations of measured concentration at each location in space are a natural consequence of hydrologic and transport processes and measurement error. Nonetheless, the concentrations at each point within a so-called stable plume tend to fluctuate around an average, representative value for that point, instead of showing an increasing or decreasing trend. These average concentrations are, in effect, representative of the steady concentrations that would be observed in a theoretical system.

Domenico (1987) used an analytical solution to the transient form of the advection-dispersion equation to illustrate that the steady concentrations produced solely by transverse dispersion occur in areas some distance upgradient of the plume's advective front, which is defined as the product of average linear velocity and the time since the onset of contamination in the groundwater. The distance separating the downgradient extent of steady concentrations from the advective front is small in cases where the influence of longitudinal dispersion is relatively minor in comparison to the influence of advection (Domenico 1987). The length of a stable plume created by transverse mixing processes and the concentrations within the plume can also be calculated directly using analytical solutions to the steady-state version of the advection-dispersion transport equation (e.g., Domenico and Palciauskus 1982, Domenico and Robbins 1985, Leij and Bradford 1994). The mathematical derivations of the steady-state models assume that transverse concentration gradients determine the width of the plume and that longitudinal dispersion is an insignificant process.

In most real-world situations, a relatively long transport distance is necessary in order for transverse mixing, by itself, to produce a steady-state plume with border concentrations that are inconsequential. At LM sites, this might require transport distances of a mile or more. Though groundwater flow paths at most LM sites might not meet this requirement, the available transport distance downgradient of the contaminant source at a few sites is sufficiently long for development of effectively stable plumes.

F3.6 Sorption and Retardation

Sorption is one form of the "contaminant sinks" in Equation **(4)** that can cause the mass of a contaminant in solution to decrease. "Sorption" is a general term that encompasses four general processes known as absorption, adsorption, ion exchange, and desorption (McCutcheon et al. 1993). Absorption refers to the incorporation of a chemical into the interior of a solid. Adsorption signifies the attraction of a dissolved chemical to the surface of solid particles, and ion exchange is a specific form of adsorption involving the charge-for-charge replacement of an ionic species on a solid surface by other ionic species in solution. Desorption, in which the

affected chemical dissolves back into the aqueous phase, is the opposite of each of the above adsorption mechanisms. In much of the literature dealing with subsurface transport, it has become generally accepted to use the term sorption as if it specifically represents adsorption (Mercer and Waddell 1993).

The phenomenon of adsorption, in which contaminants leave the dissolved state and affix to the surface of solid materials composing a porous medium, is commonly conceptualized as a partitioning process (i.e., a mass-transfer process) between phases. Chemicals once dissolved in water are said to partition from the aqueous phase to the solid phase (McCutcheon et al. 1993). Because the contaminant is being removed from solution, the adsorptive process effectively reduces the aqueous-phase concentration of the contaminant.

Several relationships can be used to mathematically describe the relative distribution of a contaminant between dissolved and adsorbed states. The most common relationship used in transport modeling assumes linear, equilibrium adsorption. In this context, “equilibrium” means that there is a unique, one-to-one relationship between the aqueous-phase and solid-phase concentrations of the contaminant. This relationship allows the propensity for a chemical to adsorb to solid materials to be described in terms of a soil-water distribution coefficient (Freeze and Cherry 1979):

$$S = K_d C_w \qquad \textbf{(11)}$$

where S = the quantity of chemical mass adsorbed on the solids surface (mass/mass),
K_d = the soil-water distribution coefficient (volume/mass), and
C_w = the dissolved chemical (contaminant) concentration (mass/volume).

The parameter K_d is also sometimes referred to as a soil-water partition coefficient (EPA 1996). The larger the K_d value, the greater the tendency is for the contaminant to adsorb to subsurface media.

Equation **(11)** is representative of a linear isotherm. A sorption isotherm is a curve through several experimentally derived points relating adsorbed concentration to dissolved concentration at a specific temperature (Freeze and Cherry 1979). Contaminant transport in some media may not conform to a linear isotherm, and is better simulated using nonlinear expressions. The Freundlich and Langmuir isotherms are examples of mathematical models that are sometimes used to represent adsorption in nonlinear sorption fields (Mercer and Waddell 1993).

Adsorption slows the downgradient movement of a contaminant in groundwater in comparison to the movement provided by advection and dispersion. Consequently, transport of the contaminant is described as being retarded. In effect, equilibrium partitioning of the contaminant between phases causes its rate of advance to be slower than the average groundwater flow velocity. This is manifested in a concentration-versus-distance profile along the plume's length that is upgradient of the profile resulting from no sorption. Figure F-1a shows the concentration profile attributed to the combined effects of advection, dispersion, and sorption (processes A + D + S) in a 1-D plume fed by a continuous source. In a 1-D plume supplied by a pulse source (Figure F-1b), the combination of these three processes not only retards plume migration but also reduces the peak concentration in the plume.

A retardation factor, which measures the ratio of the average groundwater velocity to the average velocity of a sorbing chemical, can be determined from the chemical's K_d (Freeze and Cherry 1979)

$$R = 1 + \frac{K_d \rho_b}{n} \qquad \textbf{(12)}$$

where: R = the retardation factor (dimensionless),
ρ_b = dry soil bulk density (mass/volume), and
n = porosity (dimensionless).

The structure of Equation **(12)** dictates that R will always have a value that is greater than or equal to 1. An R value greater than 1 signifies that the contaminant migration is retarded relative to the movement of groundwater. Stated another way, an R value greater than 1 signifies that contaminant migration is retarded relative to the average linear velocity of the groundwater.

Contaminant transport models that simulate advective-dispersive transport with sorption defined by Equations **(11)** and **(12)** are described as simulators of linear, equilibrium adsorption, or linear, equilibrium sorption. More commonly, a model of this kind is referred to as a simulator based on the K_d approach, or simply a K_d model. K_d models are still considered to be Fickian because the governing transport equation is identical to the classical ADE with the exception that the average linear velocity and the hydrodynamic dispersion coefficient are reduced by a factor equal to R.

The mechanisms by which dissolved species adsorb to solids vary depending on the type of chemical in solution and the porous media through which transport is occurring. Inorganic chemicals such as metals are adsorbed primarily because of the positive electric charges they carry or chemical reactions that bind them to solid surfaces. Inorganics are particularly adsorbed by hydrous ferric oxide and clay minerals, which typically have very large surface areas and carry an overall negative electric charge. Inorganic chemical K_ds can be measured in laboratory experiments or determined through field tracer studies (Domenico and Schwartz 1997).

From a theoretical perspective, equilibrium sorption does not attenuate the long-term concentration of a contaminant at a given location if the plume is supplied by a continuous contaminant source. This is because the contaminant will eventually arrive at the downgradient location with the same concentration it would have if it were not affected by sorption (i.e., if it were a non-reactive contaminant). In contrast, attenuation of the long-term concentration at a given location due to sorption is possible in a plume fed by a pulse source because the peak concentration in such a plume decreases with increasing transport distance (see Figure F-1b).

F3.7 Accounting for Variable Sorption

Contaminant transport models based on the K_d approach were adopted decades ago as a mathematical convenience, primarily in the interest of simplifying the simulation of advective-dispersive transport of adsorbing contaminants. Though this simplification has made prediction of contaminant fate more efficient, the results of K_d models do not comport with real-world conditions. This is partly because contaminant sorption is a non-equilibrium (kinetic) process rather than an equilibrium process. In addition, the amount of contaminant adsorbed to the

aquifer medium is not solely a function of the contaminant's aqueous-phase concentration, as assumed in Equation (**11),** but also the chemistry of the groundwater and the mineralogy of the aquifer solids. When the variable water chemistry of a groundwater system is taken into account along with the mineral composition of the sediment composing a porous medium, researchers tend to find that the K_d for a specific chemical can vary greatly in both space and time. Accordingly, models that allow for a spatially and temporally variable K_d dependent on ambient aquifer conditions are likely to provide more realistic appraisals of groundwater remedies.

To overcome the limitations of uranium transport models that adopt a constant K_d, models based on surface complexation theory (e.g., Davis and Curtis 2003) have been developed. A considerable amount of aquifer sediment characterization is necessary for the development of a surface complexation model (SCM) for a specific site. But such characterization can prove worthwhile if the SCM accurately accounts for variable sorption as affected by the geochemical characteristics of a groundwater system.

Studies focused on the development of surface complexation models addressing the sorption of hexavalent uranium at LM sites show that uranium K_d values are strongly affected by water pH and the aqueous-phase concentrations of uranium, calcium, and bicarbonate. These studies have demonstrated that equilibrium uranium K_ds for a given site can vary by more than an order magnitude and that uranium transport is considerably more retarded than was previously assumed. They also tend to suggest that the solid-phase uranium available in alluvial aquifers as a contaminant source is much larger than was estimated on the basis of characterization activities at the LM sites.

F3.8 Secondary Sources and Contaminant Tailing

Monitoring of contaminant plumes in groundwater during the past few decades indicates that aqueous-phase concentrations tend to attenuate at much slower rates than predicted by advective-dispersive transport models. This is generally attributed to slow release of contamination from secondary sources in the aquifers containing the plumes. Secondary contaminant sources are distinguished from primary sources in that they consist of contamination beneath or downgradient of the original source of contamination, which was usually at or near the ground surface. The contaminant mass in the secondary sources was left in the subsurface in earlier days of site contamination, when both the contaminant concentrations and the rate of contaminant mass loading to the subsurface were especially high.

Secondary sources can consist of low-permeability sediments in which groundwater velocities are particularly low; intraparticle storage of contaminants in the fractures and dead-end pores of individual sediment grains (intraparticle porosity); adsorbed mass that is released back to groundwater at rates much slower than the rate at which contamination was originally taken out of solution; and solid-phase minerals containing the contaminant that precipitated out of solution due to differences in water chemistry between the primary source fluids and the ambient groundwater chemistry. Because secondary sources release contaminant mass back to groundwater at slow rates, aqueous concentrations in the subsurface tend to remain relatively constant for many years, and often at levels that exceed the applicable groundwater standard. This is manifested as “contaminant tailing” in temporal concentration plots for monitoring wells located downgradient of the original source (Figure F-5). The slow release of secondary contamination to groundwater is sometimes referred to as back-diffusion.

Expected cleanup times for contaminated aquifers are commonly predicted using advective-dispersive transport simulations with Fickian models based on the classical ADE, and linear equilibrium sorption is often assumed to govern the exchange of contaminant mass between the solid and aqueous phases (i.e., the K_d approach). As illustrated in Figure F-5, such models cannot capture the slow, delayed release of contaminant mass from secondary sources and are thus incapable of simulating the contaminant tailing observed at monitoring wells. Consequently, the predicted cleanup times for plumes using model simulation tend to be grossly over-optimistic.

Despite the apparent shortcomings of Fickian models, it is still common for a groundwater modeler to rely on a calibrated K_d model to estimate the remediation time for an aquifer. As a consequence, a modeler can predict full plume remediation within a decade or so, only to realize several years beyond the predicted cleanup the presence of persistently high contaminant concentrations (i.e., contaminant tailing). Moreover, new predictive transport simulations using a revised K_d model are shown to be no more reliable than before. Though there are potentially multiple reasons for such poor predictive performance, reliance on Fickian models assuming equilibrium sorption provides the primary explanation for the overly optimistic projections. In effect, the modeler, by applying a K_d model to evaluate contaminant removal, has vastly underestimated the total contaminant mass that must be flushed from the subsurface to achieve aquifer cleanup. Models capable of simulating non-equilibrium contaminant transport are necessary for capturing contaminant tailing attributed to secondary sources.

A type of model used to simulate non-equilibrium transport assumes that the groundwater system consists of two distinct pore domains, with linear contaminant transfer between them. One domain represents the more permeable sediments in an aquifer that, when connected form preferential pathways (mobile domain) in which contaminant migration is rapid. The second domain (immobile domain) represents media that slowly feed contaminants to the preferential pathways, such as low-permeability sediments or intraparticle porosity. Simulators of this type, which are referred to as dual-porosity, dual-permeability, or dual-domain models, assume that the linear exchange of mass between the domains can be handled with a single, constant mass transfer coefficient. The mass transfer coefficient is typically treated as a model calibration variable. An example of a non-equilibrium model that uses analytical solutions to the governing equations of dual-domain transport is found in Leij and Toride (1997).

More-sophisticated modeling techniques have been developed over the past few decades to improve simulation of the effects of non-equilibrium exchange of contaminant mass between domains. Rather than labeling them as non-equilibrium simulators, these methods are generally referred to as non-Fickian transport models because they attempt to overcome fundamental shortcomings of models based on the classical ADE. Three non-Fickian methods have been sufficiently developed to be of practical use for this purpose, including the continuous time random walk method (e.g., Berkowitz et al. 2006), the fractional advection-dispersion equation (fADE) method (e.g., Benson et al. 2000), and the multi-rate mass transfer (MRMT) method (e.g., Haggerty and Gorelick 1995).

The flow domain in an MRMT model consists of a mobile zone and any number of immobile zones. Transport in the mobile zone conforms to the classical ADE. However, mass transport between the immobile domains and the mobile domain is a diffusion process, enabling the

MRMT model to capture non-Fickian phenomena. The mathematical formulation of a MRMT model produces multiple equations that are solved simultaneously to produce, at each time step, a contaminant concentration in the mobile domain as well as a unique concentration in each of the immobile zones. Mass transfer between each immobile zone and the mobile zone is governed by a unique mass transfer coefficient; generally, the values of the coefficients are stochastically determined via a predefined probability density function. The MRMT approach has been successfully applied to simulate non-Fickian uranium transport phenomena at DOE sites (e.g., Ma et al. 2010). Because MRMT models have been shown to be reliable for simulating contaminant tailing behavior (e.g., Zhang et al. 2007) in alluvial groundwater systems, they could prove useful for capturing recalcitrant contaminant behavior at LM sites, thereby improving the prediction of groundwater remedy performance.

F4.0 References

ASTM (American Society for Testing and Materials), 1995. Standard Guide for Risk-Based Corrective Action Applied at Petroleum Release Sites, ASTM Designation: E 1739-95, West Conshohocken, Pennsylvania.

Anderson, M.P., 1984. "Movement of Contaminants in Groundwater: Groundwater Transport—Advection and Dispersion," in *Groundwater Contamination: Studies in Geophysics*, National Academy Press, pp 37–45.

Bear, J., 1972. *Dynamics of Fluids in Porous Media*, Elsevier, New York.

Bear, J., 1979. *Hydraulics of Groundwater*, McGraw-Hill, New York.

Benson, D.A., S.W. Wheatcraft, and M.M. Meerschaert, 2000. "Application of a fractional advection-dispersion equation," *Water Resources Research*, 36(6):1403–1412.

Berkowitz, B.A., A. Cortis, M. Dentz, and H. Scher, 2006. "Modeling non-Fickian transport in geological formations as a continuous time random walk," *Reviews of Geophysics*, 44(2), RG2003.

Cherry, J.A., R.W. Gillham, and J.F. Barker, 1984. "Contaminants in Groundwater: Chemical Processes," in *Groundwater Contamination: Studies in Geophysics*, National Academy Press, pp 46–64.

Cirpka, O.A., and S. Attinger, 2003. "Effective dispersion in heterogeneous media under random transient flow conditions," *Water Resources Research*, 39(9), SBH 9-1 - 9-15.

Cirpka, O.A., E.O. Frind, and R. Helmig, 1999. Numerical simulation of biodegradation controlled by transverse mixing, *Journal of Contaminant Hydrology*, 40(2):159–182.

Davis, J.A., and G.P. Curtis, 2003. *Application of Surface Complexation Modeling to Describe Uranium(VI) Adsorption and Retardation at the Uranium Mill Tailings Site at Naturita, Colorado*, U.S. Nuclear Regulatory Commission, NUREG/CR-6820.

Domenico, P.A., and V.V. Palciauskas, 1982. “Alternative Boundaries in Solid Waste Management,” *Ground Water*, 20(3):303–311.

Domenico, P.A., and G.A. Robbins, 1985. “A New Method of Contaminant Plume Analysis,” *Ground Water*, 23(4):476–485.

Domenico, P.A., 1987. “An analytical model for multidimensional transport of a decaying contaminant species,” *Journal of Hydrology*, 91(1-2):49–58.

Domenico, P.A., and F.W. Schwartz, 1997. *Physical and Chemical Hydrogeology*, 2nd Ed., John Wiley & Sons Inc.

EPA (U.S. Environmental Protection Agency), 1986a. *Background Document for the Ground-Water Screening Procedure to Support 40 CFR Part 269—Land Disposal*, EPA/530-SW-86-047, January.

EPA (U.S. Environmental Protection Agency), 1986b. “Hazardous Waste Management System—Land Disposal Restrictions,” Final rule, *Federal Register*, 51(216):40572–40654.

EPA (U.S. Environmental Protection Agency), 1996. “Soil Screening Guidance: Technical Background Document, Second Edition,” Office of Emergency and Remedial Response, 9355.4-17A.

Falta, R.W., M.B. Stacy, A.N.M. Ahsanuzzaman, M.Wang, and R.C. Earle, 2007. *REMChlor, Remediation Model for Chlorinated Solvents, User's Manual, Version 1.0*, U.S. Environmental Protection Agency, http://www.epa.gov/ada/csmos/models/remchlor.html, accessed 24 October 2014.

Freeze, R.A., and J.A. Cherry, 1979. *Groundwater*, Prentice-Hall, Englewood Cliffs, N.J.

Gelhar L.W., C. Welty, and K.R. Rehfeldt, 1992. “A critical review of data on field-scale dispersion in aquifers, *Water Resources Research*, 19(1):161–180.

Goode, D.J., and L.F. Konikow, 2000. “Apparent dispersion in transient groundwater flow,” *Water Resources Research*, 26(10): 2339–2351.

Haggerty, R., and S.M. Gorelick, 1995. “Multiple-rate mass transfer for modeling diffusion and surface reactions in media with pore-scale heterogeneity,” *Water Resources Research*, 31(10):2383–2400.

Harleman, D.R., and R.R. Rumer, 1963. “Longitudinal and lateral dispersion in an isotropic porous medium,” *Journal of Fluid Mechanics*, 16:385–394.

Karanovic, M., C.J. Neville, and C.B. Andrews, 2007. BIOSCREEN-AT: BIOSCREEN with an Exact Analytical Solution, *Ground Water*, 45(2), p. 242-245.

Keely, J.F., M.D. Piwoni, and J.T. Wilson, 1986. “Evolving concepts of subsurface contaminant transport,” *Journal of Water Pollution Control Federation*, v. 58.

Konikow, L.F., 2011. “The Secret to Successful Solute-Transport Modeling,” *Ground Water*, 49(2):144–159.

Leij, F.J., and S.A. Bradford, 1994. *3DADE: A Computer Program for Evaluating Three-Dimensional Equilibrium Solute Transport in Porous Media*, U.S. Salinity Laboratory, Agricultural Research Service, U.S. Department of Agriculture, Research Report No. 134.

Leij, F.J. and N. Toride, 1997. *N3DADE: A computer program for evaluating three-dimensional nonequilibrium solute transport in porous media*, U.S. Salinity Laboratory Research Report 143, Riverside, CA.

Ma, R., C. Zheng, H. Prommer, J. Greskowiak, C. Liu, J. Zachara, and M. Rockhold, 2010. “A field-scale reactive transport model for U(VI) migration influenced by coupled multirate mass transfer and surface complexation reactions,” *Water Resources Research*, 46, W05509.

McCutcheon, S.C., J.L. Martin, and T.O. Barnwell Jr., 1993. “Water Quality,” in *Handbook of Hydrology*, Chapter 11, D.R. Maidment, Editor in Chief, McGraw-Hill.

Mercer, J.W., and R.K. Waddell, 1993, “Contaminant Transport in Groundwater,” In *Handbook of Hydrology*, Chapter 16, D.R. Maidment, Editor in Chief, McGraw-Hill.

Olsson, A.H., and P. Grathwohl, 2007. „Transverse Dispersion of Non-reactive Tracers in Porous Media: A new Nonlinear Relationship to Predict Dispersion Coefficients,“ *Journal of Contimant Hydrology*, 92(3-4):149–161.

Rivett, M.O., S. Feenstra, and J.A. Cherry, 2001. “A controlled field experiment on groundwater contamination by a multicomponent DNAPL: creation of the emplaced-source and overview of dissolved plume development,” *Journal of Contaminant Hydrology* 49(1-2):111–149.

Swain, E.D., and D.A. Chin, 2003. “An analytical formulation of two-dimensional groundwater dispersion induced by surficial recharge variability,” *Water Resources Research*, 39(9):17-1–17-8.

Xu, M., and Y. Eckstein, 1995. “Use of Weighted Least-Squares Method in Evaluation of the Relationship Between Dispersivity and Field Scale,” *Ground Water*, 33(6):905–908.

Zhang, Y., D.A. Benson, and B. Baeumer, 2007. “Predicting the Tails of Breakthrough Curves in Regional-Scale Alluvial Systems,” *Ground Water*, 45(4):473–484.

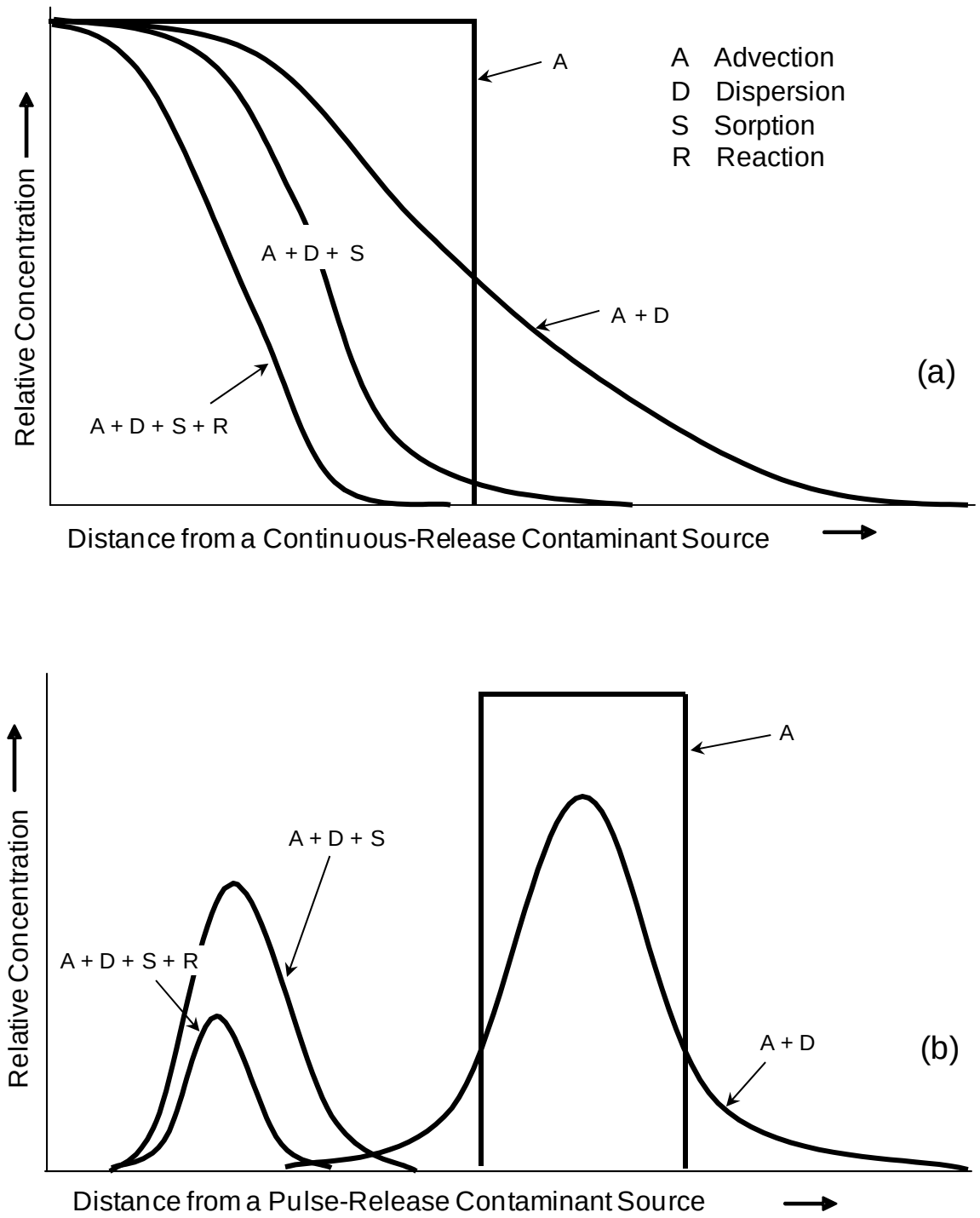

Figure F-1. Contaminant concentration profiles with distance in a one-dimensional plume fed by (a) a continuous-release and (b) a pulse-release source (after Keely et al. 1986).

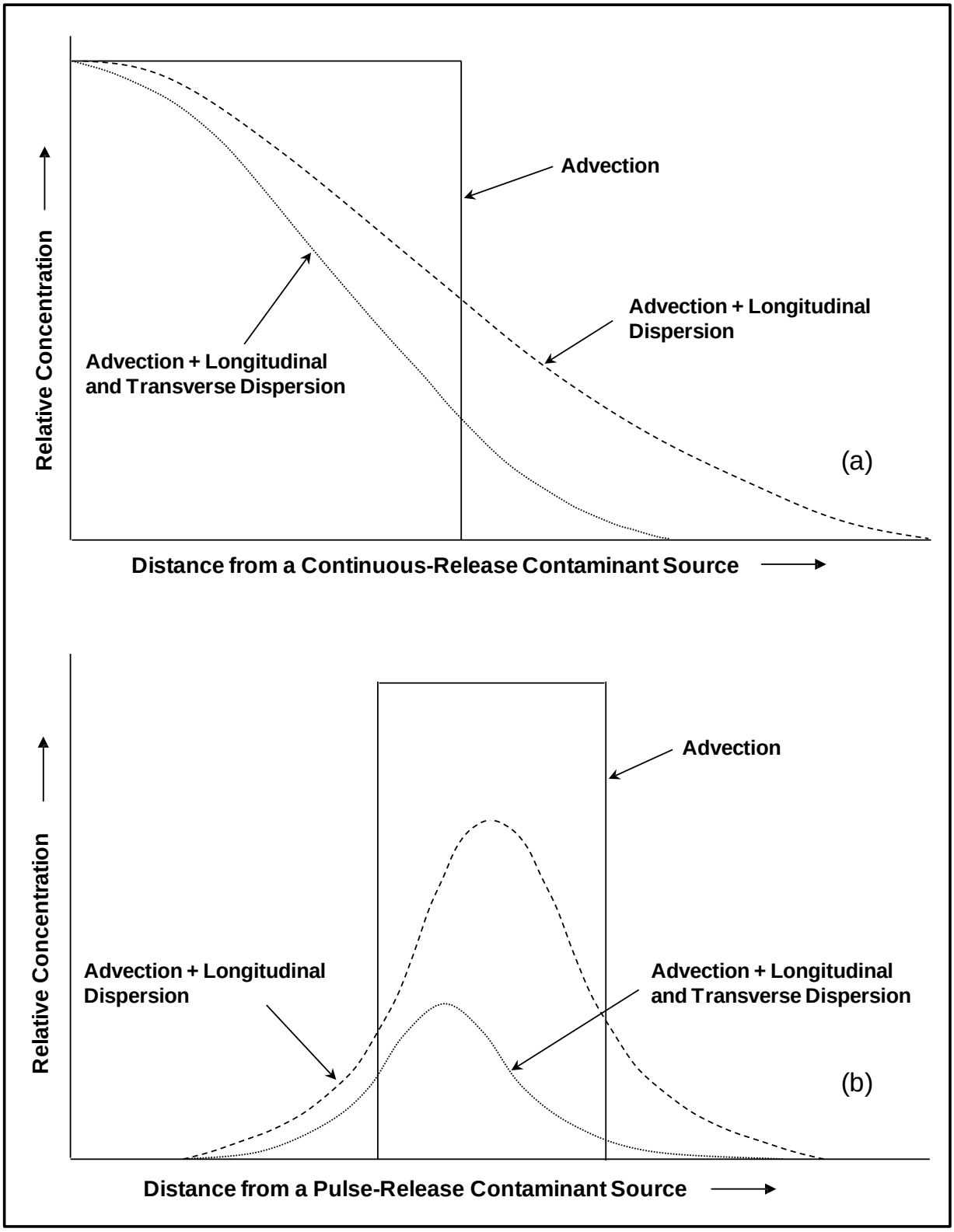

Figure F-2. Relative effects of longitudinal and transverse dispersion on contaminant concentrations along the centerline of a two-dimensional contaminant plume fed by (a) a continuous source and (b) a pulse source.

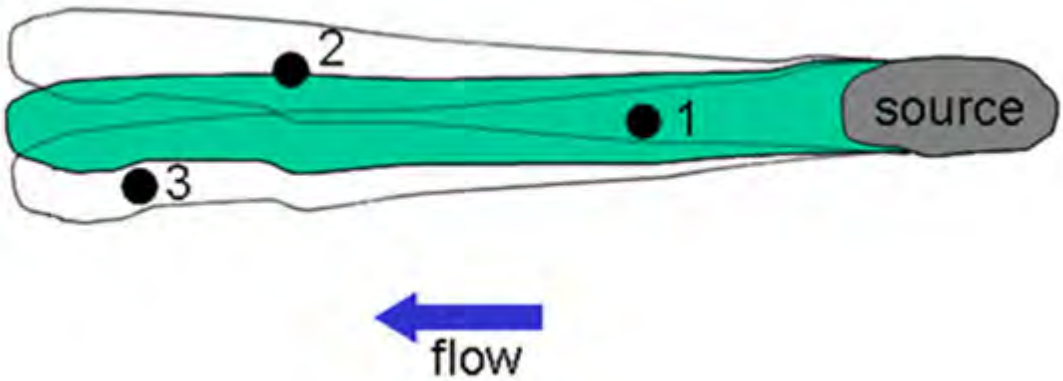

Figure F-3. Schematic illustration of how changing flow direction in a transient flow system produces an apparent dispersion in directions transverse to the average flow direction

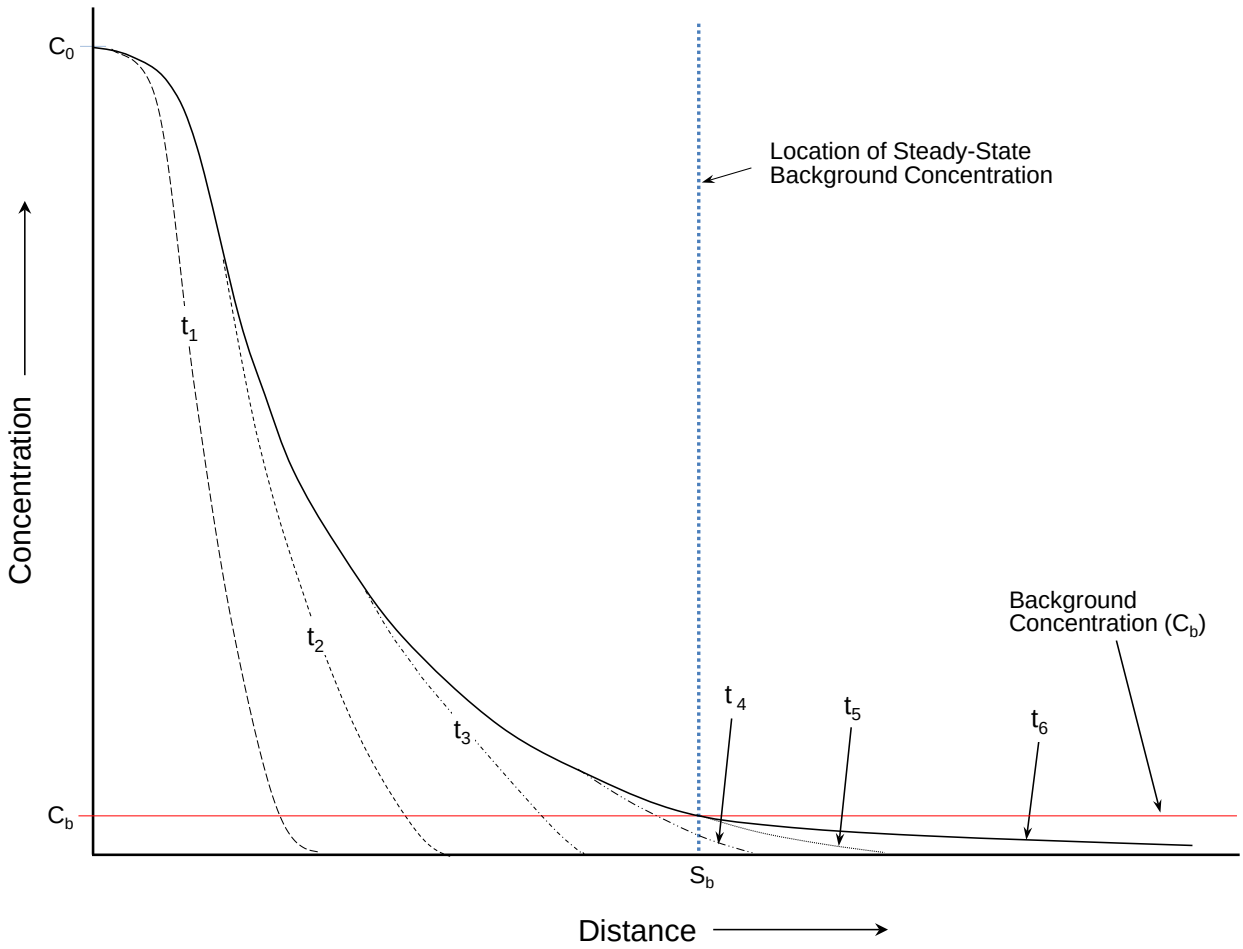

Figure F-4. Graphical Depiction of Contaminant Plume Evolution—Concentration Profiles Along the Plume Centerline at Successive Times t_1 Through t_6

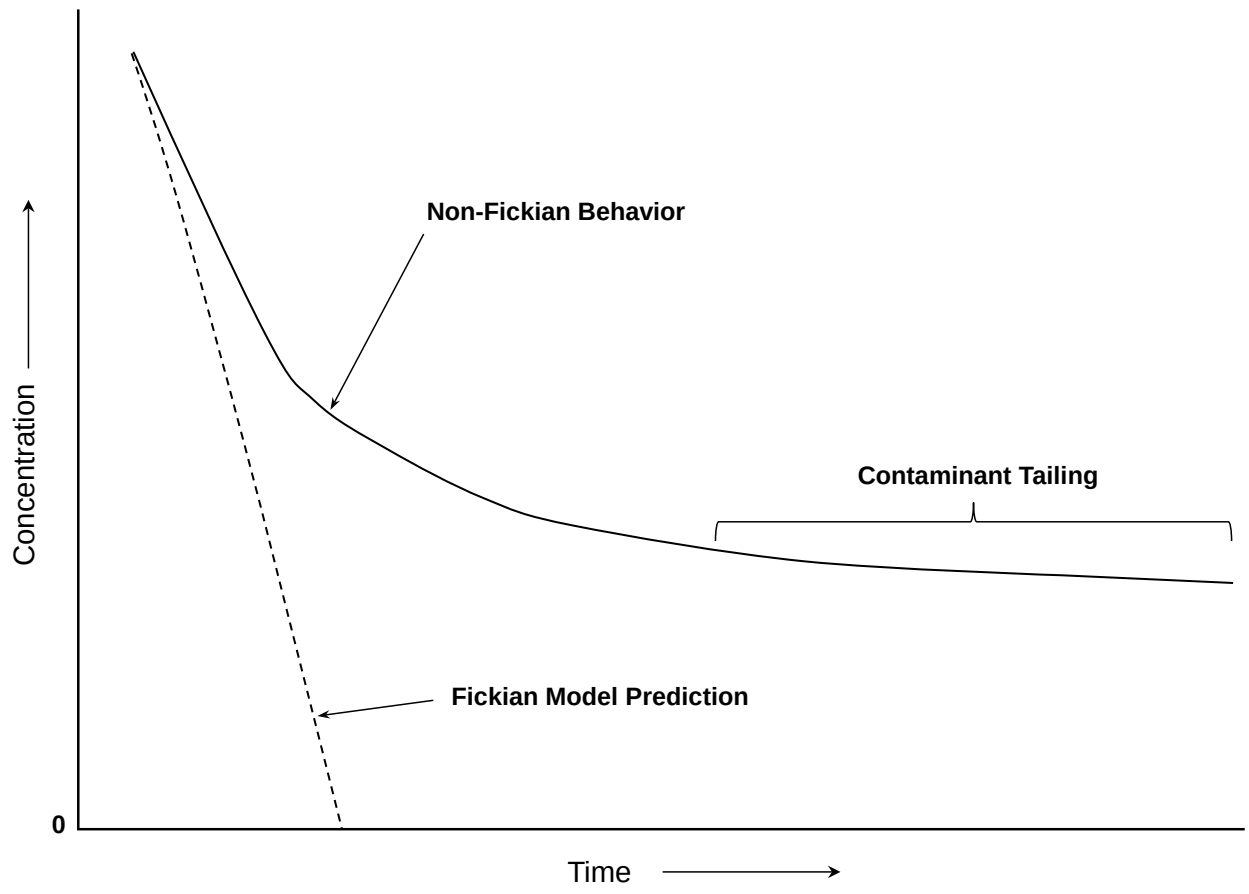

Figure F-5. Late-Time Non-Fickian Behavior and Contaminant Tailing at Monitoring Wells Due to Rate-Limited Mass Transfer from Secondary Sources

Plates

Plate 1 Conceptual Model Study Area

Plate 2 Geologic Map of the Study Area

Plate 3 Geologic Map of the Bluewater Site

Plate 4 Study Area Geologic Cross Sections A-A′ and B-B′

Plate 5 Site Geologic Cross Sections A-A′, B-B′, and C-C′

Plate 6 Site Geologic Cross Sections D-D′, E-E′, and F-F′

Plate 7 Well Locations

This page intentionally left blank

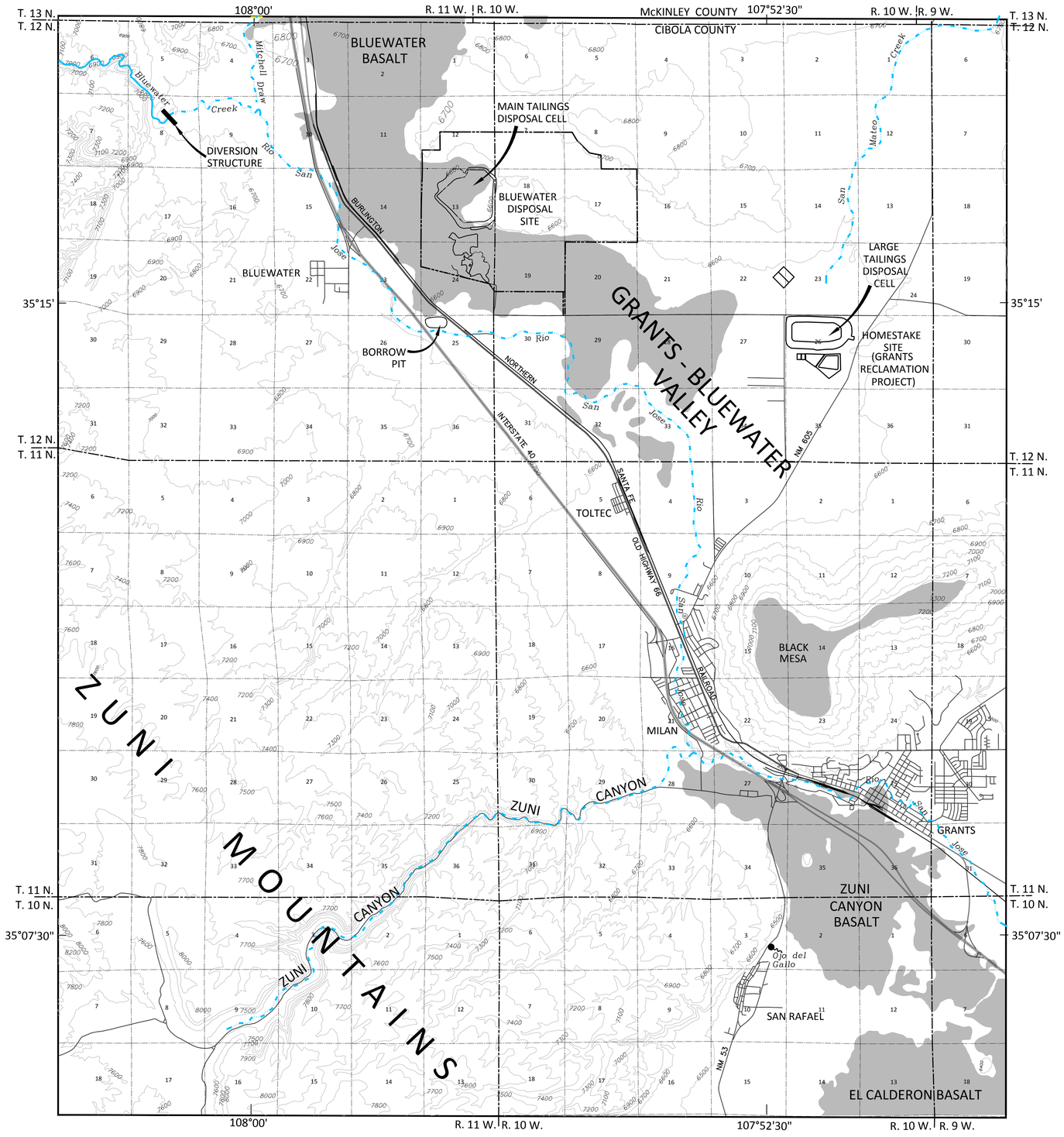

LEGEND

- BASALT
- PERENNIAL STREAM
- EPHEMERAL STREAM
- 7000 ELEVATION CONTOUR (FEET ABOVE MEAN SEA LEVEL)

N

SCALE IN FEET

4000 2000 0 4000 8000 12000

SCALE 1" = 4000' or 1:48,000

U.S. DEPARTMENT OF ENERGY GRAND JUNCTION, COLORADO	Work Performed by The S.M. Stoller Corporation Under DOE Contract No. DE-AM01-07LM00060
Plate 1	CONCEPTUAL MODEL STUDY AREA
DATE PREPARED: 3/17/2014	FILENAME: S1139500

M:\LTS\111\0024\12\000\S11395\S1139500.DWG 06/03/14 2:51pm atencioj

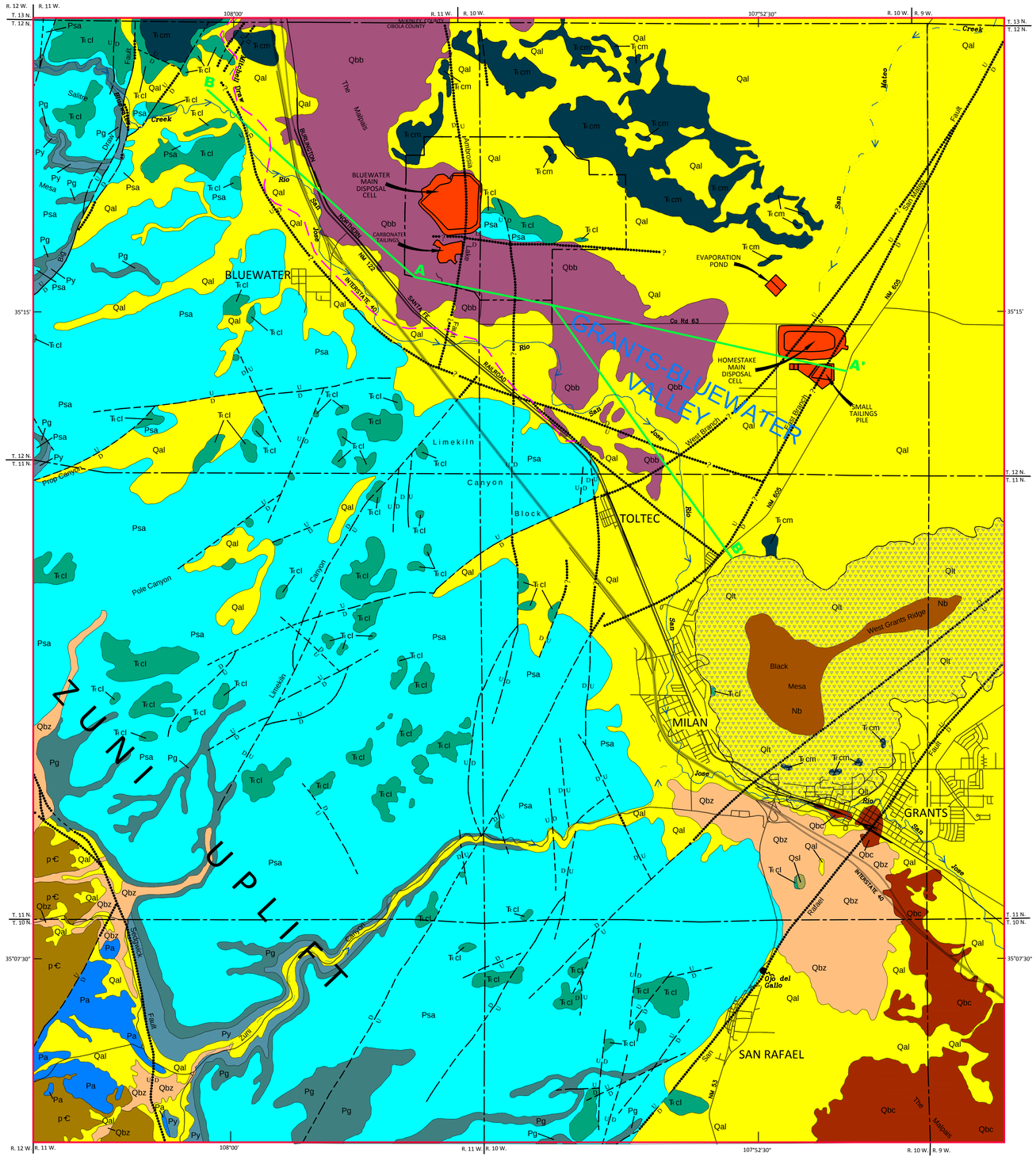

7.5 MINUTE TOPOGRAPHIC MAPS REPRESENTED ON THE REGIONAL GEOLOGIC MAP

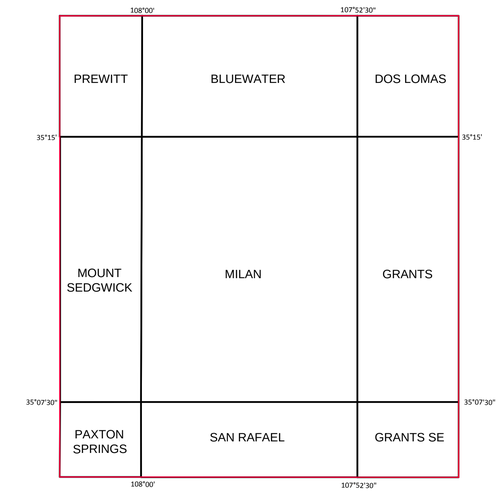

Explanation

- Uranium mill tailings disposal cell and other tailings areas

QUATERNARY
- Qal — Unconsolidated silt, clay, sand, and gravel
- Basalt Flow:
  - Qbz — Zuni Canyon
  - Qbb — Bluewater
  - Qbc — El Calderon
- Qlt — Landslide and talus material
- Qsl — Spring-deposited limestone

NEOGENE
- Nb — Basalt capping Black Mesa

UPPER TRIASSIC — Chinle Formation
- TRcm — Middle part; includes Sonsela Sandstone Bed of Petrified Forest Member
- TRcl — Lower part; may include thin Moenkopi Formation

LOWER PERMIAN
- Psa — San Andres Limestone
- Pg — Glorieta Sandstone
- Py — Yeso Formation
- Pa — Abo Formation

PRECAMBRIAN
- p€ — Granite, gneiss, and schist

Contact, approximate location

Fault; solid where certain, dashed where approximately located, dotted where concealed, and queried where uncertain. U is upthrown side and D is downthrown side.

Bluewater Title II Site Boundary

Ojo del Gallo — Spring and Name

Stream: solid where perennial, dashed where intermittent, showing direction of flow

Approximate southwestern edge of Bluewater Basalt beneath Qal

B — B' Line of Cross Section

Modified from U.S. Geological Survey Professional Paper 386-D, Plate 1

N

SCALE IN FEET
4000 2000 0 4000 8000 12000
SCALE 1" = 4000' or 1:48,000

U.S. DEPARTMENT OF ENERGY GRAND JUNCTION, COLORADO	Work Performed by The S.M. Stoller Corporation Under DOE Contract No. DE-AM01-07LM00060
Plate 2 — GEOLOGIC MAP OF THE STUDY AREA	
DATE PREPARED: 06/12/2014	FILENAME: S1138200

M:\LTS\111\0024\12\000\S11382\S1138200.DWG 06/12/14 10:57am whitneyj

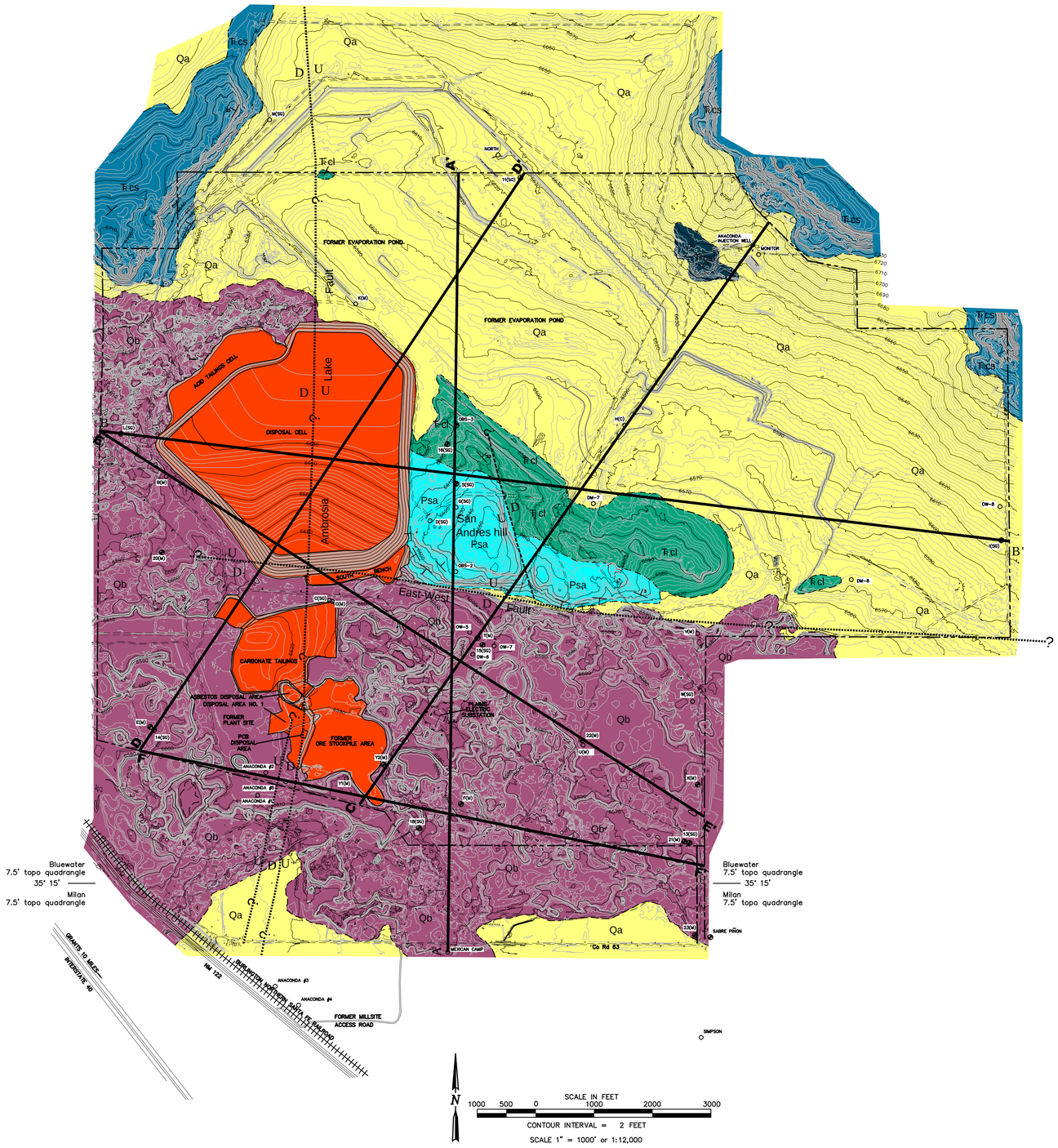

Explanation

Disposal cell and other tailings and stockpile areas

QUATERNARY

- Qa — Alluvium (includes artificial fill and disturbed land, colluvium, dune sand, and talus)
- Qb — Bluewater Basalt
- Qab — Ancestral Rio San Jose Alluvium: pre–Bluewater Basalt, not exposed but shown in cross sections

UPPER TRIASSIC — Chinle Formation

- Ŧcs — Main part of Sonsela Sandstone Bed of Petrified Forest Member
- Lower sandstone bed in the Sonsela Sandstone Bed of Petrified Forest Member
- Ŧcl — Lower beds of Chinle Formation; may include thin Moenkopi Formation

LOWER PERMIAN

- Psa — San Andres Limestone

Contact, approximate location

25 — Strike and dip (where measured) of beds

U D ...?... — Fault, solid where certain, dashed where approximately located, dotted where concealed, and queried where uncertain. U is upthrown side and D is downthrown side.

A — A' — Line of cross section

Site boundary

18(SG) — Active well and number in San Andres Limestone and/or Glorieta Sandstone

23(M) — Active well and number in Alluvium of Ancestral Rio San Jose

OW-8 — Abandoned well and name/number

Geology modified from:

1967 USGS Map GQ–679
by R. E. Thaden and E. J. Ostling
2013 NMBGMR OF Geologic Map 236
by G.C. Rawling
2012 NMBGMR OF Geologic Map 231
by G.C. Rawling

U.S. DEPARTMENT OF ENERGY GRAND JUNCTION, COLORADO	Work Performed by The S.M. Stoller Corporation Under DOE Contract No. DE–AM01–07LM00060
Plate 3	GEOLOGIC MAP OF THE BLUEWATER SITE
DATE PREPARED: 6/12/2014	FILENAME: S1138500

M:\LTS\111\0024\12\000\S11385\S1138500.DWG 06/12/14 11:14am whitney

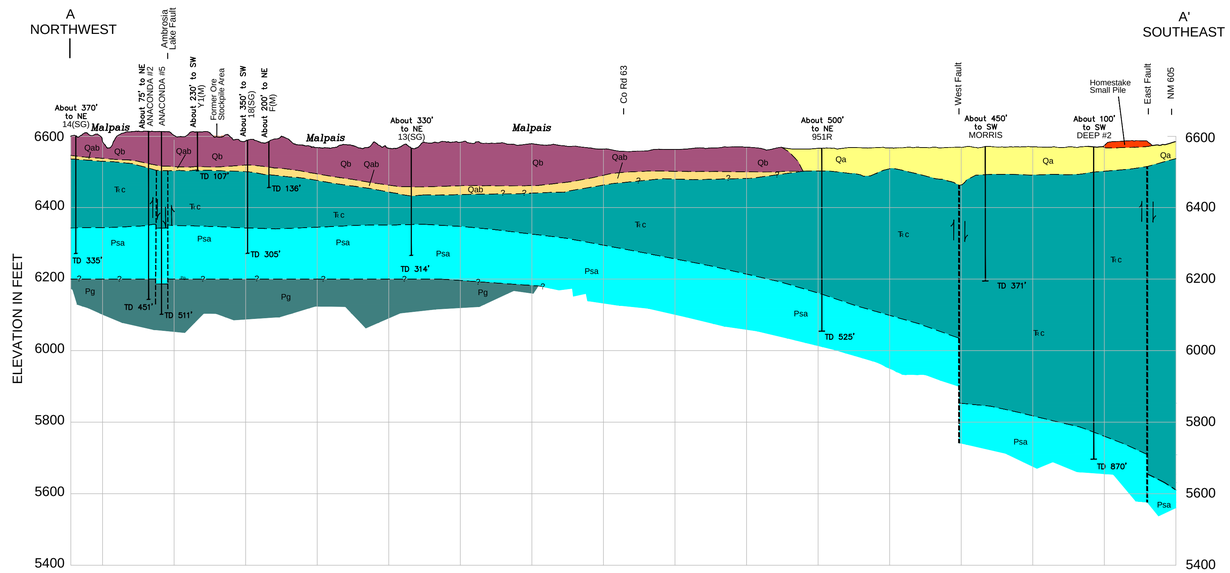

Explanation

- Disposal cell and other tailings and stockpile areas
- Qls Landslide material

QUATERNARY

- Qa Alluvium (includes artificial fill and disturbed land, colluvium, dune sand, and talus)
- Qb Bluewater Basalt
- Qab Ancestral Rio San Jose Alluvium

UPPER TRIASSIC

Chinle Formation — Tr c Undifferentiated

LOWER PERMIAN

- Psa San Andres Limestone
- Pg Glorieta Sandstone

Normal fault, arrows show direction of movement

Geologic contact, question marked where uncertain

Horizontal scale: 1" = 2000'
Vertical scale: 1" = 100'

Vertical exaggeration X10

About 180' to E F(M) — TD 136'

Monitor well, distance and direction from cross section line, and total depth of well.

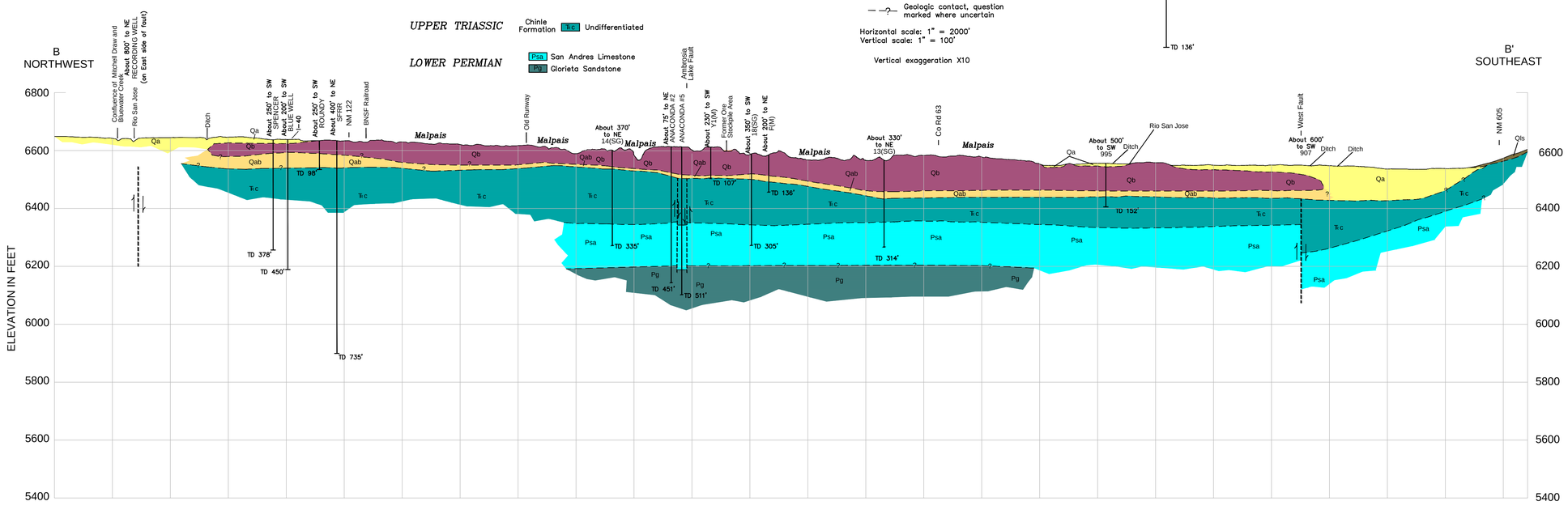

U.S. DEPARTMENT OF ENERGY GRAND JUNCTION, COLORADO	Work Performed by The S.M. Stoller Corporation Under DOE Contract No. DE-AM01-07LM00060
PLATE 4	STUDY AREA GEOLOGIC CROSS SECTIONS A–A' AND B–B'
DATE PREPARED: 6/11/2014	FILENAME: S1139400

M:\LTS\111\0024\12\000\S11394\S1139400.DWG 06/11/14 2:53pm whitneyj

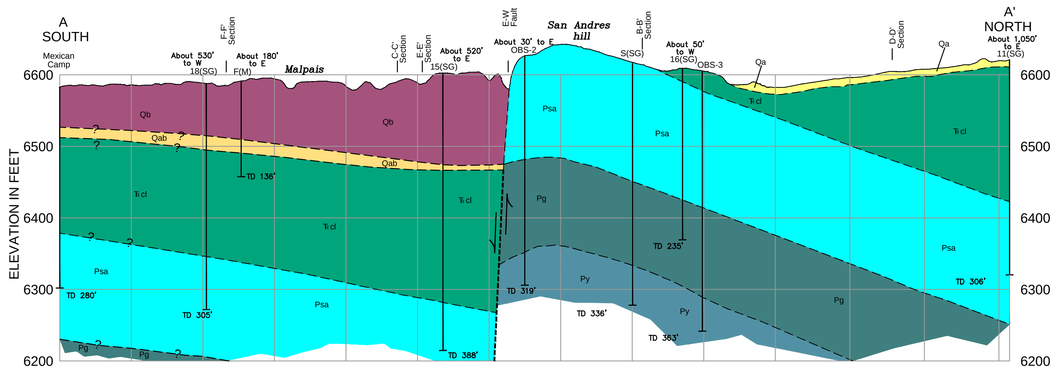

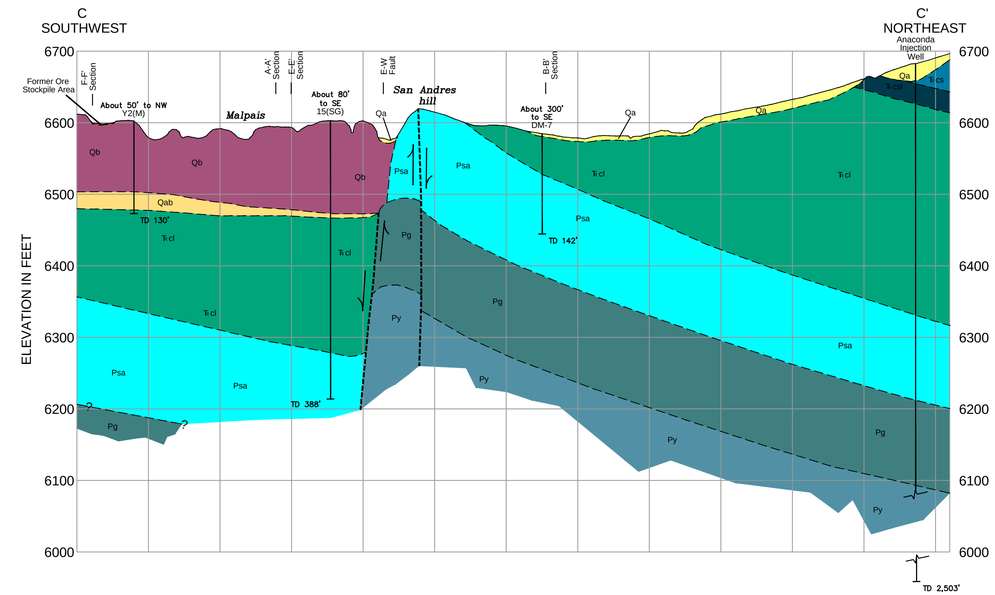

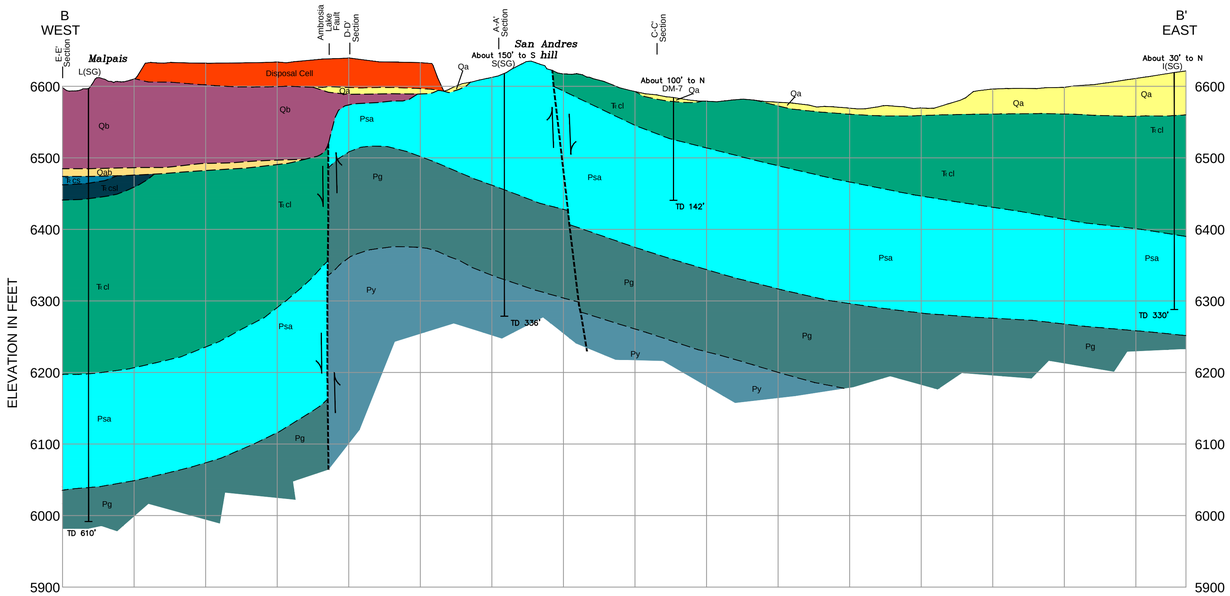

Explanation

Disposal cell and other tailings and stockpile areas

QUATERNARY

- Qa — Alluvium (includes artificial fill and disturbed land, colluvium, dune sand, and talus)
- Qb — Bluewater Basalt
- Qab — Ancestral Rio San Jose Alluvium

UPPER TRIASSIC

Chinle Formation

- Tr cs — Main part of Sonsela Sandstone Bed of Petrified Forest Member
- Tr cs — Lower sandstone bed in the Sonsela Sandstone Bed of Petrified Forest Member
- Tr cl — Lower beds of Chinle Formation

LOWER PERMIAN

- Psa — San Andres Limestone
- Pg — Glorieta Sandstone
- Py — Yeso Formation

Normal fault, arrows show direction of movement

Geologic contact, question marked where uncertain

Horizontal scale: 1" = 1000'
Vertical scale: 1" = 100'

Vertical exaggeration X10

About 180' to E
F(M)
TD 136'

Monitor well, distance and direction from cross section line, and total depth of well.

U.S. DEPARTMENT OF ENERGY GRAND JUNCTION, COLORADO	Work Performed by The S.M. Stoller Corporation Under DOE Contract No. DE-AM01-07LM00060
Plate 5	SITE GEOLOGIC CROSS SECTIONS A–A', B–B,' AND C–C'
DATE PREPARED: 6/11/2014	FILENAME: S1138800

M:\LTS\111\0024\12\000\S11388\S1138800.DWG 06/12/14 11:36am whitneyj

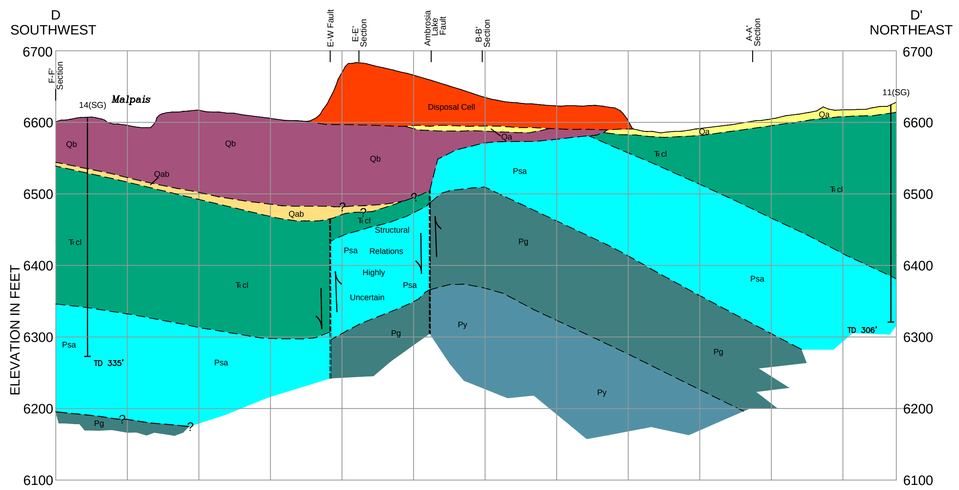

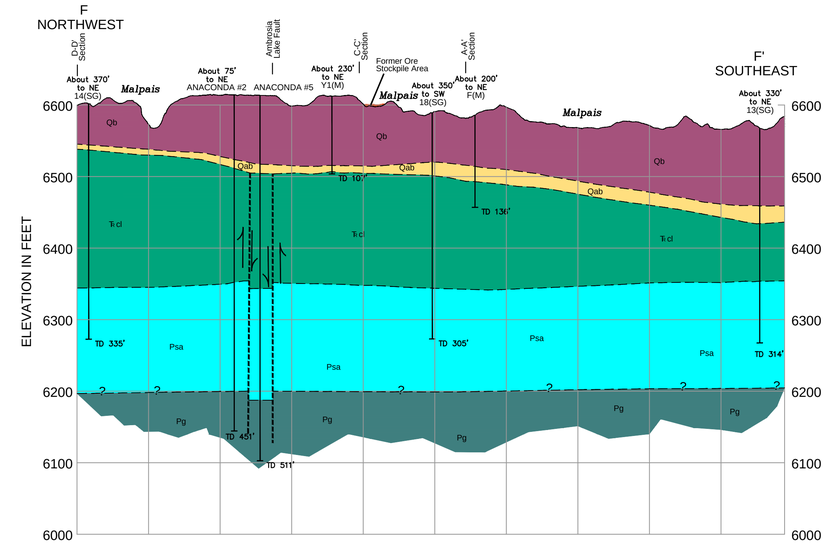

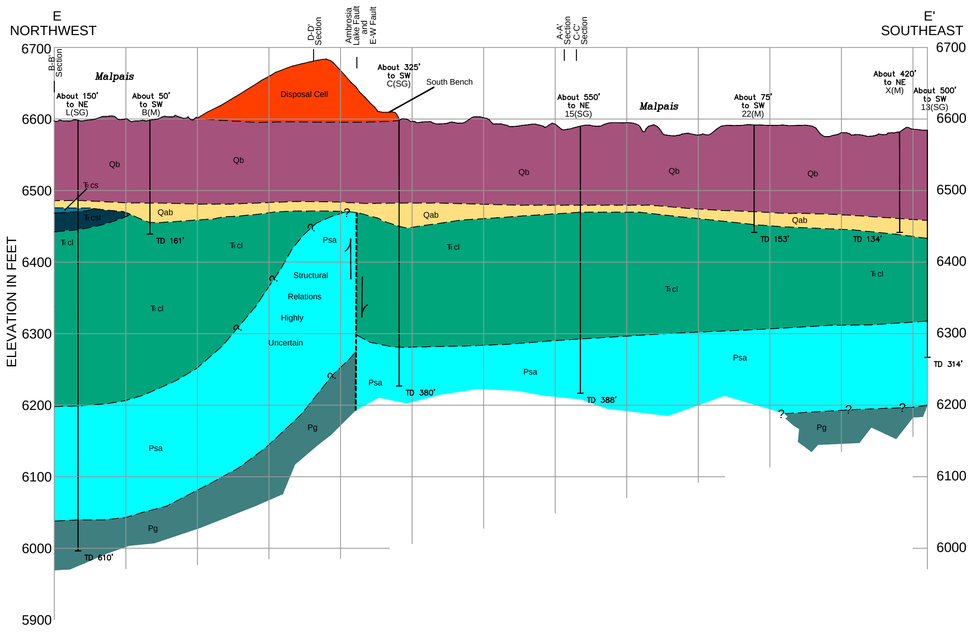

Explanation

Disposal cell and other tailings and stockpile areas

QUATERNARY

- Qa — Alluvium (includes artificial fill and disturbed land, colluvium, dune sand, and talus)
- Qb — Bluewater Basalt
- Qab — Ancestral Rio San Jose Alluvium

UPPER TRIASSIC

Chinle Formation

- Tr cs — Main part of Sonsela Sandstone Bed of Petrified Forest Member
- Tr cl — Lower sandstone bed in the Sonsela Sandstone Bed of Petrified Forest Member
- Tr cl — Lower beds of Chinle Formation

LOWER PERMIAN

- Psa — San Andres Limestone
- Pg — Glorieta Sandstone
- Py — Yeso Formation

Normal fault, arrows show direction of movement

Geologic contact, question marked where uncertain

Horizontal scale: 1" = 1000'
Vertical scale: 1" = 100'

Vertical exaggeration X10

About 180' to E F(M) — TD 136'

Monitor well, distance and direction from cross section line, and total depth of well.

U.S. DEPARTMENT OF ENERGY GRAND JUNCTION, COLORADO	Work Performed by The S.M. Stoller Corporation Under DOE Contract No. DE-AM01-07LM00060
Plate 6	SITE GEOLOGIC CROSS SECTIONS D-D' E-E', AND F-F'
DATE PREPARED: 6/12/2014	FILENAME: S1138900

M:\LTS\111\0024\12\000\S11389\S1138900.DWG 06/12/14 11:43am whitneyj

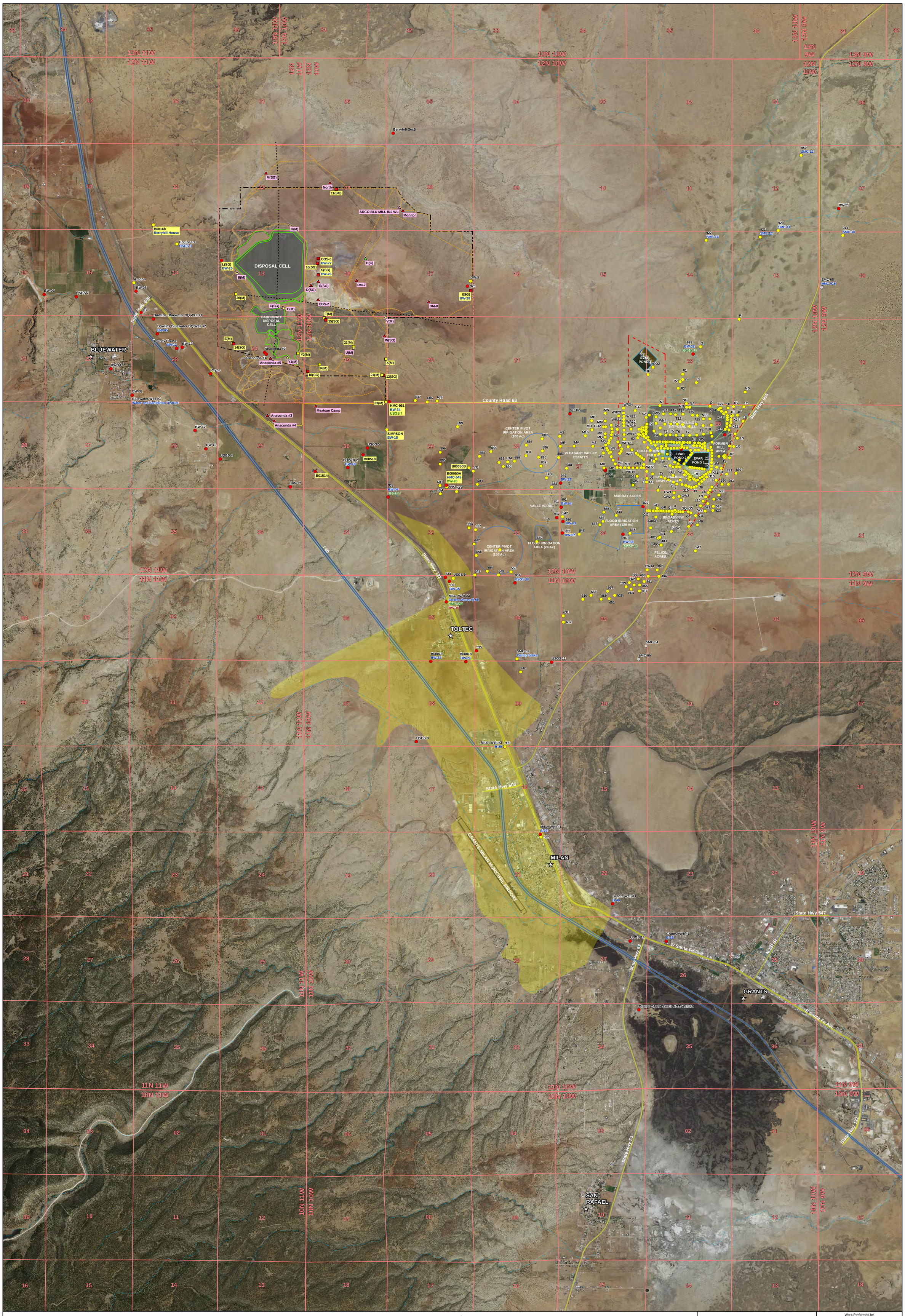

DOE-Owned Well
- Alluvium
- San Andres

Non-DOE-Owned Well
- Alluvium
- San Andres
- Unknown

Decommissioned Well
- Alluvium
- Chinle
- Precambrian (Other)
- San Andres

Y2(M) *Wells regularly and/or recently sampled by DOE are highlighted in yellow. These include some distal residential (non-DOE) wells (e.g.,B00518, also shown in Figure 5).*

Y1(M) *Decommissioned wells highlighted in pink.*

Explanation of Well Label Colors (see note):
LOCATION CODE
ALTERNATE LABEL 1
ALTERNATE LABEL 2
ALTERNATE LABEL 3

Note:
Several wells are referred to by different names or numbers depending on the study or data source. In these cases, well labels are shown in different colors (alternate labels), with black initial labels denoting the primary well reference used in this report. Detailed cross-reference information is provided in Appendix B. Given the focus of this study, this map shows locations of only those Homestake wells screened in the alluvial and San Andres aquifers (see Appendix B). For information on Homestake wells screened in the Chinle aquifer, the reader is referred to Homestake's annual reports.

- Homestake NRC License Boundary
- Homestake Tailings Pile
- Homestake Pond
- Homestake Irrigation Area
- Homestake Features
- Township
- Section
- 18 Section Number

Bluewater Site Features
- Site Boundary
- Dirt Road
- Disposal Cell or Cover
- Concealed Fault

- Municipalities
- Railroad
- Interstate Highway
- State Highway
- River
- Approximate Area Where Alluvium Directly Overlies San Andres Limestone

N

SCALE IN MILES
½ ¼ 0 ½ 1

U.S. DEPARTMENT OF ENERGY
GRAND JUNCTION, COLORADO

Work Performed by
S.M. Stoller Corporation
Under DOE Contract
No. DE-AM01-07LM00060

Plate 7
Well Locations

DATE PREPARED: June 24, 2014

FILENAME: S1154500-D+

\\lm\ess\EnvProjects\EBM\LTS\111\0024\12\000\S11545\S1154500-D+.mxd coatesc 24 June 2014 11:39:34 AM

This page intentionally left blank